FIELD-BASED EVALUATION OF PROCESSES AND MODELS FOR SOIL VAPOUR INTRUSION INTO BUILDINGS

By

IAN HERS

B.A.Sc., The University of British Columbia, 1986

M.A.Sc., The University of British Columbia, 1989

A THESIS SUBMITTED IN PARTIAL FULFILLMENT OF THE REQUIREMENTS FOR THE DEGREE OF

DOCTOR OF PHILOSOPHY

In

THE FACULTY OF GRADUATE STUDIES

Department of Civil Engineering

We accept this thesis as conforming to the required standard

.....

THE UNIVERSITY OF BRITISH COLUMBIA

August, 2004

© Ian Hers, 2004

ABSTRACT

This thesis presents the results of research on the validation of models used to evaluate the intrusion of subsurface volatile organic compounds (VOCs) into buildings, often referred to as the "soil vapour transport to indoor air pathway". Evaluation of this exposure pathway is important in the context of risk-based corrective action for contaminated sites. The study scope addresses both the fate and transport of VOCs in the unsaturated zone, and intrusion of VOCs through the subsurface building envelope (i.e., foundation). The primary approach adopted to investigate and validate models was to obtain extensive field monitoring data on VOC vapour transport and intrusion, obtained at a former petro-chemical plant site ("Chatterton" site). The Chatterton site, located near Vancouver, B.C., Canada, is contaminated with benzene, toluene and xylenes (BTX).

To facilitate measurement of BTX intrusion, a small building (greenhouse) with controlled properties was constructed. A number of experiments were conducted to evaluate vadose zone processes and vapour intrusion for different greenhouse depressurization conditions. When the greenhouse was not subject to sustained fan-induced depressurization, there was significant aerobic biodegradation of BTX vapours between approximately 0.4 m and 0.8 m depth below the greenhouse, and subslab BTX vapour concentrations were low. When the greenhouse was depressurized to –10 pascals (Pa), the subslab BTX vapour concentrations were elevated, and significant vapour intrusion was measured using both tracer and flux chamber techniques, which was inferred to be a result of an upward BTX vapour flux that exceeded biodegradation capacity based on oxygen availability.

A comprehensive analysis of case studies providing information on soil vapour intrusion was completed. This analysis, together with the Chatterton site results, were evaluated for key trends and factors affecting soil vapour intrusion. The vapour attenuation factors estimated based on field case studies were compared to those predicted using several screening level models, including the Johnson and Ettinger Model, a widely used model for this exposure pathway.

The validation of screening models using field data is complicated in that model predictions can vary greatly depending on the model and input parameters used. Further, soil vapour fate and transport and intrusion into buildings is a complex process affected by numerous factors (soil properties, house conditions, and environmental factors); therefore, vapour intrusion will vary significantly depending on site specific conditions. The results of the model comparisons to field data indicated that screening level models, typically used for this exposure pathway, were found to generally yield conservative results (i.e., overpredict vapour intrusion); however, there were a few important exceptions.

A multi-dimensional numerical model for vapour transport, which incorporated diffusion, biodegradation, sorption and soil gas advection, was also developed. Good comparisons between model predicted and measured vapour attenuation were obtained based on conditions observed at the Chatterton site.

TABLE OF CONTENTS

Abstract ii

Table of Contents iii

List of Tables viii

List of Figures x

Acknowledgements xv

Chapter 1 **Introduction** 1
Key Issues and Research Relevancy 1
Conceptual Site Model 2
Predictive Models and Framework for Their Use 3
Model Validation 3
Data Gaps and Questions Left to Be Answered 4
Purpose, Objectives and Scope 5
Background Information and Overview of Research Program 6
Structure of this Thesis 7
References 9

Chapter 2 **Evaluation of Soil Vapour Sampling and Analysis Techniques** 11
Introduction 12
Background Information Review 12
Probe Design for Soil Gas Collection 12
Sampling Collection and Handling 13
Analytical Techniques 14
Field Screening Methods 14
Laboratory Analytical Techniques 14
Evaluation of Experimental Methods 15
Rationale 15
Overview of Soil Gas Sampling and Analysis Methods at Chatterton Site 16
Tedlar Bag Permeation Study 17
Methods 17
Results 17
Syringe Sorption Study 17
Methods 17
Results 18
PVC Sorption Study 18
Methods 18
Results 18
Light Gas Analysis Study 20
Methods 20
Results 20

Consistency of Soil Gas with Biogeochemical Processes 22
BTX Analytical Quality Control Study 23
Methods 23
Results 24
Discussion of Experimental Techniques and Lessons Learned 24
Probe Design 24
Sampling Collection and Analysis 25
Analytical Techniques 26
Field Screening Methods 26
Laboratory Analytical Techniques 26
Conclusions 28
References 29

Chapter 3 **Measurement of In *situ* Gas-Phase Diffusion Coefficients** 31
Introduction 32
Background 33
Theory 35
Methods 37
Results 40
Sensitivity Analyses 44
Conclusions 44
References 46

Chapter 4 **Evaluation of Vadose Zone Biodegradation of BTX Vapours** 47
Introduction 48
Intrinsic Biodegradation 48
Processes and Effect of Building 48
Biodegradation Models and Kinetics 49
Evaluation of Biodegradation Potential 50
BTEX Attenuation 50
Geochemical Indicators 51
Laboratory Studies 52
Field study 52
Overview 52
Site Description 56
Methods 53
Baseline Soil Testing Results 55
Soil Gas Monitoring Results 56
Estimation of Field Biodegradation Rates 59
Comparison to Other Case Studies 60
Numerical Simulation of Vadose Zone BTX Transport 62
Model Description 62
Comparison to Analytical Solutions 65
Comparison of Biodegradation Models No. 1, 2, 3 and 4 (1-D Diffusion and Biodecay) 66
Comparison to Chatterton Vapour Profiles (2-D Diffusion and Biodecay) 68

Sensitivity Analysis Adjacent to Building at Chatterton site (1-D Diffusion and Biodecay) 71
Evaluation of Advective Transport at Chatterton site (1-D Diffusion, Advection and Biodecay) 72
Conclusions 74
References 75

Chapter 5 Measurement of BTX Vapour Intrusion into an Experimental Building 77
Introduction 78
Background Review and Case Studies 78
Soil Gas Models 79
Analytical Models 79
Numerical Models 80
Emperical Methods 81
Experimental Methods 81
Research Site Description 81
Description of Greenhouse, Soil Gas Probes and Soil-Air Permeability Testing 82
Soil Gas, Pressure, Temperature and Oxygen Monitoring Methods 83
Flux Chamber 84
Soil Gas Flow Rate and BTX Flux into Greenhouse Measured Using Tracer Test 85
Soil Gas Flow Rate into Greenhouse Measured Using Flux Chamber 86
BTX Flux Rates into Greenhouse Measured Using Flux Chamber 86
Experimental Results 87
Overview Soil Gas Intrusion Testing Program 87
Soil Air Permeability 87
Soil Gas Flow Rate and BTX Flux into Greenhouse Measured Using Tracer Test 88
Soil Gas Flow Rates Measured Using Flux Chamber 88
BTX Flux Rates into Building Measured Using Flux Chamber 93
Non Depressurized Condition 93
Subslab Oxygen, Pressure and Weather Monitoring 94
Depressurized Condition 94
Comparison to Model Predictions 95
Discussion 98
Conclusions 99
References 100

Chapter 6 Comparision, Validation and Use of Models for Predicting Indoor Air Quality From Soil and Groundwater Contamination 102
Introduction 103
Model Review 104
Introduction 104
Source Zone Model Attributes 104
Unsaturated Zone Model Attributes 106

Diffusion and Advection 106
Biodegradation 106
Building Foundation Model Attributes 108
Diffusion 108
Advection 108
Selection of Models for Validation 109
Model Validation - Effect of Transport Processes 110
Model Validation - Model Sensitivity and Effect of Parameter Uncertainty 112
Sensitivity Analysis 112
Effect of Parameter Uncertainty 113
Effect of Uncertainty in Soil Moisture Content and Bulk Density 115
Model Validation – Comparisons Based On Field Data 117
Description of Case Study Sites 118
Biodegradation Rates 119
Soil Gas Advection and Flow into Buildings 119
Soil Vapour Intrusion into Buildings 121
Chatterton Site Results 121
Comparisons of Measured and Predicted Vapour Attenuation Ratios 124
Proposed Tiered Framework, Discussion and Guidance 125
Proposed Tiered Framework 125
Advection Potential 127
Source Depletion 128
Biodegradation 129
Concluding Thoughts 129
References 130

Chapter 7 Evaluation of the Johnson and Ettinger Model for Prediction of Indoor Air Quality 132
Introduction 133
J&E Model Input Parameters, Sensitivity and Uncertainty 133
Estimation of Effective Diffusion Coefficient (Air-Filled and Total Porosity) 133
Estimation of Soil Gas Advection Rate (Q_{soil}) 135
J&E Model Sensitivity for Key Input Parameters 137
Sensitivity of α_p to Q_{soil} 139
Sensitivity of α_p to Crack Ratio 139
Sensitivity of α_p to Air-Filled Porosity (Moisture Content) 140
J&E Model Uncertainty for Range of Values 140
Field-Based Methods For Evaluation Of Vapour Intrusion 143
Results And Discussion Of Field Studies And Model Predictions 144
Indoor VOC Method 144
Measured Vapour Attenuation Ratios at Petroleum Hydrocarbon Sites. 148
Comparison to Model Predictions for Petroleum Hydrocarbon Sites 149
Measured Vapour Attenuation Ratios at Chlorinated Solvent Sites 149
Comparison to Model Predictions for Chlorinated Solvent Sites 151
Tracer Method 151

Flux Chamber Method 151
Regulatory Implications 152
Conclusions and Recommendations 153
References 155

Chapter 8 **The Use Of Indoor Air Measurements to Evaluate Exposure And Risk from Subsurface VOCs** 157
Introduction 158
Mechanisms for Soil Vapour Intrusion 158
Process Overview 158
Building Underpressurization and Ventilation 160
Indoor Air Quality 162
Issues for the Use of Indoor Air Measurements to Quantify Soil Vapour Sources 168
Significance Of Subsurface Relative To Indoor VOC Sources 171
Conclusions 176
References 176

Chapter 9 **Conclusions** 180
Evaluation of soil vapour sampling and analysis techniques 180
Measurement of in situ gas-phase diffusion coefficients 180
Evaluation of vadose zone biodegradation of BTX vapours 181
Measurement of BTX Vapour Intrusion into an Experimental Building 181
Comparison, validation and use of models for predicting indoor air quality from soil and groundwater contamination 182
Evaluation of the Johnson and Ettinger model for prediction of indoor air quality 183
The use of indoor air measurements to evaluate exposure and risk from subsurface VOCs 183
Significant research Contributions 184
Recommendations for Further research 184

LIST OF TABLES

Chapter 2.	Table 2.1	Summary of Quality Control Testing for BTX Analyses 24
Chapter 3.	Table 3.1	Comparison of measured and empirical gas-phase tortuosity factor from laboratory diffusion studies 34
	Table 3.2	Thermal conductivity of selected gases 38
	Table 3.3	Effect of soil gas containing CO_2 on Mark 9822 helium detector response 39
	Table 3.4	Measured mass required and beta parameter for push-pull tests 42
	Table 3.5	Measured *in situ* effective diffusion coefficients based on push-pull tests 43
Chapter 4.	Table 4.1	Results of nitrogen, sulpher and SOM analyses in soil 56
	Table 4.2	Measured aerobic biodegradation rates from field studies 61
	Table 4.3	Input Parameters for Comparison of Biodegradation Models 67
Chapter 5.	Table 5.1	Summary of Soil Gas Intrusion Test Cases 89
	Table 5.2	Results of Soil Gas Intrusion Tests 90
	Table 5.3	BTX Flux Chamber Concentrations and Flux into Greenhouse at Edge Cracks 93
Chapter 6.	Table 6.1	Summary of Model Characteristics 105
	Table 6.2	Default Generic Values for Input Parameters (Benzene) 110
	Table 6.3	Model Comparisons for Varying Processes 111
	Table 6.4	Sensitivity of Predicted Vapour Attenuation Ratio to Parameter Uncertainty for Hypothetical Site (diffusion & advection model case) 114
	Table 6.5	Effect of Parameter Uncertainty on Tortuosity Factor Estimates ... 115
	Table 6.6	Field Data Summary for Model Validation 117
	Table 6.7	Comparison of Measured and Predicted Soil Gas Flow Rates into Building 120
	Table 6.8	Comparison of Measured Soil Gas Flow Rates into Buildings 120
	Table 6.9	Recommended Soil Vapour Model Attributes 126
Chapter 7.	Table 7.1	Comparison of measured and model-predicted soil gas flow rates into buildings 138
	Table 7.2	Qualitative summary of sensitive parameters for the J&E model .. 138
	Table 7.3	Uncertainty analysis for nomalized effective diffusion coefficient 142
	Table 7.4	Measured and Model-Predicted Vapour Attenuation Ratios 147
Chapter 8.	Table 8.1	Survey of Building Depressurization Relative to Atmospheric Pressure 161
	Table 8.2	Survey of Building Ventilation Rates 163

Table 8.3 Dominant Sources of Selected VOCs (adapted from Davis and Otson, 1993; Otson and Fellin, 1992) 165
Table 8.4 Compilation of Indoor Air Quality Data 166
Table 8.5 Assumed Soil Vapour Concentrations at Contaminated Source used for Modeling 174
Table 8.6 Exposure and Risk Factors 174

LIST OF FIGURES

Chapter 1	Figure 1.1	Conceptual Site Model for Soil Vapour Intrusion into Buildings 2
Chapter 2.	Figure 2.1	Soil Gas Probes and Sampling Train Used At Chatterton Site.....16
	Figure 2.2	Results of Tedlar Bag Permeation Study: O_2 and N_2
Concentrations		16
	Figure 2.3	Results of Syringe Desorption Study: Gas Chromatograph Benzene Area Counts 18
	Figure 2.4	Results of PVC Sorption Study: Benzene, TCE and M-Xylene Concentrations in Soil Vapour Samples 19
	Figure 2.5	Comparisons of O_2, CO_2 and CH_4 Concentrations Measured Using Landtec GA-90 and GC/TCD Analysis 21
	Figure 2.6	Results of Light Gas Analysis Study: Light Gas Concentration Adjacent To Building During Dry Season Measured By Landtec GA-90 (Summer 1998) 21
	Figure 2.7	Results of Light Gas Analysis Study: Light Gas Concentration Below Building Measured By Landtec GA-9023
Chapter 3.	Figure 3.1	Predicted Spherical Helium Diffusion from Point and Finite Source 37
	Figure 3.2	Possible Helium Concentration When CO_2 replaces O_2.....39
	Figure 3.3	Calibration of Mark 9822 helium detector.....41
	Figure 3.4	Site plan 41
	Figure 3.5	Moisture Content Below Building.....42
	Figure 3.6	Sensitivity Analysis for Effective Diffusion Coefficient (Based on Equations 7 and 10) 45
Chapter 4.	Figure 4.1	Simplified Vadose Zone Biogeochemical Model 51
	Figure 4.2	Site Plan 54
	Figure 4.3	Soil Moisture Content Below and Adjacent To Building (Approximate Total Porosity Values are Provided in Table 4.3) 55
	Figure 4.4	Benzene Vapour Concentrations Below and adjacent To Building (MC = Moisture Content) 57
	Figure 4.5	BTX Vapour and Light Gas Concentrations Below Building (MC = Moisture Content) 58
	Figure 4.6	Oxygen Gas Concentrations Below and Adjacent to Building.....58
	Figure 4.7	Comparison of Field Degradation Rates to Published Data in DeVaull et al. (1997) (used with permission).....61
	Figure 4.8	Model Domain and Boundary Conditions Used for 2-D Simulations 64
	Figure 4.9	Comparison of Numerical and Analytical Comparison of Numerical and Analytical Solutions for Steady-State Conditions (input parameters: Cg(source) = 15 mg/L, $\theta w = 0.14$, $\theta = 0.36$, $H' = 0.23$, $k_w 1 = 1.2\ hr^{-1}$, $U = 5.6x10^{-6}$ m/s, α_l =0.1 m, U = specific discharge,

al = longitudinal dispersivity, Pe = Peclet number, all other symbols defined in text) 66
Figure 4.10 Comparison of Biodegradation Models for Uniform and Non-Uniform Soil Conditions Using 1-D Diffusion and Reaction Model (Steady-State Conditions, IR = Instantaneous Reaction) 67
Figure 4.11 Moisture Content Profile Used in Numerical Simulations (see Table 4.3 for Porosity Values) 69
Figure 4.12 Predicted Vapour Concentrations Below Centre of Building for 2-D Diffusion With Reaction (Model No. 4) – wet (winter) conditions ($\eta = 0.001$, $\tau_{dust} = 1$) 69
Figure 4.13 Comparison of model-predicted and measured vapour concentrations from Fig. 4 and 6 for 2-D diffusion and reaction (model no. 4) (h=0.001, $\tau_{dust} = 1.0$) (approximate steady-state conditions at 3 months) 70
Figure 4.14 Effect of slab open area and tortuosity on predicted vapour concentrations below centre of building for 2-D diffusion with reaction (model no. 4) – wet (winter) conditions (approximately steady state conditions at 3 months) 71
Figure 4.15 1-D diffusion & reaction (Model No. 4) model sensitivity for (i) critical layer (0.88-0.92 m) moisture content (constant moderate biodegradation rate), (ii) biodegradation rate +/-60% of moderate rate (constant measured moisture content), & (iii) soil profile volumetric moisture constant +/-0.03 (constant biodegradation rate) (steady-state conditions) 73
Figure 4.16 Comparison of Measured and Model-Predicted Vapour Concentrations Below Building for 2-D Advection, Diffusion, and Reaction (model no. 4) (Moderate Biodegradation Rate, η=0.001, tdust=1.0, k=10 darcy, ΔP=5 Pa. ΔL=1.4m, Initial Concentrations for Advection Case Are Steady-State Diffusion and Biodegradation Concentrations) 73

Chapter 5. Figure 5.1 Schematic of Concrete Slab and Soil Vapour and Flux Chamber Testing Locations 82
Figure 5.2 Cross-Section of Greenhouse (pressures measured December 1, 1997 during greenhouse depressurization to -40 Pa, Case 3 conditions) ..83
Figure 5.3 Schematic of Flux Chamber 85
Figure 5.4 Flux Chamber Soil Gas Flow Rates Through South Edge Crack 91
Figure 5.5 Flux Chamber Soil Gas Flow Rates Through Hair Line Cracks 92
Figure 5.6 Concrete Core Through Hair Line Crack 92
Figure 5.7 Subslab Oxygen below greenhouse – Fall 1997 (O_2 probe located near probe SG-BMW) 94
Figure 5.8 Subslab Oxygen Monitoring – Summer 1998. (O_2 Probe located near probe SG-BMW) 95
Figure 5.9 Results of Modflow Modeling a) Domain and Permeabilities, b) Flow Vectors and Equipotentials 97

Chapter 6.

Figure 6.1 Results of Sensitivity Analysis for Selected Parameters (solid lines are diffusion only models, dashed lines are for diffusion and advection model) 113

Figure 6.2 Results of Monte Carlo Probabilistic Analysis for Benzene Vapour Attenuation Rate (SVIM model, Table 6.4 inputs, triangular distributions, 5000 trials) 115

Figure 6.3 Measured Vapour Attenuation Ratio based on Hydrocarbon Intrusion Monitoring at Chatterton Site (no significant difference in indoor & outdoor concentrations obtained for natural cases) 121

Figure 6.4 Measured Benzene Vapour Profile Below Centre of Building at Chatterton Site (ΔP=depressurization, T=time from start of depressurization to sampling) 122

Figure 6.5 Comparison of Measured and Predicted Vapour Attenuation Ratio 123

Figure 6.6 Conceptual Framework for Use of Models for Soil Vapour to Indoor Air Pathway (Tier 1 = diffusion only; Tier 2 =, diffusion & advection) (Possible depth ranges: shallow<~1 m, intermediate~1 to 5 m, deep>~5m) 126

Figure 6.7 Influence of Advective Transport on Vapour Attenuation Ratio (SVIM model modified to use Flow to Perimeter Crack model, ΔP=5Pa, Table 6.2 parameters) 128

Chapter 7.

Figure 7.1 Conceptual Simplification of Water Retention Curve for Purposes of Estimating Moisture Contents And Capillary Rise ($\theta_{W,R}$, $\theta_{W,FC}$, $\theta_{W,CZ}$, $\theta_{W,S}$ are the residual, field capacity, capillary zone and saturated water contents) 134

Figure 7.2 Sensitivity of Soil Gas Flow to Perimeter Crack Model (used in J&E model) to (a) soil-air permeability (k_a), (b) depth to perimeter crack (z_{crack}) and (c) crack ratio (η). X_{crack} = perimeter crack length, A_b = subsurface foundation area) 136

Figure 7.3 Sensitivity of Vapour Attenuation Ratio (Benzene) to Soil Gas Flow Rate (Q) into Building using Perimeter Crack Model. Height = building height, Dry dust-filled concrete cracks with total porosity = 0.3, ACH = air exchanges per hour (other symbols previously defined Q = Q_{soil}) 137

Figure 7.4 Sensitivity of Vapour Attenuation Ratio (Benzene) to Soil Gas Flow Rate (Q) using Perimeter Crack Model and Foundation Crack Ratio (n) (other symbols previously defined) 139

Figure 7.5 Sensitivity of Vapour Attenuation Ratio (Benzene) to Water-filled Porosity (Pa). Other symbols previously defined 140

Figure 7.6 Predicted Vapour Attenuation Ratio (benzene) for vapour Concentrations at Source and Indoor Air Using Johnson and Ettinger (1991) model. Figure adapted from Johnson et at., 1998. Dry dust-filled cracks: total porosity = 0.3; Moist dust-filled cracks: water-filled porosity = 0.1 and total porosity = 0.3 141

Figure 7.7a Comparison Between Measured and J&E Model-Predicted Vapour Attenuation Ratio (benzene). Upper and lower bound curves from Figure 7.6 are included. Dashed lines indicate that α_m is upper bound value. Symbols are best estimate α_p values 145
Figure 7.7b Comparison Between Measured and J&E Model-Predicted Vapour Attenuation Ratio (benzene). Upper and lower bound curves from Figure 7.6 are included. Dashed lines indicate that α_m is upper bound.....146

Chapter 8. Figure 8.1 Possible Conceptual Model For Soil Vapour Intrusion Into Building.....159
Figure 8.2 Predicted Vapour Attenuation Between Benzene Vapour Concentrations at Source and Indoor Air Using Johnson And Ettinger (1991) Model. Figure Adapted From Johnson et al., 1998. Shaded Region Considered To Encompass Majority Of Sites. Height = building mixing height, Qsoil = Advective flow rate into building for coarse-grained soils, Dry dust-filled cracks, total porosity = 0.3; moist dust-filled cracks, water-filled porosity = 0.1, total porosity = 0.3; η = crack ratio 172
Figure 8.3 Model-Predicted Vapour-Derived Indoor Air Concentration for (a) benzene, (b) TCE and (c) TVOC. The Soil Vapour Component of the Indoor Air Concentration Was Predicted Using The Johnson and Ettinger (1991) model.....173
Figure 8.4 Predicted Incremental Lifetime Cancer Risks Using Soil Vapour-Derived Indoor Air Concentrations In Figure 8.3 For (A) Benzene And (B) TCE.....175

LIST OF APPENDICES

Appendix I – Soil Vapour and Indoor Air Analysis 186

Appendix II – Equation for Vadose Zone Chemical Transport 247

Appendix III – Analysis of Moisture Content Data 250

Appendix IV – 2-D Finite Difference Numerical Model Code 258

Appendix V – Evaluation of Building Parameters 284

Appendix VI – Background Information on Chatterton Research Site and Photographs 287

Appendix VII – *In situ* Respiration Test Data 303

ACKNOWLEDGEMENTS

This research project was sponsored by the Science Council of B.C. and Golder Associates Ltd. (Golder). Funding was provided by twelve industry, governmental and consulting groups:

- Alberta Environmental Protection
- American Petroleum Institute
- B.C. Environment
- B.C. Science Council
- Canadian Association of Petroleum Producers
- Canada Mortgage and Housing Corporation
- Canadian Petroleum Products Institute
- Chatterton Petrochemical
- Dow Chemical
- Golder Associates Ltd.
- National Science and Engineering Research Council
- Ontario Ministry of Environment

In-kind support (field laboratory) was provided by Analytical Laboratory Services (ALS) of Vancouver, BC.

This thesis would not have been possible without the encouragement and guidance of Reidar Zapf-Gilje. The support of the research committee, Loretta Li (Supervisor), Jim Atwater (Co-supervisor), Leslie Smith and Reidar Zapf-Gilje, is gratefully acknowledged. I would also like to thank Rob Dellatolla, David Jacubak and Scott Hannam for their assistance with the field program.

This thesis is dedicated to Leanne, Meghan, Nathaniel, Jonathan and Benjamin. I love you all. Special thanks are given to our parents for their on-going support.

CHAPTER 1

INTRODUCTION

This thesis presents the results of research on the validation of models used to evaluate the intrusion of subsurface volatile organic compounds (VOCs) into buildings, often referred to as the "soil vapour transport to indoor air pathway". Vapour intrusion into occupied buildings, when significant, has potential implications for human health arising from inhalation exposure to subsurface vapours. Models are commonly used to predict indoor air concentrations from vapour intrusion.

The primary approach followed to investigate and validate models was to collect extensive field monitoring data on VOC vapour transport and intrusion, obtained at the former "Chatterton" petro-chemical plant site. Soil and groundwater at this site, located near Vancouver, B.C., Canada, is contaminated with benzene, toluene and m&p-xylene (BTX).

This thesis is presented as a series of papers together with an introduction and conclusion. Supplementary information is provided in appendices. The introduction begins with a summary of key issues and why research on this topic is relevant and needed. Next, the research purpose and objectives are stated, and an overview of the research program is provided. The introduction concludes with a brief description of the thesis papers, which provides a "road-map" in terms of content, and interconnection between various aspects of the research program.

KEY ISSUES AND RESEARCH RELEVANCY

Numerous sites across North America have been impacted by VOCs. Some are urban brownfield sites, which increasingly are being developed for commercial or residential use. At numerous sites, groundwater contaminated with VOCs has migrated below existing structures including several well-documented sites where contaminated groundwater has migrated below hundreds of homes (see Chapter 7) (Johnson, 2002).

Soil vapour intrusion into occupied buildings is considered a *potential* exposure pathway at most sites with VOC contamination. Therefore, this pathway is now routinely addressed as part of many human health risk assessments. Until recently, there were questions as to whether subsurface VOC intrusion into buildings was a significant exposure pathway (except in obvious cases where contamination was very near or in direct contact with the building). There is now a conclusive body of case study evidence indicating that soil vapour intrusion is a *complete* or *operable* exposure pathway at a significant number of sites. Vapour intrusion has been documented for a relatively wide range in site conditions in terms of contamination depth, soil properties, and house types. The evidence for significant soil vapour intrusion is strongest for sites contaminated with chlorinated solvents, and less so for petroleum hydrocarbon contaminated sites (Fitzpatrick and Fitzgerald, 1996; Chapter 7 this thesis).

Human health risks due to the inhalation of vapours can, in some cases, greatly exceed those traditionally considered for risk-based groundwater clean-up programs. In part, this can be attributed to the relatively large volume of air a person breathes per day (about 20 m^3/day

according to USEPA guidance) relative to the amount of groundwater ingested (about 2 L/day). When there are potentially unacceptable health risks, there are implications in terms of risk communication, response by those affected, and vapour intrusion mitigation.

Predictive modeling is often needed to assess the vapour intrusion pathway. While indoor air quality testing may be an option (for a plume below an existing building), it is subject to background interference from the same VOCs that are found in soil and groundwater. As the number of published case study sites increase, the use of empirical data to assess vapour intrusion is emerging as an alternative but complementary approach to predictive modeling.

Conceptual Site Model

The conceptual site model (CSM) for the vapour intrusion pathway is complex (Figure 1.1). The source of vapour contamination may reside in groundwater as a dissolved plume, and/or be present in unsaturated zone deposits either as a non-aqueous phase liquid (NAPL) or sorbed-phase contaminant. Vadose processes that can affect vapour transport toward a building include chemical diffusion, biodegradation or biotransformation, and sorption. Geologic deposits tend to be heterogeneous leading to variable transport rates. Closer to the building and ground surface, advective processes can become significant, driven by pressure gradients created by factors that lead to depressurization of the building, or fluctuations in atmospheric pressure. Cracks or openings in the building foundation and subsurface utilities are potential pathways for vapour migration into the building. There is a large variation in building types and foundation characteristics. Once inside the building, subsurface vapours are mixed and diluted through ventilation, and may interact with building surfaces. The above processes are subject to temporal changes caused by seasonal weather patterns.

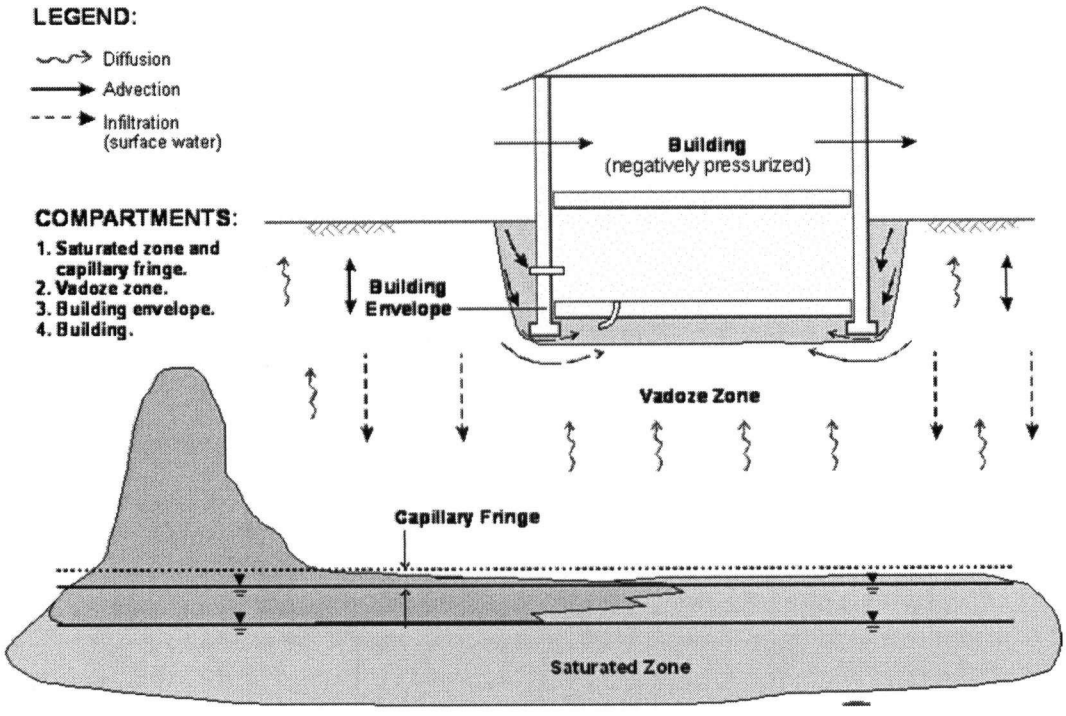

Figure 1.1. Conceptual Site Model for Soil Vapour Intrusion into Buildings

In light of the above CSM, it follows that accurate quantitative prediction of vapour intrusion is difficult. What also becomes clear is that depending on the model and input parameters used, predicted indoor air concentrations can vary over many orders-of-magnitude. A key challenge for model use is to develop a framework that provides for sufficient conservatism in terms of protection of public health, but that also has sufficient power or ability to adequately discriminate between sites (i.e., a model that predicts risk in virtually all instances is meaningless).

Predictive Models and Framework for Their Use

Over the past decade several predictive models for the vapour intrusion exposure pathway have been developed. Typically, screening level models incorporating analytical or semi-analytical solutions for steady-state one-dimensional vapour transport are used for risk assessment purposes. Most models follow the heurestic framework put forth by Johnson and Ettinger (1991) and involve a compartmental solution to chemical diffusion in soil below a building, coupled with diffusion and advection through the building foundation (*i.e.*, subsurface building envelope). More recent modeling developments include consideration of biodegradation, sorption and transient vapour transport (Sanders and Stern, 1994; Jeng *et al.*, 1996; Johnson *et al.*, 1998). In addition, there have been several models developed in the UK with a greater emphasis on building properties (Ferguson *et al.*, 1995). Multi-dimensional numerical models have also been adapted to simulate this pathway. In Canada and the U.S., the Johnson and Ettinger (1991) model (or variants thereof) has become the model of choice. This is reflected in federal regulatory guidance (Canadian Council of Ministers of the Environment Canada Wide Standards for Petroleum Hydrocarbon Compounds (CWS-PHC) (2000), and the USEPA Draft Subsurface Vapour Intrusion (VI) Guidance (2002). Several provinces and states have also adopted the Johnson and Ettinger model for regulatory purposes (e.g., Atlantic provinces in Canada, Michigan, Massachusetts).

There is an emerging recognition that models must be used in the context of an appropriate framework for site assessment and decision making. This, for example, is reflected in the USEPA VI Guidance, which provides a three-tiered framework for initial qualitative screening of sites that is followed by a secondary screening and site-specific assessment tier. The VI Guidance addresses the applicability of mathematical modeling relative to the CSM, and selection or measurement of input parameters needed for modeling. There is also recognition by practioners that at some sites, the use of more advanced site assessment techniques, relative to soil and groundwater assessments, are warranted including, for example, subslab soil vapour sampling, soil-air permeability testing, and monitoring of gases such as oxygen and carbon dioxide (to evaluate biodegradation).

Model Validation

Model validation is a process that begins with the development of a CSM. Sensitivity analysis can yield important insights into model characteristics and can help identify important model inputs. Ultimately, the "litmus test" is a model's ability to adequately predict real-world conditions. For this reason, field-based studies are a critical component of the model validation process, although theoretical and laboratory studies can be used in a complementary manner to better understand certain processes. Ideally, model validation should be a process where the

predictive capabilities of a model are tested using multiple independent cases over the expected range of conditions for model use. Model "validation" for this research is considered a process by which the predictive capabilities of a model are evaluated. It does not mean that a model is fully validated under all circumstances, which would be an unrealistic goal. Other pertinant issues include include (i) model verification, which is the determination of whether a model solves equations correctly, (ii) practicality of model use, and (iii) model acceptance by the regulatory and scientific community.

Field-based studies that that can be used to validate models vary significantly in purpose, scope and quality. There are only a few detailed research studies specifically addressing intrusion of VOCs such as chlorinated solvents or petroleum hydrocarbons into buildings (Kliest, 1987; Hogdson, 1992; Fischer *et al.*, 1996; Laubacher *et al.,* 1997; Olson and Corsi, 2001). These studies have provide insight on the importance of specific processes (e.g., soil gas advection, biodegradation), and in a few cases have enabled the estimation of vapour attenuation ratio (the ratio of indoor air to vapour concentration near the contamination source) and comparisons to model predictions.

There are a larger number of sites where groundwater, soil vapour (in some cases) and indoor air quality data has been obtained enabling the estimation of vapour attenuation ratios. Some of the available information has been summarized in technical papers (e.g., Fitzpatrick and Fitzgerald, 1996; Johnson *et al.*, 2002). While useful correlations have been developed using this data, site characterization information has generally been limited therefore making this data less useful for model validation and evaluation of vapour intrusion processes. Several field studies have indicated vadose zone biodegradation can result in significant attenuation of hydrocarbon vapours (Ostendorf and Kampbell, 1991; Ririe and Sweeney, 1995, DeVaull et al., 1997). However, there are only limited field studies of the interaction between buildings and subsurface processes that affect biodegradation.

There is a relatively extensive body of radon research including several studies involving in-depth testing of radon intrusion into homes (Nazaroff et al., 1997; Garbesi et al., 1993). The radon studies are significant since they have contributed to an enhanced understanding of mechanisms for soil gas intrusion into a building, including the influence of building underpressurization and advective soil gas flow, experimental methods (e.g., tracer tests), and models for prediction of soil gas intrusion.

DATA GAPS AND QUESTIONS TO BE ANSWERED

The following data gaps and questions to be answered were identified:

1. There are only limited field-based research studies of VOC intrusion. Only a few have been integrated studies involving an evaluation of the complete vapour intrusion pathway including characterization of contamination source, vadose zone fate and transport, migration through the building foundation, and mixing of vapours in indoor air.

2. There is only limited understanding of the interaction between buildings and subsurface processes affecting vapour transport such as soil gas advection, subslab oxygen transport and biodegradation.

3. The influence of seasonal factors on soil vapour concentrations and vapour intrusion is not well understood. Longer term studies evaluating seasonal effects have been limited.

4. While some case studies have been summarized, there have been few, if any, published studies involving a rigorous and comprehensive evaluation of the available case study database, estimation of vapour attenuation ratios, and comparison to model predictions.

5. The reliability of screening level models, such as the Johnson and Ettinger (1991) model, for prediction of soil vapour intrusion while improving, is still not well understood.

6. Protocols and guidance for certain test methods pertaining to the vapour intrusion pathway (e.g., soil vapour, flux chamber testing) are relatively limited.

7. There has been only limited use of multi-dimensional numerical computer models for the prediction of vapour intrusion into buildings.

The above data gaps were addressed through a comprehensive, multi-year research program. The research is significant in terms of its breadth, extensive monitoring, new experimental methods, in-depth validation of screening models, and development of new numerical models.

PURPOSE, OBJECTIVES AND SCOPE

The primary purpose of the research program is to contribute to the validation of existing soil vapour intrusion models through a comprehensive field-based study and review of available case studies. Secondary goals are to develop new or adapted models and experimental methods that could be used to evaluate the vapour intrusion pathway.

Specific objectives for the research program were:

1) Evaluate the reliability of screening level models (e.g., Johnson and Ettinger model) for prediction of soil vapour intrusion.

2) Obtain data that would enable evaluation of the interaction between a building and subsurface processes such as advection, diffusion and biodegradation.

3) Investigate the influence of building depressurization on soil vapour intrusion.

4) Obtain longer-term data to evaluate the influence of seasonal factors.

5) Develop new or adapted field methods to evaluate specific vapour intrusion processes and provide insight on method practicality.

6) Develop a multi-dimensional numerical model for this pathway, and compare the results to screening-level models.

7) Develop a framework for model use and application that could assist stakeholders in decision making.

The above objectives were supported through a comprehensive and integrated field study evaluating both vadose zone processes and soil vapour intrusion into an experimental greenhouse constructed at the Chatterton research site.

BACKGROUND INFORMATION AND OVERVIEW OF RESEARCH PROGRAM

The individual chapters of this thesis provide a description of research program site, experimental scope and methods. Relevant background information and an overview of the research program is provided below. Additional background information and photographs are provided in Appendix VI.

The Chatterton site, located in Delta, B.C., Canada, is contaminated with benzene, toluene and xylenes (BTX). The plant was in operation until 1992. The source of BTX contamination was spills and leaks from above-ground storage tanks, piping and valves. The specific area of the site chosen for the research program testing was located south of the main plant and source area for BTX releases, and down-gradient with respect to groundwater flow. Prior to the research program being initiated, the site had been subjected to a relatively comprehensive field investigation program. The main characteristics of the research site were as follows:

- flat, grass covered area;
- soil stratigraphy consisting of a surface sandy silt layer up to 0.3 m thick, underlain by relatively uniform fine to medium sand fill to 3.5 m depth, underlain by native silt;
- variable water table with historical fluctuations between about 1.5 m and 3 m depth below ground surface;
- well-defined non-aqueous phase liquid (NAPL) smear zone between about 1.5 m and 3 m depth;
- total benzene, toluene and xylene (BTX) concentrations generally in the several hundred to thousands parts per million range in soil samples collected between about 1.5 m and 3 m depth;
- approximate proportions by weight for the BTX compounds were 70 percent toluene, 20 percent benzene and 10 percent xylene, and;
- No separate-phase product was observed in monitoring wells in this area of the site.

The rationale for why this site was chosen for the study included site availability, relatively homogeneous soil properties, and no shallow contamination sources (i.e., above 1.5 m depth).

The research program consisted of an extensive field testing and monitoring program over a two-year period complemented by laboratory testing, analysis and modeling. The site program began with a baseline investigation of soil properties (porosity, bulk density, field capacity, air-entry tension, grain size, organic carbon, nutrient levels, microbial enumeration) and testing of BTX concentrations in groundwater, soil, and soil vapour. Following construction of the

greenhouse, extensive vertical profiling of soil vapour concentrations both below and adjacent to the greenhouse was conducted on a regular basis. In addition, numerous other monitoring data were obtained (e.g., oxygen, carbon dioxide, methane, pressure, temperature, barometric pressure, wind speed, rainfall, soil moisture) and tests were conducted (in situ biological respiration, push-pull tracer tests to measure in situ diffusion coefficient, soil-air permeability).

Vapour intrusion into the greenhouse was measured for six different cases, corresponding to different conditions for greenhouse depressurization and foundation crack area. Two cases were for a non-mechanically depressurized condition where the time-averaged pressure difference between indoor and outdoor air was approximately zero. For three cases, a fan was used to depressurize the greenhouse with tests conducted at -2.5 pascals (Pa), -10 Pa, and -30 Pa. For all six cases, indoor air concentrations (and other data) were obtained obtained enabling estimation of vapour intrusion rates. For selected cases, flux chambers were used to both measure soil gas flow and BTX flux into the greenhouse. Extensive quality control (QC) testing, and several "mini-studies" to evaluate QC issues were also performed.

The project modeling scope included (i) evaluation of available screening-level models and development of new screening model for vapour intrusion (SVIM model, Chapter 6) ; (ii) development of a two-dimensional finite difference model for hydrocarbon vapour diffusion, advection, dispersion and biodegradation (Chapter 4), and (iii) evaluation of analytical models and adaption of MODFLOW for simulation of soil gas flow into a building (Chapter 5).

STRUCTURE OF THIS THESIS

The results of the research program are documented in seven technical papers and associated appendices. Technical papers allowed for rapid dissemination of research results to the consortium sponsoring this project, and was also important since vapour intrusion is a rapidly developing field. Significant contributions are made in the areas of field methods, new models for this pathway (conceptual and quantitative), comprehensive information on model validation, and a protocol for the application of vapour intrusion models. The purpose and scope of each paper is summarized below:

Chapter 2 – Evaluation of soil vapour sampling and analysis techniques – The paper provides both a general discussion of soil vapour sampling and analysis issues, and describes and presents result for the program implemented at the Chatterton site. The paper includes several studies conducted to evaluate testing and quality control issues such as cross-contamination, soil vapour probe materials and use of field screening instruments for gas analysis. The appendix to this paper includes standard operating procedures, raw data for the BTX analyses, and results of the baseline field investigation not reported elsewhere.

Chapter 3 – Measurement of in situ gas-phase diffusion coefficients – The purpose of this study was to use push pull tests, conducted using an inert tracer, to predict *in situ* diffusion coefficients, and to compare the results to empirical predictions. Theoretical equations used to calculate diffusion coefficients, field methods and quality control issues are discussed. The measured in situ diffusion coefficients were subsequently used as input for biodegradation modeling described below.

Chapter 4 – Evaluation of vadose zone biodegradation of BTX vapours – This paper focusses on field monitoring and modeling used to evaluate the biodegradation of BTX vapours below and adjacent to the greenhouse. A review of biodegradation studies and rate constants is initially provided. A two-dimensional finite difference numerical model is used to simulate diffusion, advection, sorption and biodegradation. Through comparisons of model-predicted to measured BTX vapour profiles, first-order biodegradation rate constants for BTX vapour are estimated, and insight into key factors (oxygen availability, advection) affecting biodegradation rates are obtained. The appendix to this paper includes additional discussion and modeling investigating the relationship between moisture content and biodegradation.

Chapter 5 – Measurement of BTX Vapour Intrusion into an Experimental Building – This paper describes the testing program conducted to measure BTX vapour intrusion and soil gas flow into the greenhouse. A number of tracer and flux chamber experiments were designed and implemented. The measured rates were then compared to model predicted results. Both an analytical model and groundwater numerical model (MODFLOW), adapted to simulate soil gas flow, were used to predict soil gas flow rates into the greenhouse. Although the focus of this study were conditions near to the building foundation, the biodegradation of vapours, investigated in detail in Chapter 4, had an important effect on BTX vapour intrusion.

Chapter 6 – Comparision, validation and use of models for predicting indoor air quality from soil and groundwater contamination – The purpose of this paper is to provide information and guidance on the use of available screening level models to predict indoor air quality from soil and groundwater contamination. An extensive review of model attributes followed by evaluation of model sensitivity and uncertainty for different models is initially provided. Measured VOC intrusion and soil gas flow rates (primarily those derived from the Chatterton study) are compared to model-predicted rates to assist in the validation process. The paper concludes with a protocol that provides guidance on the application of models within a tiered risk-based framework.

Chapter 7 – Evaluation of the Johnson and Ettinger model for prediction of indoor air quality – This paper evaluates the use of the Johnson and Ettinger model for prediction of vapour intrusion and indoor air quality. The paper consists of three main parts: (i) detailed evaluation of measured vapour attenuation factors for chlorinated solvent and petroleum hydrocarbon sites, including several recent unpublished studies, (ii) estimation of input parameters for the Johnson and Ettinger model, and (iii) comparison of measured vapour attenuation rates to those predicted using the Johnson and Ettinger model. The paper concludes with a assessment of the reliability of the Johnson and Ettinger model for predictive purposes.

Chapter 8 – The use of indoor air measurements to evaluate exposure and risk from subsurface VOCs – The purpose of this paper is to identify and evaluate issues for the use of indoor air quality (IAQ) data to evaluate exposure and risk from soil vapour intrusion. A key point is that there are numerous sources of background VOCs, which can be problematic when the objective is to quantify the sub-surface derived vapour component. To provide added perspective, the risks arising from subsurface VOCs, predicted using standard models equations for soil vapour transport and intrusion, are compared to those associated with background indoor sources. Also included is an extensive compilation of building depressurization values and

ventilation rates, which represent a valuable database of information for vapour intrusion modeling.

The thesis ends with the key conclusions drawn from the technical papers and recommendations addressing remaining data gaps and research needs.

REFERENCES

American Society for Testing and Materials. 1995. Standard Guide for Risk-Based Corrective Action Applied at Petroleum Release Sites (E-1739-95).

Canadian Council of Ministers of the Environment (CCME), 2000. Canada Wide Standards for Petroleum Hydrocarbon Compounds, June.

DeVaull, G., R.A. Ettinger, J.P. Salanitro, and J. Gustafson. 1997. Benzene, toluene, ethylbenzene and xylenes degradation in vadose zone soils during vapour transport: first-order rate constants. Proceedings of 1997 Petroleum Hydrocarbons and Organic Chemicals in Ground Water, API/NGWA, Houston, Texas, November, 365-379.

Ferguson, C.C., V.V. Krylov, and P.T. McGrath. 1995. Contamination of Indoor Air by Toxic Soil Vapours: a Screening Risk Assessment Model. *Building and Environment.* 30(3): 375-383.

Fischer, M.L., A.J. Bentley, K.A. Dunkin, A.T. Hodgson, W.W. Nazaroff, R.G. Sextro, and J.M. Daisay. 1996. Factors affecting indoor air concentrations of volatile organic compounds at a site of subsurface gasoline contamination. *Environ. Sci. Technol.*, 30: 2948-2957.

Fitzpatrick, N.A. and J.J. Fitzgerald. 1996. An Evaluatoin of Vapour Intrusion into Buildings Through a Study of Field. Presented at the 11th Annual Conference on Contaminated Soils. University of Massachusetts (Amherst). October.

Garbesi, K., R.G. Sextro, W.J. Fisk, M.P. Modera, and K.L. Revzan. 1993. Soil-Gas Entry into an Experimental Basement: Model Measurement Comparisons and Seasonal Effects. *Environ. Sci. Technol.* 27(3): 466-473.

Hodgson, A.T., 1992. Soil-Gas Contamination and Entry of Volatile Organic Compounds into a House Near a Landfill, *Journal of the Air and Waste Management Association*, 29: 277-283, March.

Jeng, C.Y, V.J. Kremesec, Jr., and H.S. Primack. 1996. Models of hydrocarbon vapour diffusion through soil and transport into buildings. Proceedings of 1996 Petroleum Hydrocarbon and Organic Chemicals in Ground Water, API/NGWA, Houston, Texas, November 13-15, 319-338.

Johnson, P.C. and R. Ettinger. 1991. Heuristic Model for Predicting the Intrusion Rate of Contaminant Vapours into Buildings. *Environ. Sci. Technol.* 25 (8):1445-1452.

Johnson, P.C., W. Kemblowski, and R.L. Johnson. 1998. Assessing the Significance of Subsurface Contaminant Vapour Migration to Enclosed Spaces – site specific alternatives to generic estimates. API Publication.

Johnson, P.C. 2002. Migration of Soil Gas Vapours to Indoor Air. Determining Vapour Attenuation Factors Using Screening-Level Model and Field Data from the CDOT MTL, API Bulletin 16, April.

Jury, W.A., D. Russo, G. Streile, H. El Abd. 1990. Evaluation of volatilization by organic chemicals residing below the soil surface. *Water Resources Research*, 26(1):13-20.

Kliest, J., T. Fast, J.S.M. Bolij, H. van de Wiel and H. Bloemen. 1989. The Relationship Between Soil Contaminated with Volatile Organic Compounds and Indoor Air Pollution. *Environment International*, 15, 419-425.

Laubacher, R.C., P. Bartholomae, P. Velasco, and H.J. Reisinger. 1997. An evaluation of the vapour profile in the vadose zone above a gasoline plume. Proceedings of 1997 Petroleum Hydrocarbon and Organic Chemicals in Ground Water, Houston, Texas, November, 396-409.

Nazaroff, W.W., S.R. Lewis, S.M. Doyle, B.A. Moed, and A.V. Nero. 1987. "Experiments on Pollutant Transport from Soil into Residential Basements by Pressure Driven Airflow", *Environmental Science and Technology*, 21:459-466.

Olson, D.A. and R. Corsi. 2001. Characterizing exposure to chemicals from soil vapour intrusion using two-compartment model. *Atmospheric Environment* 35:4201-4209.

Ostendorf, D.W. and D. H. Kampbell. 1991. Biodegradation of hydrocarbon vapours in the unsaturated zone. *Water Resources Research*, 27 (4):453-462.

Ririe, T. and B. Sweeney. 1995. API Conference. Fate and Transport of Volatile Hydrocarbons in the Vadose Zone. In Proceedings of the 1995 Petroleum Hydrocarbon and Organic Chemicals in Groundwater: Prevention, Detection and Remediation Conference, Houston, Texas, November 29 to December 1:529-542.

Sanders, P. and A. H. Stern. 1994. Calculation of Soil Cleanup Criteria for Carcinogenic Volatile Organic Compounds as Controlled by the Soil-To-Indoor Air Exposure Pathway. *Environmental Toxicology and Chemistry*, 13 (8): 1367-1373.

USEPA, 2002. Draft Subsurface Vapour Intrusion Guidance. OWSER.

CHAPTER 2

EVALUATION OF SOIL GAS SAMPLING AND ANALYSIS TECHNIQUES AT A FORMER PETROCHEMICAL PLANT SITE

This chapter was accepted for publication in *Environmental Technology*[1] in October 2003.

ABSTRACT

Methods for soil gas sampling and analysis are evaluated as part of a research study on soil vapour intrusion into buildings, conducted at a former petro-chemical plant site ("Chatterton site"). The evaluation process was designed to provide information on reliability and selection of appropriate methods for soil gas sampling and analysis, and was based on literature review of data and methods, and experiments completed as part of the research study. The broader context of this work is that soil gas characterization is increasingly being used for input into risk assessment for contaminated sites, particularly when evaluating the potential intrusion of soil vapour into buildings. There are only a limited number of research studies and protocols addressing soil gas sampling and analysis. There is significant variability in soil gas probe design and sample collection and analysis methods used by practitioners. The experimental studies conducted to evaluate soil gas methods address the permeation or leakage of gases from Tedlar bags, time-dependent sorption of VOC-vapours onto probe surfaces and sampling devices, and analytical and quality control issues for light gas and VOC analyses. Through this work, common techniques for soil gas collection and analysis are described together with implications for data quality arising from the different methods used. Some of the potential pitfalls that can affect soil gas testing are identified, and recommendations and guidance for improved protocols are provided.

KEY WORDS: soil vapour, diffusion, biodegradation, first-order decay, numerical model, BTX

[1] Hers, I., Hannam, S. and Li, L.

INTRODUCTION

This paper evaluates methods for soil gas sampling and analysis as part of a research study on soil vapour intrusion into buildings conducted at a former petro-chemical plant site ("Chatterton site") (Hers and Zapf-Gilje, 1998, Hers *et al.*, 2000). The evaluation process was designed to provide information on reliability and selection of appropriate methods for soil gas sampling and analysis. To meet this objective, test data and methods cited in the literature were reviewed, and several experiments designed to address data gaps pertaining to soil gas techniques were completed. The analytical context for this work are both VOCs associated with contaminants, and light gases such as oxygen (O_2), carbon dioxide (CO_2) and methane (CH_4), which are often used to assess biotransformation processes.

The broader context for this work is the collection and analysis of soil gas samples is often required as part of human health risk assessments of contaminated sites or when implementing a risk-based corrective action approach (ASTM, 1995; Johnson *et al.*, 1998). The early application of soil gas data was primarily to provide an indirect indication of potential volatile organic compound (VOC) contamination in soil or groundwater, and thus enhance the site characterization process (Marrin and Kerfoot, 1988). The more recent use of soil gas monitoring for risk assessment is different in purpose, and sampling and analysis requirements are generally more stringent since soil gas data is used to predict possible exposure concentrations in indoor or outdoor air. In contrast to soil and groundwater media, the collection and analysis of soil gas has received less in-depth scrutiny, and the few published protocols or guidance that are available (ASTM, 1992; San Diego County, 2002) are, in the authors opinion, not widely followed. There is significant variability in soil gas sampling probe design, sample collection and analysis methods and relatively few research studies where different soil gas sampling and analysis techniques have been evaluated.

Based on the results of the experiments conducted as part of the Chatterton study and the literature review, practical recommendations and guidance for soil gas collection and analysis are provided. The benefits of this paper are new data and insights into important factors affecting soil gas quality, and improved protocols for the collection of high quality, representative data.

BACKGROUND INFORMATION REVIEW

Soil gas testing can be divided into three steps consisting of probe installation, sample collection and handling, and analysis. The methods commonly used by practitioners and laboratories, and published studies evaluating soil gas characterization are reviewed below. Only active soil gas sampling methods are considered since passive methods do not provide for concentration data (i.e., information usually needed for risk assessment).

Probe Design for Soil Gas Collection

One of four basic probe types are used to collect soil gas: (i) driven probes, (ii) probes installed using direct-push methods, (iii) probes installed in drilled boreholes, and (iv) monitoring wells screened across the water table. Driven probes in their simplest form are hollow steel bars with an internal diameter typically ranging between 12.5 and 25 mm (often referred to as ground probes). The bars include a loosely fitting conical tip that is pushed a short

distance further into the formation using an inner rod, once the probe is driven to its desired depth. Several holes may also be drilled near the base of the probe to increase the area over which soil gas can be drawn into the probe.

More sophisticated driven probes include a retractable drive tip connected to a system of threaded steel rods. The retractable tip is pulled back to expose a relatively short screened section allowing multiple soil gas samples to be collected from one probe hole, as the probe is driven. Screened sections of the probe are often constructed using stainless steel. In some cases, small diameter tubing constructed of stainless steel, Teflon (i.e., Polytetrafluoroethylene (PTFE)), or polyethylene is situated inside the outer rods to reduce the purge volume and minimize the potential for cross-contamination at rod joints. More recently, direct push technology has been used to install permanent soil gas implants. One proprietary design is a 6.25 to 12.5 mm diameter stainless steel screen that is 150 mm long. For some systems, implants are installed post-run after the desired depth is reached by lowering the implant down the hollow rods and attaching it to a detachable anchor drive point.

The design of probes that are installed in boreholes varies widely and include probes constructed of steel (3.2 mm ID) (Schroedl and Kerfoot, 1990), Teflon (6.3 mm ID) (Yeates and Nielson, 1988) and PVC (30 mm ID, No. 30 slot screen) connected to narrow diameter vinyl tubing (Van Sciver, 1992). The authors are also aware of numerous instances where soil gas samples have been collected from conventional 50 mm diameter groundwater monitoring wells that have screens that extend above the water table.

Sampling Collection and Handling

Soil gas samples are typically collected by applying a vacuum to the distal end of the probe. Sample collection devices can include gas-tight syringes, glass cylinders, Tedlar bags, sorbent tubes, and Summa evacuated steel canisters. Tedlar is a proprietary plastic with properties similar to Teflon. The selection of a collection device is influenced by analytical requirements, discussed in a separate section below.

Purge flow rates reported in the literature vary widely and range from 20 ml min^{-1} (Smith *et al.*, 1996) to 2 to 3 l min^{-1} (Rizvi and Fleischacker, 1992). Purge volumes also vary with some practitioners advocating only minimal purging corresponding to about 1 to 1 ½ probe volumes (Ririe *et al.*, 1998). Cody (2003) reported purge volumes on the basis of a differential equation for the sequential and complete mixing of VOCs over each time step within the entire volume under consideration (probe and tubing). On the basis of this equation, the estimated concentration within the probe volume reaches 90 % of the input concentration after purging about three volumes.

Christy and Spradlin (1992) evaluated the effect of purging by repeated purging, and then sampling in succession from a single probe and found that toluene concentrations decreased by a factor of 2 to 4 from the beginning to end of the purging process, which involved the removal of about 5 to 8 probe volumes. Ririe and Sweeney (1998) measured a slight decrease in CO_2, and increase in O_2 with increasing purge volume at a hydrocarbon-contaminated site.

After purging has been completed, the air-sampling pump is typically turned off and the vacuum is allowed to dissipate. In high permeability deposits this occurs almost instantaneously; however, in low permeability deposits this can take several minutes or longer (Christy and Spradlin, 1992). The vacuum generated during purging, and length of time for the vacuum to dissipate can provide a qualitative indication of the soil permeability and whether the probe is plugged. If a vacuum persists for a long period of time, it may be difficult to obtain a representative soil gas sample. When Tedlar bags are used to collect soil gas samples, a vacuum chamber can be used to avoid passing the gas sample through a pump. Since Summa canisters are under sub-atmospheric pressure, an option for this method is to collect the soil gas sample by directly connecting the canister to the probe, thus avoiding drawing the gas through the sampling pump.

There are only a few published studies of the effect of sample device and storage time on sample quality. Wang *et al.* (1996) found that for samples collected in Tedlar bags, between 16.5 and 25.6 % of the toluene, dichloroethylene (DCE) and trichloroethylene (TCE) vapours were lost over the first 24 hours after sampling. The loss was due to sorption and bag leakage. Andiro and Butler (1991) report that approximately 16 % of the methanol vapour concentration in 60-litre Tedlar bags was lost over a 24-hour period, and that the apparent vapour loss increased as the water vapour content increased. Smith *et al.* (1996) compared TCE vapour concentrations for samples collected with absorbent tubes (Supelco Inc. Carbotrap 300) and glass cylinders. They found that concentration differences were less than 5 %, and concluded that high quality samples could be obtained using both methods.

Analytical Techniques

Field Screening Methods

Soil gas surveys commonly utilize field instruments such as photoionization detectors (PIDs) and multi-gas detectors for light gases (*e.g.*, CO_2, O_2, CH_4) as an initial screening step. Aelion *et al.* (1996) tested duplicate soil vapour samples using field instruments and by gas chromatographic (GC) methods and found a poor correlation (r^2=0.45) between volatile hydrocarbons, measured using a platinum catalyst type sensor, and BTEX, measured by a GC/flame ionization detector (FID). The correlation between CO_2, measured using a non-dispersive infrared analyzer and measured by a GC/thermal conductivity detector (TCD) was fair (r^2=0.83). Possible reasons given for the poor correlation were variation in relative humidity, and a wide range in BTEX vapour concentrations. Robbins *et al.* (1990) demonstrated that several factors including flow rate restrictions, relative humidity, CO_2 concentrations, and detector non-linearity have a significant effect on total PID and FID concentrations, when used to measure hydrocarbon vapours.

Laboratory Analytical Techniques

Selection of laboratory analytical techniques for quantification of individual VOCs will depend on project and data quality objectives. An initial investigation of site contamination may involve the collection of syringe or glass bomb samples followed by direct injection and quantification using a GC/PID or FID. For risk assessment studies, low detection limits and more rigorous quality control requirements often require that samples be collected using either sorbent tubes or Summa stainless steel canisters and quantification by GC/MS (e.g., EPA

Methods TO-2, TO-14, TO-15, TO-17). In a comprehensive review, Harrington *et al.* (1998) point out that while air methods are similar to purge and trap methods for groundwater, air methods are less prescriptive, and there are also fundamental differences in terms of calibration standards, methods and materials used to clean sampling equipment and prevent cross-contamination, and the training required to ensure proper quality controls are followed.

Sorbents commonly used consist of charcoal, polymeric and/or carbonaceous resins which are either thermally desorbed or extracted with a solvent such as carbon disulphide. Some tubes contain multiple compartments containing materials with differing sorptive properties (e.g., graphitized carbon black, carbon molecular sieve), designed to optimize the collection process. There are wide variations in sorbent properties. Since soil vapour typically has a relative humidity of close to 100 %, hydrophobic sorbents are preferred since sorbed water reduces the retention of VOCs, and because water vapour can affect the GC analysis (Harper, 1994). Polar VOC compounds can also partition into the water phase reducing recovery. Other issues for sorbent sampling include sorbent pore size and uniformity, possible reactions between the sorbent and adsorbed molecules, and slow breakdown of certain polymeric sorbents and release of aromatic hydrocarbons (Harper, 1994).

Thermal desorption involves rapidly heating the sorbent to desorb the VOC, while passing an inert carrier gas through the tube. The VOCs are carried by the gas and concentrated on a smaller downstream trap, which usually is cryogenically cooled. For thermal desorption, the whole sample is analyzed at one time without the possibility of replicate analyses. In contrast, replicate analyses can performed on the extract for sorbent tubes that are chemically desorbed. While methods based on chemical extraction are typically not as sensitive as thermal desorption, reduced sensitivity may not be an issue for quantification of VOCs in soil vapour (i.e., as opposed to ambient air).

Positive aspects of stainless steel canister sampling and GC/MS analysis include collection of relatively large "whole air" samples (e.g., typically six litres), low sensitivity and ability to take multiple aliquots from canister samples. Potential disadvantages for canister samples with elevated water vapour are problems caused during cryogenic focussing prior to analysis, although an alternate method of multiple focussing using non-cooled sorbent tubes can reduce problems associated with water vapour.

EVALUATION OF EXPERIMENTAL METHODS

Rationale

The background information review identified several issues relating to sampling protocols and quality control. In part to address these issues, five soil gas studies were conducted during the Chatterton research program. These studies helped to evaluate method reliability and selection. The studies were an evaluation of time-dependent change in light gas concentrations in Tedlar bags ("Tedlar bag permeation study"), evaluation of BTX sorption on syringes ("syringe sorption study"), evaluation of VOC sorption onto PVC probes ("PVC sorption study"), comparison between light gas concentrations measured using a field detector and gas chromatographic (GC) analyses ("light gas analysis study"), and evaluation of analytical quality control for BTX vapour testing ("BTX analytical quality control study").

Overview of Soil Gas Sampling and Analysis Methods at Chatterton Site

The research program at the Chatterton site has included extensive monitoring of BTX vapour and light gas concentrations (Hers and Zapf-Gilje, 1998). Near-surface soil at the site consists of a thin surface layer up to 0.3 m thick consisting of sandy silt to fine sand with trace organic matter, underlain by dredged river sand with trace silt that extends to about 3.5 m depth. Soil gas samples were obtained from either 6.25 mm or 12 mm internal diameter hollow steel probes with 50 mm long perforated or slotted tips. Probes were equipped with dedicated miniature inert 3-way valves, one port had a 30 cm by 0.75 mm stainless steel tube connected (inserted in probe), while the other two ports had Teflon luer lock male connectors (sample collection and probe purging) (Figure 2.1). Probes were driven to the desired depths (between 0.15 m and 1.8 m depth).

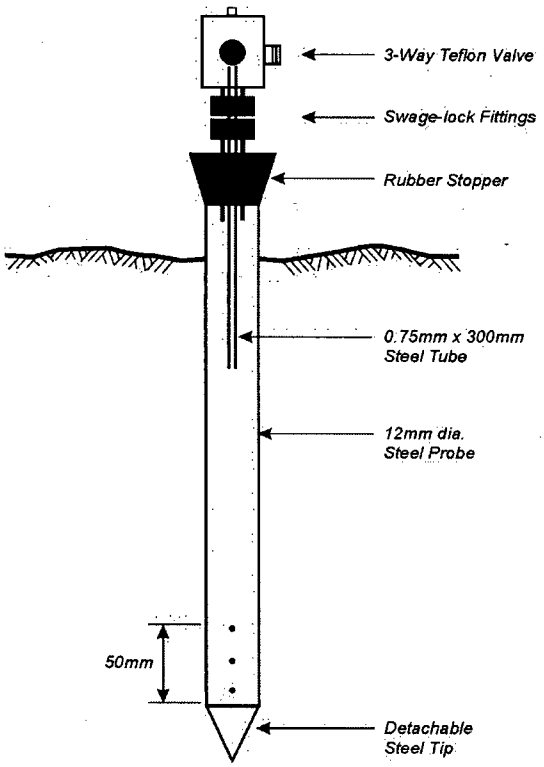

Figure 2.1. Soil gas probes and sampling train used at Chatterton site.

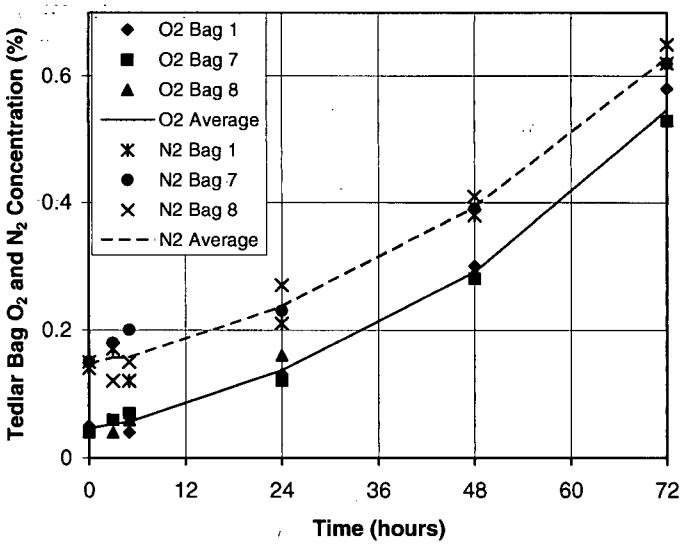

Figure 2.2. Results of Tedlar bag permeation study: O_2 and N_2

The sampling procedure was as follows: (i) the probe was purged by removing 1 ½ probe-air volumes; (ii) the air-sampling pump was turned off and the vacuum was allowed to dissipate, and (iii) a soil gas sample was collected (Figure 2.1). The purging and sampling rate was 150 ml min^{-1}. Vacuums dissipated within one second. Soil gas samples for BTX analyses were collected in a 5 ml syringe (described in detail below) or Supelco Inc. Carbotrap 300 sorbent tubes. Samples for light gas analyses were collected in 500 ml SKC Inc. Tedlar bags (Series 232). Samples were analyzed for BTX using a SRI 8610 GC/PID. Samples were analyzed for

light gases using a HP 5880 GC with TCD and FID detector, or using a Landtec Control Technologies GA-90 field portable gas detector. Samples for BTX analysis were analyzed within four hours of collection, while samples for light gas analysis were analyzed within 48 hours of collection.

Tedlar Bag Permeation Study

Methods

The purpose of the Tedlar bag diffusion study was to measure the possible intrusion of atmospheric air into bags over time. The study was conducted by filling one-litre SKC Inc. Series 232 Tedlar bags to approximately 80 % capacity with ultra-high purity (UHP) helium. At five minutes and three, five, 24, 48 and 72 hours after filling, sub-samples were collected from the bag septum using a 5 ml VICI Series A-2 gas syringe and analyzed for nitrogen (N_2) and O_2 using a HP 5890 Gas Chromatograph equipped with thermal conductivity detector (TCD), flame ionization detector (FID) , and build-in gas sampling and back flush valves. Separate bags were used for tests at each time period (*i.e.*, consecutive sub-samples were not taken from one bag). Three Tedlar bags were tested for each time period (Figure 2.2).

Results

Nitrogen and O_2 concentrations remained relatively constant over the first five hours of the experiment, and were on average about 0.15 % for N_2 and 0.05 % for O_2. After five hours, N_2 and O_2 concentrations began to increase with the rate of increase showing a slight exponential rise in time. The rate of increase was slightly greater for O_2 than N_2. At 72 hours, the average N_2 and O_2 concentrations were 0.63 and 0.55 %, respectively. The permeation of atmospheric air into the Tedlar bags tested was negligible over the first 24 hours but began to approach significant levels at 72 hours. The increase in O_2 would be of concern when accurate light gas data are required to evaluate biodegradation conditions. The implication is that Tedlar bags used for light gas analyses should be analyzed within about 24 to 48 hours.

Syringe Sorption Study

Methods

Five milliliter soil gas/headspace syringes constructed by SGE (Australia) (Part No. 5MAX-HASV) with glass syringe barrels, Teflon coated gas-tight plunger, push-button valve, with Teflon luer lock male connector were used to collect soil gas samples from the Chatterton site. After prolonged use of the syringes in high BTX concentration areas, elevated concentrations started to be measured in blanks (*i.e.*, syringes filled with helium). The time between sample collection and analysis, and blank collection and analysis was normally approximately the same. The elevated concentrations in blanks initiated an evaluation of the time-dependent desorption of benzene from the syringes (Figure 2.3). This was conducted by filling the syringe barrel with UHP helium and then waiting varying lengths of time before analysis using a SRI 8610 GC/PID.

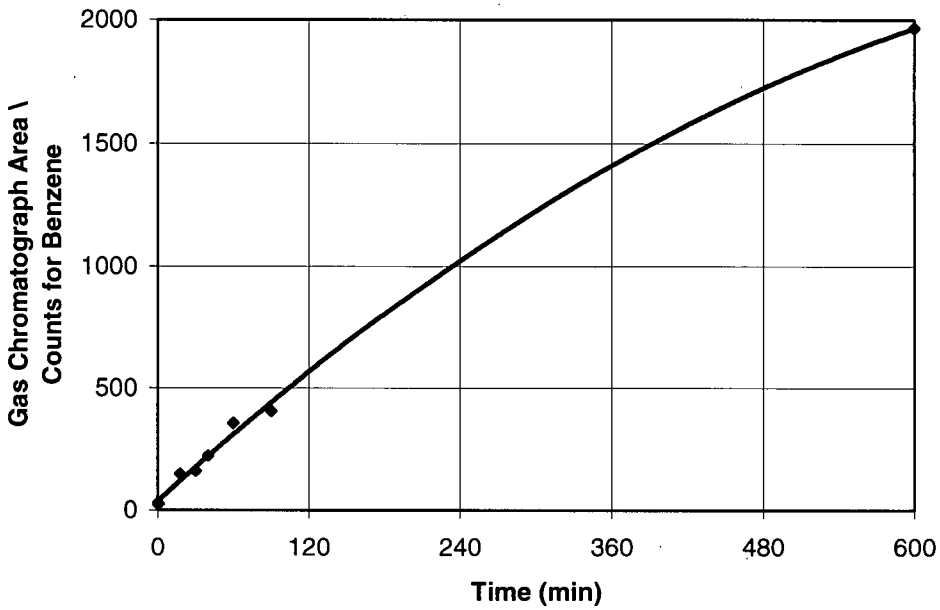

Figure 2.3. Results of syringe desorption study: Gas chromatograph benzene area counts.

Results

A progressive increase in benzene concentrations over time was measured indicating that significant adsorption of BTX had occurred, and that desorption was a time-dependent process (Figure 2.3). The implication is that blanks testing after only a few minutes would erroneously indicate a non-contaminated sampling device.

PVC Sorption Study

Methods

A laboratory study was conducted to evaluate whether sorption onto the walls of a PVC probe has a significant effect on VOC vapour concentrations. PVC probes are often used to collect soil gas samples. The study was performed using three PVC probes, each installed in a sand-filled bucket. Initially, two probes were placed in buckets containing sand contaminated with benzene, m-xylene, and TCE ("Probes No. 1 and 2"). One control probe was placed in a non-contaminated bucket ("Probe No. 3"). Probe sorption was evaluated for the two soil gas probes in contact with VOC vapours. After four weeks, one of the probes was removed and placed in a non-contaminated environment and desorption was evaluated over a 6-week period. The progression from a contaminated to non-contaminated environment could conceivably approximate field conditions where vapour concentrations are reduced through remediation of the contamination source and/or rise in the water table (*i.e.*, submergence of a residual contamination source).

The set-up for probes No. 1 and 2 was as follows: (i) 60 ml each of benzene, m-xylene and TCE was added to 1.19 litres of water, (ii) the water and contaminants were briefly mixed with 7.92 litres of sand, (iii) the sand was placed in a clean 20-litre food-grade plastic pail (corresponding height in pail was 0.15 m), (iii) a 100 mm diameter hole was created in the sand in the pail, (iv) a 0.6 m long soil gas probe constructed of pre-washed environmental quality

50 mm diameter PVC with a 0.15 m long No. 20 slot screened section and bottom cap was placed in the hole, (iv) the space surrounding the probe and the remainder of the pail was filled with moist clean silica sand, (v) the probe top was completed with a cap and ¼ inch diameter polyethylene tube assembly, and (vi) the top of the plastic pail was covered with plastic. The water-filled and total soil porosity were approximately 0.15 and 0.40. Probe No. 3 was identical to Probes No. 1 and 2, except that no contaminants were added. One pail just containing non-contaminated silica sand was also set up. After four weeks, Probe No. 2 was pulled from the contaminated pail and inserted into the pail that just contained non-contaminated sand.

Soil gas samples were collected from the probes on a weekly, or more frequent, basis. After purging approximately one probe volume, a sample was collected using either a 1 or 5 ml gas-tight syringe. Soil gas samples were analyzed using a SRI 8610 GC/PID.

Results

The vapour testing results indicate that during the first four weeks of the study, VOC concentrations for Probes #1 and #2 were highly elevated, and, as expected, concentrations in the blank (Probes #3) were near to the detection limit (Figure 2.4). The first four weeks of testing indicated a slight reduction in vapour concentrations for Probe #2, which may have been a result of contaminant mass depletion through purging and volatilization.

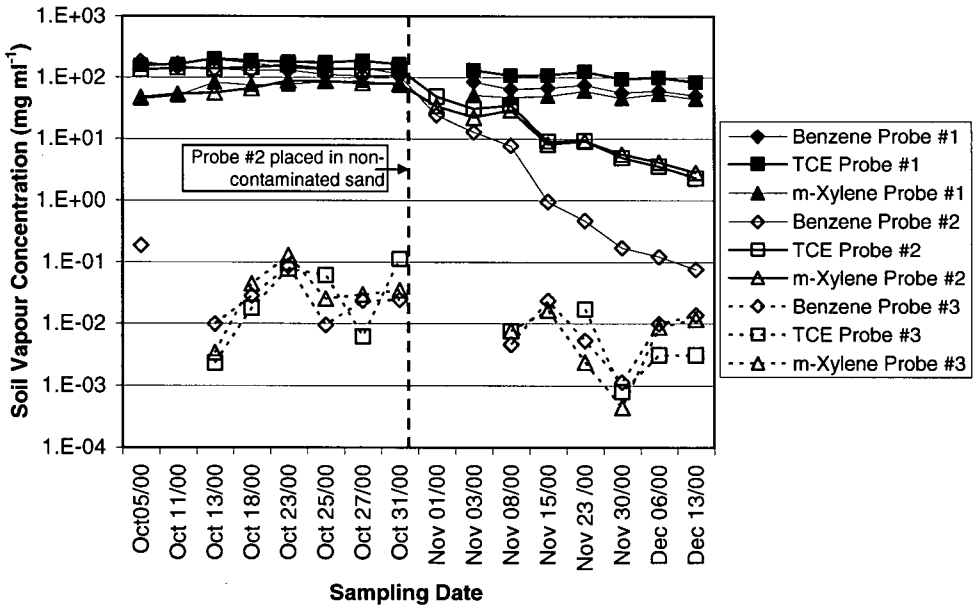

Figure 2.4. Results of PVC sorption study: Benzene, TCE and m-Xylene concentrations in soil vapour samples.

Vapour concentrations for Probe #2 decreased steadily after it was placed in the non-contaminated pail and after six weeks there was a 25-fold to 800-fold reduction in concentration relative to baseline concentrations. However, vapour concentrations after six weeks remained much higher than background concentrations in the non-contaminated pail indicating a significant mass of chemicals was undergoing time-dependent desorption. The concentration

decrease over time was greatest for benzene, which we infer to be due to a smaller mass of chemical initially sorbed to the PVC and a faster desorption rate. The study indicates that the mass of VOC vapours sorbing in or onto PVC can be significant, and that sorption and desorption processes could bias vapour testing results. Steel probes were used for the Chatterton study.

Light Gas Analysis Study

Methods

To investigate the differences between field and laboratory methods, two samples taken consecutively from the same probe were analyzed. The first sample was tested in the field using a Landtec GA-90 gas detector, which utilizes a galvanic cell for O_2 and infrared detector for CO_2 and CH_4. The Landtec was calibrated to O_2 using atmospheric air (*i.e.*, O_2 equal to 20.9 %) and to CO_2 and CH_4 using a mixture of 15 % CO_2 and 15 % CH_4 (balance N_2). The O_2 calibration was periodically checked using 4 % O_2 (balance N_2). The Landtec O_2 readings for this standard consistently ranged between 3.5 and 3.8 %. The second sample collected was analyzed using a HP 5880 GC with TCD and FID detector. Two capillary columns were used to separate the compounds within the GC/TCD-FID consisting of a (i) HP Plot molecular sieve 5A 30 m by 0.53 mm column or (ii) JW GSQ 30 m by 0.53 mm column. These columns were connected in-series using a gas valve.

Results

A relatively good comparison was obtained between the Landtec and GC results for CO_2 (r^2 = 0.95) (Figure 2.5). A good correlation was also obtained between the Landtec and GC results for O_2 (r^2=0.99). However, O_2 concentrations by GC methodology were consistently higher than the Landtec concentrations. Possible reasons for this difference include a (i) downward bias in the Landtec concentrations due to non-linear response (Landtec was always calibrated to an O_2 concentration of 20.9 %), (ii) upward bias in GC concentrations due to permeation of O_2 into Tedlar bags, and (iii) slight increase in O_2 concentrations during purging since the GC sample was always collected after the field sample. In total, these factors could potentially contribute to an O_2 difference as high as 1.5 % and therefore do not fully account for the difference observed, which was up to 3 %. While there is no readily apparent reason for this difference, the lower Landtec O_2 concentrations are consistent with the vadose zone model biogeochemical model for the Chatterton site as elaborated below.

(a) (b) (c)

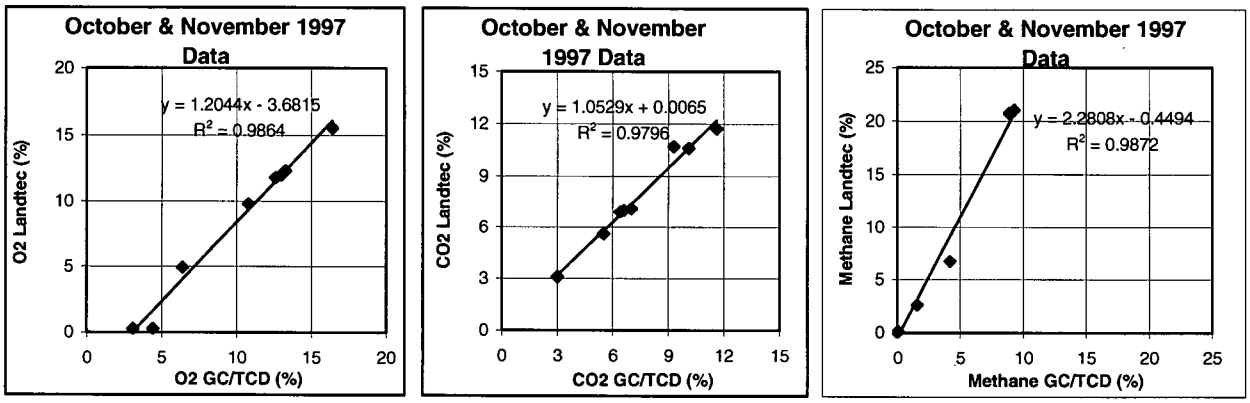

Figure 2.5. Comparisons of O_2, CO_2 and CH_4 Concentrations Measured Using Landtec GA-90 and GC/TCD Analysis

A good correlation was also obtained between Landtec and GC results for CH_4 (r^2=0.99). However, there was a significant upward bias in the Landtec CH_4 concentrations. The Landtec GA-90 "methane" infrared detector detects hydrocarbons with a stretching (vibrational) frequency between 3.2 and 3.45 μm. Benzene and toluene also have stretching values within this range, and therefore, the elevated Landtec methane concentrations are likely due to benzene and toluene vapours. When BTX concentrations were high, the Landtec concentrations were corrected using the correlation in Figure 2.5 (Corrected CH_4 = (Landtec CH_4 – 0.15) / 2.75)). The corrected CH_4 concentrations are approximate values that are only accurate to a few %. The use of the Landtec field detector was considered appropriate for the Chatterton study.

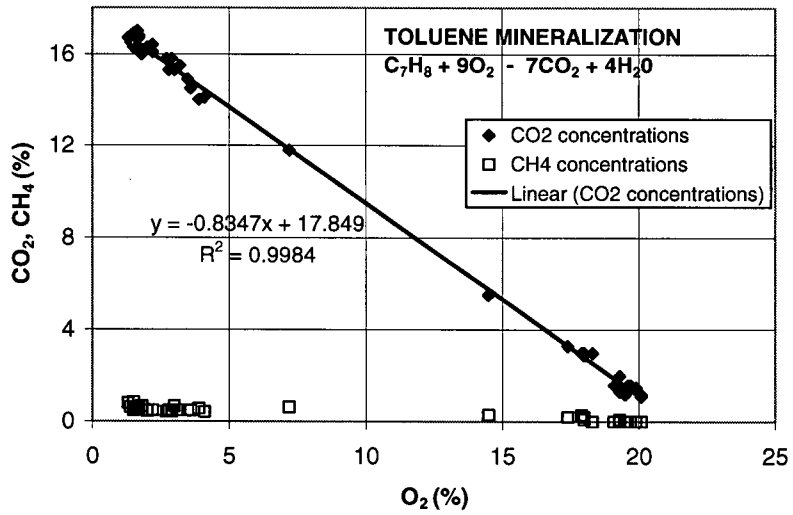

Figure 2.6. Results of light gas analysis study: Light gas concentration adjacent to building during dry season measured by Landtec GA-90 (summer 1998).

Consistency of Soil Gas with Biogeochemical Processes

Comprehensive monitoring at the Chatterton site indicates an aerobic zone, where biodegradation of BTX vapours and oxidation of CH_4 is occurring, and an anoxic or anaerobic zone (Hers and Zapf-Gilje, 1998; Hers *et al.*, 2000). Under anoxic or anaerobic conditions, low O_2 concentrations (less than 2 %) would be expected as indicated by monitoring at other sites (Jeng *et al.*, 1996; Ririe and Sweeney, 1995; Li, 1995). Soil gas samples with Landtec O_2 concentrations below 1 % were generally from the anoxic or anaerobic zone and therefore at levels consistent with inferred biogeochemical processes.

The internal consistency of the light gas levels, relative to biodegradation processes at the Chatterton site, was checked by evaluating soil gas concentrations measured below a building (greenhouse) and an adjacent grass-covered area. Soil gas concentrations between 0.15 m and 1.5 m depth were measured at 0.15 m to 0.3 m intervals in both areas. Additional information on soil gas monitoring and biodegradation modeling are provided in Hers and Zapf-Gilje (1998) and Hers *et al.* (2000).

Below the grass-covered area, the soil moisture contents were relatively low during the relatively dry summer season. As a result, atmospheric O_2 readily diffused into soil resulting in aerobic biodegradation. A plot of the summer O_2 versus CO_2 concentrations indicated a linear relationship (r^2=0.998), which is consistent with aerobic biodegradation of BTX (Figure 2.6). The slope of the CO_2 and O_2 relationship (0.83) is close to the stochiometric relationship for the complete aerobic mineralization of toluene, which states that 0.88 moles of CO_2 is produced for each mole of O_2 consumed. Toluene comprises over 80 % of the hydrocarbon mass present at the Chatterton site.

Below the building, the biogeochemical model appears to be more complex since both CH_4 and CO_2 concentrations are elevated when O_2 concentrations are low, suggesting both aerobic and anaerobic processes are operational below the building (Figure 2.7). The concrete slab of the building is a partial barrier to atmospheric O_2 diffusion into subsoil. As a result, anaerobic processes appear to be more significant below the building compared to adjacent to the building. In the presence of O_2, CH_4 will be oxidized generating CO_2. Under anaerobic conditions, the generation of methane through methanogenesis could result, and if hydrogen gas were present, methane could be generated through CO_2 reduction. The slope of the CO_2 and O_2 relationship decreases at low O_2 and elevated CH_4 concentrations (Figure 2.7). The reduced slope is approximately consistant with the stoichiometry for methane oxidation where 0.5 moles of CO_2 is produced for every mole of O_2 consumed.

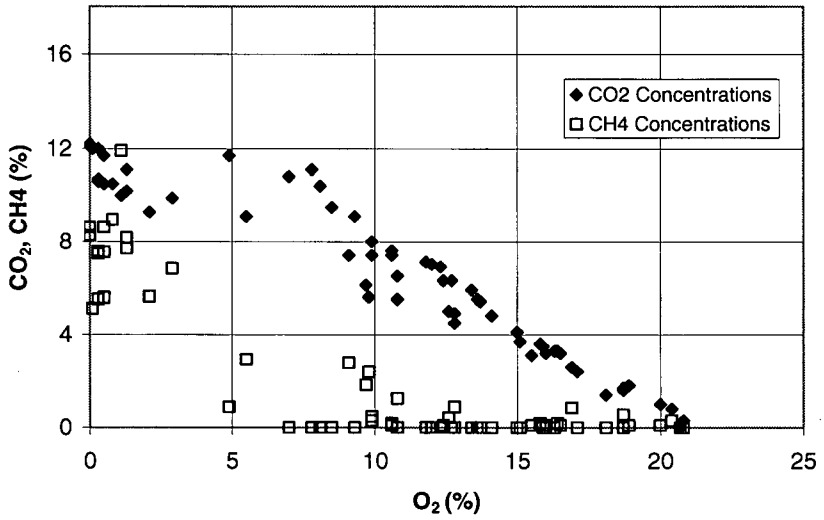

Figure 2.7. Results of light gas analysis study: Light gas concentration below building measured by Landtec GA-90.

BTX Analytical Quality Control Study

Methods

Soil gas samples were analyzed for BTX vapours using a SRI 8610 GC/PID. The GC/PID capillary column was a DB-624 30 m by 0.53 mm column with a methylated phenoxy stationary phase (1.8 μm thickness). The CG carrier gas was ultra-high purity (UHP) helium and the flow rate was 8 ml min^{-1}. Syringes samples were directly injected into the GC. Sorbent tubes were initially desorbed onto a focusing tube using a thermal tube desorber (Dynatherm Analytical Instruments, Inc. Model 850), which in turn was desorbed and passed through the GC. The GC oven temperature ramp implemented for BTX analysis was a constant 50°C for two minutes followed by 5°C/minute increase to 85°C followed by a two minute hold at the upper temperature. Calibration standards consisted of 1 μl of 100, 250, 500 and 1,000 ng μl^{-1} benzene, toluene and xylene (individual concentrations) in pentane. Since the boiling point of pentane is 36°C, the pentane based calibration standards would have readily volatilized in the injection port (at 50°C). Standards were directly injected in the GC using a 10 μl syringe while vapour samples were injected using a 5 ml syringe. A 0.2 ml vapour sample was the minimum volume that could be accurately injected into the GC (using 5 ml syringes) while a 5 ml sample was the maximum volume that could be run without excessive broadening of the chromatogram peaks. In part, the maximum sample volume is controlled by the relatively small volume of the GC column (about 6.6 ml).

Replicate soil gas samples obtained from the same probe were analyzed for BTX to evaluate sampling and analysis variability. Replicates consisted of either two or three samples obtained within about 15 to 60 minutes. Prior to collecting each sample, the probe was purged. The BTX recovery was evaluated by injecting a known mass of 3-fluorotoluene (surrogate) into the sorbent tube (typically 5 μl of 50 ng μl^{-1} 3-fluorotoluene), and then measuring the response.

Results

The replicate precision was assessed using the relative standard deviation (RSD) (standard deviation divided by mean), since at some locations more than two replicates were analyzed. The relative percent difference (RPD) is more commonly used, and when two samples are analyzed, is 1.41 X greater than the RSD. The recovery was calculated as a percentage of the initial injected mass (Table 2.1). The median RSD of 14 to 29 %, which corresponds to a RPD between 20 and 40 %, is greater than the regulatory acceptable levels for duplicate laboratory water analyses (RPD of about 20 %). However, for this study, the RSD incorporates the combined variability associated with laboratory analysis, and sampling and short-term variation in soil vapour concentrations since replicate samples were concurrently collected in separate syringes. The analytical precision (RSD) and bias (recovery) was considered acceptable for purposes of this research project

Table 2.1: Summary of Quality Control Testing for BTX Analyses

QC Measure	Compound	No. QC Samples	Minimum	Maximum	Arithmetic Mean	Median
Precision (% RSD)	Benzene	22	0.52	108	28	14
Precision (% RSD)	Toluene	22	0.86	119	33	26
Precision (% RSD)	M&p-Xylene	18	1.9	68	30	29
Recovery (%)	3-fluoro-toluene	26	19	138	80	85

DISCUSSION OF EXPERIMENTAL TECHNIQUES AND LESSONS LEARNED

Experimental techniques, lessons learned and recommended practice for soil gas sampling and analysis, based on both the results of the experimental studies and broader literature review, are discussed below.

Probe Design

Site geology and depth requirements can dictate the type of probe installed. Driven probes have the potential advantage of less disturbance compared to methods involving drilling, and are generally less expensive than probes installed in boreholes. However, our experience with driven ground probes is that the side perforations in some instances become smeared with fine-grained soil during installation making it difficult to draw a soil gas sample. There is greater flexibility in the design of probes installed in boreholes.

Factors that potentially affect the quality of soil gas samples include the probe material, internal area of probe in contact with the sample, the screened length, cross-sectional area of the screened or open portion of the probe, the probe volume and opportunity for leaks or short-circuiting from the surface. The probe material combined with the internal area of the probe in contact with the sample potentially has implications in terms of sorption of VOCs and possible time-dependent desorption of VOCs into a clean air stream.

There is little quantitative information on the best type of sample tubing to use. The results of the PVC sorption study suggest that VOC sorption into PVC can be significant. While further testing of other material types is required to evaluate relative sorption characteristics, PVC may not be an appropriate probe and tubing material for vapour sampling. Teflon is sometimes cited as the plastic of choice, but others indicate that Teflon is porous and a poor choice of tubing material for vapour sampling (Kreamer, 2001). Although Teflon has also been the material of choice for sampling containers and tubing used by environmental laboratories, it's selectivity in removing organics from samples and standards has increasingly been noted over the past few years as being problematic. This has resulted in the introduction and use new relatively inert tubing manufactured from PEEK, Tefzel (ETFE-polymer), fused-silica glass, and HDPE. However, most of these materials are not readily available for use in soil gas surveys. Based on currently available materials, Teflon or high density polyethylene (HDPE) appear to have reasonable sorption characteristics compared to other types of plastic.

To obtain representative soil gas samples, the relative open area over the perforated or screened section of the probe should be maximized and sufficiently large to provide for unimpeded flow of soil gas into the probe. However, the probe volume and filter pack volume should be kept relatively small to minimize purge volumes and the surface area over which sorption could occur. Smaller probe volumes also reduce the potential for non-representative samples due to over-purging and disturbance of equilibrium soil vapour concentrations, and possible short-circuiting. Especially for deeper probes, consideration should be given to systems that employ an implant connected to smaller diameter tubing. Suggested probe diameter for most applications is 25 mm or less. Since an overly large filter pack may alter the local vapour concentrations, installation of small diameter probes in large diameter boreholes should be avoided.

The screened length of the probe is important since usually the investigation objective is to measure concentrations representative of a discrete point in the unsaturated zone. Several studies have indicated that hydrocarbon vapour concentrations can change several orders-of-magnitude over short vertical distances (*i.e.*, on the order of 0.3 m) (Fischer *et al.*, 1996; Hers and Zapf-Gilje, 1998). For this reason, soil gas probes with relatively short screens (i.e., 300 mm or less) are recommended for most applications. Soil vapour sampling from groundwater monitoring wells is not recommended except to provide approximate screening information.

Short-circuiting of atmospheric air to the probe can result between the probe and soil, and leakage of soil gas and/or atmospheric air can occur at probe joints. Prevention of short-circuiting and leaks is particularly important for low permeability soil deposits. The surface seal integrity can be tested by introducing a tracer gas (e.g., propane, butane) around the probe at the contact with the ground surface and then analyzing the collected soil gas samples for the tracer gas (Hartman, 2002).

Sampling Collection and Analysis

Critical factors affecting soil gas sample quality include sampling collection methodology, sample losses and cross-contamination. The purge volume and rate can affect soil vapour concentrations over time. Sample losses can occur as a result of contaminant condensation within the sampling device or tubing, solution into condensed water, sorption onto sampling

device materials, leakage out of the sampling container and chemical change. Cross-contamination can result from intrusion of atmospheric air into the container, incomplete decontamination of the sampling device or sampling train. Several studies have suggested that sorption to and leakage from Tedlar bags can result in relatively large VOC losses over short time periods. When used for light gases, the Chatterton research program permeation study suggests that Tedlar bags can provide acceptable results when analyzed within 24 to 48 hours. Longer holding times for Tedlar bags could result in oxygen concentrations with an upward bias. Sorption of BTX onto sampling equipment (Teflon coated gas-tight syringe barrel) can be significant as demonstrated by the syringe study, highlighting the importance of decontamination of sampling devices.

Typically, soil vapour sampling protocols due not include probe development prior to purging and sampling (i.e., as conducted for groundwater sampling). It some cases, it may also be prudent to develop or "condition" probes prior to purging and sampling, particularly if the probe surface area is large or if drilling fluids (air or water) are used during the drilling process. We are aware of one project where soil vapour probes were installed in deep boreholes advanced using an air rotary drill rig, and where probe development, consisting of the removal of air introduced into the formation, was needed to obtain representative results.

The purging volume and rate should be based on a number of factors including considerations relating to the mixing of VOCs in the probe, and the desired representative soil gas volume to be tested. While based on a complete sequential mixing equation upwards of three probe volumes should be purged (Cody, 2003), for narrow diameter tubing fewer purge volumes are likely needed to obtain a representative sample due to reduced mixing resulting from more of a "plug flow" phenomena. If local vapour concentrations adjacent to the probe tip are required, it is recommended that purge volumes be minimized (about 1 ½ volumes). It is recommended that the vacuum be measured using a manometer and that vacuums generated be allowed to fully dissipate before collecting samples. Relatively low flow sampling rates should generally be employed (*i.e.*, on order of 100 to 200 ml min-1) to minimize short-circuiting. The fittings between tubing and pump should be tight. Consistency in sampling is important to obtain repeatable results.

Sampling devices should be consistent with analytes and data quality objectives (*e.g.*, Tedlar bags would generally be inappropriate for VOCs). Quality control procedures must be carefully adhered to including the use of low sorptive materials for sampling trains dedicated to individual probes, thorough decontamination procedures, and appropriate holding times. Tape should never be used for sampling train connections. It is recommended that syringe samples be analyzed within a few hours of collection. While there is little guidance in terms of appropriate sample storage procedures, a reasonable approach is to keep samples dark to avoid photooxidation losses and to prevent excessive changes in temperature relative to the *in situ* soil gas temperature.

Analytical Techniques

Field Screening Methods

The use of hand-held detectors for measuring total hydrocarbon and light gas concentrations at contaminated sites has become common. While these types of detectors are potentially valuable for site screening, the limitations associated with these instruments, including non-

specificity to compounds of possible interest, and effect of environmental factors and sampling methods, should be clearly understood (*e.g.*, Robbins *et al.*, 1990). The light gas study demonstrated that while a relatively good correlation between the Landtec GA-90 field detector and GC methods was obtained for CO_2, the Landtec CH_4 results appeared to be affected by non-specificity to CH_4 and elevated BTX vapour concentrations. The use of field detectors such as the Landtec GA-90 is considered appropriate provided that instrument limitations are recognized and data is corrected. It is also noted that detector technology continues to evolve and, in the case of the Landtec, an optical sensor that is highly specific to methane (wavelength=3.322 μm) is now available. The light gas study also showed how an understanding of biogeochemical processes can be used to evaluate the quality of gas measurements. Oxygen concentrations near atmospheric levels within hydrocarbon source zones, or lack of an inversely proportional O_2 versus CO_2 relationship (for soil zones where aerobic biodegradation is occurring) may be indicative of short-circuiting of air to the probe or equipment problems.

Laboratory Analytical Techniques

There are a wide range of options for sampling containers and laboratory analytical methods for quantification of individual VOCs. Method selection will typically depend on the target VOCs, data quality objectives and cost considerations. For the Chatterton site research study, the collection of samples using syringes and sorbents, and analysis by GC/PID methodology was found to be effective. For risk assessment studies, it is important that quality control requirements and detection limits be carefully considered.

The authors have reviewed data for relatively numerous projects where the soil gas data quality was suspect. Problems have included for sorbent tubes the selective breakthrough of certain compounds and poor sample recovery due to excessive moisture, for Summa canisters the improper cleaning of canisters and contaminant carry-over, and elevated levels of non-target compounds associated with poor probe design (i.e., use of tape) and cross-contamination from nearby above-ground use of petroleum products. Some measures that can be taken to improve data quality are discussed below.

Detection Limits: For risk assessments, the measured vapour concentrations are often used to predict indoor air concentrations. Appropriate detection limits can be back-calculated using risk-based target indoor air concentrations combined with expected dilution factors between soil vapour and indoor air. Guidance on dilution factors can be found in US EPA (2002), Hers *et al.* (2002) and Johnson *et al.* (1998).

Sorbent Selection: Should be based on VOC type, desired detection limit, and data quality objectives. Due to elevated humidity in soil vapour, some sorbents used for air sampling are not appropriate for soil vapour. For low level analysis of soil vapour, older sorbent materials such as coconut shell charcoal have been largely replaced by newer sorbents such as processed synthetic carbon, or molecular sieve materials.

Sorbent Sampling Volume: Should be carefully determined through consideration of the expected VOC concentration and mass, the sorption capacity and required detection limits. For highly volatile compounds such as vinyl chloride the use of sorbent tubes can be challenging due to limited capacity of the sorbent to retain vinyl chloride. Field screening of VOC concentrations

using a PID can be used to guide the calculation of the sample volume. It is recommended that two tubes in series be analyzed to evaluate possible breakthrough, for at least of portion of the samples collected.

Blanks: For all methods, it is recommended that the analytical laboratory demonstrate, for at least a portion of the sample containers, that the sampling device (canister, sorbent tube) is clean to below the required detection limits, prior to sampling and analysis. Method blank and spike samples should be analyzed, and depending on the project, transport blanks and background samples may also be warranted. A field method blank can be collected by drawing atmospheric air or inert gas through the sampling train and probe to be sampled, prior to installation.

CONCLUSIONS

Soil gas sampling and analysis was an important component of the Chatteron research study. Acquiring good quality, representative soil gas data requires careful attention to probe design, sampling containers and methods, and analytical methods. For this reason, several experiments were conducted to evaluate methods for soil gas testing. The broader context for the studies and recommendations provided in this paper is that there is significant variability in soil gas probe design and sample collection and analysis methods used by practitioners, and there is a need for improved protocols for soil gas sampling and analysis. The results of the research program experiments and our background review indicate that significant issues for soil gas testing sampling include probe design and possible short-circuiting of atmospheric air, sorption of VOCs onto probe materials, contamination of sampling containers, and possible gas leakage from Tedlar bags. Some of the key issues that need to be addressed for soil gas program design include the probe size, material and installation method, purging volume and rate, the sampling and analysis method (sorbent tube versus "whole air" canister samples), and quality control procedures and checks.

Although not the focus of this paper, soil properties and environmental factors should also be considered in the design of a soil gas sampling program. Soil gas samples from shallow depths can be affected by infiltration of rain water, fluctuations in temperature and barometric pressure. In some cases, there can be significant concentration attenuation of hydrocarbon vapours due to fine-grained high moisture content layers (representing a diffusive barrier) and/or biodegradation of hydrocarbon vapours (Hers *et al.*, 2000). As a result of concentration variability, the use of closely spaced vertical network of probes may be warranted.

REFERENCES

Aelion, C.M., J.N. Shaw, R.P. Ray, M.A. Widdowson, and H.W. Reeves. 1996. Simplified Methods for Monitoring Petroleum-Contaminated Groundwater and Soil Vapour. *J. of Soil Contamination.* 5(3): 225-241.

American Society for Testing and Materials (ASTM), 1992. Standard Guide for Soil Gas Monitoring in the Vadose Zone. D-5314-92.

American Society for Testing and Materials (ASTM), 1995. Standard Guide for Risk-Based Corrective Action Applied at Petroleum Release Sites. E-1739-95.

Andiro, J.M. and J.W. Butler. 1991. A study of the stability of methanol-fueled vehicle emissions in Tedlar bags. *Environ. Sci. Technol.* 25: 1644-1646.

Christy, T.M. and S.C. Spradlin. 1992. The Use of Small Diameter Probing Equipment for Contaminated Site Investigation. In: *Proc. of the Sixth National Outdoor Action Conference.* May 11-13, Las Vegas, NV. 87-101.

Cody, R. 2003. Soil Vapour Sampling and Analysis: Sources of Random and Systematic Error in the Characterization of Low Level Organohalide Sources. In: *US EPA Seminar on Indoor Air Intrusion*, January 14-15, 2003. Fairmont Hotel, Dallas, Tx.

Fischer, M.L., A.J. Bentley, K.A. Dunkin, A.T. Hodgson, W.W. Nazaroff, R.G. Sextro, and J.M. Daisey. 1996. Factors Affecting Indoor Air Concentrations of Volatile Organic Compounds at a Site of Subsurface Gasoline Contamination. *Environ. Sci. Technol.*, 30 (10): 2948-2957.

Harper, M., 1994. Novel Sorbents for Sampling Organic Vapours. *Analyst*, January, Vol. 119.

Harrington, D., Tekmar-Dohrman, Introduction to Air Toxics Analyses, Rev3.10-98 Tekmar-Dohrman (1998).

Hartman, B., 2002. How to Collect Reliable Soil-Gas Data for Risk-Based Applications, Part 1: Active Soil-Gas Method. *LUSTLine Bulletin*, 42, October

Hers, I. and R. Zapf-Gilje. 1998 Canadian consortium research project – field validation of soil gas transport to indoor air pathway. In: *Proc. 1998 Petrol. Hydro. and Org. Chem. in Ground Water*, API/NGWA, Houston, Tx., Nov. 11-13:251-266.

Hers, I., J. Atwater, L. Li, and R. Zapf-Gilje. 2000. Evaluation of vadose zone biodegradation of BTX vapours. *Journal of Contaminant Hydrology*, 46: 233-264.

Hers, I., D. Evans, R. Zapf-Gilje, and L. Li. 2002. Comparison, Validation and Use of Models for Predicting Indoor Air Quality from Soil and Groundwater Contamination. *J. of Soil and Sediment Contamination.* 11 (4): 491-527.

Jeng, C.Y, V.J. Kremesec, Jr., and H.S. Primack. 1996. Models of Hydrocarbon Vapour Diffusion through Soil and Transport into Buildings. In: *Proc. 1996 Petrol. Hydro. and Org. Chem. in Ground Water*, API/NGWA, Houston, Tx., November 13-15, 319-338.

Johnson, P.C., W. Kemblowski, and R.L. Johnson. 1998. Assessing the Significance of Subsurface Contaminant Vapour Migration to Enclosed Spaces – Site Specific Alternatives to Generic Estimates. API Publication 4674, December.

Kreamer, D., 2001. Field Innovation Forum: Down the Rabbit Hole with Alice – Sucking Soil Gas All the Way. *Ground Water Monitoring and Remediation.* Fall.

Li, D.X., 1995. Bioventing feasibility assessment and system design using subsurface oxygen sensors. *J. of Air & Waste Management Association.* 45: 762-769.

Marrin, D.L. and H.B. Kerfoot. 1988. Soil-gas surveying techniques. *Environ. Sci. Technol.* 22(7): 740-745.

Robbins, G.A., B.G. Deyo, M.R. Temple, J.D. Stuart, and M.J. Lacy. 1990. Soil-Gas Surveying for Subsurface Gasoline Contamination Using Total Organic Vapour Detection Instruments Part I. Theory and Laboratory Experimentation. *GWMR.* Summer.

Ririe, T. and R. Sweeney. 1995. Fate and Transport of Volatile Hydrocarbons in the Vadose Zone. In: *Proc. 1995 Petrol. Hydro. and Org. Chem. in Groundwater.* API/NGWA, Houston, Tx., Nov. 29 to Dec. 1, 529-542.

Ririe, T., R. Sweeney, S. Daughery, and P. Peuron. 1998. A Vapour Transport Model That is Consistent with Field and Laboratory Data. In: *Proc. 1998 Petrol. Hydro. and Org. Chem. in Groundwater*, API/NGWA, Houston, Tx., Nov. 11 to 13, 299-308.

Ririe, T. and R. Sweeney. 1998. Sampling/Analysis Protocols for Vapour-Phase Investigations. Petroleum Environmental Research Forum Soil Vapour to Indoor Air Workshop, Feb. 6-7.

Schroedl, S.R. and H.B. Kerfoot. 1990. Long-term Soil-Gas Monitoring of Underground Storage Tanks. In: *Proc. 1990 Petrol. Hydro. & Org. Chem. in Ground Water*, API/NGWA, Houston, Tx., Nov. 15-17.

San Diego County, 2002. San Diego County Site Assessment Manual http://www.co.san-diego.ca.us/cntydepts/landuse/env_health/lwq/sam/pdf_files/presentations/soilvapour_guide.pdf.

Smith, J.A., C.T. Chiou, J.A. Kammer, and D.E. Kile. 1990. *Environ. Sci. Technol.*, 24: 676-683.

Smith, J.A., A.M. Tisdale, and H.J. Cho. 1996. Quantification of Natural Vapour Fluxes of Trichloroethene in the Unsaturated Zone at Picatinny Arsenal, New Jersey. *Environ. Sci. Technol.* 30: 2243-2250.

U.S. EPA, 2002. Draft Guidance for Evaluating the Vapour Intrusion to Indoor Air Pathway from Groundwater and Soils. December.

Van Sciver, C. 1992. Monitoring a Methane Plume at a Sanitary Landfill Utilizing Cost Efficient Soil and Gas Techniques. *Hazardous Materials Control.* September/October.

Wang, Y., T.S. Raihala, A.P. Jackman, and R. St. John. 1996. Use of Tedlar Bags in VOC Testing and Storage: Evidence of Significant VOC Losses., 30: 3115-3117.

Yeates, G.L. and D.M. Nielsen. 1998. Design and Implementation of an Effective Soil Gas Monitoring Program for Four-dimensional Monitoring of Volatile Organics in the Subsurface. In: *Proc. 1998 Petrol. Hydro. and Org. Chem. in Ground Water*, API/NGWA, Houston, Tx., Nov. 14-16.

CHAPTER 3

MEASUREMENT OF *IN SITU* GAS-PHASE DIFFUSION COEFFICIENTS

This chapter was published in *Environmental Technology.* 21: 631-640 (2000)[2].

ABSTRACT

Vadose zone *in situ* diffusion coefficients were measured at a former petro-chemical plant ("Chatterton" research site) using a push-pull test and helium tracer. The test is relatively simple to perform, utilizes relatively inexpensive materials and field equipment, and requires only a few hours to complete each series of tests. *In situ* diffusion coefficients are derived using an analytical solution for spherical diffusion from a point source, assuming instantaneous injection of the tracer. The results of push-pull tests conducted at the Chatterton research site indicate that measured effective diffusion coefficients in sand fill with moisture content between 5 and 12% (by weight) ranged from about 0.01 to 0.07 cm^2sec^{-1}. A good comparison was obtained between the measured gas-phase tortuosity factor and that predicted using a common empirical relationship with measured tortuosity factors consistently about twice the predicted values. While further comparisons need to be conducted for various moisture contents and different soil types, the results of this study suggest that the push-pull test is an effective tool for estimating diffusion coefficients and can be used to validate empirical relationships for diffusion coefficient.

KEY WORDS: soil gas, diffusion coefficient, tracer, helium, vadose zone.

[2] Hers, I., Zapf-Gilje, R., Li, L. and Atwater, J.

INTRODUCTION

Gas-phase diffusion is an important vadose zone transport mechanism for volatile chemicals. Prediction of gas-phase diffusion is integral for human health risk assessment at contaminated sites, where estimation of potential exposure for the soil gas transport to indoor and/or outdoor air pathways is often required (ASTM, 1995). In addition, quantification of diffusion coefficients may be important for *in situ* remediation projects involving soil vapour extraction and bioventing, where diffusion from low permeability soil zones may represent a rate-limiting process.

Diffusion occurs as a result of the movement of chemicals as influenced by their kinetic energy. In most cases, predictive relationships assume a Fickian model where diffusive transport through a porous medium is a function of the concentration gradient, temperature, fluid viscosity and tortuosity. Diffusive transport rates in air are several orders-of-magnitude higher than those in water, and therefore consideration of liquid-phase diffusive transport is generally only important when moisture contents are very close to saturation levels. The soil tortuosity is dependent on the porosity, moisture content, pore geometry, horizontal and vertical soil layering and other potential macroscopic features such as dessication cracking (Batterman, 1995). It is noted that in some cases, transport may not be adequately described by a Fickian model. These include surface-hindered or Knudson diffusion which may be important for fine-grained soils where molecular collisions with pore walls prevail over collisions between molecules (Lin, 1994) and when multi-component gas-phase concentrations are very high. In this case, gas-phase diffusion is intrinsically coupled with viscous gas-flow arising from varying partial pressures of the gas mixture (Thorstenson and Pollock, 1989).

The effective diffusion coefficient is typically estimated using the chemical-specific diffusion coefficient in air and water and a factor to account for porous medium tortuosity. In many cases, relatively simple empirical correlations based on relationships between the tortuosity factor, moisture content and soil porosity are used (Millington and Quirk, 1961). The Millington and Quirk model is typically used when simulating diffusive vapour transport (Johnson and Ettinger, 1991; ASTM, 1995; Lowell and Ekland, 2004). *In situ* or laboratory diffusion coefficients are rarely measured since to date such tests have not been straightforward, and perhaps due to an implicit assumption that empirically derived diffusion coefficients are sufficiently accurate for their intended purpose. Higher accuracy estimates of *in situ* diffusion coefficient may be warranted for risk assessment where accurate estimates of chemical flux are desired, or when there is a need to separate diffusive transport from other transport processes (*e.g.*, biodegradation).

This paper presents *in situ* diffusion coefficients estimated using a relatively simple push-pull test using a non-reactive tracer (helium) (Johnson *et al.*, 1998). Diffusion testing was conducted at the former "Chatterton" petro-chemical plant site located near Vancouver, B.C., Canada, a site contaminated with benzene, toluene and xylene, and represents one component of a comprehensive research program investigating the soil gas transport to indoor air pathway. The contribution of this work is to provide a simple and inexpensive technique for *in situ* measurement of diffusion coefficients, and to provide a comparison between measured and predicted diffusion coefficients.

BACKGROUND

Determination of diffusion coefficients has primarily been conducted using laboratory tests where steady-state chemical flux is measured in soil cores or packed soil columns. Field tests have generally involved evaluation of the transient variation in gas concentrations through sequential (in time) extraction of small quantities of gas, relative to the initial volume of tracer injected (Lai *et al.*, 1976; Roltson and Brown, 1977; Jellick and Schable, 1986). For these studies, gas samples were obtained using hyperdermic type needles and analyzed using gas chromatographic methods. For the transient method, the diffusion coefficient is determined using a least squares or similar fitting technique that minimizes the difference in predicted and measured gas concentrations based on an analytical solution for transient diffusion. The primary advantage of the push-pull test is a decreased sensitivity to potential errors since a much larger gas sample is extracted and analyzed resulting in a diffusion coefficient that represents transport integrated over a spherical volume. The relative merits of transient and push-pull type tests are further described in a recent publication (Johnson *et al.*, 1996).

The results of several laboratory-based studies where diffusion coefficients and tortuosity factors (see definition below) were estimated and are compared to empirically-predicted values in Table 3.1. The rationale for comparing tortuosity factors, as opposed to effective diffusion coefficients, is that the tortuosity factor is theoretically a function on soil properties only, whereas the effective diffusion coefficient is a function of chemical and soil properties and therefore subject to somewhat greater variability. Empirical tortuosity factors (τ_g) that have been proposed include:

- $\tau_g = \phi_g^{10/3}/\phi^2$ (Millington, R.J. and Quirk, J.M., 1961) (henceforth referred to as the "Millington and Quirk" relationship);
- $\tau_g = \phi_g^4/\phi^{5/2}$ (Currie, 1970) ("Currie relationship"), and;
- $\tau_g = 0.66\phi_g$ (Penman, 1940) ("Penman relationship"),

where θ_g and θ are the gas-phase and total porosity (L^3L^{-3}), respectively. The comparisons indicate that under laboratory conditions the common Millington and Quirk relationship generally underpredicts the tortuosity factor, and that the deviation between measured and predicted values increases with moisture content. At higher moisture contents, the difference between predicted and measured tortuosity factor may be as much as one order-of-magnitude. Under certain conditions it appears that the Penman relationship provides improved predictive capabilities.

Few field studies have included comparisons of measured to predicted diffusivities or tortuosity factors using different empirical models (Lahvis and Baehr, 1996; Lai *et al.*, 1976). One field study involved estimation of *in situ* diffusivity by model calibration with transient carbon dioxide production (Lahvis and Baehr, 1996). Comparison of *in situ* diffusivities through model calibration with those estimated using the Millington and Quirk relationship indicated that the empirical values were about three-times higher than the field-derived values for sand but two times less for clay (Lahvis and Baehr, 1996). In a second field study, a tortuosity factor of $1.66\phi_g$ provided a reasonable approximation of measured field and laboratory values for small-scale oxygen diffusion (Lai *et al.*, 1976).

Table 3.1. Comparison of measured and empirical gas-phase tortuosity factor from laboratory diffusion studies.

Soil Type	Chemical	Total Porosity	Air-filled Porosity	Experimental Tortuosity	Calculated Gas-Phase Tortuosity Factor		
					Penman (1940)	Millington & Quirk (1961)	Currie (1970)
Fine Silty Loam[1]	Methane	0.40	0.040	0.0025	0.027	0.00014	0.000025
Pachappa Loam[2]	Toluene	0.50	0.36	0.22	0.24	0.14	0.099
Pachappa Loam	Freon	0.50	0.26	0.11	0.17	0.04	0.024
Pachappa Loam	Freon	0.50	0.33	0.20	0.22	0.10	0.065
Pachappa Loam	Freon	0.50	0.43	0.28	0.28	0.23	0.18
Fine Sand[3]	TCE	0.38	0.38	0.34/0.37	0.26	0.28	0.24
Fine Sand	TCE	0.38	0.31	0.21/0.20	0.20	0.13	0.10
Fine Sand	TCE	0.38	0.23	0.15/0.091	0.15	0.051	0.03
Fine Sand	TCE	0.38	0.15	0.085/0.052	0.10	0.013	0.0061
Fine Sand	TCE	0.38	0.08	0.032/0.034	0.051	0.0013	0.00038
Concrete Sand[4]	Hexane	0.26	0.26	0.18	0.17	0.17	0.13
Concrete Sand	Benzene	0.26	0.26	0.17	0.18	0.17	0.14
Concrete Sand	Iso-octane	0.26	0.26	0.17	0.17	0.17	0.13
Silt Loam[5]	Toluene	0.48	0.44	0.23	0.29	0.28	0.23
Silt Loam	Toluene	0.52	0.40	0.32	0.27	0.17	0.13
Silt Loam	Toluene	0.51	0.33	0.24	0.22	0.10	0.06
Silt Loam	TCE	0.40	0.38	0.31	0.25	0.25	0.21
Silt Loam	TCE	0.39	0.26	0.17	0.17	0.07	0.05
Silt Loam	TCE	0.39	0.20	0.11	0.13	0.03	0.02

References: [1] Johnson and Perrott (1991); [2] Jin et al. (1994); [3] Batterman et al. (1995); [4] Baehr and Bruell (1990); [5] Arands et al. (1997)

Note: For study 5, assumed free-air diffusion coefficients used for calculation were Dair toluene=0.078 cm^2sec^{-1}, Dair TCE=0.083 cm^2sec^{-1}

THEORY

One-dimensional transient gas-phase diffusion (*i.e.*, Fick's second law) of a non-reactive chemical in a homogenous porous media can be expressed as:

$$\Theta_g R \frac{\partial C_g}{\partial_t} = \frac{\partial}{\partial Z}\left[\left(\Theta_g D_g + \Theta_w \frac{D_w}{H'}\right)\frac{\partial C_g}{\partial Z}\right] \tag{1}$$

where, R is the retardation factor (*dimensionless*), C_g is the soil gas concentration ($mol\ L^{-3}$), t is the time (T) and D_g and D_w are the gas- and aqueous-phase diffusion coefficients ($L^2\ T^{-1}$) (Appendix I). Assuming local equilibrium partitioning between the solid (sorbed) and soil water, and soil water and soil gas phases, and linear isotherms, the retardation factor can be expressed as:

$$R = 1 + \frac{\theta_w}{\theta_g H'} + \frac{\rho_b K_d}{\theta_g H'} \tag{2}$$

where θ_w is the water-filled porosity (L^3L^{-3}), ρ_b is the bulk density of the soil (ML^{-3}), K_d is the distribution coefficient (L^3M^{-1}) and $H`$ is Henry's Law Constant (*dimensionless*). In many cases, an effective gas-phase diffusion coefficient (D^{eff}) is defined that includes both the gas-phase porosity and diffusion coefficient. The effective diffusion coefficient is dependent on the tortuosity factor, and free-air and free-water diffusion coefficients, as follows:

$$D_g^{eff} = \theta_g D_g = \tau_g D_{air} \tag{3}$$

$$D_w = \Theta_w \frac{D_w}{H'} = \tau_w D_{water} \tag{4}$$

where τ_g and τ_w are factors to account for tortuosity (*dimensionless*) and D_{air} and D_{water} are the free-air and free-water diffusion coefficients (L^2T^{-1}). The free-air diffusion coefficient for helium in air can be estimated using an equation for binary diffusion coefficient (Fuller *et al.*, 1966):

$$D_{AB} = \frac{10^{-3} T^{1.75}\left[(M_A + M_B)/M_A M_B\right]^{1/2}}{P\left[(\Sigma v)_A^{1/3} + (\Sigma v)_B^{1/3}\right]^2} \tag{5}$$

where D_{AB} is the binary diffusion coefficient of gas A in gas B, T is temperature (K), P is pressure (*atmospheres*), M_A and M_B are molecular weights of A and B, and v_A and v_B are atomic diffusion volumes. Equations below exclude diffusion through soil water from the transport formulation since free-water diffusion coefficients are about four orders-of-magnitude less than free-air diffusion coefficients. Aqueous-phase diffusion should be included for moisture contents close to saturation levels.

Analytical solutions for several initial and boundary conditions have been derived (Crank, 1956). The analytical solution for spherical gas-phase diffusion, assuming a point source of mass M_o (M), released at $t = 0$ in a porous medium with uniform and homogenous properties, is:

$$C_v(r,t) = \frac{M_o / \left[\theta_g + \theta_w / H' + Q_b K_d / H'\right]}{8\pi^{3/2} t^{3/2} D_{sorp}^{3/2}} \, e \, \frac{-r^2}{4 D_{sorp} t} \tag{6}$$

$$D_{sorp} = \frac{D_g^{eff}}{\theta_g + \theta_w / H' + \rho_b K_d / H'} \tag{7}$$

where $C_v(r,t)$ is the concentration at any distance r (L) from the point source, and D_{sorp} is the "sorption-corrected" effective diffusion coefficient ($L^2 T^{-1}$). In the case where a small volume of tracer gas is injected at a point source, the measured fraction of the initial mass of tracer recovered (η) at time t_s is set equal to the predicted fraction obtained by integrating equation 6 over a known spherical volume (corresponding to volume of gas withdrawn). This manipulation enables calculation of D_{sorp} using the following equations, which were obtained from Johnson *et al.* (1998):

$$\eta = M(t_s)/M_o = \langle C_v \rangle V_s / C_v^{\circ} V_o \tag{8}$$

$$\eta = erf\left(B^{1/2}\right) - \left(\frac{2B^{1/2}}{\sqrt{\pi}}\right) e^{-B} \tag{9}$$

$$B = \frac{1}{4 D_{sorp} t_s} \left[\frac{3V_s}{4\pi\theta_g}\right]^{2/3} \tag{10}$$

where $M(t_s)$ is the mass recovered, M_o is the mass injected, C_v is the concentration in gas recovered, V_s is the volume of gas recovered, C_v^o is the concentration in gas injected, and V_o is the volume of gas injected. The point source assumption is reasonably approximated for $V_o/V_s <$ 0.1 and $\eta < 0.1$. Using equations 7 and 10, the effective diffusivity can be estimated provided that soil porosity and moisture content are known or can be approximated.

The equation for one-dimensional gas-phase diffusion can also be solved analytically for an initial finite source consisting of radius R_o, assuming that the injected tracer uniformly displaces soil gas (Johnson *et al.*, 1998):

$$Cv(r,t) = \frac{C_v^o}{2}\left\{erf\left[\frac{R_o + r}{2\sqrt{D_{sorp} t}}\right] + erf\left[\frac{R_o - r}{2\sqrt{D_{sorp} t}}\right]\right\} - \frac{C_v^o}{r}\sqrt{\frac{D_{sorp} t}{\pi}}\left\{\exp\left[\frac{-(R_o - r)^2}{4 D_{sorp} t}\right] - \exp\left[\frac{-(R_o + r)^2}{4 D_{sorp} t}\right]\right\} \tag{11}$$

Diffusion characteristics of helium were evaluated for initial concentrations and volumes corresponding to the test conditions used for the push-pull test for both a point and finite source *i.e.*, equations 6 and 11). The results, presented in Figure 3.1, indicate that predicted helium concentrations decrease rapidly with distance from source and time. The comparison of the point and finite source solutions indicates that the differences in concentrations were greatest for short time periods and distances from source. As time increased, the two solutions converged to almost identical concentrations.

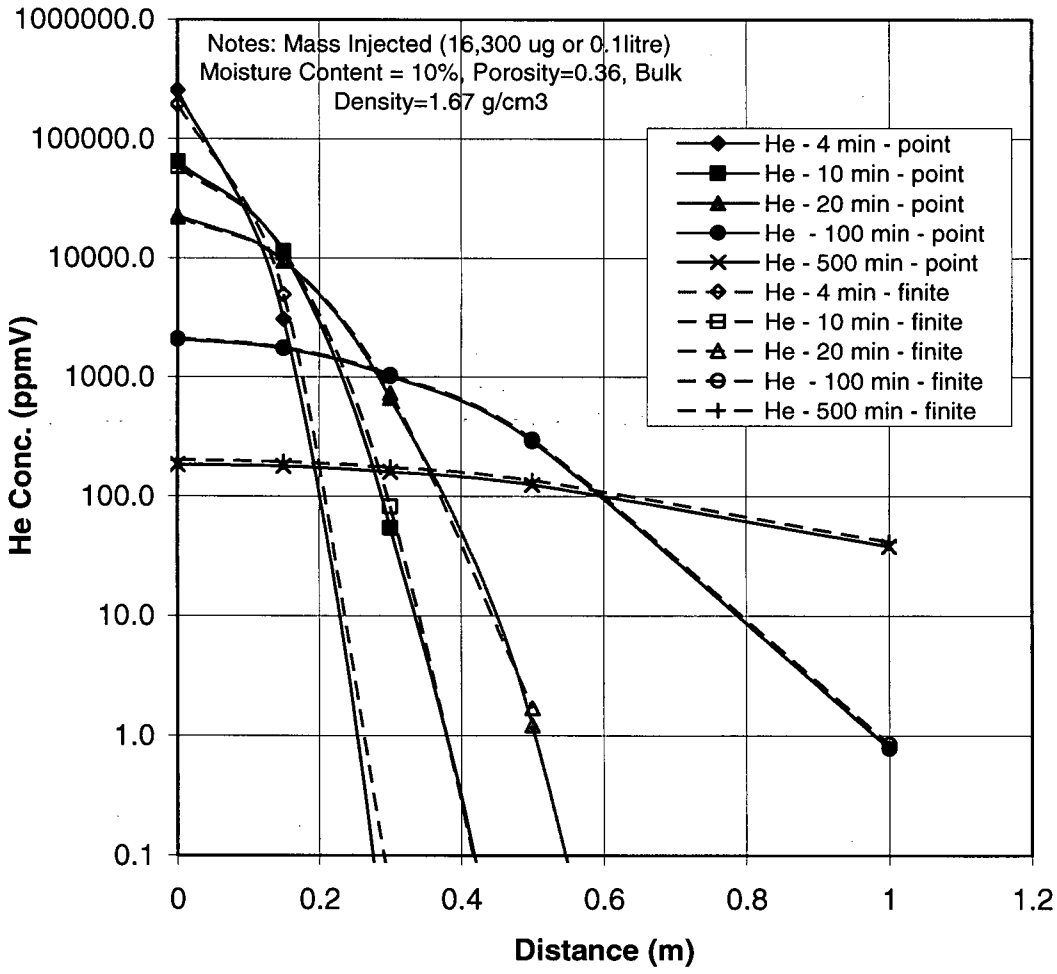

Figure 3.1. Predicted spherical helium diffusion from point and finite source.

Methods

In situ diffusion coefficients were measured at probes designed to collect soil gas samples using a previously published push-pull test protocol with several slight modifications (Johnson *et al.*, 1998). Soil gas probes consisted of 13 mm I.D. hollow-steel probes with an inner 6 mm polyethylene tubing. Once driven to the desired depth, the conical probe tip was rammed a further 10 mm below the bottom of the probe using an inner rod creating a small air cavity.

Helium concentrations were measured using a field portable Mark Products Inc. Model 9822 detector. The Mark 9822 detector uses a thermal conductivity detector with a carbon graphite filter located upstream of the detector. According to the manufacturer, the filter was designed primarily to remove methane and heavier organic compounds. The detector utilizes the contrast in thermal conductivity between nitrogen (N_2) and oxygen (O_2), the primary components in air, and helium which has a much higher thermal conductivity. The thermal conductivities of several gases are provided in Table 3.2.

Table 3.2. Thermal conductivity of selected gases.

Gas	Thermal Conductivity (cal ^{o}C cm^{-3} sec^{-1}))x10^{-6}
Air	60.34
CO_2	37.61
CO	57.86
C_2H_6	47.94
He	352.1
H_2	433.92
O_2	61.58
N_2	60.34

Source: Thermal conductivities are from CRC Handbook of Chemistry and Physics, 66th Ed., CRC Press, 1985-86

Of potential concern is the possible interference of carbon dioxide (CO_2) and other light gases with helium quantification. For example, if CO_2 were to replace O_2 in the gas mixture, helium concentrations would be negatively biased, assuming CO_2 was not filtered out by the carbon graphite.

The manufacturer indicates that no testing has been conducted to determine whether the filter would also remove CO_2. Gas-phase adsorption is affected by several factors including properties of the chemical and adsorbent material. For a non-polar molecule such as CO_2, molecular attraction and adsorption likely occurs primarily through Van der Waals force. The possible effect of carbon dioxide on detector response was theoretically evaluated assuming that CO_2 was not filtered out, and that CO_2 replaced O_2 in the air and helium mixture. Assuming a linear response relative to the thermal conductivities provided in Table 3.2, the hypothetical measured helium detector response is compared to the "true" response (*i.e.*, for a gas mixture excluding CO_2) in Figure 3.2. As shown, relatively significant deviations occur for helium concentrations below about 1%.

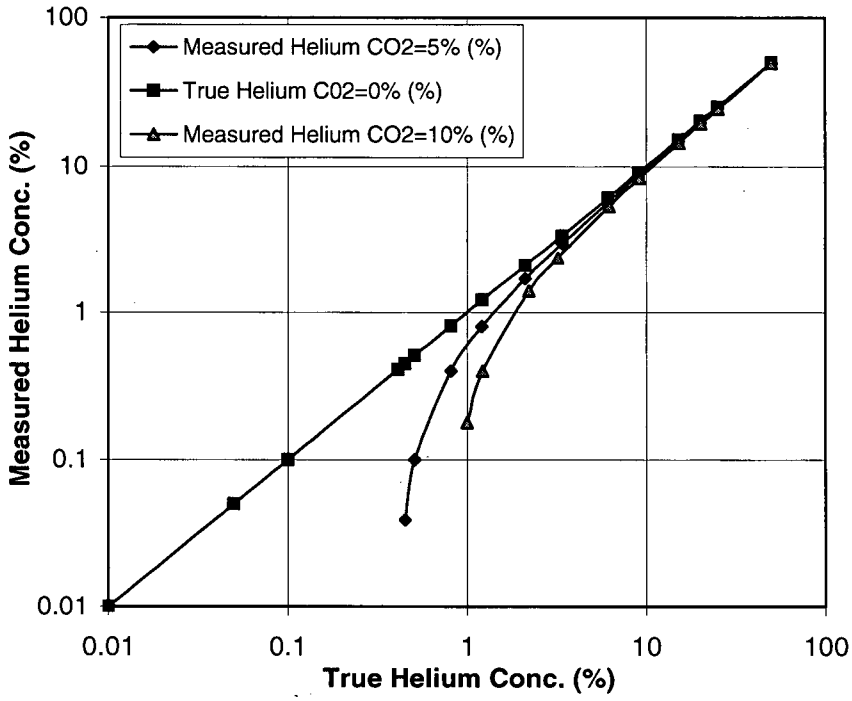

Figure 3.2. Possible helium concentration when CO_2 replaces O_2.

The effect of CO_2 on helium response was further evaluated by comparing measured helium concentrations for a known standard, after calibrating the detector to air, to measured helium concentrations in the same standard after calibrating the detector using soil gas containing elevated CO_2. The results, presented in Table 3.3, indicate that CO_2 may have affected the helium response for these tests. When calibrated using soil gas, the CO_2 concentrations were higher, a result of a decreased detector response for baseline conditions.

Table 3.3. Effect of soil gas containing CO_2 on Mark 9822 helium detector response.

Helium Standard Conc. (Air and He) (%)	**Helium Concentration: Calibrated to Soil Gas** (%)	**Helium Concentration: Calibrated to Air** (%)
1	1.9	0.76
2	3.7	2.3
5	6.6	5.3
20	24	23

Notes: 1) Standard comprised of helium and air.
2) Soil gas comprised of CO_2 = 16.8%, CH_4 = 3.9%, O_2 = 0.5%. Other potential gases (N_2, hydrocarbons) were not quantified.

As indicated below, soil gas near the probe tip was "purged" through injection of air. As a result, CO_2 concentrations were likely low, and therefore no significant effect on helium detector

response was anticipated. Evaluation of the effect of CO_2 on helium detector response should be conducted in cases where CO_2 concentrations are elevated.

The protocol used for the push-pull tests consisted of the following:

1. Purge soil gas in region of soil gas probe tip by injecting a minimum of 15 litres of air.

2. Collect one-litre soil gas sample in one-litre Tedlar™ bag (*i.e.*, "blank") and measure helium concentration. Inject additional air if helium concentration is above instrument detection limit (0.01%).

3. Partially fill an evacuated one-litre Tedlar™ bag with industrial (*i.e.*, welding) grade helium. The helium volume placed into bag should be 0.1 litre plus the volume of the probe. Inject helium into soil.

4. Immediately extract from the same probe a 1-litre soil gas sample into a bag and measure helium concentration.

5. Repeat Steps #1 through #4 except wait for periods of 2, 5, 10 and 15 minutes before withdrawing a soil gas sample.

Purging of soil gas was conducted using an air flow rate of 0.5 to 1 litre min^{-1} while gas injection and extraction was conducted using a flow rate of 0.5 litre min^{-1}. Gas injection and extraction was conducted using calibrated battery-powered air sampling pumps. Each round of tests at a particular depth took approximately two hours to complete.

Before conducting the push-pull tests, the helium detector calibration was checked using standards comprised of air and helium mixtures prepared in Tedlar™ bags. As shown in Figure 3.3, a relatively good comparison was obtained between the measured concentrations and prepared standards. After the initial comprehensive calibration check, instrument response was periodically checked prior to use.

RESULTS

In situ diffusion coefficients were measured at five soil gas probes installed at varying depths below the approximate centre of a research greenhouse constructed at the Chatterton site, and at one nearby probe installed in an open lightly vegetated area (Figure 3.4). Soils at the site consist of a relatively uniform dredged river sand fill with less than 5 percent silt content. During testing, the depth to the water table was approximately 2.5 m below ground surface. Testing was conducted in August 1998 during sunny and warm weather (*i.e.*, daytime high temperatures of 22 to 27°C).

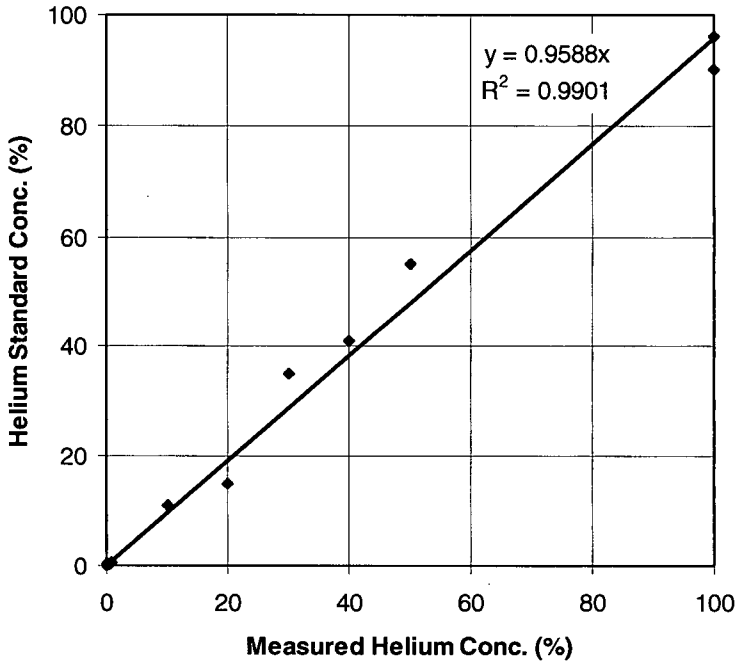

Figure 3.3. Calibration of Mark 9822 helium detector.

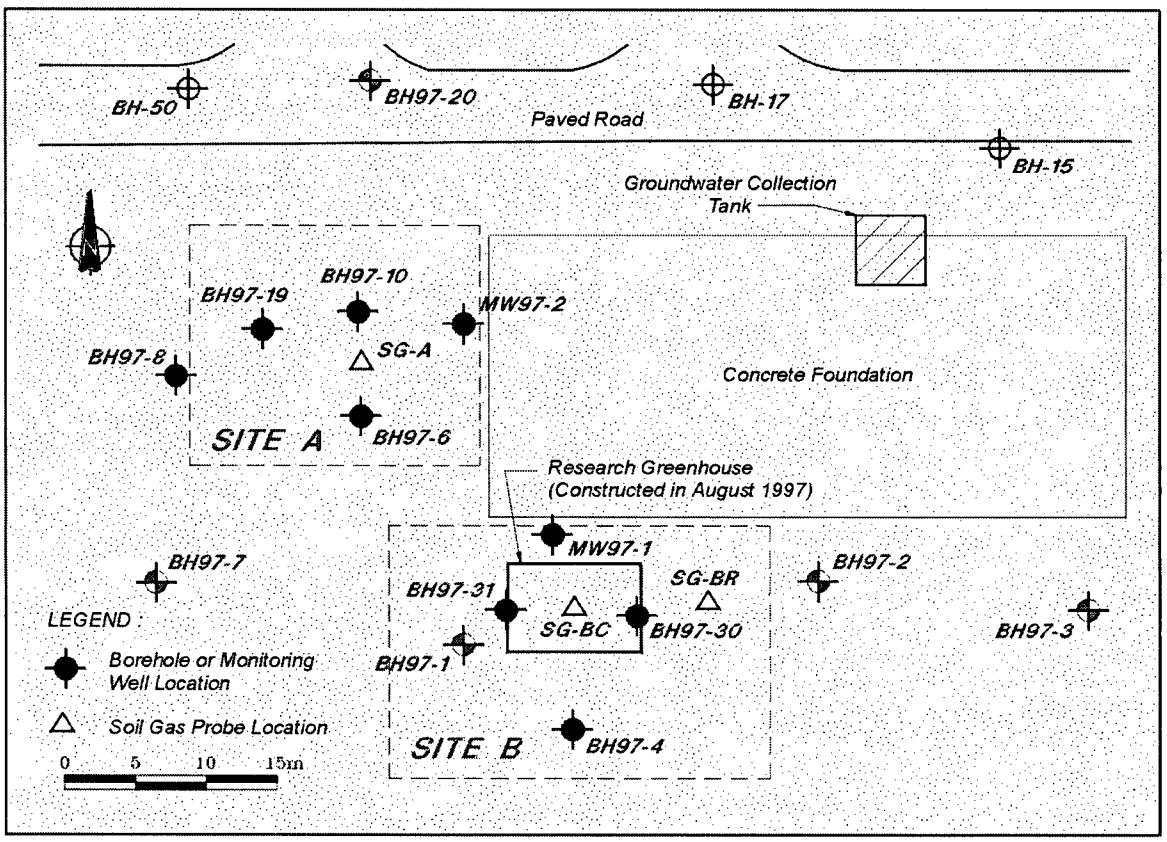

Figure 3.4. Site plan.

The measured mass recovered, effective diffusivity and gas-phase tortuosity factors are presented in Tables 3.4 and 3.5. Tortuosity factors were calculated using equation 3. The elapsed time between injection and extraction (*i.e.*, t in equation 10) was the difference between the mid-points of the extraction and injection time. The moisture contents used to calculate the effective diffusivity were obtained from gravimetric moisture content determinations for several soil cores obtained within 2 m of the soil gas probe clusters. The approximate mean moisture content for each depth based on the data shown in Figure 3.5 was used in the calculations. Based on the range of measured moisture contents, the measurement scale for the diffusion coefficient is a sphere with radius on the order of 9 to 11 cm.

Table 3.4. Measured mass required and beta parameter for push-pull tests.

		Time=1.24 min		Time=3.24 min		Time=6.24 min		Time=11.2 min		Time=16.2 min	
Location	**Depth (m)**	**η**	**β**	**η**	**β**	**η**	**β**	**η**	**β**	**η**	**β**
SG-A	0.60	0.46	1.08	0.24	0.59	0.08	0.25	0.046	0.16	0.031	0.13
SG-BC	0.3	0.30	0.71	0.15	0.40	0.09	0.26	0.029	0.12	0.023	0.10
SG-BC	0.45	0.50	1.18	0.32	0.76	0.24	0.59	0.17	0.44	0.073	0.23
SG-BC	0.58	0.57	1.38	0.46	1.08	0.23	0.57	0.15	0.40	0.086	0.26
SG-BC	0.75	0.96	4.15	0.61	1.51	0.46	1.08	0.30	0.71	0.21	0.52
SG-BC	0.9	0.48	1.13	0.30	0.71	0.16	0.42	0.11	0.31	-	-

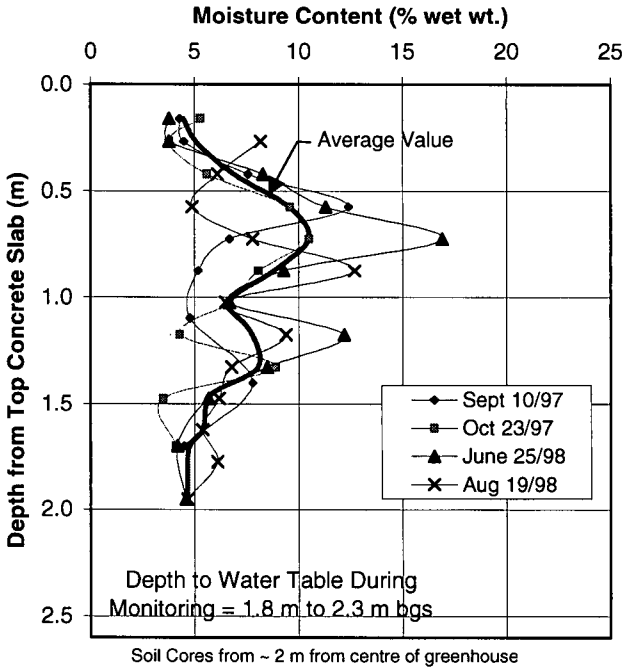

Figure 3.5. Moisture content below building.

Table 3.5. Measured *in situ* effective diffusion coefficients based on push-pull tests.[1]

Location	Depth	MC	τ_g	Measured Eff. Diffusivity - Varying Extraction Times					Mean[2] Effective Diffusivity	Mean Measured Tortuosity Factor	Predicted Tortuosity Factor[4] (M&Q, '61)
				Time= 1.24 min	Time= 3.24 min	Time= 6.24 min	Time= 11.2 min	Time= 16.2 min			
	(m)	(% wt.)		(cm^2sec^{-1})	(cm^2sec^{-1})	(cm^2sec^{-1})	(cm^2sec^{-1})	(cm^2sec^{-1})	(cm^2sec^{-1})		
SG-A	0.60	6.9	0.24	0.075	0.053	0.063	0.056	0.049	0.055	0.17	0.069
SG-BC	0.3	5	0.27	0.12	0.081	0.064	0.078	0.063	0.071	0.22	0.10
SG-BC	0.45	8	0.22	0.067	0.040	0.027	0.020	0.026	0.028	0.085	0.053
SG-BC	0.58	10	0.19	0.054	0.027	0.026	0.021	0.022	0.024	0.072	0.031
SG-BC	0.75	12	0.16	0.017	0.018	0.013	0.011	0.010	0.013	0.039	0.016
SG-BC	0.9	7	0.24	0.072	0.043	0.038	0.028	-	0.037	0.11	0.067

[1] Physical/chemical properties for Helium: $D_{air} = 0.33\ cm^2sec^{-1}$, H (dimensionless) = 121; $K_d = 0.002$

[2] Arithmetic mean based on results for time equal to 3.24, 6.24, 11.2 and 16.2 minutes

[3] MC = moisture content, MC are approximate values based on data in Figure 3.5, total porosity = 0.356.

4 Predicted tortuosity factor based on Millington and Quirk relationship.

The measured effective diffusivities for each depth were relatively consistent for elapsed extraction times equal to or greater than 3.24 minutes. The effective diffusivity for the 1.24 minute test was generally higher than those for longer times possibly due to experimentally inaccuracies compounded by the short duration over which the test was conducted, and deviations from the point source assumption incorporated in the analytical solution to the gas diffusion equation. The test precision for extraction times equal to or greater than 3.24 minutes, as characterized by the relative standard deviation (RSD), was on the order of 20%.

As expected, the effective diffusion coefficients decreased with increasing moisture. In addition, a good comparison was obtained between the measured gas-phase tortuosity factor and that predicted using the Millington and Quirk relationship with measured tortuosity factors consistently about twice the predicted values.

SENSITIVITY ANALYSES

A sensitivity analysis was conducted for key input parameters by individual varying inputs while keeping remaining parameters constant. The baseline values were η equal to 0.1, t_s equal to 500 seconds, ϕ_g equal to 0.19, H' equal to 121, and K_d equal to 0.002. The input values were varied +/- 40% of the baseline values. The results, presented in Figure 3.6, indicate that the diffusion coefficient is most sensitive to time, followed by fraction of mass recovered. The results were relatively insensitive to gas-filled porosity for the input values chosen with a 40% variation in gas-filled porosity resulting in only a 25% variation in the effective diffusion coefficient. The relatively low sensitivity of effective diffusion coefficient to variation in gas-filled porosity for the push-pull test enables a reasonably accurate effective diffusion coefficient to be estimated even when direct moisture content measurements are not available (Johnson *et al.*, 1998).

CONCLUSIONS

Vadose zone *in situ* diffusion coefficients were measured at the Chatterton research site using a push-pull test and helium tracer. The test is relatively simple to perform, utilizes relatively inexpensive materials and equipment, and requires only a few hours to complete each series of tests. Appropriate pre-cautions and care must be taken during the test to account for possible effects of soil gas on detector response (*i.e.*, through purging or calibration), and gas volumes and time must be measured as accurately as possible.

In situ diffusion coefficients were obtained using an analytical solution for spherical diffusion from a point source, assuming instantaneous injection of the tracer. The results of several push-pull tests conducted at the Chatterton research site indicate that measured effective diffusivity coefficients in sand ranged from about 0.01 to 0.07 cm^2sec^{-1}. A good comparison was obtained between the measured gas-phase tortuosity factor and that predicted using the Millington and Quirk relationship (*i.e.*, $\tau_g = \phi_g^{10/3}/\phi^2$) with measured tortuosity factors consistently about twice the predicted values. The results indicate the Millington and Quirk relationship, which is commonly used to account for tortuosity, is appropriate over the range of moisture contents evaluated.

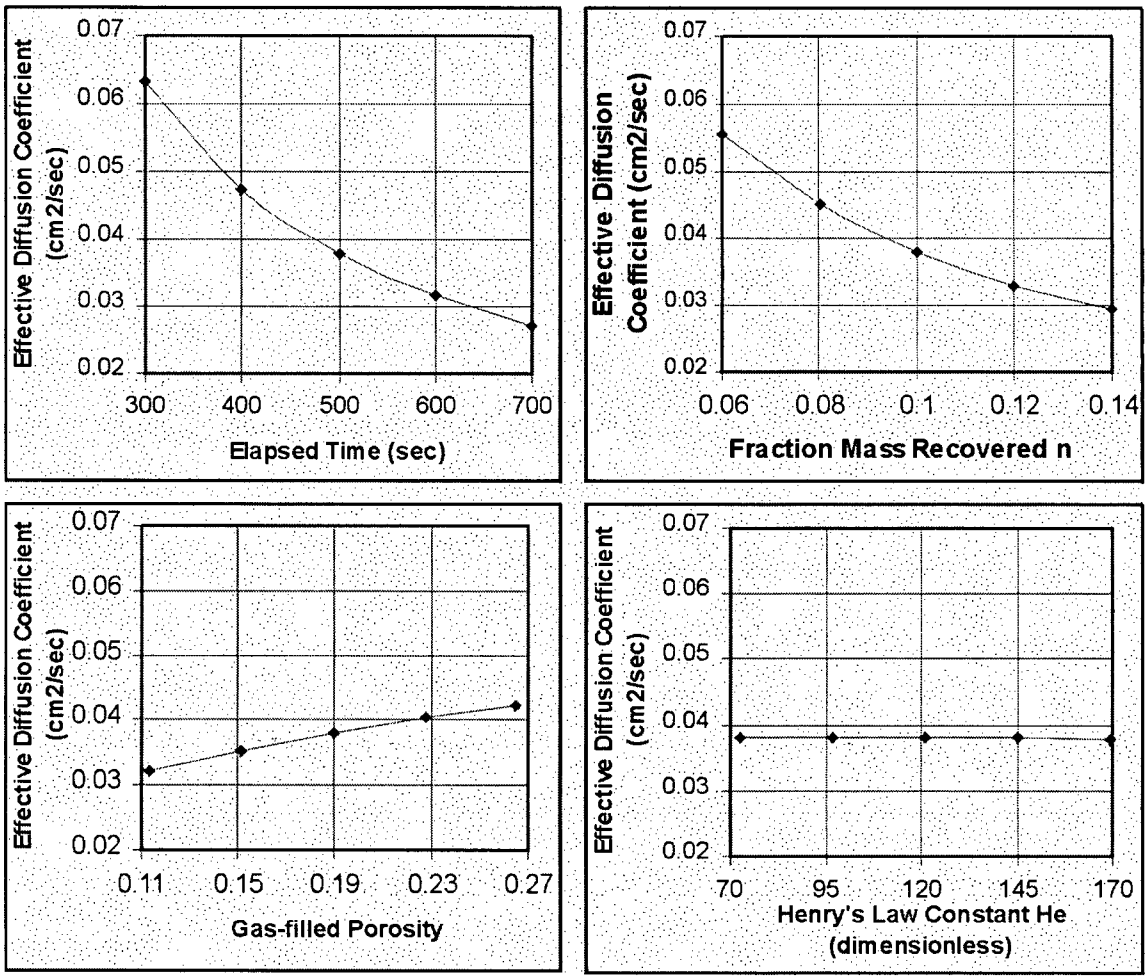

Figure 3:6. Sensitivity analysis for effective diffusion coefficient (based on equations 7 and 10).

Measurement of *in situ* diffusion coefficient may be warranted in cases where accurate estimates of diffusion coefficient are required for risk assessment purposes, or when evaluating vadose zone natural attenuation (*e.g.*, biodegradation rates). In this context, they represent a valuable component of the research currently being conducted to evaluate the soil gas transport to air pathway at the Chatterton site. While further comparisons need to be conducted for various moisture contents and different soil types, the results of this study suggest that use of the Millington and Quirk empirical relationship may be reasonable in many situations, in light of the experimental accuracy of the push-pull test and relative effect of other factors affecting VOC fate and transport.

REFERENCES

American Society for Testing and Materials (ASTM). 1995. Standard Guide for Risk-Based Corrective Action Applied at Petroleum Release Sites, E1739-95.

Batterman, S. 1995. Hydrocarbon vapour transport in low moisture soils. *Environmental Science and Technology*, 29(1): 171-180.

Crank, J. 1956. The mathematics of diffusion. Oxford Clarendon Press.

Currie, J.A. 1970. Sorption and transport processes. *SCI Monogr.* 27: 152-171.

Fuller, E.N., P.D. Schettler, and J.C. Giddings. 1966. *Ind. Eng. Chem.* 58(5): 18.

Jellick, G.J. and R.R. Schabel. 1986. Evaluation of a field method for determining the gas diffusion coefficient in soils. *Soil Sci. Soc. Am. J,* Vol. 50.

Johnson, P.C., C. Bruce, R.L. Johnson, and M.W. Kemblowski. 1998. In situ measurement of effective vapour-phase porous media diffusion coefficients. *Accepted for Publication, Environ. Sci Technol.*

Lahvis, M.A. and A.L. Baehr. 1996. Estimation of rates of aerobic hydrocarbon biodegradation by simulation of gas transport in the unsaturated zone. *Water Resources Research.* 32(7): 2231-2249, July.

Lai, S., J.M. Tiedje, and E. Erickson. 1976. In situ measurements of gas diffusion coefficients in soils. *Soil. Sci. Soc. Amer. J,*. 40.

Lin, T. 1994. Transport and sorption of volatile organic compounds and water vapour within dry soil drains. E*nvironmental Science and Technology.* 28: 322-330.

Lowell, P.S. and B.E. Eklund. 2004. VOC Emission Fluxes as a Function of Lateral Distance from the Source. *Environmental Progress*, 25 (1): 52-58.

Millington, R.J. and J.M. Quirk. 1961. Permeability of porous solids. *Trans. Farady Soc:*, 1200-1207.

Penman, H.L. 1940. Gas and vapour movements in the soil. I. The diffusion of vapours through porous solids. *J. Agric. Sci. (Cambridge),* 30:437-462.

Roltson, D.E. and B.D. Brown. 1977. Measurement of soil gaseous diffusion coefficients by a transient-site methods with time-dependent surface condition. *Soil Sc. Soc. Am. J.* 41.

Thorstenson, D.C., and D.W. Pollock. 1989. Gas transport in unsaturated porous media: The adequacy of Fick's Law. *Review of Geophysics.* 27(1), February.

CHAPTER 4

EVALUATION OF VADOSE ZONE BIODEGRADATION OF BTX VAPOURS

This chapter was published in *J. of Contaminant Hydrogeology*. 46:233-264. 2000.[3]

ABSTRACT

Soil vapour transport to indoor air is an important potential exposure pathway at many sites impacted by subsurface volatile organic compounds (VOCs). The inclusion of biodegradation in vadose zone transport models for benzene, toluene and xylene (BTX) and fuel hydrocarbons has been proposed; however, there is still significant uncertainty regarding biodegradation rates, and the local effects of buildings or ground surface cover on fate and transport processes. The objective of this study was to evaluate biodegradation processes through comprehensive monitoring at a site contaminated with BTX and model simulation. Study methods included extensive vertical profiling of BTX vapour and light gas (oxygen and carbon dioxide) concentrations and moisture content, and semi-continuous monitoring of oxygen and pressure below a building floor slab. Significant vadose zone biodegradation over a relatively small depth interval was observed. Based on the observed soil vapour profile, first-order biodegradation rates were estimated by fitting an analytical solution for diffusion and biodecay to the data. Degradation rates were found to compare well to other reported laboratory and field data. A two-dimensional numerical model incorporating vapour-phase diffusion, advection, sorption and biodegradation was used to simulate the effect of a building floor slab on transport processes. Model results demonstrate the sensitivity of vapour-phase BTX and oxygen transport to partial barriers to diffusion (e.g., building foundation) and highlight the importance of using a model that ties biodecay to oxygen availability. In addition, depressurization within a building and advective transport are shown to have a potentially significant effect on BTX fate in soil below the building.

KEY WORDS: soil vapour, diffusion, biodegradation, first-order decay, numerical model, BTX

[3] Hers, I., Atwater, J., Li, L. and Zapf-Gilje, R.

INTRODUCTION

Soil vapour transport to indoor air is an important exposure pathway at many sites impacted by volatile organic compounds (VOCs). Relatively simple screening-level models are often used to quantify potential exposure and risk (ASTM, 1995); however, there is significant uncertainty surrounding processes and factors affecting this pathway, and the accuracy of models used. To address this limitation, a comprehensive field-based research program is being conducted at a former petro-chemical plant site impacted by benzene, toluene and m&p-xylene (BTX) releases, located near Vancouver, B.C. ("Chatterton" research site). As shown in this paper, monitoring at the Chatterton site indicates that intrinsic biodegradation is an important vadose zone process.

Evidence for vadose zone biodegradation of BTX or fuel hydrocarbons has been seen at a limited number of field sites (e.g., Ostendorf and Kampbell, 1991; Ririe and Sweeney, 1995; Franzmann *et al.*, 1999). Several analytical models for hydrocarbon vapour transport that include biodegradation have been proposed. These include a model incorporating vapour-phase and aqueous-phase diffusion and aqueous-phase advection, subject to sorption and first-order decay (Jury *et al.*, 1990), and a model for steady-state vapour-phase diffusion, subject to first-order decay (Johnson *et al.*, 1988; DeVaull *et al.*, 2002). Incorporating biodecay in models simulating soil vapour transport to indoor air, in some instances, reduces predicted exposure concentrations by several orders-of-magnitude. Therefore, sound evaluation of biodegradation potential is essential.

There remains considerable uncertainty in terms of vadose zone biodegradation rates for organic chemicals. There are only a few comprehensive field-based assessments of biodegradation potential for petroleum hydrocarbons. Further, there has been little direct evaluation of the local effect of a building or ground surface cover on soil gas transport and rates of hydrocarbon vapour biodegradation. The focus of this work is to evaluate BTX biodegradation processes and rates through comprehensive analysis of field data combined with model simulation, in the context of the exposure pathway of soil vapour transport to indoor air. The objective is to gain new insight on biodegradation processes and kinetics, and to contribute to improved modeling methods. The paper is presented in three parts; (i) overview of intrinsic biodegradation processes, kinetics and case studies, (ii) presentation of monitoring data from the Chatterton site and derivation of field biodegradation rates, and (iii) description of a numerical model developed for this project and comparison of model-predicted to measured soil vapour transport.

INTRINSIC BIODEGRADATION

Processes and Effect of Building

Diffusion, sorption and biodegradation, for non-recalcitrant VOCs, are generally thought to have the most significant effect on VOC fate and transport within the vadose zone. Biodegradation is an important natural attenuation mechanism since it is the only process whereby there is a reduction in total hydrocarbon mass. More than 200 species of bacteria, yeast and fungi capable of degrading petroleum hydrocarbons have been identified, with *Pseudomonas spp.* and *Corynebacterium spp.* thought to be two major bacterial agents (Fan and Krishnamurthy, 1995). Aerobic biodegradation of petroleum hydrocarbons will occur in the vadose zone providing there is sufficient O_2, indigenous microbes that produce enzymes capable

of degrading the compound of interest, soil moisture, nutrients, and appropriate pH, temperature and salinity conditions, and no inhibiting materials. DeVaull (1997) suggests that O_2 levels above 4 percent (as gas) and 1 to 2 mg/L nitrate (as nitrogen in pore water) will sustain aerobic biodegradation. Anoxic and/or anaerobic biodegradation can also potentially occur in the vadose zone depending on types of electron acceptors present, pH conditions and oxidation-reduction potential.

Conceptually, there are several ways in which a building (or other similar surface barrier) could affect intrinsic biodegradation. For aerobic degradation of VOCs, the ability of O_2 to diffuse, or be transported through advection to below the building is of critical importance. Oxygen replenishment will be a function of the diffusivity and permeability of near surface soils and the subsurface building structure, and gradients driving these processes. Advective transport of soil gas through shallow soil can occur as a result of changes in atmospheric pressure and temperature gradients (Massman and Farrier, 1992).

A building or other low permeability structure will also eliminate surface water infiltration below the structure footprint and potentially promote long-term drying of the soil. While there is little direct study of the effect of soil moisture on intrinsic biodegradation, bioventing studies suggest that biodegradation rates are significantly reduced for low moisture contents (Zwick *et al.*, 1995). A laboratory study indicated that biodegradation of toluene by *Pseudomonas putida* was affected by matric potential with about 35 to 60 % reduction in cell growth and first-order biodegradation rate when the matric suction was increased from 0 to 1.5 MPa (Holden *et al.*, 1997). The permanent wilting point is the soil moisture content at a matric suction of about 1.5 MPa.

Biodegradation Models and Kinetics

Biodegradation kinetics for petroleum hydrocarbons can be simulated using several models including (i) first-order or zero-order decay models, (ii) models based on Monod-kinetics, and (iii) instantaneous reaction models.

A first-order (*i.e.*, exponential) decay model can be represented as follows:

$$dS/dt = k\,S \qquad t_{1/2} = ln\,(2)\,/\,k \tag{1}$$

where S is the substrate concentration ($M\,L^{-3}$), k is the first-order rate constant (T^{-1}), and $t_{1/2}$ is the half-life (T). A first-order decay constant assumes that both the O_2 and hydrocarbon-degrading microbes are available in excess, and that only the hydrocarbon substrate is rate limiting. A zero-order model assumes a constant biodegradation rate, and that the O_2 and/or hydrocarbon-degrading microbes are rate-limiting.

In some cases, kinetics based on equations proposed by Monod (1949) provide for a more accurate representation of biodegradation. The Monod model describes the growth of a pure culture of microorganisms suspended in liquid through the utilization of a single rate-limiting substrate (Bekins *et al.*, 1998). One simplified expression ("Monod-no-growth") given by Simpkins and Alexander (1984) is:

$$dS/dt = k_1\,S\,/\,(K_S + S) \qquad k_1 = u_{max}\,B\,/\,Y \tag{2}$$

where k_1 is the substrate utilization rate ($ML^{-3}T^{-1}$), K_S is the half-saturation constant or hydrocarbon concentration at which the biodegradation rate is half its maximum value (ML^{-3}), u_{max} is the maximum specific growth rate of the biomass (T^{-1}), B is the biomass concentration (ML^{-3}), and Y is the biomass yield (M *biomass* M^{-1} *substrate*). When hydrocarbon substrate concentrations are high (*i.e.*, $S >> K_S$), equation 2 approximates a zero-order expression. Conversely, when hydrocarbon substrate concentrations are low (*i.e*,. $S<<K_S$), equation 2 approximates a first-order expression. A dual-Monod equation can be used to represent substrate utilization as a function of both biomass concentration and electron acceptor concentration (Kissel, 1985). The dual-Monod equation can be expressed as:

$$dS/dt = k_1 S / (K_S + S) (A / (K_A + A)) \quad (3)$$

where A is the concentration of the electron acceptor ($M\ L^{-3}$) and K_A is the electron acceptor concentration at which the utilization rate is half the maximum ($M\ L^{-3}$). Coupled transport equations for the primary substrate and electron acceptor can be linked through the Monod expressions and stochiometric ratio of the electron acceptor to substrate consumed (MacQuarrie *et al.*, 1990). A practical disadvantage of the Monod-kinetics model is that input parameters can be difficult to obtain.

The instantaneous-reaction model couples hydrocarbon vapour transport with O_2 or alternative electron acceptor concentrations. Two factors that control the biodegradation rate for the instantaneous-reaction model are: (i) the electron acceptor utilization factor for hydrocarbon mineralization (estimated from stochiometric relationships), and (ii) the electron acceptor transport rate from source areas and mixing with the hydrocarbon-impacted soil vapour. Additional considerations for biodegradation modeling are multi-component effects and appropriate use of reaction models where there is competing utilization of O_2.

Evaluation of Biodegradation Potential

Multiple lines of evidence should be considered when evaluating vadose zone intrinsic biodegradation, as typically conducted for dissolved hydrocarbon fate in groundwater. Lines of evidence include: (i) field measurements indicating that hydrocarbon vapour concentrations are being attenuated beyond levels that would be expected for other non-destructive mechanisms, (ii) geochemical data showing the depletion of electron acceptors and generation of metabolic by-products, and (iii) laboratory studies (*e.g.*, microcosm, column studies).

BTEX Attenuation

There have been several field studies where vertical profiling has enabled evaluation of BTEX attenuation. Fischer *et al.* (1996) reported that hydrocarbon vapour concentrations below an at-grade building decreased sharply over a small vertical interval (0.1 to 0.7 m depth). The authors suggested that a partial physical barrier to vertical transport (*i.e.*, high moisture content zone) in combination with biodegradation accounted for the steep gradient. Contrasting results were presented by Laubacher *et al.* (1997) where vapour profiling was performed below and adjacent to a house with a basement. Testing directly below the basement floor slab indicated elevated BTEX vapour concentrations and low O_2 concentrations (less than one percent). In contrast, BTEX vapour concentrations adjacent to the house (*i.e.*, at the same depth) were two

orders-of-magnitude lower, and O_2 levels were about 14 percent. The Laubacher *et al.* (1997) study is significant since it suggests that hydrocarbon vapour can accumulate below a building.

Several studies have involved monitoring at sites not covered by buildings. Ririe and Sweeney (1995) present data showing that BTEX vapour concentrations decreased sharply with decreasing depth. Complimentary geochemical data was obtained to demonstrate biodegradation was occurring. Ostendorf and Kampbell (1991) present similar data for a site contaminated with aviation fuel and derive kinetic biodegradation rate constants using a coupled diffusive hydrocarbon and O_2 transport model calibrated using field data.

Geochemical Indicators

Geochemical data are often good indicators of biodecay. A simplified vadose zone biogeochemical model is presented in Figure 4.1. For each process, the main reactants and final metabolic end products are shown. Aerobic biodegradation or oxidation of hydrocarbons will result in the consumption of O_2 and generation of CO_2. Oxygen concentrations in hydrocarbon source zones are generally below 1 to 2 % (Jeng *et al.*, 1996; Ririe and Sweeney, 1995; Li, 1995). While there is ample evidence for aerobic processes, anoxic and anaerobic processes are not as well understood. Hydrogen gas has been measured near the interface between the oxic and anoxic zones at hydrocarbon-contaminated sites (Ririe and Sweeney, 1995). Hydrogen gas may form through the breakdown of volatile fatty acids (VFAs), and in turn may be oxidized in the sub-oxic zone by knall-gas bacteria (Burlage *et al.*, 1998). Hydrocarbon mineralization through denitrifying, sulphate-reducing or iron-reducing bacteria could also occur, although there is little, if any, field data to verify this process for the vadose zone. Under anaerobic conditions, the generation of methane through methanogenesis could also result, as documented for groundwater studies (Wiedemeier *et al.*, 1995).

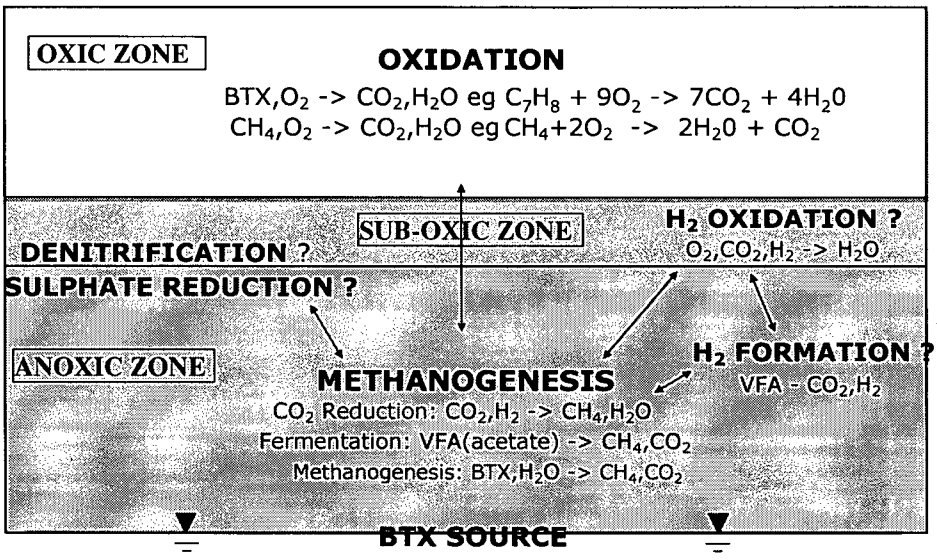

Figure 4.1. Simplified vadose zone biogeochemical model
(VFA=Volatile fatty acids)

The interpretation of geochemical data can be problematic in that there are natural sources of CO_2 and methane. Natural sources of CO_2 include organic matter, plant root respiration and marine carbonates. Natural sources of methane include biogenic generation through fermentation of acetate and thermogenic sources. Several researchers have proposed the use of stable isotope ratios for carbon and radiocarbon (^{14}C) content of metabolic endproducts to evaluate the source of these gases (Van der Velde *et al.*, 1995).

Laboratory Studies

DeVaull *et al.* (1997) present a detailed analysis of BTEX biodegradation rate constants based on a review of seven laboratory studies and one field study designed to simulate unsaturated soil conditions. Significant variability in first-order rate constants was observed; for example, k based on aqueous concentrations ranged from 0.002 to 35 hr^{-1}. The use of Monod-type kinetics (equation 2) provided an improved fit to the experimental data (k_1 = 0.9 mg/L-hr, K_S = 0.2 mg/L) suggesting that a first-order model is inappropriate when hydrocarbon concentrations increase beyond a certain point. Bekins *et al.* (1998) concluded that when toluene concentrations exceed K_s, it may be better to use a zero-order, as opposed to first-order rate expression to model intrinsic biodegradation.

As described by DeVaull *et al.* (1997), insight into biodegradation kinetics can be gained by considering O_2 saturation limits in water, and diffusion rate limitations for micro-scale transfer of dissolved O_2 through the cell walls of hydrocarbon-degrading bacteria. To further evaluate the effect of O_2 limitations, the use of a qualitative indicator termed biodegradation capacity (*BC*, dimensionless) is proposed and is defined as:

$$BC = DO / (SR * S) \quad (4)$$

where *DO* is the dissolved O_2 concentration in soil water ($M\ L^{-3}$), and *SR* is the stochiometric ratio for complete mineralization (by use of O_2) of hydrocarbon to CO_2 and water ($M\text{-}O_2\ M\text{-}hydrocarbon^{-1}$). When hydrocarbon concentrations are sufficiently low, the available O_2 will be high relative to consumptive requirements. As hydrocarbon concentrations increase, *BC* will decrease with rate limitations becoming more important as *BC* approaches unity. An example calculation is provided below for a single-chemical substrate consisting of benzene, which has a *SR* of about 3 mg-O_2/mg-benzene. Equilibrium partitioning between phases and a temperature of 20°C yields a DO concentration of about 8 mg/L in soil moisture, in equilibrium with approximately 20 % O_2 by volume in soil gas. The benzene concentration in soil water, corresponding to a *BC* equal to unity, is about 2.7 mg/L (concentration in vapour is 0.48 mg/L). This calculation suggests that first-order biodegradation kinetics may not be applicable for BTEX concentrations in excess of a few milligrams per litre since O_2 is no longer available in excess relative to the hydrocarbon concentrations.

FIELD STUDY

Overview

Biodegradation processes were evaluated through a comprehensive multi-year testing program conducted at the Chatterton research site. The testing scope has included baseline analyses of soil samples, soil gas monitoring below and adjacent to a building (greenhouse),

semi-continuous monitoring of O_2 and pressure below the building slab, monitoring of environmental conditions (*e.g.*, temperature, barometric pressure) and *in situ* respiration tests. Pertinent methods and results are described below with additional information provided in Hers and Zapf-Gilje (1998).

Site Description

The former Chatterton petrochemical plant is located in Delta, B.C. Near-surface soil in the plant area consists of fill (about 3.5 m thick) underlain by native silt. In most areas, the fill consists of a thin surface layer up to 0.3 m thick consisting of sandy silt to fine sand with trace organic matter, underlain by dredged river sand. The surface unit is henceforth referred to as the "crust". The depth to the water table generally ranges from 1.5 to 2.5 m below ground surface. Releases of BTX from sources removed from the study site and lateral migration on the water table have resulted in an extensive zone of residual non-aqueous phase liquid (NAPL). The NAPL is distributed vertically over an approximate 1 m interval, which corresponds to the approximate water table fluctuation. No other hydrocarbon compounds are present at the plant site. Some testing at a nearby non-contaminated reference site with similar soils was also conducted for comparative purposes. Average annual precipitation at a nearby weather station (*i.e.*, 7 km from site), considered to approximate site conditions, is 1240 mm (Richmond Nature Park).

Methods

Continuous soil cores were initially obtained in March 1997 from 12 boreholes drilled using a Geoprobe™ sampler (Figure 4.2). Multiple soil samples from each borehole, obtained at 0.15 to 0.3 m intervals, were generally analyzed for BTX, grain size, moisture content, porosity and soil organic matter (SOM). Soil samples from the BTX contaminated area and from the reference site were also analyzed for various species of nitrogen (nitrate, nitrite, and total Kjeldahl nitrogen (TKN)) and sulphur. Soil samples representing a broad range of BTX concentrations were enumerated for total heterotrophic bacteria (THB) and BTX-degrading bacteria (BTXB) using the most-probable number (MPN) method (Haines *et al*, 1996).

A small building (greenhouse) was subsequently constructed for research purposes in August 1997 (Figure 4.2). The building was fastened to a 6.1 by 9.3 m at-grade concrete slab of 125 mm nominal thickness. The slab was constructed with a 2-mm wide crack located approximately 0.5 m from the edge of the slab. Steel inserts were subsequently used to vary the open area of the edge crack. The crust below the building was replaced with sand fill and the foundation slab during construction.

Multiple soil gas monitoring events, and testing of soil moisture content was conducted between March 1997 and February 1999 to assess the effect of seasonal changes on soil vapour fate and transport (Figure 4.3). Soil gas probes consisted of either 6.25 mm or 12.5 mm internal diameter hollow steel rods with 50 mm long perforated or slotted tips driven to the desired depth. Multiple soil gas probes were installed at 0.15 to 0.3 m intervals below the approximate centre of the building and adjacent to the building. Soil gas samples obtained for BTX analyses were collected using gas-tight glass and Teflon syringes while gas samples obtained for light gas

analyses (O_2, CO_2 and CH_4) were collected using syringes or 500 ml TedlarTM bags. Samples were analyzed for BTX using a SRI 8610 gas chromatograph with photoionization detector (GC/PID). The GC/PID capillary column was a DB-624 30 m by 0.53 mm column with a methylated phenoxy stationary phase (1.8 μm thickness). Samples were analyzed for light gases using a HP 5880 GC with thermal conductivity or flame ionization detector (TCD or FID), or using a Landtec Control Technologies GA-90 field portable gas detector. One of two capillary columns were used for the GC/TCD consisting of a (i) HP Plot molecular sieve 5A 30 m by 0.53 mm column or (ii) JW GSQ 30 m by 0.53 mm column.

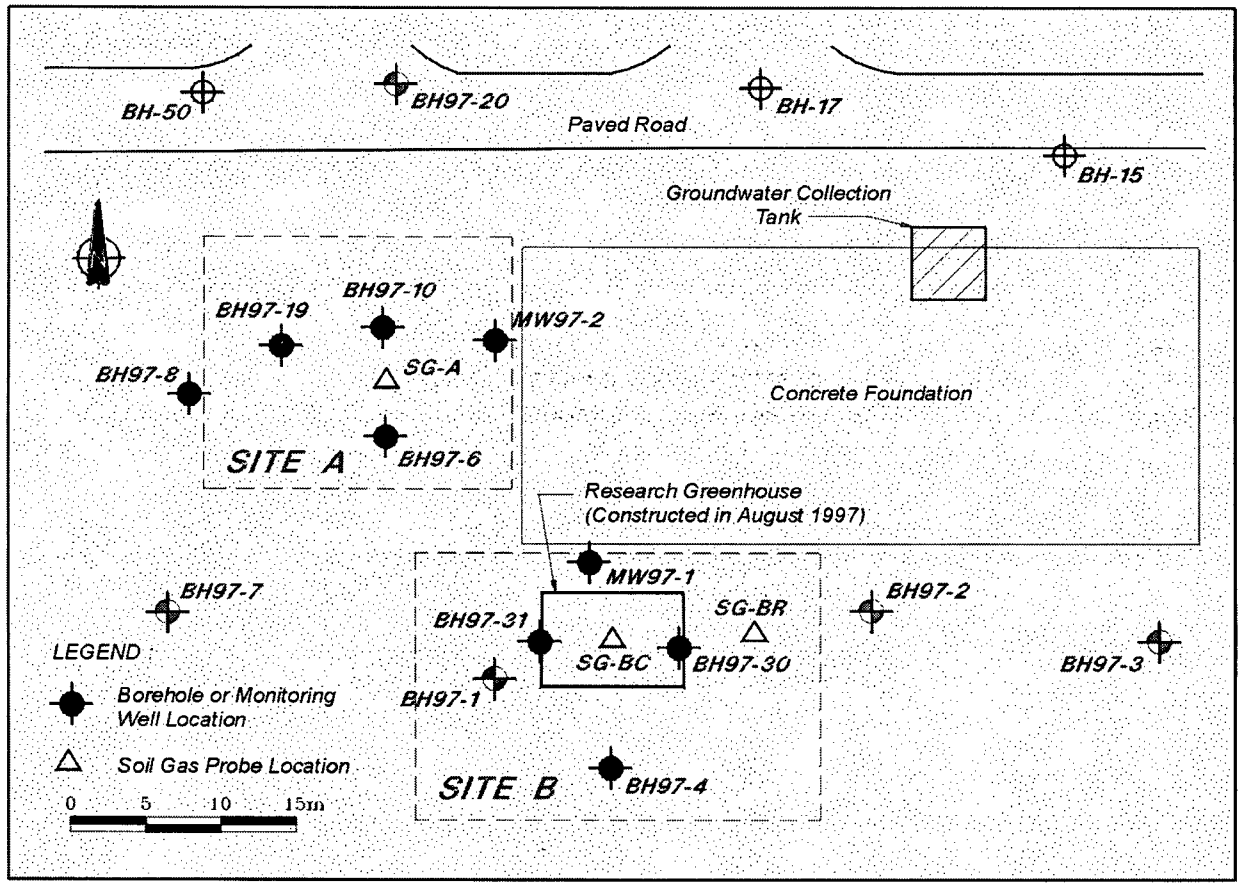

Figure 4.2. Site plan.

A Datawrite Research Co. Model XT252 electrochemical cell and datalogger was used to measure O_2 concentrations below the building slab near location SG-BC (Figure 4.2). Differential pressures between the building, atmosphere and various soil gas probes (*i.e.*, representative of soil pressures adjacent to probe openings) were measured using Setra Systems Model 264 differential pressure transducers with a full-scale range of 63 Pa, and accuracy equal to approximately 1 percent of the full-scale range.

To further investigate biodegradation processes, an *in situ* respiration test was conducted north of the building at probe cluster SG-A (Figure 4.2, Appendix VII). The test was conducted by injecting air with helium tracer over a 24-hour period (U.S. EPA, 1995). After injection was stopped, the O_2, CO_2 and helium concentrations were monitored over multiple depth levels for a

monitored over multiple depth levels for a two-day period. Helium concentrations remained relatively constant indicating O_2 depletion was likely due to biological processes, as opposed to O_2 transport away from the test location.

Baseline Soil Testing Results

Elevated BTX concentrations, indicative of residual NAPL, were measured below 1.4 to 1.5 m depth below ground surface. The residual NAPL layer is at least 1 m thick, and at least 0.5 m was exposed above the water table during the testing program. Above 1.4 to 1.5 m depth, the BTX concentrations in soil decreased sharply.

The medium sand fill is relatively uniform with a silt (less than 0.074 mm, U.S.S classification) content ranging from 1.7 to 5.5 % for samples composited over 0.15 m intervals. Visual examination of continuous soil cores indicated a thin silty fine sand layer (*i.e.*, few millimeters thick) at about 0.92 m depth near vapour probes (SG-BR) adjacent to the building (Figure 4.2). Multiple cores indicate that this fine layer is locally continuous on the scale of a few meters, but was not observed below the building. The fine layer has implications for BTX vapour transport as discussed in the modeling section of this paper. Soil moisture contents below the building were at moderate levels and correspond to residual saturations (relative to soil pore volume) between 25 and 58 % (Figure 4.3). On average, moisture contents below the building appear to be highest between about 0.6 and 0.9 m depth. Greater variability in soil moisture content is observed in boreholes adjacent to the building.

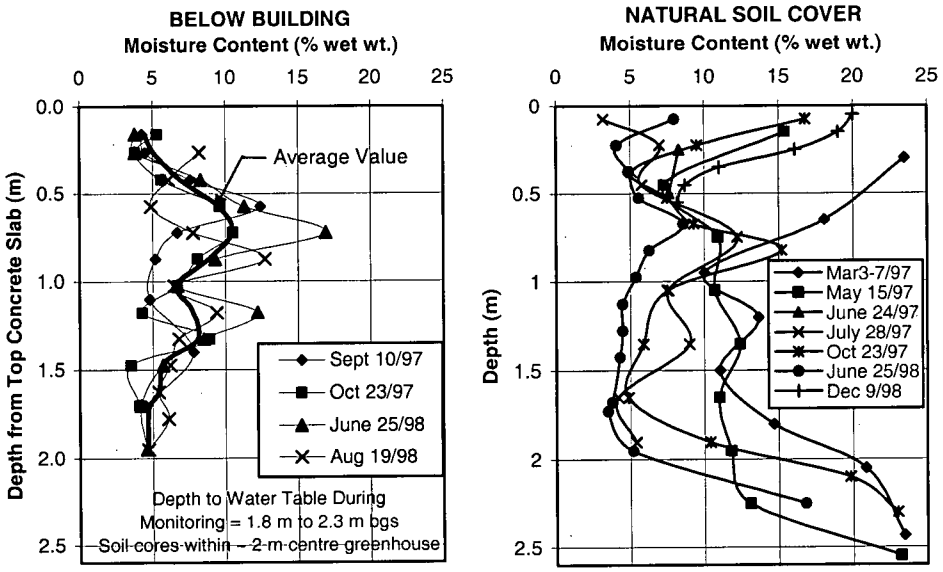

Figure 4.3. Soil moisture content below and adjacent to building (approximate total porosity values are provided in Table 3).

The nitrogen and sulphur testing indicated that the total Kjeldahl nitrogen (TKN) concentrations were elevated within the zone of inferred greatest biological activity based on O_2 depletion, relative to shallower and deeper zones and the reference site. In addition, nitrate was depleted relative to the reference site (Table 4.1). Sulphide concentrations were, in contrast,

anaerobic reactions. The soil organic matter content (SOM) was relatively consistent and ranged from 0.55 to 0.70 %, except for one sample from 0.88 to 0.92 m depth where the SOM was 0.97 %. This sample was collected immediately above the thin fine-grained soil layer and corresponds to the depth where a significant decrease in O_2 concentrations was observed. The TKN concentrations were highest in the sample from 0.9 to 1.05 m depth. Although much more sophisticated methods are available for biomass characterisation (*e.g.*, Franzmann *et al.*, 1999), the elevated TKN and SOM levels near 0.9 m depth may provide a crude indication of biomass formation and where biological activity is occurring.

Table 4.1. Results of nitrogen, sulpher and SOM analyses in soil

Depth (m)	Nitrate (mg/kg)	Nitrite (mg/kg)	TKN[1] (mg/kg)	Total N[2] (mg/kg)	Sulphate (mg/kg)	Sulphide (mg/kg)	SOM (%)
Adjacent Building[3]							
0.3-0.45	N/A	N/A	N/A	N/A	N/A	N/A	0.57
0.45-0.6	0.06	0.01	3.2	3.3	<10	1.3	0.60
0.6-0.75	<0.05	0.01	3.1	3.1	<10	1.0	0.71
0.75-0.9	<0.05	0.02	6.7	6.7	<10	1.1	0.55
0.88-0.92	N/A	N/A	N/A	N/A	N/A	N/A	0.97
0.9-1.05	<0.05	0.01	21.9	21.9	<10	1.3	0.66
1.05-1.2	<0.05	<0.01	10.3	10.3	<10	1.1	0.48
1.2-1.35	0.06	0.01	8.6	8.7	<10	0.5	0.70
1.35-1.5	N/A	N/A	N/A	N/A	N/A	N/A	0.55
Reference Site							
Location 1 0.45-0.9	0.24	<0.02	<0.5	0.24	<10	0.2	N/A
Location 2 0.45-0.9	0.24	<0.02	0.6	0.30	<10	0.3	N/A

[1] TKN = Total Kjeldahl Nitrogen

[2] Total N ~ TKN + nitrate + nitrite; Organic N ~ TKN - ammonia

[3] Samples collected 1 m north of SG-BR probe cluster on June 2, 1999 (from one soil core).

The THB counts ranged from 4.9E+02 CFU/g to 1.7E+09 CFU/g (geometric mean of 6.4E+05) while the BTXB counts ranged from no growth (less than 50 CFU/g) to 1.1E+06 (geometric mean of 1.3E+03). There was no correlation between THB or BTXB counts with BTX concentrations, or inferred zones of biodegradation based on soil vapour monitoring and *in situ* respiration testing. Franzmann *et al.* (1999) likewise found a poor correlation between microbial numbers, calculated from the phospholipid content, and BTEX contamination within an aquifer.

Soil Gas Monitoring Results

Soil vapour benzene concentrations at probes (SG-BC) below the building (greenhouse), and at probes (SG-BR) not covered by a building (*i.e.*, below the present building before it was constructed, or adjacent to the building) are presented in Figure 4.4. The benzene concentration profiles below the centre of the greenhouse were relatively consistent over time and are characterized by high concentrations at depth, significant attenuation (about 3 orders-of magnitude) between about 0.4 to 0.8 m depth, and lower but variable concentrations within 0.4 m depth below slab surface. The measured vapour concentrations below 1 m depth are within a factor of two and one half of those predicted assuming equilibrium partitioning between the NAPL and vapour phases, and vapour pressure adjusting using the mole fraction and Raoult's Law. The benzene concentration profiles for the no building case were somewhat more

variable than those below the building. Postulated causes include variation in surface water infiltration and moisture content, and advective soil gas pumping caused by barometric pressure and/or temperature fluctuations. Similar results were obtained for toluene and *m&p*-xylene below and adjacent to the building; results for one typical monitoring round are presented in Figure 4.5.

The O_2 concentrations below the centre of the building, and at probes not covered by the building are presented in Figure 4.6. The O_2 concentrations below the building were relatively consistent over time and indicate significant O_2 consumption is likely occurring between about 0.6 to 0.9 m depth. Oxygen levels in near surface soil below the centre of the building slab were depleted and ranged between approximately 8 and 13 %. Carbon dioxide concentrations above 0.9 m depth generally ranged from 6 to 9 %, while below 0.9 m the concentrations generally ranged between 10 and 13 %. Methane concentrations were also high (*i.e.*, at percent levels) below about 0.9 m depth (Figure 4.5).

The O_2 concentration profiles for the no building case exhibited greater variability. The O_2 concentration profiles after a relatively long period of dry weather (September 1998 monitoring rounds) were consistent and showed a significant decline between about 0.7 m and 0.9 m depth. In contrast, O_2 concentrations during wet periods (November 1998) indicated greater variability with lower concentrations at shallow depths. Rainfall during the week prior to each sampling event in November 1998 exceeded 30 mm. Lower O_2 concentrations at shallow depths may have been a result of reduced O_2 flux through the surface crust due to high moisture content, and O_2 depletion at depth through biological activity. Oxygen concentrations at a non-contaminated reference site with similar soils were within 1.0 % of atmospheric levels while CO_2 concentrations were equal to or below 0.1 % throughout the soil column.

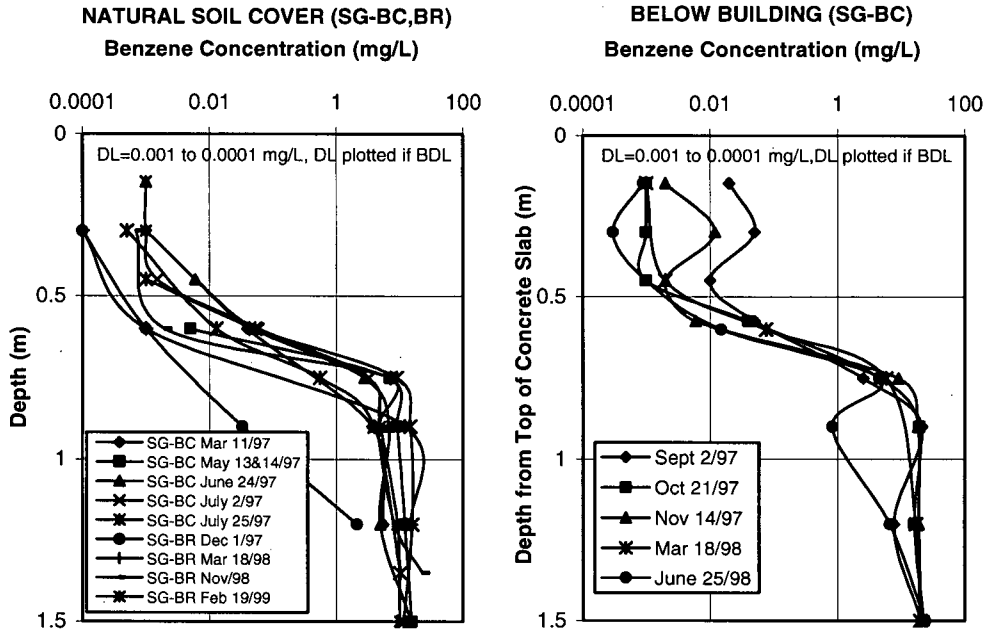

Figure 4.4. Benzene vapour concentrations below and adjacent to building (MC = moisture content).

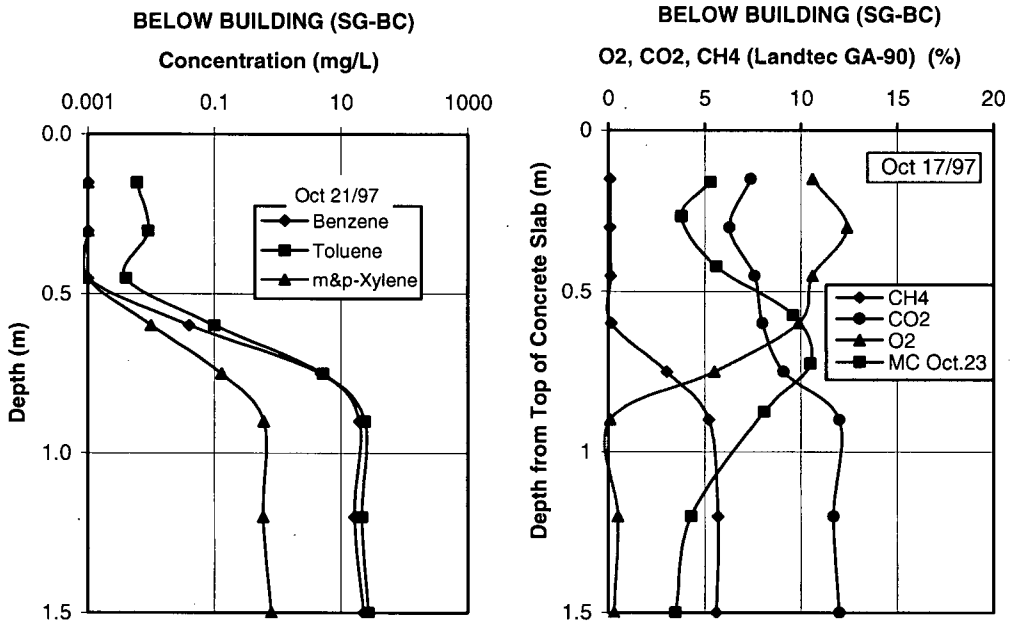

Figure 4.5. BTX vapour and light gas concentrations below building (MC = moisture content.

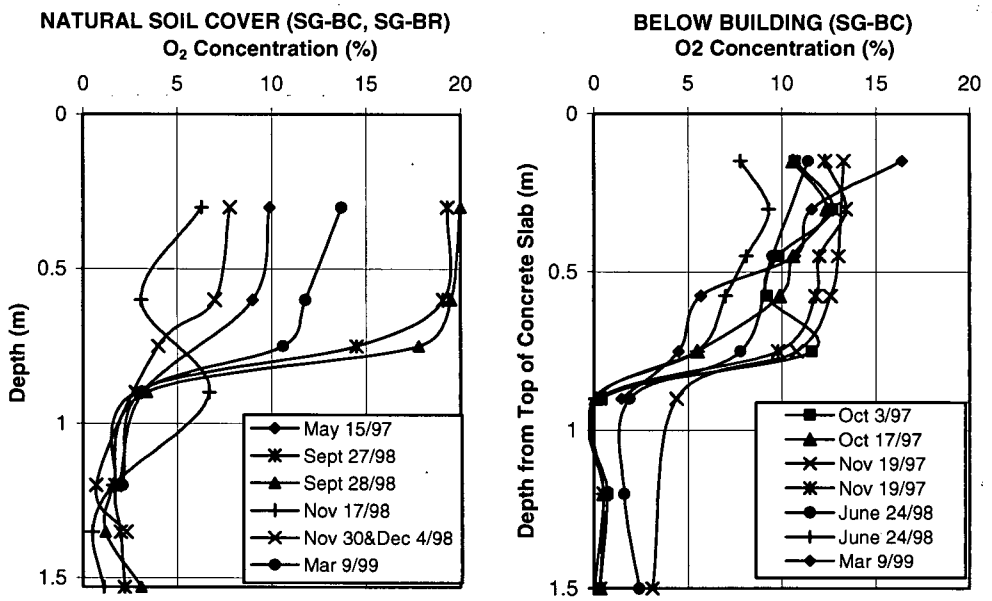

Figure 4.6. Oxygen gas concentrations below and adjacent to building.

The semi-continuous O_2 monitoring below the slab indicated diurnal changes in concentrations (up to 2 %) due to temperature fluctuations and day-long to week-long O_2 trends that appear to be correlated to barometric pressure. Pressure monitoring indicating that significant effects from diurnal and atmospheric pressure changes were limited to above 0.3 m

depth beneath the building slab. As discussed in subsequent sections of this paper, advective processes may be important in terms of O_2 replenishment directly below the slab.

Estimation of Field Biodegradation Rates

Monitoring at the Chatterton site suggests that processes affecting fate and transport below the building can be divided in three zones based on depth below ground surface consisting of primarily diffusion in the deep zone, biodegradation and diffusion in the mid-depth zone, and advection, biodegradation and diffusion in the shallow zone. First-order degradation coefficients were estimated for the mid-depth zone by fitting model-predicted BTX concentrations, based on an analytical solution for one-dimensional steady-state diffusion and reaction, to measured BTX concentrations. The vapour profile between about 0.5 to 0.8 m depth was used since BTX attenuation was significant and approximately log-linear over this interval. The BTX vapour profiles below and adjacent to the building were also consistent over time suggesting approximate steady-state conditions (Figure 4.4). A first-order model was considered appropriate based on the log-linear BTX vapour profile and presence of sufficient O_2 for biodegradation based on the biodegradation capacity (BC).

Steady-state vapour-phase diffusion and reaction for a homogeneous soil can be represented by the following equation:

$$D_g^{eff} \, \partial^2 C_g / \partial Z^2 = G = (k_w^1 \, \theta_w / H') \, C_g \tag{5}$$

where D_g^{eff} is the effective vapour-phase diffusion coefficient ($L^2 \, T^1$), C_g is the vapour concentration ($mol \, L^{-3}$), G is the first-order rate of mass consumption ($mol \, L^{-3} \, T^1$), k_w^1 is the first-order degradation rate based on the pore-water concentration (T^1), θ_w is the water-filled porosity ($L^3 L^{-3}$), and H' is Henry's Law Constant (*dimensionless*). Assuming the top and bottom boundary conditions can be represented by constant concentrations, an analytical solution can be derived that enables calculation of a Damkohler number, or the ratio of the degradation rate over the diffusion rate (DeVaull *et al.*, 1997), as follows:

$$\frac{C_g(Z)}{C_g(Z=0)} = \frac{\left(e^{-\alpha} - \beta\right)e^{\alpha Z/L} + \left(\beta - e^{\alpha}\right)e^{-\alpha Z/L}}{e^{-\alpha} - e^{\alpha}}, \quad \alpha > 0 \tag{6}$$

$$D_{am} = \alpha^2 = \text{Degradation Rate / Diffusion Rate} = k_w^1 \, \theta_w \, L^2 / (H' \, D_g^{eff}) \tag{7}$$

where D_{am} is the dimensionless Damkohler number, L is the domain length over which transport occurs (L) and β is the vapour concentration at distance L.

For the Chatterton site, the effective diffusion coefficient was calculated using the measured tortuosity factor obtained from *in situ* push-pull tracer tests using helium (Hers *et al.*, 1999) and the free-air diffusion coefficient. Between 0.5 and 0.8 m depth, the mean D_g^{eff} was 0.044 cm^2/sec while θ_w and θ were equal to 0.18 and 0.36, respectively. Using the above input values, the estimated first-order degradation rate constants based on soil pore water concentrations (k_w^1) were on the order of 1.2 hr^{-1} for benzene, 0.9 hr^{-1} for toluene and 0.5 hr^{-1} for *m&p*-xylene.

Zero-order biodegradation rates (k_w^0, $mol\ L^{-3}\ T^{1}$) were estimated from *in situ* respiration tests using the method in U.S. EPA (1995). Respiration tests were conducted for the lower part of the mid-depth zone, and deep zone described above. A zero-order model was considered appropriate based on approximately linear O_2 consumption curves and since total BTX concentrations in vapour exceeded about 1 mg/L at the respiration test locations. The zero-order total hydrocarbon (*i.e.*, BTX) degradation rates in pore water ranged between 0.8 and 6 mg/L-hr and were highest at 0.9 m depth, which again was consistent with the depth interval over which the highest biodegradation rates are expected.

A relatively good comparison is obtained between the first- and zero-order rates measured at the Chatterton site and published biodegradation rates based on laboratory and field studies, compiled by DeVaull *et al.* (1997) (Figure 4.7). In addition, the Chatterton site total BTX first-order rate intersects the zero-order rate at a pore-water concentration of about 2 mg/L, which is consistent with the biodegradation model described in Section 2.3.3. Together the first-order degradation rates (from vapour profiles), and zero-order degradation rates (from the *in situ* respiration tests), provide a practical field-based method to approximate the relationship between biodegradation rate and concentration based on Monod kinetics.

Comparison to Other Case Studies

The estimated Damkohler numbers and first-order aerobic biodegradation rates for the Chatterton site and several other case studies are presented in Table 4.2. The degradation rates are highly sensitive to the Damkohler number, effective diffusion coefficient and moisture content. Biodegradation rates are overestimated when there are thin unquantified high moisture content layers, since these layers represent a partial barrier to diffusive transport. At sites where there are unresolved moisture content effects, fitted biodegradation rates are, in effect, lumped parameters. Due to the various sources of uncertainty, the estimated biodegradation rates (k_w^1) should be considered order-of-magnitude estimates.

The vadose zone first-order degradation rates are about two to four orders-of-magnitude higher than those obtained for dissolved BTEX plumes in groundwater (Wiedemeier *et al.*, 1996). While the vadose zone biodegradation rates are high compared to saturated zone rates, they are on the same order or lower than rates obtained for biofilters, suggesting that vadose zone rates given in Table 4.2 may be reasonable. For example, Andreoni *et al.* (1997) report a toluene removal rate of 6 mg/L-hr for a biofilter constructed of wood bark, while Conti *et al.* (1999) report a toluene removal rate of 135 mg/L-hr for a biofilter constructed of peat beads.

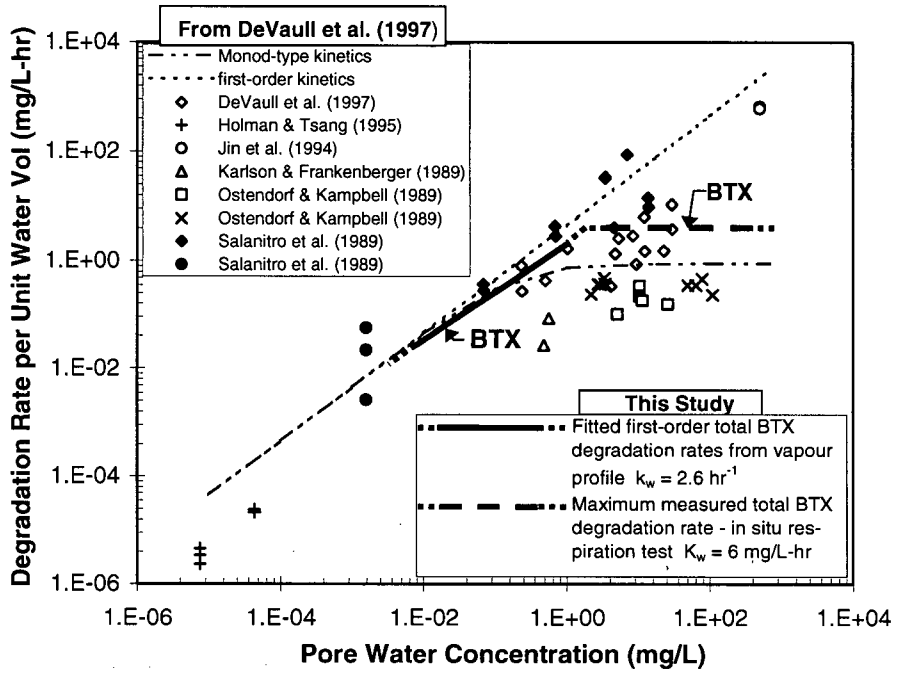

Figure 4.7. Comparison of field degradation rates to published data in DeVaull et al. (1997) (used with permission).

Table 4.2. Measured aerobic biodegradation rates from field studies

Site	Chemical Class	Chemical	Biodegradation Layer Thickness (m)	Damkohler Number (D_{am})	First-order Degradation Rate (water-(phase)(hr^{-1})
Chatterton (this paper)	BTX	Benzene	0.3	7.4+/-1	0.5-2.0 (1.2)[3]
		Toluene	0.3	6.05+/-1	0.3-1.5 (0.9)[3]
		m&p-xylene	0.3	5.2+/-1	0.2-0.8 (0.5)[3]
Alameda Fischer *et al.* (1996)	Gasoline	iso-pentane	0.2	~6[1]	~2[1]
Traverse City Ostendorf & Kampbell (1991)	Aviation Fuel	Total Hydrocarbon	3	4	~0.01[2]
California Ririe and Sweeney (1995)	Gasoline	Benzene	2	9	0.4[2]

Notes:

[1] Degradation rate overestimated due to likely presence of low moisture content layer (i.e., physical barrier).

[2] Order-of-magnitude estimate due to significant uncertainty in air-filled and total porosity, and physical-chemical properties.

[3] Range and best estimate (in parentheses) based on probable range of values for Damkohler Number and moisture content.

NUMERICAL SIMULATION OF VADOSE ZONE BTX TRANSPORT

A two-dimensional numerical model (VADBIO) for multispecies transport in the unsaturated zone was developed to compare various types of biodegradation models, and was based on conditions observed at the Chatterton site. The VADBIO model was used to evaluate the effects of a building, variations in moisture content, and advection on biodegradation processes and kinetics.

Model Description

The differential equation for vadose zone chemical transport incorporating two-dimensional diffusion, gas-phase advection, absorption and first- or zero-order reaction, assuming equilibrium chemical partitioning between the vapour, aqueous and sorbed phases, and linear isotherms, for a single chemical species may be written as follows:

$$\Theta_g R \frac{\partial C_g}{\partial t} = \frac{\partial}{\partial x}\left\{D_{xx}\frac{\partial C_g}{\partial x}\right\} + \frac{\partial}{\partial x}\left\{D_{xy}\frac{\partial C_g}{\partial y}\right\} - \frac{\partial}{\partial x}\left\{\Theta_g (V_g)_x C_g\right\} + \frac{\partial}{\partial y}\left\{D_{yx}\frac{\partial C_g}{\partial x}\right\} + \frac{\partial}{\partial y}\left\{D_{yy}\frac{\partial C_g}{\partial y}\right\} - \frac{\partial}{\partial y}\left\{\Theta_g (V_g)_y C_g\right\} - G \tag{8}$$

$$D_{xx} = \Theta_g\left(\alpha_L \frac{(V_g)_x^2}{V} + \alpha_{TH}\frac{(V_g)_y^2}{V}\right) + \Theta_g D_g + \frac{\Theta_w}{H'} D_w \tag{9a}$$

$$D_{xy} = D_{yx} = \Theta_g\left((\alpha_L - \alpha_{TH})\frac{(V_g)_x (V_g)_y}{V}\right) + \Theta_g D_g + \frac{\Theta_w}{H'} D_w \tag{9b}$$

$$D_{yy} = \Theta_g\left(\alpha_{TH}\frac{(V_g)_x^2}{V} + \alpha_L \frac{(V_g)_y^2}{V}\right) + \Theta_g D_g + \frac{\Theta_w}{H'} D_w \tag{9c}$$

$$V = \sqrt{(V_g)_x^2 + (V_g)_y^2} \tag{9d}$$

$$G = k_w{}^1 \frac{\Theta_w}{H'} C_g \ \text{(1st order)}; \qquad G = k_w{}^0 \ \text{(zero order)} \tag{10}$$

$$R = 1 + \frac{\Theta_w}{\Theta_g H'} + \frac{\rho_b K_d}{\Theta_g H'} \tag{11}$$

where θ_g is the gas-phase porosity (L^3L^{-3}), R is the retardation coefficient (*dimensionless*), D_{xx}, D_{xy}, D_{yx} and D_{yy} comprise the dispersion tensor ($L^2\,T^{-1}$), $(V_g)_x$, $(V_g)_y$ are the gas-phase velocities ($L\,T^{-1}$), α_L, α_{TH} are the longitudinal and transverse dispersivities (L), D_g and D_w are the vapour- and aqeous-phase diffusion coefficients ($L^2\,T^{-1}$), ρ_b is the dry bulk density of the soil (ML^{-3}) and K_d is the distribution coefficient between the sorbed and aqueous phases (L^3M^{-1}).

The VADBIO model simulates vapour-phase hydrocarbon transport described by equations 8 to 11 and models biodegradation processes using four different methods:

1. First-order biodecay (m*odel no.1*).
2. Combined first and zero-order biodecay. For lower concentrations where the substrate concentration limits biodecay, a first-order process is assumed, while above a critical concentration, a zero-order process is assumed (m*odel no. 2*).
3. Instantaneous-reaction model where the hydrocarbon and O_2 concentrations are sequentially computed, and at each time step combined using superposition to simulate the reaction between O_2 and hydrocarbon compounds. The O_2 consumed is linked to hydrocarbon degraded through the stochiometric ratio for complete mineralization of the hydrocarbon compound using the following equations:

$$H(t+1) = H(t) - O(t) / SR \; ; \; O(t+1) = 0 \; (zero) \quad \text{where } H(t) > O(t) / SR \tag{12}$$

$$O(t+1) = O(t) - H(t) * SR \; ; \; H(t+1) = 0 \; (zero) \quad \text{where } O(t) > H(t) * SR \tag{13}$$

   where H is the total hydrocarbon concentration, O is the O_2 concentration and SR is the average stochiometric ratio of O_2 to hydrocarbon consumed. The instantaneous reaction model is appropriate for single hydrocarbon compounds, or multiple compounds with similar SR values (*e.g.*, BTEX) (m*odel no. 3*).

4. Combined first- and zero-order biodecay as described above except that the O_2 availability in soil at each time step is checked by simultaneously solving the O_2 transport equation. The mass of O_2 consumed is obtained using the stochiometric relationship for complete mineralization and the mass of hydrocarbon degraded by either a first- or zero-order process (m*odel no. 4*).

The numerical model solution assumes a rectangular domain and hydrocarbon transport from a subsurface source at the base of the domain to ground surface (Figure 4.8). Boundary conditions for hydrocarbon transport are as follows:

1. Bottom layer: constant or time-varying concentrations (Dirichlet condition). Possible compositional changes in NAPL and source vapour concentrations over time are not accounted for in this version of the model.
2. Top layer: constant concentration equal to atmospheric hydrocarbon concentration, which assumes chemicals are subject to instantaneous mixing and dilution in the atmosphere.

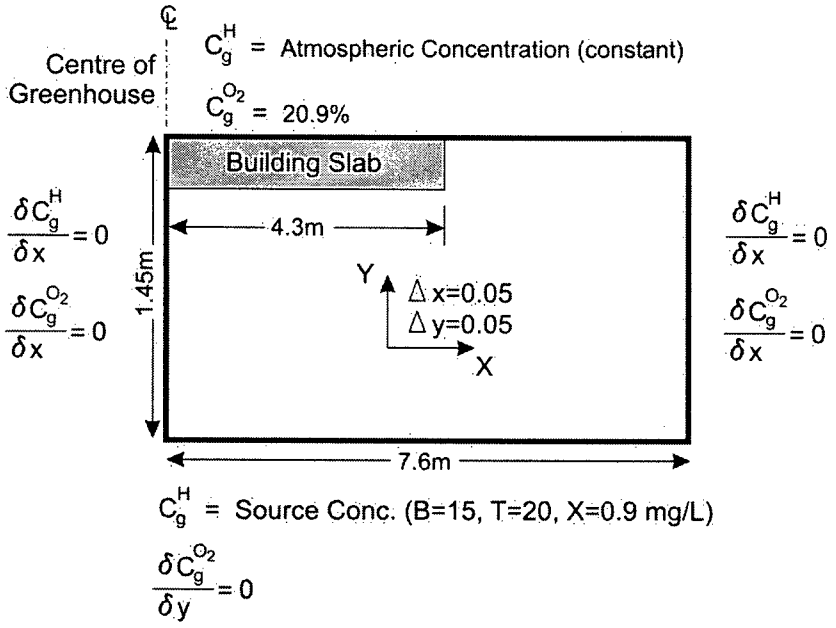

Figure 4.8. Model domain and boundary conditions used for 2-D simulations.

The boundary conditions for O_2 transport are as follows:

1. Bottom layer: constant flux set equal to zero (Neumann condition).
2. Top layer: constant atmospheric concentration with time (20.9%).

Initial conditions used for simulations presented in this paper are hydrocarbon concentrations equal to average atmospheric concentrations (except at the bottom boundary), and O_2 concentrations equal to 20.9 % (except at the bottom boundary).

The model allows for input of variable soil properties and an at-grade building with cracked floor slab. The effective diffusion coefficient for soil is calculated using the Millington and Quirk (1961) relationship:

$$D_g^{eff} = \theta_g D_g = \tau_g D_{air} = (\theta_g^{10/3} / \theta^2) * D_{air} \quad (14)$$

$$D_w^{eff} = \theta_w D_w / H' = \tau_w D_{water} = (\theta_w^{10/3} / (\theta^2 H')) * D_{water} \quad (15)$$

where τ_g and τ_w are the gas-phase and aqueous-phase tortuosity factors. Diffusion through the building slab occurs primarily through cracks and other openings, and through intact concrete. The approach for simulations presented in this paper is to assume that diffusion only occurs through cracks, but to use a somewhat conservative crack ratio to account for possible diffusion through intact concrete. Radon research suggests that diffusion through both cracks and intact concrete can be significant (Renken & Rosenberg, 1995; Nielson *et al.*,1997). Little research on hydrocarbon diffusion through building foundations has been conducted. Since discretization of crack-sized openings requires too fine a model grid, diffusion through concrete is modeled assuming that a rough estimate of the bulk tortuosity of the concrete slab can be obtained as follows:

$$D_{gcon}^{eff} = (A_c \, \tau_{dust} / A_b) \; * D_{air} \qquad (16)$$

where D_{gcon}^{eff} is the effective diffusion coefficient of the concrete, A_c is the area of the cracks in concrete, τ_{dust} is the tortuosity factor for dirt-filled cracks and A_b is the building slab area. The model output includes concentration versus time data, and calculated hydrocarbon flux across the top boundary of the model domain.

The numerical solution utilizes a forward, or explicit, temporal discretization scheme. The scheme is subject to the following stability constraints:

$$\Delta t < (\Delta X)^2 / (2 \, *(D_g^{eff} + D_w^{eff})); \quad \Delta t < (\Delta Y)^2 / (2 \, *(D_g^{eff} + D_w^{eff})); \quad \Delta t < 1 / k_w \qquad (17)$$

where ΔX and ΔY are the grid block size in the x and y directions.

The VADBIO model is similar to the R-UNSAT computer model developed by the U.S. Geological Survey (Lahvis and Baehr, 1997). The main difference relates to advection in that VADBIO only incorporates gas-phase transport while R-UNSAT only incorporates aqueous-phase transport. The VADBIO model includes additional options for biodegradation modeling and incorporation of building slab properties whereas R-UNSAT has greater flexibility in terms of boundary conditions, and includes an analytical model.

Comparison to Analytical Solutions

Model-predicted benzene transport was compared to analytical solutions for: (i) steady-state one-dimensional diffusion with first-order decay (equation 6), and (ii) one-dimensional uniform soil gas flow, two dimensional dispersion (and diffusion) and first-order decay for a finite, constant source, as adapted from the extended pulse model (approximate solution) by Domenico (1987). The diffusion solution (equation 6) assumes constant concentrations at the top and bottom boundary, while the advection (Domenico) solution assumes a finite, constant source combined with an infinite flow domain. A homogeneous, isotropic porous media is assumed by both models. For the diffusion model case, the numerical solution closely approximates the analytical solution for a grid size equal to or less than 0.05 m (Figure 4.9). For the advection model case, the numerical solution closely approximates the analytical solution for the grid sizes evaluated. Subsequent model simulations in this paper use a grid size equal to or less than 0.05 m.

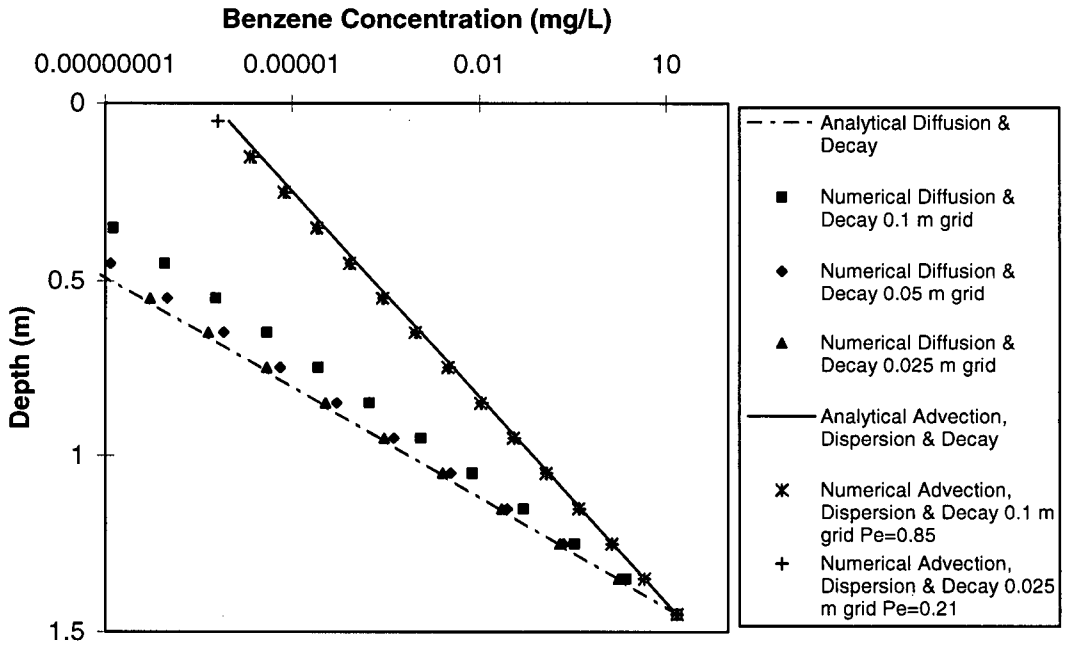

Figure 4.9. Comparison of numerical and analytical solutions for steady-state conditions. (input parameters: $C_g(source)$ = 15 mg/L, θ_w = 0.14, θ = 0.36, H' = 0.23, k_w^1 = 1.2 hr^{-1}, U = 5.6x10^{-6} m/s, α_l = 0.1 m, U = specific discharge, α_l = longitudinal dispersivity, Pe = Peclet number, all other symbols defined in text)

Comparison of Biodegradation Models No. 1, 2, 3 and 4 (1-D Diffusion and Biodecay)

The numerical solutions for the four biodegradation models were compared for steady-state one-dimensional diffusion of BTX with biodecay with results presented in Figure 4.10. Two cases were simulated: (i) a uniform soil with relatively low soil moisture content (θ_w equal to 0.14, θ equal to 0.36), and (ii) a two-layer soil profile with a relatively high moisture content for the surface layer (θ_w equal to 0.28, θ equal to 0.36). Model input parameters are provided in Table 4.3. The first-order degradation rates were estimated by fitting the analytical model previously described to measured hydrocarbon vapour profiles at the Chatterton site while the zero-order rates were obtained from *in situ* respiration tests. Individual zero-order rates for BTX constituents were assumed to be in the same proportions as the first-order rates.

For the uniform soil layer case, all biodegradation models predict a sharp decrease in benzene concentration just above the BTX source and an approximate linear decrease in O_2 concentrations over the depth range. No significant difference was obtained between model no. 2 (first- and zero-order) and model no. 4, which incorporates an O_2 availability check, since biodegradation is not limited by O_2 availability over most of the soil profile. Results for model no. 3 (instantaneous reaction) showed a sharper decrease in benzene concentration than models no. 2 and 4 since again O_2 is not rate limiting. For the two soil layer case (*i.e.*, high surface soil moisture content), there was a significant difference in models no. 2 and 4 since biodegradation at depth is limited by O_2 availability, but there was virtually no difference between models no. 3 and 4 for benzene vapour concentrations above 1 mg/L. The results highlight the importance of

O_2 diffusion rates (and hence moisture content) and selection of a biodegradation model that incorporates appropriate reaction kinetics combined with O_2 availability (*e.g.*, model no. 4).

Table 4.3. Input Parameters for Comparison of Biodegradation Models

Parameter		Comparison of Bio Models		Chatterton Comparisons	
		Sand	Crust (0.2m)	Sand	Crust (0.2m)
Soil Properties	Water-filled Porosity (-)	0.14	0.28	variable	variable
	Total Porosity (-)	0.36	0.36	0.36	0.403
	Organic Carbon Content (-)	0.006	0.006	0.006	0.006
	Bulk Density(g/cm^3)	1.67	1.67	1.67	1.58
		Benzene	toluene	*m&p*-xylene	Oxygen
Chemical Properties	Henry's Law Constant (-)	0.23	0.28	0.23	31.6
	Diffusion Coef in Air (m^2/sec)	8.44E-06	7.60E-06	7.00E-06	2.06E-05
	Diffusion Coef in Water (m^2/sec)	1.00E-09	9.4E-10	8.5E-10	1.00E-09
	Partitioning coef (log K_{oc}) (cm^3/g)	1.96	2.12	2.56	1
Concentrations	Cg(x,y,t=0) (mg/L)	0	0	0	279
	Cg(x,y=0,t) (mg/L)	15	20	0.9	Variable
	Cg(x,y=1.4,t) (mg/L)	0.000005	0.00001	0.000003	279
Biodegradation Rates	First-order rates (k_w^1) (hr^{-1})	1.2	0.9	0.5	N/A
	Zero-order rates (k_w^0) (mg/L-hr)	1.36	1.06	0.56	N/A
	Average stochiometric ratio	3.1	3.1	3.1	N/A

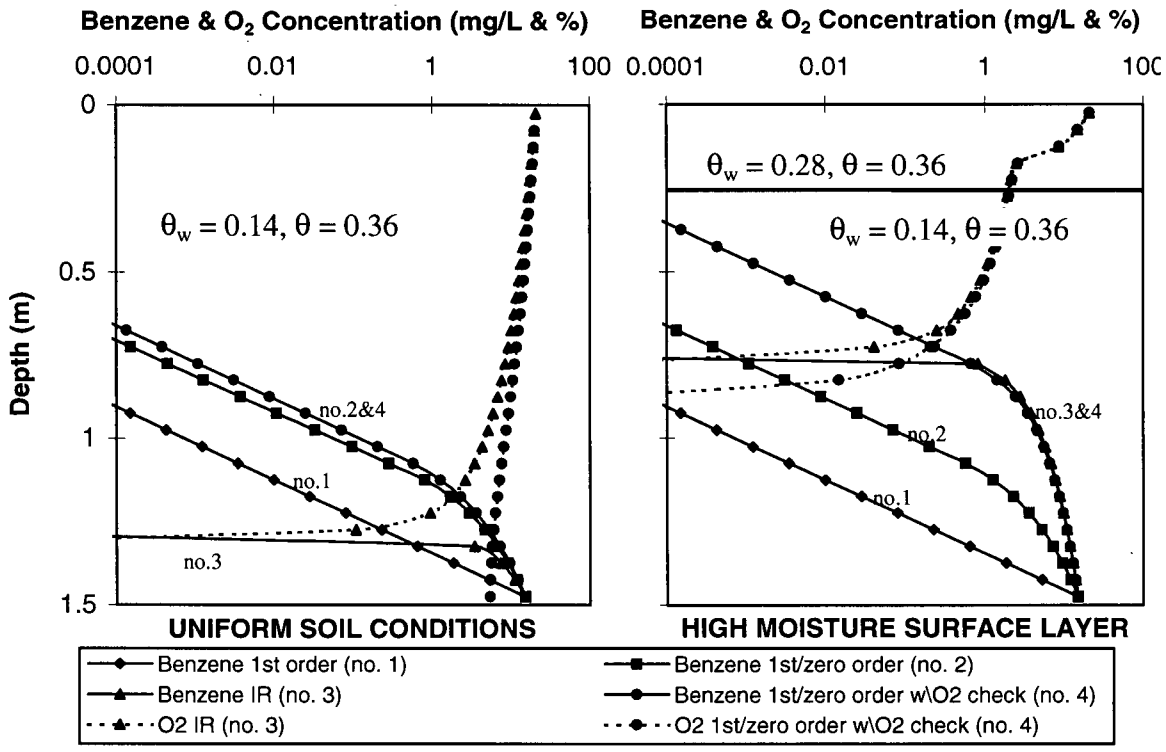

Figure 4.10. Comparison of biodegradation models for uniform and non-uniform soil conditions using 1-D diffusion and reaction model (steady-state conditions, IR = instantaneous reaction).

Comparison to Chatterton Vapour Profiles (2-D Diffusion and Biodecay)

Model-predicted and measured soil vapour concentrations for the Chatterton site were compared using the biodegradation model incorporating first- and zero-order biodegradation with O_2 availability check (model no. 4). Two additional refinements were made to the model for the purposes of simulations presented in this section. First, biodegradation was turned off once O_2 concentrations reached 1.5 % since biodegradation rates are significantly reduced at low concentrations (DeVaull, 1997). Second, biodegradation was turned off once hydrocarbon concentrations reached atmospheric levels. The justification for this refinement is that there is insufficient substrate to support biodegradation at low hydrocarbon concentrations. Estimation of the precise concentration at which biodegradation becomes substrate limiting is beyond the scope of this assessment; however, an arbitrary cut-off point equal to atmospheric concentrations was considered sufficiently accurate for the purposes of these simulations.

Input parameters were identical to those given in Table 4.3 except that soil moisture was varied, and an at-grade building slab was simulated over a portion of the model domain (Figure 4.8). Due to the dilution that occurs through building ventilation, BTX concentrations inside the building (*i.e.*, top left boundary condition) were assumed to be equal to atmospheric concentrations. The model domain was chosen to simulate conditions at the Chatterton site. Since vapour transport is likely symetrical in relation to the building slab, only half the building is incorporated in the domain; the left edge of the model domain corresponds to concentrations below the centre of the building while the right edge corresponds to concentrations adjacent to the building. The ratio of the crack area to building slab area ($\eta = A_c/A_b$) ranged from 0.0003 to 0.001, and τ_{dust} was varied between 0.25 and 1. The lower values for η and τ_{dust} represent an estimate of the crack ratio based on measurements of visible cracks while the upper values for η and τ_{dust} are considered conservative estimates that take into account micro-scale cracks and pores through which diffusion can occur.

Two scenarios were simulated corresponding to approximate measured moisture content conditions during dry periods in summer and early fall (Case 1) and during wet periods in late fall and winter (Case 2). The moisture content profiles used for the simulations are provided in Figure 4.11. As shown, the most significant difference in moisture content is for the surface crust, which tends to retain moisture for longer periods of time during wet periods. The crust is not present below the greenhouse since it was replaced by the foundation slab and sand fill. Laterally constant moisture contents were assumed for the simulations. Based on the measured moisture content variation (Figure 4.3), it is recognized that the moisture content profile adjacent to the building is approximate.

The predicted benzene and oxygen concentrations below the centre of the building for simulations corresponding to 0.5, 1, 2 and 3 months are presented in Figure 4.12 (Case 2 only). Both predicted and measured concentrations below (centre) and adjacent to the building at 3 months are presented in Figure 4.13 (Case 1 and 2). The upper ranges of the crack ratio and tortuosity factor were chosen for these simulations. The time to reach approximate steady-state conditions varies depending on moisture content and location. Approximate steady-state conditions were reached in about one month adjacent to the building for Case 1 (dry summer) conditions (results not shown). As shown in Figure 4.12, benzene concentrations below the building were still slowly increasing after three months for Case 2 (wet winter) conditions.

Lateral O_2 diffusion from adjacent to the building has a slight effect on O_2 concentrations below the centre of the building. The 2-D O_2 concentrations were about 0.1 % higher than 1-D O_2 concentrations, for Case 1 conditions.

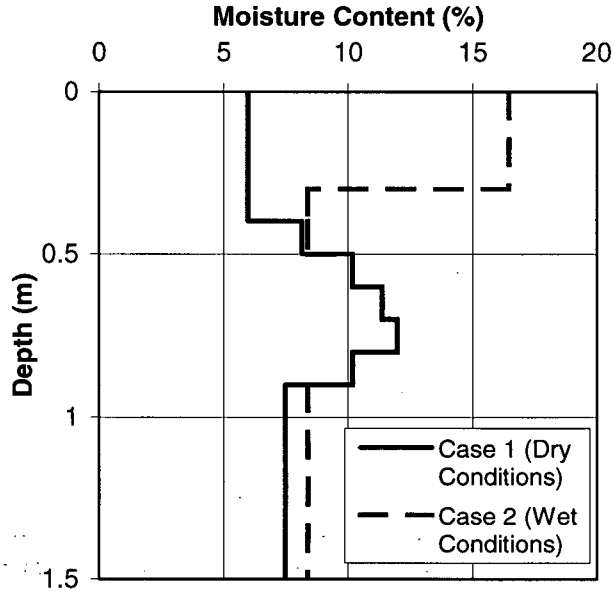

Figure 4.11. Moisture content profile used in numerical simulations (see Table 4.3 for porosity values).

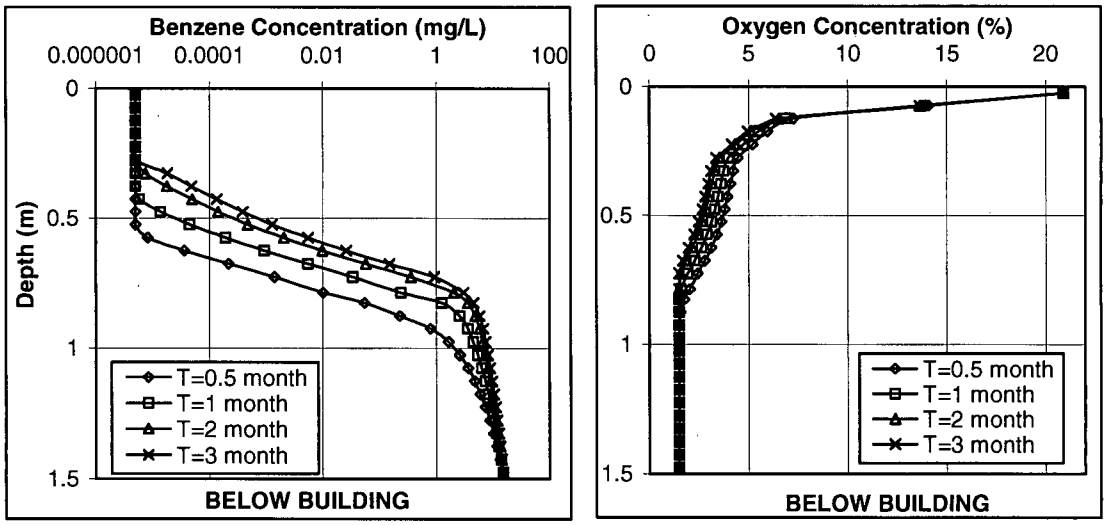

Figure 4.12. Predicted vapour concentrations below centre of building for 2-D diffusion with reaction (Model No. 4) – wet (winter) conditions ($\eta = 0.001$, $\tau_{dust} = 1$).

For Case 1, there is a significant difference between the benzene and O_2 concentrations below and adjacent to the building (Figure 4.13). This is a result of the much higher diffusive O_2 flux through the surface crust, compared to the concrete slab. For Case 2, there is less of a difference between the benzene and O_2 concentrations below and adjacent to the building since the diffusivity through the crust is lower. Adjacent to the building, there is a difference in O_2

profiles for wet and dry conditions but virtually no difference between the benzene concentration profiles. This lack of sensitivity of benzene to moisture content is caused by O_2 levels that remain sufficiently elevated for biodegradation to occur.

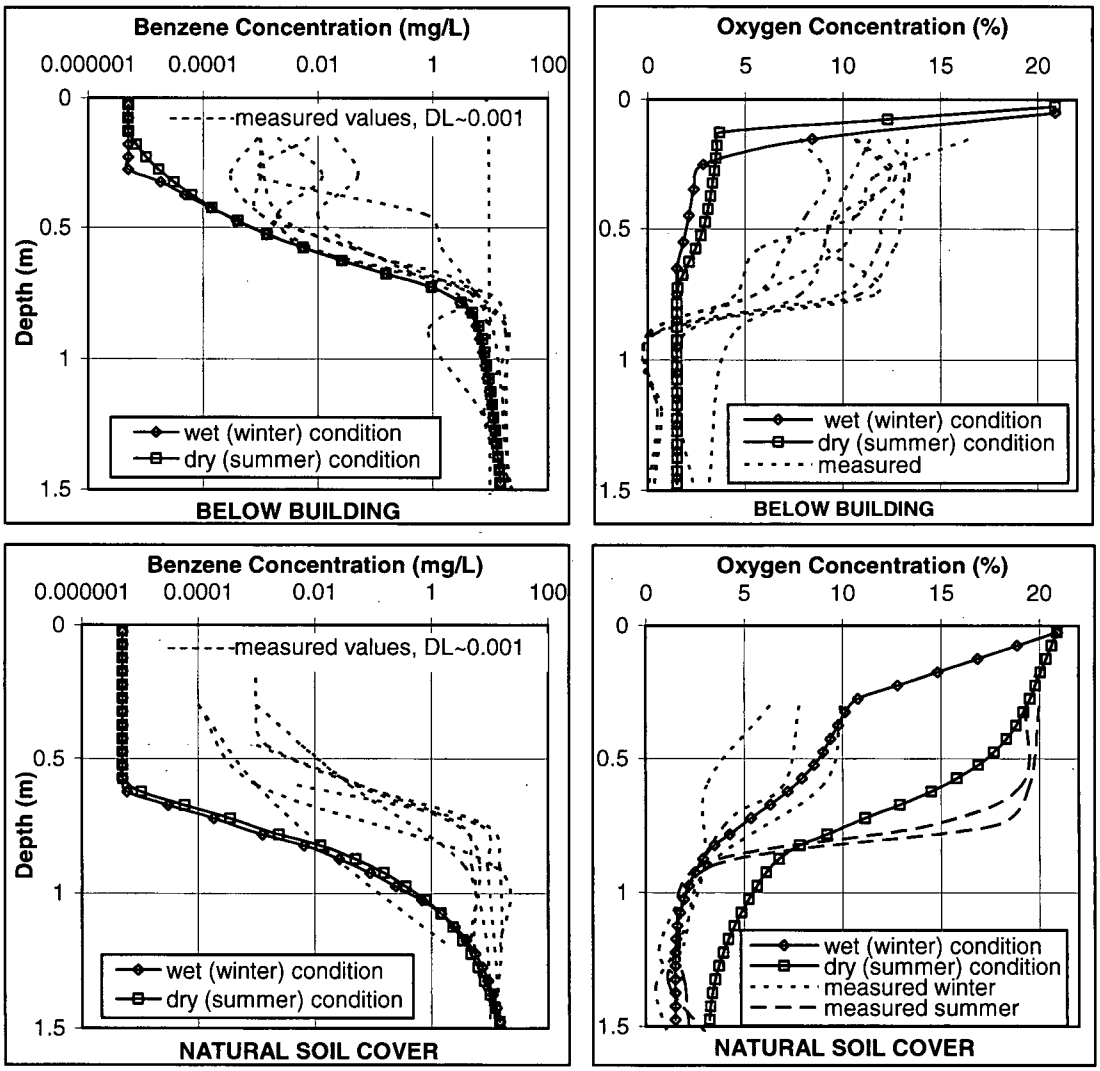

Figure 4.13. Comparison of model-predicted and measured vapour concentrations from Figure 4.4 and 4.6 for 2-D diffusion and reaction (model no. 4) ($\eta = 0.001$, $\tau_{dust} = 1.0$) (approximate steady-state conditions at 3 months)

The results are highly sensitive to the diffusivity of the building slab and O_2 flux (Figure 4.14). For the upper range of values chosen for η and τ_{dust}, concentrations are low below the slab, but sufficient O_2 remains to degrade benzene. However, a slight decrease in τ_{dust} from 1.0 to 0.5 results in the depletion of O_2 and a significant increase in benzene concentrations below the foundation slab. Measured O_2 concentrations were higher than predicted below the building, even for the highest crack area used. The elevated O_2 concentrations below the building may be a result of natural pressure-driven advective soil gas flow (*i.e.*, pumping) in shallow foundation soils resulting from variation in temperature and barometric pressure. Monitoring indicated that these pressure gradients caused the greenhouse to either be over pressurized or under pressurized

relative to subsurface soil pressures. Short-term diurnal temperature-induced pressure variations were as high as 2 to 3 Pa during the summer months; however, time-averaged net pressure gradients were negligible (see Chapter 5).

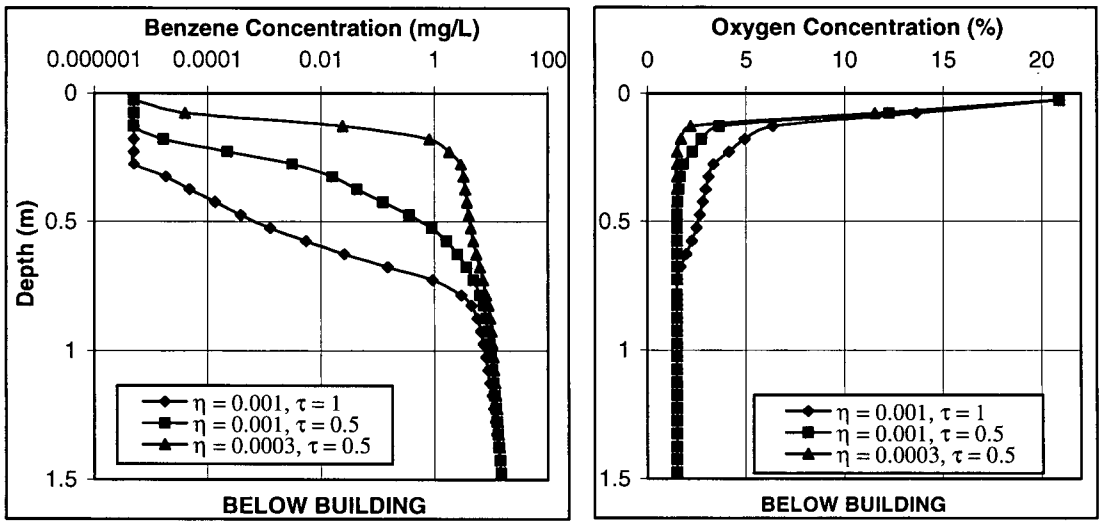

Figure 4.14. Effect of slab open area and tortuosity factor on predicted vapour concentratiosn below centre of building for 2-D diffusion with reaction (model no. 4) – wet (winter) conditions (approximately steady state conditions at 3 months).

Overall, the predictive capabilities of the model used are considered good based on the above results. Model-predicted vapour profiles were generally similar in shape to measured profiles, indicating the effect of seasonal moisture content variation and building slab can be approximately simulated. The observed differences between model-predicted and measured vapour concentrations may be related to uncertainty in moisture content and/or biodegradation rate. These factors are further investigated below.

Sensitivity Analysis Adjacent to Building at Chatterton site (1-D Diffusion and Biodecay)

Sensitivity analysis was conducted to evaluate the effect of moisture content and biodegradation rate variation on predicted vapour concentrations, using the model incorporating first- and zero-order biodegradation with O_2 availability check (model no. 4) and a vertical model grid of 0.04 m. Using this analysis, biodegradation rates were refined through both comparison to measured O_2 and benzene profiles.

Additional detailed soil sampling and moisture content testing, and soil vapour testing were conducted in May and June 1999 to provide data required for modeling. This testing was conducted adjacent to the building. As described in Section 3.4, a thin silty fine sand layer is present at 0.92 m depth. This fine sand layer corresponds to the depth where a sharp decrease in O_2 was observed adjacent to the building (Figure 4.6). About 4 cm of sand above the silt layer had a higher moisture content than sand above and below this layer. Samples for moisture content consisted of composite samples collected at 0.15 m intervals, except for the 0.04 m thick layer (with higher moisture content) from 0.88 to 0.92 m.

The following parameters were individually varied as part of the sensitivity analysis:

1. *Critical layer moisture content (0.88 to 0.92 m).* The volumetric moisture content was varied between 0.2 and 0.32 m^3m^{-3} (measured value was 0.23 m^3m^{-3}). The rationale for focusing on this layer is that the uncertainty in diffusivity is likely greatest for this zone and the thin fine sand layer directly below. The moisture content for the remainder of the soil profile was kept constant and was that measured in May 1999.
2. *Entire soil profile moisture content*: The volumetric moisture content was varied +/- 0.03 m^3m^{-3} of the values measured in May 1999.
3. *Biodegradation rates*: Both the first- and zero-order biodegradation rates were varied by +/- 60 % of the mean values provided in Table 4.2, since this range corresponding to the approximate variation in fitted rates (see Section 3.6). The biodegradation rates corresponding to the range used are described as "low", "moderate" and "high".

The model-predicted benzene and O_2 concentrations, and measured profiles are provided in Figure 4.15. As shown, the results are most sensitive to biodegradation rate and soil profile moisture content, and only slightly sensitive to moisture content for the critical layer, based on the range of values chosen. In general, a relatively good comparison is obtained between the model-predicted and measured benzene and oxygen values. Since different factors provide similar results (*e.g.*, low soil profile moisture content versus low biodegradation rate), it is not possible to conclusively identify which combination of parameters provides the best fit. Qualitatively, a moderate to high biodegradation rate, a relatively high critical layer moisture content, and the measured soil moisture profile result in the best match between model-predicted and measured O_2 concentrations. It also appears that variable biodegradation rates would have improved the fit with low biodegradation rates at depths below 0.9 m depth, and moderate to high biodegradation rates above 0.9 m depth more representative of actual conditions.

The detailed modeling results highlight the importance of careful sampling, and demonstrate that good comparisons can be obtained between measured and model-predicted values using appropriate input values. The sensitivity analysis is also significant in that the range of biodegradation rates given in Section 3.7 is further supported.

Evaluation of Advective Transport at Chatterton site (1-D Diffusion, Advection and Biodecay)

Advective chemical transport, in combination with diffusion and biodegradation (model no. 4) was evaluated below the centre of the greenhouse building at the Chatterton site. On several occasions, the building has been mechanically depressurized in order to evaluate the effect on subsurface BTX fate and transport, and intrusion into the building. By adjusting the ventilation rate, building underpressurizations of between 10 and 30 Pa have been achieved. Sustained depressurization had a significant effect on BTX vapour profiles below the centre of the building, as indicated in Figure 4.16. The two depressurization tests incorporate different time periods between the start of the depressurization experiment and sampling; therefore, the test results are likely affected by transient vapour fate and transport and gradual build-up of vapour concentrations below the foundation slab. This may be the reason for higher concentrations for the test conducted at -10 Pa.

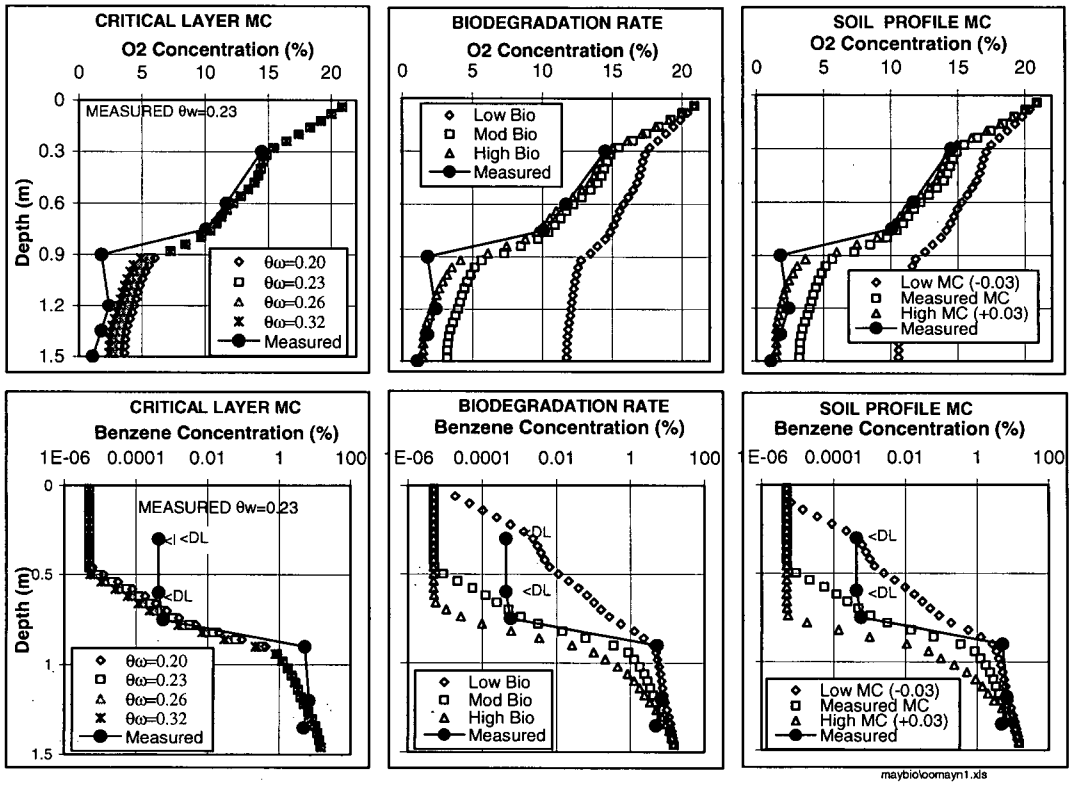

Figure 4.15. 1-D diffusion & reaction (Model No. 4) model sensitivity for (i) critical layer (0.88-0.92 m) moisture content (constant moderate biodegration rate), (ii) biodegradation rate +/-60% of moderate rate (constant measured moisture content), & (iii) soil profile volumetric moisture constant +/-0.03 (constant biodegradation rate) (steady-state conditions).

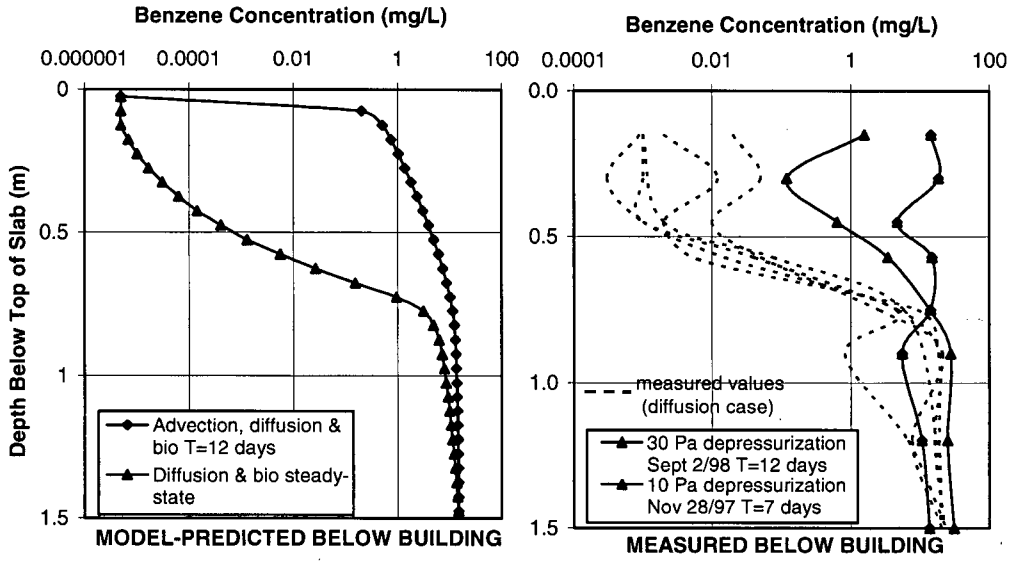

Figure 4.16. Comparison of measured and model-predicted vapour concentrations below building for 2-D advection, diffusion, and reaction (model no. 4) (moderate biodegradation rate, $\eta = 0.001$, $\tau_{dust} = 1.0$, $k = 10$ darcy, $\Delta P = 5$ Pa. $\Delta L = 1.4$m, initial concentrations for advection case are steady-state diffusion and biodegradation concentrations)

Advective soil gas transport was simplistically assumed to be uniform and 1-D in direction (*i.e.*, vertically upwards) below the centre of building. Model simulations presented in Figure 4.16 are intended to simulate the –10 Pa test. The soil gas specific discharge was estimated using a pressure gradient equal to –10 Pa divided by the depth (1.4 m). The soil air permeability used was $1x10^{-11}$ m^2 (~10 darcy), and was based on *in situ* permeability tests (Hers and Zapf-Gilje, 1998). The assumed longitudinal dispersivity was 0.1 m. The model-predicted results indicate that advective transport potentially has a significant effect on BTX and O_2 concentrations, and that O_2 below the building is depleted in a few days.

The evaluation of advective transport is preliminary and work is on-going to develop a calibrated 2-D soil gas flow model, to be used in conjunction with the chemical transport model. Initial measurements and model predictions presented in this paper suggest that advective transport can be significant relative to diffusive transport only, when there is shallow contamination, permeable soils and pressure-coupling between the building and underlying soils. It is also noted that the sustained depressurization of the building also likely prevented natural advective pumping to occur. Advective pumping may be the cause of the elevated O_2 levels below the building, as described in Section 4.4.

CONCLUSIONS

The results of monitoring and model simulations indicate that biodegradation through aerobic respiration is an important attenuation process at the Chatterton research site. Measured first- and zero-order BTX degradation rates were relatively high and similar to those reported in other published laboratory and field studies. Through use of the measured BTX concentration profile and the results of an *in situ* respiration test, a novel bi-linear method for approximating Monod-kinetics is presented. Model simulations obtained using a 2-D numerical model incorporating diffusion, sorption and biodecay indicated that both biodegradation kinetics (*i.e.*, first- versus zero-order) and consideration of O_2 transport and availability to mineralize hydrocarbons is critical. Due to the high BTX concentrations at the Chatterton site, first-order rates overestimate biodegradation above a critical BTX concentration.

Diffusive O_2 transport in porous media is primarily controlled by moisture content and varies over several orders-of-magnitude. For this reason, both seasonal variations in precipitation and infiltration, and variations in soil type and water retention can have a significant effect on O_2 diffusivity, biodegradation, and hence hydrocarbon concentrations. Diffusive O_2 transport through materials such as concrete building slabs is more complex but generally thought to be relatively low compared to the effective diffusivity in porous media, except when the moisture content in soil is close to saturation levels. It is clear that building characteristics and size, and the surface cover adjacent to buildings will have a significant effect on diffusive O_2 transport.

Model-predictions and measurements suggest that advective processes may also have an important effect on BTX fate and transport below the building at the Chatterton site. Under natural conditions, soil gas pumping through variation in barometric pressure and temperature may be resulting in O_2 replenishment below the building. During sustained and relatively high building depressurization, advective chemical transport results in much higher BTX concentrations at shallow depths.

Implications for risk assessment for the soil vapour transport to indoor air pathway are several-fold. First, there is clear evidence from this and other studies that vadose zone biodegradation rates for BTEX or other readily degraded hydrocarbon compounds can, in many cases, be significant, and that predictive models should include the possibility of including bioattenuation. The challenge lies primarily in determining when inclusion of biodegradation is appropriate, particularly when the objective is to predict future exposure and risk prior to changes in site conditions. It is suggested that biodegradation modeling should include careful site-specific consideration of soil types, possible seasonal variation in moisture conditions, potential future construction of barriers that would reduce O_2 transport to subsurface soils, and advective processes.

REFERENCES

Andreoni, V., G. Origgi, M. Colombo, E. Calcaterra, and A. Colombi. 1997. Characterization of a biofilter treating toluene contaminated air. *Biodegradation* 7:397-404.

American Society for Testing and Materials (1995). Standard Guide for Risk-Based Corrective Action Applied at Petroleum Release Sites (E-1739-95).

Bekins, B.A., E. Warren, and E.M. Godsy. 1998. A comparison of zero-order, first-order and monod biotransformation models. *Groundwater*, 36 (2), March-April.

Burlage, R.S., R. Atlas, D. Stahl, G. Geesey, and G. Sayler. (editors), 1998. Techniques in Microbial Ecology. Oxford University Press, New York, Oxford.

Conrad, M.E., P.F. Daley, M.L. Ficher, B.B. Buchanan, T. Leighton, and M. Kashgarian. 1997. Combined ^{14}C and del^{13}C monitoring of in Situ biodegradation of petroleum hydrocarbons. *Environ. Sci. Technol.*, 31(5):1463-1469.

Craig, H. 1957. Isotopic standards for carbon and oxygen and correction factors for mass-spectrometric analysis of CO_2. *Geochem-Cosmochmin Acta*, 12: 133-149.

DeVaull, G., 1997. Biological and other loss mechanisms associated with gasoline volatilization from in-situ soils. Presentation at Petroleum Environmental Research Forum (PERF) Workshop, Brea California, February 6 and 7.

DeVaull, G., R.A. Ettinger, J.P. Salanitro, and J. Gustafson., 1997. Benzene, toluene, ethylbenzene and xylenes degradation in vadose zone soils during vapour transport: first-order rate constants. Proceedings of 1997 Petroleum Hydrocarbons and Organic Chemicals in Ground Water, API/NGWA, Houston, Texas, November, 365-379.

DeVaull, G., R. Ettinger, J. Gustafson. 2002. Chemical Vapor Intrusion from Soil or Groundwater to Indoor Air: Significance of Unsaturated Zone Biodegradation of Aromatic Hydrocarbons, *Soil and Sediment Contamination*, Vol. 11, No. 4, pp. 625-641.

Domenico, P.A. 1987. An analytical model for multidimensional transport of decaying species. *J. of Hydrology*, 91 (1/2):47-58.

Fan, C-Y. and S. Krishnamurthy. 1995. Enzymes for enhancing bioremediation of petroleum-contaminated soils: a brief review. *J.Air & Waste Manage. Assoc.* 45:453-460.

Fischer, M.L., A.J. Bentley, K.A. Dunkin, A.T. Hodgson, W.W. Nazaroff, R.G. Sextro, and J.M. Daisay. 1996. Factors affecting indoor air concentrations of volatile organic compounds at a site of subsurface gasoline contamination. *Environ. Sci. Technol.* 30:2948-2957.

Franzmann, P.D., L.R. Zappia, T.R. Power, G.B. Davis, and B.M. Patterson. 1999. Microbial mineralisation of benzene and characterisation of microbial biomass in soil above hydrocarbon-contaminated groundwater. *FEMS Microbiology Ecology.* 30:67-76.

Haines, J.R., B.A. Wrenn, E.L. Holder, K.L. Strohmeier, R.T. Herrington, and A.D. Venosa. 1996. Measurement of hydrocarbon-degrading microbial populations by a 96-well plate most-probable number procedure. *Journal of Industrial Microbiology.* 16:6-41.

Hers, I. and R. Zapf-Gilje. 1998. Canadian consortium research project – field validation of soil gas transport to indoor air pathway. Proceedings of 1998 Petroleum Hydrocarbon and Organic Chemicals in Ground Water, API/NGWA, Houston, Texas, November 11-13, 251-266.

Hers, I., R. Zapf-Gilje, L. Li, and J. Atwater. 1999. Measurement of in situ gas-phase diffusion coefficient. *Environmental Technology,* **21**, 631-640.

Holden, P.A., L.J. Halverson, and M.K. Firestone. (1997). Water stress effects on toluene biodegradation by *Pseudomonas putida*. Biodegradation 8, 143-151.

Jeng, C.Y, V.J. Kremesec, Jr., and H.S. Primack. 1996. Models of hydrocarbon vapour diffusion through soil and transport into buildings. Proceedings of 1996 Petroleum Hydrocarbon and Organic Chemicals in Ground Water, API/NGWA, Houston, Texas, November 13-15, 319-338.

Johnson, P.C., W. Kemblowski, and R.L. Johnson. 1998. Assessing the Significance of Subsurface Contaminant Vapour Migration to Enclosed Spaces – site specific alternatives to generic estimates. API Publication.

Jury, W.A., D. Russo, G. Streile, H. El Abd. 1990. Evaluation of volatilization by organic chemicals residing below the soil surface. *Water Resources Research.* 26(1):13-20.

Laubacher, R.C., P. Bartholomae, P. Velasco, and H.J. Reisinger. 1997. An evaluation of the vapour profile in the vadose zone above a gasoline plume. Proceedings of 1997 Petroleum Hydrocarbon and Organic Chemicals in Ground Water, Houston, Texas, November, 396-409.

Li, D.X., 1995. Bioventing feasibility assessment and system design using subsurface oxygen sensors. *Air & Waste Management Association.* 45:762-769.

Kissel, J.C., 1985. Numerical simulation of mixed-culture biofilms. Ph.D. thesis, Stanford University, Stanford, California.

MacQuarrie, K.T.B., E.A. Sudicky, E.O. Frind. 1990. Simulation of biodegradable organic contaminants in groundwater 1. Numerical formulation in principal directions. *Water Resources Research.* 26 (2):207-222.

Massman, J. and D.F. Farrier. 1992. Effects of atmospheric pressures on gas transport in the vadose zone. *Water Resources Research.* 28 (3):777-791.

Millington, R.J. and Quirck., 1961. Permeability of porous solids. *Trans. Farady Soc.* 1200-1207.

Monod, J. 1949. The growth of bacterial cultures. *Annual Review of Microbiology.* 3:371-394.

Nielson, K.K., V.C. Rogers, R.B. Holt, T.D. Pugh, W.A. Grondzik, and R.J. de Meijer. (1997). Radon penetration of concrete slab cracks, joints, pipe penetrations, and sealants. *Health Physics.*

Ostendorf, D.W. and D.H. Kampbell. 1991. Biodegradation of hydrocarbon vapours in the unsaturated zone. *Water Resources Research.* 27 (4):453-462.

Renken, K.J. and T. Rosenberg. 1995. Laboratory measurement of the transport of radon gas through concrete samples. *Health Physics.* 68 (6):800-808.

Ririe, T. and R. Sweeney. 1995. Fate and transport of volatile hydrocarbons in the vadose zone. Proceedings of 1995 Petroleum Hydrocarbon and Organic Chemicals in Groundwater, Houston, Texas, 529-542.

Simpkins, S., and M. Alexander. 1984. Models for mineralization kinetics with the variables of substrate concentration and population density. *Applied and Environmental Microbiology.* 47 (6):1299-1306.

U.S. EPA. 1995. Bioventing Principles and Practice. EPA/540/R-95/534a. September.

Van der Velde, K.D., M.C. Marley, J. Studer, and D.M. Wagner. 1995. Stable carbon isotope analysis to verify bioremediation and bioattenuation. Monitoring and Verification of Bioremediation, Ed. Robert Hinchee, Gregory Douglas and Say Kee Ong, Batelle Press, Columbus, Ohio.

Wiedemeier, T.H., Miller, R.N., Wilson, J.T. and Kampbell, D.H., 1995. Significance of anaerobic processes for the intrinsic bioremediation of fuel hydrocarbons. Proceedings of 1995 Petroleum Hydrocarbon and Organic Chemicals in Ground Water, API, Houston, Texas, November, 49-61.

Wiedemeier, T.H., M.A. Swanson, J.T. Wilson, D.H. Kampbell, Miller and J.E. Hansen. 1996. Approximation of biodegradation rate constants for monoaromatic hydrocarbons (BTEX) in ground water. *Ground Water Monitoring and Remediation.* Summer:186-194.

Wu, G., B. Conti, A. Leroux, and R. Brzezinski. 1999. A high performance biofilter for VOC emission control. *J. Air & Waste Manage. Assoc.* 49:185-192.

Zwick, T.C., A. Leeson, R.E. Hinchee, R.E. Hoeppel, L. Bowling. 1995. Soil moisture effects during bioventing in fuel-contaminated arid soils. In Third International In Situ and On-Site Bioreclamation Symposium. Vol. 3(2). In Situ Aeration. San Diego, California, Batelle Press.

CHAPTER 5

MEASUREMENT OF BTX VAPOUR INTRUSION INTO AN EXPERIMENTAL BUILDING

This chapter is in preparation for submission for journal publication.

ABSTRACT

Measurements of vapour intrusion were used to evaluate subsurface vapour intrusion at a site contaminated with benzene, toluene and xylene (BTX). Although models are now commonly used to predict vapour intrusion for human health risk assessment, there have been only few comprehensive studies involving direct measurement techniques. These studies are important from a methods development perspective and for model validation purposes. Research methods included construction of an experimental greenhouse followed by measurement of soil gas flow and BTX flux into the greenhouse using tracer test and flux chamber techniques. Results indicate subslab vapour concentrations were low and no vapour intrusion was detectable for the non-depressurized greenhouse case. Significant vapour levels and intrusion were measured when the greenhouse was depressurized to –10 and –30 Pa. At –2.5 Pa depressurization, vapour levels below the middle of the greenhouse were elevated; however, concentrations remained low near the foundation slab edge crack, which was where most soil gas intrusion into the greenhouse occurred. As a result, no detectable vapour intrusion could be detected for the –2.5 Pa case. The soil gas flow rates into the depressurized greenhouse (-10 and –30 Pa cases), backcalculated from the tracer tests, were on the order of 0.35 to 2.8 L/min (0.001 and 0.005 L/min-Pa-m^2). The flux chamber tests gave similar results when scaled to account for the estimated total crack length. The soil gas flow rates predicted by an analytical model for flow to a perimeter edge crack and a groundwater model (MODFLOW) adapted to simulate soil gas flow were also similar to measured values. Advection and aerobic biodegradation processes had a significant effect on the soil vapour regime, as evidenced by subslab oxygen monitoring.

KEY WORDS: flux chamber, tracer, soil gas, intrusion, BTX, building

INTRODUCTION

The use of predictive models to evaluate the potential for soil vapour intrusion into buildings has become commonplace over the past decade (ASTM, 1995; CCME, 2000). Modeling of soil vapour intrusion is typically performed when implementing a risk-based corrective action approach at sites where soil or groundwater is contaminated with volatile organic compounds (VOCs). In contrast, measurement of soil vapour intrusion into buildings is rare with only a limited number of published studies, most of which address radon intrusion research (Nazaroff *et al.*, 1987; Garbesi and Sextro, 1989; Hodgson *et. al*, 1992; Garbesi *et al.*, 1993; Fischer *et al.*, 1996, Olson and Corsi, 2001). Consequently, there is little experience with both direct measurement techniques (*e.g.*, flux chambers), and the use of VOC measurements and tracer tests, which involve estimating intrusion rates from concentration data. While measurement of VOC intrusion is challenging and not routinely conducted, these types of tests can provide insight on processes for vapour intrusion and be used to evaluate predictive models.

The primary purpose of this paper is to describe the use of dynamic flux chamber and tracer tests for the estimation of VOC-vapour mass flux and soil gas flow into a greenhouse building constructed for research purposes at a former petro-chemical plant ("Chatterton research site") impacted by benzene, toluene and m&p-xylene (BTX) releases. In addition, measured soil gas flow rates are compared to those predicted using analytical models and a numerical model for groundwater flow (MODFLOW), which was adapted to enable prediction of soil gas flow. The paper concludes with practical implications for the prediction of soil vapour intrusion into buildings, as derived from these aspects of the research program. The benefits of this work are new or adapted methods for the measurement and prediction of vapour intrusion into buildings, and insight on the importance of building depressurization, soil gas advection and biodegradation on vapour intrusion. Other related aspects published include general research program information (Hers and Zapf-Gilje, 1998), biodegradation of BTX vapours (Hers *et al.*, 2000), and model validation (Hers *et al.*, 2002, 2003).

BACKGROUND REVIEW AND CASE STUDIES

Multiple processes within the vadose zone ("far-field") and subsurface building envelope and nearby soil ("near-field") influence soil vapour intrusion into buildings at sites contaminated with subsurface VOCs. These processes include volatilization, diffusion, advection, biodegradation and sorption. Several field studies at VOC-contaminated sites suggest that soil gas advection into a depressurized building can result in much higher flux rates compared to those predicted by diffusion alone, provided that the soil air permeability is sufficiently high and vapour contamination source is relatively shallow. (Hodgson *et. al*, 1992; Adomait, 1992). Several radon studies also suggest that VOC intrusion by advection is typically a much more significant process than diffusion (Garbesi and Sextro, 1989; Nazaroff, 1992).

Advective soil gas flow through the building envelope can occur through untrapped drains, perimeter cracks at the building wall and floor slab interface, service penetrations, expansion joints and other cracks, if present. The perimeter or "edge" crack between the building wall and floor slab is typically the most significant pathway for soil gas entry, for residential construction (Figley and Snodgrass, 1992). Positive pressure gradients between soil and building (*i.e.*, higher pressures in soil) can develop through mechanisms that lower the pressure in a building such as

ventilation system operation, temperature differences between indoor or outdoor air (e.g., stack effect through rise of warm air in a building) and wind-loading (Nazaroff, 1992).

Transient atmospheric pressure fluctuations were shown to have a small effect on time-averaged advective radon entry, contributing about the same amount of radon flux as diffusion, for a study involving an experimental basement (Robinson and Sextro, 1997). For sustained indoor-outdoor pressure differences greater than 1.5 Pa, the radon flux increased significantly and the atmospheric pressure fluctuations had essentially no effect on the time–averaged radon entry rate. A study of methane and VOC intrusion into a townhouse complex in Kitchener, Ontario, measured cross-foundation pressure differences and found that rapid changes in barometric pressure generated transient cross-slab pressures of up to 500 Pa when the subslab foundation layer was not well vented to atmosphere (*i.e.*, confined by low permeability material) (Fugler and Adomait, 1997). Negligible cross-slab pressures were generated for houses with well vented subslab foundation soils.

Several studies have involved the estimation of soil gas flow into buildings under sustained depressurization by injecting an inert tracer not found in ambient air (sulfur hexafluoride, SF_6) below a building followed by indoor air measurements. The soil gas flow rate (Q) and flow rate normalized to foundation area and pressure difference ($Q/Area*\Delta P$) for three tracer studies involving the use of SF_6 are summarized below:

- Soil gas flow rate of about 20 L/min at -20 Pa depressurization (0.04 L/min-m^2-Pa) estimated for a small-scale test basement (Garbesi *et al.*, 1993).
- Soil gas flow rate of 4.5 L/min at –10 Pa depressurization (0.009 L/min-m^2-Pa) estimated for a small commercial slab-at-grade building (Fischer *et al.*, 1996).
- Soil gas flow rates between 2.5 and 6.7 L/min for tests conducted at –1.6 Pa, -3.65 Pa, -6.02 and –6.22 Pa (0.03 to 0.05 L/min-m^2-Pa) estimated based on results for two relatively small houses with basements (Olson and Corsi, 2001).

Most published flux chamber protocols and studies (Kienbusch, 1986; Eklund and Schmidt, 1990) are for estimation of gaseous emissions from land surfaces, as opposed to vapour intrusion into buildings. One study of vapour intrusion through a foundation slab indicated indoor air concentrations predicted using a flux chamber were within a factor of four of the measured air concentrations (Schmidt and Zdeb, 1998). This study found it important to conduct a thorough survey of potential emission sources, account for the crack length, and perform a sufficient number of flux measurements to generate a representative emission rate into the structure.

SOIL GAS MODELS

Analytical Models

Screening models used to estimate indoor air quality from sub-surface VOCs are typically analytical or semi-analytical solutions for steady-state one-dimensional vapour transport, which couple diffusion through the vadose zone with diffusion and soil gas advection through the building foundation. Three analytical models that have been proposed for prediction of soil gas advection into buildings are discussed below.

The ***Perimeter Crack Model*** is commonly used in conjunction with the Johnson and Ettinger (1991) model. This model is an analytical solution for two-dimensional soil gas flow to a small horizontal drain intended to simulate flow to an edge crack along the perimeter of a building (Nazaroff, 1992):

$$Q_{soil} = \frac{2\pi\, k_a\, \Delta P\, X_{crack}}{\mu \ln\left(\frac{2\, z_{crack}}{r_{crack}}\right)} \qquad \eta = \frac{r_{crack}\; X_{crack}}{A_B} \tag{1a,b}$$

where Q_{soil} is the soil gas flow (L^3T^{-1}), k_a the soil gas permeability (L^2), ΔP the pressure difference ($M\, L^{-1}\, T^{-2}$), X_{crack} the perimeter crack length (L), μ is the gas viscosity ($M\, L^{-1}\, T^{-1}$), z_{crack} the depth to crack (L), r_{crack} is the crack width (L), η the ratio of cracks to total sub-surface foundation area (*i.e.*, base and walls), and A_B the subsurface foundation area (L^2). Equation 1a is similar to the Thiem equation for steady-state groundwater flow to a horizontal drain. The Perimeter Crack Model takes into account both the properties of the soil and foundation crack.

The ***Parallel Plate Model***, based on the Hagen-Poiseuille Relationship, is an analytical solution for one-dimensional soil gas flow between smooth parallel plates intended to simulate flow through cracks in a building foundation (Hers *et al.*, 1997):

$$Q_{slab} = \frac{k_{slab}\, b\, w\, \Delta P}{L_c} \tag{2}$$

$$w = \frac{2A_b}{S_C} \qquad k_{slab} = \frac{b^2}{12\,\mu} \qquad \eta = \frac{b}{S_C} \tag{3a,b,c}$$

where Q_{slab} is the soil gas flow (L^3T^{-1}), k_{slab} the foundation slab permeability (L^2), b the crack width (L), S_C the crack spacing (L), w the crack width (L), L_c the foundation (concrete) thickness (L). The Parallel Plate Model only takes into account the foundation slab properties.

An analytical solution for one-dimensional soil gas flow, which does not take into account foundation characteristics, is the third model. The soil gas flow regime is either formulated in terms of one-dimensional upward flow to a foundation slab (Ferguson *et al.*, 1995), or radial flow to a depressurized sphere representing a basement (Rezvan *et al.*, 1988). The pressure gradient is the building depressurisation divided by the distance over which advection occurs.

Numerical Models

Numerical models have been developed for radon research purposes. For example, a three-dimensional finite difference model for radon advection and diffusion in soil coupled with an analytical solution for advection through an edge crack situated at the floor/wall interface was developed to simulate radon intrusion (Loureiro, 1990). This study found that for intrinsic permeabilities (k) below about $1\text{x}10^{-12}$ m^2, diffusive radon transport dominated, while for k values above $1\text{x}10^{-12}$ m^2, advective transport dominated. As discussed later in this paper,

numerical groundwater flow models such as MODFLOW have been adapted to predict soil gas flow, although to our knowledge, these types of models have not been used to predict soil gas intrusion into a building.

Empirical Methods

A method utilized for radon assessments is the equivalent leakage area (ELA) method (Figley, 1997). The ELA is obtained by developing an empirical relationship between the soil gas flow into a building and building depressurization, as follows. First, the leakage into a building or across an individual element (*e.g.*, foundation crack) is measured as a function of pressure, with C_b and n being fitted constants (n is 0.5 for turbulent flow and 1 for laminar flow):

$$Q_b = C_b * \Delta P^n \tag{4}$$

where Q_b is the soil gas flow into building. If the leakage into a building or room is measured, it must be scaled to reflect only the soil gas component. Next, the flow for an equivalent opening or orifice (Q_e) is estimated:

$$Q_c = C_e * ELA * (2g * \Delta H)^{0.5} \qquad \Delta H = \frac{\Delta P}{\rho * g} \tag{5a,b}$$

where ρ is the air density [$M\,L^{-3}$], and g the gravitational constant [$L\,T^{-2}$].

The *ELA* is obtained by setting Q_b equal to Q_e. The *ELA* is dependent on the flow coefficient C_e used, and the pressure difference. In Canada, these parameters have been standardized to C_e equal to 0.61 and ΔP equal to 10 Pa (CSGB, 1986) while in the US, the standard values are C_e equal to 1 and ΔP equal to 4 Pa (Grimsrud *et al.*, 1982). Due to the often non-linear relationship between flow and pressure, the *ELA* is specific to the reference pressure chosen (CSGB, 1986; Grimsrud *et al.*, 1982). The *ELA* approach can be used to develop a general predictive equation for soil gas flow (Q_s) through the building foundation (Figley, 1997), as follows:

$$Q_s = 3.6\left(C\ \Delta P^n\right) \qquad C = \frac{ELA}{\{0.0001157(\rho)^{0.5}\ 10^{n-0.5}\}} \tag{6a,b}$$

where C is a gas flow coefficient ($L^3T^1\ Pa^{-n}$). While the *ELA* framework is not used to analyze data for this study, there are important insights that can be gained from this area of research. For one detailed air leakage study of ten homes, the largest *ELAs* were for untrapped open floor drains (8.5 cm^2 to 50 cm^2) (Figley and Snodgrass, 1992). Somewhat lower *ELAs* were otained for floor/wall edge cracks (0.15 cm^2 to 16 cm^2), while the lowest *ELAs* were measured for hairline cracks surrounding utility penetrations. Depending on the crack properties, soil gas flow may be turbulent resulting in a non-linear pressure versus flow relationship.

EXPERIMENTAL METHODS

Research Site Description

The former Chatterton petrochemical plant is located in Delta, B.C. Near-surface soil in the plant area consists of fill (about 3.5 m thick) underlain by native silt. The fill is comprised of sandy silt to fine sand with trace organic matter (up to 0.3 m thick), underlain by dredged river

sand. The depth to the water table ranges from 1.5 to 2.5 m below ground surface. Releases of BTX from sources removed from the study site combined with lateral migration on the water table resulted in a distinct zone of residual non-aqueous phase liquid (NAPL) distributed vertically over an approximate 1 m interval (i.e., approximate water table fluctuation). No other hydrocarbon compounds are present at the plant site. Average annual precipitation at a nearby weather station (*i.e.*, 7 km from site), considered to approximate site conditions, is 1240 mm (Richmond Nature Park).

Description of Greenhouse, Soil Gas Probes and Soil-Air Permeability Testing

A small greenhouse with internal volume of 125 m^3 was constructed at the Chatterton site for research purposes in August 1997 (Figure 5.1). A greenhouse-type building was selected due to cost considerations. The greenhouse was constructed using an aluminum frame covered with plastic and mechanically ventilated using a wall-mounted fan with two sets of air-inlet louvres installed at the opposite wall from the fan. The greenhouse ventilation rate (fan exhaust) was measured using a rotometer. Multiple rotometer measurements over a grid pattern were made to obtain an average air flow rate. The greenhouse was fastened to a 6.1 by 9.3 m at-grade concrete slab of 125 mm nominal thickness. The edge of the concrete slab was poured on top of a wood strip footing, intended to simulate the footings that often extend to greater depths at the edge of a slab (Figure 5.2). The surface sandy silt to fine sand below the building footprint was replaced with sand fill and the foundation slab during construction. The sand fill placed below the foundation slab was dredged river sand similar in gradation to the underlying fill. The sand fill directly below the slab was compacted to approximately 90% Modified Proctor maximum dry density (ASTM D1557).

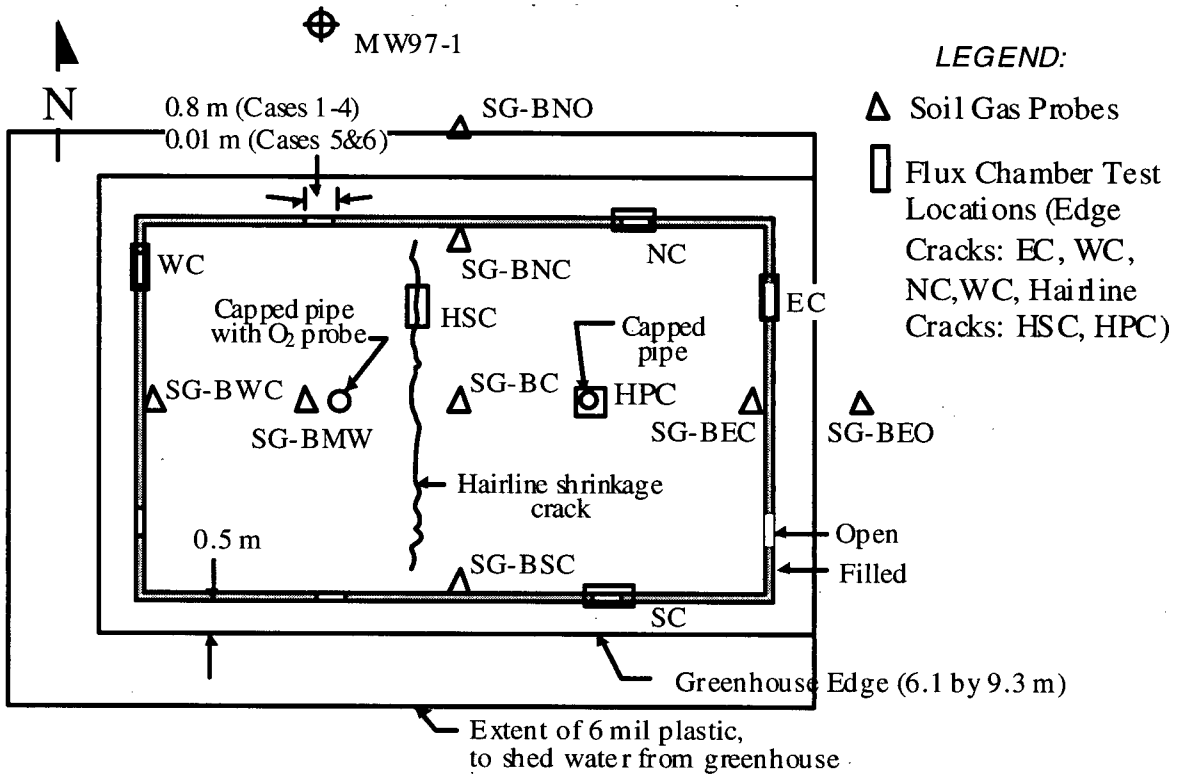

Figure 5.1. Schematic of Concrete Slab and Soil Vapour and Flux Chamber Testing Locations

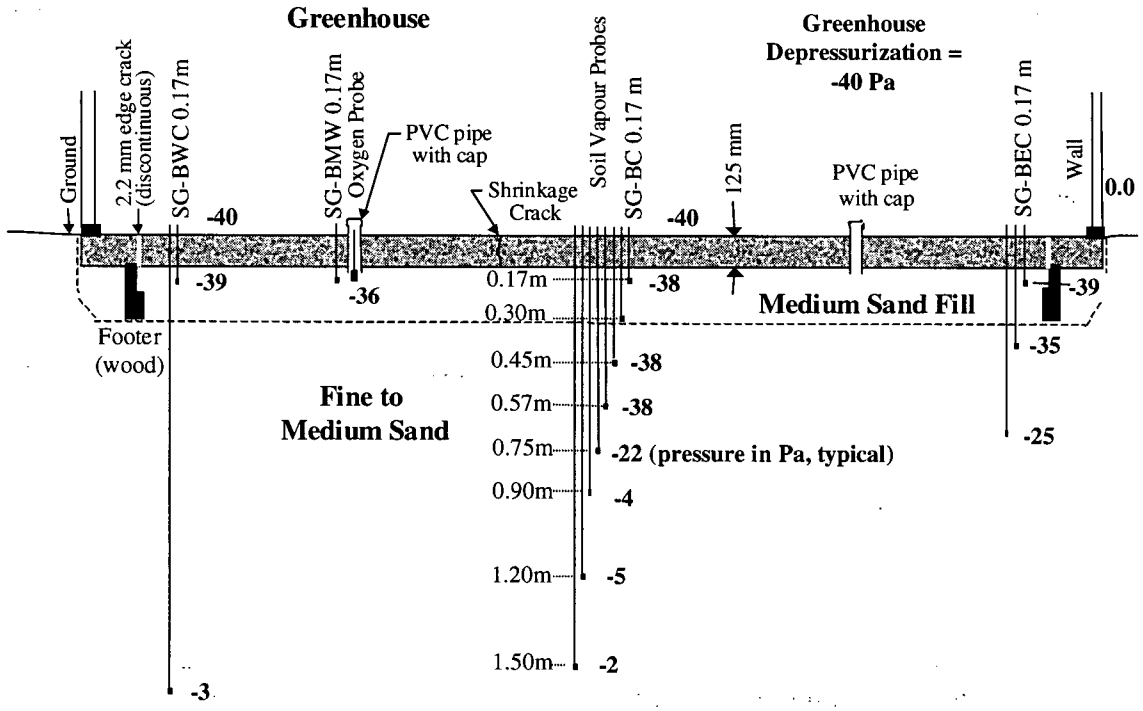

Figure 5.2. Cross-Section of Greenhouse (pressures measured December 1, 1997 during greenhouse depressurization to -40 Pa, Case 3 conditions)

The concrete slab was constructed with an approximate 2.2-mm wide crack near the edge of the slab. The edge crack was formed using steel plates that were pulled just before the concrete set. Steel plates and infilling using cement grout were subsequently used to vary the open portion of the edge crack. Within a few weeks of pouring the slab, an approximate north-south trending hairline shrinkage crack developed. The crack, which bi-sected the entire width of the slab, is consistent with shrinkage that would be expected for a 9.3 m long slab. Upon close scrutiny, several hairline cracks were observed primarily near the edges of the slab. These hairline cracks were less prominent than the main shrinkage crack.

Prior to pouring the slab, numerous steel soil gas probes and two 100 mm diameter PVC pipes were installed. Soil gas probes were constructed of either 6.25 mm or 12.5 mm internal diameter hollow steel with 50 mm long perforated or slotted tips, and were driven to the desired depth. At each probe cluster below the building, a shallow probe was installed between 0.15 m and 0.2 m below the top of slab. Additional deeper probes were installed at typically 0.15 to 0.3 m intervals at most probe cluster locations. Probes were equipped with dedicated miniature inert 3-way valves, one port was connected to a 30 cm by 0.75 mm stainless steel tube inserted in the probe, while the other two ports had Teflon luer lock male connectors. The PVC pipes extended 0.05 m below the bottom of the concrete slab and were fitted with a slip cap.

Soil-air permeability tests were conducted at soil gas probes according to the method described in Garbesi *et al.* (1996). This test measures soil air permeability within a small radius

of the probe tip (0.1 m is suggested by Fischer *et al.* (1996)). Tests were conducted using a range of flow rates (3.1 to 12.6 cm^3/sec) and pressures (43 to 160 Pa).

Soil Gas, Pressure, Temperature and Oxygen Monitoring Methods

Soil gas samples were collected in gas-tight glass and Teflon syringes while indoor and outdoor air samples were collected using sorbent tubes (Carbotrap 300, Supelco Inc.). The sorbent tube sampling flow rate ranged between 125 and 200 ml/min. The sampling flow rate was checked before and after sampling using 1-10-100 ml soap film flowmeters (Hewlett Packard) and varied by less than five percent. The sampling duration ranged between 30 and 1200 minutes, and depending on the anticipated BTX concentration. Shorter times were used for the greenhouse samples when BTX concentrations were elevated. Syringe and sorbent samples were analyzed for BTEX using a SRI 8610 gas chromatograph with photoionization detector (GC/PID). The GC/PID capillary column was a DB-624 30 m by 0.53 mm column with a methylated phenoxy stationary phase (1.8 μm thickness). Sorbent tubes were initially desorbed onto a focussing tube using a Dynatherm Analytical Instruments Model 850 thermal tube desorber. The focussing tube was subsequently desorbed allowing compounds to be introduced into the GC. The quality control program for this testing is described in Hers *et al.* (2003).

Differential pressures between inside and outside air, and soil gas probes (*i.e.*, representative of soil pressures adjacent to probe openings) were measured using a micromanometer (Microtector, Dwyer) and two differential pressure transducers (Model 264, Setra Systems). One pressure transducer had a full-scale range of 63 Pa while the second had a full-scale range of 125 Pa. The reported accuracy for both was one percent of the full-scale range. A Datawrite Research Co. Model XT252 electrochemical cell and datalogger was used to measure O_2 concentrations below the building slab near location SG-BMW (Figures 5.1 and 5.2).

Flux Chambers

Two flux chambers were constructed to measure soil gas flow rates and BTX flux through the slab (Figure 3). The flux chambers were constructed primarily of stainless steel with internal dimensions of 910 mm by 90 mm by 90 mm (7.4 litre volume), and 340 mm by 200 mm by 90 mm (6.1 litre). A 35 mm wide steel flange was located at the base of the flux chamber. A 3 mm thick nitrile or rubber strip was used to seal the chamber to the concrete slab, or to a stainless steel base plate used during blank tests. At each location where slab soil gas intrusion tests were conducted, eight bolts were installed into the concrete by drilling holes and then grouting the bolts in. The seal between the flux chamber and concrete was checked using a feeler gauge, and nuts were tightened until no gaps were detected. Flux chamber valves consisted of fine adjustment steel needle values while tubing consisted of Teflon except for a short portion of vinyl tubing at the peristaltic pump (Manostat Varistaltic V/P-1A). When sampling with air replacement (valve #4 open, valve #3 closed), air passed through an activated carbon filter (replacement with an inert gas was deemed impractical). Air flow rates were measured using 1-10-100 ml soap film flowmeters. Each flux chamber was also equipped with threading ports that could be used to measure pressure.

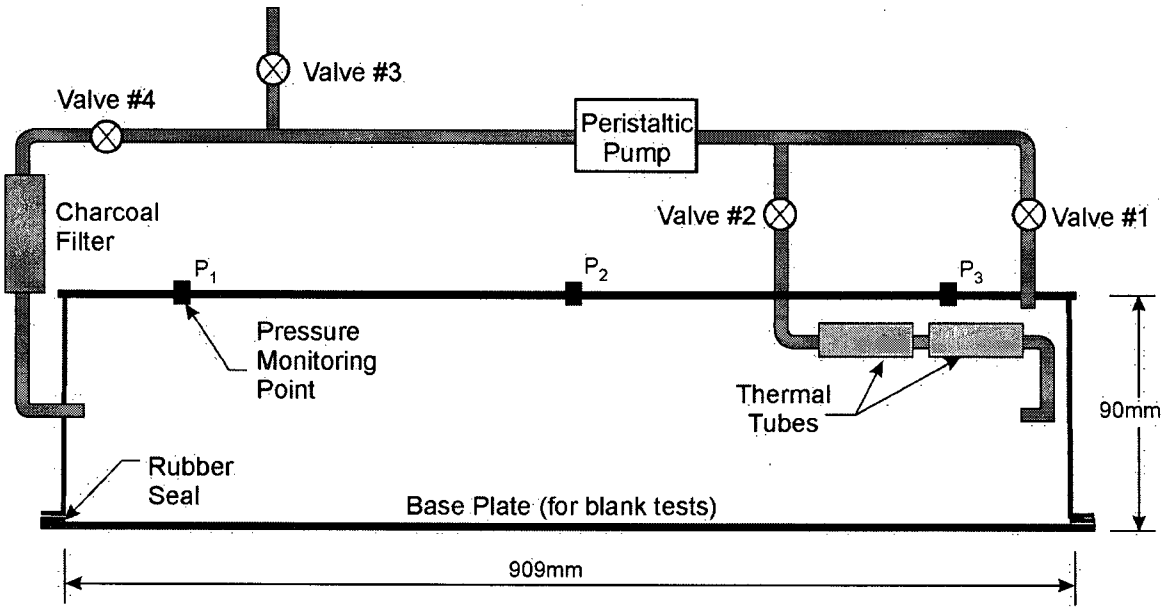

Figure 5.3. Schematic of Flux Chamber

Soil Gas Flow Rate and BTX Flux into Greenhouse Measured Using Tracer Test

For each test case the following was measured: BTEX concentrations in indoor air and outdoor air, BTEX vapour concentrations at six shallow soil gas probes located directly below the slab (SG-BC, SG-BEC, SG-BSC, SG-BWC, SG-BNC, SG-BMW, Figure 5.1), the pressure difference between both indoor and outdoor air, and indoor air and sub-slab soil gas, indoor temperature, and greenhouse ventilation rate (for the depressurized condition). For some cases, sub-slab oxygen concentrations and soil temperatures were also measured. Between two and four indoor and outdoor air samples were analyzed for each test case. Indoor air samples for the non depressurized cases were collected in the approximate middle of the greenhouse. For the sustained depressurization cases, indoor air samples were collected 1.5 m from the fan inlet at approximately the same height.

The soil gas flow rate and BTX flux were estimated using the mean indoor, outdoor and subslab BTX vapour concentrations, and building ventilation rate (*i.e.*, mass balance approach). Assuming diffusive mass flux is negligible compared to advective mass flux, the following mass balance holds:

$$Q_{soil} * C_{subslab\ vapour} = C_{indoor}\,(Q_{soil} + Q_{build}) \quad (7)$$

Assuming that $Q_{build} >> Q_{soil}$ results in:

$$Q_{soil} \sim Q_{build}\, C_{indoor}/C_{sub\text{-}slab\ vapour} \quad (8)$$

$$Flux = Q_{soil} * C_{sub\text{-}slab\ vapour} \quad (9)$$

Uniform mixing of BTX in the greenhouse is assumed. The use of BTX as a tracer is subject to potential interference through sorption and the presence of background levels in ambient air.

Soil Gas Flow Rate into Greenhouse Measured Using Flux Chamber

The soil gas flow rate into the greenhouse through the edge crack was measured at four locations. The procedure used was: (i) bolt-down flux chamber over edge crack, (ii) depressurize greenhouse to desired level using ventilation fan, (iii) draw air through flux chamber using peristaltic pump with valves #1 and 3 open and valve #4 closed, (iv) adjust chamber air flow rate until the pressure in the flux chamber and greenhouse was approximately the same, (v) measure the flux chamber air flow rate. Differential pressures were measured using a micromanometer. Equilibration of pressure between the flux chamber and greenhouse minimizes possible local pressure and flow perturbations, and hence inaccurate soil gas flow estimates (Figley *et al.*, 1991).

A similar procedure was used to measure flows through shrinkage and hairline cracks except that sampling with partial replacement with flux chamber air. By partially opening valves #3 and #4 (Figure 5.3), The inflow rate to the chamber was adjusted to less than the outflow rate. Sampling with partial replacement was needed to facilitate larger air flow rates, since the peristaltic pump was not capable of providing accurate stable flows below about 200 ml/min.

At selected crack locations, the differential pressure between the flux chamber and greenhouse was also measured for varying flux chamber air flow rates. When the chamber flow rate was very low, the pressure in the chamber was lower than that in the greenhouse. For higher flow rates, the pressure in the chamber was higher than in the greenhouse. By taking a number of measurements and plotting the results, the soil gas flow rate at the zero differential pressure intercept was estimated. The flow rate and pressure variability was evaluated by taking repeat measurements for each flow rate and depressurization. Potential leakage through flux chamber valves was evaluated by sealing the flux chamber to the steel base plate, and measuring the vacuum in the flux chamber as a function of flow rate.

BTX Flux Rates into Greenhouse Measured Using Flux Chamber

The BTX flux rate through edge and shrinkage/hairline cracks was obtained by measuring (i) the mass of BTX retained in sorbent tubes (Carbotrap 300, Supelco), or (ii) the BTX concentration in Tedlar bags and multiplying by the flux chamber flow rate. The BTX concentrations in flux chamber air were estimated by dividing the BTX mass by the volume of air drawn through the sorbent tube.

Extensive testing of blanks was conducted prior to initiating the flux chamber testing program. The blank tests were conducted by securing a stainless steel base plate to the chamber and sampling with complete air replacement (i.e., valve #3 closed, valve #4 open). Multiple blanks runs interspersed with chamber decontamination were continued until the BTX concentrations in air were appropriately the same or less than those in outdoor air. To achieve these levels, it was found that extensive decontamination of all materials (chamber, seal, tubing, valves) was required. The decontamination protocol consisted of a hot-water and soap wash, rinse and low temperature (70°C) bake for at least two days.

The flux chamber was bolted to the concrete over the edge crack and sealed using a rubber gasket. Five chamber volumes were initially purged at 5 L/min (valve #1 open). For Case 1 (no

depressurization), sampling with complete replacement at a flow rate between 150 and 300 ml/min was used (valves #1 and #3 closed, valve #2 and #4 open). The sorbent samples were collected over 240 to 1200 minutes. During the tests, the differential pressure between the chamber and greenhouse was periodically measured using a micromanometer. No pressure gradient was detected between the flux chamber and greenhouse. For the Case 4 edge crack tests (-10 Pa depressurization), sampling without replacement at a flow rate of 500 ml/min was used (valves #1 and 4 closed, valve #2 and 3 open). Previous testing had indicated that the pressure in the flux chamber and greenhouse were equal at an approximate chamber flow rate of 500 ml/min. The sorbent samples were collected over 60 to 1200 minutes. For the Case 4 shrinkage crack test (-10 Pa depressurization), sampling with partial replacement was used (valve #1 closed, valve #2 open, values #3 and 4 partially open). The valves were adjusted until the net flow rate (flow out – flow in) was 10 ml/min.

EXPERIMENTAL RESULTS

Overview Soil Gas Intrusion Testing Program

Soil gas flow rates and BTX flux into the greenhouse were measured using flux chamber and tracer test methods for the test cases described in Table 5.1. For the no greenhouse depressurization case, the louvres were open, and the door was periodically opened providing some natural ventilation. For the sustained depressurization cases, the differential pressure between indoor and outdoor air was frequently measured (at least twice daily) and the fan-speed was adjusted as required to ensure that the mean differential pressure was approximately equal to the target pressure. The differential pressure between indoor and outdoor air, during sustained depressurization, was found to vary by up to +/- 1.5 Pa. A preliminary depressurization test with a continuous 2.2 mm wide edge crack indicated that soil gas flow rates through the slab were high with little pressure drop across the slab. For this reason, portions of the crack were sealed with concrete grout. For Cases 1 to 4 there were eight 0.8 m long open edge cracks, which corresponded to a crack ratio of about 0.0003 (Table 5.1, Figure 5.1). For Cases 5 and 6, steel inserts were placed in the edge crack further reducing the edge crack length to 0.08 m and crack ratio to about 0.0001. The estimated crack length and crack ratio are approximate.

Soil Air Permeability

The measured soil-air permeability at each soil gas probe location varied between 30 and 60 % depending on pressure, which ranged between 43 to 160 Pa. Correcting for density and gas slippage (Klinkenberg) effects did not significantly reduce the pressure-dependent variation in permeability observed.

The soil-air permeability was measured at six probes below the greenhouse at depths between 0.15 m and 1.5 m below the slab. The mean soil air permeability (over the range of test pressures) ranged between 5.6×10^{-12} m^2 (1.2 m) and 2.7×10^{-11} m^2 (0.15 m). While the soil moisture content was not concurrently measured at the same time as soil-air permeability, the high soil-air permeability at the shallow 0.15 m probe below the slab may have been due to low moisture content, which was lowest in soil immediately below the slab.

Soil Gas Flow Rate and BTX Flux into Greenhouse Measured Using Tracer Test

The soil vapour, indoor and outdoor air concentrations, and soil gas flow rate (Q_{soil}) and BTX flux estimated using equations 8 and 9 are presented in Table 5.2. The subslab soil vapour concentrations near the edge crack for Case 2 (no depressurization) and Case 6 (-2.5 Pa depressurization) were low and in most cases less than about 1 ug/L. The subslab vapour concentrations for Cases 3, 4 and 5 (depressurization of –10 and –30 Pa), while variable, were elevated and generally much higher than for Cases 2 and 6. The subslab vapour concentrations near the middle of the slab were significantly higher than those measured at the edge crack.

Statistical hypothesis testing indicated that the mean indoor and outdoor concentrations were significantly different for Cases 3, 4 and 5, when evaluated using a two-tailed test and significance level of 0.05. The differences in indoor and outdoor concentrations were not statistically significant for the non depressurized greenhouse (Cases 1 and 2), and for –2.5 Pa depressurization (Case 6), although it is recognized that only a limited number of samples were analyzed. The Q_{soil} into the greenhouse, estimated using equation 8, ranged between 0.35 and 2.8 L/min, while the benzene and toluene mass flux ranged between 0.86 and 10 mg/min for Cases 3, 4 and 5. There did not appear to be a relationship between soil gas flow rate, and depressurization and crack ratio, although the difference in crack ratio was not significant. The highest estimated soil gas flow rates were obtained for a moderate depressurization (-10 Pa) and lowest crack ratio (Case 5). This may reflect the approximate nature of the tracer test or other factors discussed below.

Soil Gas Flow Rates Measured Using Flux Chamber

Soil gas flow rates at four edge crack locations were measured for a greenhouse depressurization of -10 Pa (Case 4) (Figure 5.1). Each edge crack was 0.8 m long and 2.2 mm wide (the flux chamber length was 0.9 m). The measured flow rates per crack at pressure equilization were on the order of 0.4 to 0.6 L/min.

Detailed measurements of flux chamber air flow rate versus depressurization were made at three locations: (i) south edge crack, (ii) shrinkage crack that bi-sected the slab, and (iii) capped PVC pipe. A small hairline crack surrounded a portion of the PVC pipe. The flux chamber was sealed over the capped PVC pipe.

Table 5.1. Summary of Soil Intrusion Test Cases

case no.	condition	date	ventilation rate (m^3/min)	estimated length edge cracks (m) Width = 2.2 mm	estimated length hairline cracks (m) Width ~ 0.1 mm	crack ratio η	flux chamber tests	tracer tests
1	no depressurization	nov. 97	N/A	6.4	48	0.00033	yes	yes
2	no depressurization	june/july 98	N/A	6.4	48	0.00033	no	yes
3	- 30 Pa depressurization	nov. 97	30	6.4	48	0.00033	yes	yes
4	- 10 Pa depressurization	aug./sept. 98	10	6.4	48	0.00033	yes	yes
5	- 10 Pa depressurization	nov./dec. 98	10	0.08	61	0.00011	no	yes
6	-2.5 Pa depressurization	aug. 99	4	0.08	61	0.00011	no	yes

Notes: Crack ratio is the open crack area divided by the slab area.
The hairline crack width is assumed

Table 5.2. Results of Soil Gas Intrusion Tests

		Case 1 No Depressurization η = 0.00033		Case 2 No Depressurization η = 0.00033		Case 3 ΔP = -30 Pa η = 0.00033 Q_b=30 m^3/min		Case 4 ΔP = -10 Pa η = 0.00033 Q_b=10 m^3/min		Case 5 ΔP = -10 Pa η = 0.00011 Q_b=10 m^3/min		Case 6 ΔP = -2.5 Pa η = 0.00011 Q_b=4 m^3/min	
	Location	**Benzene**	**Toluene**	**Benzene**	**Toluene**	**Benzene**	**Toluene**	**Benzene**	**Toluene**	**Benzene**	**Toluene**	**Benzene**	**Toluene**
Subslab Soil Vapour Conc. (ug/L)													
Middle Probes	SG-BC 0.15 m	-	-	<1	6	1580	5300	14430	19970	12980	16640	3814	3693
	SG-BMW 0.17 m	-	-	220	730	16820	19400	9370	14330	9380	13870	793	1538
Edge Crack Probes	SG-BNC 0.17 m	-	-	<1	1	8	240	130	140	2000	3060	<0.05	0.26
	SG-BSC 0.17 m	-	-	1	5	160	500	2410	4000	6420	9040	<0.05	0.21
	SG-BEC 0.17m	-	-	1	4	1030	3650	3.0	9.0	1130	880	<0.05	0.16
	SG-BWC 0.17m	-	-	<1	1	330	1410	24	11	430	770	<0.05	0.23
Subslab Soil Vapour	Weighted Average			28	93	2491	3813	3296	4808	4042.5	5533	576	654
Indoor Air Conc. (ug/L)	Average	0.018	0.061	0.0014	0.0099	0.044	0.21	0.29	1.72	1.48	2.55	0.0040	0.00589
	RSD	95	68	79	51	104	21	36	31	23	25	54	61
Outdoor Air Conc. (ug/L)	Average	0.010	0.022	-	-	0.015	0.060	0.0045	0.019	-	-	0.00157	0.00169
	RSD	79	97	-	-	80	76	69	67	-	-	172	148
In - Out Air Conc. (ug/L)	Average	0.0072	0.035	-	-	0.029	0.15	0.29	1.70	1.48	2.55	0.0024	0.0042
Soil Gas Flow Rate (L/min)		N/A	N/A	N/A	N/A	0.35	1.2	0.52	2.1	2.2	2.8	N/A	N/A
BTX Flux Rate (mg/min)		N/A	N/A	N/A	N/A	0.86	4.4	1.7	10	8.9	15	N/A	N/A

The edge crack tests indicate that pressure equalization between the flux chamber and greenhouse was achieved using a chamber sampling flow rate of about 1 to 2 L/min at -20 Pa greenhouse depressurization (July 31st test) and 2 to 3 L/min at -30 Pa (July 20th test) (Figure 5.4). The error bars for the pressure readings correspond to +/- 2 standard deviations, based on the average standard deviation measured for ten sets of four repeat measurements. Scaling the -20 and -30 Pa depressurization results to -10 Pa suggests that a chamber flow rate of about 0.5 to 1 L/min would have provided for pressure equalization.

The shrinkage crack and PVC pipe tests indicate that it was not possible to measure the flux chamber air flow rate at pressure equalization. It appears that the air flow rate at zero pressure differential was less than 0.02 L/min (Figure 5.5). Qualitatively, it can be stated that the air flow rate through shrinkage and hairline cracks is much less that for the edge crack; however, these small cracks do transmit some air flow when compared to the air leakage test for a sealed flux chamber. A photograph of a concrete core subsequently taken from the hairline crack testing location suggests a continuous crack through the concrete (Figure 5.6).

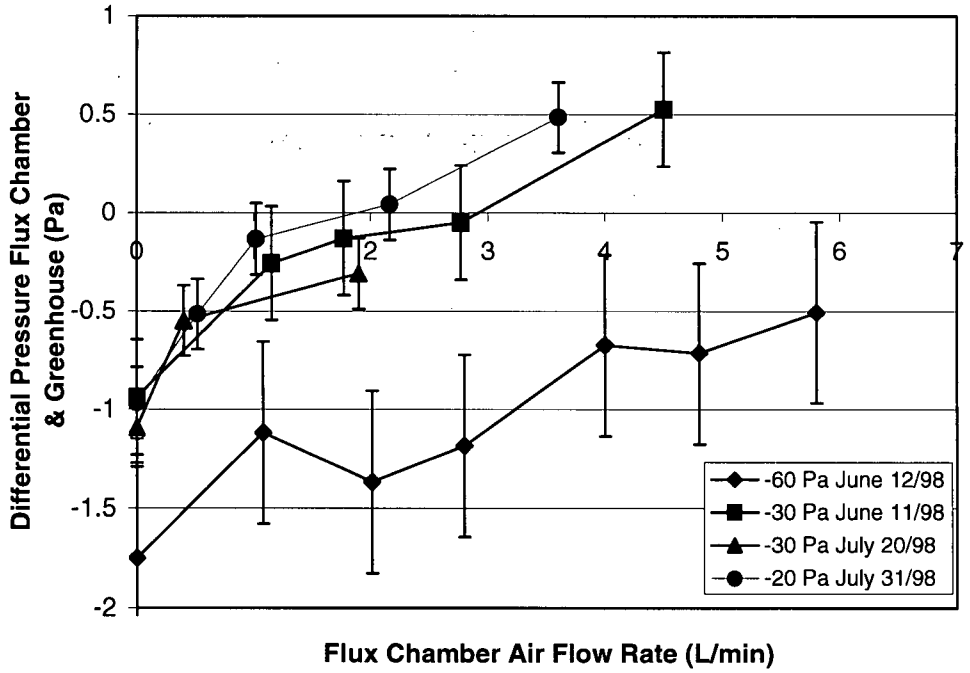

Figure 5.4. Flux Chamber Soil Gas Flow Rates Through South Edge Crack

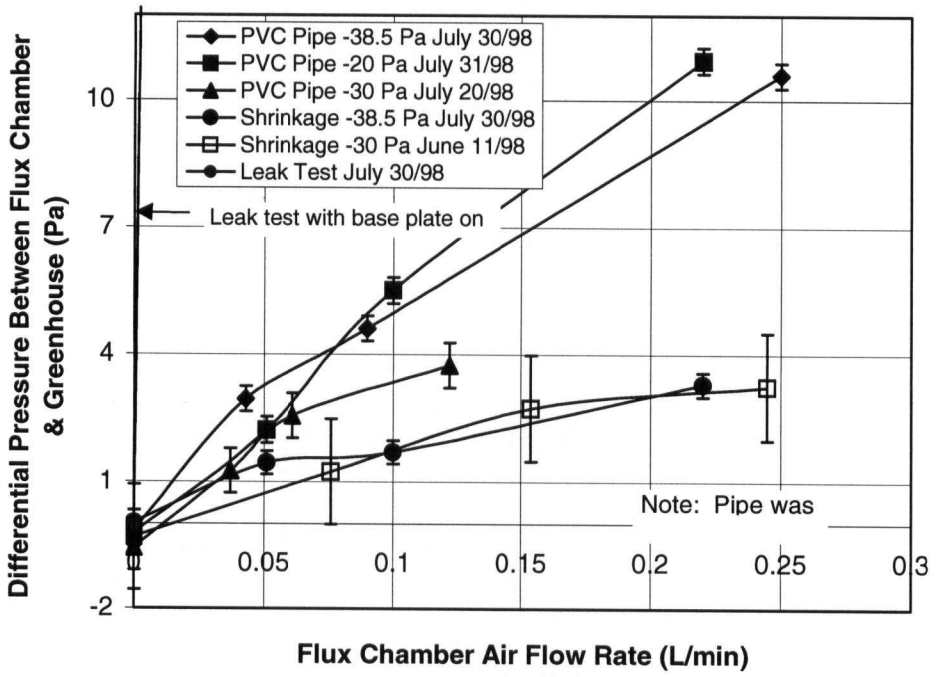

Figure 5.5. Flux Chamber Soil Gas Flow Rates Through Hair Line Cracks (note, PVC pipe was capped during test)

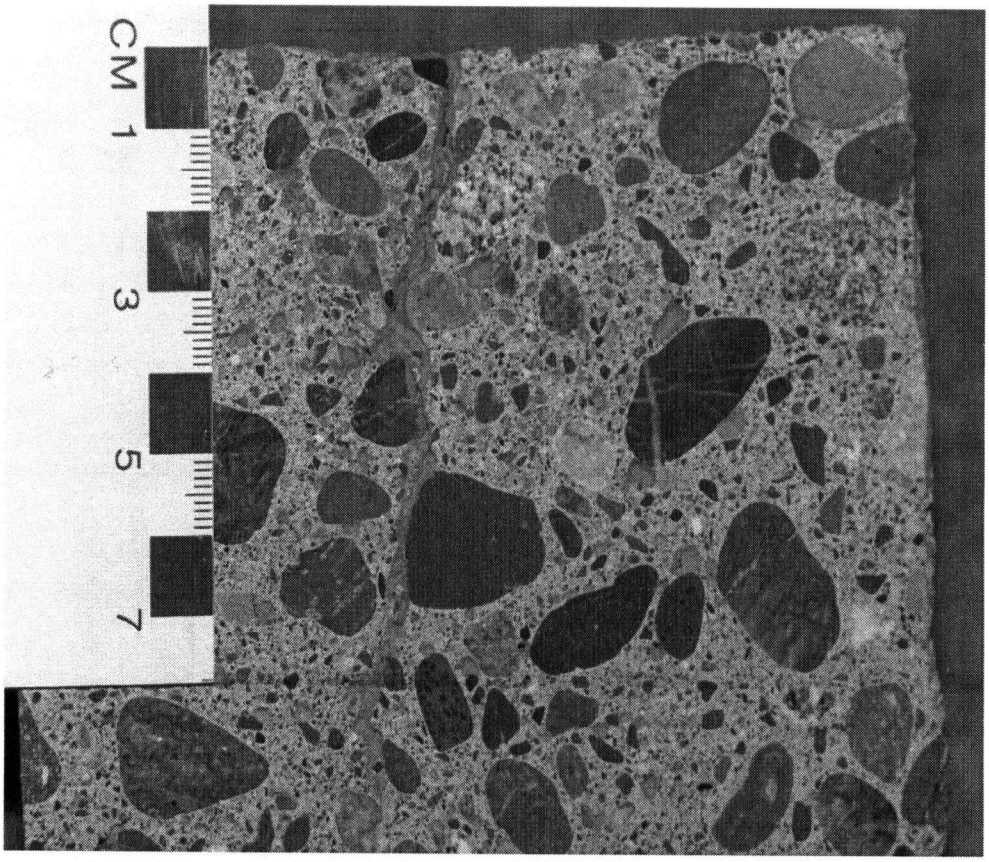

Figure 5.6. Concrete Core Through Hair Line Crack

BTX Flux Rates into Building Measured Using Flux Chamber

The BTX mass flux rates were measured at four edge crack locations for the non depressurized (Case #1) and –10 Pa depressurization (Case #4) conditions (Table 5.3). For the non-depressurized greenhouse (Case 1), the benzene and toluene concentrations in the flux chamber were low and similar to or less than the outdoor air (background) concentrations. For the edge crack and –10 Pa depressurized condition (Case 4), the benzene and toluene concentrations in air ranged between 20 and 637 ug/L. The benzene and toluene mass flux rates per individual edge crack ranged between 10 and 368 ug/min (Table 5.3).

The BTX flux was also measured through the shrinkage crack for –10 Pa depressurization. Significantly lower concentrations and flux were measured. The benzene and toluene flux chamber concentrations were both 1.3 ug/L. The benzene and toluene mass flux for the shinkage crack was 1.5 and 1.4 ug/min, respectively.

Non Depressurized Condition

For the non-depressurized condition, the subslab oxygen concentrations (SG-BMW) generally ranged between about 5 and 14 percent. Monitoring during the fall of 1997 (non-depressurized condition) indicated that during periods of rainfall the oxygen concentrations below the slab decreased while during dry periods the oxygen concentration increased (Figure 5.7).

Table 5.3. BTX Flux Chamber Concentrations and Flux into Greenhouse at Edge Cracks

	Case 1 No Depressurization		Case 4 -10 Pa Depressurization	
	Benzene	**Toluene**	**Benzene**	**Toluene**
Average Concentration (ug/L)				
East	0.0024	0.0046	24	47
West	0.00028	0.0025	20	31
South	0.00022	0.0018	380	423
North	0.0011	0.0089	913	637
Average Flux (ug/min)				
East	N/A	N/A	10	20
West	N/A	N/A	13	19
South	N/A	N/A	148	165
North	N/A	N/A	368	257
Total 4 Edge Cracks	N/A	N/A	539	460

Note: Case 1 utilized sorbent tube (1 measurement per crack location)
Case 3 utilized Tedlar bags (3 to 5 measurements per crack location, RSDs ranged between 3 and 40 %).

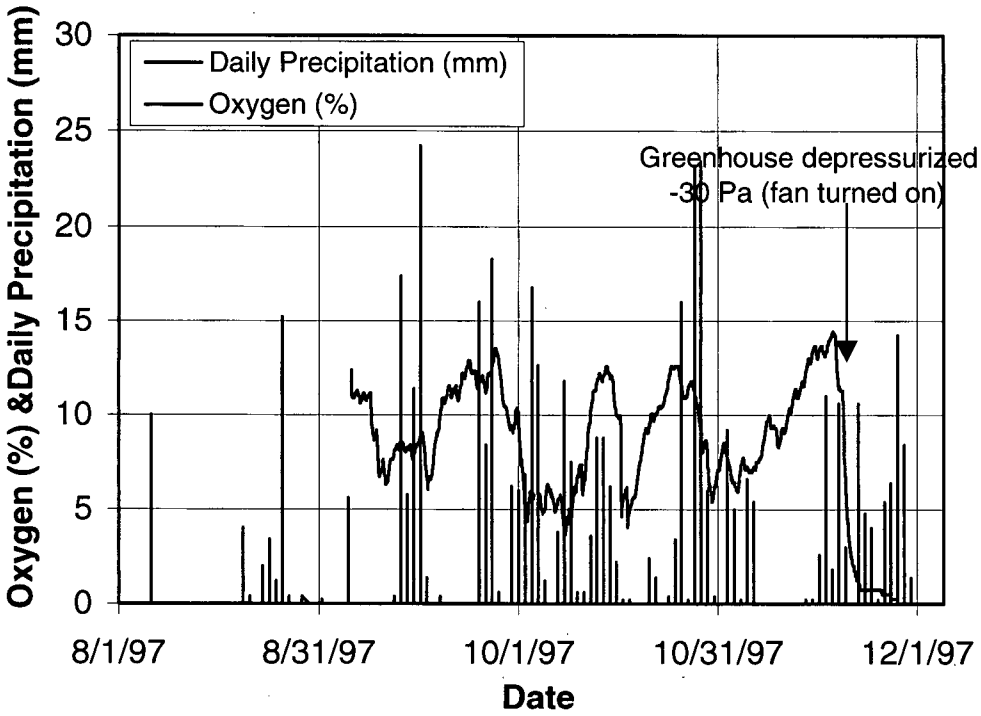

Figure 5.7. Subslab Oxygen below greenhouse – Fall 1997 (O_2 probe located near probe SG-BMW)

Subslab Oxygen, Pressure and Weather Monitoring

Monitoring during the summer of 1998 indicated diurnal fluctuations in subslab oxygen of up to 1 percent correlated to changes in pressure of up to 3 Pa due to daytime heating of the greenhouse (Figure 5.8). Qualitatively, there appeared to be an inverse relationship between the temperature and pressure in the greenhouse (relative to outdoor air) and the subslab oxygen concentrations. As the temperature and pressure increased during daytime hours, the oxygen decreased.

Depressurized Condition

Monitoring conducted for a greenhouse depressurization of –40 Pa (December, 1997) indicated the average pressure gradient across the slab was about 1 Pa at the edge crack probes, about 2 Pa at the centre probe (SG-BC), and about 4 Pa at the probe near the oxygen sensor (SG-MW) (Figure 5.2). The higher gradient across the slab at SG-BMW suggests a less permeable slab in this area. The results indicate that most of the pressure drop is across the soil (as opposed to slab) with significant pressure coupling between the greenhouse and underlying sand to a depth of about 0.75 m based on the centre probes. The negative pressures (-2 Pa, -3 Pa) at the deep soil gas probes (1.5 m) may be an artifact of inaccurate pressure measurements.

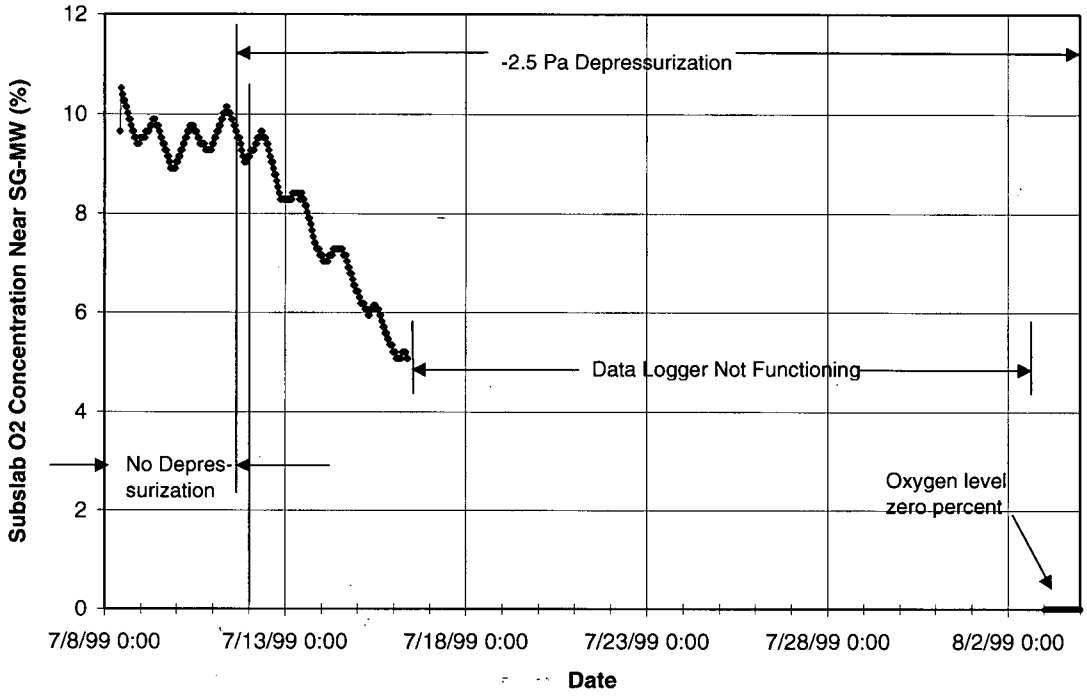

Figure 5.8. Subslab Oxygen Monitoring – Summer 1998.
(O_2 Probe located near probe SG-BMW).

The oxygen monitoring indicated that when the greenhouse was subject to sustained depressurization (–30 Pa), the subslab oxygen (SG-BMW) decreased to less than 0.5 % within about three days and remained low (Figure 5.7). The decrease in subslab oxygen during depressurization of the greenhouse to –2.5 Pa was more gradual (Figure 5.8). Although there is missing data due to a malfunctioning data logger, it appears that it would have taken about nine to ten days for oxygen to have been depleted. The slower oxygen depletion at –2.5 Pa depressurization is possibly a result of a lower rate of BTX flux to shallow soil below the greenhouse.

COMPARISON TO MODEL PREDICTIONS

The Flow to Perimeter Crack Model (equation 1a) was used to estimate the soil gas flow rate into the greenhouse for input parameters corresponding to Case 4. The Q_{soil} was estimated for both the edge cracks (r_{crack} = 2.2 mm, X_{crack} = 640 cm, Z_{crack} = 30 cm) and hairline cracks (r_{crack} = 0.1 mm, X_{crack} = 4800 cm, Z_{crack} = 30 cm). The building depressurization was 10 Pa and estimated soil-air permeability based on tests was $1x10^{-11}$ m^2 (10 Darcy). The estimated Q_{soil} was 2.4 L/min for the edge cracks and 11.6 L/min for the hairline cracks. In comparison, the tracer test Q_{soil} was 0.5 to 2.1 L/min for Case 4. The Perimeter Crack Model is most sensitive to soil air permeability, building depressurization and crack length (X_{crack}), but is not sensitive to crack width. For this reason, the model-predicted flows for the hairline crack are higher than the edge crack flows even though the edge crack area is 3X the hairline crack area (141 cm^2 versus 48 cm^2). The higher predicted flows through the hairline crack are suspect when compared to the tracer test values and open area available for soil gas advection, and suggest that the

Perimeter Crack Model is less accurate when used to predict soil gas flow through small hairline cracks.

The numerical model MODFLOW was also used to simulate soil gas flow through the greenhouse concrete slab through analogy of the groundwater and airflow equations (ASTM D5719-95, Guo and Neville, 1998). This is accomplished through substitution of air-phase parameters and variables into the groundwater flow equations. The one-dimensional groundwater flow equation for a homogeneous, isotropic porous media is:

$$K \frac{\partial^2 h}{\partial X^2} = S_S \frac{\partial h}{\partial t} \tag{11}$$

where K denotes the hydraulic conductivity [$L\ T^{-1}$], h the hydraulic head [L], and S_s the specific storage [L^{-1}]. Groundwater flow models typically assume fluid compressibility to be negligible. Airflow models incorporate air compressibility according to the ideal gas law. The resulting nonlinear air flow equation is linearized by expressing it in terms of air pressure squared as suggested by Muskat and Botset (1931) for modeling gas reservoirs. The linearized form of the air flow equation can be written as:

$$k \frac{\partial^2 P^2}{\partial X^2} = \frac{\theta_g \mu}{P_o} \frac{\partial P^2}{\partial t} \tag{12}$$

where k is the air permeability [L^2], μ the air viscosity [$ML^{-1}T^{-1}$], θ_g the air filled porosity, and P_o the ambient (atmospheric) pressure [$ML^{-1}T^{-2}$]. If one first divides both sides of equation 2 by μ, and multiplies both sides by gas density ρ and gravitational constant g, equations 11 and 12 are identical if the following relationships are recognized:

$$h \Leftrightarrow P^2$$

$$S_a \Leftrightarrow \theta_g \rho g / P_o$$

$$K \Leftrightarrow k \rho g / \mu$$

where S_a is the air storage coefficient [L^{-1}]. The simplifying assumptions needed to arrive at the linear airflow equation include Darcy's Law is valid for air flow, the elevation component of pneumatic head is neglected, isothermal conditions are assumed, the ideal gas law is assumed for gas compressibility, and the Klinkenberg effect is neglected.

The MODFLOW model was used to simulate soil gas flow into the greenhouse when depressurized for Cases 4 and 5 (Figure 5.9). The surface outside and inside the greenhouse was represented using constant head boundaries. The difference in head was equivalent to 10 Pa. The soil-air permeability was estimated using the field tests described earlier, except for the surface soil layer (Unit 1), which was an assumed value for a silty sand to fine sand.

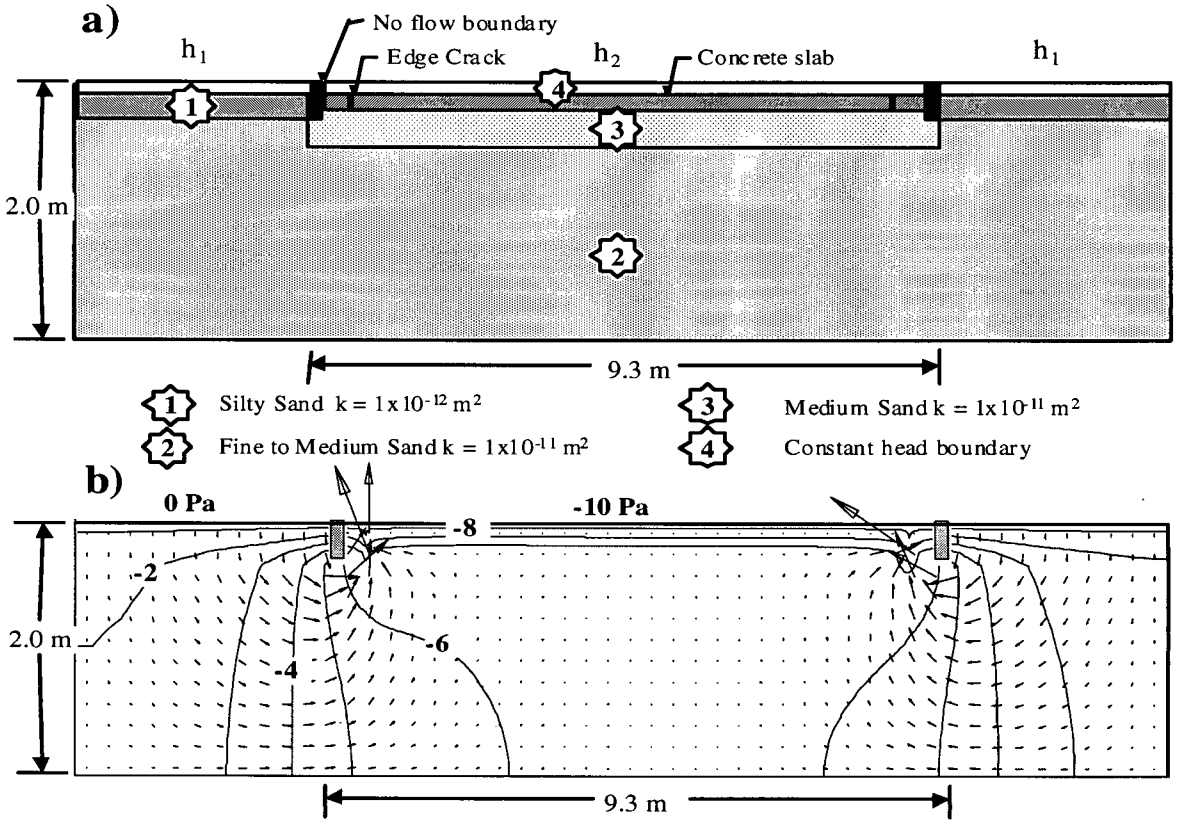

Figure 5.9. Results of Modflow Modeling
a) Domain and Permeabilities, b) Flow Vectors and Equipotentials

The simulation of air flow through the concrete slab presented significant challenges. The approach taken was to estimate separate permeability values for the (i) edge crack, and (ii) concrete slab including hairline cracks. The permeability of the edge and hairline crack was estimated using the Hagen-Poiseuille relationship. The air conductivity for laminar flow between two parallel plates is:

$$K^{HP} = \rho g b^2 / 12 \mu \tag{13}$$

The edge crack (2.2 mm wide) was too narrow to simulate using MODFLOW. As an approximation, a larger crack was incorporated in the MODFLOW domain, but the air conductivity of the edge crack (K^{HP}_{EC}) was scaled using a linear relationship, as follows:

$$K^{MODFLOW}_{EC} = K^{HP}_{EC} * Area_{Edge\ Crack} / Area_{MODFLOW\ Edge\ Crack} \tag{14}$$

The permeability of a concrete slab with hairline cracks is considered impossible to accurately estimate. As a crude approximation, the air permeability for a hairline crack (K^{HP}_{HC}) was scaled using the ratio of the hairline crack to total slab area to obtain the permeability of the slab, as follows:

$$K^{MODFLOW}_{SLAB} = K^{HP}_{HC} * Area_{Hairline\ Crack} / Area_{SLAB} \tag{15}$$

The MODFLOW predicted air flow vectors indicate most soil gas flow into the greenhouse is through the edge crack. For Case 4, the predicted Q_{soil} through the edge crack was 4.5 L/min, while the Q_{soil} through the slab (hairline cracks) was 0.3 L/min. For Case 5, the predicted Q_{soil} through the edge crack was 4 L/min, while the air flow through the slab was 0.4 L/min. These values are on the same order as the Q_{soil} predicted by tracer test, which ranged between 0.5 and 2.8 L/min.

The MODFLOW simulations indicate that most of the pressure drop between ambient and greenhouse air is across the soil (as opposed to slab), which is consistent with pressure monitoring presented earlier. In addition, the results indicate that partial sealing of the edge crack did not significantly reduce the soil gas flow rate.

DISCUSSION

The tracer test results show the importance of building depressurization and advective flux on soil vapour intrusion into the greenhouse. For the non depressurized case, the difference between indoor and outdoor concentrations was not significant and sub-slab vapour concentrations were low. While the experimental results discussed in this paper are limited to the near-field conditions below and inside the greenhouse, the research study also included extensive deeper soil vapour testing (Hers *et al.*, 2000). This testing indicated for the non-depressurized case there was significant bioattenuation of BTX vapours between about 0.4 and 0.8 m depth below the slab, and a significant reduction of oxygen levels over the same depth interval. Although the greenhouse was not mechanically depressurized, there were still short-term pressure fluctuations of up to 3 Pa due to temperature variations, and possibly also due to barometric pressure changes and wind loading. However, there was no net positive pressure gradient between subslab soil and the greenhouse. As described below, *sustained* depressurization of the greenhouse was required before there were significant changes to the subslab vapour concentrations and vapour intrusion into the greenhouse.

For the –2.5 Pa case, the subslab BTX vapour concentrations near the edge crack remained low, which is inferred to be a result of aerobic biodegradation. Near to the middle of the greenhouse, the subslab vapour concentrations were elevated suggesting the biodegradation capacity based on oxygen transport was exceeded in this area. There was no significant difference between the indoor and outdoor concentrations for the –2.5 Pa case. Since most of the advective soil gas flow into the greenhouse is through the edge crack, the indoor air concentrations were controlled by the low subslab vapour concentrations near the edge crack, and not the elevated levels closer to the middle of the slab. The results highlight the lateral variability in subslab BTX concentrations and influence of vapour biodegradation.

For the –10 and –30 Pa cases, the subslab BTX vapour concentrations were elevated both near the middle and edges of the slab, and the indoor air concentrations were much higher than outdoor air concentrations. In addition, the oxygen was depleted below the slab. The likely reason for the high subslab vapour concentrations and low oxygen concentrations is that the upward advective flux of BTX vapours exceeded the biodegradation capacity based on transport of oxygen to below the slab. In addition, the sustained depressurization would have prevented the temperature- and pressure-induced pumping of air into and out of the subslab soil below the greenhouse.

The oxygen monitoring provides insight into the complex relationship between fate and transport of BTX vapour and oxygen, biodegradation of BTX vapours, and temperature and seasonal weather fluctuations. This is seen through (i) longer term fluctuations in oxygen correlated to rainfall patterns, (ii) diurnal fluctuations in oxygen correlated to variation in greenhouse temperature and pressure, and (iii) the decrease in subslab oxygen when the greenhouse was depressurized. The longer-term monitoring (Fall 1997) showed subslab oxygen concentrations decreased during periods of sustained wet weather, but increased during dry weather. We believe the reason for this trend is related to oxygen transport rates through surface soil to below the foundation slab combined with consumption of oxygen through BTX biodegradation. During periods of rain, the soil moisture is higher in the finer-grained surface soils, which causes oxygen transport through either diffusion or advection to be lower resulting in decreased oxygen below the slab.

The diurnal variation in subslab oxygen concentrations (up to one percent) for the non depressurized condition was likely caused by pressure fluctuations and movement of gas below the greenhouse. When the pressure in the greenhouse decreased, the subslab oxygen level increased possibly as a result of atmospheric air entering subslab soil adjacent to greenhouse and then moving toward the centre of the greenhouse toward the zone of lower pressure. An increase in pressure resulted in a decrease in oxygen, which may have been due to movement of subslab soil gas towards the edges of the slab, and replacement with deeper soil gas with lower oxygen concentrations. The subslab oxygen levels decreased rapidly when the greenhouse was depressurized to -10 and –30 Pa. A more gradual decrease was seen at –2.5 Pa depressurization again highlighting the relationship between advection and biodegradation.

The tracer test method provided a means of estimating both the soil gas flow rate, and BTX mass flux into the greenhouse. While the use of BTX as a tracer has limitations, the predicted soil gas flow rates (0.35 to 2.8 L/min) were similar to those estimated using the flux chamber (about 4 L/min for all edge cracks) and predicted using an analytical and numerical model (2.4 to 4.5 min for the edge crack). The flux chamber flow rate was obtained by scaling individual measurements (about 0.5 L/min per edge crack) assuming eight open edge cracks. The consistent soil gas flow values suggest the tracer tests provided fairly reliable "order-of-magnitude" measurements of flow. In addition, the tracer soil gas flow rates, when normalized to pressure and foundation area, ranged between 0.001 and 0.005 L/min-Pa-m^2, which is somewhat less than the rates reported for the three studies summarized earlier.

CONCLUSIONS

A comprehensive field program was conducted to evaluate soil vapour intrusion into an experimental greenhouse constructed at a site with high levels of BTX contamination. Several different tests were designed to evaluate both soil gas flow and BTX mass flux into the greenhouse under varying depressurization conditions. The foundation slab edge crack and crack ratio, and greenhouse depressurizations (excluding the –30 Pa test), were intended to simulate possible conditions for a residential dwelling.

The tracer and flux chamber tests indicated that for the non-depressurized condition where vapour diffusion is a dominant process, the subslab vapour concentrations below the greenhouse remained low, and based on similar indoor and outdoor air concentrations there was no

significant vapour intrusion. There was pressure-induced movement or pumping of soil gas as evidenced by subslab oxygen fluctuations. However, the soil gas pumping did not result in measureable vapour intrusion into the greenhouse.

Sustained depressurization (-10 to –30 Pa) was required before there were significant changes to the subslab vapour regime, and measureable intrusion into the greenhouse. The tracer test method (mass balance approach) provided order of magnitude estimates of the soil gas flow rate, which ranged between 0.35 and 2.8 L/min (normalized value) for benzene and toluene. The -2.5 Pa test case, which indicated low subslab vapour concentrations near the edge of the slab, but not near the middle, highlighted the sensitivity of vapour intrusion to advective and biodegradation processes, and the presence of sufficient oxygen below the slab.

The flux chamber tests, while considered successful, were challenging to implement. Important methodology issues were extensive chamber decontamination needed to avoid cross-contamination, establishing appropriate flow rates based on pressure equilibration between the chamber and greenhouse, and scaling of individual chamber test results to the entire greenhouse. As expected, the soil gas flow and BTX flux was significant through the edge crack; however, in contrast flows and flux through the hairline cracks were negligible.

The modeling study indicated the Perimeter Crack Model and adapted MODFLOW simulations predicted similar edge crack soil gas flow rates to measured values. However, the Perimeter Crack Model predicted relatively high flow rates through the hairline cracks that were not consistent with the field measurements suggesting this model may be less accurate for hairline cracks. Although preliminary, the MODFLOW results suggest that a combination of numerical modeling for soil gas flow combined with an analytical model for crack flow can be used to better understand controlling factors (e.g., soil-air versus foundation slab permeability) for soil gas intrusion, and possibly for evaluation of vapour intrusion mitigation measures (e.g., slab sealing, subslab depressurization). Sensitivity analysis is required to further evaluate the performance of numerical soil gas flow models.

REFERENCES

Adomait, M. July 1992. "Soil Gas Containing VOCs Entering Homes Near Hazardous Lands", *Canada Mortgage and Housing Corporation.*

American Society for Testing and Materials (ASTM). 1995. Standard Guide for Simulation of Subsurface Airflow Using Ground-Water Flow Modeling Codes, ASTM D5719-95.

Canadian General Standards Board (CSGB). 1986. Determination of the Airtightness of Building Envelopes by the Fan Depressurization Method. CAN/CSGB-149.10-M86.

Eklund,B. and C. Schmidt. 1990. Estimation of Baseline Air Emissinos at Superfund Sites, Air/Superfund National Technical Guidance Study Series, Vol. II, August 1990, EPA-450/1-89-002a.

Ferguson, C.C., V.V. Krylov, and P.T. McGrath, 1995. Contamination of Indoor Air by Toxic Soil Vapours: a Screening Risk Assessment Model. *Building and Environment.* 30(3): 375-383.

Figley, D.A. 1997. A Guide for Estimating Indoor Concentrations of Soil Gas Pollutants in Houses. Prepared for CMHC.

Figley, D.A., and L.J. Snodgrass. June 21-26, 1992. "Comparative Foundation Air Leakage Performance of Ten Residential Concrete Basements", *Proceedings of the 85th Annual Meeting of Air and Waste Management Association.*

Figley, D.A., R.S. Dumont, and L.J. Snodgrass. 1991. Air Leakage Distribution Characteristics for Two Residential Concrete Foundations. In Proc. 84th Annual Meeting of the Air and Waste Management Assoc., Vancouver, B.C., June 16 to 21.

Fischer, M.L., A.J. Bentley, K.A. Dunkin, A.T. Hodgson, W.W. Nazaroff, R.G. Sextro, and J.M. Daisey. 1996. Factors Affecting Indoor Air Concentrations of Volatile Organic Compounds at a Site of Subsurface Gasoline Contamination. *Environ. Sci. Technol.* 30 (10): 2948-2957.

Fugler, D. and M. Adomait. 1997. Indoor Infiltration of Volatile Organic Contaminants: Measured Soil Gas Entry Rates and Other Research Results for Canadian Houses. J. of Soil. Contamination. 6 (1), 9-13.

Garbesi, K. and R.G. Sextro. 1989. Modeling and Field Evidence of Pressure-Driven Entry of Soil Gas into a House through Permeable Below-Grade Walls. *Environ. Sci. Technol.* 23(12):1481-1487.

Garbesi, K., R.G. Sextro, W.J. Fisk, M.P. Modera, and K.L. Revzan. 1993. Soil-Gas Entry into an Experimental Basement: Model Measurement Comparisons and Seasonal Effects. *Environ. Sci. Technol.* 27(3): 466-473.

Garbesi, K., R.G. Sextro, A.L. Robinson, J.D. Wooley, J.A. Owens, and W.W. Nazaroff. (1996). *Water Resources Research.* 32: 547-560.

Grimsrud, D.T., M.H. Sherman, and R.C. Sonderegger. 1982. Calculating Infiltration: Implications for a Construction Quality Standard. In: Proc. Amer. Soc. of Heating, Refrigeration, and Air-Conditioning Engineers and the U.S. Department of Energy Conference: Thermal Performance of the Exterior Envelopes of Buildings II. Las Vegas, NV., December.

Guo, W. and C.J. Neville. 1998. Adaptation of MODFLOW for Transient Air Flow Simulation. In Proc. Modflow '98 Volume 1, Golden, Co. October 4-8. Colorado School of Mines.

Hers, I. and R. Zapf-Gilje. 1998. Canadian consortium research project – field validation of soil gas transport to indoor air pathway. In Proc. 1998 Petrol. Hydro. and Org. Chem. in Ground Water. API/NGWA, Houston, Tx., Nov. 11-13: 251-266.

Hers, I., J. Atwater, L. Li and R. Zapf-Gilje. 2000. Evaluation of Vadose Zone Biodegradation of BTX Vapours. *Journal of Contaminant Hydrology*, 46: 233-264.

Hers, I., D. Evans, R. Zapf-Gilje and L. Li. 2002. Comparison, Validation and Use of Models for Predicting Indoor Air Quality from Soil and Groundwater Contamination. Journal of Soil and Sediment Contamination, 11 (4): 491-527.

Hers, I., L. Li and S. Hannam. 2003. Evaluation of Sampling and Analysis Techniques for Soil Gas at a Petro-Chemical Plant Site. Accepted for Publication by Environmental Technology. October.

Hodgson, A.T., 1992. Soil-Gas Contamination and Entry of Volatile Organic Compounds into a House Near a Landfill, *Journal of the Air and Waste Management Association*, 29: 277-283, March.

Johnson, P.C. and R. Ettinger. 1991. Heuristic Model for Predicting the Intrusion Rate of Contaminant Vapours into Buildings. *Environ. Sci. Technol.* 25 (8): 1445-1452.

Kienbusch, M.R. 1986. Measurement of Gaseous Emission Rates from Land Surfaces Using an Emission Isolation Flux Chamber, Users Guide, EPA/600/8-86/008, NTIS #PB86-223161.

Muskat and Botset (1931)

Nazaroff, W.W. May 1992. "Radon Transport from Soil to Air", *Review of Geophysics.* 30 (2): 137-160.

Nazaroff, W.W., H. Feustel, A.V. Nero, K.L. Revzan, D.T. Grimsrud, M.A. Essling, and R.E. Toohey. 1985. "Radon Transport into a Detached One-Story House with a Basement" *Atmospheric Environment.* 19(1): 31-46.

Nazaroff, W.W., S.R. Lewis, S.M. Doyle, B.A. Moed, and A.V. Nero. 1987. "Experiments on Pollutant Transport from Soil into Residential Basements by Pressure Driven Airflow", *Environmental Science and Technology.* 21: 459-466.

Olson, D.A. and R. Corsi. 2001. Characterizing exposure to chemicals from soil vapour intrusion using two-compartment model. *Atmospheric Environment.* 35: 4201-4209.

Robinson, A.L. and R. Sextro (1997). Radon Entry into Buildings Driven by Atmospheric Pressure Fluctuations. *Environ. Sci. Technol.* 31: 1742-1748.

Schmidt, C. and T.F. Zdeb. 1998. Direct measurement of indoor infiltration using flux chambers. In Proc. of 91th Annual Meeting of AWMA.

CHAPTER 6

COMPARISON, VALIDATION AND USE OF MODELS FOR PREDICTING INDOOR AIR QUALITY FROM SOIL AND GROUNDWATER CONTAMINATION

This chapter was published in *J. of Soil and Sediment Contamination*. 11(4): 491-527 (2002).[4]

The use of models to predict indoor air quality and health risk for the soil vapour transport to indoor air pathway is commonplace; however, there is significant uncertainty surrounding processes and factors affecting this pathway, and the accuracy of models used. Available screening models were evaluated through a review of model characteristics and sensitivity, and through comparisons to measured conditions at field sites. Model simulations and comparisons to field data indicate that the vapour attenuation ratio (α) is highly sensitive to certain processes (e.g., biodegradation and advection) and input parameters. Comparisons of model predicted to measured α values indicate that models based on the Johnson and Ettinger (1991) framework in most cases result in predictions that are conservative by up to one to two orders-of-magnitude for field sites that were assessed, providing that appropriate input parameters are used. However, for sites where the advection potential is high, these models may not be conservative. The potential for advective transport of vapours into building may be significant for sites with shallow contamination, high permeability soil and foundation and high building underpressurization. The paper concludes with possible tiered management framework for the soil vapour pathway.

KEY WORDS: soil vapour building, intrusion, advection, biodegradation, models

[4] Hers, I., Evans, D., Zapf-Gilje and Li, L.

INTRODUCTION

The implementation of risk-based corrective action at contaminated sites is now commonplace. Soil vapour intrusion into buildings is a potential pathway at all sites impacted by subsurface volatile organic compounds (VOCs). Over the past decade several predictive models for this pathway have been developed, and guidelines or regulations for this pathway have been promulgated or are under consideration in several countries throughout North America and Europe. Several organizations and regulatory bodies in North America (Canadian Council of Ministers of the Environment (CCME) and ASTM) have adopted a tiered approach for this pathway, while others have intentionally not included soil vapour intrusion due to the relatively high degree of uncertainty in models (*e.g.*, British Columbia).

Predictive models used for this pathway are typically relatively simple screening level models incorporating analytical or semi-analytical solutions for steady-state one-dimensional vapour transport. Most models follow the heurestic framework put forth by Johnson and Ettinger (1991) and involve a compartmental solution to chemical diffusion in soil below a building, coupled with diffusion, and in some cases advection, through the building foundation (*i.e.*, subsurface building envelope). Recent modeling developments include consideration of biodegradation, sorption and transient vapour transport. Multi-dimensional numerical models have also been developed for this pathway and may be appropriate in certain instances (Hers *et al.*, 2000; Mendoza, 1999).

There is significant uncertainty associated with the simulation of the soil vapour transport to indoor air pathway, and therefore a need for more in-depth analysis of key processes and factors affecting this pathway and testing of models through comparisons to field data. Screening level models commonly used are thought by many to incorporate conservative assumptions; however, to-date, there are only a limited number of field studies that can be used to validate models and test assumptions (Fitzpatrick and Fitzgerald, 1995; Fischer *et al.*, 1996; Laubacher *et al.*, 1997).

The purpose of this paper is to evaluate model suitability through comparison and validation, and to develop a framework for model use. Models considered are analytical or semi-analytical since this class of model is relatively simple to use, they have reasonable input requirements and can be incorporated into a tiered framework. Specifically, the paper consists of three parts: (i) review of available screening level models and selection of models for validation, (ii) model validation through evaluation of sensitivity, uncertainty and comparison of model predictions to conditions measured at field sites, and (iii) guidance on model application in the context of a tiered framework. The model validation data presented in this paper is primarily monitoring conducted by the authors over a two-year period at a former petro-chemical plant impacted by benzene, toluene and m&p-xylene (BTX) releases, although information for four other petroleum hydrocarbon sites, and radon intrusion research has also been reviewed. Detailed information is included to enable both independent verification of the evaluation process and to provide readers with a database of information.

The benefits of this work are new insights in terms of model sensitivity, uncertainty and the predictive capabilities of the models reviewed. A model framework, consistent with those commonly used for groundwater assessments, is provided but is modified to account for unique aspects associated with the soil vapour pathway.

MODEL REVIEW

Introduction

The contents, benefits, limitations and suitability of eleven analytical or semi-analytical models for soil vapour transport to indoor air were reviewed (Table 6.1). Seven models are based on the Johnson and Ettinger (1991) framework and couple steady-state diffusion in soil with diffusion, and in some cases, advection through the subsurface building envelope. Two are steady-state models (Ferguson and Modified Ferguson) that assume contamination is directly below the building and where the focus is on foundation and building characteristics (Ferguson *et al.*, 1995; Krylov and Ferguson, 1998). Several steady-state models also include biodegradation and/or depletion or decay of the chemical source (*e.g.*, Johnson *et al.*, 1998). One model is an analytical solution for one-dimensional transient transport of chemicals incorporating vapour- and aqueous-phase diffusion, and aqueous-phase advection, subject to sorption and first-order decay, as proposed by Jury *et al.* (1990) and adapted by Sanders and Stern (1994). The Jury model does not include transport through the building foundation and when used for the indoor pathway, a dirt floor foundation is assumed.

Nine models use a simple "box" model to calculate the indoor air concentration (*i.e.*, uniform and instantaneous mixing of chemicals within the building enclosure). Inputs to the model are the building ventilation rate, enclosure height and chemical flux from sub-surface sources. The Modified Ferguson model includes fate and transport in the building through consideration of possible sources and sinks for volatile chemicals. Most models also allow the estimation of human health risks and calculation of risk-based remediation criteria based on acceptable air concentrations. Model attributes are described below with reference to fate and transport processes within each compartment (*i.e.*, source zone, unsaturated zone and building foundation).

Source Zone Model Attributes

The partitioning relationships used by all models assume local equilibrium conditions, linear isotherms and reversible partitioning of chemicals between the absorbed, aqueous and vapour phases (in absence of non-aqueous phase liquid (NAPL)). Absorption of non-ionic hydrocarbons occurs primarily through partitioning into soil organic matter (Chiou, 1987). When the soil moisture content is unusually low, as characterized by a relative humidity below 100 %, and when the organic carbon fraction is less than about 0.1 %, the partitioning relationships may become inaccurate resulting in greater uncertainty in source zone concentrations (Bouchard *et al.*, 1987; Schwarzenbach *et al.*, 1993). Several models (SVIM, VAPEX4, VOLASOIL) also incorporate partitioning from a residual hydrocarbon phase (NAPL) and adjust the predicted vapour concentration for a multi-component mixture based on Raoult's Law. Based on this relationship, the vapour concentration is constant regardless of concentration once the aqueous phase chemical solubility is reached and NAPL begins to form (*i.e.*, the so-called NAPL saturation concentration).

Several models allow for the depletion or decay of a chemical source. The SVIM model approximates the change in flux and concentration through repeated calculations for discrete time steps based on a mass balance that assumes quasi steady-state conditions. This leads to downward migration of the VOC source boundary (*i.e.*, peeling of onion analogy). The GSI and VAPEX4 models use a different method where the total mass available to be volatilized is

Table 6.1. Summary of Model Characteristics

Model Name	Reference	Diffu -sion	Multi-Layer[1]	Biodegr adation	Advec-tion Soil[2]	Advec-Tion Slab	Source Depletion	Model Type & Comments
Johnson -Ettinger	Johnson & Ettinger ('91)	Yes	Yes	No	No	Yes	Yes	Mathematical equations
GSI (Tier 2 RB CA Tool Kit)	ASTM ('95)	Yes	No	No	No	No[4]	Yes	Computer spreadsheet by Groundwater Services Inc. (commercially available)
SVIM (V. 2, '99)	Hers *et al.* ('97)	Yes	Yes	No	Yes	Yes	Yes	Computer spreadsheet by Golder Associates Ltd.
Unocal	Daugherty ('91 & 97), Ryrie *et al.* ('98)	Yes	No	Yes	No	No	No	Computer spreadsheet, modification of Orange County Health Care Agency (OCHCA) (California, USA) model
Modified Johnson	Johnson *et al.* ('98)	Yes	Yes	Yes	No	Yes	No	Mathematical equations, nomographs
RISC	N/A	Yes	Yes	Yes[5]	No	Yes	No	Computer windows-based model by Spense Environmental Engineering (developed for British Petroleum) (commercially available)
VAPEX4 (V. 4, 1999)	N/A	Yes	Yes	Yes	No	Yes	Yes	Computer model by Environmental Systems & Technologies Inc. (commercially available)
Ferguson	Ferguson *et al.* ('95)	Yes[3]	N/A	N/A	N/A	Yes	Yes	Computer spreadsheet model
Modified Ferguson	Krylov & Ferguson ('98)	Yes[3]	N/A	N/A	N/A	Yes	Yes	Computer spreadsheet model
VOLASOIL	Waitz *et al.* ('96)	Yes	No	No	Yes	Yes	No	Computer Windows-based model by Dutch National Institute of Public Health & Environment (RIVM) (commercially available)
Jury	Jury *et al.* ('90)	Yes	No	Yes	No	N/A	Yes	Mathematical equations

[1] Variable moisture content layers [2] Advective vapour-phase transport in soil [3] No diffusion through soil included

[4] The GSI RBCA Tool Kit for Chemical Releases (1999) supercedes the Tier 2 Tool Kit and includes advection through the slab (not used for this study)

[5] Dominant layer model (Johnson *et al.*, 1998), an O_2-limited, first-order biodegradation model currently being added (Lyn Spense, personal communication)

initially estimated. If the mass volatilized over the averaging time for vapour flux is less than the available mass, the volatilization rate is calculated using the Johnson-Ettinger model assuming an infinite mass. If the mass volatilized exceeds the available mass, the steady-state chemical flux into the building is simply the available total mass divided by the averaging time (*i.e.*, it is apportioned over time assuming constant steady-state transport). When the mass volatilized exceeds the available mass, the GSI model automatically defaults to the source depletion model, and peak concentrations and time for depletion to occur are not calculated. The Ferguson models include source decay as a first-order reaction rate mechanism.

Unsaturated Zone Model Attributes

Diffusion and Advection

Chemical transport through diffusion requires the calculation of an effective diffusivity (D^{eff}; L^2T^{-1}), which in all cases is estimated using an empirical relationship proposed by Millington and Quirk (1961):

$$D^{eff} = D_a\tau_a + \frac{D_w}{H'}\tau_w \qquad (1)$$

$$\tau_a = \frac{\phi_a^{\frac{10}{3}}}{\phi^2} \qquad \tau_w = \frac{\phi_w^{\frac{10}{3}}}{\phi^2} \qquad (2a,b)$$

where D_a and D_w are the free-air and free-water diffusion coefficients (L^2T^{-1}), τ_a and τ_w are the soil air phase and soil water phase tortuosity factors (*dimensionless*), θ_a, θ_w and θ are the volumetric air-filled, water-filled and total porosity (*dimensionless*), and H' is the Henry's Law Constant (*dimensionless*). In several models (listed in Table 6.1), an average depth-integrated effective diffusivity is calculated using the following relationship:

$$(D^{eff})_T = L_T * \left[\sum \frac{L_i}{(D^{eff})_i}\right]^{-1} \qquad (3)$$

where $(D^{eff})_T$ is the the overall effective diffusivity, L_T is the total soil thickness (L) and L_i is the thickness of individual soil layers (L).

One model (VAPEX4) modifies the effective diffusion coefficient to include the effects of dispersion through barometric pumping. Only the VOLASOIL model considers one-dimensional advective chemical transport in the unsaturated zone, in addition to advective transport through the building foundation.

Biodegradation

The Unocal and Modified Johnson models incorporate biodegradation through an analytical solution for one-dimensional vapour-phase transport subject to diffusion and first-order biodegradation. The RISC model has incorporated the Modified Johnson dominant layer biodegradation model. Steady-state vapour-phase diffusion and biodegradation for a homogenous soil can be represented by the following equation:

$$D_g^{eff} \frac{\delta^2 C_g}{\delta z^2} = G \tag{4}$$

where D_g^{eff} is the effective vapour-phase diffusion coefficient, C_g is the vapour concentration ($mol\ L^{-3}$) and G is the rate of mass consumption or biodegradation ($mol\ L^{-3}\ T^{-1}$). Assuming concentrations at the top and bottom boundaries are constant, an analytical solution can be derived that enables calculation of a dimensionless Damkohler number (D_{am}), or the ratio of the degradation rate over the diffusion rate (DeVaull *et al.*, 1997), as follows:

$$\frac{C_g(z)}{C_g(z=0)} = \frac{(e^{-\varepsilon} - \beta) \bullet e^{\varepsilon \bullet \frac{Z}{L}} + (\beta - e^{\varepsilon}) \bullet e^{-\varepsilon \frac{Z}{L}}}{e^{-\varepsilon} - e^{\varepsilon}}, \varepsilon > 0 \tag{5}$$

$$D_{am} = \varepsilon^2 = \frac{Degradation\ Rate}{Diffusion\ Rate} = \frac{k_w^{\ 1} \theta_w L^2}{H' D_g^{\ eff}} \tag{6}$$

where $k_w^{\ 1}$ is the first-order degradation rate based on pore-water concentration (T^{-1}), L is the domain length over which transport occurs (L), and β is the vapour concentration at distance L. Hydrocarbon-vapour concentration profiles are used to obtain fitted, and hence site-specific decay constants. The use of log concentration plots for fitting measured to predicted data has been found to be effective for D_{am} numbers in excess of about five, while normal plots have been used for D_{am} values below five (Ryrie *et al.*, 1998; Hers *et al.*, 2000).

The Unocal model assumes that biodegradation occurs over the entire vertical depth profile. The Modified Johnson model assumes biodegradation only occurs in the middle or "dominant" layer of a three-layer system. The rationale for the "dominant layer model" is that observations at several sites indicate that hydrocarbon vapour and oxygen (O_2) concentrations decrease significantly over a well-defined vertical layer. Conversely, the rate of decrease in concentration is much less above, and below this dominant layer.

The VAPEX4 biodegradation model assumes that the soil compartment is a uniform well-mixed reactor, and that the net upward flux is the diffusive flux minus the biodegradation flux. The biodegradation flux can be estimated from *in-situ* respiration tests. Alternately, it is based on estimates of O_2 transfer from air and subsurface flux through diffusion and aqueous-phase advection (*i.e.*, infiltration) coupled with a mass balance between the mass of O_2 needed to degrade an equivalent mass of hydrocarbon.

The Jury model includes a first-order decay term with transport and decay formulated in terms of total concentrations. More recently, Jeng *et al.* (1996) presented a similar solution formulated in terms of vapour concentrations with the degradation term applied to the aqueous phase, which more accurately represents the biodegradation process. The Jury Model assumes a non-constant chemical source over time. This may be non-conservative when there is a large mass of subsurface hydrocarbon present and when concentrations over a relatively long period of time are of interest.

Building Foundation Model Attributes

There are substantial differences in the way models predict hydrocarbon vapour intrusion through the building foundation. The key processes are diffusion and advection, as described below.

Diffusion

For the Johnson-Ettinger, GSI, RISC and VAPEX4 models, diffusive transport is limited to that occurring through dirt-filled cracks in the concrete foundation slab. The SVIM model provides for both diffusive transport through dirt-filled cracks and intact concrete. Diffusion through intact concrete (*i.e.*, non-cracked portion) is supported by findings from several studies on radon diffusion (Rogers *et al.*, 1994; Renken and Rosenberg, 1995; Nielson *et al.*, 1997).

The GSI and SVIM models calculate the effective diffusivity of the dirt-filled cracks using equations 1 and 2, and allow the user to enter site-specific water-filled porosity and total porosity values. The RISC model uses the same equation but assumes dirt in cracks is dry and the dirt porosity 0.25. These defaults can not be changed by the user.

The two Ferguson models do not explicitly model diffusion through cracks or intact concrete but instead require a single empirical diffusivity value for a multi-layered foundation material. Due to the uncertainty in transport processes through the building foundation, the Unocal model does not explicitly model transport through the building foundation but instead uses an empirical 'slab attenuation factor'. The recommended slab attenuation factors are 0.01 for residences, and 0.001 for commercial buildings, or newly cast concrete floors (Daugherty, 1997).

Advection

Soil gas advection through near surface soil and the building foundation is incorporated using a variety of methods, as follows:

1. ***Flow to Perimeter Crack Model (Johnson-Ettinger, RISC, VAPEX4 models)***: An analytical solution for two-dimensional soil gas flow to a small horizontal drain is used to simulate flow to an edge crack located at the perimeter of a building (Nazaroff, 1992):

$$Q = \frac{2\pi\, k_a\, \Delta P\, X_{crack}}{\mu \ln\left(\frac{2 z_{crack}}{r_{crack}}\right)}, \qquad \frac{r_{crack}}{z_{crack}} << 1 \tag{7}$$

where Q is the soil gas flow (L^3T^{-1}), k_a is the soil gas permeability (L^2), ΔP is the pressure difference, X_{crack} is the perimeter crack length (L), μ is the gas viscosity ($M\,L^{-1}\,T^{-1}$), z_{crack} is the crack width (L) and r_{crack} (L) is the crack radius. The ratio of cracks to total sub-surface foundation area (*i.e.*, base and walls) (η) can be expressed as:

$$\eta = \frac{r_{crack}\, X_{crack}}{A_B} \tag{8}$$

where A_B is the subsurface foundation area (L^2). This model takes into consideration both flow through soil, and the foundation.

2. ***Flow Through Foundation Model (SVIM, VOLASOIL models):*** An analytical solution for one-dimensional soil gas flow through a cracked building foundation is used. The permeability is estimated using the Hagen-Poiseuille relationship for flow between smooth parallel plates (SVIM) or cylindrical tubes (VOLASOIL), which represent concrete cracks or holes. The Hagen-Poiseuille relationship is based on laminar flow between two surfaces and does not take into account resistance to air flow from soil, or edge effects associated with the soil–crack interface. The equations used by the SVIM model are:

$$Q_{slab} = \frac{k_{slab} b\, w\, \Delta P}{L_c} \tag{9}$$

$$k_{slab} = \frac{b^2}{12\mu} \qquad \eta = \frac{b}{S_C} \qquad w = \frac{2A_b}{S_C} \tag{10a,b,c}$$

where Q_{slab} is the soil gas flow (L^3T^1), k_{slab} is the foundation slab permeability (L^2), b is the crack width (L), S_C is the crack spacing (L), w is the crack length (L), L_c is the foundation (concrete) thickness (L). The Q_{slab} is proportional to b^3 and is only applicable for narrow crack widths.

3. ***Flow through Soil Model (VOLASOIL, Ferguson models)***: An analytical solution for one-dimensional upward soil gas flow through the unsaturated zone and/or building foundation is used. The pressure gradient input into the models is the building underpressurisation divided by the depth over which advection occurs.

An additional method that is utilized for radon intrusion assessments is the equivalent leakage area (ELA) method (CSGB, 1986; Grimsrud *et al.*, 1982). The ELA is not directly related to the η parameter used in the above models.

Most models for soil vapour intrusion assume a ground-bearing slab as part of a basement or at-grade structure. The Ferguson and VOLASOIL models also incorporate the effects of a suspended floor slab or crawlspace, and the Modified Ferguson model can simulate the effect of ventilation of several floor layers. Possible advective flow through service ducts, open drains or other preferential flow pathways is not explicitly considered by any of the models reviewed.

Selection of Models for Validation

Model validation is addressed below through evaluation of model processes, sensitivity and uncertainty analysis, and comparisons to field data. Three models (GSI, RISC and SVIM) were chosen for validation purposes (limited comparisons are also shown for the VOLASOIL model). The GSI model is based on ASTM guidance, is widely used and includes diffusion and source depletion processes. The RISC and SVIM models include additional features consisting of biodegradation, advection and multi-layer capabilities. The three models collectively incorporate key transport processes and represented a manageable number of models in terms of implementing the validation process.

MODEL VALIDATION - EFFECT OF TRANSPORT PROCESSES

Models were initially compared for a hypothetical generic contamination scenario and diffusive transport only in order to evaluate model variability for simple baseline conditions. Next, various processes were added to evaluate their effect on attenuation. The input parameters used represent possible values for a residence with an at-grade ground-bearing slab located at a site with sandy soil and shallow gasoline contamination (Table 6.2). The contaminant considered was limited to benzene, for which a soil (total) concentration of 5 mg/kg was assumed. Benzene is a volatile and toxic chemical and therefore is a critical parameter for many risk assessments. Information sources and values for parameters used in models are further described in Appendix I.

Table 6.2. Default Generic Values for Input Parameters (Benzene)

Information	Model[6]	Value	Information	Model[6]	Value
Physico-chemical Properties[1]			***Building Properties***		
Benzene MW (g/mol)	G,R,S,V	78.1	Volume (m^3)	G,R,S,V	300
Gasoline MW (g/mol)	R	107	Height (m)	G,R,S,	3
Wt. fraction benzene (%)	-	0.01	Area (m^2)	G,R,S,V	100
Mole Fraction Benzene	S	0.0137	Air exchange rate (1/d)	G,R,S,V	10
Vapour Pressure (mm Hg)	R,S,V	76	***Advection Case***		
Henry's Law Constant (-)	G,R,S,V	0.22	Underpressurization (Pa)	R,S	3
Solubility ($mg\ L^{-1}$) (mg/L)	G,R,S,V	1750	Depth to perimeter crack (m)[4]	R	0.6
Log Koc	G,R,S,V	1.92	Length of perimeter crack (m)[4]	R	40
Free-air diffusivity (cm^2/s)	G,R,S,V	8.7E-02	Crack Width (m)[5]	S	0.001
Water diffusivity (cm^2/s)	G,R,S,V	1.1E-05	Crack spacing (m)	S	2
Contamination Properties			Advective depth of influence (m)	S	0.3
Depth to contamination (m)	G,R,S,V	1.5	***High Moisture Layer Case***		
Contamination Area (m^2)	G,R,S,V	100	Total porosity (-)	R,S	0.3
Background air conc. (ug/L)	S	0	Water-filled porosity (-)	R,S	0.25
Soil Properties			Thickness (m)	R,S	0.3
Total porosity (-)	G,R,S,V	0.3	***Biodegradation Case***		
Water-filled porosity (-)	G,R,S,V	0.1	First-order constant (H_2O) (1/hr)	R	0.5
Fraction organic carbon (f_{oc})	G,R,S,V	0.03	Dominant layer thickness (m)	R	0.38
Soil dry bulk density (g/cm^3)	G,R,S,V	1.7	Upper/lower layer thickness (m)	R	0.56
Soil-air permeability (m^2)	R,S,F,V	1.0E-11	***Non-ventilated Crawlspace Case***		
Soil Temperature (K)	S	283	Depth to crawlspace base (m)	V	0.4
Foundation Properties			Volume of crawlspace (m^3)	V	50
Total porosity cracks (-)[2]	G,S,V	0.3	***Ventilated Crawlspace Case***		
Water-filled porosity cracks[2]	G,S	0.1	Ventilation Rate (hr^{-1}) (1/hr)	V	0.8
Total porosity cracks (-)	R	0.25	Total number openings floor (N)	V	10
Water-filled porosity cracks	R	0.0	Total area openings floor (m^2)	V	0.1
Tortuosity factor concrete (-)[3]	S	1.1E-3	ΔP building-crawlspace (Pa)	V	2
Concrete thickness (m)	G,R,S,V	0.15	ΔP Crawlspace – Soil (Pa)	V	2
Subsurface area building (m^2)	G,R,S,V	100	***Source Depletion Case***		
Ratio crack / foundation area	G,R,S	0.001	Soil contamination thickness (m)	G,S	1.0

Notes:
1. Properties for benzene unless otherwise noted
2. For dirt-filled cracks
3. For intact (not cracked) concrete
4 Flow to horizontal perimeter (edge) crack model
5. Flow through foundation model
6. G=GSI; R=RISC; S=SVIM; V=VOLASOIL

The vapour attenuation ratio (α), defined as the predicted indoor air concentration divided by the source vapour concentration, was estimated for each of the models. For models that do not directly provide equilibrium vapour concentrations at source, the source vapour concentration was estimated using:

$$C_g = C_t \rho_b / (K_{oc} f_{oc} \rho_b / H' + \theta_w / H' + \theta_a) \quad (11)$$

where C_t is the soil (total) concentration (MM^{-1}), ρ_b is the bulk density (ML^{-3}), f_{oc} is the organic carbon fraction (dimensionless) and K_{oc} is the organic carbon-water partitioning coefficient (L^3M^{-1}).

Initially, identical properties for concrete cracks were used to evaluate diffusion only through dry dirt-filled concrete cracks (θ= 0.25) resulting in identical α values (2.6E-05) for the GSI, SVIM and RISC models (Table 6.3, diffusion only case). Next, model simulations were run to investigate the effect of slight variations in concrete properties. The resulting variation in α for the GSI, RISC and SVIM models (between about four and 19 times) is due to the different sub-model and input parameters used to represent diffusion through the building foundation. For the GSI and RISC models, diffusion is limited to dirt-filled cracks, while the SVIM model also allows for diffusion through intact concrete. Moist dirt in cracks (θ_w = 0.1, θ= 0.3) was assumed for the GSI and SVIM models while the default for the RISC model is dry dirt (θ= 0.25). The reason for the high α value for the VOLASOIL model is not readily apparent.

Table 6.3. Model Comparisions for Varying Processes[1]

	Vapour Attenuation Ratio			
Process Added	**GSI**	**SVIM**	**RISC**	**VOLASOIL**
Diffusion Only (dry cracks only)	2.6E-05[2]	2.6E-05	2.6E-05	
Diffusion Only (variable slab properties)	8.5E-06[2]	1.6E-04	2.6E-05	1.0E-03
Advection through Foundation		8.2E-04	6.0E-04	
High Moisture Content Layer		3.5E-05	7.4E-06	
Biodegradation			7.4E-08	
Non-ventilated Crawlspace				9.8E-04
Ventilated Crawlspace & Advection				2.1E-10
Contaminant Source Depletion		6.E-06[3]		

[1] See Table 2 for default input parameters

[2] Averaging time of one year

[3] Average value over 25 year period as risk to benzene is modelled as life time average cancer risk

Several processes and conditions were then evaluated for one set of input assumptions to indicate general trends in terms of effect on α values (Table 6.2). The processes and conditions considered were advection, biodegradation, water-filled porosity, building crawlspace ventilation

and chemical source depletion. The results, presented in Table 6.3, indicate that including advection through the foundation resulted in a three- to 23-fold increase in α values relative to the diffusion only case. Conversely, simulation of all other processes resulted in a decrease in α values. A modest decrease in α was obtained when water-filled porosity was increased from 0.1 to 0.25 while a significant decrease was obtained when biodegradation was modeled. The first-order biodegradation rate (0.5 hr^{-1}) chosen was based on monitoring results for the Chatterton site, as subsequently described in this paper. A significant decrease in α was also obtained when a ventilated crawlspace was simulated using the VOLASOIL model. Source depletion resulted in a moderate decrease in time-averaged α relative to peak values; a further reduction in α would have been obtained had a lower organic carbon fraction been assumed since higher source vapour concentrations would have been predicted.

Based on the input parameters chosen, the most important processes relative to the diffusion only case were biodegradation and ventilation of a crawlspace. Moderately important processes were advection, while the least important were simulation of a high moisture content layer and source depletion.

MODEL VALIDATION - MODEL SENSITIVITY AND EFFECT OF PARAMETER UNCERTAINTY

Model sensitivity for benzene was evaluated for the diffusion only and diffusion and advection model cases while the effect of parameter uncertainty was evaluated for the diffusion and advection model case. Sensitivity and uncertainty analysis help determine which input parameters have the greatest effect on results and are most important.

Sensitivity Analysis

The sensitivity analysis was conducted by varying input parameters, one variable at a time, while keeping remaining variables constant (equal to values in Table 6.2). Sensitivity to the following input parameters was evaluated: vapour concentration, f_{oc}, θ_w, η, contamination depth, H', D_a, first-order decay constant, building underpressurization, building ventilation rate (air exchanges per hour or *AEH*), building height (*H*) and soil-air permeability (Figure 6.1, selected parameters only). The sensitivity analysis was conducted for the predicted indoor air concentration, as opposed to α, since the version of the GSI model used does not directly provide α.

The sensitivity depends on the model under consideration and reference input values since the variation in indoor concentration for most input parameters is non-linear. The relative sensitivity, defined as the ratio of percent variation in model output (concentration) to model input (*i.e.*, slope of curves shown in Figure 6.1) is, in general, greatest for soil concentration, soil properties (θ_w, f_{oc}), physico-chemical properties (H', D_a) and building properties (*H*, *AEH*), and is least for foundation properties (η, *b*) and contamination depth (except at very shallow depth). For the diffusion only case, the GSI and RISC models are only slightly sensitive to soil properties since the diffusive flux through the building foundation is limited to cracks and therefore the crack ratio, as opposed to soil properties, controls the overall flux into the building. The SVIM model shows greater sensitivity to soil properties for the diffusion only case since diffusion occurs through both cracks and intact concrete. Except for depth to contamination, the

addition of advection as a model process reduces the sensitivity of the indoor concentration to the above parameters (Figure 6.1).

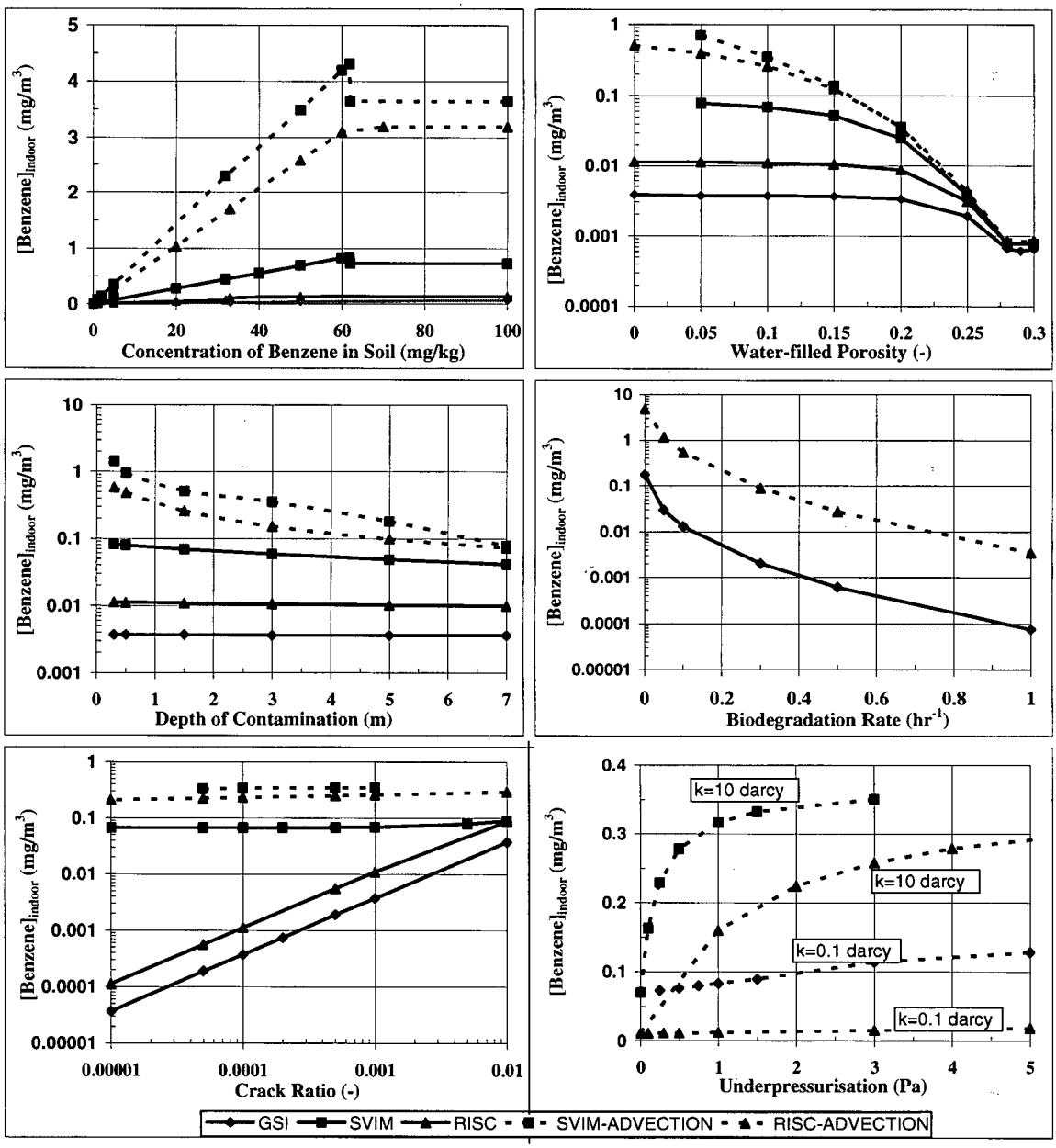

Figure 6.1. Results of Sensitivity Analysis for Selected Parameters (solid lines are diffusion only models, dashed lines are for diffusion and advection model).

Effect of Parameter Uncertainty

The effect of parameter uncertainty on model predictions, as opposed to relative sensitivity, has greater relevance when evaluating model characteristics since parameter uncertainty is variable. For example, soil permeability and building crack ratio may vary over several orders-

of-magnitude whereas some physico-chemical parameters may vary only slightly. The effect of parameter uncertainty was evaluated by choosing an input parameter range felt to represent the possible uncertainty in values for a hypothetical site that is reasonably well characterized. Vapour attenuation ratios were predicted by individually varying input parameters relative to base case conditions. It is recognized that selection of the input parameter ranges is subjective and will vary depending on the site conditions and chemical under consideration. The variation in benzene α for the RISC and SVIM models, for diffusive and advective transport, is presented in Table 6.4. The GSI model was not used since the version used did not include advection (see Table 6.1). The highest variation in output (α) was obtained for concentration, soil properties and AEH. A moderate degree of variability was associated with underpressurization, and only slight variability was predicted for contamination depth, building foundation properties and physico-chemical properties, for the input ranges chosen.

Table 6.4. Sensitivity of Predicted Vapour Attenuation Ratio to Parameter Uncertainty for Hypothetical Site (diffusion & advection model case)

Parameter	Best Estimate	Variation in input (%)	Variation in Output (%)[1]	
			SVIM	RISC
Contaminant Data				
Soil concentration (mg/kg)	5	+/-50	+50 / -50	+50 / -50
Depth to contamination (m)	1.5	+/- 3	+3.0 / -3.0	+0.4 / -0.4
Physico-Chemical Properties				
Henry's Law constant (-)	0.22	+/-8	+9.2 / -8.9	+8.0 / -8.0
Free-air diffusivity (cm^2/s)	0.087	+/-8	+6.6 / -6.3	+8.3 / -8.3
Soil Properties (Sandy Soil)				
Total porosity (-)	0.3	+/-17	+50 / -43	+25/-32
Water-filled porosity (-)	0.1	+/-50	+101 / -61	+100 / -52
Fraction organic carbon (-)	0.03	+/-33	+100 / -30	+100 / -23
Soil dry bulk density (g/cm^3)	1.7	+/-6	< +/- 1.0	< +/- 1.0
Soil-air permeability ($10^{-12}m^2$)	10	+/-70	+3 / -24	+ 25 / -23
Foundation / Advection Properties				
Tortuosity factor concrete (-)	1E-08	+/-1 OM[2]	+6.0/<-1.0	N/A
Total porosity dirt-filled cracks (-)	0.3	+/-50	< +/- 1.0	N/A
Water-filled porosity of cracks (-)	0.1	+40/-80	< +/- 1.0	N/A
Concrete thickness (m)	0.15	+/-13	< +/- 1.0	< +/- 1.0
Ratio crack to foundation area (-)	0.001	+/-1 OM	<+1.0/-3.0	+13 / -10
Underpressurisation (Pa)	3	+/-67	<+1.0/-5.0	+13 / -38
Depth to perimeter crack (m)	0.6	+/-20	N/A	< +1.0 / -1.4
Crack width (m)	0.001	+100/-50	<+1.0 /-22	N/A
Building Properties				
Height (m)	3	+/-20	+20 / -20	+20 / -20
Air exchanges (day^{-1})	10	+150/-50	+150 / -50	+150 / -50

Notes:
1. Output is Predicted Vapour Attenuation Ratio
2. OM = order-of-magnitude

The uncertainty in indoor air concentrations due to the combined variability in selected input parameters was also evaluated by modifying the SVIM model to include a probabilistic analysis using Crystal Ball™ (Figure 6.2). Triangular distributions were used to represent the parameter ranges given in Table 6.4. A lognormal distribution for α was obtained and the range in α

corresponding to the 10th and 90th percentiles was 3.4E-4 to 1.2E-3 (factor of 3.5). The results indicate that for the SVIM model parameter uncertainty representing a well-characterized site results in α that varies over about one order-of-magnitude. While overall uncertainty is a function of both model and parameter uncertainty, this degree of parameter uncertainty is not considered excessive relative to other sources of uncertainty associated with human health risk estimation.

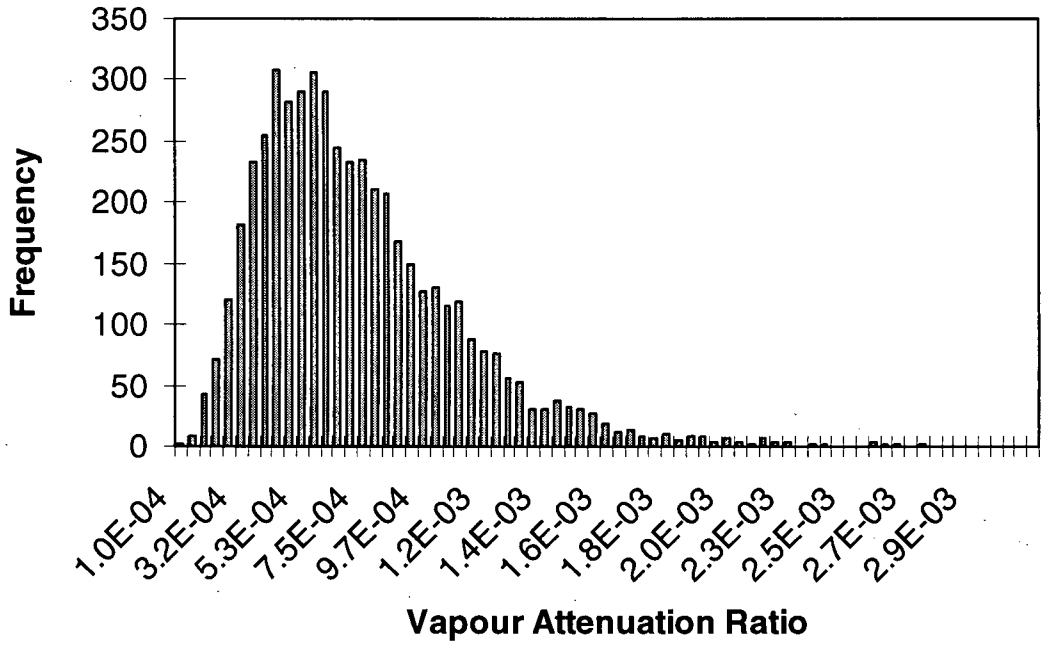

Figure 6.2. Results of Monte Carlo Probabilistic Analysis for Benzene Vapour Attenuation Rate (SVIM model, Table 6.4 inputs, triangular distributions, 5000 trials)

Effect of Uncertainty in Soil Moisture Content and Bulk Density

For the above analysis, the total and air-filled porosity were directly input and then used to calculate the tortuosity factor using the empirical relationships in equations 1 and 2. However, the total and air-filled porosity are often estimated using the particle density (ρ_s) and gravimetric moisture content (MC, % dry weight), as follows:

$$\theta = 1 - \frac{\rho_b}{\rho_s} \qquad \theta_a = \theta - \rho_b MC \qquad (12)$$

Using these equations, the uncertainty in tortuosity factor is a function of the combined uncertainty in bulk density, soil particle density and moisture content. This uncertainty increases as the moisture content increases due the power functions incorporated in the equation for the tortuosity factor (Equation 2).

To investigate the effect of parameter uncertainty specifically associated with these parameters, a probabilistic analysis using Crystal Ball™ was conducted for a scenario involving

low, moderate and high moisture contents (Table 6.5). The assumed variation in bulk density and moisture content (10 %) is considered representative of that which might be expected for a carefully conducted investigation and a relatively uniform soil deposit. The input distributions were assumed to be triangular. The simulation results indicate that the tortuosity factor, calculated using equation 2, is subject to a significant degree of uncertainty, which increases with moisture content. The variation in tortuosity factor, when defined as the range between the 10^{th} and 90^{th} percentile, ranges from +/- 31 % for the low moisture content scenario to over two orders-of-magnitude for the high moisture content scenario. When compared to alternate empirical equations for tortuosity factor, the variation introduced by uncertainty in moisture content and bulk density is on the same order or greater than that represented by the alternate empirical equations. This points to the importance of obtaining accurate geotechnical properties for input into models.

Table 6.5. Effect of Parameter Uncertainty on Tortuosity Factor Estimates[4]

	Assumed Variation for Each Case[2]	Values		
		Low MC[3] Case	Moderate MC Case	High MC Case
Input Values				
Bulk density (kg/L)	+/-10 %	1.7	1.7	1.7
Moisture content (gravimetric) (%)	+/-10 %	6	12	18
Total Porosity	N/A	0.36	0.36	0.36
Output Values				
Mean air-filled porosity	N/A	0.26	0.15	0.052
Mean tortuosity factor	N/A	0.084	0.016	0.00080
10^{th} percentile tortuosity factor	N/A	0.058	0.0087	0.000035
90^{th} percentile tortuosity factor	N/A	0.11	0.025	0.0045

Notes:
2. Assumed triangular distributions, for high moisture content case, distributions were truncated to prevent negative values
3. MC = moisture content
4. Assumed soil particle density = 2.65 kg/L (fixed)

Measurement of *in-situ* diffusion coefficients or laboratory measurements represent alternative methods for estimating tortuosity factors, and may be appropriate when accurate estimates are required. One *in-situ* method is a push-pull test involving injection and extraction of a non-reactive tracer gas such as sulpher hexafluoride or helium (Johnson *et al.*, 1998). Push-pull tests using helium were conducted at the Chatterton site. A good comparison was obtained between the measured tortuosity and that predicted using the Millington and Quirk (1961) relationship with measured values consistently about twice the predicted values (Hers and Zapf-Gilje, 1998). Published test results of *in-situ* diffusion coefficients are limited and therefore it is not possible to verify whether this test can be reliably used for a wide range of soil types.

MODEL VALIDATION – COMPARISONS BASED ON FIELD DATA

Model validation is conducted in four parts consisting of description of case study sites, derivation of biodegradation rates, evaluation of soil gas advection followed by comparison of measured and model-predicted indoor air concentrations for three models (GSI, RISC and SVIM). The first three sections provide the context needed for the model comparisons. Model validation focuses on published field data from five sites affected by BTEX or petroleum hydrocarbons, which are the Chatterton site located near Vancouver, B.C. (Hers and Zapf-Gilje, 1998; Chapter 5), Paulsboro site (Laubacher *et al.*, 1997), Traverse City site (Ostendorf and Kampbell, 1991), Alameda Naval site (Fisher *et al.*, 1996) and California site (Ryrie and Sweeney, 1995; Ryrie *et al.*, 1998). Information on radon sites is also reviewed when relevant. Conditions at the five case study sites are summarized in Table 6.6.

Table 6.6. Field Data Summary for Model Validation[5]

	Chatterton Site	Paulsboro	Traverse City	Alameda Naval	California Site
Contaminant Data					
Contamination type	BTX	Gasoline	Aviation Fuel	Gasoline	Gasoline
Contamination depth (m)	1.35 (NAPL)	2.74	4.0	0.7	~3
Source soil concentrations (mg/kg)	B,T,X=500, 5500,450[2]	N/A	N/A	N/A	N/A
Source groundwater concentrations (mg/L)	N/A	B,T;E,X,TPH=9.6 ,18,1.6,9.5,58[2]	N/A	N/A	Product on water-table
Soil Vapour Data					
Hydrocarbon attenuation	~4 OM[2]	<1 to 4-5 OM adj	1.5 OM	2 -3 OM	≥ 3 OM
Hydrocarbon conc. near source (mg/m^3)	B,T,X=15000, 20000,900[2]	B,T,E,X=576, 1466,224,764	TPH=1600-10000 ppm	B,T,isoP=200, 200,28000	B=270-300
O_2 conc. near source (%)	0-3	1-6	0.2-3.8	1.5-3	0.5-2
CH_4 conc. near source	1-12%	~250 ppmv	N/A	100 g/m3	3-7 %
Soil Properties					
Soil type	Uniform sand	Sand, some silt	Fine uniform sand	Uniform sand	Sand, some thin clayey silt layers
Soil cover outside bldg	Lightly vegetated	N/A	Unpaved	Partially paved	Partially paved
Total porosity (-)	0.36	0.39	0.35	0.36	~0.3
Air-filled porosity (-)	0.21	0.23	0.27	0.22	~0.25
Fraction organic carbon (-)	0.0065	0.0006	N/A	0.006	N/A
Dry bulk density (g/cm^3)	1.66	1.7	N/A	1.6	N/A
Soil air k (10^{-12} m^2)	10	**10**	N/A	10	N/A
Depth to Groundwater (m)	2-2.5	5.8	~4.0	1.0-1.9	~3
Foundation Properties					
Foundation type	Slab-on-grade	Basement	N/A	Slab-on-grade	N/A
Building area (m^2)	57	39	N/A	50	N/A
Crack ratio (η) (-)	0.0001- 0.00033	**0.0001**	N/A	**0.0001**	N/A
Depth perimeter crack (m)	0.3	2.13	N/A	**0.2**	N/A
Crack width (SVIM)(mm)	2.2	**0.2**	N/A	**0.2**	N/A
Crack spacing (SVIM)(m)	13.3 – 44	**4**	N/A	**4**	N/A
Building Properties					
Height (m)	2.19	2.74	N/A	2.4	N/A
Dimensions (m)	6.1 by 9.3	4 by 9.8	N/A	6 by 8.3	N/A
Ventilation (1/day)	**10,** 115, 345	**10**	N/A	50	N/A
Building ΔP (Pa)	0, 2.5, 10, 30	**5**	N/A	3[3]	N/A

	Chatterton Site	Paulsboro	Traverse City	Alameda Naval	California Site
Contaminant Data					
Biodegradation[7]					
Dominant layer thick (m)	0.3	N/A	3	0.2	2
Damkohler Number (-)	B,T,X=7.4+/-1 ,6.05+/-1, 5.2+/-1	N/A	4	~6[4]	9
1st order fitted decay constant (water phase) (1/hr)	B,T,X=0.5-2 (1.2) ,0.3-1.5(0.9), 0.2-0.8(0.5)[5]	N/A	~0.01[6]	~2[4]	~0.4[6]

Notes:
5. Parameters that are assumed are in bold type, mean values given unless otherwise noted, see Table 6.2 for other parameters
2. B=benzene, T=toluene, E=ethylbenzene, X=xylene, TPH=total petroleum hydrocarbon, isoP=isopentane, OM=order-of-magnitude, adj=adjacent
3. Estimated based on wind loading (building was not mechanically ventilated)
4. Degradation over-estimated due to likely presence of low moisture content layer (i.e., physical barrier)
5. Range and best estimate
6. Order-of-magnitude estimate due to significant uncertainty in air-filled and total porosity and physico-chemical properties
7. For details see Hers et al., 2000.

Description of Case Study Sites

The source BTX vapour concentrations at the Chatterton site were high (1 to 20 mg/L) since no other hydrocarbon compounds are present. Predicted vapour concentrations based on partitioning between the immiscible-phase and vapour adjusted for mole fraction, were about two times higher than measured concentrations when vapour pressures representative of *in-situ* temperatures were used (10 to 15°C). The source BTEX concentrations at three gasoline-contaminated sites were several hundred to thousand ug/L. For the Paulsboro site, predicted BTEX vapour concentrations were two to four times higher than those measured, based on partitioning between the groundwater (*i.e.*, dissolved concentrations) and vapour phases. The difference in predicted and measured vapour concentrations may be a result of non-representative physico-chemical properties or non uniform NAPL distribution in soil. Comparisons were not conducted for the remaining sites due to insufficient data.

With the exception of monitoring below the building at the Paulsboro site, the hydrocarbon vapour profiles exhibited significant attenuation with decreasing depth. The depth to contamination below the building foundations ranged from about 1.35 to 4 m, and soil at all sites consists primarily of sand. Biodegradation was demonstrated to be a primary process for vapour attenuation. At the Paulsboro site (only site with basement), the BTEX vapour concentrations directly below the foundation slab were elevated and O_2 concentrations were low (less than one percent). In contrast, BTEX vapour concentrations adjacent to the house (*i.e.*, at the same depth) were two orders-of-magnitude lower, and O_2 levels were about 14 percent. The Paulsboro site study is significant since it suggests that hydrocarbon vapour can accumulate below a building. None of the case study sites evaluated had vapour profiles consistent with steady-state diffusion for a uniform soil deposit (*i.e.*, linearly increasing vapour concentrations with depth), which is the condition described by the GSI model.

Biodegradation Rates

Aerobic biodegradation rates are dependent on O_2 transport, and determination of these rates is complicated by other processes that are occurring at the same time (*e.g.*, diffusion, sorption and advection). Providing that O_2 is not rate limiting, BTEX biodegradation appears to approximate a first-order process for BTEX concentrations below about 1 mg/L (DeVaull *et al.*, 1997; Hers *et al.*, 2000). Damkohler numbers and first-order aerobic biodegradation rates for four case study sites were estimated by fitting measured hydrocarbon vapour profiles to an analytical solution for one-dimensional diffusion and decay (Equations 5 and 6) (Table 6.5). The degradation rates are highly sensitive to the Damkohler number, effective diffusivity and moisture content. For the Alameda site, degradation rates are likely overestimated due to the probable presence of a thin but unquantified high moisture content layer and possible effect of advection in shallow soil. For the Alameda site, the biodegradation rate in part incorporates the effect of a diffusive barrier. Since in practice it is difficult to detect thin higher moisture content layers in soil deposits, the fitted biodegradation rate may, in effect, be a lumped parameter that includes unresolved moisture content effects. Due to the various sources of uncertainty, the estimated biodegradation rates should be considered order-of-magnitude estimates.

Soil Gas Advection and Flow into Buildings

Several studies have indicated pressure coupling occurs between a building and soil when there is sustained building underpressurisation relative to atmospheric air. For example, Garbesi *et al.* (1993) report a pressure coupling between soil and experimental basement (*i.e.*, relative to that between the basement and atmosphere) equal to 96 % directly below the slab, between 29 and 44 % at 1 m below the basement floor slab, and between 0.7 and 27 % at a horizontal distance of 2 m from the basement wall. At the Chatterton site, the pressure coupling immediately below the building floor slab ranged from 90 to 95 % and at a depth of 0.5 m was on the order of 50 % (Chapter 5). These results indicate that advective soil gas transport can extend to several meters from the building foundation.

Measured soil gas flow rates into a building were compared to predicted rates for the Flow to "Perimeter Crack" model (used in RISC) and Flow through Foundation or "Parallel Plate" model (used in SVIM) to provide insight on the accuracy of simple flow models (Table 6.7). Soil gas flow and intrusion rates into the building were generally measured by a mass balance approach using hydrocarbon constituents, radon or injected tracer (*e.g.*, sulphur hexafluoride) (Chapter 5). Due to unavoidable experimental limitations, flow rates are order-of-magnitude estimates. The comparisons in Table 6.7 reveal that the predicted rates are generally within an order-of-magnitude of measured rates. The flow rates are highly sensitive to crack width for the Parallel Plate model. When flow through soil and a foundation is viewed in terms of a series resistance model, the Perimeter Crack model may be more appropriate when the primary resistance to flow is associated with soil (*i.e.*, foundation is less important). Alternatively, the Parallel Plate model may be more important when the primary resistance to flow is associated with the foundation (*i.e.*, soil is less important). The Perimeter Crack model appears to provide for better comparisons to measured data, and is considered preferable in most cases since it is more robust and less affected by foundation properties.

Table 6.7. Comparison of Measured and Predicted Soil Gas Flow Rates into Building

Site	Foundation Type	ΔP (Pa)	η	b (FF model) (mm)	$k_{soil-air}$ (Darcy)	Soil Gas Flow Rates into Building: Measured w\ Tracer (L/min)	Predicted: FPC (RISC) (L/min)	Predicted: FF (SVIM) (L/min)
Chatterton Site	Slab-on-grade	30	0.00033	2.2	10	2.7	29	172
		10	0.00033	2.2	10	4.2	9.6	57
		10	0.0001	2.2	10	2.9	8.2	50
Alameda Site	Slab-on-grade	3	**0.0001**	**0.2 & 1** [3]	10	1.4 [4]	2.4	0.53 & 7.5 [3]
Central California Site Garbesi & Sextro (1989)	Filled hollow block basement w\coating	30	**0.0001**	**0.2 & 1**	3	67	8.3	29 & 109
Ben Lomond Garbesi *et al*.(1993)	Experimental Basement	10	0.00075	3	6	9.7	2.3	16
Spokane Valley Houses Revzan *et al*. (1991)	Poured Concrete Basements	5	**0.0001**	**0.2 & 1**	200	102	110	18 & 374

Notes:

1) Values in bold print were assumed, all other values were measured

2) ΔP=building underpressurization, η=crack ratio, b = crack width, FPC = Flow to Perimeter Crack, FF = Flow through Foundation model

3) When two values provided for predicted soil gas flow rate, first is for 0.2 mm crack, second is for 1 mm crack width.

4) Estimated based on wind loading

Field monitoring at the Chatterton and Alameda sites, and tracer tests at several radon research sites also provide insight on the importance of advective soil gas intrusion into a building relative to the building ventilation rate (Table 6.8). Excluding the apartment site, the ratio of soil gas intrusion rate to ventilation rate (Q_{soil}/Q_b), and soil gas intrusion rate normalized by pressure and foundation area ($Q_{soil}/(\Delta P*A)$ range over one order-of-magnitude. The important implication of these results is that the inferred indoor air concentrations are at least 1000 times less than concentrations directly below the building slab, assuming advection is the primary mechanism for vapour intrusion. These results support the minimum indoor air to source vapour attenuation ratio of about 0.001 estimated by Johnson *et al.* (1998) using the Johnson and Ettinger model.

Table 6.8. Comparison of Measured Soil Gas Flow Rates into Buildings

Reference	Building	Foundation Type & Construction	Q_{soil}/Q_b	$Q_{soil}/(\Delta P*A)$ (L/min-Pa-m2)
Apartment site, Vancouver B.C. (in-progress by author)	Below ground parkade	Basement Poured Concrete	0.00005	0.002
Chatterton Site	Small building (greenhouse)	Slab-on-grade, poured concrete, 2-mm edge crack	0.0003 to 0.0006	0.005 to 0.01
Alameda Site	Small building	Slab-on-grade, poured concrete	0.0002 to 0.0004	0.006
Central California Site Garbesi and Sextro (1989)	House	Basement, poured slab, block walls w\ asphalt coating	~0.001	0.02
Ben Lomand Site, CA Garbesi *et al.* (1993)	Experimental basement	Basement, poured slab with 3-mm wide edge crack	N/A	0.04

Notes:

1. Qsoil = Soil gas advective flow into building enclosure, Qb = building ventilation rate
2. ΔP = building depressurization relative to atmosphere, A = subsurface building foundation area

Soil Vapour Intrusion into Buildings

Chatterton Site Results

Extensive testing was conducted at the Chatterton site to measure soil vapour intrusion into an experimental building (greenhouse) constructed at the site. The building was fastened to a 6.1 by 9.3 m at-grade concrete slab constructed with an adjustable length 2-mm wide perimeter edge crack. An edge crack of variable size is often present at the interface between a floor slab and foundation wall, for residential construction. Monitoring of soil gas intrusion into the greenhouse was conducted under natural conditions (*i.e.*, no fan-induced depressurization) and depressurized conditions. During natural conditions, temperature differences and barometric pressure changes caused the building to be either over- or under-pressurized relative to subsurface pressures and caused advective pumping of soil gas to occur. The diurnal temperature-induced pressure variations were as high as 2 to 3 pascals (Pa) during the summer months, however, time-averaged pressure gradients (ΔP) were negligible. Vapour intrusion for the depressurized condition was measured for sustained depressurizations of 2.5, 10 and 30 Pa. Possible routes of soil gas entry through the building envelope were the partially sealed edge crack, possible hairline cracks surrounding 28 soil gas probes and two capped PVC drain pipes penetrating the concrete slab. In addition, a small north-south trending shrinkage crack bisects the approximate middle of the slab.

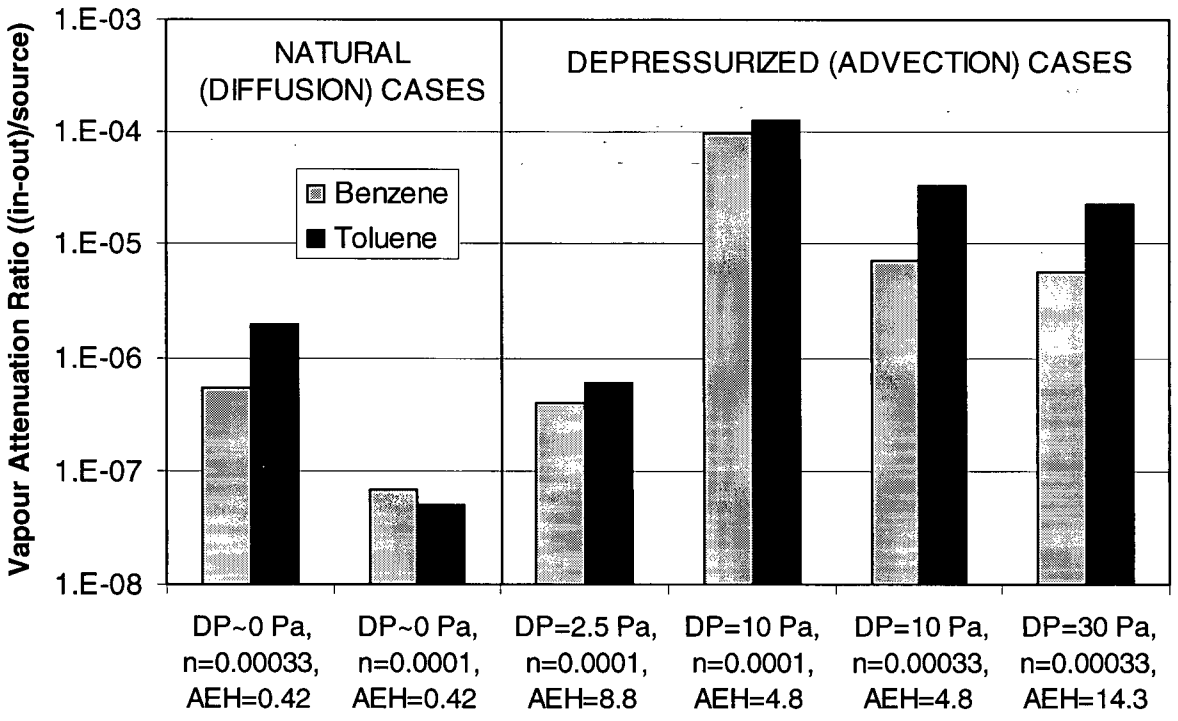

Figure 6.3. Measured Vapour Attenuation Ratio based on Hydrocarbon Intrusion Monitoring at Chatterton Site (no significant difference in indoor & outdoor concentrations obtained for natural cases)

The BTX vapour flux into the building was estimated using (i) a mass balance approach where the measured indoor, outdoor and sub-slab vapour concentrations, and measured

ventilation rates were input into a box mixing model, and (ii) direct measurements using a flux chamber. Vapour concentrations were measured at six locations directly below the slab, and a minimum of three time-composited indoor and outdoor samples were analyzed for each case. The methods used and results are described in greater detail in Chapter 5 with a summary provided below.

The measured attenuation ratios for benzene, defined as:

$$\alpha_m = \text{(indoor air conc.- outdoor air conc.) / vapour conc. at contamination source} \quad (13)$$

are presented in Figure 6.3. For the two natural cases, which are expected to represent primarily diffusive transport, there was no statistically significant difference between outdoor air concentrations, and indoor air or flux chamber concentrations. For the depressurized cases, which are expected to reflect primarily advective transport, there was a slight difference in indoor and outdoor air concentrations for the 2.5 Pa case (3X to 4X) and generally a large difference for the 10 and 30 Pa cases (3X to over 100X). The depressurized cases can not be directly compared due to variable ventilation rates. This, in part, explains why α_m was lower for the 30 Pa compared to 10 Pa case. The ventilation rates values are higher than those typically encountered in buildings (Appendix I); however, for model validation purposes these rates are considered acceptable.

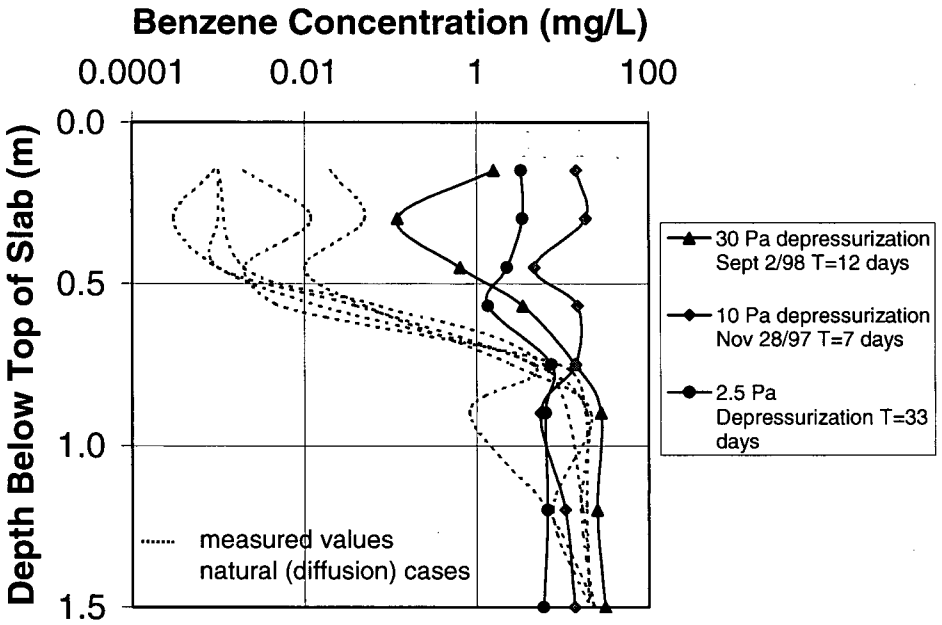

Figure 6.4. Measured Benzene Vapour Profile Below Centre of Building at Chatterton Site (ΔP=depressurization, T=time from start of depressurization to sampling)

The vapour concentrations below the building also provide insight into the effect of building depressurization on vapour migration. The vapour concentrations below the centre of the building are shown for the natural and depressurized cases in Figure 6.4. There is significant attenuation of benzene vapour concentrations under natural conditions, however, very little

attenuation under depressurized conditions indicating a build-up of vapours below the building. Higher vapour concentrations directly below the building for the 10 Pa, compared to 30 Pa case, may be due to transient effects since the time duration between the start of the depressurization experiment and vapour sampling varied (Figure 6.4), or other factors such as differences in relative transport rates for BTX and oxygen.

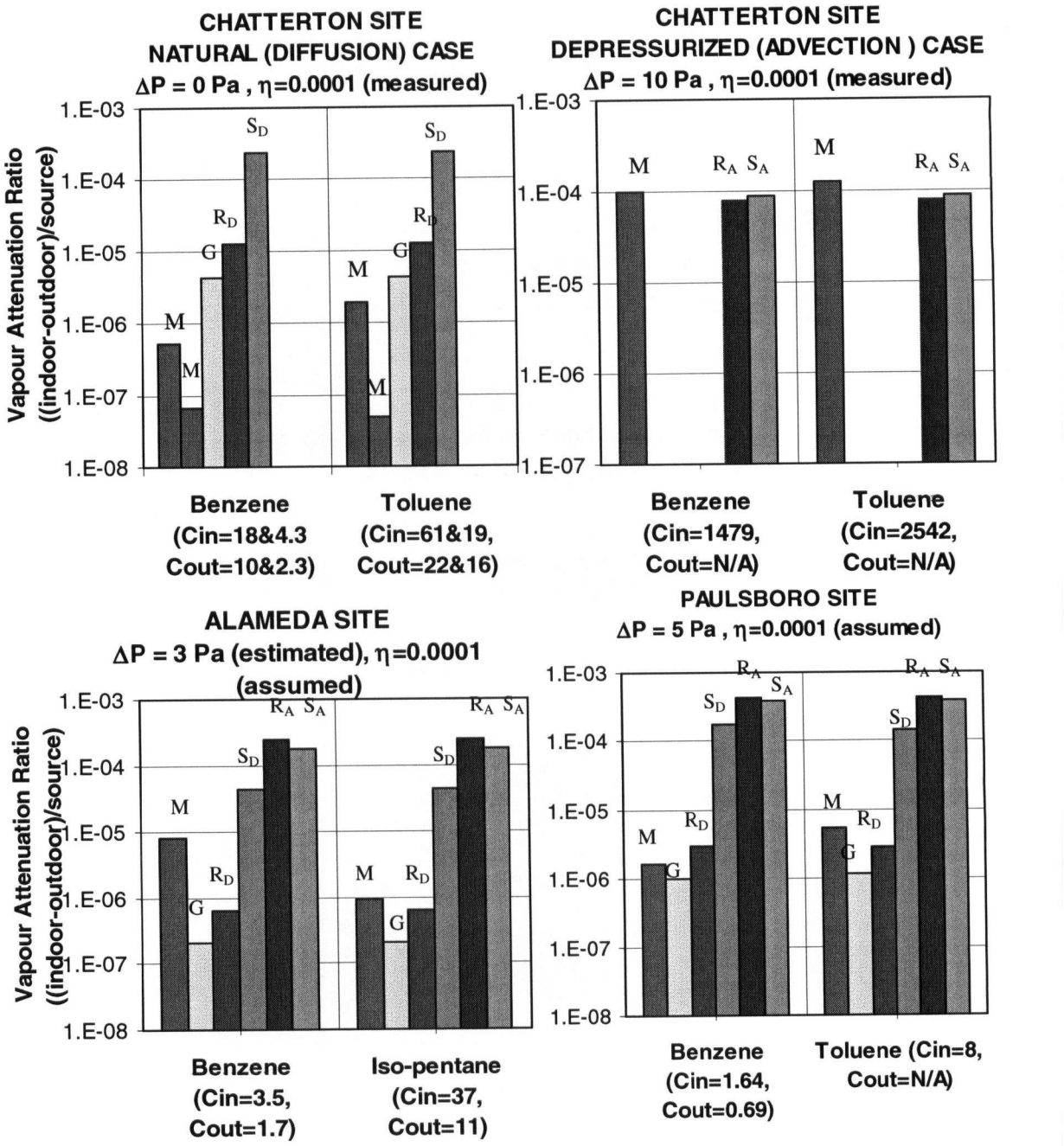

Figure 6.5. Comparison of Measured and Predicted Vapour Attenuation Ratio (M = measured, G = GSI model (diffusion only), S_D = SVIM w\ diffusion only, S_A = SVIM w\ advection, R_D = RISC w\ diffusion, R_A = RISC w\ advection)

Of note is that the vapour concentrations below the centre of the building were elevated for the 2.5 Pa case; however, indoor air concentrations were only slightly higher than outdoor air concentrations indicating non-significant flux relative to results obtained for higher depressurizations. The reason for the low flux for the 2.5 Pa case is that vapour concentrations below the building edge crack were low and close to ambient levels, whereas for the 10 and 30 Pa cases, concentrations were elevated below the entire building slab. Flux chamber testing indicated that the majority of soil gas flow into the building is through non-sealed portions of the edge crack. The results suggest that for the 2.5 Pa case, O_2 transport and biodegradation rates are sufficient to degrade BTX vapours near the edge of the building; however, for the 10 Pa case, biodegradative capacity is exceeded as a result of the higher advective soil gas flow rates and a flow zone which extends from the foundation to near to the contamination source.

Comparisons of Measured and Predicted Vapour Attenuation Ratios

Measured and predicted vapour attenuation ratios (α_m and α_p) were compared for the Chatterton, Alameda and Paulsboro sites (Figure 6.5). For the Chatterton natural (diffusion) cases, and Alameda and Paulsboro sites, the indoor and outdoor concentrations were similar and generally at background levels; therefore, comparisons are qualitative and only provide a general indication of the predictive capabilities of the models used. For the Paulsboro and Alameda sites only a limited number of samples were generally analyzed, and building properties (η, ΔP and AEH) were not directly measured. Due to the uncertainty in ΔP, the diffusion only and diffusion and advection models were compared on the same plot for the Paulsboro and Alameda sites (Figure 6.5).

For the Chatterton natural cases, the building ventilation rate (*i.e.*, through an open door and louvres) could not be measured and was assumed. This assumed natural ventilation rate was 12 to 34 times lower than ventilation rates for the depressurized cases. This difference in ventilation rates is the reason why the SVIM model predicts higher α_p for the natural condition case than for the depressurized case. The key findings of the model comparisons are summarized below.

1. For the Chatterton natural (diffusion) cases, the diffusion only models yield α_p values that exceed α_m by at least two orders-of-magnitude indicating predictions are conservative.

2. For the Chatterton depressurized (advection) cases, α_p for the diffusion and advection models is very close to α_m.

3. For the Alameda and Paulsboro sites, the diffusion only models result in α_p values that are on the same order or lower than α_m (for GSI and RISC). Differences in the diffusion model for the concrete slab and input assumptions result in significantly higher SVIM α_p when compared to GSI and RISC models (see Section 3). For these sites, models incorporating both diffusion and advection result in α_p values that are at least one order-of-magnitude greater than α_m.

4. Although there is only limited validation data and a high level of uncertainty, it appears that diffusion only models could result in non-conservative predictions when only diffusion through cracks is simulated and a low crack ratio is chosen.

5. When there is shallow contamination, permeable soils and relatively high, sustained building underpressurization (*i.e.*, similar to Chatterton site), models incorporating diffusion and advective transport through the foundation only may not be conservative. These conditions would be expected at only a small number of sites.

PROPOSED TIERED FRAMEWORK, DISCUSSION AND GUIDANCE

The objective of this work has been to evaluate available screening level models and provide guidance on suitable models, input parameters and a tiered framework for model use. Integral to this evaluation is an understanding of the key processes and input parameters that control hydrocarbon vapour intrusion into buildings, and the differences between models. Key processes include diffusion, advection and biodegradation, for BTEX and petroleum hydrocarbon vapours. Important input parameters include depth to contamination, moisture content, soil permeability and building underpressurization. As described in this paper, various transport processes and site conditions have a large influence on vapour intrusion into buildings and indoor air concentrations.

Proposed Tiered Framework

Several organizations and regulatory bodies in North America (*e.g.*, CCME, ASTM) have adopted a tiered approach where model and input complexity increases for successive tiers. Typically, Tier 1 involves the use of a simple model and default input parameters to derive risk-based screening levels. For Tier 2, additional site-specific factors and possibly a more complex model would be used, while for Tier 3, model requirements would be defined as part of a site-specific assessment. Implicit in this framework is that Tier 1 is the most conservative tier. The conventional use of a tiered assessment framework is challenged by process variability and model sensitivity to certain parameters. For example, it is clear from model comparisons presented earlier that a simple Tier 1 model based on diffusion only may not always represent the most conservative solution.

A proposed conceptual framework for the soil vapour transport to indoor air pathway is developed on the basis of depth to contamination, "advection potential", which is primarily a function of soil air permeability and building underpressurization, and "diffusion potential", which is primarily a function of soil moisture and type (Figure 6.6). Recommended model attributes for each tier are presented in Table 6.9.

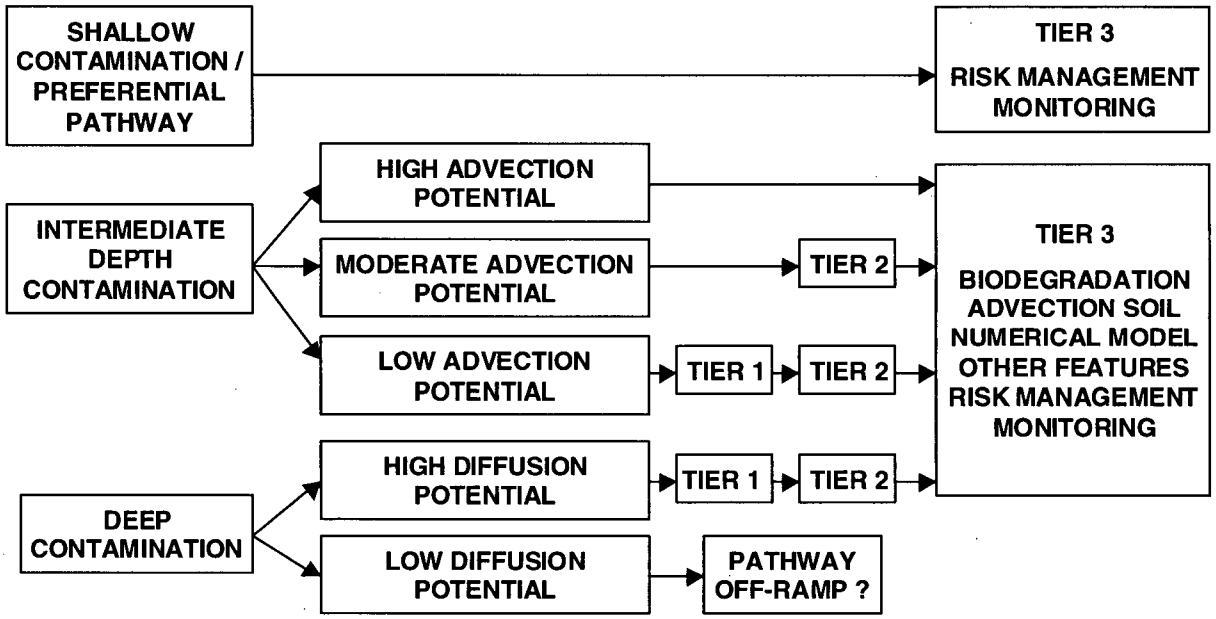

Figure 6.6: Conceptual Framework for Use of Models for Soil Vapour to Indoor Air Pathway (Tier 1 = diffusion only; Tier 2 =, diffusion & advection) (Possible depth ranges: shallow<~1 m, intermediate~1 to 5 m, deep>~5m)

Table 6.9. Recommended Soil Vapour Model Attributes

Tier One		*Tier Two (continued)*	
Input soil concentrations	✔	Moisture content multiple soil layers	✔
Input groundwater concentrations	✔	Advection through building foundation[2]	✔
Equilibrium 3-phase linear partitioning	✔	Source depletion	✔
Diffusion in soil	✔	*Tier Three (possible options)*	
Diffusion through dirt-filled concrete cracks	✔	Biodegradation	✔
Diffusion through intact concrete[1]	✔	Sub-model for estimating ΔP	✔
Mixing in building enclosure (box model)	✔	Sub-model for estimating ventilation	✔
Tier Two		Sub-model crawlspace effects	✔
Input soil vapour concentrations	✔	Advective chemical transport in soil	✔
NAPL partitioning (NAPL and vapour)	✔	Other	✔

[1] Not required when appropriate minimum crack ratio used
[2] Recommend Flow to Perimeter Crack model

Tier 1 represents a simple screening assessment with minimum data requirements and is based on diffusive transport only. A Tier 1 model may be appropriate for sites with low advection potential and would be expected to yield conservative predictions providing that reasonable input parameters are used. For models that only allow for diffusion through concrete cracks, a reasonable range for crack ratio may be 0.0001 to 0.001, based on model comparisons presented in this paper.

The Tier 2 model incorporates both diffusion and advection through the building foundation and may be appropriate for intermediate depth contamination combined with moderate advection potential. A Tier 2 model should allow for NAPL to vapour partitioning, direct input of vapour

concentrations and source depletion. Since moisture content has a large effect on vapour flux, the capability to simulate multiple soil layers should also be included, and in some cases, it may important to predict the long-term effect of a building on the potential drying of soil.

The Tier 3 assessment or mitigation scope would depend on the site conditions. When contamination is shallow and/or there are preferential pathways, predictive models are considered unreliable. Therefore, the appropriate response would generally consist of risk management measures and/or indoor air monitoring, unless it could be shown that the contamination source concentrations were not significant. A Tier 3 assessment could also be appropriate for sites with intermediate depth contamination but high advection potential, or if other processes such as biodegradation are modeled. As additional data on hydrocarbon vapour biodegradation becomes available, it may be possible to incorporate biodegradation modeling as part of a Tier 2 assessment.

There may also be opportunity to eliminate sites from further consideration (*i.e.*, provide for a pathway "off-ramp") as part of initial screening based on site information combined with a preponderance of case study evidence indicating that the conditions will not result in unacceptable risks. This may, for example, apply to sites with a deep groundwater table, deep contamination and extensive fine-grained soil deposits. Further guidance is provided below with respect to several key Tier 2 and 3 issues, including several potential limitations associated with screening models.

Advection Potential

To gain further insight in the relative importance of advection, the SVIM model modified to use the Perimeter Crack model was used to predict α for varying soil air permeability and contamination depth (Figure 6.7). A fixed ΔP of 5 Pa was used. Underpressurizations of between 3 and 10 Pa (relative to ambient air) are common in residences during the heating season in Canada and parts of the USA due to temperature differences between indoor and outdoor air and the effects of mechanical ventilation (Appendix I). Advective chemical transport was limited to that occurring through the building foundation. The model predictions provide a basis for screening sites for advection potential and determination of the appropriate tier. For example, the advection potential would likely be low if the soil air permeability was less than about 0.1 Darcy (10^{-13} m^2) or if contamination depth was greater than about 5 m. For reference purposes, a soil air permeability of 0.1 Darcy corresponds approximately to a silty fine sand whereas a permeability of 10 Darcy corresponds approximately to a medium sand.

Advective chemical transport in soil is not included in screening models commonly used in North America, but may be appropriate as part of a Tier 3 assessment for a limited number of sites. The VOLASOIL model (Waitz *et al.*, 1996) provides a simple method of including advective transport in soil through an equation for one-dimensional steady-state vapour-phase chemical flux in soil due to diffusion and advection:

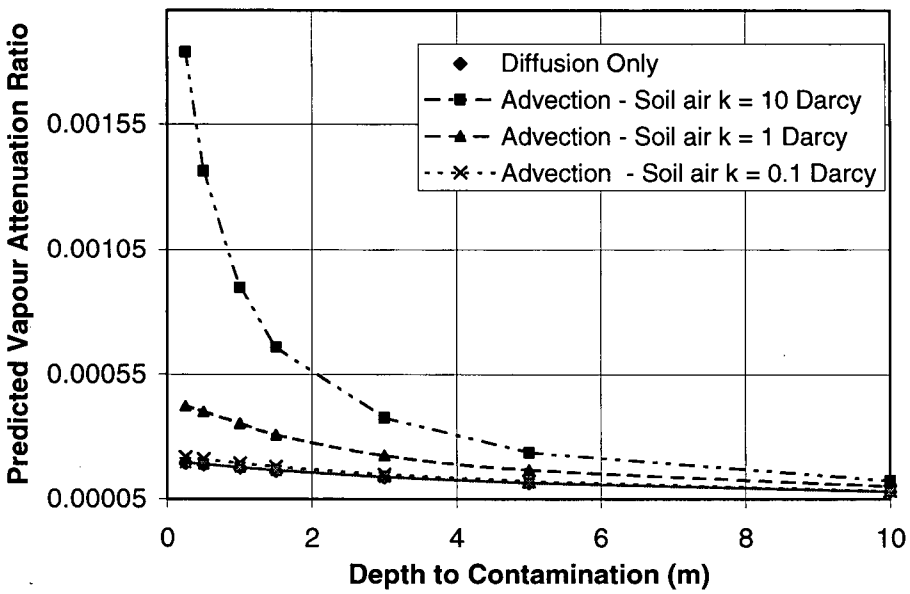

Figure 6.7. Influence of Advective Transport on Vapour Attenuation Ratio (SVIM model modified to use Flow to Perimeter Crack model, ΔP = 5Pa, Table 2 parameters)

$$J_{soil} = - D_g \, \delta C_g / \delta z + F_g \, C_g \qquad (14)$$

where J_{soil} is the flux, D_g is the diffusion coefficient and C_g is the soil vapour concentration. Based on equation 14, the analytical solution for chemical flux is:

$$J_{soil} = - F_g \, (C_{gs} - C_{gbs} \, exp \, [F_g L_s / D_g^{eff}]) / (exp[F_g L_s / D_g^{eff}] - 1) \qquad (15)$$

where C_{gs} and C_{gbs} are the soil vapour concentrations at source and below the building slab, F_g is the advective soil gas flow rate and L_s is the distance over which advective flow occurs. The SVIM model was adapted to include advective vapour transport in soil. Model simulations indicate that α_p continues to increase linearly with increasing underpressurization and does not approach an asymptotic limit, which is the trend predicted by models that couple diffusion in soil with diffusion and advection through the foundation (see Figure 6.1). The above equations are a highly simplified approximation of boundary conditions and flow regime, and likely represent an upper range or worst case estimate of advective chemical transport in soil due to building effects.

Source Depletion

The GSI and VAPEX4 models require input of an averaging time for vapour flux to estimate source depletion. The averaging time for vapour flux is related to human health risk assessment methodology and is often set to the exposure duration (*e.g.*, 25 to 30 years), since toxicity factors are based on long-term exposure. When a small mass of chemical is input into the model, source depletion can result in a time-averaged concentration that, particularly for highly volatile

chemicals, is significantly lower than the peak concentration. This may be problematic when time-averaged concentrations are compared to toxicity factors based on approximately constant long-term exposure concentrations. When the GSI or VAPEX4 models are used, it is recommended that a range of averaging times and/or source masses be used to investigate the effect of source depletion on indoor air concentrations, and that appropriate adjustments be made, as warranted.

Biodegradation

Factors affecting biodegradation rates for BTEX and petroleum vapours are O_2 transport, and possibly soil moisture content if drying occurs. Oxygen transport below a building is affected by building properties, nearby surface barriers and barometric and/or temperature-induced pumping. There is some evidence that a significant reduction in biodegradation rates occur for soil moisture lower than the permanent wilting point of soil (Zwick *et al.*, 1995; Holden *et al.*, 1997). In general, the biodegradation potential is expected to decrease as the ratio of building area (or width) to contamination depth increases.

Providing there is sufficient evidence for biodegradation it may be appropriate to add a first-order decay function to screening models (*e.g.*, RISC) on a site-specific basis. In this context, Johnson *et al.* (1998) highlight the importance of obtaining supporting information including a conceptual model consistent with hydrocarbon loss through biodegradation, O_2 and carbon dioxide profiles, and vapour concentrations with depth for a compound recalcitrant to biodegradation. Biodegradation kinetics should be carefully evaluated since predicted fluxes and concentrations are highly sensitive to the rate chosen. When changes to site conditions could occur (*e.g.*, building construction), it is also important to evaluate whether biodegradation can be relied upon in the future. The use of fitted first-order biodegradation rates implicitly assume that O_2 is not rate limiting. An alternate and potentially more rigorous approach is to solve the coupled hydrocarbon vapour and O_2 transport equation combined with first-order biodecay and O_2 consumption, for appropriate boundary conditions.

CONCLUDING THOUGHTS

In closing, knowledge of vadose zone processes and vapour intrusion into buildings has improved over the past decade and in many cases available screening models can be reliably used. Model comparisons presented in this paper for petroleum hydrocarbon sites suggest that models incorporating diffusion and advection based on the Johnson and Ettinger (1991) framework will, in most cases, result in predictions that are conservative by up to one to two orders-of-magnitude providing that appropriate input parameters are used. Models should be used with caution and appropriate adjustments made when the advection potential is relatively high. Despite advances made, model and parameter uncertainty remains significant and there are opportunities for further research on advective vapour intrusion, interaction between building and vadose zone (*e.g.*, gas pumping, ΔP effects), biodegradation models and kinetics, and specific issues relating to chlorinated solvents.

REFERENCES

American Society for Testing and Materials (ASTM). 1995. Standard Guide for Risk-Based Corrective Action Applied at Petroleum Release Sites. E-1739-95.

American Society of Heating, Refrigerating, and Air-Conditioning Engineers, *ASHRAE Handbook-1985 Fundamentals.*, Chap. 22, Atlanta, GA.

Bouchard, D.C., C.G. Enfield, and M.D. Piwoni. 1987. Transport Processes Involving Organic Chemicals. In: Soil Sci. Amer. Special Pub. No. 22, Eds. B.L. Sawhney and K. Brown.

Canadian General Standards Board (CSGB). 1986. Determination of the Airtightness of Building Envelopes by the Fan Depressurization Method. CAN/CSGB-149.10-M86.

Chiou, C.T. 1987. Theoretical Considerations of the Partition Uptake of Nonionic Organic Compounds by Soil Organic Matter. In: Soil Sci. Amer. Special Pub. No. 22. Eds. B.L. Sawhney and K. Brown.

Daugherty, S. 1991. Regulatory Approaches to Hydrocarbon Contamination from Underground Storage Tanks. In: *Hydrocarbon Contaminated Soils and Groundwater.* Eds. Paul T. Kostecki and Edward Calabrese, Lewis Publishers.

Daugherty, S. 1997. Use of Subsurface Vapour to Indoor Air Exposure Models by a Local Health Agency: Historical Development and Issues Encountered. In: Proc. Petroleum Environmental Research Forum (PERF) Symposium. Brea, California, February 6 and 7.

DeVaull, G., R.A. Ettinger, J.P. Salanitro, and J. Gustafson. 1997. Benzene, toluene, ethylbenzene and xylenes degradation in vadose zone soils during vapour transport: first-order rate constants. In: Proc. 1997 Petrol. Hydro. and Org. Chem. in Ground Water. API/NGWA, Houston, Tx., Nov.:365-379.

Ferguson, C.C., Krylov, V.V., and McGrath, P.T. 1995. Contamination of Indoor Air by Toxic Soil Vapours: a Screening Risk Assessment Model. *Building and Environment.* 30(3):375-383.

Figley, D.A., L.J. Snodgrass. 1992. Comparative Foundation Air Leakage Performance of Ten Residential Concrete Basements. In: Proc. 85th Annual Meeting of Air and Waste Management Assoc. June 21-26.

Figley, D.A. 1997. A Guide for Estimating Indoor Concentrations of Soil Gas Pollutants in Houses. Prepared for CMHC.

Fischer, M.L., A.J. Bentley, K.A. Dunkin, A.T. Hodgson, W.W. Nazaroff, R.G. Sextro, and J.M. Daisey. 1996. Factors Affecting Indoor Air Concentrations of Volatile Organic Compounds at a Site of Subsurface Gasoline Contamination. *Environ. Sci. Technol.* 30 (10):2948-2957.

Fitzpatrick, N.A. and J.J. Fitzgerald. 1997. An Evaluation of Vapour Intrusion into Buildings through a Study of Field Data. Massachusetts Department of Environmental Protection.

Garbesi, K. and R.G. Sextro. 1989. Modeling and Field Evidence of Pressure-Driven Entry of Soil Gas into a House through Permeable Below-Grade Walls. *Environ. Sci. Technol.* 23(12):1481-1487.

Garbesi, K., R.G. Sextro, W.J. Fisk, M.P. Modera, and K.L. Revzan. 1993. Soil-Gas Entry into an Experimental Basement: Model Measurement Comparisons and Seasonal Effects. *Environ. Sci. Technol.* 27(3):466-473.

Grimsrud, D.T., M.H. Sherman, and R.C. Sonderegger. 1982. Calculating Infiltration: Implications for a Construction Quality Standard. In: Proc. Amer. Soc. of Heating, Refrigeration, and Air-Conditioning Engineers and the U.S. Department of Energy Conference: Thermal Performance of the Exterior Envelopes of Buildings II. Las Vegas, NV., December.

Hers, I., R. Zapf-Gilje, R. Petrovic, M. Macfarlane, and R. McLenehan. 1997. Prediction of Risk-Based Screening Levels for Infiltration of Volatile Sub-surface Contaminants into Buildings. Environ. Tox. and Risk Assessment (6th Vol.), ASTM STP 1317. Eds: F. J. Dwyer, T. Doane, and M. L. Hinman.

Hers, I. and R. Zapf-Gilje. 1998. Canadian consortium research project – field validation of soil gas transport to indoor air pathway. In: Proc. 1998 Petrol. Hydro. and Org. Chem. in Ground Water. API/NGWA, Houston, Tx., Nov. 11-13:251-266.

Hers, I., J. Atwater, L. Li and R. Zapf-Gilje. 2000. Evaluation of Vadose Zone BTX Biodegradation. *Journal of Contaminant Hydrology.* 46:233-264.

Hodgson, A.T., 1992. Soil-Gas Contamination and Entry of Volatile Organic Compounds into a House Near a Landfill, *J. Air and Waste Management Assoc.* 29:277-283. March.

Holden, P.A., L.J. Halverson, and M.K. Firestone. (1997). Water stress effects on toluene biodegradation by *Pseudomonas putida. Biodegradation.* 8:143-151.

Jeng, C.Y, V.J. Kremesec, Jr., and H.S. Primack. 1996. Models of Hydrocarbon Vapour Diffusion through Soil and Transport into Buildings. In: Proc. 1996 Petrol. Hydro. and Org. Chem. in Ground Water. API/NGWA, Houston, Tx., November 13-15:319-338.

Johnson, P.C. and R. Ettinger. 1991. Heuristic Model for Predicting the Intrusion Rate of Contaminant Vapours into Buildings. *Environ. Sci. Technol.* 25 (8):1445-1452.

Johnson, P.C., W. Kemblowski, and R.L. Johnson. 1998. Assessing the Significance of Subsurface Contaminant Vapour Migration to Enclosed Spaces – Site Specific Alternatives to Generic Estimates. API Publication 4674, December.

Jury, W.A., D. Russo, G. Streile, and H. El Abd. 1990. Evaluation of Volatilization by Organic Chemicals residing Below the Soil Surface, *Water Resources Research.* 26(1):13-20.

Krylov, V.V., and C.C. Ferguson. 1998. Contamination of Indoor Air by Toxic Soil Vapours: the effects of Subfloor Ventilation and Other Protective Measures. *Building and Environment.* 33(6):331-347.

Laubacher, R.C., P. Bartholomae, P. Velasco and H.J. Reisinger. 1997. An evaluation of the Vapour Profile in the Vadose Zone Above a Gasoline Plume. In: Proc. 1997 Petrol. Hydro. and Org. Chem. in Groundwater, API/NWGA, Houston, Tx., pp. 396-409.

Mendoza, C.A. personal communication, adaptation of VapourT model described in Mendoza, C.A., Frind, E.O. March 1990. "Advective-Dispersive Transport of Dense Organic Vapours in the Unsaturated Zone 1. Model Development", *Water Resources Research.* 26(3):379-387.

Millington, R.J. and J.M. Quirck. 1961. Permeability of Porous Solids. Trans. Farady Soc. 1200-1207.

Mueller Associates, Syscon Co., and Brookhaven National Laboratory, 1988. Handbook of Radon in Buildings. Hemisphere Publishing Co. New York, NY.

Nazaroff, W.W., H. Feustel, A.V. Nero, K.L. Revzan, D.T. Grimsrud, M.A. Essling, and R.E. Toohey. 1985. Radon Transport into a Detached One-Story House with a Basement. *Atmospheric Environ.* 19(1):31-46.

Nazaroff, W.W., 1992. Radon Transport from Soil to Air. *Review of Geophysics.* 30(2):137-160.

Nielson, K.K., V.C. Rogers, R.B. Holt, T.D. Pugh, W.A. Grondzik, and R.J. de Meijer. 1997. Radon Penetration of Concrete Slab Cracks, Joints, Pipe Penetrations, and Sealants. *Health Physics.* 73(4):668-678.

Ostendorf, D.W. and D.H. Kampbell. 1991. Biodegradation of Hydrocarbon Vapours in the Unsaturated Zone. *Water Resources Research.* 27 (4):453-462.

Renken, K.J and T. Rosenberg. 1995. Laboratory Measurements of the Transport of Radon Gas through Concrete Samples. *Health Physics.* 68(6):800-808.

Revzan, K.L., W.J. Fisk, A.J. Gadgil. 1991. Modeling Radon Entry into Houses with Basements: Model Description and Verification. *Indoor Air.* 2:173-189.

Rodgers, V.C., K.K. Neilson, R.B. Hold, R. Snoddy. 1994. Radon Diffusion Coefficients for Residential Concrete. *Health Physics.* 67(3):261-265.

Ryrie, T. and R. Sweeney. 1995. Fate and Transport of Volatile Hydrocarbons in the Vadose Zone. In: Proc. 1995 Petrol. Hydro. and Org. Chem. in Groundwater. API/NGWA, Houston, Tx., Nov. 29 to Dec. 1, pp. 529-542.

Ryrie, T., R. Sweeney, S. Daughery and P. Peuron. 1998. A Vapour Transport Model That is Consistent with Field and Laboratory Data. In: Proc. 1998 Petrol. Hydro. and Org. Chem. in Groundwater. API/NGWA, Houston, Tx., Nov. 11 to 13, pp. 299-308.

Sanders, P.A. and A.H. Stern. 1994. Calculation of Soil Cleanup Criteria for Carcinogenic Volatile Organic Chemicals as Controlled by the Soil-to-Indoor Air Exposure Pathway. *Environ. Tox. Chem.* 13(8):1367-1373.

Scanada Consultants Limited. 1993. Field Testing of House Characteristics, Report to CMHC. October.

Schwarzenbach, R.P., P.M. Gschwend and D.M. Imboden. 1993. *Environmental Organic Chemistry.* John Wiley and Sons Inc., New York, pp. 616.

U.S. EPA, 1992. Assessing Potential Indoor Air Impacts for Superfund Sites, Air/Superfund National Technical Guidance Study Series. EPA 451/R-92-002.

Waitz, M.F.W., J.I. Freijer, P. Keule and F.A. Swartjes. 1996. The VOLASOIL risk assessment model based on CSOIL for soils contaminated with volatile compounds. National Institute of Public Health and the Environment, Bilthoven, The Netherlands.

Zwick, T.C., A. Leeson, R.E. Hinchee, R.E. Hoeppel, and L. Bowling. 1995. Soil Moisture Effects During Bioventing in Fuel-Contaminated Arid Soils. In: In Situ Aeration: Air Sparging, Bioventing and Related Remediation Processes. Batelle Press, Coulmbus, pp. 333-340

CHAPTER 7

EVALUATION OF THE JOHNSON AND ETTINGER MODEL FOR PREDICTION OF INDOOR AIR QUALITY

This chapter was published in *Groundwater Monitoring and Remediation*, Summer, 2003.[5]

ABSTRACT

Screening level models are now commonly used to estimate vapour intrusion for subsurface volatile organic compounds (VOCs). Significant uncertainty is associated with processes and models, and to date, there has only been limited field-based evaluation of models for this pathway. To address these limitations, a comprehensive evaluation of the Johnson and Ettinger (J&E) model is provided through sensitivity analysis, comparisons of model-predicted to measured vapour intrusion for eleven petroleum hydrocarbon and chlorinated solvent sites, and review of radon and flux chamber studies. Significant intrusion was measured at five of twelve sites with measured vapour attenuation ratios (α_m's) (indoor air/source vapour) ranging from about $1x10^{-6}$ to $1x10^{-4}$. Higher attenuation ratios were measured for studies using radon, inert tracers and flux chambers; however, these ratios are conservative due to boundary conditions and tracer properties which are different than those at most VOC-contaminated sites. Reasonable predictions were obtained using the J&E model with comparisons indicating that model-predicted vapour attenuation ratios (α_p's) were on the same order, or less than the α_m's. For several sites, the α_m's were about two orders of magnitude less than the α_p's indicating that the J&E model is conservative in these cases. The model comparisons highlight the importance in using appropriate input parameters for the J&E model. The regulatory implications associated with use of the J&E model to derive screening criteria are also discussed.

KEY WORDS: vapour, attenuation, intrusion, validation, hydrocarbon, chlorinated solvents

[5] Hers, I., Zapf-Gilje, R., Johnson, P.C. and Li, L.

INTRODUCTION

The use of models to predict indoor air quality associated with volatile organic compound (VOC) contamination in soil and ground water is now commonplace (ASTM 1995; Johnson *et al.* 1998, Hers *et al.* 2002). Screening models typically used for this pathway are the Johnson and Ettinger (1991) model (henceforth referred to as the J&E model), or variants there of. Processes controlling the intrusion of VOC vapours into buildings are not well understood, the accuracy of J&E model is uncertain, and there have only been limited comparisons of model predictions to field data. There are also substantial differences in the way in which the J&E model is used for regulatory purposes.

To address these limitations, this paper presents a comprehensive evaluation of the J&E model based on theoretical considerations and field data from petroleum hydrocarbon and chlorinated solvent sites, and radon and flux chamber studies. Data sources are published studies, consultant or agency reports, and a field-based research program conducted by the authors. Included in the data sets analyzed are several recent ground breaking investigations at chlorinated solvent sites.

The paper begins with an analysis of methods for estimating input parameters for the J&E model, and their effect on model sensitivity and uncertainty. This analysis provides the needed context for the methods employed to interpret the field data used for this study. It is also important since, in our view, it is essential that model attributes and potential limitations be understood before using field data to evaluate the predictive capabilities of a model. Field-based methods for the evaluation of vapour attenuation ratio (α), defined as the indoor air concentration divided by the source vapour concentration, are evaluated next. The primary focus is α_m from eleven sites with petroleum hydrocarbon and chlorinated solvent contamination. Information from tracer studies using radon or an injected tracer such as sulpher hexafluoride (SF_6), and flux chamber studies are also reviewed. The measured α_m from field studies are compared to α_p predicted using the J&E model. Trends in the data are qualitatively evaluated and possible factors affecting vapour intrusion are considered. The paper also comments on the use of the J&E model to derive regulatory screening criteria.

J&E MODEL INPUT PARAMETERS, SENSITIVITY AND UNCERTAINTY

The basic form of the J&E model couples one-dimensional steady-state diffusion through soil, and diffusion and advection through a building envelope (i.e., foundation). A simple "box" model, which assumes uniform and instantaneous mixing of chemicals within the building enclosure, is used to estimate the indoor air concentration. Model sensitivity and uncertainty analysis, and input needed for comparisons of model predictions to field data all require estimation of effective diffusion coefficient and soil gas advection rates. Since the available data varied, different methods were used to estimate these input parameters and interpret field data. The estimation methods subsequently used in this paper are discussed below.

Estimation of Effective Diffusion Coefficient (Air-Filled and Total Porosity)

The J&E model utilizes the Millington and Quirck (1961) relationship to estimate the effective diffusion coefficient (D_T^{eff}), as follows:

$$D_T^{eff} = (\theta_a^{(10/3)} / \theta^2) * D_{air} + 1/H' * (\theta_w^{(10/3)} / \theta^2) * D_{water} \quad (1)$$

where θ_a , θ_w and θ are the air-filled, water-filled and total porosity, D_{air} and D_{water} are free-air and free-water diffusion coefficients, and H' is the dimensionless Henry's Law Constant.

A common method for estimating air-filled and total porosity directly uses the measured soil moisture content and bulk density. A potential disadvantage is that soil disturbance during sampling can lead to inaccurate moisture, density, and hence, porosity estimates. Samples obtained adjacent to buildings may not be representative of conditions below buildings due to the drying of soil that can occur.

A second method involves the use of the van Genuchten (VG) model (van Genuchten, 1980) to predict the water retention parameters for U.S. Soil Conservation Service (SCS) soil types, based on VG model curve-fit parameters computed by Schaap and Leij (1998) ("Simplified VG Method"). This method, developed by Environmental Quality Management Inc. (EQM) (2000), is incorporated in U.S. EPA guidance for this pathway. The VG model parameters are, in turn, used to develop a simplified step function for water-filled porosity (Figure 7.1). The capillary zone ($\theta_{w,cz}$) water-filled porosity is equal to the moisture content at the inflection point in the water retention curve where $d\theta_w/dh$ is maximal, as suggested by Waitz *et al.* (1996) (where θ_w and h equal the water-filled porosity and matric suction, respectively). Vapour-phase diffusion becomes negligible once the water-filled porosity exceeds the $\theta_{w,cz}$. The height of the capillary zone is estimated using an equation for capillary rise in a tube (Fetter 1994), and mean particle size for the SCS soil textural classifications (Nielson and Rogers 1990). The water-filled porosity above the capillary zone is user defined; we suggest a practical range below a building is between the residual water content and field capacity.

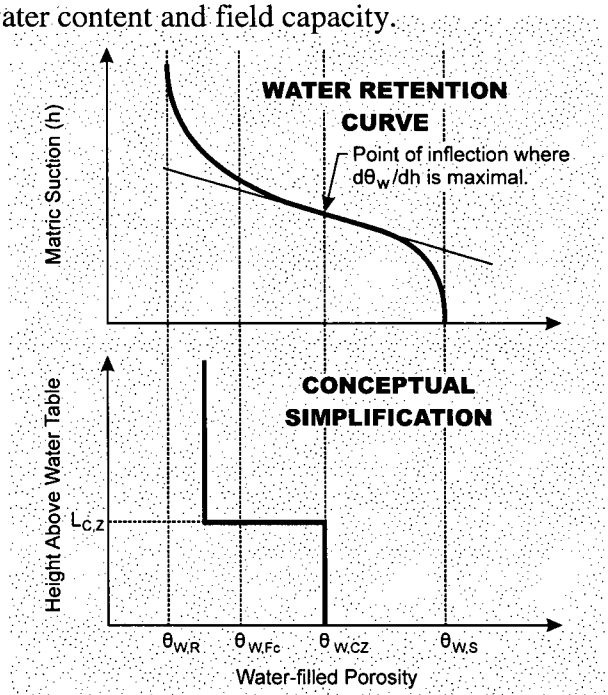

Figure 7.1. Conceptual simplification of water retention curve for purposes of estimating moisture contents and capillary rise ($\theta_{W,R}$, $\theta_{W,FC}$, $\theta_{W,CZ}$, $\theta_{W,S}$ are the residual, field capacity, capillary zone and saturated water contents).

The simplified VG model likely predicts lower than actual water-filled porosity in soil, for the capillary transition zone (Figure 7.1). Since diffusion rates are much higher in air than water, this simplification likely results in conservative (high) diffusion estimates through the capillary transition zone. However, this conservatism may be counter-balanced by non-representative assumptions for the ground water contamination source. The common paradigm for prediction of cross-media VOC transport is that dissolved chemicals are present below a static water table, and that transport through the capillary transition zone is limited to vapour- and aqueous-phase diffusion. In reality there will be some lateral ground water flow and dispersive mixing of chemicals in the tension-saturated zone, and vertical movement of chemicals as a result of water table fluctuations. There is limited information on VOC migration in the capillary transition zone. One study, involving a large chamber, showed that the pore-water concentrations in the tension-saturated zone were similar to those below the water table, and showed a sharp decline in concentrations near the top of the tension-saturated zone (McCarthy and Johnson 1993). The implication is that a more representative top boundary for dissolved ground water contaminants may be some distance above the water table.

Estimation of Soil Gas Advection Rate (Q_{soil})

The method often used with the J&E model for estimating the soil gas advection rate (Q_{soil}) through the building envelope is an analytical solution for two-dimensional soil gas flow to a small horizontal drain (Nazaroff 1992). This model is used to simulate gas flow to an edge crack located at the perimeter of a building ("Perimeter Crack Model"). The Q_{soil} ($L^3T^{1)}$ is estimated as follows:

$$Q_{soil} = \frac{2\pi k_a \Delta P X_{crack}}{\mu \ln\left(\frac{2 z_{crack}}{r_{crack}}\right)} \qquad (2)$$

where k_a is the soil-air permeability (L^2), ΔP is the pressure difference between the building and ambient air, X_{crack} is the perimeter crack length (L), μ is the gas viscosity ($M\,L^{-1}\,T^{-1}$), z_{crack} is the depth to edge crack (L) and r_{crack} is the crack radius (L). The ratio of cracks to total sub-surface foundation area (i.e., base and walls) (η) can be expressed as:

$$\eta = \frac{r_{crack} \quad X_{crack}}{A_B} \qquad (3)$$

where A_B is the subsurface foundation area (L^2). The Perimeter Crack model accounts for both soil gas flow through soil and the foundation, but is most sensitive to the soil-air permeability based on the analysis presented in Figure 7.2. For the range of values chosen for k_a, η, ΔP and z_{crack}, by far the greatest variation is obtained for k_a with the predicted Q_{soil} ranging between about 0.001 and 100 L/min.

One method of estimating soil-air permeability is to use published values for saturated hydraulic conductivity and water retention parameters for a particular soil type (EQM 2000). This method involves the following steps: (i) obtain saturated hydraulic conductivity for soil texture type (Schaap and Leij 1998), (ii) estimate intrinsic permeability from saturated hydraulic

conductivity, (iii) estimate effective total fluid saturation at field capacity, and (iv) estimate relative air permeability using the relationship proposed by Parker *et al.* (1987), and (v) calculate effective soil-air permeability (relative air permeability multiplied by intrinsic permeability). The soil-air permeability can also be measured in the field (Garbesi and Sextro 1995; Hers and Zapf-Gilje 1998) but this type of testing is rarely performed.

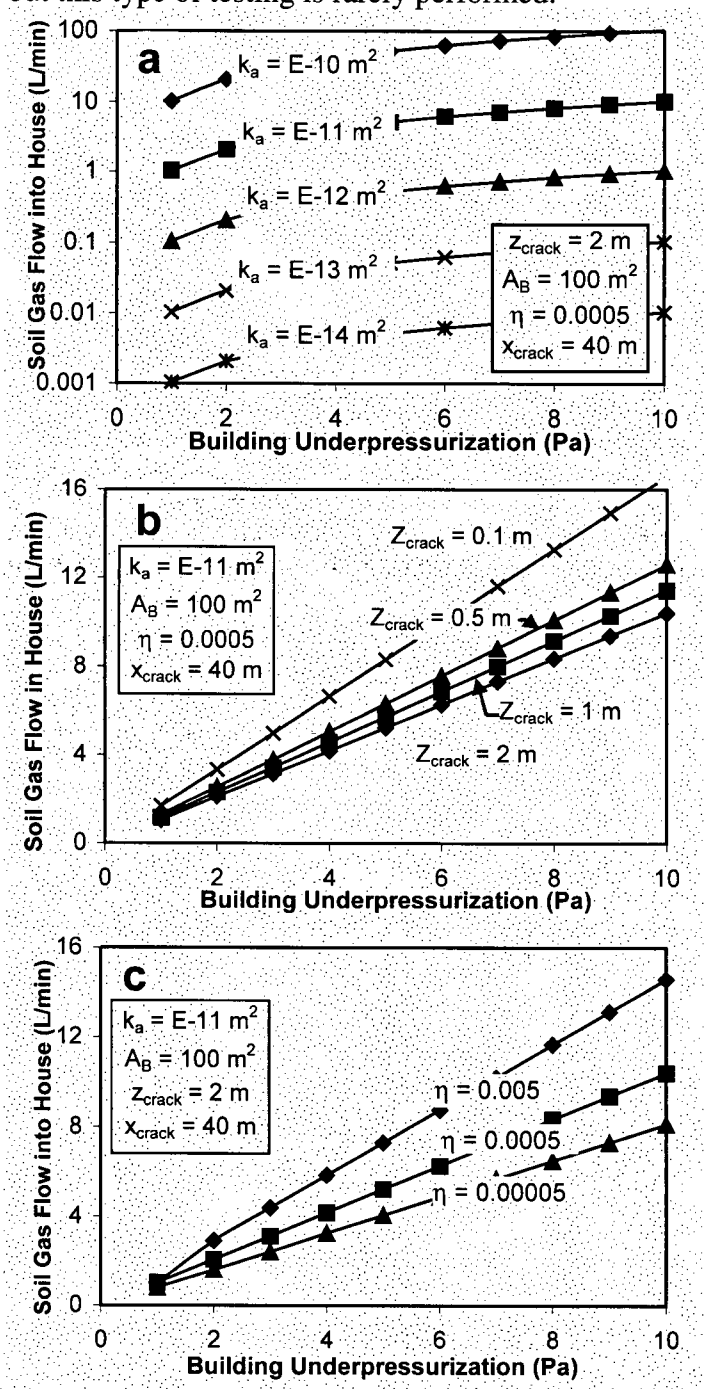

Figure 7.2. Sensitivity of soil gas flow to perimeter crack model (used in J&E model) to (a) *soil-air permeability (k_a), (b) depth to perimeter crack (z_{crack}) and (c) crack ratio* (η). X_{crack} = perimeter crack length, A_b = subsurface foundation area.

The Q_{soil} can also be estimated from a tracer test mass balance. When soil gas advection is the primary mechanism for tracer intrusion into a building, the Q_{soil} can be estimated by measuring the concentrations of a chemical tracer in indoor air, outdoor air and in soil vapour below a building, and measuring the building ventilation rate (Hers *et al.* 2002; Fischer *et al.* 1996; Garbesi *et al.* 1993; Rezvan *et al.* 1991; Garbesi and Sextro, 1989). The Q_{soil} values measured using this technique are compared to predicted rates using the Perimeter Crack model, for sites with coarse-grained soils (Table 7.1). The Perimeter Crack model predictions are both higher and lower than the measured values, but overall are within one order of magnitude of the measured values. Although the Q_{soil} predicted by models and measured using field tracer tests are uncertain, the results suggest that a "typical" range for houses on coarse-grained soils is on the order of 1 to 10 L/min.

J&E Model Sensitivity for Key Input Parameters

The sensitivity of the benzene α_p predicted by the J&E model is evaluated as a function of soil gas flow (Q_{soil}), the effective diffusion coefficient (D_T^{eff}) and contamination depth (L_T) (Figure 7.3). The D_T^{eff}/L_T ratio captures the influence of soil properties and depth to contamination source on α_p. For BTEX and most chlorinated solvent compounds, chemical-specific variation in the D_T^{eff}/L_T ratio is not significant since the free-air diffusion coefficients vary by only a factor of two, and the Henry's Law Constants vary by a factor of ten (D_T^{eff}/L_T is less sensitive to H' than D_{air}). Since the effective diffusion coefficient is calculated using the Millington and Quirck (1961) relationship, the soil properties of relevance are the air-filled and total porosity. A high D_T^{eff}/L_T ratio is associated with dry soils and/or shallow contamination while a low D_T^{eff}/L_T ratio is associated with wet soils and/or deep contamination. Based on the analysis in the sections below, sensitive parameters for the J&E model are also qualitatively summarized in Table 7.2.

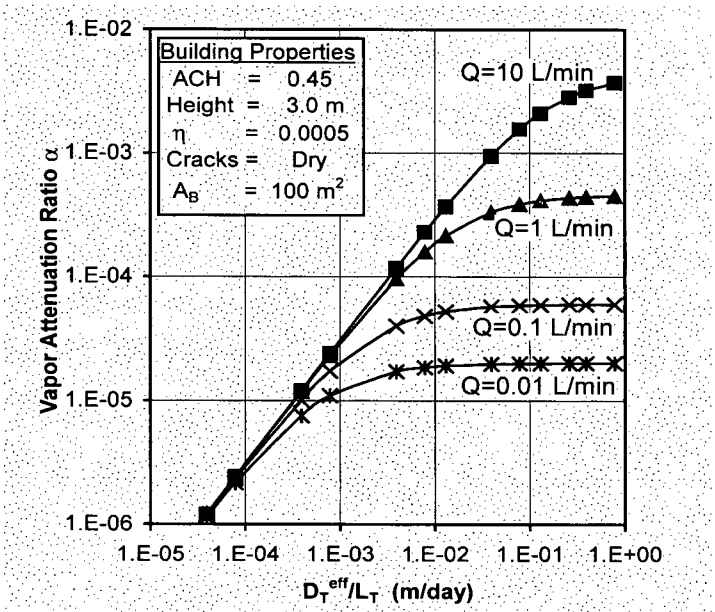

Figure 7.3. Sensitivity of Vapour Attenuation Ratio (Benzene) to Soil Gas Flow Rate (Q) into Building using Perimeter Crack Model. Height = building height, Dry dust-filled concrete cracks with total porosity = 0.3, ACH = air exchanges per hour $Q = Q_{soil}$ (other symbols previously defined)

Table 7.1. Comparison of measured and model-predicted soil gas flow rates into buildings

Site	Foundation Type	ΔP (Pa)	Subsurface Foundation Area (m^2)	Crack Ratio η	Depth to Perimeter Crack (m)	$k_{soil-air}$ (Darcy)	Soil Gas Flow Rates Measured Tracer (L/min)	Soil Gas Flow Rates Predicted PCM (L/min)
Chatterton Site (Hers et al. 2000)	Slab-on-grade	30	57	0.00033	0.3	10	2.7	29
	Slab-on-grade	10	57	0.00033	0.3	10	4.2	9.6
	Slab-on-grade	10	57	0.0001	0.3	10	2.9	8.2
Alameda Site Fischer et al. (1996)	Slab-on-grade	3	50	**0.0001**	**0.2**	10	1.4	2.4
Central California Site Garbesi & Sextro (1989)	Filled hollow block basement w\coating	30	128	**0.0001**	2.5	3	67	8.3
Ben Lomond Garbesi et al. (1993)	Experimental basement	10	26	0.00075	1.8	6	9.7	2.3
Spokane Valley Houses Revzan et al. (1991)	Poured concrete basements	5	**220**	**0.0001**	2	200	102	110

Notes: Bold print values assumed, all other values measured, ΔP = building underpressurization, PCM = Perimeter Crack Model

Table 7.2. Qualitative summary of sensitive parameters for the J&E model

Parameter	Building Depressurized (advection & diffusion)	Building Not Depressurized (diffusion only)
High D_T^{eff}/L_T (shallow &/or dry soil)	Q_{soil} (advection controlled)	Building Foundation Cracks
Moderate D_T^{eff}/L_T	Q_{soil} & Moisture Content (MC)	Building Foundation Cracks & MC
Low D_T^{eff}/L_T (deep and/or wet soil)	Moisture Content (diffusion controlled)	Moisture Content (MC)

Note: Indoor air concentrations are directly proportional to source concentrations, building mixing height and ventilation rate.

Sensitivity of α_p to Q_{soil}

For sensitivity analysis purposes, a Q_{soil} range of 0.01 to 10 L/min was chosen since it is considered representative of most houses or small buildings. The results indicate that Q_{soil} begins to have a significant influence on α_p when D_T^{eff}/L_T values are moderate to relatively large (greater than about 0.001 m/day) (Figure 7.3). The J&E model is described to be advection controlled for this scenario. When D_T^{eff}/L_T is relatively small (less than about 0.001 m/day), α_p is not sensitive to Q_{soil}. The J&E model is described to be diffusion controlled for this scenario. The D_T^{eff}/L_T for case studies subsequently evaluated in this paper ranged from about 0.002 to 0.1 m/day. For these D_T^{eff}/L_T values, the maximum error in prediction caused by a four order of magnitude variation in Q_{soil} ranges from 3X to 100X.

Sensitivity of α_p to Crack Ratio

The influence of crack ratio (η) on α_p was evaluated for two different Q_{soil} values (Figure 7.4). For Q_{soil} equal to 10 L/min, α_p is not sensitive to η. When Q_{soil} is equal to 0.01 L/min, a two order of magnitude change in η causes up to 25X change in α_p. The sensitivity of α_p to η increases as Q_{soil} decreases, with sensitivity highest for the diffusion only case (i.e., $Q_{soil} = 0$). The crack ratio is of little importance for smaller D_T^{eff}/L_T or Q_{soil} greater than about 1 L/min, which means that for the majority of sites crack ratio will not be important.

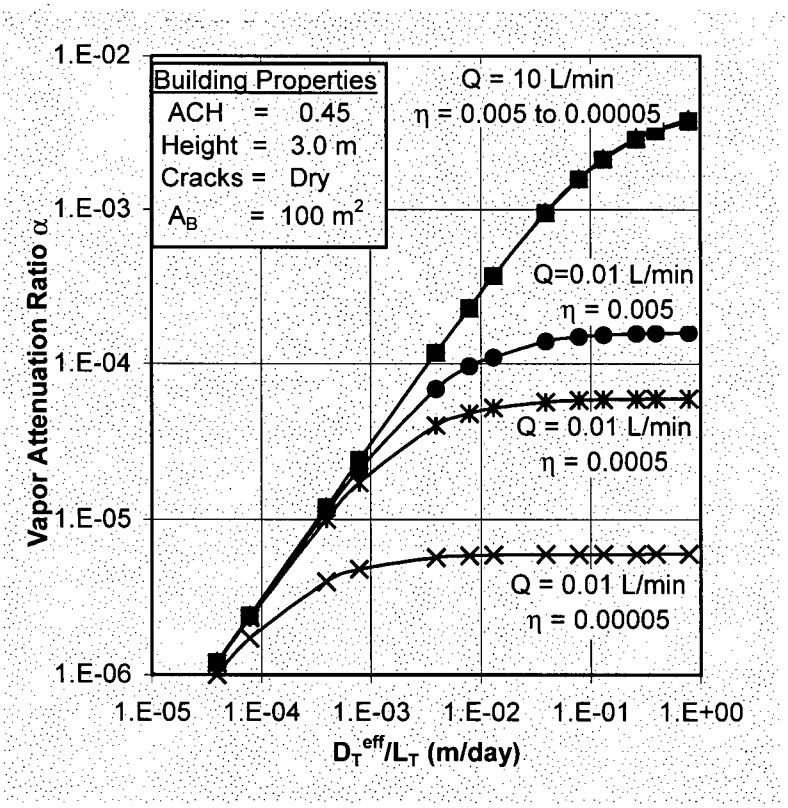

Figure 7.4. Sensitivity of Vapour Attenuation Ratio (Benzene) to Soil Gas Flow Rate (Q) using Perimeter Crack Model and Foundation Crack Ratio (η) (other symbols previously defined).

Sensitivity of α_p to Air-Filled Porosity (Moisture Content)

The effect of air-filled porosity and depth to contamination was evaluated for a soil with moisture contents ranging from 3.6 to 15.6 percent (dry weight) and a constant total porosity of 0.3 (Figure 7.5). This variation in moisture content is potentially representative of the difference between a dry soil below a building compared to a wet soil within the capillary transition zone. The corresponding air-filled porosities are between 0.04 and 0.26. A Q_{soil} value of 10 L/min was assumed. For a constant depth to contamination, a 4X change in moisture content causes about or more than two orders of magnitude change in α_p. For a constant moisture content, α_p becomes sensitive to depth to contamination, at shallow depths. It is clear that soil layers with high moisture content will have a significant effect on the diffusive flux and vapour intrusion.

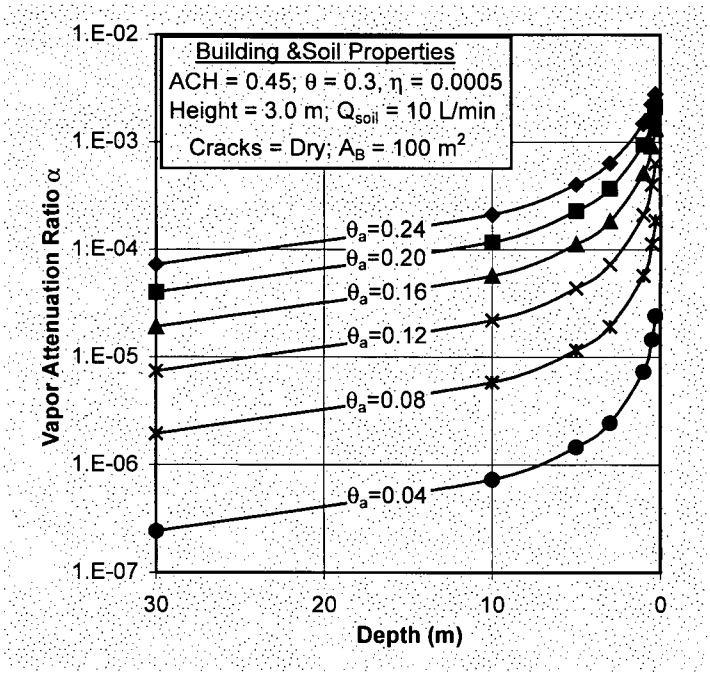

Figure 7.5. Sensitivity of Vapour Attenuation Ratio (Benzene) to Water-filled Porosity (Pa). Other symbols previously defined.

J&E Model Uncertainty for Range of Values

Vapour attenuation ratios predicted by the J&E model are provided for a range of soil gas advection rates and building properties, as a function of D_T^{eff}/L_T (Figure 7.6). For illustrative purposes, upper and lower soil gas advection rates were estimated for four U.S. SCS soil textures (Sand, Loamy Sand, Sandy Loam and Silt) using published values for saturated hydraulic conductivity and the Perimeter Crack Model (i.e., method described above). The soil type only applies to soil immediately adjacent to the building, since the radius-of-influence for soil gas advection is relatively limited. The estimated Q_{soil} values are highly uncertain; however, we note that the predicted values for Sand (1 to 10 L/min) are consistent with the results of tracer tests for coarse-grained soils. The uncertainty in Q_{soil} increases for finer-grained soils since the influence of permeable soil layers and preferential pathways (e.g., utility backfill) becomes more important. It is suggested that the Q_{soil} for Sand be used when near the foundation soil is not well characterized.

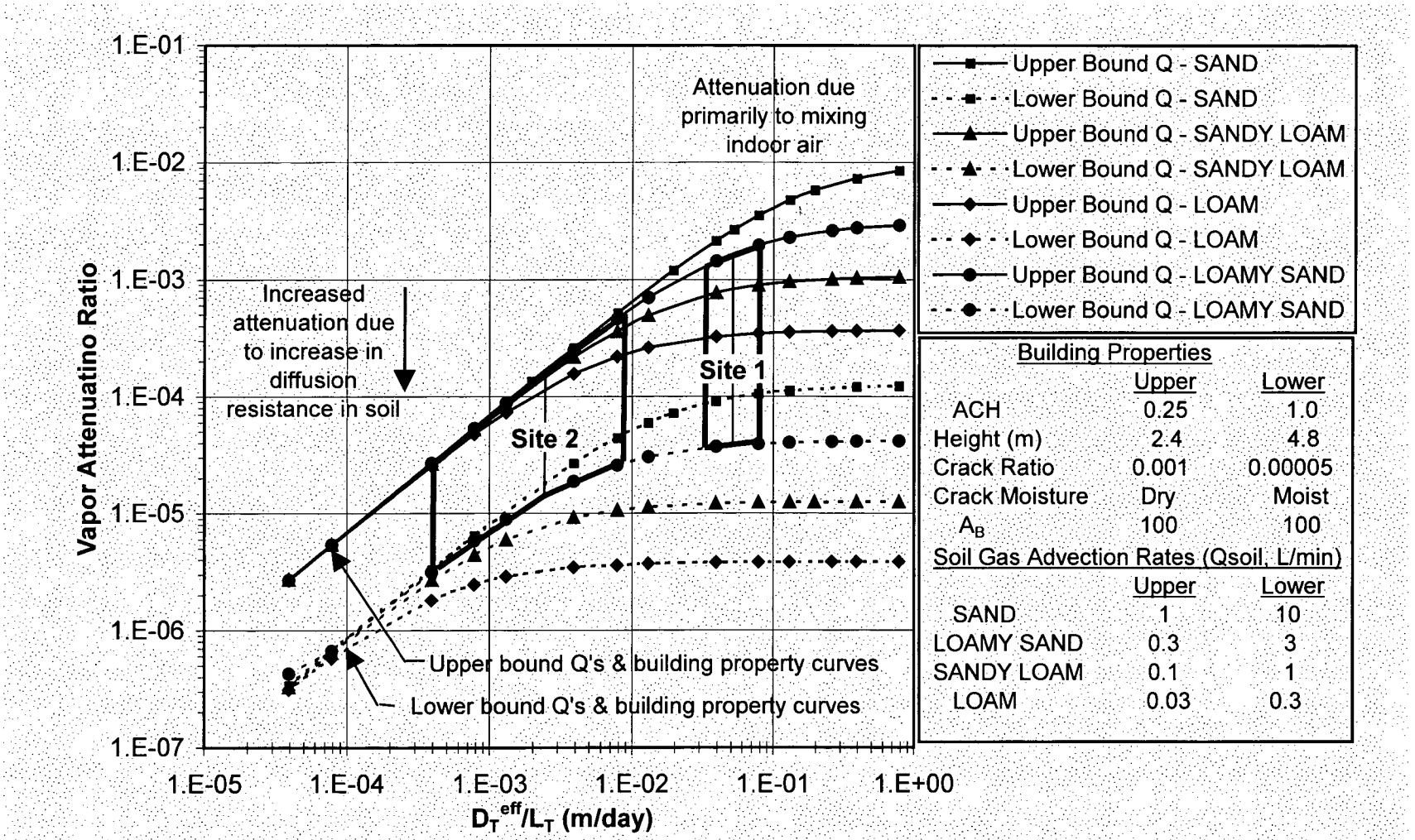

Building Properties	Upper	Lower
ACH	0.25	1.0
Height (m)	2.4	4.8
Crack Ratio	0.001	0.00005
Crack Moisture	Dry	Moist
A_B	100	100

Soil Gas Advection Rates (Qsoil, L/min)	Upper	Lower
SAND	1	10
LOAMY SAND	0.3	3
SANDY LOAM	0.1	1
LOAM	0.03	0.3

Figure 7.6: Predicted vapour attenuation ratio (benzene) for vapour concentrations at source and indoor air using Johnson and Ettinger (1991) model. Figure adapted from Johnson et at., 1998. Dry dust-filled cracks: total porosity = 0.3; Moist dust-filled cracks: water-filled porosity = 0.1 and total porosity = 0.3

The building properties input to the model are the crack ratio, dust-filled crack moisture content, building height, building air exchanges and building foundation size. The upper and lower building properties given are subjectively considered to represent the range of values that would be encountered at most sites, based on available information and the author's experience (Hers and Zapf-Gilje 1998; Hers *et al.* 2000, 2002). The subsurface foundation area is for a house with a shallow basement or slab-on-grade foundation. Slightly lower α_p's would be predicted for a deep basement with larger foundation area.

The graphs in Figure 7.6 illustrate the effect of variation in Q_{soil} and building properties on vapour attenuation ratio, but do not address uncertainty in D_T^{eff}/L_T, which is primarily due to soil moisture content. To gain insight into uncertainty in model predictions due to moisture content, a possible range in D_T^{eff}/L_T was evaluated for two hypothetical scenarios. The first scenario ("Site 1") assumes a shallow soil vapour source (1.5 m depth) situated well above the water table. The second scenario ("Site 2") assumes a relatively deep water table (6 m depth) and contamination that is limited to a dissolved ground water plume. Both sites were assumed to have uniform SCS Loamy Sand soil. The approach taken was to first obtain a plausible best estimate, and upper and lower range for D_T^{eff}/L_T. For Site 1, a constant air-filled porosity half way between the residual water content and field capacity was assumed. For Site 2, the Simplified VG Method, as described above, was used to estimate the air-filled and total porosity for the capillary zone. As shown in Table 7.3, the resulting porosities are expressed as relative water saturation values where $S = \theta_w/\theta$ and $\theta_a = \theta(1\text{-}S)$. The reason for using relative saturation values in the uncertainty analysis is that the air-filled and total porosity are expected to be strongly correlated. Therefore, uncertainty would be over-estimated if these parameters are allowed to vary independently. This is prevented through the use of the relative saturation values. The uncertainty ranges given for total porosity and relative saturation are considered reasonable values for a well-characterized site.

Table 7:3. Uncertainty analysis for normalized effective diffusion coefficient

Parameters	Best Estimate Values Site 1	Site 2	Uncer-tainty
Input Parameters			
Contamination location	Above wt	Dissolved in Gdw	N/A
Contamination depth (m)	1.5	6.0	constant
U.S. SCS soil classification	Sandy	Sandy	N/A
Total porosity (θ)	0.390	0.390	+/- 10 %
S_R (θ_w/θ) above CZ (S)	0.265	0.265	+/- 25 %
Height of CZ (L_{cz}) (m)	N/A	0.250	+/- 25 %
S_R (θ_w/θ) in CZ (S_{cz})	N/A	0.821	+12/-10 %
Calculated Values			
D_T^{eff}/L_T lower est. (m/day)	0.0325	0.00038	-
D_T^{eff}/L_T best est. (m/day)	0.0512	0.00248	-
D_T^{eff}/L_T upper est. (m/day)	0.0775	0.00861	-
D_T^{eff}/L_T upper/lower range	2.4	23	-

Notes: CZ = capillary zone, SR = relative saturation
Gdw = Groundwater, WT = water table

Using the best estimate values and uncertainty ranges, the best estimate, lower and upper ranges are provided for the normalized effective diffusion coefficient (D_T^{eff}/L_T) (Table 7.3 and Figure 7.6). For Site 1, the upper and lower D_T^{eff}/L_T values vary by a factor of 2.4. For Site 2, the uncertainty is greater (factor of 23) since the sensitivity of D_T^{eff}/L_T to air-filled porosity within the capillary zone is high since moisture content is also high.

The overall uncertainty in the vapour attenuation ratio will be dependent on the available data. If there is only information on the contamination depth, the range in α_p can vary three to four orders of magnitude. When information on soil properties is also available, the uncertainty in D_T^{eff}/L_T and Q_{soil} is reduced resulting in α_p that vary over two orders of magnitude (Figure 7.6). When good quality site-specific data is available for both soil properties (e.g., moisture content) and building properties (e.g., ventilation rate, mixing height), it may be possible to reduce the uncertainty in α_p to about one order of magnitude.

FIELD-BASED METHODS FOR EVALUATION OF VAPOUR INTRUSION

Three different field-based approaches or methods are used to evaluate vapour intrusion: (1) indoor VOC method, (2) tracer method and (3) flux chamber method. The *indoor VOC method* involves measurement of VOC concentrations in indoor air, and at the contamination source. The α_m will vary depending on the contamination scenario. For sites with dissolved ground water plumes, the α_m is calculated using a predicted source vapour concentration (i.e., directly above the water table) estimated using the Henry's Law Constant assuming equilibrium partitioning between the dissolved and vapour phases. When measured source vapour concentrations are available, the α_m can be directly calculated. Since some deviation from equilibrium conditions would be expected, the α_m's estimated using ground water and soil vapour data are not directly comparable. A key challenge for this approach is that there are numerous other 'background" sources of VOCs in indoor and outdoor air for most chemicals of concern at contaminated sites (Hers *et al.* 2001). The intrusion of soil vapour into buildings is also highly dependent on site specific conditions, and may vary over time. These factors complicate the interpretation of indoor air measurements when the goal is to deduce the subsurface-derived component.

The *tracer method* involves measurement of the indoor air concentration of a tracer injected below ground (SF_6), or a natural tracer such as radon (e.g., Fisher *et al.* 1996; Garbesi *et al.* 1993). The measured vapour intrusion for the tracer is, in turn, used to infer intrusion for the VOC of interest. Key factors affecting this approach are that boundary conditions for a tracer injected below a building may be different than those for the VOC of interest (*e.g.*, if contamination is relatively deep) and that typically, an essentially inert tracer is used. When compared to the tracer, the mass loss or attenuation through sorption and/or biodegradation will be greater for most VOCs of interest. For these reasons, the tracer method will typically provide a conservative estimate of intrusion.

The *flux chamber* method involves measurement of soil gas flow and/or VOC flux through cracks or openings in a building foundation. There are only a few published reports documenting the use of flux chambers to measure VOC flux into buildings (e.g., Figley and Snodgrass 1992; Hers and Zapf-Gilje 1998). Challenges for this approach are that these tests are

difficult and costly to perform, and the uncertainty associated with "scaling up" the results for a small crack to an entire building.

RESULTS AND DISCUSSION OF FIELD STUDIES AND MODEL PREDICTIONS

Indoor VOC Method

Vapour attenuation ratios are evaluated for eleven sites. The sites represent studies available to the authors with reasonable quality field data, and are for residential houses, ground-floor apartments or small commercial buildings. Site characteristics and estimated input parameters are summarized, and measured and J&E model-predicted vapour attenuation ratios (α_m and α_p) are compared (Tables 7.4 and 7.5, Figure 7.7). In most cases, the vapour attenuation ratios are estimated by the authors using site data; in a few cases, the ratios given in references cited in Table 7.4 are reported. This has lead to differences in the statistical estimators used to characterize the variability in α_m and α_p. For completeness, the vapour attenuation ratios reported for several Massachusetts sites are also included in Table 7.4; these sites are not included in the eleven case study sites discussed below.

The quality and quantity of site characterization data, and ability to distinguish measured indoor air concentrations from background VOC sources varies from site to site. For three sites, the VOC concentrations in a relatively large number of houses above the contaminant plume were significantly greater than house concentrations in background areas, resulting in fairly reliable α_m estimates. For the remaining sites, either the vapour-derived VOC concentrations in indoor air were only significant in a small subset of houses above the contaminant plume, or there was no significant difference between above plume and background indoor air concentrations. The vapour attenuation ratio is not "measurable" when there is no significant vapour-derived component; however, the indoor air concentrations can be used to calculate upper bound α_m values, represented as "less than" values in Table 7.4, and dashed lines in Figure 7.7.

For each site (except Chatterton), a predictive "envelope" for α_p was generated. A best estimate D_T^{eff}/L_T was directly calculated when reasonably good quality moisture content data was available. When good quality data was not available, the U.S. SCS soil texture class was inferred based on soil descriptions and the Simplified VG Method was used to calculate D_T^{eff}/L_T. We recognize that inference of soil texture is approximate and subjective. The upper and lower bound D_T^{eff}/L_T values were approximated using the same variability calculated for the two hypothetical sites discussed earlier (Table 7.3). The upper and lower bounds for Q_{soil} and building properties are the curves presented in Figure 7.6. A Q_{soil} range of 1 to 10 L/min (i.e., representative of Sand) was assumed for all sites (except Virginia) since either coarse soils were present below building foundations, or there was no information on soil type (in these cases Sand was assumed to be present below foundations). Based on the fine-grained near-foundation soils at the Virginia site, a Q_{soil} range of 0.03 to 0.3 L/min (i.e., representative of loam) was assumed. When there was sufficient information on building properties and soil gas advection potential, the J&E model-predicted α_p was also estimated (represented as symbols on Figure 7.7). For the Chatterton site, only the best estimate α_p were plotted since testing at this site involved an experimental building and test cases not representative of generalized predictive envelopes in Figure 7.6.

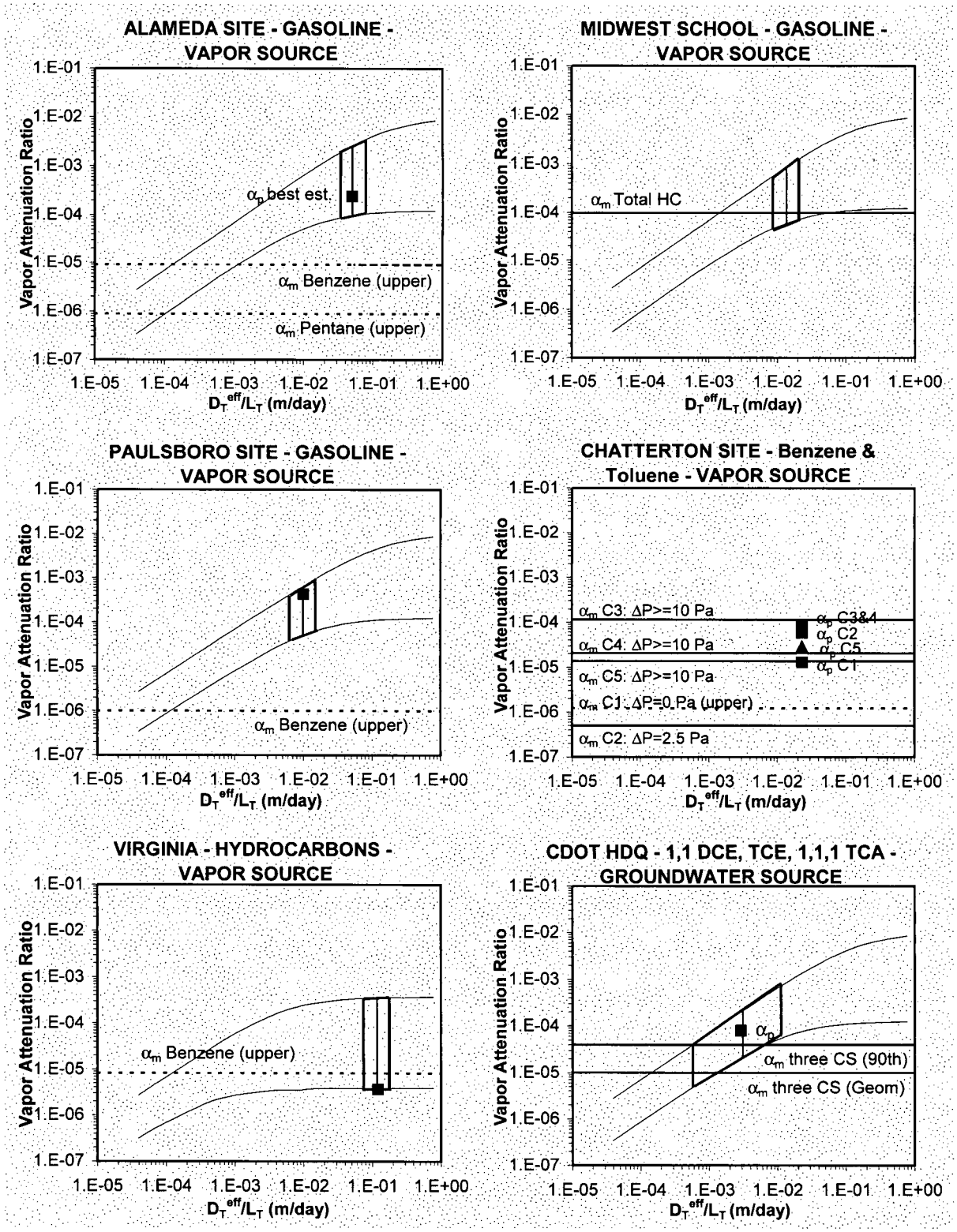

Figure 7.7a. Comparison Between Measured and J&E Model-Predicted Vapour Attenuation Ratio (benzene). Upper and lower bound curves from Figure 7.6 are included. Dashed lines indicate that α_m is upper bound value. Symbols are best estimate α_p values.

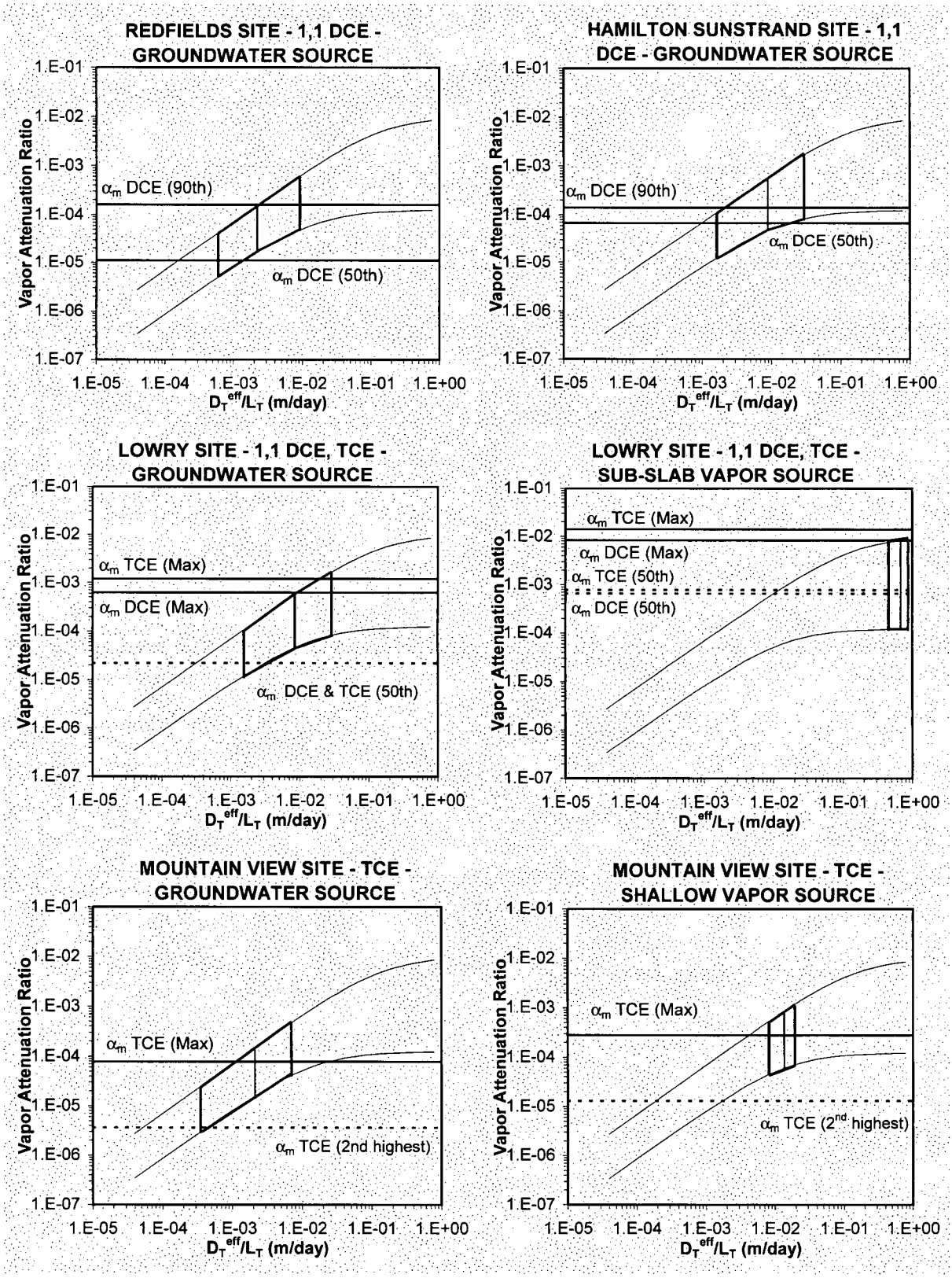

Figure 7.7b. Comparison Between Measured and J&E Model-Predicted Vapour Attenuation Ratio (benzene). Upper and lower bound curves from Figure 7.6 are included. Dashed lines indicate that α_m is upper bound.

Table 7.4. Measured and Model-Predicted Vapour Attenuation Ratios

Site & Reference	Contaminant or Tracer	Building and Foundation Type	Soil Conditions	Depth (m)[1]	Chemical	Source Concentration (ug/L)	N Indoor Air[2]	α_m Statistic	Measured α_m	J&E model α_p[3]	Comments
Indoor VOC Method											
"Virginia (Motiva) Site", Fan and Quinn (2000)	petroleum HC, NAPL above water	SFR, basements, attached garages, cement block foundations	claystone saprolite k ~ 0.01 darcy	0.5	benzene	V: 410	13	50th	<8.3E-6	3.70E-06	
"Chatterton Site" Delta, B.C. Canada Hers et al. (1998) Hers et al.(2000a)	BTX petrochemical plant, NAPL above water table	research greenhouse slab-on-grade poured concrete 2 mm edge crack	surface silt to f. sand, underlain by m.sand with k ~ 10 darcies	1.4	benzene	V: 15,000	3-4	Avg	< 5.3E-7	1.3E-05	C1: ΔP= 0 Pa, η = 3.3E-4
					toluene	V: 20,000	3-4	Avg	< 1.9E-6	1.3E-05	C1: ΔP= 0 Pa, η = 3.3E-4
					benzene	V: 15,000	3-4	Avg	4.0E-07	5.9E-05	C2: ΔP= 2.5 Pa, η = 1E-4
					toluene	V: 20,000	3-4	Avg	5.9E-07	5.9E-05	C2: ΔP= 2.5 Pa, η = 1E-4
					benzene	V: 15,000	3-4	Avg	9.9E-05	7.8E-05	C3: ΔP= 10 Pa, η = 1E-4
					toluene	V: 20,000	3-4	Avg	1.3E-04	7.8E-05	C3: ΔP= 10 Pa, η = 1E-4
					benzene	V: 15,000	3-4	Avg	7.2E-06	8.0E-05	C4: ΔP= 10 Pa, η = 3.3E-4
					toluene	V: 20,000	3-4	Avg	3.4E-05	8.0E-05	C4: ΔP= 10 Pa, η = 3.3E-4
					benzene	V: 15,000	3-4	Avg	5.8E-06	2.9E-05	C5: ΔP= 30 Pa, η = 3.3E-4
					toluene	V: 20,000	3-4	Avg	2.2E-05	2.9E-05	C5: ΔP= 30 Pa, η = 3.3E-4
"Paulsboro Site", NJ USA, Laubacher et al. (1997)	gasoline NAPL above water table	SFR basement	sand, some silt	2.74	benzene	V: 576	15	Avg	<1.6E-6	4.3E-04	
"Alameda (Air Station) Site", CA, USA Fischer et al.(1996)	gasoline NAPL above water table	small commercial building, slab-on-grade poured concrete	sand k ~ 1 to 3 darcy	0.7	benzene	V: 200	1	N/A	<9E-6	2.45E-04	
				0.7	iso-pentene	V: 28,000	1	N/A	< 9E-7	2.46E-04	
"Mass. DEP Sites" USA, Fitzpatrick & Fitzgerald (1996)	petroleum hydrocarbon	N/A (3 sites)	N/A	N/A	benzene	N/A	-	N/A	1E-5 to 4E-5	INS INS	
"Midwest School Site" USA, Moseley and Meyer (1992)	petroleum HC NAPL above water table	Built 50's, at-grade construction, crawlspace, large paved area	sand & gravel, discontinuous clay lenses	~ 3	benzene	N/A	N/A	N/A	HC-like odours ~~ 1E-4	INS	crawlspace conc.: benzene ~ 8.3 mg/m^3, Total HC ~ 500 mg/m^3
					total HC						
"CDOT HDQ Site" Colorado, USA Johnson et al. (2000)	chlorinated solvents, dissolved plume	mostly apartments, few SFRs, mostly slab-on-grade, few crawlspaces & basements, AC mostly window units, heating natural gas,baseboard, and/or fireplaces	weathered & fractured claystone above water table	4.6	1,1 DCE	G: 10-10,000	115-150	Geom 90th	4.8E-06 2.0E-05		a_m values for houses above plume with DCE groundwater concentration > 10 ug/L
					1,1 DCE	G: 10-10,000					
					TCE	G: 3-3,000	115-150	Geom 90th	1.4E-05 7.0E-05		
					TCE	G: 3-3,000					
					1,1,1 TCA	G: 10-1,000	115-150	Geom 90th	1.7E-05 6.6E-05		
					1,1,1 TCA	G: 10-1,000					
					above 3 CS		115-150	Geom 90th	1.2E-05 5.2E-05	8.6E-05 2.4E-04[4]	average for 3 chlorinated solvents (CS)
					above 3 CS						
"Redfields Site" Colorado, USA Envirogroup (1999)	chlorinated solvents, dissolved plume	SFRs, built 50's and 60's, mostly basements or crawlspaces, no combustion air intakes	clay & silt, some sand layers, mostly sand or silt near WT	6.1 to 7.3	1,1 DCE	G: 10-1,000	65	50th Avg 90th	1.50E-05 7.60E-05 1.20E-04	INS	a_m values for houses above plume with DCE groundwater concentration > 10 ug/L
					1,1 DCE	G: 10-1,000					
					1,1 DCE	G: 10-1,000	65	90th			
Hamilton Site Colorado, USA (2001), unpublished	chlorinated solvents, dissolved plume	SFRs built 50's most basements	primarily sand & & gravel, some clay & silt layers	9.7 to 11	1,1 DCE	G: 15-30	32	50th	6.80E-05	INS	Gravel at water table
						G: 15-30	32	90th	1.40E-04		
"Lowry (Air Force Base) Site" Colorado, USA Versar (2000)	chlorinated solvents, dissolved	SFR: mostly basements some crawlspaces	silty sand to silt, generally silty sand near water table	6.1 to 7	1,1 DCE	G: 1.4-1.9	>50	50th	2.20E-05	INS	max G a_m = 6.2E-04
					TCE	G: 120-170	>50	50th	2.20E-05		max G a_m = 1.2E-03
					1,1 DCE	V: > 29	>50	50th	6.50E-04		max V_{SS} a_m = 8.3E-03
					TCE	V: > 1,000	>50	50th	7.70E-04		max V_{SS} a_m = 1.4E-02
"Mountain View Site" California, USA Wu (2000)	chlorinated solvents, leachfield & dissolved[5]	SFRs, built 1998, at-grade construction with moisture vapor barrier	mostly silty/ clayey sand & gravel, some sand or silt lenses	1.5	TCE	V: 84	14	Max	2.80E-04	INS	a_m shallow vapour
						V: 84	14	2nd[6]	<1.3E-5		
				10.7	TCE	G: 735	14	Max	7.80E-05		a_m groundwater, depth to groundwater = 10.7 m
						G: 735	14	2nd	<3.6E-5		
"Mass. DEP Sites" USA, Fitzpatrick & Fitzgerald (1996)	chlorinated solvents	N/A (19 sites)	N/A	N/A	CS	N/A	N/A	N/A	2E-6 to to 1E-1	INS	high a_m associated with highly permeable building envelopes (earthern floor, block walls & sumps)
Tracer and Flux Chamber Tests											
"Central California Site", Garbesi & Sextro (1989)	SF_6	SFR, basement poured slab, block walls coated with asphalt	sandy loam to loamy sand, k = 0.1 to 10 darcies	sub-slab	SF_6	N/A	N/A	N/A	~ 1E-3	N/A	ΔP = 30 Pa
"Alameda Site" Fischer et al. (1996)	SF_6	small commercial, slab on-grade, concrete	sand, k = 1 to 3 darcy	sub-slab	SF_6	N/A	N/A	N/A	2E-4 to 4E-4	N/A	ΔP ~ 3 (estimate based on wind loading)
U.S. Sites Little et al.(1992)	radon	SFRs	N/A	sub-slab	radon	N/A	N/A	N/A	1.6E-3[7]	N/A	
"Spokane River Valley Sites", WA, USA, Rezvan et al. (1992)	radon	SFRs (14), 8 houses slab-on-grade, 6 basement	highly permeable sand & gravel, k ~ 200 darcies	sub-slab	radon	N/A	N/A	N/A	~ 7.9E-3 to to 4.5E-2	N/A	winter conditions, mean house volume = 500 m^3, ACH = 0.5/hr

Notes: 1 Depth to contamination from underside of foundation slab; 2 N = Number of indoor air samples tested; 3 Best estimate unless otherwise noted; 4 Upper range; 5 Contamination likely in unsaturated zone; 6 2nd highest α_m value; 7 Alpha (α) estimated using mean radon content of soil combined with appropriate emanation constant divided

Measured Vapour Attenuation Ratios at Petroleum Hydrocarbon Sites

Case study sites with petroleum hydrocarbon contamination have coarse-grained soils (except for the Virgina Site) and shallow to moderate depths to contamination (0.5 to 3 m). Extensive residual non-aqueous phase liquid (NAPL) is present above the water table at the Chatterton site. There is evidence for some residual NAPL above the water table at the Alameda, Paulsboro, Virginia and Midwest School sites. Indoor air testing was limited to a single or small number of buildings at each case study site. For petroleum sites, near-source vapour concentrations are available and therefore the α_m is directly calculated ("vapour α_m").

At the Virginia, Chatterton (depressurization (ΔP = 0 Pa case), Paulsboro and Alameda sites, there was no difference between indoor air concentrations measured in building(s) above the plume and in background areas indicating that the α_m's are unknown. For these sites, the α_m's calculated using the measured indoor air concentrations are upper bound values and range from < 4.0×10^{-7} to < 9.0×10^{-6}. For the Chatterton ΔP = 2.5 Pa case, there was a statistically significant difference in indoor and background indoor air concentrations, however, the α_m remained low (4.0×10^{-7} to 5.9×10^{-7}). For the Chatterton ΔP = 10 and 30 Pa cases, there was a significant increase in indoor air concentrations and α_m's.

At the Midwest School site, hydrocarbon-like odours were noted indoors during a period of relatively heavy rains and high water table in September 1992. Subsequent analysis of indoor air during October 1992 indicated that hydrocarbon concentrations in indoor air were elevated but could not be conclusively distinguished from background sources at this time. However, the benzene (8 mg/m^3) and total hydrocarbon concentrations (500 mg/m^3) in an unventilated crawlspace below the ground floor were well above background levels. Based on a rough estimate of the source vapour concentrations and odour thresholds for hydrocarbons, the α_m may have been on the order of 1×10^{-4}.

Field data, including soil vapour profiles, indicate there was significant bioattenuation of hydrocarbon vapours for the Alameda and Chatterton (ΔP = 0 and 2.5 Pa cases) sites. This is consistent with other studies indicating that biodegradation can result in significant vadose zone attenuation of hydrocarbon vapours provided sufficient O_2 is present (Ostendorf and Kampbell 1991; Ririe and Sweeney 1995). For higher underpressurizations (10 and 30 Pa), hydrocarbon vapour concentrations were elevated due to increased vapour flux from deeper soil, and reduced travel times (Hers *et al.* 2000). The relatively high α_m's at the Chatterton site are due to combined effect of shallow contamination, relatively permeable soils, and high building underpressurizations.

The Paulsboro and Midwest School sites had elevated hydrocarbon vapour levels directly below the building slab. For the Midwest School site, we speculate that elevated indoor hydrocarbon concentrations may have been a result of limited biodegradation due to a large building and paved area, which reduced oxygen recharge, combined with factors that contributed to vapour intrusion into the building. These factors include building construction (i.e., crawlspace) and/or a sanitary sewer that was located near the water table within the hydrocarbon plume, which may have acted as a preferential pathway. At the Virginia site contamination was shallow but no significant vapour intrusion was measured possibly due to presence of fine-grained soils and/or building construction (i.e., "tight" foundations).

Comparison to Model Predictions for Petroleum Hydrocarbon Sites

Comparisons for the Chatterton (ΔP = 0 and 2.5 Pa cases), Paulsboro and Alameda sites indicate that the best estimate α_p's are one to two orders of magnitude higher than the measured or upper bound α_m's indicating the J&E model results in conservative predictions for these sites. Comparisons for the Chatterton (ΔP = 10 and 30 Pa cases) and Virginia sites indicate the best estimate α_p's are similar to the α_m's. The high soil gas advection rates for the Chatterton site resulted in significant vapour intrusion rates and hence similar α_p and α_m. For the Virginia site, the α_p is lower than at other sites due to the influence of the fine-grained soils. For the Midwest site, the predictive envelope for α_p also intersects the α_m; however, the α_m is highly uncertain.

Measured Vapour Attenuation Ratios at Chlorinated Solvent Sites

At four case study sites with chlorinated solvent contamination (CDOT, Redfields, Hamilton and Lowry), dissolved plumes have migrated below houses (Table 7.4). The depth to the water table at these sites ranged from about 4.8 to 10.7 m below ground surface. The ground water plumes at these sites are relatively long and narrow resulting in significant spatial variability in dissolved ground water concentrations. At the fifth site (Mountain View), houses were constructed on top of a former leach field where chlorinated solvents had been disposed of. Therefore, in addition to ground water, shallow soil is likely contaminated at this site. Soil grain size at the sites is variable (Table 7.4). For all sites, the α_m are estimated using vapour concentrations predicted from ground water data ("ground water α_m"). For the Lowry and Mountain View sites, soil vapour data was also available; therefore, the α_m is also directly calculated using vapour data (unless otherwise noted the α_m given below are for the ground water source scenario).

For the CDOT site, the differences in three chlorinated solvent concentrations (1,1 DCE, TCE and 1,1,1 TCA) in houses above the plume and at background locations are statistically significant. However, the ground water and indoor air data was found to be unreliable at the periphery of the plume and therefore low ground water and indoor air concentrations were removed from the database prior to calculating the α_m's. The resulting database is comprised of several hundred tests from apartments and houses. The methodology used to estimate α_m is further described in Johnson *et al.* (2000). The geometric mean and 90th percentile α_m's for the CDOT site are 1.0×10^{-5} and 5.2×10^{-5}. Analysis of the intrusion database for the site indicated no strong correlation between seasons and α_m, or difference between basement and slab-on-grade construction (personal communication, Dr. Jeff Kurtz, EMSI, Inc.).

For the Redfields site, the difference in 1,1 DCE concentrations in houses above the plume and at background locations are statistically significant. A data screening procedure similar to that used for the CDOT site resulted in α_m only being estimated in areas where the 1,1 DCE concentrations in ground water exceeded 10 ug/L. A visual interpolation method was used to estimate ground water concentrations below houses. The resulting database is comprised of 65 houses nearest to the Redfields site. The 50th and 90th percentile α_m's for the Redfields site are 1.1×10^{-5} and 1.2×10^{-4}. Synoptic data for the Redfields site indicated a slight correlation between indoor 1,1 DCE concentrations and season, for some houses, with winter-time values that were

two to three times higher than summer-time values (personal communication, Mr. David Folkes, Envirogroup, Inc., 2000).

For the Hamilton site, the difference in 1,1 DCE concentrations in houses above the plume and at background locations are statistically significant. Since ground water data was limited, the attenuation ratio analysis is for a strip of 32 houses parallel and closest to the long axis of the plume (and wells) in the area with 1,1 DCE concentrations above about 10 ug/L. The 50th and 90th percentile α_m's for the Hamilton site are $6.8x10^{-5}$ and $1.4x10^{-4}$.

At the Lowry site, the database evaluated consists of over a year of quarterly testing at 13 houses above and near the periphery of the plume. Concurrent testing of indoor air, and sub-slab vapour concentrations for houses with slab-on-grade or basement construction, and crawlspace air for houses with crawlspaces was conducted. At one house, the maximum TCE and 1,1 DCE concentrations in indoor air were 51 ug/m^3 and 0.91 ug/m^3, suggesting significant vapour intrusion. At three other houses, the TCE concentrations in indoor air were mostly between 5 and 15 ug/m^3. Compared to published background data for TCE (Hers *et al.* 2001) and data for houses along the periphery of the plume, it is possible that concentrations at these three houses included a soil vapour-derived component. The indoor air concentrations were at background levels in remaining houses.

Measured vapour attenuation ratios are estimated for a subset of four Lowry houses with nearby ground water data. For this data subset, the maximum indoor air TCE concentration was 51 ug/m^3, but exceeded 5 ug/m^3 in only one house. Therefore, most α_m's are upper bound values. When all data are used, the 50th percentile and maximum ground water α_m's are $2.2x10^{-5}$ and $1.2x10^{-3}$ for TCE, and $2.2x10^{-5}$ and $6.2x10^{-4}$ for 1,1 DCE. The maximum, as opposed to 90th percentile α_m, was calculated due to the relatively limited number of tests for this site. The Lowry sub-slab vapour concentrations were highly variable and elevated below certain houses (e.g., TCE up to 10,000 ug/m^3), but near background levels below other houses above the plume. An analysis of the house data subset where indoor air TCE concentrations exceeded 5 ug/m^3 and/or sub-slab TCE concentrations exceeded 1,000 ug/m^3 indicated that the 50th percentile and maximum sub-slab vapour α_m are $7.7x10^{-4}$ and $1.4x10^{-2}$. Available synoptic data for the Lowry site indicated no significant seasonal variation in sub-slab or indoor air concentrations.

At the Mountain View site, indoor air in seven houses above the contaminated area, and two "background" houses in a non-contaminated area was tested on two occasions. The indoor TCE concentration in one house was 12 and 25 ug/m^3, while the TCE concentrations in remaining houses ranged were at background levels (0.26 to 1.1 ug/m^3) (Wu 2000). The maximum ground water α_m is $7.8x10^{-5}$ while the shallow vapour maximum α_m is $2.8x10^{-4}$.

When all five sites are evaluated the results can be summarized as follows. The 50th percentile (or geometric mean) and 90th percentile (or maximum) α_m values for the ground water to indoor air pathway were remarkably similar for all sites (approximately $1x10^{-5}$ and $1x10^{-4}$, respectively). For individual sites, there is significant house-to-house variability in α_m (e.g., two order of magnitude difference for Redfields site); however, based on the available data there appear to be only slight, if any, seasonally induced variations in vapour intrusion, and similar intrusion rates for houses with basement and slab-on-grade construction. Potential sources of variability in α_m include inaccurate estimation of water table ground water concentrations below

houses, geological heterogeneity, differences in house construction and depressurization, and differences in ventilation rates and house activities during indoor air testing. At the Lowry and Mountain View sites, no significant vapour intrusion could be measured for most houses. One likely reason for the generally non-significant intrusion is that ground water concentrations are lower at these sites, compared to the CDOT, Redfields and Hamilton sites. Another possible factor for the Mountain View site is the building construction, which consists of at-grade foundation slab with (moisture) vapour barrier. Overall, the results suggest that geologic conditions and diffusion rates have the greatest influence on vapour intrusion rates at the chlorinated solvent sites, and that building factors are less important.

Comparison to Model Predictions for Chlorinated Solvent Sites

Comparisons for sites with the most reliable data (CDOT, Redfields and Hamilton) indicates that the predictive envelope for the α_p intersects the α_m. The centroid of the predictive envelope is in all cases higher than the 50th percentile α_m suggesting, on average, the J&E model would result in conservative predictions. For the CDOT site, the best estimate α_p is about eight times higher than the 50th percentile α_m. For the Lowry site, the predictive envelope is below the α_m for one house with significant vapour intrusion indicating a non-conservative prediction in this case. For the Mountain View site, the predictive envelope for α_p intersects the maximum α_m. Overall, the J&E model in most cases results in conservative predictions (i.e., α_p is higher than α_m). However, the comparisons highlight the potential for non-conservative predictions if a combination of low Q_{soil} and low D_T^{eff}/L_T are used.

Tracer Method

There are several sites where tracer tests can be used to estimate α, which range from about $2x10^{-4}$ at the Alameda Site to $4.5x10^{-2}$ at the Spokane River (Valley) Sites (Table 7.4). The Spokane River sites were calculated using an assumed average house volume (500 m^3) and building ventilation rate (air changes per hour (ACH = 0.5 hr^{-1})) and therefore are approximate. Soils at the Spokane River site are very permeable and α is based on winter conditions (i.e., highest expected seasonal building depressurization); therefore the α's for this site are considered an upper range value. It should be remembered that tracer studies represent α values for near-field boundary conditions, and therefore are not representative of intrusion at many sites contaminated with VOCs. The tracer test α values are, however, consistent with the upper range of the J&E model predictions (Figure 7.6).

Flux Chamber Method

A method that has been utilized for radon assessments is the equivalent leakage area (ELA) method (Grimsrud *et al.* 1982; CSGB 1986). The ELA is obtained by developing an empirical relationship between the soil gas flow into a building and building depressurization. Soil gas flows are measured using flux chambers and mass flow meters. In one study involving multiple measurements of soil gas flow through various building foundation cracks at ten houses in Saskatchewan, Canada, the total house foundation ELA for the foundation edge cracks and utility penetrations ranged from 0.15 to 16.4 cm^2 (Figley and Snodgrass 1992). The contribution to total ELA from untrapped floor drains, present at a few houses, was excluded from this analysis since untrapped drains are uncommon in newer construction. For example, the National

Building Code of Canada (1995) requires sealing of floor drainage systems that have the potential to allow soil gas entry (Section 9.13.8.3).

The measured total ELA can be used to estimate soil gas intrusion rates using the method in Figley (1997). A building depressurization representative of severe winter conditions (10 Pa), as proposed by Figley (1997), and possible values for the house volume (500 m^3) and building ventilation rate (0.3 ACH) produces α values between $3.6x10^{-4}$ and $3.8x10^{-2}$. The α obtained in this manner is conservative because it assumes an unlimited and uniform soil vapour source directly below the foundation slab (i.e., contaminants in vapour are replenished as fast as they are swept into the building).

Flux chamber tests have also been used to measure VOC flux rates through concrete cracks (Schmidt and Zdeb 1997; Hers and Zapf-Gilje 1998). Both studies indicated detectable VOCs were measured in soil gas transmitted through cracks, and the study by Hers and Zapf-Gilje (1998) indicated that the scaled up flux for the entire building was of the same order as flux measured by the indoor VOC method.

REGULATORY IMPLICATIONS

The J&E model is widely used for regulatory and guidance purposes in North America. Several agencies have developed generic screening criteria for the vapour intrusion pathway (Massachusetts, 1993; Michigan, 1998; Connecticut, 1998). Semi-generic soil standards have been developed in Canada based on two different soil types (fine- and coarse-grained) and two building types (CCME, 2000). Guidance recently developed as part of the U.S. EPA Environmental Indicator (EI) program consists of a multi-tiered framework to evaluate the soil vapour intrusion pathway (U.S. EPA 2001). A primary (initial) screening step is used to identify sites with significant potential for vapour intrusion (e.g., odors, product in sumps or directly below foundation), and where indoor air monitoring and/or engineering controls is warranted. A secondary screening step involves the use of semi-generic curves for α, based on soil type and depth, and target breathing concentrations in indoor air to back calculate acceptable source ground water and soil vapour concentrations. Depending on the results of the secondary screening, there is the option to conduct a site-specific pathway assessment.

Derivation of regulatory criteria requires the prediction of cross-media transfer of contaminants, and vapour transport and intrusion into buildings. For the regulatory agencies cited above (excluding Massachusetts), cross-media transfer between VOCs in ground water and soil vapour is predicted using the Henry's Law Constant assuming equilibrium partitioning. Under the Massachusetts guidance, the Henry's Law Constant is divided by ten to account for source vapour concentrations that are typically lower than those predicted assuming equilibrium partitioning. The vapour attenuation ratios incorporated into regulatory criteria depend on whether the assumed contamination scenario is a dissolved ground water plume or an unsaturated zone contamination source. For a ground water source, the α incorporates vapour transport through both the capillary transition zone and unsaturated zone. For an unsaturated zone source, the α incorporates transport through just the unsaturated zone. For the agencies cited above, the ground water source α's range from $4.6x10^{-6}$ to $1.5x10^{-3}$ while the vapour source α's range from $3.9x10^{-7}$ to $6.2x10^{-3}$. An analysis of the above regulatory criteria indicates that

the key factor affecting the α is the Q_{soil} value chosen or estimated for predictive purposes. Of lessor importance is the assumed generic or semi-generic soil type.

When vapour attenuation ratios incorporated in regulatory criteria are compared to measured ratios for field studies presented in this paper, it is apparent that the low end of the regulatory range may not be conservative for some sites. Of greatest concern would be sites with non-biodegradable chemicals, shallow to moderate depth contamination and high advection potential (i.e., coarse soil, high building underpressurization).

CONCLUSIONS AND RECOMMENDATIONS

A comprehensive evaluation of the J&E model characteristics and sensitivity, and comparisons of measured to model-predicted vapour attenuation ratios (α_m and α_p) have been provided for residential houses, ground-floor apartments and small commercial buildings. Based on this analysis, the following conclusions can be drawn:

1. The J&E model is moderately to highly sensitive to soil gas advection rate into the building (Q_{soil}), at D_T^{eff}/L_T values above about $1x10^{-3}$. Except when Q_{soil} is low, the J&E model is relatively insensitive to building foundation properties. At best, the range or uncertainty in J&E model predictions is about one order of magnitude when relatively good quality site-specific data is available.
2. Estimation of effective diffusion coefficient is subject to considerable uncertainty. Some of this uncertainty can be reduced through better site characterization, including careful lithological descriptions, testing of moisture content, grain size distribution and water retention, and appropriate consideration of the effect of surface barriers on soil moisture content.
3. Several radon and VOC tracer studies indicate that measured Q_{soil} values at coarse-grained soil sites, for single family residences, ranged from about 1 to 10 L/min. Depending on the input values chosen, much lower Q_{soil} values can be predicted using the soil gas advection model typically used in conjunction with the J&E model.
4. There are only a limited number of high quality and comprehensive field studies that can be used to help validate models for the vapour intrusion pathway.
5. For petroleum hydrocarbon sites, the vapour α_m's for the Chatterton site (high ΔP cases) and Midwest site were on the order of $1x10^{-5}$ to $1x10^{-4}$ (the Midwest value is uncertain). For the remaining cases and sites, the possible upper bound vapour α_m's ranged from about $5x10^{-7}$ to $1x10^{-5}$.
6. For chlorinated solvent sites, the ground water α_m's were on the order of $1x10^{-6}$ to $1x10^{-4}$ for the three sites with the most reliable data sets (CDOT, Redfields and Hamilton). For one site with a smaller and somewhat less reliable data set (Lowry), the maximum ground water α_m was approximately $1x10^{-3}$ while the maximum sub-slab vapour α_m was approximately $1x10^{-2}$.
7. For the tracer and flux chamber studies, the α_m's were on the order of $1x10^{-4}$ to $1x10^{-2}$. In the context of VOC intrusion, these α_m represent conservative upper bounds due to boundary conditions and tracer properties that are generally different than those at VOC-contaminated sites.

8. For almost all case studies, the best estimate J&E model-predicted α_p's were one to two orders of magnitude less than the 50th percentile or median α_m's, indicating that when best estimate and "average" conditions are evaluated, the J&E model predictions are conservative. There were a few cases studies where the best estimate α_p was less than the 90th percentile or maximum α_m indicating the J&E model predictions are non-conservative for a small subset of houses or apartments. The comparisons also highlight the potential for non-conservative model predictions if a combination of low Q_{soil} and low D_T^{eff}/L_T are used.

The observed variability in α_m between different field sites, and individual houses at some sites, highlights the complexity of processes affecting vapour intrusion. Numerous factors potentially affect the vapour intrusion pathway including biodegradation, chemical transformation, sorption, contaminant source depletion, geologic heterogeneity, soil properties (moisture content, permeability, organic carbon content), building properties, meteorological conditions, and building ventilation rates. In light of this complexity, it is important to recognize the vapour intrusion modeling paradigm typically followed is a compartmental model for steady-state one-dimensional diffusion through soil, and diffusion and advection through a building foundation having an idealized edge or perimeter crack (J&E model). Often, a homogeneous soil is assumed, although it is relatively easy to model diffusion for multiple soil layers assuming site information is available (Johnson *et al.* 1998). Simulation of vapour transport through the building foundation and mixing of VOCs within the building airspace is highly simplified. Although not used for this study, it is noted that the J&E model has been modified to include first-order biodegradation for a dominant soil layer (Johnson *et al.* 1998) and oxygen-limited first-order biodegradation (Johnson *et al.* 2001).

Notwithstanding the above, the question remains: Can the J&E model (or other similar screening models) be reliably used for the vapour intrusion pathway? Our answer is a qualified yes, provided that appropriate input values are used and the model sensitivity, uncertainty and limitations are recognized. The answer may also depend on what the model is used for. For example, the use of the J&E model to set generic criteria is problematic due to model sensitivity and uncertainty, and the wide range in possible site conditions. In our opinion, a semi-generic approach that incorporates site-specific information on critical factors affecting vapour intrusion (e.g., Q_{soil} and soil properties) improves on a single criteria approach. The technically preferred approach is to use J&E model on a fully site-specific basis, and to calibrate model predictions using soil vapour profiles, and when possible, indoor air data. In all cases, an appropriate framework for model use, and understanding of model characteristics is essential when using models for regulatory purposes.

Several data gaps and sources of uncertainty remain. Additional field-based studies should be conducted to evaluate the vapour intrusion pathway for different site conditions, and to more fully assess specific factors affecting vapour intrusion. Data that would contribute to a more in-depth pathway analysis include soil properties such as moisture content and porosity, soil vapour concentration profiles below buildings, building properties such as depressurization, and meteorological data. Further evaluation of biodegradation kinetics for hydrocarbon vapours, effect of surface barriers (e.g., buildings) on biodegradation, and chlorinated solvent transformation processes are also needed.

REFERENCES

American Society for Testing and Materials (ASTM). 1995. *Standard Guide for Risk-Based Corrective Action Applied at Petroleum Release Sites*. E-1739-95.

Canadian General Standards Board (CSGB). 1986. *Determination of the Airtightness of Building Envelopes by the Fan Depressurization Method*. CAN/CSGB-149.10-M86.

Canadian Council for Ministers of the Environment (CCME), 2000. *Canada Wide Standards for Petroleum Hydrocarbon Compounds in Soil*. June 2000.

Carsel, R.F. and R.S. Parrish. 1988. Developing joint probability distributions of soil water retention characteristics. *Water Resources Research* 24(5): 755-769.

Connecticut Department of Environmental Protection, 1998. *Residential Volatilization Criterion*. RCSA 22a-133k, Appendix E.

Domenico, P.A. and F.W. Schwartz. 1998. *Physical and Chemical Hydrogeology*. New York, John Wiley and Sons.

EnviroGroup Limited (Envirogroup). 1999. *Indoor Air Assessment Report – Redfield Rifle Scope Site*. April.

Environmental Quality Management, Inc. 2000. *User's Guide for The Johnson and Ettinger (1991) Model for Subsurface Vapour Intrusion into Buildings (Revised)*. Prepared for E.H. Pechan and Associates, Inc. Submitted to U.S. EPA. December 2000.

Fan, A. and E.A. Quinn. 2000. Case Study: Residential Indoor Air Assessment Above a Hydrocarbon Plume. Presentation to U.S. EPA EI Forum, RCRA National Conference, Washington, D.C., August 15.

Fetter, C.W. 1994. *Applied Hydrogeology*. 3rd Ed. Englewood Cliffs, New Jersey: Prentice-Hall, Inc.

Figley, D.A. and L.J. Snodgrass. 1992. Comparative Foundation Air Leakage Performance of Ten Residential Concrete Basements. *In Proc. 85th Annual Meeting of Air and Waste Management Assoc.*, June 21-26.

Figley, D.A. 1997. *A Guide for Estimating Indoor Concentrations of Soil Gas Pollutants in Houses*. Report prepared for CMHC.

Fischer, M.L., A.J. Bentley, K.A. Dunkin, A.T. Hodgson, W.W. Nazaroff, R.G. Sextro, J.M. Daisey. 1996. Factors Affecting Indoor Air Concentrations of Volatile Organic Compounds at a Site of Subsurface Gasoline Contamination. *Environ. Sci. Technol.* 30(10): 2948-2957.

Garbesi, K. and R.G. Sextro, R.G. Modeling and Field Evidence of Pressure-Driven Entry of Soil Gas into a House through Permeable Below-Grade Walls. *Environ. Sci. Technol.* 23(12): 1481-1487.

Garbesi, K., R.G. Sextro, W.J. Fisk, M.P. Modera, K.L. Revzan. 1993. Soil-Gas Entry into an Experimental Basement: Model Measurement Comparisons and Seasonal Effects. *Environ. Sci. Technol.* 27(3): 466-473.

Grimsrud, D.T., M.H. Sherman and R.C. Sonderegger, R.C. 1982. Calculating Infiltration: Implications for a Construction Quality Standard. *In Proc. Amer. Soc. of Heating, Refrigeration, and Air-Conditioning Engineers and the U.S. Department of Energy Conference: Thermal Performance of the Exterior Envelopes of Buildings II*. Las Vegas, NV., December.

Hers, I. and R. Zapf-Gilje. 1998. Canadian consortium research project – field validation of soil gas transport to indoor air pathway. *In Proc. 1998 Petrol. Hydro. and Org. Chem. in Ground Water*. API/NGWA, Houston, Tx., Nov. 11-13: 251-266.

Hers, I., J. Atwater, L. Li and R. Zapf-Gilje. 2000. Evaluation of Vadose Zone Biodegradation of BTX Vapours. *Journal of Contaminant Hydrology*, 46: 233-264.

Hers, I., R. Zapf-Gilje, L. Li and J. Atwater. 2001. The use of indoor air measurements to evaluate exposure and risk from subsurface VOCs. *J. Air & Waste Manage. Assoc. 51:174-185.*

Hers, I., R. Zapf-Gilje, D. Evans and L. Li. 2002. Comparison, Validation and Use of Models for Predicting Indoor Air Quality from Soil and Groundwater Contamination. *Journal of Soil and Sediment Contamination*, 11(4): 491-527.

Johnson, P.C. and R. Ettinger. 1991. Heuristic Model for Predicting the Intrusion Rate of Contaminant Vapours into Buildings. *Environ. Sci. Technol.* 25(8): 1445-1452.

Johnson, P.C., W. Kemblowski and R.L. Johnson. 1998. Assessing the Significance of Subsurface Contaminant Vapour Migration to Enclosed Spaces – Site Specific Alternatives to Generic Estimates. API Publication 4674, December.

Johnson, P.C., J. Kurtz, R. Bryan and R. Ettinger. 2000. In-Depth Review of Colorado (CDOT facility) Data. Presentation at U.S. EPA RCRA EI Forum, August 15 & 16, Washington, D.C.

Johnson, P.C., V.A. Hermes and S. Roggemans 2001. An Oxygen-Limited Hydrocarbon Vapour Mitration Attenuation Screening Model. Submitted to *Environ. Sci. Technol.*

Laubacher, R.C., P. Bartholomae, P. Velasco and H.J. Reisinger, H.J. 1997. An evaluation of the Vapour Profile in the Vadose Zone Above a Gasoline Plume. *In Proc. 1997 Petrol. Hydro. and Org. Chem. in Ground Water.* API/NWGA, Houston, Tx.: 396-409.

Massachusetts Department of Environmental Protection, 1993. Massachusetts Contingency Plan (GW-2 Standards), 310 CMR 40.0000, 1993 and as amended.

McCarthy, K.L and R.L. Johnson, 1993. Transport of Volatile Organic Compounds Across the Capillary Fringe. Water Resources Research 29(6): 1675-1683.

Michigan Department of Environment Quality (DEQ) 1998. *Part 201 Generic Groundwater and Soil Volatilization to Indoor Air Inhalation Criteria: Technical Support Document.* August 31, 1998.

Millington, R.J. and J.M. Quirck. 1961. Permeability of Porous Solids. *Trans. Farady Soc.,* 1200-1207.

Moseley, C.L. and M.R. Meyer. Petroleum Contamination of an Elementary School: A Case History Involving Air, Soil-Gas and Groundwater Monitoring. *Environ. Sci. Technol.* 26(2): 185-192.

Nazaroff, W.W., 1992. Radon Transport from Soil to Air. *Review of Geophysics* 30(2): 137-160.

Ostendorf, D.W. and D.H. Kampbell. 1991. Biodegradation of Hydrocarbon Vapours in the Unsaturated Zone. *Water Resources Research* 27(4): 453-462.

Parker, J.C., R.J. Lenhard and T. Kuppusamy. 1987. A parametric model for constitutive properties go
verning multiphase flow in porous media. *Water Resources Research* 23(4): 618-624.

Revzan, K.L., W.J. Fisk and A.J. Gadgil. 1991. Modeling Radon Entry into Houses with Basements: Model Description and Verification. *Indoor Air* 2, 173-189.

Ririe, T. and R. Sweeney. 1995. Fate and Transport of Volatile Hydrocarbons in the Vadose Zone. *In Proc. 1995 Petrol. Hydro. and Org. Chem. in Ground Water.* API/NGWA, Houston, Tx., Nov. 29 to Dec. 1: 529-542.

Schmidt, C.E. and T.F. Zdeb. 1998. Direct Measurement of Indoor Infiltration Through a Concrete Slab Using the US EPA Flux Chamber. In Proc. 1998 Air and Waste Management Assoc. Paper #98, TA9C.01.

U.S. EPA 2001. *Draft Supplemental Guidance for Evaluating the Vapour Intrusion to Indoor Air Pathway*, RCRA Corrective Action Environmental Indicator Program. October.

U.S. EPA 1996. *Soil Screening Guidance: Technical Background Document.* Office of Solid Waste and Emergency Response. EPA/540/R-95/128.

Versar, Inc. (Versar) 2000. *Draft Final Operable Unit 5 – Groundwater. Ground-to-Indoor Air VOC Migration Pathway Investigation Report.* January.

Waitz, M.F.W., J.I. Freijer, P. Keule and F.A. Swartjes. 1996. *The VOLASOIL risk assessment model based on CSOIL for soils contaminated with volatile compounds.* National Institute of Public Health and the Environment, Bilthoven, The Netherlands.

Wu, J. 2000. Feasibility of Indoor Air Testing (Former GTE Property) Mountain View, California – Case Example. Presentation at U.S. EPA RCRA EI Forum, August 15 & 16, Washington, D.C.

CHAPTER 8

THE USE OF INDOOR AIR MEASUREMENTS TO EVALUATE INTRUSION OF SUBSURFACE VOC VAPOURS INTO BUILDINGS

This chapter was published in *J. Air & Waste Manage. Assoc.* 51: 174-185 (2001).[6]

ABSTRACT

The implementation of a risk based corrective action approach often requires consideration of soil vapour migration into buildings and potential inhalation exposure and risk to human health. Due to the uncertainty associated with models for this pathway, there may be a desire to analyze indoor air samples to validate model predictions, and this approach is followed on a somewhat frequent basis at sites where risks are considered potentially significant. Indoor air testing can be problematic for a number of reasons. First of all, soil vapour intrusion into buildings is complex, highly dependent on site specific conditions, and may vary over time, complicating the interpretation of indoor air measurements when the goal is to deduce the subsurface-derived component. An extensive survey of indoor air quality data sets highlights the variability in indoor volatile organic compound (VOC) concentrations and numerous sources that can lead to elevated VOC levels. The contribution from soil vapour is likely to be small relative to VOCs from other sources for most sites. In light of these challenges, we discuss how studies that use indoor air testing to assess subsurface risks could be improved. To provide added perspective, we conclude by comparing indoor air concentrations and risks arising from subsurface VOCs, predicted using standard model equations for soil vapour fate and intrusion into buildings, to those associated with indoor sources. The key implication of this paper is that the use of indoor air concentrations to deduce the subsurface-derived vapour component is not straightforward, and that an integrated approach that recognizes the factors that affect soil vapour intrusion and indoor air quality is needed. Since there are several other significant sources of VOCs beside soil vapour, distinguishing the vapour component from other sources will, in practice, be difficult. Model predictions suggest that the soil vapour derived exposure and risk could range from being much less than to much greater than the risk associated with other VOC sources. Further development of protocols for indoor air sampling and validation of predictive models for soil vapour intrusion are needed to improve risk assessments for this exposure pathway.

KEY WORDS: air exchanges, air quality, ventilation, VOC, vapour, intrustion, buildings

[6] Hers, I., Zapf-Gilje, Li, L. and Atwater, J.

INTRODUCTION

The implementation of risk-based corrective action at contaminated sites is now commonplace. Soil vapour intrusion into buildings is a potential exposure pathway at many sites impacted by subsurface volatile organic compounds (VOCs), and this pathway is included in many regulatory standards and guidance documents pertaining to risk-based clean-up (e.g., ASTM, 1995; CCME, 2000). There is significant uncertainty associated with mechanisms for intrusion of VOCs into buildings, and consequently, with models used for this exposure pathway. In the face of this uncertainty, there may be a desire to analyze indoor air samples to validate model predictions, and this approach is followed on a somewhat frequent basis at sites where risks are considered to be potentially significant (e.g., Fitzpatrick and Fitzgerald, 1995; Moseley and Meyer, 1992). Indoor air testing can be problematic in terms of sampling methodology and data interpretation since typically there will also be indoor and outdoor sources of the VOC under consideration. In addition, the generation and fate of VOCs in indoor air are highly variable and building specific (Tichenor *et al.*, 1990; Davis and Otson, 1996). While numerous studies on indoor air VOCs have been conducted, there is little information or guidance on the use of indoor air sampling to evaluate subsurface contamination VOCs sources, or evaluation of the relative significance of subsurface versus indoor or outdoor air VOC sources.

The purpose of this paper is to provide an integrated overview on soil vapour intrusion and VOCs in buildings, and contribute to an improved understanding of critical mechanisms affecting VOC concentrations in buildings and appropriate sampling strategies. Mechanisms for soil vapour intrusion are initially evaluated since this context is important in the design and interpretation of indoor air testing programs. Next, we provide an overview of the factors that contribute to indoor air quality, and compile measured VOC concentrations in indoor air from a number of sources. Possible improvements to indoor air sampling that is used to characterize subsurface sources are discussed, and essential complimentary measurements are identified. To provide added perspective on the relative importance of subsurface versus indoor air VOC sources, we conclude by comparing indoor air concentrations and risks arising from subsurface VOCs, predicted using standard equations for soil vapour fate and intrusion into buildings, to those associated with indoor sources. The focus of this paper is assessment of residential buildings.

MECHANISMS FOR SOIL VAPOUR INTRUSION

Process Overview

Two compartments are defined to enhance our conceptual understanding of processes: the far-field consisting of vadose zone soil, and the near-field, consisting of the subsurface building envelope (foundation) and nearby soil (Figure 8.1). If the depth to the contamination source below the building is significant, vadose zone processes such as diffusion, sorption and biodegradation (for benzene, toluene, ethylbenzene and xylenes (BTEX) and petroleum vapours) will likely have the greatest influence on VOC mass flux into a building. In this case, the VOC mass flux will be controlled by far-field processes potentially resulting in non-significant concentrations below the building. Of greater concern for the soil vapour intrusion pathway are sites with relatively shallow VOC contamination, where it appears that VOC mass flux through pressure-driven advective transport of soil gas into buildings can be significant (Fitzpatrick and

Fitzgerald, 1996). In this case, intrusion would be controlled by near-field processes. Several radon studies also suggest that radon intrusion by advection is typically a more significant process than diffusion (Nazaroff *et al.*, 1985; Garbesi and Sextro, 1993; Robinson and Sextro, 1997). The most significant factors affecting the near-field compartment would therefore tend to be building underpressurization, the permeability of the building envelope and nearby soil, and depth to contamination.

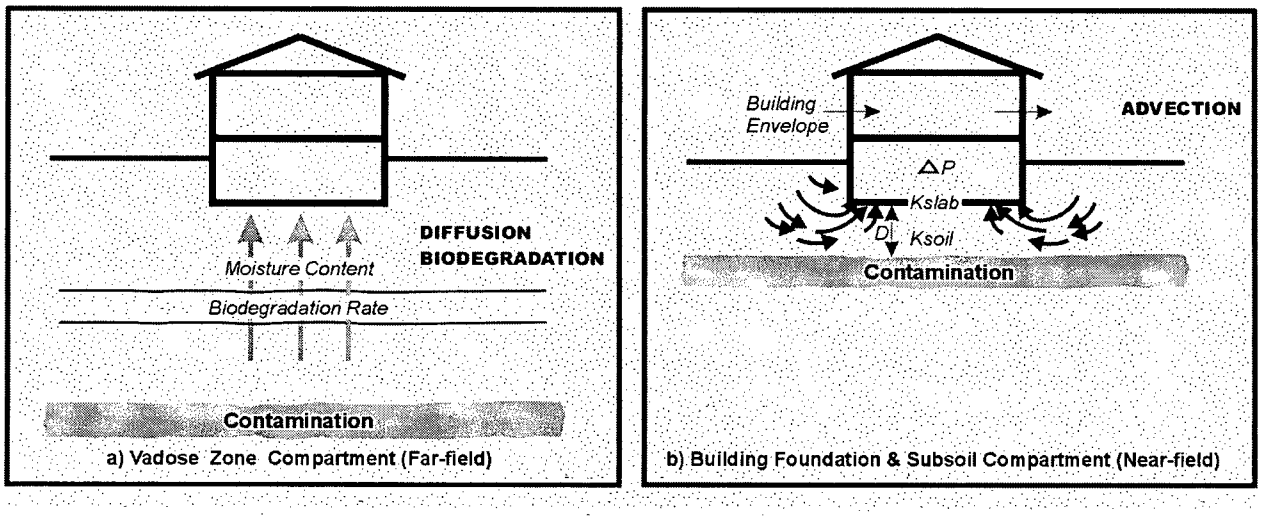

Figure 8.1. Possible conceptual model for soil vapour intrusion into building.

Advective soil gas transport can occur through untrapped drains, perimeter cracks at the building wall and floor slab interface, service penetrations, expansion joints and other cracks, if present. Driving forces for advection are pressure gradients caused by building underpressurization, changes in barometric pressure and diurnal fluctuations in temperature (Adomait and Fugler, 1997). The subsurface pressure and soil gas flow regime adjacent to, and through the building envelope, will be highly site specific and dependent on building construction, soil permeability and potential preferential pathways such as utility corridors. Building construction factors that may be significant include whether a basement, crawlspace and/or water vapour barrier is present, and type of concrete (poured cement or cement block).

Positive soil-to-building pressure gradients can potentially have a significant effect on soil gas intrusion, as illustrated by several examples below. A study evaluating radon entry into a house near Chicago, IL, found higher building underpressurizations and radon entry rates during winter compared to summer months and an advective radon flux that was greater than the diffusive flux (Nazaroff *et al.*, 1985). Another study found that average indoor radon levels were 12 times higher during winter, compared to summer, for 14 houses constructed on permeable soils in Spokane, Washington, USA (Turk *et al.*, 1987). The inferred reason for the difference was building underpressurization caused by the stack effect. A study of methane and VOC intrusion into a townhouse complex in Kitchener, Ontario, Canada indicated that large short-duration cross-foundation pressure differences (up to 500 Pa) developed when barometric pressure decreased rapidly, and when the sub-slab foundation layer was not well vented to atmosphere (i.e., confined by low permeability material) (Adomait and Fugler, 1997). Consistently higher indoor VOC and methane concentrations were measured in townhouses during positive pressure gradients, for two cycles of measurements (one cycle is a negative and

positive pressure gradient). Another study compared the effect of atmospheric pressure fluctuations and sustained depressurization on advective radon entry into an experimental basement, and found that for sustained indoor-outdoor pressure differences greater than 1.5 Pa, atmospheric pressure fluctuations had essentially no effect on the time–averaged radon entry rate (i.e., sustained depressurization was much more important) (Robinson and Sextro, 1997). While it appears that short-term variation in atmospheric pressure can cause advective soil gas flow into a building, the most important determinant is whether there are conditions for sustained building depressurization arising from the stack effect, unbalanced mechanical ventilation systems, or possibly wind loading (Nazaroff *et al.*, 1985, Turk *et al.*, 1987, Nazaroff, 1992, Scanada, 1993; Robinson and Sextro, 1997).

Building Underpressurization and Ventilation

Building underpressurization is considered in greater detail since it can be the most significant driving force for VOC intrusion at sites with shallow contamination. Building ventilation rates are important since they can affect background indoor VOC concentrations (Fellin and Otson, 1993; Gusdorf and Hamlin, 1995). Background concentrations are defined in this paper as not being related to soil vapour. In addition, both parameters are required when estimating model-predicted indoor VOC concentrations associated with soil vapour intrusion. Ventilation and building underpressurization are often linked in that forces that cause building underpressurization (*e.g.*, stack effect arising from temperature differences) can result in ventilation, and conversely unbalanced mechanical ventilation systems or forced-air heating systems with leaking ducts can cause buildings to be underpressurized (SRC, 1995). It is noted that ventilation systems for commercial buildings in Canada and the U.S. are often designed to produce positive pressures in buildings relative to outdoor air thereby reducing the potential for significant soil vapour intrusion (Nazaroff, 1992).

Building underpressurization is controlled by a combination of wind-loading, temperature differences between indoor and outdoor air (*i.e.*, stack effect), forced-air mechanical ventilation systems, operation of furnaces and fireplaces, and appliance fans. Measured mean indoor-outdoor pressure differences for houses with basements, during the heating season, typically range from 2 to 10 Pa (Nazaroff *et al.*, 1985; Nazaroff 1992, Scanada Consultants Ltd., 1993; Figley, 1997; Waitz *et al.*, 1996) although this pressure difference can be as high as 15 Pa (Figley, 1997) (Table 8.1). The climatic conditions required for the higher pressure differences are severe winter conditions in Canada (Figley, 1997). There is little data specifically for slab-on-grade structures, although studies by Scanada Consultants Limited (1993) and Fischer *et al.* (1996) suggest that a building underpressurization between 2 and 4 Pa may be reasonable for such structures. Based on literature values and his experience Figley (1997) proposed values for underpressurization based on buildings types (Table 8.1). While simple empirical relationships can be used to estimate building underpressurization due to wind-loading and temperature differences between indoor and outdoor air (e.g., Nazaroff, 1992), such estimates may be unreliable due the complex mechanisms for building underpressurization.

Table 8.1. Survey of Building Depressurization Relative to Atmospheric Pressure

Reference	Data Type	Location	Building Type & Number	Measurement Date	Measurement Statistic	Depressurization (Pa)	Comments
19 [1]	Measured	Netherlands	Houses with Crawlspace	N/A		~ 2 ~ 2	Between indoor space and crawlspace Between crawlspace and soil
14	Measured	Canada	Houses: Halifax (12), Ottawa/Hull (16), Winnipeg(12) ,Vancouver (12)	Winter 93	range average for house	-5 to 15 0.5 to 8.5	Mix older & newer houses, most houses had forced air heating system & basement, depressurization correlated to house construction (full, partial basement, slab on grade) & climate
9	Measured	Spokane River Valley, WASH, USA	House (14)	Winter	average	2 to 6	
7	Measured	Chicago, Ill., USA	House (1)	Feb 17 to June 1, 1982	range	0.6 to 4.3	Basement ΔP decreased between Feb. & June 1
20	Predicted	Alameda, California, USA	Small commercial building (1)	N/A	range	1 to 4	Predicted based on wind loading
8	Predicted	Portland, Or	2-storey house with basement	N/A		~ 2 ~ 2	Predicted based on wind Predicted based on stack effect
47	General reference	N/A	Houses	N/A		up to 10	upper range associated with extreme weather conditions
18	Guidance	Canada	slab-on-grade house slab-on-grade house 1 to 2 storey house 1 to 2 storey house 3 storey house 3 storey house	N/A	range range range range range range	1 to 3 3 to 5 4 to 6 8 to 10 7 to 9 13 to 15	range mild to severe winter, without chimney range mild to severe winter, with chimney range mild to severe winter, without chimney range mild to severe winter, with chimney range mild to severe winter, without chimney range mild to severe winter, with chimney

Notes: [1] references Put and Meijer, 1989 (report in Dutch)

[2] if the house has a fresh air intake duct or combustion air supply, reduce differential pressures by 2 Pa. If the house has a fireplace, central exhaust system or other large or frequently used exhaust equipment, increase the differential pressures by 2 Pa.

Ventilation has three components consisting of (i) infiltration, or uncontrolled leakage of air into a building through openings in the building envelope, (ii) natural ventilation through open windows and doors, and (iii) mechanical ventilation provided by fans (Nazaroff, 1992). Ventilation rates reported in the literature vary significantly (Table 8.2). Two broad trends suggested by the data are a general reduction in ventilation rates over the past two decades and lower ventilation rates for houses in cold climates (e.g., compare U.S. and Canadian data). In regions with relatively cold climates, the recent trend has been to construct "air-tight" houses with reduced ventilation rates to minimize energy consumption and costs (e.g., "R-2000" houses in Canada; Gusdorf and Hamlin, 1995). For houses with high energy efficient systems and that typically have mechanical ventilation supplied through a heat recovery ventilator, ventilation rates may be as little as 0.1 air exchange per hour (*ACH*) (Fellin and Otson, 1996). Reported ventilation rates also vary seasonally. In some cases, winter ventilation rates can exceed those measured in the summer since pressure gradients caused by differences in indoor and outdoor temperature result in higher ventilation rates (SRC, 1995). Summer ventilation rates will typically depend largely on natural ventilation and hence occupant use patterns (Lamb *et al.*, 1985; Walkinshaw, 1987).

Standards in Canada and the U.S. both specify minimum ventilation rates for residential dwellings. In Canada, the CSA F326 standard for a 3 bedroom house with unfinished basement is an outside air exchange of 70 L/s, or about 0.5 *ACH* for a 100 m^2 bungalow with 100 m^2 basement (SRC, 1995). In the US, the ASHRAE 62-89 standard recommends an outside air ventilation rate of not less than 7.5 L/s per person, and also not less than 0.35 *ACH*. It appears that mechanical ventilation systems are quite frequently operated at less than the design or installed capacity (SRC, 1995; Figley, 1997; Hamlin and Gusdorf, 1995).

While we are not aware of studies involving detailed evaluation of the interaction between ventilation rate and building depressurization, we would intuitively expect the air exchange rate to increase as the building depressurization, due to stack effect, increased. In contrast, if the mechanical ventilation rate were to be decreased, we would expect the building depressurization due to possible unbalanced flows, to also decrease, all other factors being equal. For these reasons, we suggest that it would be overly conservative to select very high building underpressurizations together with very low ventilation rates when using models to predict indoor air quality from subsurface VOC contamination.

INDOOR AIR QUALITY

Indoor VOC concentrations are affected by numerous factors including indoor, outdoor and potentially subsurface sources, air exchange between the building and outdoors, air movement within the building, interactions between the VOC and indoor sources, and chemical reactions (Tichenor *et al.*, 1990). Human activity and environmental factors such as temperature and relative humidity can also affect VOC levels. Elevated VOC concentrations in indoor air have been associated with adverse health effects such as sensatory irritation, and a broad-ranging and complex set of symptoms known as Sick Building Syndrome (SBS) (Andersson *et al.*, 1997).

Table 8.2. Survey of Building Ventilation Rates

Reference	Data Type	Location	Building Type & Number	Measurement Date	Measurement Statistic	Air Exchange (ach)	Comments
Otson and Zhu, 1997	Measured PFT	Greater Toronto, ONT, Canada	Houses (44)	Feb. 12 to Apr. 9, 1996	average median	0.45 0.4	
Murray and Burmaster, 1995	Measured PFT	U.S. Region 1 U.S. Region 2 U.S. Region 3 U.S. Region 4 U.S. Region 1 U.S. Region 1 U.S. Region 1 U.S. Region 1	Houses (467) Houses (1496) Houses (332) Houses (1549) Houses (161) Houses (254) Houses (5) Houses (47)	All seasons All seasons All seasons All seasons Winter Spring Summer Fall	mean mean mean mean mean mean mean mean	0.4 0.55 0.55 0.98 0.36 0.44 0.82 0.25	5th and 95th percentile = 0.1, 0.95 5th and 95th percentile = 0.14, 1.38 5th and 95th percentile = 0.15, 1.25 5th and 95th percentile = 0.21, 2.82 5th and 95th percentile = 0.08, 0.90 5th and 95th percentile = 0.14, 1.06 5th and 95th percentile = 0.27, 2.01 5th and 95th percentile = 0.1, 0.58
SRC, 1995	Measured PFT	Saskatoon, SASK, Canada	Houses (20)	1993 - 1994 (9 months)	minimum average maximum	0.08 0.2 0.43	all houses had natural gas forced air heating systems and chimneys connected to the natural gas furnaces
Fellin and Otson, 1993	Measured PFT	Canada	Houses (24)	1992 to 1993	average	0.34	most measurements in fall and winter months
SRC, 1992	Measured PFT	Saskatoon, Regina SASK, Tillsonburg, ONT, Canada	Houses (44)	Jan. 14 to Feb. 11, 1991	average median	0.34 0.31	
Rothweiler et al., 1992	Measured N_2O	Switzerland	Houses (10)	N/A	10th percentile 50th percentile 90th percentile	0.06 0.16 2.06	new houses or renovated houses
Panadian et al., 1993	Measured PFT	USA	Houses (4000)	Mostly 80's early 90's	average average average average average average average average	2 3.3 0.6 0.4 0.5 1.9 5.4 0.4	all regions (std. dev. = 3.3) southwest northeast northwest winter, all regions spring, all regions summer, all regions fall, all regions
Lewis and Zweidinger, 1992	Measured SF_6	Boise, Idaho, USA	Houses (10)	Nov. 15, 1986 to Feb. 4, 1987	average median	0.45 0.45	
Mailahn et al., 1989.	Measured PFT&HFB	Berlin, Germany	Houses (10)	Sept. 1986 to Apr. 1987	average median	1.01 1.02	older houses had statistically significant higher ach (1.2) then newer houses (0.88)
Mueller et al., 1988.	Measured	USA	Houses	N/A	typical range	0.5 - 1.5 0.5 - 0.8	typical houses new or energy efficient houses, some as low as 0.2
Walkinshaw, 1987	Measured	ONT, Canada	Houses (70) R-2000 Houses (?)		range range	0.06 - 0.77 0.34 - 0.37	lowest ach occurred in summer with windows closed in R-2000 houses
Boman and Lyberg, 1986.	Measured	Sweden	Detached & row houses 3-storey appartments	1974-1982 1974-1982	average average	0.17 0.78	no mechanical ventilation, 1975 and later no mechanical ventilation, with fireplace, 1940-1960
Gerry et al., 1986	Measured		Houses (typical) Recently built houses		typical range typical range	0.7 - 1.1 0.5 - 0.8	
Parker, 1986	Measured	Bangor, Washington	2-storey, four unit building (4)		range	0.24 - 0.91	electric heating
Lamb, 1985	Measured PFT	Eastern Washington, USA	Houses (10)		range	0.3 - 1.0	during typical meterological conditions extended use of doors caused ach to exceed 3
ASHRAE, 1985	Measured	USA	Houses	N/A	typical range median	0.2 to 2 0.5, 0.9	median values for 2 studies
Grimsrud et al., 1982	Mostly Predicted	North America	Houses (312)	N/A	average median	0.63 0.5	mostly predicted using LBL model (stack & wind effect)
Gusdorf and Hamlin, 1995	Predicted AIM-2 HOT-2000	Canada	Houses (47)	Annual Average	average median minimum maximum	0.36 0.34 0.14 0.68	R-2000 houses, high energy efficiency houses use heat recovery ventilators
Ekberg (1994)	Measured SF_6	Malmo, Goteburg, Sweden	Office buildings (4)	Jan. 90 to Dec. 91	range	3.2 to 4	measured during periods of mechanical ventilation
Sheldon et al., 1988	Measured SF_6	Washington D.C., USA	Old-age home School Office Office	Winter 83 1983 July 1983 Sept. 1983		1.72 +/-0.41 0.85 +/- 0.31 0.61+0.32 0.52+0.25	high ach attributed to excessive heating and cold outdoor temperatures
CMHC, 1997	Guidance	Canada	Wood frame pre 1945 Wood frame 1946-1960 Wood frame 1961-1980 Airtight new house	N/A N/A N/A N/A	typical range typical range typical range typical range typical range typical range	0.5-1 None 0.2-0.4 None 0.15-0.3 0.05-0.1	Estimated heating season natural ventilation Estimated mechanical ventilation Estimated heating season natural ventilation Estimated mechanical ventilation maybe 0.2 intermittent 0.3 installed capacity
Otson et al., 1996	Guidance	Canada	Houses	N/A	low typical	0.1 0.3	low typical

Notes: 1. PFT = perfluorocarbon tracer, HCB = hexafluorobenzene, SF_6 = sulphur hexafluoride, N_2O = nitrous oxide

2. Region 1: heating degree days > 7000 (coldest region), Region 2: 5,500 < heating degree days < 7,000
Region 3: 2,500 < heating degree days < 5,500, Region 4: heating degree days < 2,500

There are numerous indoor sources of VOCs including building and construction products, furniture, carpets, textiles, household cleaners, sealants, glues, adhesives, paints, waxes, lubricants, heating systems (*i.e.*, fuels), cooking vapours, human bioeffluents, personal care products, molds and fungi (SRC, 1992). Specific sources of indoor VOCs, that are also common subsurface contaminants, are listed in Table 8.3. The VOC emission rate varies widely depending on the material and time, and numerous studies have involved the use of small-scale environmental test chambers to evaluate emission rates (*e.g.*, Figley *et al.*, 1996; European Commission, 1995). Data from chamber tests are often fitted to empirical models such as first-order decay models to provide a means to predict indoor air quality. More sophisticated models for mass transfer such as gas-phase-limited mass transfer, or within material diffusion-limited emissions have also been proposed (e.g., Sparks *et al.*, 1996; Gustafsson, 1992). In a few cases, larger-scale test rooms or houses have been used to validate models developed (e.g., Tichenor *et al.*, 1990). The interaction between VOCs and building surfaces is complex. Sinks such as wallboard, ceiling tile, carpet and upholstery are important in controlling VOC levels over extended periods. During high concentration periods, adsorption of VOCs can reduce peak concentrations; however, accumulated VOCs can be released as indoor air concentrations decrease, or as a result of changes in temperature or other environmental factors (Fellin and Otson, 1996).

Several indoor air quality studies providing information for houses are summarized below. The VOC concentrations for typical chemicals of concern at contaminated sites have been extracted from these studies and are presented in Table 8.4. Indoor VOC concentrations were measured in 757 homes from various parts of Canada as part of a comprehensive Health Canada study between 1991 and 1992 (Otson *et al.*, 1993). Samples were collected using passive devices and concentrations were quantified by GC/MS. The arithmetic mean total VOC (TVOC) concentration was 829 $\mu g/m^3$ based on identified compounds, however, the concentration was estimated to be as high as 1.4 mg/m^3 if non-identified compounds were to be included (*i.e.*, estimate based on area under the gas chromatograph trace). The mean indoor benzene concentration for this study was 5.4 $\mu g/m^3$. Davis and Otson (1996), based on this study, concluded that toluene, ethylbenzene, xylenes, decane, and dichlorobenzene were chemicals with a high likelihood of originating from indoor sources, benzene had a medium likelihood while tetrachloroethylene, trichloroethylene and hexane had a low likelihood of indoor sources.

The U.S. EPA conducted a comprehensive evaluation of personal (i.e., mostly indoor) air quality for several urban centres, located primarily in industrialized areas (Elizabeth-Bayonne, New Jersey and Los Angeles, California) (Wallace, 1987). Passive personal air samplers were used to measure VOC concentrations. The mean concentrations for several compounds (e.g., benzene) were somewhat higher for this study when compared to others summarized in Table 8.4. Personal air values generally exceeded outdoor air values by ratios of 2 to 5 (Wallace, 1987). Shah and Singh (1988) summarized VOC concentrations for numerous U.S. studies for all indoor air settings, with the majority of sites corresponding to residential and commercial types. The mean and median indoor benzene concentrations for this study were 16.5 and 10 $\mu g/m^3$, respectively.

Table 8.3 . Dominant Sources of Selected VOCs (adapted from Davis and Otson, 1993; Otson and Fellin, 1992).

Source	Benzene	Toluene	Ethylbenzene	Xylenes	Styrene	Trimethybenzenes	Naphthalene	Trichloroethylene	Tetrachloroethylene	Trichloroethanes	Chlorobenzenes	Decane
Latex paints	X	X				X						
Alkyl paints										X	X	
Carpets	X	X			X	X						
Glued carpets	X	X			X	X					X	X
Wood burning		X		X	X	X	X					
Foam board											X	
Paint removers		X										
Spray products				X								
Adhesives/tape		X			X			X				X
Room deodorizers											X	
Tobacco smoke	X	X	X	X	X							
Gasoline/driving	X	X		X	X	X						
Solvents		X	X									
Dry cleaning									X			

Note: Dominant or key sources of VOCs based on factorial analysis between documented sources in homes and concentrations for Health Canada study. There are other sources of VOCs listed. VOCs selected for table are those commonly found at contaminated sites.

Indoor air concentrations were measured in 44 homes in the greater Toronto area (Ontario, Canada) between February 12 and April 9, 1996 using similar methods as the Health Canada study (Otson and Zhu, 1997). The mean TVOC concentration was 132 $\mu g/m^3$ for this study (based on 20 identified compounds). The mean indoor/outdoor (I/O) ratios for VOCs generally ranged between 1 and 6, and was 1.79 for benzene.

Several studies indicate that VOC concentrations in indoor air can be very high in new buildings (Rothweiler *et al.*, 1992; Andersson *et al.*, 1997). For example, TVOC concentrations in new and recently renovated buildings in Switzerland ranged from 1.6 to 31.7 mg/m^3 and were particularly high in buildings with low ventilation rates. Many of the individual compounds detected had I/O ratios that were much higher than one and were attributed to materials such as glues, sealants, carpets, and paints. One exception was benzene which had an I/O ratio of about one. A Dutch study of 300 homes found that VOC concentrations were significantly higher in

newer houses (Lebret *et al.*, 1986). The I/O ratios for this study ranged from 1 to 10 for most compounds. Recent data on chlorinated solvent background concentrations in indoor air are provided in Kurtz and Folkes (2002) and Foster et al. (2002).

Table 8.4. Compilation of Indoor Air Quality Data (page 1)

Study	Date & Time	Statistic	Number	Concentrations in Indoor Air: Benzene	Toluene	Ethyl-benzene	m,p-Xylene	o-Xylene	Styrene	1,3,5-Trime-thybenzene	Naph-thalene
Lowry AFB Study (Versar, 2000)[7]											
Colorado	1997 - 1998	Median	12-26	-	-	-	-	-	-	-	-
		Arithmetic Mean	12-26	-	-	-	-	-	-	-	-
		Maximum	12-26	-	-	-	-	-	-	-	-
Redfields Colorado Study (Envirogroup, 1999)[7]											
Redfields, Denver	1999	Median	55-78	-	-	-	-	-	-	-	-
Colorado		Arithmetic Mean	55-78	-	-	-	-	-	-	-	-
		90th percentile	55-78	-	-	-	-	-	-	-	-
		Maximum	55-78	-	-	-	-	-	-	-	-
Denver Colorado Study (Walsh, 1999)[7]											
Denver, Colorado	1997-1999	Lognormal Mean	55-415	4.71	-	-	-	-	-	-	-
		95% Tolerance Limit	55-415	12.2	-	-	-	-	-	-	-
		Maximum	55-415	41	-	-	-	-	-	-	-
Health Canada Study (Davis and Otson, 1996)[1]											
Across Canada	1991, 1992	Arithmetic Mean	757	5.4	40.8	8.2	20.7	5.6	0.3	2.7	-
	All seasons	Maximum	757	67.9	5730	540	1470	320	130	640	-
U.S. EPA TEAM Study (U.S. EPA, 1987)[2]											
Elizabeth-Bayonne,	Fall 1981	Arithmetic Mean	340	28	-	19	52	16	8.9	-	-
New Jersey	Fall 1981	Maximum	85	120	-	320	120	46	54	-	-
	Summer 1982	Arithmetic Mean	150	-	-	9.2	37	12	2.1	-	-
	Summer 1982	Maximum	71	-	-	180	150	100	10	-	-
	Winter 1983	Arithmetic Mean	49	-	-	12	36	13	2.4	-	-
	Winter 1983	Maximum	8	-	-	32	63	24	11	-	-
Los Angeles, California	Feb-84	Arithmetic Mean	110	18	-	11	28	13	3.6	-	-
	Feb-84	Maximum	25	49	-	29	58	34	9	-	-
Los Angeles, California	May-84	Arithmetic Mean	50	9.2	-	7.4	24	7.2	1.8	-	-
	May-84	Maximum	25	29	-	35	94	29	5	-	-
Contra Costa, California	Jun-84	Arithmetic Mean	67	7.5	-	3.7	11	4.4	1	-	-
	Jun-84	Maximum	10	22	-	9	26	11	4	-	-
U.S. National Survey (Shah and Singh, 1988)											
Across U.S.A	pre 1988	Median	96-2278	10.0	6.3	4.8	-	-	-	1.4	-
		Arithmetic Mean	96-2278	16.5	27.9	12.4	-	-	-	2.8	-
		Upper Quartile	96-2278	21.1	28.8	9.3	-	-	-	4.0	-
Dutch Study (Lebret et al., 1985)[3]											
Ede, Netherlands	Winter 81/82	Median	100	7	40	3	12	-	-	2	-
Post war		Maximum	100	148	697	45	178	-	-	99	-
Rotterdam, Netherlands	Winter 82/83	Median	100	7	23	2	9	-	-	1	-
Pre war		Maximum	100	24	526	117	159	-	-	37	-
Ede, Netherlands	Winter 82/83	Median	100	5	43	2	10	-	-	2	-
< 6 years		Maximum	100	53	2252	138	753	-	-	93	-
Greater Toronto Study (Otson and Zhu, 1997)[4]											
Greater Toronto	Feb. 12-Apr. 9, 1996	Arithmetic Mean	44	3.42	15.2	1.58	-	-	-	0.53	4.81
		Maximum	44	45.8	186	20.9	-	-	-	1.47	83.4
Saskatchewan and Ontario Study (SRC, 1992)[5]											
Regina, Saskatoon, SA	Jan. 14, 1991 -	Arithmetic Mean	44	15	23.9	9.6	21.6	5.7	4.1	5.1	7.2
Tillsonburg, Ontario	Feb 11, 1991	Maximum	44	42.3	110.5	32.9	74.2	20.3	11.3	15	30
Tennessee Houses (Oak Ridge National Laboratory, 1988)[6]											
East Tennessee Houses	Aug 84 to Jan 85	Median	8	7.5	38.5	6.5	18.5	6	-	-	-
		Maximum	8	30	111	82	302	323	-	-	-

Notes:

1. OVM 3500 (3M Co.) passive samplers, 24 hour samples, quantified by GC/MSD
2. Personal air samplers using Tenax, arithmetic mean of 12 hour daytime and 12 hour nighttime samples, quantified by GC/MS
3. Charcoal tubes, 5 to 7 day samples at 100 ml/min, GC/FID and GC/MS
4. OVM 3500 passive samplers, 24 hour samples, quantified by GC/MSD
5. OVM 3500 passive samplers, 24 hour samples, quantified by GC/MSD, 20 houses in Sask (Regina and Saskatoon), 24 in Tillsonburg, Ontario
6. Sorbent tubes consisting of Tenax or Tenax-carbonaceous mixtures quantified by GCMS
7. SummaTM steel canisters and EPA Method TO-14 or TO-15.
8. - = not tested or below detection limit

Table 8.4. Compilation of Indoor Air Quality Data (page 2)

Concentrations in Indoor Air									
1,1,1-Trichloroethane	m,p-Dichlorobenzene	Carbon Tetrachloride	n-Hexane	n-Heptane	n-Octane	n-Nonane	n-Decane	n-Undecane	n-Dodecane
-	-	-	-	-	-	-	-	-	-
-	-	-	-	-	-	-	-	-	-
-	-	-	-	-	-	-	-	-	-
1.55	-	-	-	-	-	-	-	-	-
4.45	-	-	-	-	-	-	-	-	-
9	-	-	-	-	-	-	-	-	-
78	-	-	-	-	-	-	-	-	-
1.89	-	-	-	-	-	-	-	-	-
6.98	-	-	-	-	-	-	-	-	-
78	-	-	-	-	-	-	-	-	-
-	18.9	-	1.2	-	-	-	31.4	-	-
-	1390	-	124	-	-	-	6450	-	-
94	45	9.3	-	-	-	-	-	-	-
880	920	14	-	-	-	-	-	-	-
67	50	1	-	-	-	-	-	-	-
120	1600	6	-	-	-	-	-	-	-
45	71	1	-	-	-	-	-	-	-
170	120	-	-	-	-	-	-	-	-
96	18	1	-	-	5.8	-	5.8	5.2	2.5
200	210	3	-	-	38	-	11	11	10
44	13	0.8	-	-	4.3	-	3.5	4.2	2.1
94	170	1	-	-	20	-	17	76	57
16	5.5	1.3	-	-	2.3	-	2	2.7	2.1
14	9	3	-	-	2	-	26	16	5
10.0	1.7	0.0	-	-	2.4	3.7	1.6	1.8	-
267.4	24.0	2.6	-	-	4.1	6.1	4.5	4.8	-
30.1	5.6	0.9	-	-	4.3	6.3	4.1	3.8	-
-	2	-	4	3	2	4	9	5	2
-	139	-	107	68	60	269	433	191	118
-	<0.6	-	5	3	1	3	8	3	1
-	355	-	338	30	36	278	807	229	40
-	<0.6	-	3	2	1	6	14	9	4
-	246	-	178	556	533	407	905	445	96
-	53.4	-	5.24	-	-	-	6.85	-	-
-	1600	-	108	-	-	-	91.9	-	-
-	12.8	-	14.5	-	-	-	-	-	14.7
-	337.5	-	99.4	-	-	-	-	-	91.9
3.5	0.75	0.5	9	-	-	-	-	-	-
18	34	4	113	-	-	-	-	-	-

ISSUES FOR THE USE OF INDOOR AIR MEASUREMENTS TO QUANTIFY SOIL VAPOUR SOURCES

The sampling and analysis methods used for indoor air quality studies referenced in Table 8.4 were mostly passive or active collection of VOCs on sorbents followed by GC/MC analysis. Sorbents consisted of charcoal, Tenax (poly (2,6-diphenyl phenylene oxide)) or multi-bed sorbent tubes containing graphitized carbons and carbon molecular sieve sorbents. Samples collected using sorbent tubes were often collected over two 12 hour periods to obtain "daytime" and "nighttime" samples, or over a 24 hour period. The recent trend in the U.S.A. is the collection of indoor air samples using Summa passivated stainless steel canisters and analysis by U.S. EPA Method TO-14 or TO-15, as reflected by protocols developed or under development by Commonwealth of Massachusetts (Massachusetts, 2000) and State of Colorado (personal communication, Sheila Gaston, Colorado Department of Health). The concerns surrounding use of sorbant tubes include chemical breakthrough, cross-contamination and detection limits that are not sufficiently low.

While the mechanics of sample collection and analysis are not overly difficult, the design of an indoor air sampling program and interpretation of data to quantify potential soil vapour sources and risk is a challenging undertaking. Some considerations that we believe will result in improved assessments are discussed below.

Recognize the high background VOC concentrations in air and concentration variability: We are aware of only a very limited number of published studies where the soil vapour derived component of indoor air has been thoroughly evaluated. In one study, it was shown that the mean indoor benzene concentration in houses directly above a benzene vapour plume was less than that in nearby control houses in an uncontaminated area (Laubacher, 1997). Although there is limited data, the contribution of VOCs from subsurface sources relative to indoor sources is expected to be small for most chemicals and sites. Therefore, it is important to recognize the high degree of variability in indoor air quality when designing an air testing program.

Reported TVOC concentrations, in particular, vary significantly and range from less than 0.5 mg/m^3 for identified compounds (Lebret *et al.*, 1986; Otson and Zhu, 1997; U.S. Wallace, 1987; Shah and Singh, 1988) to about 1.4 mg/m^3 for the Health Canada study if unidentified compounds are included. This range excludes studies of new houses. The variability in part is due to the TVOC definition (identified versus non-identified compounds) and differing analytical methods. For example, polar organics may be lost or underestimated when charcoal or Tenax is used (Rothweiler *et al.*, 1992).

The most important determinants affecting indoor air quality are building materials and age, and factors relating to occupant use. The design of a background study would obviously need to take these factors into account. Ventilation rates can also affect indoor air concentrations, and therefore indoor air data collected over various times of the year may not be directly comparable. For example, the Health Canada study indicated that for outdoor temperature ranges of $< 0^{\circ}C$, 0 to $15^{\circ}C$ and $> 15^{\circ}C$, respectively, the mean indoor concentrations for individual VOCs (26 compounds) were 10.3, 9.8 and 5.0 $\mu g/m^3$ (Fellin and Otson, 1993). While these concentration differences were not statistically significant, the trend suggests that the VOC

concentrations were affected by outdoor temperature. The apparent difference in VOC concentration was interpreted to be, in part, a result of lower natural ventilation rates during winter months. The trend toward "air-tight" houses and reduced ventilation rates in regions with a cold climate may also be a relevant consideration. Reduced ventilation rates can affect background indoor VOC concentrations, but will not necessarily affect the soil vapour component of indoor concentrations since building underpressurization and VOC intrusion may also decrease in conjunction with a reduction in ventilation rates. In some cases, mechanical ventilation systems are also designed to minimize their influence on building pressurization.

Recognize the temporal variation in soil gas intrusion: Since soil gas advection appears to be the most significant mechanism for VOC intrusion into buildings, there may be diurnal variations in intrusion due to daily temperature fluctuations, longer term variations due to changes in barometric pressure, and seasonal variations due to differences in temperature and/or ventilation system operation. As proposed by Adomait and Fugler (1997), the collection of indoor air samples during both periods of positive and negative soil-to-building pressure gradients may actually provide a means to distinguish between indoor and subsurface sources.

Complementary data is essential: We consider obtaining complementary data to assist in the interpretation of indoor air data as essential since the "blind use" of measured indoor air concentrations may lead to erroneous conclusions with respect to the VOC source. Measurement data and information that are relatively important and easy to obtain are:

1. Pressure gradients between the basement (or ground floor) and atmospheric air, measured at the time of sampling. Several studies indicates that building depressurization can result in signficant soil gas intrusion through advection (Nazaroff *et al.*, 1985; Adomait and Fugler, 1997; Hers and Zapf-Gilje, 1998).
2. Collection of seasonal data when conditions suggest seasonal effects could be significant. For example, for houses in cold climate areas, vapour intrusion rates for an advection dominated system (i.e., controlled by near-field processes) would be expected to be highest during winter months due to the stack effect.
3. Description of building features (age, basement, garage), foundations (construction, any visible cracks, drains, sumps, utility connections), heating, ventilation, and air conditioning system type and operation, and occupant use during sampling. If ventilation rates are highly uncertain, tracer tests to measure building ventilation rates can also be considered.
4. Meterological data such as precipitation, temperature, barometric pressure and wind speed. This data is relatively inexpensive to obtain, and can be used to evaluate pressure gradients.

In comparison to the expense and effort required to obtain high quality indoor air data, obtaining the above data is considered relatively straightforward and cost effective.

Soil vapour concentrations below a building and cross-foundation slab pressures can be highly useful in that it provides a direct indication of vapour sources and advection potential. Obtaining this data may be problematic at ocupied houses due to the intrusive nature of such measurements. Nevertheless, it is suggested that this data be obtained at least at a sub-set of the buildings under consideration, whenever possible. In some cases, soil vapour measurements are

obtained at similar depths to the building ground floor slab in an attempt to infer sub-slab vapour concentrations. Several studies have shown that there can be significant differences between soil vapour concentrations below and adjacent to a building (*e.g.*, Laubacher *et al.*, 1997; Hers and Zapf-Gilje, 1998); therefore this approach is not recommended.

Use of natural tracers: The use of natural tracers to distinguish between subsurface and building sources may be possible when subsurface transformations result in chemicals that are not normally found indoors. For example, cis-1,2-dichloroethylene (DCE), a degradation product of trichloroethylene (TCE), was either not detected or quantified in the indoor air quality studies studies reviewed above, suggesting that background DCE concentrations in air are low. For a site where both TCE and DCE are measured in soil vapour, and DCE is detected in indoor air, a mass balance approach could be used to approximate the TCE concentrations in indoor air as follows. Assuming VOCs are well-mixed, the following mass balance equation for a house, or portion of a house (e.g., basement) is obtained:

$$V\frac{\partial C_i}{\partial t} = C_o Q_{in} + M_{sv} - C_i Q_{out} + S_i - R_i \qquad (1)$$

where V is the house volume (L^3), C_i and C_o are the indoor and outdoor VOC concentrations which in this case are for DCE ($M\,L^{-3}$), Q_{in} is the air flow entering the house, M_{sv} is the mass flux of soil vapour VOC entering the house ($M\,T^{-1}$), Q_{out} is the air flow leaving the house ($L^3\,T^{-1}$), S_i is the source term and and R_i is the removal (sink) term. If the soil gas flow (Q_{sg}) entering the house is small relative to the building air exchange, if steady state conditions prevail and if there are no sources or sinks, the air flow and mass flux of the soil vapour tracer (DCE) can be estimated as follows:

$$Q_{out} = Q_{sg} + Q_{in} \sim Q_{in} \sim V\,ACH \qquad (2)$$

$$M_{sv}^{DCE} = V\,ACH\,(C_i^{DCE} - C_o^{DCE}) \qquad (3)$$

where ACH is the air changes per hour (L^3/T per L^3). The mass flux of the chemical of interest (TCE), and indoor air concentration associated with a soil vapour source are estimated using the relative concentrations measured in soil vapour:

$$M_{sv}^{TCE} = M_{sv}^{DCE}\,C_{sv}^{TCE}/C_{sv}^{DCE} \qquad (4)$$

$$C_i^{TCE} = M_{sv}^{TCE}/(V\,ACH) \qquad (5)$$

where C_{sv}^{TCE} and C_{sv}^{DCE} are concentrations of TCE and DCE in soil vapour ($M\,L^{-3}$). When near-foundation soil vapour measurements are available and advection is the dominant mechanism for vapour intrusion, eq. 4 is likely a reasonable approximation. If diffusion, sorption and other processes are important, this relationship would only be accurate if chemical fate and transport were similar between the tracer and chemical of interest.

SIGNIFICANCE OF SUBSURFACE RELATIVE TO INDOOR VOC SOURCES

The potential significance of intrusion of soil vapour containing VOCs into buildings, relative to background indoor air sources, is evaluated using a slightly modified version of the Johnson and Ettinger (1991) model. This model is commonly used to predict indoor air concentrations from subsurface contamination sources. Model predictions are made for a range of soil and building properties, and a single vapour concentration at the contamination source (i.e., single source strength).

The Johnson and Ettinger modeling results are given as a function of the vapour attenuation ratio (α) and the ratio of effective diffusion coefficient (D_T^{eff}) to depth to contamination (L_T) (Figure 8.1). The α value is defined as the indoor air concentration divided by the source vapour concentration. The D_T^{eff}/L_T ratio captures the influence of soil properties and depth to contamination source on α. Since free-air diffusion coefficients vary by only a factor of two for most volatile chemicals, chemical-specific variation in the D_T^{eff}/L_T ratio will be of little consequence, in most cases.

The influence of building foundation and building properties are represented by a possible "upper" and "lower" range of input values, considered representative of most sites (Figure 8.2). These values were subjectively chosen based on the author's research and review of other studies (Hers and Zapf-Gilje, 1998, Hers *et al.*, 2003). The building mixing height is the height over which mixing of soil vapour contaminants take place. The assumed range corresponds to a one-storey to two-storey house. The slight modification to the model is that the advective soil gas flow rate (Q_{soil}) is directly input and not estimated using the equation provided in Johnson and Ettinger (1991). The Q_{soil} range is roughly based on measured values from tracer tests at several sites for coarse-grained (sand to gravel) soils (Hers *et al.*, 2003). The modeling assumes a soil contamination source above the water table. The highest α values are estimated when there is shallow contamination, dry soil (*i.e.*, high air-filled porosity), high advective soil gas flow rates into the building, and low ventilation rates.

Model predicted indoor air concentrations from soil vapour are estimated for benzene, TCE and TVOC (Figure 8.3). The assumed source vapour concentrations are possible "typical" values based on reported concentrations for several studies (Table 8.5). The assumed background indoor air concentrations are mean concentrations measured for the Health Canada study (Davis and Otson, 1996).

The incremental lifetime cancer risk (*ILCR*) are estimated for benzene and TCE using reported Health Canada Tumourigenic Concentrations corresponding to five percent cancer incidence (TC_{05}) (Health Canada, 1996). The Tumourigenic Concentrations are based on neoplastic effects in animal species, and animal to human conversions that incorporate inhalation to body weight ratios. These conversions are based on variations in breathing rates and body weights between rodents and the age group for humans for which this ratio is greatest (i.e., 5 to 11 year olds). Health Canada considers benzene as a Group 1 – Carcinogenic chemical while TCE is classified as Group 2 – Probably Carcinogenic (Health Canada, 1996). The *ILCR* is calculated as follows:

$$ILCR = 0.05\ C\ ET\ EF\ /\ (TC_{05}\ UCF) \qquad (6)$$

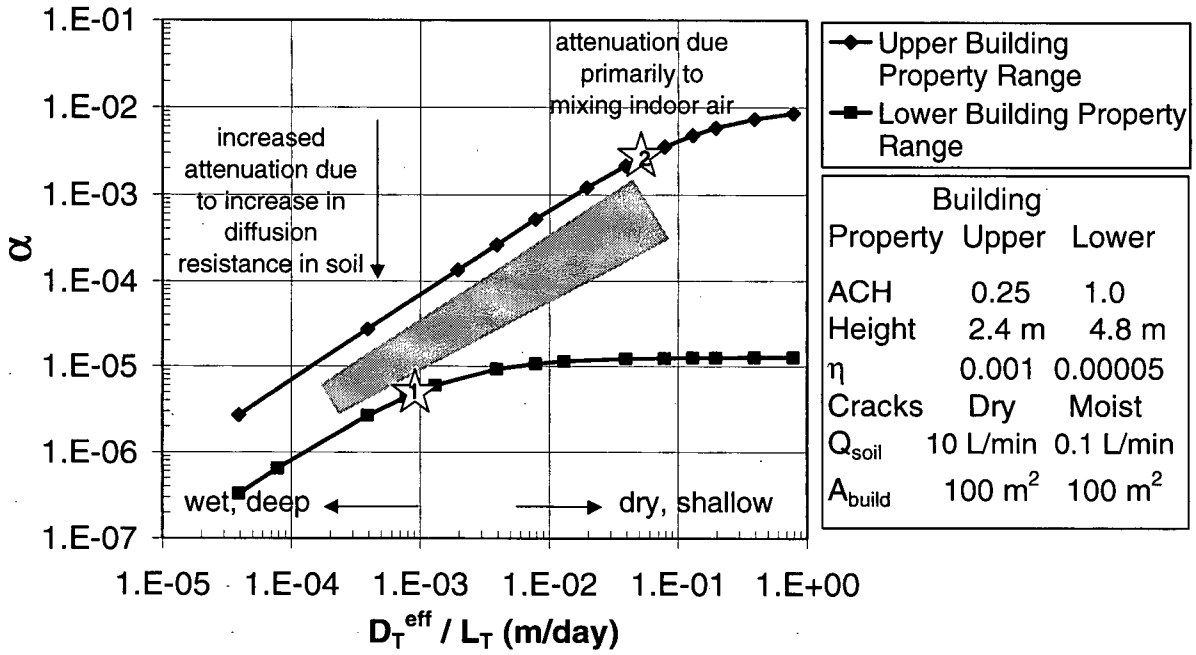

Figure 8.2. Predicted vapour attenuation between benzene vapour concentrations at source and indoor air using Johnson and Ettinger (1991) model. Figure adapted from Johnson *et al.*, 1998. Shaded region considered to encompass majority of sites. Height = building mixing height, *Qsoil* = Advective flow rate into building for coarse-grained soils, Dry dust-filled cracks, total porosity = 0.3; moist dust-filled cracks, water-filled porosity = 0.1, total porosity = 0.3; η = crack ratio

with C equal to the indoor air concentration and other exposure and risk parameters defined in Table 8.6. The ILCR is estimated using both the predicted indoor air concentration derived from soil vapour, and the background benzene and TCE concentrations measured for the Health Canada study (Davis and Otson, 1996) (Figure 8.4). While regulatory promulgated toxicity values for TVOCs are not available, numerous studies have attempted to evaluate health effects associated with TVOC (Andersson *et al.*, 1997). For example, Molhave and co-workers reported sensory effects at a TVOC concentration of 1.7 mg/m^3 (Molhave *et al.*, 1993), dose effects for odour starting at 3 mg/m^3 and reduced well-being above 25 mg/m^3 TVOC (Molhave *et al.*, 1991).

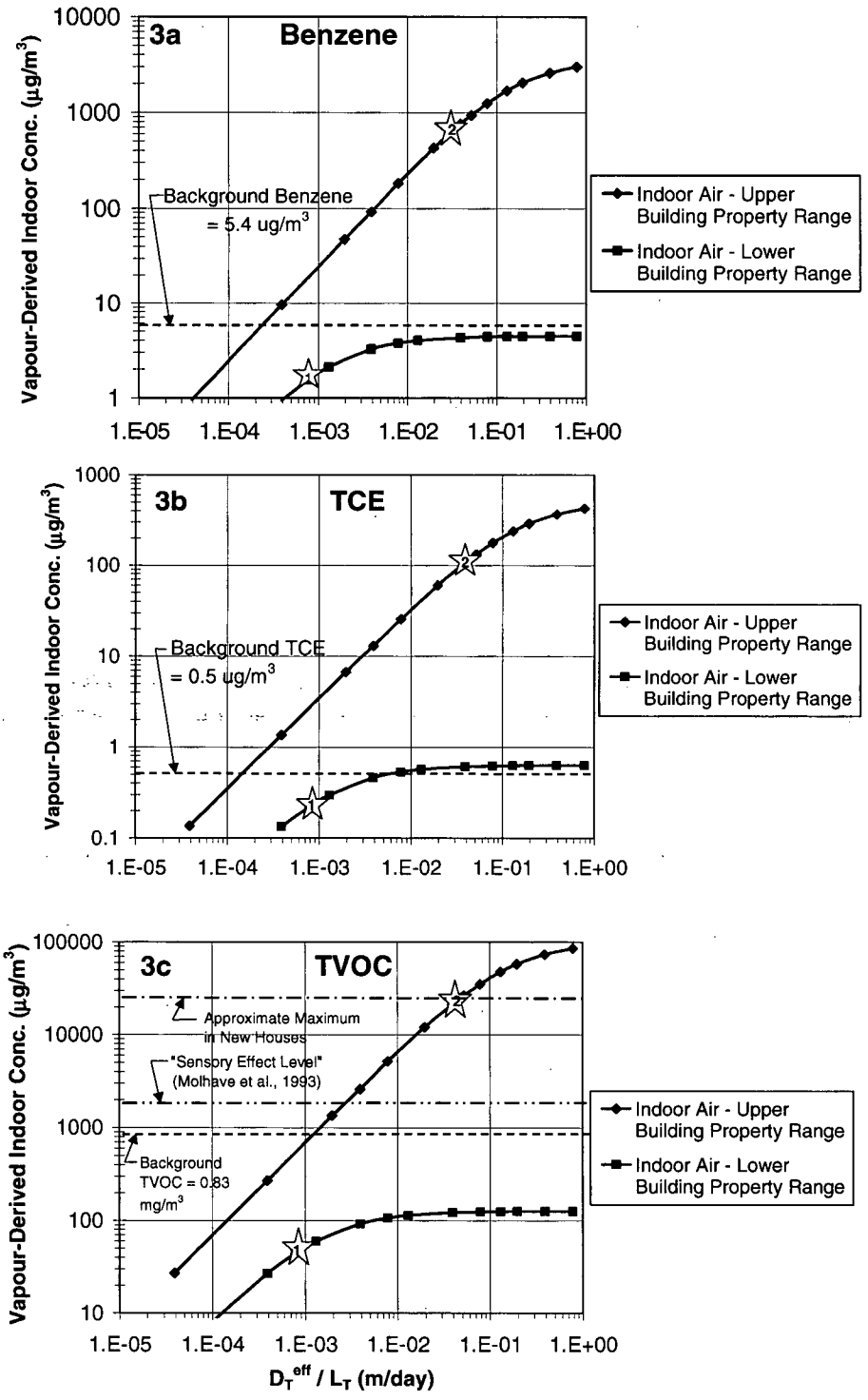

Figure 8.3. Model-predicted vapour-derived indoor air concentrations for (a) benzene, (b) TCE and (c) TVOC. The soil vapour component of the indoor air concentration was predicted using the Johnson and Ettinger (1991) model.

Table 8.5. Assumed Contamination Source Soil Vapour Concentrations Used for Modeling

Chemical	Reference	Contamination Type[1]	Approx. Measured Vapour Concentrations (ug/L)[2]
Benzene	Fischer et al., 1996	Gasoline	200
	Laubacher et al., 1997	Gasoline	576
	Ryrie & Sweeney (1995)	Gasoline	270 to 300
Assumed Benzene Source Vapour Concentration			**350**
TCE	McNeel et al. (1997)		18
	Smith et al. (1996)	PCE, TCE	3
	Golder Associates Ltd.[3]	PCE, TCE	50
Assumed TCE Source Vapour Concentration			**25**
TVOC	Fischer et al., 1996	Gasoline	40000
	Ostendorf and Kampbell (1991)	Aviation Fuel	6400 to 40000
	Moseley and Meyer (1992)	Gasoline	1000
	Tillman et al. (1990)	Gasoline	10000
Assumed TVOC Source Vapour Concentration			**10000**

Notes:

1 Vapour concentrations for all sites were measured near to the water table. For gasoline and aviation fuel sites, residual NAPL was in close proximity to probes (i.e., above water table). For chlorinated solvent sites, vapour probes were near source locations, however presense of residual NAPL above water table is less certain (concentrations may reflect a dissolved groundwater source)

2 Most values are peak vapour concentrations, however, in some cases, only limited soil vapour data was available

3 Golder Associates Ltd. internal report

Table 8.6. Exposure and Risk Factors

Factor	Value
Exposure Time ET (hr/day)	20
Exposure Frequency EF (day/year)	350
Exposure Duration ED (year)	30
Averaging Time Carcinogens (years)	75
Unit Conversion Factor UCF (hr to year)	8760
Benzene TC_{05} (mg/m^3)[1]	15
TCE TC_{05} (mg/m^3)[1]	140

Notes:

1 Health Canada (1996). TCE TC_{05} is average of 3 reported values.

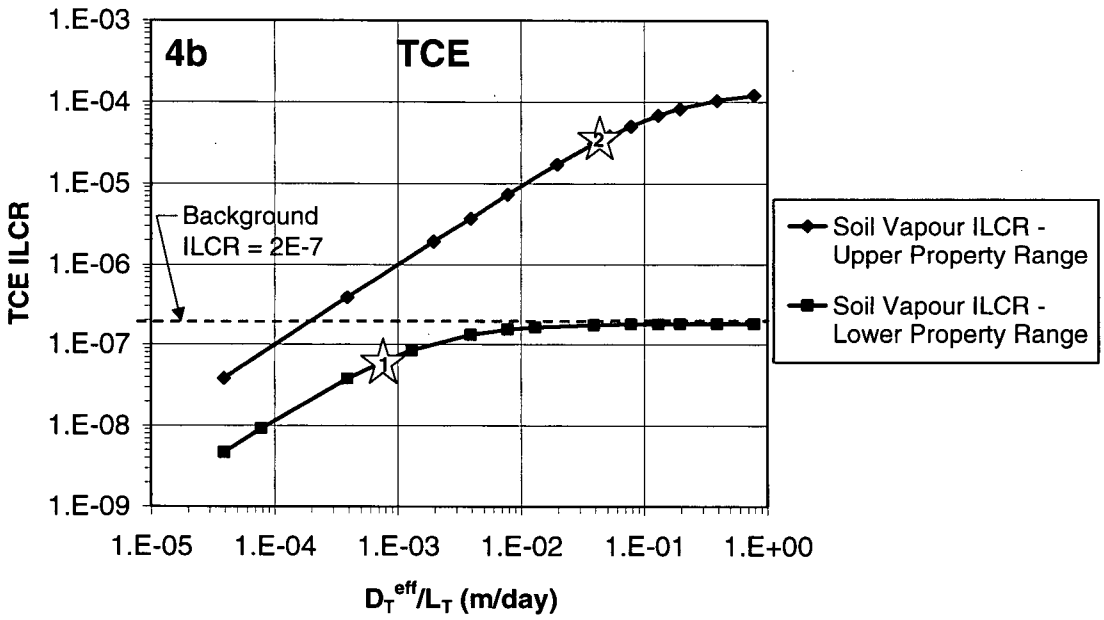

Figure 8.4. Predicted incremental lifetime cancer risks using soil vapour-derived indoor air concentrations in Figure 8.3 for (a) benzene and (b) TCE.

The significance of the model predictions are compared for two hypothetical sites with identical contamination sources and the source vapour concentrations in Table 8.5, but with differing site characteristics, as follows:

Site 1: Depth to contamination = 5 m
Moist soil (water-filled porosity = 0.2)
Low advection potential = Lower range building properties (Figure 8.2)

Site 2: Depth to contamination = 1 m
Dry soil (water-filled porosity = 0.1)
High advection potential = Higher range building properties (Figure 8.2)

In both cases, the total soil porosity is taken to be 0.3.

Model parameters for Sites 1 and 2 are shown on Figure 8.2. As shown, the α values for Sites 1 and 2 are about 7E-06 and 3E-03, respectively. The importance of advection potential and building properties (i.e., the essential "complementary" data described earlier) is highlighted in Figure 8.2. The implication of the Site 1 results is that the model-predicted indoor VOC concentrations from soil vapour are less than the background indoor concentrations. Of note is that the background ILCR for benzene is relatively high (1.4E-5). For Site 2, the predicted indoor benzene and TCE concentrations from soil vapour are over two orders-of-magnitude greater than background indoor air concentrations. For TVOC, the difference between indoor concentrations from soil vapour and background sources is not as great, and the soil vapour derived indoor air concentration is similar to maximum TVOC levels expected for new houses. The model-predictions for Site 2 suggest that soil vapour related risks may be significant for sites with shallow contamination and high advection potential. This conclusion is predicated upon

theoretical model predictions for possible vapour source strengths, and does not consider how well the Johnson and Ettinger (1991) model predicts soil vapour transport and intrusion into buildings. Since the accuracy and validation of models for this pathway goes beyond the intended scope of this paper, the reader is referred to Johnson *et al.* (1998) and Hers *et al.* (2003).

CONCLUSIONS

Soil vapour intrusion into buildings is complex, highly dependent on site specific conditions, and can vary over time. There are numerous other significant sources of VOCs beyond soil vapour, and the reported range in background indoor VOC concentrations is large. Understanding mechanisms for soil gas intrusion is important when indoor air measurements are used to deduce the subsurface-derived component since, for most sites, the contribution from soil vapour is likely to be small relative to other sources. Model predicted indoor air concentrations from soil vapour are compared to background indoor concentrations and show that the relative importance of soil vapour will depend on site specific conditions. For deep contamination where diffusive transport is the dominant process (far-field condition, Figure 8.1), indoor air concentrations and risk from soil vapour will tend to be insignificant relative to risks associated with background indoor VOCs. In contrast, for shallow contamination where advective transport is the dominant process (near-field condition, Figure 8.1), model predictions suggest that indoor air concentrations and risk from soil vapour could be significant. Since distinguishing the subsurface vapour component from background indoor sources will, in practice, be difficult for most sites appropriate sampling strategies should be used. This includes collection of essential complementary data and information on pressure gradients, seasonal data, house characteristics, meteorological data, and whenever possible, sub-slab vapour concentrations.

Further work is required to evaluate how best indoor air measurements can be used to quantify potential exposure and risk from subsurface VOCs. This includes studies that generate high quality and comprehensive data sets for soil vapour, indoor air in impacted and background areas, and information on factors that affect soil vapour intrusion and indoor air quality. Also needed is further development of protocols for indoor air sampling when the goal is to estimate vapour-derived indoor air concentrations.

REFERENCES

Adomait, M.; D. Fugler. A Method to Evaluate Soil Gas VOC Influx into Houses. In *Proc. of Air and Waste Management Associations's 90th Annual Meeting and Exhibition*, June 8-13, 1997, Toronto, Ontario, Canada.

American Society for Testing and Materials (ASTM). *Standard Guide for Risk-Based Corrective Action Applied at Petroleum Release Sites*. E-1739-95, 1995.

Anderrson, K.; J.V. Bakke, O. Bjorseth, C.G. Bornehag, G. Clausen, J.K. Hongslo, M. Kjellman, S. Kjaergaard, F. Levy, L. Molhave, S. Skerving, and J. Sundell. TVOC and Health in Non-industrial Indoor Environments. *Indoor Air*. 1997, 7:78-91.

Boman, C.A.; M.D. Lyberg. Analysis of Air Change Rates in Swedish Residential Buildings. In *Measured Air Leakage of Buildings: A Symposium*. ASTM STP 904. ASTM, West Conshohocken, PA., 1986.

Canadian Council of Ministers of the Environment (CCME). *Draft Canada Wide Standards for Petroleum Hydrocarbons*, June, 2000.

Davis, C.S.; R. Otson. The Canadian Indoor Air Quality (CIAQ) and the Canadian Source Profile (CISP) Databases. *Indoor Environment*. 1993. 3:39-47.

Davis, C.S.; R. Otson. Estimation of Emissions of Volatile Organic Compounds (VOCs) from Canadian Residences. In *Volatile Organic Compounds in the Environment*, ASTM STP 1261, W.Wang, J. Schnoor, and J. Doi, Eds., American Society for Testing and Materials, 1996, pp. 55-65.

Ekberg, L.E. Volatile Organic Compounds in Office Buildings. *Atmospheric Environment.* 1994. 28 (22):3571-3575.

EnviroGroup Limited. Indoor Air Assessment Report – Redfield Rifle Scope Site. April 1999.

European Commission. Determination of VOCs emitted from indoor materials and products. In *Second interlaboratory comparison of small chamber measurements.* Report No. 16. Published by Joint Research Centre – Environmental Institute, Ispra (Italy), Report EUR 16284 EN, 1995.

Fellin, P.; R. Otson. Seasonal trends of Volatile Organic Compounds (VOCs) in Canadian Homes. Proc. *Indoor Air '93: 6th International Conference on Indoor Air Quality and Climate.* Helsinki, Finland, 1993..

Fellin, P.; R. Otson. The Effectiveness of Selected Materials in Moderation of Indoor VOC Levels, In *Volatile Organic Compounds in the Environment*, ASTM STP 1261, W.Wang, J. Schnoor, and J. Doi, Eds., American Society for Testing and Materials, 1996, pp. 135-146.

Figley, D.; J. Makahon, R. Dumont, and T. Mayo. Development of a VOC Emission Database for Building Materials., Unpublished Manuscript, 1996.

Figley, D.A. A Guide for Estimating Indoor Concentrations of Soil Gas Pollutants in Houses. Prepared for CMHC, 1997.

Fischer, M.L.; A.J. Bentley, K.A. Dunkin, A.T. Hodgson, W.W. Nazaroff, R.G. Sextro, and J.M. Daisey. Factors Affecting Indoor Air Concentrations of Volatile Organic Compounds at a Site of Subsurface Gasoline Contamination. *Environ. Sci. Technol.*1996. 30 (10):2948-2957.

Fitzpatrick, N.A.; J.J. Fitzgerald. An Evaluation of Vapour Intrusion into Buildings Through a Study of Field Data. Proc. *11th Annual Conference on Contaminated Soils,* Amherst, Massachusetts, AEHS, October 1995.

Foster, S.J.; J. P. Kurtz, and A. K. Woodland 2003. Background Indoor Air Risks at Selected Residences in Denver Colorado. *Proc. of The Ninth International Conference on Indoor Air Quality and Climate*, The American Industrial Hygiene Association, Monterey, CA., 2002.

Garbesi, K.; R.G. Sextro, W.J. Fisk, M.P. Modera, and K.L. Revzan. Soil-Gas Entry into an Experimental Basement: Model Measurement Comparisons and Seasonal Effects. *Environ. Sci. Technol.* 1993. 27(3):466-473.

Gerry, P.A., L.L. Green, and D.O. Moses. A Comparison of the Effects of Ventilation and Other Factors for Residential Combustion Sources of Indoor Air Pollution. In: *79th Annual Meeting of the Air Pollution Control Association.* June 22-27, 1986, Minneapolis, MN.

Grimsrud, D.T.; M.H. Sherman, R.C. Sonderegger. Calculating Infiltration: Implications for a Construction Quality Standard. In: *Proc. Amer. Soc. of Heating, Refrigeration, and Air-Conditioning Engineers and the U.S. Department of Energy Conference: Thermal Performance of the Exterior Envelopes of Buildings II.* Las Vegas, NV., December 1982.

Gustafsson, H. Building materials identified as major sources for indoor air pollutants. A critical review of case studies. *Swedish Council for Building Research. Report D10*, 1992.

Gusdorf, J.; T. Hamlin, Buildings Group, Residential Programs, Energy Technology Branch. Indoor Air Quality and Ventilation Rates in R-2000 Houses. *Call-up No. 23440-95-1037.* Energy Technology Branch, CANMET, Department of Natural Resources Canada, Ottawa, Ontario, 1995 (43 pg).

Health Canada. Canadian Environmental Protection Act. Priority Substances List. Supporting Documentation. Health-Based Tolerable Daily Intakes/Concentrations and Tumourigenic Doses/Concentrations for Priority Substances. August 1996.

Hers, I.; R. Zapf-Gilje. Canadian consortium research project – field validation of soil gas transport to indoor air pathway. In. Proc. 1998 Petrol. Hydro. and Org. Chem. in Ground Water, API/NGWA, Houston, Tx., Nov. 11-13, 1998, pp. 251-266.

Hers, I.., R. Zapf-Gilje, P.C. Johnson, and L. Li. Evaluation of the Johnson and Ettinger Model for Prediction of Indoor Air Quality. *Ground Water Monitoring and Remediation*, Summer 2003.

Hodgson, A.T. Soil-Gas Contamination and Entry of Volatile Organic Compounds into a House Near a Landfill, *Journal of the Air and Waste Management Association.* 1992. 29:277-283, March.

Johnson, P.C.; R. Ettinger. Heuristic Model for Predicting the Intrusion Rate of Contaminant Vapours into Buildings. *Environ. Sci. Technol.* 1991. 25 (8):1445-1452.

Lamb, B.; H. Westberg, P. Byrant, J. Dean, and S. Mullins. Air infiltration rates in pre- and post-weatherized houses. *J. Air Pollut. Cont. Assoc.* 1985. (35):545-551.

Laubacher, R.C.; P. Bartholomae, P. Velasco, H.J. Reisinger. An evaluation of the Vapour Profile in the Vadose Zone Above a Gasoline Plume. In: *Proc. 1997 Petrol. Hydro. and Org. Chem. in Groundwater,* API/NWGA, Houston, Tx., November 1997. pp. 396-409.

Laubacher, R.C. An evaluation of the Vapour Profile in the Vadose Zone Above a Gasoline Plume. Proc. *Petroleum Environmental Research Forum (PERF) Symposium*, Brea, California, February 6 and 7, 1997.

Lebret, E.; H. Van de Wiel, H. Bos, D. Noij, and J. Boliej. Volatile Organic Compounds in Dutch Homes. *Environment International.* 1986. 12:323-332.

Lewis, C. W.; R.B. Zwiedinger. Apportionment of Residential Indoor Aerosol, VOC and Aldehyde Sources, and their source Strengths. *Atmospheric Environment.* 1990. 26A (12):2179-2184.

Kurtz, J.P. and D.J.Folkes. Background concentrations of selected chlorinated hydrocarbons in residential indoor air. *Proc. of The Ninth International Conference on Indoor Air Quality and Climate*, The American Industrial Hygiene Association, Monterey, CA., 2002.

Mailahn, W.; B. Seifert, D. Ullrich, and H. Moriske. The Use of a Passive Sampler for The Simultaneous Determination of Long-term Ventilation Rates and VOC Concentrations. *Environment International.* 1989. 15:537-544.

Massachusetts, Commonwealth of. Method for the Determination of Air-Phase Petroleum Hydrocarbons (APH). Public Comment Draft 1.0. Massachusetts Department of Environmental Protection. February 2000.

McNeel, P.; V. Dibley, and C. Atwood. Case Study Comparisons of Vapour Inhalation Risk Estimates: ASTM RBCA Model Predictions vs. Site Specific Soil Vapour Data. Proc. *1997 Petrol. Hydro. and Org. Chem. in Groundwater*, API/NWGA, Houston, Tx., November 1997, pp. 115-124.

Molhave, L.; J. Jensen, and S. Larsen. Subjective reactions to volatile organic compounds as air pollutants", *Atmospheric Environment.* 1991. 25A (7):1238-1293.

Molhave, L.; S. Kjaergaard, O. Pedersen, A. Jorgensen, and T. Pedersen. 1993. Human response to different mixtures of volatile organic compounds. Proc. *Indoor Air '93,6th International Conference on Indoor Air Quality and Climate*, Vol. 1, Helsinki, Finland, 1993, pp. 555-560.

Moseley, C.L.; M.R. Meyer. Petroleum Contamination of an Elementary School: A Case History Involving Air, Soil-Gas and Groundwater Monitoring. *Environ. Sci. Technol.* 1992. 26:185-192.

Mueller Associates; Syscon Co.; Brookhaven National Laboratory, 1988. Handbook of Radon in Buildings. Hemisphere Publishing Co., New York, NY.

Murray, D.M.; D.E. Burmaster. Residential air exchange rates in the United States: empirical and estimated parametric distributions by season and climatic region. *Risk Anal.* 1995. 15:459-465.

Nazaroff, W.W.; H. Feustel, A.V. Nero, K.L. Revzan, D.T. Grimsrud, M.A. Essling, and R.E. Toohey. Radon Transport into a Detached One-Story House with a Basement. *Atmospheric Environ.* 1985. 19(1):31-46.

Nazaroff, W.W.; S.R. Lewis, S.M. Doyle, B.A. Moed, and A.V. Nero. Experiments on Pollutant Transport from Soil into Residential Basements by Pressure-Driven Airflow. *Environ. Sci. Technol.* 1987. 21(5):459-466.

Nazaroff, W.W. Radon Transport from Soil to Air. *Review of Geophysics.* 1992. 30(2):137-160.

Ostendorf, D.W.; D.H. Kampbell. Biodegradation of Hydrocarbon Vapours in the Unsaturated Zone. *Water Resources Research.* 1991. 27 (4):453-462. April.

Oak Ridge National Laboratory. Measurement of Volatile Organic Compounds (VOC) in Eight East Tennessee Homes. *Report ORNL-6286*, September 1988.

Otson, R.; P. Fellin. Volatile Organics in the Indoor Environment: Sources and Occurrence. *Gaseous Pollutants – Characterization and Cycling*. J.O. Nriagu, Ed., Wiley, New York, 1992. pp. 335-421.

Otson, R.; P. Fellin, and Q. Tran. Investigation of VOCs in Canadian Residences. Proc. *Indoor Air '93: 6th International Conference on Indoor Air Quality and Climate.* Helsinki, Finland, 1993.

Otson, R.; F. Meth, and P. Fellin. Identification of Important Sources of Five Priority Substances in Canadian Indoor Air. Proc. Indoor Air '96, 7th International Conference on Indoor Air Quality and Climate, 1996.

Otson, R.; J. Zhu. I/O Values for Determination of the Origin of Some Indoor Organic Pollutants. Proc. *Air & Waste Managements Association's 90th Annual Meeting and Exhibition*, Toronto, Ontario, Canada, June 8 to 13, 1997.

Pandian, M.D.; W.R. Ott, and A. Fail. Residential air exchange for use in indoor air and exposure modeling studies. *J. Exp. Anal. Environ. Epidem.* 1993. 3:407-416.

Robinson, A.; R. Sextro. Radon Entry into Buildings Driven by Atmospheric Pressure Fluctuations. *Environ. Sci. Technol.* 1997. 31:1742-1748.

Rothweiler, H.; P.A. Wager, and C. Schlatter. Volatile Organic Compounds and Some Very Volatile Organic Compounds in New and Recently Renovated Buildings in Switzerland. *Atmospheric Environment.* 1992. 26A(12):2219-2225.

Saskatchewan Research Council (SRC). Volatile Organic Compound Survey and Summarization of Results. *Report I-4800-1-C-92*. Prepared for Canada Mortgage and Housing Corporation. April 1992.

Saskatchewan Research Council (SRC). Ventilation Control in Medium Air Tightness Houses. Report I-4800-21-C-94, 1995.

Scanada Consultants Limited. Field Testing of House Characteristics, Report to CMHC. October 1993.

Shah, J.J.; H.B. Singh. Distribution of volatile organic chemicals in outdoor and indoor air. *Environ. Sci. Technol*, 1988. 22(12):1381-1388.

Sheldon, L.; H. Zelon, J. Sickles, C. Eaton, T. Hartwell, and L. Wallace. Indoor Air Quality in Public Buildings: Volume II (Project Summary). *EPA/600/S6-88/009b*, September 1988.

Sparks, L.E.; B.A. Tichenor, J. Chang, and Z. Guo. Gas-Phase Mass Transfer Model of Predicting Volatile Organic Compound (VOC) Emission Rates from Indoor Pollutant Sources. *Indoor Air*. 1996. 6:31-40.

Tichenor, B.A.; L.S. Sparks, J.B. White, and M.D. Jackson. Evaluating Sources of Indoor Air Pollution. *J. Air Waste Manage. Assoc*. 1990. 40 (4):487-492, April.

Turk, B.H.; R.J. Prill, W.J. Fisk, D.T. Grimsrud, B.A. Moed, and R.G. Sextro. Radon and Remedial Action in Spokane River Valley Homes, *Lawrence Berkley Laboratory, Berkeley, CA, Vol. 1, LBL-23430*., 1987.

Wallace, L. The Total Exposure Assessment Methodology (TEAM) Study: Summary and Analysis. *EPA/600/S6-87/002*, September 1989.

Versar, Inc. Draft Final Operable Unit 5 – Groundwater. Ground-to-Indoor Air VOC Migration Pathway Investigation Report. January 2000.

Waitz, M.F.W.; J.I. Freijer, P. Keule, and F.A. Swartjes. The VOLASOIL risk assessment model based on CSOIL for soils contaminated with volatile compounds. *National Institute of Public Health and the Environment, Bilthoven*, The Netherlands, 1996.

Walkinshaw, D.S. 1987. Indoor Air Quality in Cold Climates: Hazards and Abatement Measures Summary of an APCA International Specialty Conference, *J. Air Pollut. Cont.* 1987. (36):235-241.

CHAPTER 9

CONCLUSIONS

A comprehensive, integrated research program involving extensive field monitoring, laboratory testing, analysis and model development was completed to evaluate processes and models for soil vapour intrusion into buildings. The research program was sponsored by a consortium of ten industry, governmental and consulting groups with results published in seven technical papers accepted or submitted to peer reviewed journals, each forming a chapter of this thesis. Conclusions are provided separately for each chapter of the thesis. In addition, there are specific concluding statements to address the objectives listed in the thesis introduction.

Evaluation of soil vapour sampling and analysis techniques (Chapter 2)

A survey of soil vapour sampling and analysis methods indicates wide variation in probe design, purging and sampling techniques, and analytical methods. The lack of consistent protocols and quality control procedures affects the reliability of soil gas surveys.

For this research program it was considered important to conduct several studies to evaluate methodology and quality control issues, and to contribute to protocol development (Objective #5). Contamination of soil vapour syringes and sorption onto probe materials was found to be potentially significant indicating appropriate materials should be used for soil vapour studies. Intrusion of atmospheric air into Tedlar bags could reach significant levels after about two days. Field gas detectors provided reasonably estimates of oxygen, carbon dioxide and methane levels based on comparisons to laboratory analyses, except that there was a shift in the methane results due to cross-sensitivity of the detector to other hydrocarbon compounds. The oxygen and carbon dioxide concentrations were inversely correlated, as expected for a vapour regime controlled by aerobic biodegradation. Light gas results can be used to infer whether atmospheric intrusion has affected the integrity for soil vapour samples, when the biogeochemical regime can reasonably be predicted. A field deployed gas chromagraph/photoionization detector (GC/PID) combined with syringe and sorbent tube sampling yielded high quality results for this study.

Measurement of in situ gas-phase diffusion coefficients (Chapter 3)

Push-pull tests, which involved injecting a helium tracer at soil gas, were an effective method of estimating the *in situ* diffusion coefficient. The test is relatively simple, however, appropriate pre-cautions or corrections must be made to account for possible effects of soil gas composition on helium detector response. The *in situ* diffusion coefficients in fine to medium sand below the greenhouse, estimated using an analytical solution for spherical diffusion from a point source, ranged between about 0.01 to 0.07 cm^2sec^{-1}. A good comparison was obtained between the measured gas-phase tortuosity factor (obtained from the in situ diffusion coefficient) and that predicted using the Millington and Quirk relationship (*i.e.*, $\tau_g = \phi_g^{10/3}/\phi^2$) with measured factors consistently about twice the predicted values. The *in situ* diffusion testing results indicated that Millington and Quirk relationship, which is commonly used in conjunction with the Johnson and Ettinger model, provided reasonable estimates of tortuosity factors for the sand deposits. This

research was important in terms of field protocol development (Objective #5) and contributing to validation of empirical equations for diffusion used in screening-level models (Objective #1).

Evaluation of vadose zone biodegradation of BTX vapours (Chapter 4)

Extensive vertical profiling of BTX vapour and light gas (oxygen and carbon dioxide) concentrations and monitoring of subslab oxygen and pressure below the non-depressurized greenhouse indicated over three orders-of-magnitude reduction in BTX vapour concentrations between 0.4 and 0.8 m depth below the slab. Field testing indicated elevated moisture content and soil organic matter over a thin layer suggesting enhanced biodegradation. The BTX concentrations were relatively stable over several seasons (Objective #4). When the greenhouse was depressurized to –10 and –30 Pa, the BTX vapour concentrations increased to relatively high levels with little attenuation between the subslab and deeper soil.

The monitoring and model simulations indicate that biodegradation through aerobic respiration is an important attenuation process (Objective #2). Estimated first-order biodegradation rates based on soil pore water concentrations (k_w), obtained by fitting an analytical solution for diffusion and biodecay to the vertical concentration profiles, were approximately 1.2 hr^{-1} for benzene, 0.9 hr^{-1} for toluene and 0.5 hr^{-1} for *m&p*-xylene. These rates compared well to other reported laboratory and field data. A novel bi-linear method for approximating Monod-kinetics, based on field test data, was successfully used to derive inputs required for predictive modeling.

A two-dimensional numerical model incorporating vapour-phase diffusion, advection, sorption and biodegradation, incorporating both zero- and first-order reaction kinetics, was used to simulate BTX transport and intrusion into the greenhouse (Objective #6). Model results demonstrate the sensitivity of vapour-phase BTX and oxygen transport to layers with low diffusion coefficients. When advection was included as a model process, the predicted vapour profile was similar to that measured for the –10 and –30 Pa depressurization cases (i.e., little attenuation was observed). The model simulations highlight the importance of using a model that ties biodecay to oxygen availability.

Measurement of BTX Vapour Intrusion into an Experimental Building (Chapter 5)

The greenhouse depressurization experiments indicated vapour intrusion into the greenhouse was dependent on depressurization, which in turn affected the advective flow regime and biodegradation conditions below the greenhouse. For the non-depressurized case, subslab vapour concentrations were low and no vapour intrusion was detected. Pressure-induced movement or pumping of soil gas, as evidenced by subslab oxygen fluctuations, did not result in measureable vapour intrusion into the greenhouse. Significant vapour levels and intrusion were measured when the greenhouse was depressurized to –10 and –30 Pa. At –2.5 Pa, vapour levels below the middle of the greenhouse were elevated; however, concentrations remained low near the foundation slab edge crack, which was where most soil gas intrusion occurred. As a result, no detectable vapour intrusion could be detected for the –2.5 Pa case.

The soil gas flow rates into the depressurized greenhouse (-10 and –30 Pa cases), backcalculated from the tracer tests, were on the order of 0.35 to 2.8 L/min (0.001 and 0.005 L/min-Pa-m^2). The flux chamber tests gave similar results when scaled to account for the estimated total crack

length. The soil gas flow rates predicted by an analytical model for flow to a perimeter edge crack and a groundwater model (MODFLOW) adapted to simulate soil gas flow were also similar to measured values (Objective #6). The results suggest that numerical modeling of soil gas flow into a building can provide useful insight into factors controlling soil gas advection.

Dynamic flux chamber testing, while feasible, is challenging to implement. Methodology issues include decontamination, establishing appropriate flow rates, and scaling of individual test results to the greenhouse. This study highlighted the influence of building depressurization on vapour intrusion (Objective #3) and contributed to field protocol development (Objective #5).

Comparison, validation and use of models for predicting indoor air quality from soil and groundwater contamination (Chapter 6)

Several commercially available screening models for vapour intrusion and one model developed by the author were reviewed. Most models are based on the Johnson and Ettinger model framework, but include additional processes such as biodegradation and chemical source depletion. Other models incorporate methods to simulate a crawlspace or different foundation properties. Predictions made using these models illustrate the wide range in predicted vapour attenuation ratios that result when different model processes are considered. For selected models, a sensitivity and uncertainty analysis was performed to better understand model characteristics. While sensitivity is important, the uncertainty in model inputs, which vary significantly depending on the parameter, can have a greater influence on the results. In particular, the uncertainty in gas-phase tortuosity factor (see definition above) can be significant for wetter soils based on the expected variation in moisture content and soil bulk density measurements. The uncertainty analysis for gas-phase tortuosity factor highlighted the importance of accurate geotechnical measurements (density, porosity, moisture content), or *in situ* measurements of diffusion coefficient.

Two models, based on the Johnson and Ettinger model framework, were used to predict vapour attenuation ratios. Results were compared to measured values for three sites, with the primary focus being the Chatterton site test results. The results indicated that for the Chatterton non-depressurized condition ("diffusion only case"), model predicted vapour attenuation ratios were conservative by at least one to two orders of magnitude. However, for the depressurized condition ("advection case"), the model predicted vapour attenuation ratios were similar to those measured. Based on these results, it was concluded that the advective transport of vapours into building could be significant for sites with shallow contamination, high permeability soil and foundation, and high building underpressurization. This study provided valuable information on reliability of screening level models for prediction of vapour intrusion and indicated that in most cases, a model that incorporates diffusion only, is unreliable (Objective #1).

A framework consisting of three assessment tiers is proposed based on depth to contamination and advection potential (Objective #7). Tier 1, a simple diffusion model, applies to deep contamination, or moderate depth contamination with low advection potential. Tier 2, a model for diffusion through the vadose zone, and diffusion and advection through the building foundation, applies to moderate depth contamination under most advective scenarios. For shallow contamination, defined here to be within about 1 m of the foundation, it is suggested that the use of screening models is not appropriate due to uncertainty in contamination depth (e.g.,

fluctuating water table) and possible preferential pathways. Tier 3 provides for the option for use of more sophisticated models and incorporation of model processes such as biodegradation.

Evaluation of the Johnson and Ettinger model for prediction of indoor air quality (Chapter 7)

The evaluation of the Johnson and Ettinger (J&E) model sensitivity, and comparisons of measured to model-predicted vapour attenuation ratios (α_m and α_p) for residential houses, ground-floor apartments and small commercial buildings provided valuable information on model performance and reliability (Objective #1). The J&E model is moderately to highly sensitive to soil gas advection rate into the building (Q_{soil}) for depth normalized diffusion coefficient (D_T^{eff}/L_T) values above about $1x10^{-3}$. For petroleum hydrocarbon sites, the vapour α_m's for the Chatterton site (high ΔP cases) and Midwest site were on the order of $1x10^{-5}$ to $1x10^{-4}$ (the Midwest value is uncertain). For the remaining cases and sites, the possible upper bound vapour α_m's ranged from about $5x10^{-7}$ to $1x10^{-5}$. For chlorinated solvent sites, the ground water α_m's were on the order of $1x10^{-6}$ to $1x10^{-4}$ for the three sites with the most reliable data sets (CDOT, Redfields and Hamilton). For one site with a smaller and somewhat less reliable data set (Lowry), the maximum ground water α_m was approximately $1x10^{-3}$ while the maximum sub-slab vapour α_m was approximately $1x10^{-2}$.

For almost all case studies, the best estimate J&E model-predicted α_p's were one to two orders of magnitude greater than the 50th percentile or median α_m's, indicating that when best estimate and "average" conditions are evaluated, the J&E model predictions are conservative. There were a few cases studies where the best estimate α_p was less than the 90th percentile or maximum α_m indicating the J&E model predictions are non-conservative for a small subset of houses or apartments. The comparisons show the potential for non-conservative model predictions if a combination of low Q_{soil} and low D_T^{eff}/L_T are used. The observed variability in α_m between different field sites, and individual houses at some sites, highlights the complexity of processes affecting vapour intrusion. The model comparisons to measured data suggest that J&E model can provide for reasonable order-of-magnitude estimates of indoor air quality, provided that appropriate input values are used. Due to the widely varying attenuation ratios that can be predicted, the use of the J&E model to develop generic regulatory criteria is problematic. A better framework for J&E model use is one based on site specific data.

The use of indoor air measurements to evaluate exposure and risk from subsurface VOCs (Chapter 8)

Due to the uncertainty associated with models for the vapour intrusion pathway, many advocate indoor air quality testing to validate model predictions. However, indoor air testing can be problematic. One reason is that vapour intrusion into buildings is variable and subject to temporal variations and building conditions at the time of sampling, making it difficult to obtain representative indoor air measurements. Secondly, as demonstrated by the survey of background indoor air quality, most of the same subsurface VOC found at contaminated sites are also present at elevated levels in indoor air. Although background risk is not normally evaluated as part of human health risk assessments, it is worth noting that the health risk posed by background indoor VOCs can be significant. The ventilation rate survey indicates that the building air exchange rate is influenced by building construction and seasonal factors. Reported average or median

building air exchange rates ranged between 0.17 and 5.4 hr^{-1}. The lowest ventilation rates tended to be newer high energy efficient homes. The study provided insight on background indoor air quality, a key consideration when indoor air measurements are used to evaluate model predictions, and practical information on the air exchange rate, which is needed for model input purposes (Objective #1).

Significant Research Contributions

Significant contributions were made in the following areas:

i) New or adapted field methods including push-pull tracer for estimation of *in-situ* diffusion coefficient, use of flux chambers and building tracer tests to measure vapour intrusion;

ii) New models for this pathway (conceptual and quantitative), including (i) development of a two-dimensional finite difference numerical computer model for diffusion, advection and biodegradation, (ii) adapted MODFLOW for prediction of soil gas flow into buildings, and (iii) developed analytical model for prediction of vapour intrusion.

iii) Model validation through a comprehensive analysis and comparison of model-predicted to field measured vapour attenuation ratios including data from sites across North America, and;

iv) Development of a protocol for evaluating sites and application of vapour intrusion models.

The benefit of the research is reduced uncertainty and improved methods for measurement and prediction of soil vapour intrusion into buildings. Uncertainty in assessment of soil vapor intrusion is reduced through insight gained on processes affecting intrusion (e.g., biodegradation, diffusion, advection) and model reliability. For example, the research provided valuable data on reasonable ranges of input parameters for the Johnson and Ettinger model. In addition, the comparisons of model predictions to measured vapour intrusion and attenuation factors provided an improved understanding of the predictive capabilities of the Johnson and Ettinger model, and also precluding factors or sites where use of this model may not be appropriate. This has significant benefit for practitioners conducting human health risk assessments at contaminated sites.

Recommendations for Further research:

Recommendations for further research are as follows:

1. Additional field-based studies should be conducted to evaluate the vapour intrusion pathway for different site conditions (e.g., for range of soil properties and contamination types), and to more fully assess specific factors affecting vapour intrusion such as soil properties, building types and environmental factors.

2. This study provided valuable information on vapour intrusion into a greenhouse under controlled conditions. Similar studies involving tracer testing is recommended to evaluate vapour intrusion into occupied buildings to better characterize the influence of building and foundation construction and environmental conditions.

3. More in-depth multi-dimensional modeling is recommended to evaluate the influence of buildings and heterogeneous geologic settings on vadose zone processes and vapour intrusion.

4. Additional field evaluation of biotransformation and biodegradation processes is needed for non-BTEX petroleum hydrocarbon and chlorinated solvent compounds.

5. Much of this research focused on sites with coarse-grained soil. Research at sites with fine-grained soil, or soil or bedrock with fractures, would be beneficial.

APPENDIX I

SOIL VAPOUR AND INDOOR AIR ANALYSIS DATA

Date Printed: 8/27/2004

Table I-1. Results of GC/PID Vapour and Air Testing

Sample Designation	Depth (m)	Sample Type	Sy-ringe	Syringe Wait Time Before Injection	Sample Collect Date	Sample Analysis Date	Anal-ysis Time	Injec-tion Volume (ul)	Sample Volume (L)
March 1997 Program - Site B - Before Greenhouse Built									
pid4ma14	N/A	BTEX Standard	N/A	N/A	N/A	5-Mar-97	N/A	N/A	N/A
pid4ma9	N/A	BTEX Standard	N/A	N/A	N/A	5-Mar-97	N/A	N/A	N/A
pid4ma11	N/A	BTEX Standard	N/A	N/A	N/A	5-Mar-97	N/A	N/A	N/A
pid4ma10	N/A	BTEX Standard	N/A	N/A	N/A	5-Mar-97	N/A	N/A	N/A
pid4ma15	Thermal Tube #5	Ambient Air	N/A	N/A	N/A	5-Mar-97	N/A	N/A	N/A
pid4ma12	Front Tube #1	Flux Chamber Blank #1 Closed Loop	N/A	N/A	N/A	5-Mar-97	N/A	N/A	N/A
pid4ma13	Back Tube #2	Flux Chamber Blank #1 Closed Loop	N/A	N/A	N/A	5-Mar-97	N/A	N/A	N/A
pid6mar1	N/A	New Standard NC-5	N/A	N/A	N/A	5-Mar-97	N/A	N/A	N/A
pid6mar2	Thermal Tube #4	Flux Chamber Front	N/A	N/A	N/A	5-Mar-97	N/A	N/A	N/A
pidmar4	Thermal Tube #3	on Soil Site A Back	N/A	N/A	N/A	5-Mar-97	N/A	N/A	N/A
pid6mar5	Front Tube #1	Flux Chamber Blank #2 Tube/Pump	N/A	N/A	N/A	5-Mar-97	N/A	N/A	N/A
pidmar9	Thermal Tube	Surrogate Test	N/A	N/A	N/A	5-Mar-97	N/A	N/A	N/A
pidmar8	Thermal Tube	Surrogate Test	N/A	N/A	N/A	5-Mar-97	N/A	N/A	N/A
pidma11	Thermal Tube	Surrogate Test	N/A	N/A	N/A	5-Mar-97	N/A	N/A	N/A
pidma10	Thermal Tube	Surrogate Test	N/A	N/A	N/A	5-Mar-97	N/A	N/A	N/A
td17ma17	Thermal Tube	Surrogate Test	N/A	N/A	N/A	5-Mar-97	N/A	N/A	N/A
td17ma17	Thermal Tube	Surrogate Test	N/A	N/A	N/A	5-Mar-97	N/A	N/A	N/A
50 ng std	sg11mar1	N/A	N/A	N/A	N/A	11-Mar-97	N/A	1000	N/A
100 ng std	sg11mar5	N/A	N/A	N/A	N/A	11-Mar-97	N/A	1000	N/A
250 ng std	sg11ma12	N/A	N/A	N/A	N/A	11-Mar-97	N/A	1000	N/A
500 ng std	sg11ma11	N/A	N/A	N/A	N/A	11-Mar-97	N/A	1000	N/A
100 ng std	sg11ma22	N/A	N/A	N/A	N/A	11-Mar-97	N/A	1000	N/A
Site A 0.6M QC Fail	sg11mar2	N/A	N/A	N/A	N/A	11-Mar-97	10:30	5000	N/A
Site A 0.9m QC Fail	sg11mar3	N/A	N/A	N/A	N/A	11-Mar-97	10:30	5000	N/A
Site A 1.2m QC Fail	sg11mar4	N/A	N/A	N/A	N/A	11-Mar-97	10:30	2000	N/A
Site A 1.2m QC Fail	sg11mar6	N/A	N/A	N/A	N/A	11-Mar-97	10.55	2000	N/A
Site A 0.9M	sg11mar7	N/A	N/A	N/A	N/A	11-Mar-97	10.55	500	N/A
Site A 0.6M	sg11mar8	N/A	N/A	N/A	N/A	11-Mar-97	10:55	2000	N/A
Site A 0.6m - 3rd	sg11ma20	N/A	N/A	N/A	N/A	11-Mar-97	13:35	500	N/A

Date Printed: 8/27/2004

Table I-1. Results of GC/PID Vapour and Air Testing

Sample Designation	Depth (m)	Sample Type	Sy-ringe	Syringe Wait Time Before Injection	Sample Collect Date	Sample Analysis Date	Anal-ysis Time	Injec-tion Volume (ul)	Sample Volume (L)
Site A 0.3m	sg11ma10	N/A	N/A	N/A	N/A	11-Mar-97	10:55	1000	N/A
Site A 0.3m -4th	sg11ma19	N/A	N/A	N/A	N/A	11-Mar-97	13:35	5000	N/A
Site A 1.2 m -2nd	sg11mar9	N/A	N/A	N/A	N/A	11-Mar-97	11:10	500	N/A
Site A 1.2m -3rd	sg11ma16	N/A	N/A	N/A	N/A	11-Mar-97	12:20	500	N/A
Site A 0.3m -2nd QC Fail	sg11ma13	N/A	N/A	N/A	N/A	11-Mar-97	11:10	2000	N/A
Site A 0.6m -2nd QC Fail	sg11ma14	N/A	N/A	N/A	N/A	11-Mar-97	11:10	500	N/A
Site B 1.2 m	sg11ma23	N/A	N/A	N/A	N/A	11-Mar-97	14:15	500	N/A
Site B 1.2m -2nd	sg11ma29	N/A	N/A	N/A	N/A	11-Mar-97	15:15	500	N/A
Site B 0.9m	sg11ma24	N/A	N/A	N/A	N/A	11-Mar-97	14:15	500	N/A
Site B 0.9m -2nd	sg11ma28	N/A	N/A	N/A	N/A	11-Mar-97	15:15	500	N/A
Site B 0.6m	sg11ma25	N/A	N/A	N/A	N/A	11-Mar-97	14:15	500	N/A
Site B 0.6m -2nd	sg11ma27	N/A	N/A	N/A	N/A	11-Mar-97	15:15	2000	N/A
Site B 0.3m	sg11ma26	N/A	N/A	N/A	N/A	11-Mar-97	14:15	5000	N/A
May 1997 Program - Site B - Before Greenhouse Built									
sg13may1	N/A	500 ppm BTEX Standard	N/A	N/A	N/A	13-May-97	7:59	1.6	N/A
sg13may2	N/A	250 ppm BTEX Standard	N/A	N/A	N/A	13-May-97	8:18	1.9	N/A
sg13may3	N/A	250 ppm BTEX Standard	N/A	N/A	N/A	13-May-97	9:03	1.6	N/A
sg13may4	N/A	100 ppm BTEX Standard	N/A	N/A	N/A	13-May-97	9:27	1.6	N/A
SG-BC (sg13ma24)	0.3 Syr #2	Below middle future green	N/A	N/A	N/A	13-May-97	13:56	4000	N/A
SG-BC (sg13ma25)	0.45 Syr #3	Below middle future green	N/A	N/A	N/A	13-May-97	14:08	1000	N/A
SG-BC (sg13ma26)	0.6 Syr #1 plugged ?	Below middle future green	N/A	N/A	N/A	13-May-97	14:22	500	N/A
SG-BC (sg13ma27)	0.75 Syr #2	Below middle future green	N/A	N/A	N/A	13-May-97	14:35	500	N/A
SG-BC (sg13ma28)	0.6 Syr #1 plugged ?	Below middle future green	N/A	N/A	N/A	13-May-97	14:54	3000	N/A
SG-BC (sg13ma28)	0.6 Syr #1 plugged ?	Below middle future green	N/A	N/A	N/A	13-May-97	14:54	3000	N/A
SG-BC (sg13ma29)	0.9 Syr #4	Below middle future green	N/A	N/A	N/A	13-May-97	15:06	200	N/A

Date Printed: 8/27/2004

Table I-1. Results of GC/PID Vapour and Air Testing

Sample Designation	Depth (m)	Sample Type	Sy-ringe	Syringe Wait Time Before Injection	Sample Collect Date	Sample Analysis Date	Anal-ysis Time	Injec-tion Volume (ul)	Sample Volume (L)
SG-BC (sg13ma30)	1.2, Syr #3	Below middle future green	N/A	N/A	N/A	13-May-97	15:21	200	N/A
SG-BC (sg13ma31)	1.2, Syr #5	Below middle future green	N/A	N/A	N/A	13-May-97	15:33	200	N/A
SG-BC (sg13ma32)	1.2, Syr #5	Below middle future green	N/A	N/A	N/A	13-May-97	15:33	200	N/A
June 1997 Program - Site B - Before Greenhouse Built									
sg24jun1	N/A	250 ppm BTEX standard	N/A	N/A	N/A	24-Jun-97	8:42	1.3	N/A
sg24jun2	N/A	500 ppm BTEX standard	N/A	N/A	N/A	24-Jun-97	9:17	1.45	N/A
sg24jun3	N/A	1500 ppm BTEX standard	N/A	N/A	N/A	24-Jun-97	9:31	1.4	N/A
SG-BC (sg24jun4)	0.15	Below middle future green	N/A	N/A	N/A	24-Jun-97	9:48	4000	N/A
SG-BC (sg24jun5)	0.3	Below middle future green	N/A	N/A	N/A	24-Jun-97	10:01	4000	N/A
SG-BC (sg24jun6)	0.45	Below middle future green	N/A	N/A	N/A	24-Jun-97	10:17	3000	N/A
SG-BC (sg24jun7)	0.3	Below middle future green	N/A	N/A	N/A	24-Jun-97	10:29	4000	N/A
SG-BC (sg24jun8)	0.6	Below middle future green	N/A	N/A	N/A	24-Jun-97	10:42	2000	N/A
SG-BC (sg24jun14)	0.6	Below middle future green	N/A	N/A	N/A	24-Jun-97	14:07	4000	N/A
SG-BC (sg24jun9)	0.75	Below middle future green	N/A	N/A	N/A	24-Jun-97	11:14	500	N/A
SG-BC (sg24jun17)	0.75	Below middle future green	N/A	N/A	N/A	24-Jun-97	14:52	500	N/A
SG-BC (sg24jun10)	0.9	Below middle future green	N/A	N/A	N/A	24-Jun-97	11:29	200	N/A
SG-BC (sg24jun16)	0.9	Below middle future green	N/A	N/A	N/A	24-Jun-97	14:35	500	N/A
sg24jun11	N/A	500 ppm BTEX standard	N/A	N/A	N/A	24-Jun-97	11:48	1.3	N/A
sg24jun12	N/A	1500 ppm BTEX standard	N/A	N/A	N/A	24-Jun-97	12:02	1.2	N/A
sg24jun13	N/A	1500 ppm BTEX standard	N/A	N/A	N/A	24-Jun-97	12:25	1.2	N/A
SG-BC (sg24jun18)	1.2	Below middle future green	N/A	N/A	N/A	24-Jun-97	14:52	200	N/A
SG-BC (sg24jun19)	1.2	Below middle future green	N/A	N/A	N/A	24-Jun-97	15:17	200	N/A
SG-BC (sg24jun20)	1.5	Below middle future green	N/A	N/A	N/A	24-Jun-97	15:30	200	N/A
SG-BC (sg24jun21)	1.5	Below middle future green	N/A	N/A	N/A	24-Jun-97	15:42	200	N/A
July 15 1997 Program - Site B - Before Greenhouse Built									

Date Printed: 8/27/2004

Table I-1. Results of GC/PID Vapour and Air Testing

Sample Designation	Depth (m)	Sample Type	Sy-ringe	Syringe Wait Time Before Injection	Sample Collect Date	Sample Analysis Date	Anal-ysis Time	Injec-tion Volume (ul)	Sample Volume (L)
July 15 1997 Program - Site	N/A	100 ppm BTEX standard	N/A	N/A	N/A	15-Jul-97	9:45	1.1	N/A
sg15jul15	N/A	250 ppm BTEX standard	N/A	N/A	N/A	15-Jul-97	10:04	1.2	N/A
sg15jul16	N/A	250 ppm BTEX standard	N/A	N/A	N/A	15-Jul-97	10:20	2.2	N/A
sg15jul17	N/A	1500 ppm BTEX standard	N/A	N/A	N/A	15-Jul-97	10:41	1.1	N/A
sg15jul18	N/A	1500 ppm BTEX standard	N/A	N/A	N/A	15-Jul-97	11:06	2.3	N/A
sg15jul19	N/A	100 ppm BTEX standard	N/A	N/A	N/A	15-Jul-97	11:43	1.4	N/A
sg15ju18	N/A	1500 ppm BTEX standard	N/A	N/A	N/A	15-Jul-97	N/A	1.1	N/A
sg15ju19	N/A	1500 ppm BTEX standard	N/A	N/A	N/A	15-Jul-97	N/A	1.2	N/A
sg15ju28	N/A	1500 ppm BTEX standard	N/A	N/A	N/A	15-Jul-97	N/A	1.1	N/A
sg15ju29	N/A	1500 ppm BTEX standard	N/A	N/A	N/A	15-Jul-97	N/A	1	N/A
sg15ju30	N/A	250 ppm BTEX standard	N/A	N/A	N/A	15-Jul-97	N/A	2.2	N/A
SG-BC (sg15jul19)	0.15	Below middle future green	N/A	N/A	N/A	15-Jul-97	N/A	5000	N/A
SG-BC (sg15jul10)	0.15	Below middle future green	N/A	N/A	N/A	15-Jul-97	N/A	5000	N/A
SG-BC (sg15jul11)	0.3	Below middle future green	N/A	N/A	N/A	15-Jul-97	N/A	5000	N/A
SG-BC (sg15jul12)	0.3	Below middle future green	N/A	N/A	N/A	15-Jul-97	N/A	5000	N/A
SG-BC (sg15jul13)	0.45	Below middle future green	N/A	N/A	N/A	15-Jul-97	N/A	5000	N/A
SG-BC (sg15jul14)	0.45	Below middle future green	N/A	N/A	N/A	15-Jul-97	N/A	4500	N/A
SG-BC (sg15jul15)	0.6	Below middle future green	N/A	N/A	N/A	15-Jul-97	N/A	4000	N/A
SG-BC (sg15jul16)	0.6	Below middle future green	N/A	N/A	N/A	15-Jul-97	N/A	5000	N/A
SG-BC (sg15jul20)	0.75	Below middle future green	N/A	N/A	N/A	15-Jul-97	N/A	500	N/A
SG-BC (sg15jul21)	0.75	Below middle future green	N/A	N/A	N/A	15-Jul-97	N/A	1000	N/A
SG-BC (sg15jul22)	0.9	Below middle future green	N/A	N/A	N/A	15-Jul-97	N/A	200	N/A
SG-BC (sg15jul23)	0.9	Below middle future green	N/A	N/A	N/A	15-Jul-97	N/A	500	N/A
SG-BC (sg15jul24)	1.2	Below middle future green	N/A	N/A	N/A	15-Jul-97	N/A	200	N/A
SG-BC (sg15jul25)	1.2	Below middle future green	N/A	N/A	N/A	15-Jul-97	N/A	200	N/A
SG-BC (sg15jul26)	1.5	Below middle future green	N/A	N/A	N/A	15-Jul-97	N/A	200	N/A

Date Printed: 8/27/2004

Table I-1. Results of GC/PID Vapour and Air Testing

Sample Designation	Depth (m)	Sample Type	Sy-ringe	Syringe Wait Time Before Injection	Sample Collect Date	Sample Analysis Date	Anal-ysis Time	Injec-tion Volume (ul)	Sample Volume (L)
SG-BC (sg15ju27)	1.5	Below middle future green	N/A	N/A	N/A	15-Jul-97	N/A	200	N/A
July 28 1997 Program - Site B - Before Greenhouse Built									
N/A	N/A	100 ppm BTEX standard	N/A	N/A	N/A	28-Jul-97	N/A	1	N/A
N/A	N/A	100 ppm BTEX standard	N/A	N/A	N/A	28-Jul-97	N/A	1.3	N/A
N/A	N/A	250 ppm BTEX standard	N/A	N/A	N/A	28-Jul-97	N/A	1.2	N/A
N/A	N/A	250 ppm BTEX standard	N/A	N/A	N/A	28-Jul-97	N/A	1.3	N/A
N/A	N/A	500 ppm BTEX standard	N/A	N/A	N/A	28-Jul-97	N/A	1.6	N/A
N/A	N/A	500 ppm BTEX standard	N/A	N/A	N/A	28-Jul-97	N/A	1.8	N/A
N/A	N/A	1000 ppm BTEX standard	N/A	N/A	N/A	28-Jul-97	N/A	1.2	N/A
N/A	N/A	1500 ppm BTEX standard	N/A	N/A	N/A	28-Jul-97	N/A	1.8	N/A
N/A	N/A	1500 ppm BTEX standard	N/A	N/A	N/A	28-Jul-97	N/A	2.6	N/A
N/A	N/A	1500 ppm BTEX standard	N/A	N/A	N/A	28-Jul-97	N/A	2.7	N/A
SG-BC	0.15	Below middle future green	N/A	N/A	N/A	28-Jul-97	N/A	5000	N/A
SG-BC	0.15	Below middle future green	N/A	N/A	N/A	28-Jul-97	N/A	5000	N/A
SG-BC	0.3	Below middle future green	N/A	N/A	N/A	28-Jul-97	N/A	5000	N/A
SG-BC	0.3	Below middle future green	N/A	N/A	N/A	28-Jul-97	N/A	5000	N/A
SG-BC	0.45	Below middle future green	N/A	N/A	N/A	28-Jul-97	N/A	4000	N/A
SG-BC	0.45	Below middle future green	N/A	N/A	N/A	28-Jul-97	N/A	5000	N/A
SG-BC	0.6	Below middle future green	N/A	N/A	N/A	28-Jul-97	N/A	5000	N/A
SG-BC	0.6	Below middle future green	N/A	N/A	N/A	28-Jul-97	N/A	5000	N/A
SG-BC	0.75	Below middle future green	N/A	N/A	N/A	28-Jul-97	N/A	500	N/A
SG-BC	0.75	Below middle future green	N/A	N/A	N/A	28-Jul-97	N/A	200	N/A
SG-BC	0.9	Below middle future green	N/A	N/A	N/A	28-Jul-97	N/A	200	N/A
SG-BC	0.9	Below middle future green	N/A	N/A	N/A	28-Jul-97	N/A	200	N/A

Date Printed: 8/27/2004

Table I-1. Results of GC/PID Vapour and Air Testing

Sample Designation	Depth (m)	Sample Type	Sy-ringe	Syringe Wait Time Before Injection	Sample Collect Date	Sample Analysis Date	Anal-ysis Time	Injec-tion Volume (ul)	Sample Volume (L)
SG-BC	1.2	Below middle future green	N/A	N/A	N/A	28-Jul-97	N/A	200	N/A
SG-BC	1.2	Below middle future green	N/A	N/A	N/A	28-Jul-97	N/A	200	N/A
SG-BC	1.5	Below middle future green	N/A	N/A	N/A	28-Jul-97	N/A	200	N/A
SG-BC	1.5	Below middle future green	N/A	N/A	N/A	28-Jul-97	N/A	250	N/A
September 1997 Program - Site B - After Greenhouse Built									
SG09Sep1	N/A	100 ppm BTEX standard	N/A	N/A	N/A	9-Sep-97	8:51	1.2	N/A
SG09Sep2	N/A	100 ppm BTEX standard	N/A	N/A	N/A	9-Sep-97	9:09	1.2	N/A
SG09Sep3	N/A	250 ppm BTEX standard	N/A	N/A	N/A	9-Sep-97	9:35	1.2	N/A
SG09Sep4	N/A	500 ppm BTEX standard	N/A	N/A	N/A	9-Sep-97	9:49	1.2	N/A
SG09Sep5	N/A	1000 ppm BTEX standard	N/A	N/A	N/A	9-Sep-97	10:08	1.8	N/A
SG09Sep6	N/A	1500 ppm BTEX standard	N/A	N/A	N/A	9-Sep-97	10:21	1.4	N/A
SG09Sep6	N/A	3000 ppm BTEX standard	N/A	N/A	N/A	9-Sep-97	12:54	1.2	N/A
SG-BC (SG09SE19)	0.15	Below green house	N/A	N/A	N/A	9-Sep-97	17:11	4000	N/A
SG-BC (SG09SEP9)	0.3	Below green house	N/A	N/A	N/A	9-Sep-97	13:09	1000	N/A
SG-BC (SG09SE20)	0.6	Below green house	N/A	N/A	N/A	9-Sep-97	17:23	4000	N/A
SG-BC (SG09SE11)	0.45	Below green house	N/A	N/A	N/A	9-Sep-97	13:37	4000	N/A
SG-BC (SG09SE12)	0.75	Below green house	N/A	N/A	N/A	9-Sep-97	13:50	200	N/A
SG-BC (SG09SE13)	0.9	Below green house	N/A	N/A	N/A	9-Sep-97	14:06	200	N/A
SG-BC (SG09SE14)	1.2	Below green house	N/A	N/A	N/A	9-Sep-97	14:18	200	N/A
SG-BC (SG09SE15)	1.5	Below green house	N/A	N/A	N/A	9-Sep-97	14:30	200	N/A
SG09SE16	N/A	3000 ppm BTEX standard	N/A	N/A	N/A	9-Sep-97	14:43	1.3	N/A
SG09SE18	N/A	1500 ppm BTEX standard	N/A	N/A	N/A	9-Sep-97	15:24	1.2	N/A
SG09SE21	N/A	500 ppm BTEX standard	N/A	N/A	N/A	9-Sep-97	17:35	1.4	N/A
September 1997 Program - Site B adjacent to green house - After Greenhouse Built									
SG10SE2	N/A	100 ppm BTEX standard	N/A	N/A	N/A	10-Sep-97	9:30	1.4	N/A
SG10SE3	N/A	250 ppm BTEX standard	N/A	N/A	N/A	10-Sep-97	9:43	1.4	N/A
SG10SE4	N/A	250 ppm BTEX standard	N/A	N/A	N/A	10-Sep-97	9:55	1.5	N/A
SG10SE5	N/A	1000 ppm BTEX standard	N/A	N/A	N/A	10-Sep-97	10:08	1.6	N/A

Date Printed: 8/27/2004

Table I-1. Results of GC/PID Vapour and Air Testing

Sample Designation	Depth (m)	Sample Type	Sy-ringe	Syringe Wait Time Before Injection	Sample Collect Date	Sample Analysis Date	Anal-ysis Time	Injec-tion Volume (ul)	Sample Volume (L)
SG10SE6	N/A	1500 ppm BTEX standard	N/A	N/A	N/A	10-Sep-97	10:21	1.4	N/A
SG10SE7	N/A	3000 ppm BTEX standard	N/A	N/A	N/A	10-Sep-97	10:34	1.4	N/A
0.17m South (sg10sep8)	0.17 South Probe 4	Below greenhouse	N/A	N/A	N/A	10-Sep-97	11:34	5000	N/A
0.17m East (sg10sep9)	0.17 East Probe 5	Below greenhouse	N/A	N/A	N/A	10-Sep-97	11:46	5000	N/A
0.4m South (sg10se10)	0.4 South Probe 3	Below greenhouse	N/A	N/A	N/A	10-Sep-97	12:01	4000	N/A
0.4m East (sg10se11)	0.4 East Probe 6	Below greenhouse	N/A	N/A	N/A	10-Sep-97	12:01	5000	N/A
0.7m South (sg10se14)	0.7 South Probe 2	Below greenhouse	N/A	N/A	N/A	10-Sep-97	12:52	5000	N/A
1.6m South (sg10se15)	1.6 South Probe 1	Below greenhouse	N/A	N/A	N/A	10-Sep-97	13:05	200	N/A
0.7m East (sg10se19)	0.7 East Probe 7	Below greenhouse	N/A	N/A	N/A	10-Sep-97	14:37	200	N/A
1.6 m North (sg10se23)	1.6 North Probe 8	Below greenhouse	N/A	N/A	N/A	10-Sep-97	15:38	200	N/A
0.17 m North (sg10se24)	0.17 North Probe 9	Below greenhouse	N/A	N/A	N/A	10-Sep-97	15:51	5000	N/A
0.17 m West (sg10se26)	0.17 West Probe 12	Below greenhouse	N/A	N/A	N/A	10-Sep-97	16:16	1000	N/A
1.6 m West (sg10se27)	1.6 West Probe 11	Below greenhouse	N/A	N/A	N/A	10-Sep-97	16:29	200	N/A
0.17m Centre (sg10se28	0.17m Centre Probe 10	Below greenhouse	N/A	N/A	N/A	10-Sep-97	16:41	2000	N/A
SG10SE16	N/A	500 ppm BTEX standard	N/A	N/A	N/A	10-Sep-97	13:19	1.4	N/A
SG10SE17	N/A	1500 ppm BTEX standard	N/A	N/A	N/A	10-Sep-97	13:32	1.2	N/A
SG10SE19	N/A	1500 ppm BTEX standard	N/A	N/A	N/A	10-Sep-97	13:32	1.2	N/A
SG10SE29	N/A	1500 ppm BTEX standard	N/A	N/A	N/A	10-Sep-97	16:53	1.7	N/A
SG12SEP1	N/A	100 ppm BTEX standard	N/A	N/A	N/A	12-Sep-97	9:05	1.2	N/A
SG12SEP2	N/A	500 ppm BTEX standard	N/A	N/A	N/A	12-Sep-97	9:19	1.3	N/A
SG12SEP3	N/A	1500 ppm BTEX standard	N/A	N/A	N/A	12-Sep-97	9:32	1.4	N/A
SG12SEP8	N/A	1500 ppm BTEX standard	N/A	N/A	N/A	12-Sep-97	11:41	2.4	N/A
SG12SEP11	N/A	1000 ppm BTEX standard	N/A	N/A	N/A	12-Sep-97	12:29	1.2	N/A
0.4m N Outside (SG12SEP4	0.4m North Out Probe 13	Adjacent Greenhouse	N/A	N/A	N/A	12-Sep-97	10:29	5000	N/A
0.7m N Outside (SG12SEP9	0.7m North Out Probe 14	Adjacent Greenhouse	N/A	N/A	N/A	12-Sep-97	12:00	2000	N/A
0.7m E Outside (SG12SEP6	0.7m East Out Probe 15	Adjacent Greenhouse	N/A	N/A	N/A	12-Sep-97	11:01	5000	N/A
0.4m E Outside (SG12SEP7	0.4m East Out Probe 16	Adjacent Greenhouse	N/A	N/A	N/A	12-Sep-97	11:28	5000	N/A
October 21 1997 Program - Site B - After Greenhouse Built									
SG21OCT1	N/A	100 ppm BTEX standard	N/A	N/A	N/A	21-Oct-97	11:42	1.2	N/A
SG21OCT2	N/A	250 ppm BTEX standard	N/A	N/A	N/A	21-Oct-97	11:55	1.3	N/A

Date Printed: 8/27/2004

Table I-1. Results of GC/PID Vapour and Air Testing

Sample Designation	Depth (m)	Sample Type	Sy-ringe	Syringe Wait Time Before Injection	Sample Collect Date	Sample Analysis Date	Anal-ysis Time	Injec-tion Volume (ul)	Sample Volume (L)
SG21OCT3	N/A	500 ppm BTEX standard	N/A	N/A	N/A	21-Oct-97	12:08	1.4	N/A
SG21OCT4	N/A	1000 ppm BTEX standard	N/A	N/A	N/A	21-Oct-97	12:22	1.3	N/A
SG21OC11	N/A	2000 ppm BTEX standard	N/A	N/A	N/A	21-Oct-97	14:28	2.3	N/A
SG-BC((SG21OCT5)	0.15	Below green house	N/A	N/A	N/A	21-Oct-97	13:09	5000	N/A
SG-BC((SG21OCT6)	0.3	Below green house	N/A	N/A	N/A	21-Oct-97	13:21	5000	4000
SG-BC((SG21OCT7)	0.45	Below green house	N/A	N/A	N/A	21-Oct-97	13:34	4000	N/A
SG-BC((SG21OCT8)	0.6	Below green house	N/A	N/A	N/A	21-Oct-97	13:47	4000	N/A
SG-BC((SG21OCT9)	0.75	Below green house	N/A	N/A	N/A	21-Oct-97	14:02	1000	N/A
SG-BC((SG21OC10)	0.9	Below green house	N/A	N/A	N/A	21-Oct-97	14:15	200	N/A
SG-BC((SG21OC12)	1.2	Below green house	N/A	N/A	N/A	21-Oct-97	15:59	200	N/A
SG-BC((SG21OC13)	1.5	Below green house	N/A	N/A	N/A	21-Oct-97	16:12	200	N/A
October 28/29 1997 Program - Site B - After Greenhouse Built									
SG28OC22	N/A	2000 ppm BTEX standard	N/A	N/A	N/A	28-Oct-97	18:08	2.8	N/A
SG28OC7	N/A	2000 ppm BTEX standard	N/A	N/A	N/A	28-Oct-97	12:46	2.2	N/A
SG28OC15	N/A	2000 ppm BTEX standard	N/A	N/A	N/A	28-Oct-97	16:08	1.4	N/A
SG28OC6	N/A	2000 ppm BTEX standard	N/A	N/A	N/A	28-Oct-97	12:26	1.3	N/A
SG28OC5	N/A	1500 ppm BTEX standard	N/A	N/A	N/A	28-Oct-97	12::13	1.3	N/A
SG28OC4	N/A	1000 ppm BTEX standard	N/A	N/A	N/A	28-Oct-97	11:59	1.2	N/A
SG28OC3	N/A	500 ppm BTEX standard	N/A	N/A	N/A	28-Oct-97	11:39	1.3	N/A
SG28OC2	N/A	250 ppm BTEX standard	N/A	N/A	N/A	28-Oct-97	11:26	1.4	N/A
SG28OC1	N/A	100 ppm BTEX standard	N/A	N/A	N/A	28-Oct-97	11:14	1.1	N/A
0.7m East (sg28oc23)	0.7 East Probe 4	Below greenhouse	N/A	N/A	N/A	28-Oct-97	18:22	200	N/A
0.17m West (sg28oc21)	0.17 West	Below greenhouse	N/A	N/A	N/A	28-Oct-97	17:54	3000	N/A
1.6m West (sg28oc20)	1.6 West	Below greenhouse	N/A	N/A	N/A	28-Oct-97	17:41	500	N/A
0.17 Centre (sg28oc19)	0.17 m Midwest ?	Below greenhouse	N/A	N/A	N/A	28-Oct-97	17:28	2000	N/A
0.17 North(sg28oc18)	0.17 m North ?	Below greenhouse	N/A	N/A	N/A	28-Oct-97	17:16	5000	N/A
1.6 North(sg28oc17)	1.6m North	Below greenhouse	N/A	N/A	N/A	28-Oct-97	17:03	200	N/A
0.7 East (sg28oc16)	0.7m East	Below greenhouse	N/A	N/A	N/A	28-Oct-97	16:51	1000	N/A
0.4 East (sg28oc12)	0.4m East	Below greenhouse	N/A	N/A	N/A	28-Oct-97	14:45	5000	N/A
0.7 South (sg28oc11)	0.7m South	Below greenhouse	N/A	N/A	N/A	28-Oct-97	14:23	5000	N/A
0.4 South (sg28oc10)	0.4m South	Below greenhouse	N/A	N/A	N/A	28-Oct-97	14:08	5000	N/A

Date Printed: 8/27/2004

Table I-1. Results of GC/PID Vapour and Air Testing

Sample Designation	Depth (m)	Sample Type	Sy-ringe	Syringe Wait Time Before Injection	Sample Collect Date	Sample Analysis Date	Anal-ysis Time	Injec-tion Volume (ul)	Sample Volume (L)
0.17 East (sg28oc9)	0.17m East	Below greenhouse	N/A	N/A	N/A	28-Oct-97	3:55:00 PI	5000	N/A
0.17 South (sg28oc8)	0.17m South	Below greenhouse	N/A	N/A	N/A	28-Oct-97	13:42	5000	N/A
1.6 South (sg28oc14)	1.6m South	Below greenhouse	N/A	N/A	N/A	28-Oct-97	15:50	200	N/A
0.4 North Out (sg29oc6)	0.4m North Out	Below greenhouse	N/A	N/A	N/A	29-Oct-97	15:36	5000	N/A
0.7 North Out (sg29oc8)	0.7m North Out	Below greenhouse	N/A	N/A	N/A	29-Oct-97	16:02	1000	N/A
0.4 East Out (sg29oc9)	0.4m East Out	Below greenhouse	N/A	N/A	N/A	29-Oct-97	16:16	1000	N/A
0.7 East Out (sg29oc7)	0.7m East Out	Below greenhouse	N/A	N/A	N/A	29-Oct-97	15:49	5000	N/A
SG29OC10	N/A	250 ppm BTEX standard	N/A	N/A	N/A	29-Oct-97	16:29	1.4	N/A
SG29OC2	N/A	100 ppm BTEX standard	N/A	N/A	N/A	29-Oct-97	13:51	1.2	N/A
November 28 1997 (during 30 Pa Depressurization)									
SG-BC (SG28NOV9)	0.15 m	Below greenhouse	N/A	N/A	N/A	28-Nov-97	10:59	0.5	N/A
SG-BC (SG28NO10)	0.3 m	Below greenhouse	N/A	N/A	N/A	28-Nov-97	11:26	0.5	N/A
SG-BC (SG28NO11)	0.45 m	Below greenhouse	N/A	N/A	N/A	28-Nov-97	11:38	0.5	N/A
SG-BC (SG28NO12)	0.6m	Below greenhouse	N/A	N/A	N/A	28-Nov-97	11:52	0.5	N/A
SG-BC (SG28NO14)	0.75 m	Below greenhouse	N/A	N/A	N/A	28-Nov-97	12:48	0.2	N/A
SG-BC (SG28NO15)	0.9 m	Below greenhouse	N/A	N/A	N/A	28-Nov-97	13:01	0.2	N/A
SG-BC (SG28NO15)	0.9 m	Below greenhouse	N/A	N/A	N/A	28-Nov-97	13:01	0.2	N/A
SG-BC (SG28NO16)	1.2	Below greenhouse	N/A	N/A	N/A	28-Nov-97	13:13	0.2	N/A
SG-BC (SG28NO17)	1.5	Below greenhouse	N/A	N/A	N/A	28-Nov-97	13:26	0.2	N/A
SG-BC (SG28NO18)	0.17 Mid West	Below greenhouse	N/A	N/A	N/A	28-Nov-97	13:41	0.2	N/A
SG-BC (SG28NO21)	0.17 North	Below greenhouse	N/A	N/A	N/A	28-Nov-97	16:30	5	N/A
SG-BC (SG28NO22)	0.17 East	Below greenhouse	N/A	N/A	N/A	28-Nov-97	16:42	5	N/A
SG-BC (SG28NO23)	0.17 South	Below greenhouse	N/A	N/A	N/A	28-Nov-97	16:54	3	N/A
SG-BC (SG28NO24)	0.17 West	Below greenhouse	N/A	N/A	N/A	28-Nov-97	17:07	1.5	N/A
SG28NOV1	N/A	100 ppm BTEX standard	N/A	N/A	N/A	28-Nov-97	9:17	1	N/A
SG28NOV7	N/A	Syringe Blank	N/A	N/A	N/A	28-Nov-97	10:47	5	N/A
SG28NOV2	N/A	250 ppm BTEX standard	N/A	N/A	N/A	28-Nov-97	9:31	1.2	N/A
SG28NOV3	N/A	500 ppm BTEX standard	N/A	N/A	N/A	28-Nov-97	9:43	1.4	N/A
SG28NOV4	N/A	1000 ppm BTEX standard	N/A	N/A	N/A	28-Nov-97	9:55	1.4	N/A
SG28NOV5	N/A	1500 ppm BTEX standard	N/A	N/A	N/A	28-Nov-97	10:07	1.2	N/A
SG28NOV6	N/A	1500 ppm BTEX standard	N/A	N/A	N/A	28-Nov-97	10:07	2.3	N/A

Table I-1. Results of GC/PID Vapour and Air Testing

Sample Designation	Depth (m)	Sample Type	Sy-ringe	Syringe Wait Time Before Injection	Sample Collect Date	Sample Analysis Date	Anal-ysis Time	Injec-tion Volume (ul)	Sample Volume (L)
SG28NO13	N/A	5000 ppm BTEX standard	N/A	N/A	N/A	28-Nov-97	12:08	1.2	N/A
SG28NO25	N/A	5000 ppm BTEX standard	N/A	N/A	N/A	28-Nov-97	17:20	2.2	N/A
SG28NOV7	N/A	Syringe Blank	N/A	N/A	N/A	28-Nov-97	15:57	5	N/A
December 1, 1997 10 m East of Greenhouse									
SG-BR (10mE)	1.2	Adjacent Greenhouse	N/A	N/A	N/A	1-Dec-97	16:33	5	N/A
SG-BR (10mE)	0.9	Adjacent Greenhouse	N/A	N/A	N/A	1-Dec-97	16:21	5	N/A
SG-BR (10mE)	0.6	Adjacent Greenhouse	N/A	N/A	N/A	1-Dec-97	16:09	5	N/A
SG-BR (10mE)	0.3	Adjacent Greenhouse	N/A	N/A	N/A	1-Dec-97	15:56	5	N/A
SG01DEC5	N/A	Syringe Blank	N/A	N/A	N/A	1-Dec-97	14:47	5	N/A
SG01DEC4	N/A	1000 ppm BTEX standard	N/A	N/A	N/A	1-Dec-97	14:27	1.4	N/A
SG01DEC3	N/A	500 ppm BTEX standard	N/A	N/A	N/A	1-Dec-97	14:15	1.4	N/A
SG01DEC2	N/A	250 ppm BTEX standard	N/A	N/A	N/A	1-Dec-97	14:02	1.4	N/A
SG01DEC1	N/A	100 ppm BTEX standard	N/A	N/A	N/A	1-Dec-97	13:49	1.2	N/A
SG-BR (10mE) sg03dec8	0.9	Adjacent Greenhouse	N/A	N/A	N/A	3-Dec-97	15:01	5	N/A
SG-BR (10mE) sg03dec7	0.3	Adjacent Greenhouse	N/A	N/A	N/A	3-Dec-97	15:01	5	N/A
SG-BR (10mE) sg03dec9	1.5 ? Results suspect	Adjacent Greenhouse	N/A	N/A	N/A	3-Dec-97	15:24	5	N/A
SG01DEC6	N/A	Syringe Blank	N/A	N/A	N/A	1-Dec-97	14:37	5	N/A
October 1997 Program - Flux Chamber QC Testing									
TD03OCT2 Tube 1	Flux Chamber blank	White nitrile rubber, 24 hr sample	N/A	N/A	2-Oct-97	3-Oct-97	N/A	N/A	389
TD03OCT2 Tube 2	Flux Chamber blank	White nitrile rubber, 24 hr sample	N/A	N/A	2-Oct-97	3-Oct-97	N/A	N/A	389
TD14OCT3 Tube 1	Flux Chamber blank	White nitrile rubber, 24 hr , after bakinç	N/A	N/A	13-Oct-97	14-Oct-97	N/A	N/A	401
TD14OCT4 Tube 2	Flux Chamber blank	White nitrile rubber, 24 hr , after bakinç	N/A	N/A	13-Oct-97	14-Oct-97	N/A	N/A	401
TD14OCT6 Tube 1	Indoor Air, east room	Chatterton building	N/A	N/A	14-Oct-97	14-Oct-97	N/A	N/A	63.2
TD24OCT1 Tube 2	Tube Blank		N/A	N/A	24-Oct-97	24-Oct-97	N/A	N/A	N/A
TD24OCT5 Tube 2	Indoor Air, east room	Chatterton building	N/A	N/A	24-Oct-97	24-Oct-97	N/A	N/A	53.2
TD21OCT2 Tube 1	Flux Chamber blank	Black rubber, 24 hr sample	N/A	N/A	20-Oct-97	21-Oct-97	N/A	N/A	320.4
TD21OCT3 Tube 2	Flux Chamber blank	Black rubber, 24 hr sample	N/A	N/A	20-Oct-97	21-Oct-97	N/A	N/A	320.4
TD23OCT2 Tube 4	Flux Chamber blank	Black rubber, 24 hr, clear vinyl tubing	N/A	N/A	22-Oct-97	23-Oct-97	N/A	N/A	288.7
TD23OCT3 Tube 5	Flux Chamber blank	Black rubber, 24 hr, clear vinyl tubing	N/A	N/A	22-Oct-97	23-Oct-97	N/A	N/A	288.7
TD23OCT1	N/A	500 ppm BTEX & 3FT Standard	N/A	N/A	23-Oct-97	23-Oct-97	N/A	1	N/A
TD22OCT1 Tube 4	Tube Blank		N/A	N/A	22-Oct-97	22-Oct-97	N/A	N/A	N/A

Table I-1. Results of GC/PID Vapour and Air Testing

Sample Designation	Depth (m)	Sample Type	Sy-ringe	Syringe Wait Time Before Injection	Sample Collect Date	Sample Analysis Date	Anal-ysis Time	Injec-tion Volume (ul)	Sample Volume (L)
TD22OCT1 Tube 5	Tube Blank	baked another 30 min afterwards	N/A	N/A	22-Oct-97	22-Oct-97	N/A	N/A	N/A
TD24OCT6 Tube 4	Flux Chamber blank	No rubber gasket	N/A	N/A	24-Oct-97	24-Oct-97	N/A	N/A	331.7
TD27OCT4 Tube 4	Flux Chamber blank	No gasket, baked another 30 min	N/A	N/A	27-Oct-97	27-Oct-97	N/A	N/A	331.7
TD27OCT2 Tube 5	Flux Chamber blank	No gasket, baked another 30 min	N/A	N/A	27-Oct-97	27-Oct-97	N/A	N/A	N/A
TD23OCT5 Tube 4&5	Tube Blank		N/A	N/A	23-Oct-97	23-Oct-97	N/A	N/A	N/A
TD24OCT2	N/A	250 ppm BTEX , 500 ppm 3FT Std	N/A	N/A	24-Oct-97	24-Oct-97	N/A	1	N/A
TD24OCT3	N/A	500 ppm BTEX , 500 ppm 3FT Std	N/A	N/A	24-Oct-97	24-Oct-97	N/A	1.1	N/A
TD24OCT4	N/A	1000 ppm BTEX , 500 ppm 3FT Std	N/A	N/A	24-Oct-97	24-Oct-97	N/A	1.1	N/A
TD27OCT1	N/A	1000 ppm BTEX , 500 ppm 3FT Std	N/A	N/A	27-Oct-97	27-Oct-97	N/A	1	N/A
TD27OCT3	N/A	2000 ppm BTEX , 500 ppm 3FT Std	N/A	N/A	27-Oct-97	27-Oct-97	N/A	2	N/A
TD30OCT3 Tube 4	Flux Chamber blank	ack rubber, baked 72 hr, fittings clean	N/A	N/A	30-Oct-97	30-Oct-97	N/A	N/A	341.5
TD30OCT4 Tube 5	Flux Chamber blank	ack rubber, baked 72 hr, fittings clean	N/A	N/A	30-Oct-97	30-Oct-97	N/A	N/A	341.5
TD30OCT5	N/A	1000 ppm BTEX , ? ppm 3FT Std	N/A	N/A	30-Oct-97	30-Oct-97	N/A	1.1	N/A
TD30OCT2	N/A	500 ppm BTEX , ? ppm 3FT Std	N/A	N/A	30-Oct-97	30-Oct-97	N/A	1	N/A
TD30OCT1	N/A	100 ppm BTEX , ? ppm 3FT Std	N/A	N/A	30-Oct-97	30-Oct-97	N/A	1	N/A
TD29OCT1 Tube 4&5	Tube Blank		N/A	N/A	29-Oct-97	29-Oct-97	N/A	N/A	N/A
November 1997 Program - Indoor/Outdoor and Flux Chamber Testing at Greenhouse (non-depressurized)									
TD06NO15 Tube 5	Ambient Air	Outside Greenhouse	N/A	N/A	7-Nov-97	7-Nov-97	N/A	N/A	26.1
TD06NO8 Tube 5	Ambient Air	Inside Greenhouse	N/A	N/A	7-Nov-97	7-Nov-97	N/A	N/A	34.9
TD06NO2 Tube 5	Tube Blank	Prior to collecting ambient air	N/A	N/A	6-Nov-97	6-Nov-97	N/A	N/A	N/A
TD06NO13 Tube 3	Flux Chamber - South	Over Crack	N/A	N/A	7-Nov-97	7-Nov-97	N/A	N/A	319
TD06NO4 Tube 3&4	Tube Blank	Prior to collecting flux chamber crack	N/A	N/A	6-Nov-97	6-Nov-97	N/A	N/A	N/A
TD06NO10 Tube 1	Glass Tube Blank	Prior to collecting flux chamber crack	N/A	N/A	6-Nov-97	6-Nov-97	N/A	N/A	N/A
TD06NO10 Tube 1	Glass Tube Blank	Prior to collecting flux chamber crack	N/A	N/A	5-Nov-97	5-Nov-97	N/A	N/A	N/A
TD06NO5 Tube 1	Flux Chamber Blank	Flux Chamber on Solid Concrete	N/A	N/A	6-Nov-97	6-Nov-97	N/A	N/A	418.3
TD06NO5 Tube 2	Flux Chamber Blank	Flux Chamber on Solid Concrete	N/A	N/A	6-Nov-97	6-Nov-97	N/A	N/A	418.3
TD06NO7	N/A	100 ppm BTEX , 500 ppm 3FT Std	N/A	N/A	6-Nov-97	6-Nov-97	N/A	1.1	N/A
TD06NO16	N/A	500 ppm BTEX , 500 ppm 3FT Std	N/A	N/A	7-Nov-97	7-Nov-97	N/A	1.1	N/A
TD06NOV1	N/A	500 ppm BTEX , 500 ppm 3FT Std	N/A	N/A	6-Nov-97	7-Nov-97	N/A	1.1	N/A
TD06NOV3	N/A	1000 ppm BTEX , 500 ppm 3FT Std	N/A	N/A	6-Nov-97	7-Nov-97	N/A	1	N/A
TD06NOV9	N/A	2000 ppm BTEX , 500 ppm 3FT Std	N/A	N/A	7-Nov-97	7-Nov-97	N/A	1	N/A
TD12NOV2 Tube 1	Ambient Air	Inside Greenhouse	N/A	N/A	12-Nov-97	12-Nov-97	N/A	N/A	23

Table I-1. Results of GC/PID Vapour and Air Testing

Sample Designation	Depth (m)	Sample Type	Sy-ringe	Syringe Wait Time Before Injection	Sample Collect Date	Sample Analysis Date	Anal-ysis Time	Injec-tion Volume (ul)	Sample Volume (L)
TD12NOV6 Tube 1	Ambient Air	Desorbed tube another 10 min	N/A	N/A	12-Nov-97	12-Nov-97	N/A	N/A	23
TD12NOV3 Tube 2	Ambient Air	Outside Greenhouse	N/A	N/A	12-Nov-97	12-Nov-97	N/A	N/A	22.6
TD12NOV5 Tube 2	N/A	Desorbed tube another 10 min	N/A	N/A	12-Nov-97	12-Nov-97	N/A	N/A	22.6
TD11NO3 Tube 2	Tube Blank	Prior to collecting outside air sample	N/A	N/A	11-Nov-97	11-Nov-97	N/A	N/A	N/A
TD11NOV6 Tube 4	Flux Chamber - East	Over Crack	N/A	N/A	11-Nov-97	11-Nov-97	N/A	N/A	237
TD12NOV9 Tube 5	Flux Chamber - East	Over Crack	N/A	N/A	12-Nov-97	12-Nov-97	N/A	N/A	N/A
TD12NOV4	N/A	250 ppm BTEX , 500 ppm 3FT Std	N/A	N/A	12-Nov-97	12-Nov-97	N/A	1	N/A
TD11NOV5	N/A	500 ppm BTEX , 500 ppm 3FT Std	N/A	N/A	12-Nov-97	12-Nov-97	N/A	1	N/A
TD12NOV1	N/A	1000 ppm BTEX , 500 ppm 3FT Std	N/A	N/A	12-Nov-97	12-Nov-97	N/A	1	N/A
TD10OCT2 Tube 4&5	Tube Blank	Prior to collecting east flux chamber	N/A	N/A	10-Nov-97	10-Nov-97	N/A	N/A	N/A
TD13NOV6	Flux Chamber - West	Over Crack	N/A	N/A	13-Nov-97	13-Nov-97	N/A	N/A	296
TD11NOV7 Tube 4	Tube Blank	Prior to west flux chamber sample	N/A	N/A	11-Nov-97	11-Nov-97	N/A	N/A	N/A
TD13NOV2 Tube 1	Ambient Air	Inside Greenhouse	N/A	N/A	13-Nov-97	13-Nov-97	N/A	N/A	25
TD12NOV8 Tube 1	Tube Blank	Prior to indoor air	N/A	N/A	12-Nov-97	12-Nov-97	N/A	N/A	N/A
TD13NOV3 Tube 2	Ambient Air	Outside Greenhouse	N/A	N/A	13-Nov-97	13-Nov-97	N/A	N/A	23.7
TD12NOV7 Tube 2	Tube Blank	Prior to outside air	N/A	N/A	12-Nov-97	12-Nov-97	N/A	N/A	N/A
TD13NOV4	N/A	250 ppm BTEX , 500 ppm 3FT Std	N/A	N/A	12-Nov-97	12-Nov-97	N/A	1	N/A
TD13NOV1	N/A	500 ppm BTEX , 500 ppm 3FT Std	N/A	N/A	13-Nov-97	13-Nov-97	N/A	1	N/A
TD13NOV5	N/A	2000 ppm BTEX , 500 ppm 3FT Std	N/A	N/A	13-Nov-97	13-Nov-97	N/A	1	N/A
TD13NO10	Flux Chamber - North	Over Crack	N/A	N/A	13-Nov-97	13-Nov-97	N/A	N/A	240
TD12NO10 Tube 5	Tube Blank	Prior to north flux chamber	N/A	N/A	12-Nov-97	12-Nov-97	N/A	N/A	N/A
TD17NOV2 Tube 4	Flux Chamber blank	End first week (on solide concrete)	N/A	N/A	17-Nov-97	17-Nov-97	N/A	N/A	198
	Tube Blank	Prior to flux chamber blank	N/A	N/A	13-Nov-97	13-Nov-97	N/A	N/A	N/A
March 1998 Program - Site B (Greenhouse) - Non-Depressurized Conditions									
Gasblk1	N/A	Carrier Gas Blank	N/A	N/A	N/A	18-Mar-98	10:39	N/A	N/A
S100A	N/A	100 ppm BTEX standard	N/A	N/A	N/A	16-Mar-98	11:20	1.4	N/A
S250A	N/A	250 ppm BTEX standard	N/A	N/A	N/A	16-Mar-98	11:32	1.4	N/A
S1000A	N/A	1000 ppm BTEX standard	N/A	N/A	N/A	16-Mar-98	14:33	1.1	N/A
S1000B	N/A	1000 ppm BTEX standard	N/A	N/A	N/A	16-Mar-98	14:49	2.4	N/A
S1000C	N/A	1000 ppm BTEX standard	N/A	N/A	N/A	16-Mar-98	15:53	3.1	N/A
S100B	N/A	100 ppm BTEX standard	N/A	N/A	N/A	18-Mar-98	9:00	1.2	N/A

Date Printed: 8/27/2004

Table I-1. Results of GC/PID Vapour and Air Testing

Sample Designation	Depth (m)	Sample Type	Sy-ringe	Syringe Wait Time Before Injection	Sample Collect Date	Sample Analysis Date	Anal-ysis Time	Injec-tion Volume (ul)	Sample Volume (L)
S250B	N/A	250 ppm BTEX standard	N/A	N/A	N/A	18-Mar-98	9:17	1.2	N/A
-	N/A	Sample Syringe Blk (He)	N/A	N/A	N/A	16-Mar-98	12:43	5000	N/A
-	N/A	Sample Syringe Blk (He)	N/A	N/A	N/A	16-Mar-98	12:55	5000	N/A
Syn #1 - Run1	N/A	Sample Syringe Blk (He)	#1	N/A	N/A	18-Mar-98	11:55	5000	N/A
Syn #1 - Run2	N/A	Sample Syringe Blk (He)	#1	N/A	N/A	18-Mar-98	13:02	5000	N/A
Syn #1 - Run3	N/A	Sample Syringe + Valve (air)	#1	N/A	N/A	18-Mar-98	13:28	5000	N/A
Syn #3 - Run1	N/A	Sample Syringe Blk (He)	#3	N/A	N/A	18-Mar-98	9:39	5000	N/A
Syn #3 - Run2	N/A	Sample Syringe Blk (He)	#3	N/A	N/A	18-Mar-98	10:27	5000	N/A
Syn #3 - Run3	N/A	Sample Syringe Blk (He)	#3	N/A	N/A	18-Mar-98	11:09	5000	N/A
Syn #3 - Run4	N/A	Sample Syringe + Valve (air)	#3	N/A	N/A	18-Mar-98	12:07	5000	N/A
Syn #4 - Run1	N/A	Sample Syringe Blk (He)	#4	N/A	N/A	18-Mar-98	11:42	5000	N/A
Syn #4 - Run2	N/A	Sample Syringe Blk (He)	#4	N/A	N/A	18-Mar-98	13:14	5000	N/A
Syn #5 - Run1	N/A	Sample Syringe Blk (He)	#5	N/A	N/A	18-Mar-98	12:24	5000	N/A
Syn #5 - Run2	N/A	Sample Syringe + Valve (air)	#5	N/A	N/A	18-Mar-98	12:49	5000	N/A
Syn #5 - Run3	N/A	Sample Syringe + Valve (air)	#5	N/A	N/A	18-Mar-98	13:42	5000	N/A
Syn #6 - Run1	N/A	Sample Syringe Blk (He)	#6	N/A	N/A	18-Mar-98	10:06	5000	N/A
Syn #6 - Run2	N/A	Sample Syringe Blk (He)	#6	N/A	N/A	18-Mar-98	10:52	5000	N/A
Syn #6 - Run3	N/A	Sample Syringe Blk (He)	#6	N/A	N/A	18-Mar-98	11:23	5000	N/A
Syn #6 - Run4	N/A	Sample Syringe Blk (He)	#6	N/A	N/A	18-Mar-98	12:36	5000	N/A
Syn #6 - Run5	N/A	Sample Syringe Blk (He)	#6	N/A	N/A	18-Mar-98	14:02	5000	N/A
SG-BR (10mE)	0.3	SG East of Greenhouse	N/A	N/A	16-Mar-98	16-Mar-98	13:06	5000	N/A
SG-BR (10mE)	0.6	SG East of Greenhouse	N/A	N/A	16-Mar-98	16-Mar-98	13:18	5000	N/A
SG-BR (10mE)	0.9	SG East of Greenhouse	N/A	N/A	16-Mar-98	16-Mar-98	14:06	200	N/A
SG-BR (10mE)	1.2	SG East of Greenhouse	N/A	N/A	16-Mar-98	16-Mar-98	14:19	200	N/A
SG-BC	0.15	SG Below Greenhouse	#1	N/A	18-Mar-98	18-Mar-98	14:50	5000	N/A
SG-BC	0.45	SG Below Greenhouse	#5	N/A	18-Mar-98	18-Mar-98	15:02	5000	N/A
SG-BC	0.6	SG Below Greenhouse	#3	N/A	18-Mar-98	18-Mar-98	15:15	4000	N/A
SG-BC	0.75	SG Below Greenhouse	#4	N/A	18-Mar-98	18-Mar-98	15:28	500	N/A

Date Printed: 8/27/2004

Table I-1. Results of GC/PID Vapour and Air Testing

200

Sample Designation	Depth (m)	Sample Type	Syringe	Syringe Wait Time Before Injection	Sample Collect Date	Sample Analysis Date	Analysis Time	Injection Volume (ul)	Sample Volume (L)
SG-BC	1.2	SG Below Greenhouse	#6	N/A	18-Mar-98	18-Mar-98	15:40	200	N/A
June 1998 Program - Site B (Greenhouse) - Non-Depressurized Conditions									
Standard #1	N/A	Standard	N/A	N/A	26-Jun-98	26-Jun-98	N/A	N/A	N/A
Standard #2	N/A	Standard	N/A	N/A	26-Jun-98	26-Jun-98	N/A	N/A	N/A
Standard #3	N/A	Standard	N/A	N/A	26-Jun-98	26-Jun-98	N/A	N/A	N/A
Standard #4	N/A	Standard	N/A	N/A	26-Jun-98	26-Jun-98	N/A	N/A	N/A
Standard #5	N/A	Standard	N/A	N/A	26-Jun-98	26-Jun-98	N/A	N/A	N/A
Standard #6	N/A	Standard	N/A	N/A	26-Jun-98	26-Jun-98	N/A	N/A	N/A
Standard #7	N/A	Standard	N/A	N/A	26-Jun-98	26-Jun-98	N/A	N/A	N/A
SG-BC	0.15	SG Below Greenhouse	N/A	N/A	25-Jun-98	25-Jun-98	12:48	5000	N/A
SG-BC	0.3	SG Below Greenhouse	N/A	N/A	25-Jun-98	25-Jun-98	13:03	5000	N/A
SG-EC	0.17	SG Below Greenhouse	N/A	N/A	25-Jun-98	25-Jun-98	11:05	5000	N/A
SG-EC	0.4	SG Below Greenhouse	N/A	N/A	25-Jun-98	25-Jun-98	13:24	5000	N/A
SG-SC	0.17	SG Below Greenhouse	N/A	N/A	25-Jun-98	25-Jun-98	11:23	5000	N/A
SG-SC	0.4	SG Below Greenhouse	N/A	N/A	25-Jun-98	25-Jun-98	13:38	5000	N/A
SG-WC	0.17	SG Below Greenhouse	N/A	N/A	25-Jun-98	25-Jun-98	13:38	5000	N/A
SG-NC	0.17	SG Below Greenhouse	N/A	N/A	25-Jun-98	25-Jun-98	10:51	5000	N/A
SG-O2 PROBE	0.17	SG Below Greenhouse	N/A	N/A	25-Jun-98	25-Jun-98	12:34	5000	N/A
SG-BC	0.45	SG Below Greenhouse	N/A	N/A	26-Jun-98	26-Jun-98	N/A	5000	N/A
SG-BC	0.6	SG Below Greenhouse	N/A	N/A	26-Jun-98	26-Jun-98	N/A	1000	N/A
SG-BC	0.75	SG Below Greenhouse	N/A	N/A	26-Jun-98	26-Jun-98	N/A	500	N/A
SG-BC	0.9	SG Below Greenhouse	N/A	N/A	26-Jun-98	26-Jun-98	N/A	200	N/A
SG-BC	1.2	SG Below Greenhouse	N/A	N/A	26-Jun-98	26-Jun-98	N/A	200	N/A
SG-BC	1.5	SG Below Greenhouse	N/A	N/A	26-Jun-98	26-Jun-98	N/A	200	N/A
SG-EC	0.7	SG Below Greenhouse	N/A	N/A	26-Jun-98	26-Jun-98	N/A	1000	N/A
SG-SC	0.7	SG Below Greenhouse	N/A	N/A	26-Jun-98	26-Jun-98	N/A	1000	N/A
SG-SC	1.6	SG Below Greenhouse	N/A	N/A	26-Jun-98	26-Jun-98	N/A	200	N/A
SG-WC	1.6	SG Below Greenhouse	N/A	N/A	26-Jun-98	26-Jun-98	N/A	500	N/A
SG-NC	1.6	SG Below Greenhouse	N/A	N/A	26-Jun-98	26-Jun-98	N/A	200	N/A
SG-BR (10mE)	1.2	SG Adj. Greenhouse	N/A	N/A	26-Jun-98	26-Jun-98	N/A	500	N/A

Date Printed: 8/27/2004

Table I-1. Results of GC/PID Vapour and Air Testing

Sample Designation	Depth (m)	Sample Type	Sy-ringe	Syringe Wait Time Before Injection	Sample Collect Date	Sample Analysis Date	Anal-ysis Time	Injec-tion Volume (ul)	Sample Volume (L)
December 1998 Program - Site B									
Calibration & Quality Control Tests (DYNAMIC- -10Pa)									
Syringe 1	N/A	Syringe + Valve (air) [5 min.]	#1	N/A	N/A	3-Dec-98	12:17	5000	N/A
Syringe 1	N/A	Syringe + Valve (air) [30 sec.]	#1	N/A	N/A	3-Dec-98	12:01	5000	N/A
Syringe 1	N/A	Syringe + Valve (air)[washed: 10min.]	#1	N/A	N/A	3-Dec-98	11:30	5000	N/A
60ng std	N/A	Syringe + 60ng BTX	N/A	N/A	N/A	3-Dec-98	10:44	N/A	N/A
60ng std	N/A	Syringe + 60ng BTX	N/A	N/A	N/A	3-Dec-98	13:36	N/A	N/A
300ng std	N/A	Syringe + 300ng BTX	N/A	N/A	N/A	3-Dec-98	11:03	N/A	N/A
Sorbant Tube 1	N/A	Sorbant Tube + Air	N/A	N/A	N/A	3-Dec-98	15:29	N/A	N/A
Sorbant Tube 5	N/A	Sorbant Tube + Air	N/A	N/A	N/A	3-Dec-98	13:59	1-Jul-18	N/A
800ng std	N/A	Sorbant Tube + 800ng BTX	N/A	N/A	N/A	3-Dec-98	15:00	N/A	N/A
Sorbant Tube 1	N/A	Sorbant Tube + Air	N/A	N/A	N/A	4-Dec-98	14:26	N/A	N/A
Sorbant Tube 5	N/A	Sorbant Tube + Air	N/A	N/A	N/A	4-Dec-98	13:53	N/A	N/A
800ng std	N/A	Sorbant Tube + 800ng BTX	N/A	N/A	N/A	4-Dec-98	14:59	N/A	N/A
Sorbant Tube 1	N/A	Sorbant Tube + Air	N/A	N/A	N/A	8-Dec-98	13:19	N/A	N/A
Sorbant Tube 5	N/A	Sorbant Tube + Air	N/A	N/A	N/A	8-Dec-98	10:36	N/A	N/A
Sorbant Tube 5	N/A	Sorbant Tube + Air	N/A	N/A	N/A	8-Dec-98	12:34	N/A	N/A
575ng std	N/A	Sorbant Tube + 575ng BTX	N/A	N/A	N/A	8-Dec-98	11:45	N/A	N/A
115ng std	N/A	Sorbant Tube + 115ng BTX	N/A	N/A	N/A	8-Dec-98	13:55	N/A	N/A
Sorbant Tube 5	N/A	Sorbant Tube + Air	N/A	N/A	N/A	9-Dec-98	10:00	N/A	N/A
60ng std	N/A	Sorbant Tube + 60ng BTX	N/A	N/A	N/A	9-Dec-98	11:57	N/A	N/A
550ng std	N/A	Sorbant Tube + 550ng BTX	N/A	N/A	N/A	9-Dec-98	15:01	N/A	N/A
800ng std	N/A	Sorbant Tube + 800ng BTX	N/A	N/A	N/A	9-Dec-98	11:20	N/A	N/A
2400ng std	N/A	Sorbant Tube + 2400ng BTX	N/A	N/A	N/A	9-Dec-98	13:28	N/A	N/A
Sample Tests (DYNAMIC- -10Pa)									
Indoor Sample	N/A	Indoor Air - Sorbant Tube 5	N/A	N/A	3-Dec-98	3-Dec-98	14:30	349000	N/A
SG-BR (10mE)	0.3	SG Adj. Greenhouse (Tube 1)	N/A	N/A	3-Dec-98	3-Dec-98	16:21	652000	N/A
Indoor Sample	N/A	Indoor Air - Sorbant Tube 5	N/A	N/A	4-Dec-98	4-Dec-98	16:24	364000	N/A
SG-BR (10mE)	0.6	SG Adj. Greenhouse	N/A	N/A	4-Dec-98	4-Dec-98	15:50	750000	N/A
Indoor Sample	N/A	Indoor Air - Sorbant Tube 5	N/A	N/A	8-Dec-98	8-Dec-98	11:16	384000	N/A
SG-BR (10mE)	0.3	SG Adj. Greenhouse	N/A	N/A	8-Dec-98	8-Dec-98	15:09	160000	N/A
SG-BR (10mE)	0.6	SG Adj. Greenhouse	N/A	N/A	8-Dec-98	8-Dec-98	15:40	160000	N/A

Date Printed: 8/27/2004

Table I-1. Results of GC/PID Vapour and Air Testing

Sample Designation	Depth (m)	Sample Type	Sy-ringe	Syringe Wait Time Before Injection	Sample Collect Date	Sample Analysis Date	Anal-ysis Time	Injec-tion Volume (ul)	Sample Volume (L)
Indoor Sample	N/A	Indoor Air - Sorbant Tube 5	N/A	N/A	9-Dec-98	9-Dec-98	10:48	384000	N/A
SG-BC	0.15	SG Below Greenhouse	N/A	N/A	9-Dec-98	9-Dec-98	14:45	200	N/A
SG-NC	0.17	SG Below Greenhouse	N/A	N/A	9-Dec-98	9-Dec-98	12:23	400	N/A
SG-SC	0.17	SG Below Greenhouse	N/A	N/A	9-Dec-98	9-Dec-98	12:52	200	N/A
SG-EC	0.17	SG Below Greenhouse	N/A	N/A	9-Dec-98	9-Dec-98	12:37	1000	N/A
SG-WC	0.17	SG Below Greenhouse	N/A	N/A	9-Dec-98	9-Dec-98	14:11	1000	N/A
SG-MW	0.17	SG Below Greenhouse	N/A	N/A	9-Dec-98	9-Dec-98	14:27	200	N/A
November/December 1998 Program - Site B (Greenhouse)									
Calibration & Quality Control Tests (DYNAMIC- -10Pa)									
Sorbant Tube 1	N/A	Sorbant Tube + Air	N/A	N/A	N/A	1-Dec-98	14:02	N/A	N/A
Sorbant Tube 5	N/A	Sorbant Tube + Air	N/A	N/A	N/A	1-Dec-98	13:15	N/A	N/A
Sorbant Tube 5	N/A	Sorbant Tube + Air	N/A	N/A	N/A	2-Dec-98	11:29	N/A	N/A
6400ng std	N/A	Sorbant Tube + 6400ng BTX	N/A	N/A	N/A	2-Dec-98	14:04	N/A	N/A
11000ng std	N/A	Sorbant Tube + 11000ng BTX	N/A	N/A	N/A	2-Dec-98	12:09	N/A	N/A
Syringe 1	N/A	Syringe + Valve (air)	#1	N/A	N/A	2-Dec-98	14:45	N/A	N/A
12ng std	N/A	Syringe + 12ng BTX	N/A	N/A	N/A	2-Dec-98	14:27	N/A	N/A
300ng std	N/A	Syringe + 300ng BTX	N/A	N/A	N/A	2-Dec-98	15:19	N/A	N/A
Sorbant Tube 1	N/A	Sorbant Tube + Air	N/A	N/A	N/A	30-Nov-98	10:25	N/A	N/A
Sorbant Tube 5	N/A	Sorbant Tube + Air	N/A	N/A	N/A	30-Nov-98	10:58	N/A	N/A
60ng std	N/A	Sorbant Tube + 60ng BTX	N/A	N/A	N/A	30-Nov-98	9:54	N/A	N/A
60ng std	N/A	Sorbant Tube + 60ng BTX	N/A	N/A	N/A	1-Dec-98	9:52	N/A	N/A
550ng std	N/A	Sorbant Tube + 550ng BTX	N/A	N/A	N/A	1-Dec-98	10:24	N/A	N/A
12000ng std	N/A	Sorbant Tube + 12000ng BTX	N/A	N/A	N/A	30-Nov-98	12:13	N/A	N/A
Syringe 1	N/A	Syringe + Valve (air)	#1	N/A	N/A	30-Nov-98	14:04	N/A	N/A
Syringe 2	N/A	Syringe + Valve (air)	#2	N/A	N/A	30-Nov-98	14:21	N/A	N/A
Syringe 4	N/A	Syringe + Valve (air)	#4	N/A	N/A	30-Nov-98	14:40	N/A	N/A
12ng std	N/A	Syringe + 12ng BTX	N/A	N/A	N/A	30-Nov-98	13:46	N/A	N/A
300ng std	N/A	Syringe + 300ng BTX	N/A	N/A	N/A	30-Nov-98	17:06	N/A	N/A
12000ng std	N/A	Syringe + 12000ng BTX	N/A	N/A	N/A	30-Nov-98	16:49	N/A	N/A
2400ng std	N/A	Syringe + 2400ng BTX	N/A	N/A	N/A	30-Nov-98	16:32	N/A	N/A
Sorbant Tube 1	N/A	Sorbant Tube + Air	N/A	N/A	N/A	27-Nov-98	10:12	N/A	N/A
4600ng std	N/A	Syringe + 4600ng BTX	N/A	N/A	N/A	27-Nov-98	9:46	N/A	N/A

Date Printed: 8/27/2004

Table I-1. Results of GC/PID Vapour and Air Testing

Sample Designation	Depth (m)	Sample Type	Sy-ringe	Syringe Wait Time Before Injection	Sample Collect Date	Sample Analysis Date	Anal-ysis Time	Injec-tion Volume (ul)	Sample Volume (L)
2400ng std	N/A	Syringe + 2400ng BTX	N/A	N/A	N/A	27-Nov-98	12:07	N/A	N/A
2400ng std	N/A	Syringe + 2400ng BTX	N/A	N/A	N/A	27-Nov-98	16:15	N/A	N/A
Sorbant Tube 1	N/A	Sorbant Tube + Air	N/A	N/A	N/A	24-Nov-98	11:03	N/A	N/A
Sorbant Tube 1	N/A	Sorbant Tube + Air	N/A	N/A	N/A	24-Nov-98	12:57	N/A	N/A
Sorbant Tube2	N/A	Sorbant Tube + Air	N/A	N/A	N/A	24-Nov-98	12:05	N/A	N/A
550ng std	N/A	Sorbant Tube + 550ng BTX	N/A	N/A	N/A	24-Nov-98	15:31	N/A	N/A
2400ng std	N/A	Sorbant Tube + 2400ng BTX	N/A	N/A	N/A	24-Nov-98	14:22	N/A	N/A
Sorbant Tube 1	N/A	Sorbant Tube + Air	N/A	N/A	N/A	20-Nov-98	9:20	N/A	N/A
Sorbant Tube 2	N/A	Sorbant Tube + Air	N/A	N/A	N/A	20-Nov-98	9:45	N/A	N/A
Sorbant Tube 3	N/A	Sorbant Tube + Air	N/A	N/A	N/A	20-Nov-98	10:10	N/A	N/A
60ng std	N/A	Sorbant Tube + 60ng BTX	N/A	N/A	N/A	20-Nov-98	13:03	N/A	N/A
600ng std	N/A	Sorbant Tube + 600ng BTX	N/A	N/A	N/A	20-Nov-98	13:32	N/A	N/A
2400ng std	N/A	Sorbant Tube + 2400ng BTX	N/A	N/A	N/A	20-Nov-98	15:45	N/A	N/A
4400ng std	N/A	Sorbant Tube + 4400ng BTX	N/A	N/A	N/A	20-Nov-98	15:11	N/A	N/A
12ng std	N/A	Sorbant Tube + 12ng BTX	N/A	N/A	N/A	19-Nov-98	16:49	N/A	N/A
Syringe 1	N/A	Syringe + Valve (air)	#1	N/A	N/A	19-Nov-98	15:32	N/A	N/A
Syringe 2	N/A	Syringe + Valve (air)	#2	N/A	N/A	19-Nov-98	14:10	N/A	N/A
Syringe 2	N/A	Syringe + Valve (air)	#2	N/A	N/A	19-Nov-98	15:08	N/A	N/A
Syringe 2	N/A	Syringe + Valve (air)	#2	N/A	N/A	19-Nov-98	16:11	N/A	N/A
Syringe 4	N/A	Syringe + Valve (air)	#4	N/A	N/A	19-Nov-98	15:50	N/A	N/A
12ng std	N/A	Syringe + 12ng BTX	N/A	N/A	N/A	19-Nov-98	13:53	N/A	N/A
12ng std	N/A	Syringe + 12ng BTX	N/A	N/A	N/A	19-Nov-98	16:29	N/A	N/A
60ng std	N/A	Syringe + 60ng BTX	N/A	N/A	N/A	19-Nov-98	12:02	N/A	N/A
12ng std	N/A	Syringe + 12ng BTX	N/A	N/A	N/A	18-Nov-98	14:45	N/A	N/A
60ng std	N/A	Syringe + 60ng BTX	N/A	N/A	N/A	18-Nov-98	14:26	N/A	N/A
Sample Tests (DYNAMIC- -10Pa)									
Indoor Sample	N/A	Indoor Air - Sorbant Tube	N/A	N/A	2-Dec-98	2-Dec-98	13:00	7400000	N/A
Indoor Sample	N/A	Indoor Air - Syringe	N/A	N/A	2-Dec-98	2-Dec-98	15:00	5000	N/A
Indoor Sample	N/A	Indoor Air - Sorbant Tube	N/A	N/A	1-Dec-98	1-Dec-98	16:56	6000000	N/A
Indoor Sample	N/A	Indoor Air - Sorbant Tube	N/A	N/A	30-Nov-98	1-Dec-98	11:32	5800000	N/A
Outdoor Sample	N/A	Outdoor Air - Sorbant Tube	N/A	N/A	1-Dec-98	1-Dec-98	10:56	4320000	N/A
SG-BR (10mE)	0.3	SG Below Greenhouse	N/A	N/A	30-Nov-98	30-Nov-98	15:38	5000	N/A

Table I-1. Results of GC/PID Vapour and Air Testing

Sample Designation	Depth (m)	Sample Type	Sy-ringe	Syringe Wait Time Before Injection	Sample Collect Date	Sample Analysis Date	Anal-ysis Time	Injec-tion Volume (ul)	Sample Volume (L)
SG-BR (10mE)	0.6	SG Below Greenhouse	N/A	N/A	30-Nov-98	30-Nov-98	15:55	5000	N/A
SG-BR (10mE)	0.75	SG Below Greenhouse	N/A	N/A	1-Dec-98	1-Dec-98	16:08	500	N/A
SG-BR (10mE)	0.9	SG Below Greenhouse	N/A	N/A	1-Dec-98	1-Dec-98	16:22	500	N/A
SG-BR (10mE)	1.2	SG Below Greenhouse	N/A	N/A	1-Dec-98	1-Dec-98	16:37	N/A	N/A
SG-BR (10mE)	1.35	SG Below Greenhouse	N/A	N/A	30-Nov-98	30-Nov-98	16:13	160000	N/A
SG-BC	0.15	SG Below Greenhouse	N/A	N/A	26-Nov-98	26-Nov-98	16:38	N/A	N/A
SG-BC	0.3	SG Below Greenhouse	N/A	N/A	26-Nov-98	26-Nov-98	16:54	N/A	N/A
SG-BC	0.45	SG Below Greenhouse	N/A	N/A	26-Nov-98	26-Nov-98	17:10	N/A	N/A
SG-BC	0.6	SG Below Greenhouse	N/A	N/A	27-Nov-98	27-Nov-98	11:00	N/A	N/A
SG-BC	0.75	SG Below Greenhouse	N/A	N/A	27-Nov-98	27-Nov-98	11:22	N/A	N/A
SG-BC	0.9	SG Below Greenhouse	N/A	N/A	27-Nov-98	27-Nov-98	11:40	N/A	N/A
SG-BC	1.2	SG Below Greenhouse	N/A	N/A	27-Nov-98	27-Nov-98	12:53	N/A	N/A
SG-BC	1.5	SG Below Greenhouse	N/A	N/A	27-Nov-98	27-Nov-98	13:11	N/A	N/A
SG-NC	0.17	SG Below Greenhouse	N/A	N/A	27-Nov-98	27-Nov-98	14:59	N/A	N/A
SG-SC	0.17	SG Below Greenhouse	N/A	N/A	27-Nov-98	27-Nov-98	15:15	N/A	N/A
SG-EC	0.17	SG Below Greenhouse	N/A	N/A	27-Nov-98	27-Nov-98	15:30	N/A	N/A
SG-WC	0.17	SG Below Greenhouse	N/A	N/A	27-Nov-98	27-Nov-98	15:56	N/A	N/A
SG-O2 PROBE	0.17	SG Below Greenhouse	N/A	N/A	27-Nov-98	27-Nov-98	13:30	N/A	N/A
Indoor Sample	N/A	Indoor Air - Sorbant Tube	N/A	N/A	24-Nov-98	24-Nov-98	14:53	5900000	N/A
Outdoor Sample	N/A	Outdoor Air - Sorbant Tube	N/A	N/A	24-Nov-98	24-Nov-98	16:24	2710000	N/A
Indoor Sample	N/A	Indoor Air - Sorbant Tube	N/A	N/A	20-Nov-98	20-Nov-98	14:22	1440000	N/A
Outdoor Sample	N/A	Outdoor Air - Sorbant Tube	N/A	N/A	20-Nov-98	20-Nov-98	16:15	2610000	N/A
TD26NOV4	N/A	Flux Chamber hairline crack -10 Pa	N/A	N/A	26-Nov-98	26-Nov-98	14:47	N/A	N/A
February 1999 Program - Site B (Greenhouse)									
Calibration & Quality Control Tests (STATIC-FAN OFF)									
65ng std	N/A	Syringe + 65ng BTX	N/A	N/A	N/A	22-Feb-99	9:05	N/A	N/A
70ng std	N/A	Syringe + 70ng BTX	N/A	N/A	N/A	19-Feb-99	8:49	N/A	N/A
70ng std	N/A	Syringe + 70ng BTX	N/A	N/A	N/A	19-Feb-99	9:07	N/A	N/A
350ng std	N/A	Syringe + 350ng BTX	N/A	N/A	N/A	19-Feb-99	10:21	N/A	N/A
600ng std	N/A	Syringe + 600ng BTX	N/A	N/A	N/A	19-Feb-99	15:08	N/A	N/A
1500ng std	N/A	Syringe + 1500ng BTX	N/A	N/A	N/A	22-Feb-99	9:22	N/A	N/A
1500ng std	N/A	Syringe + 1500ng BTX	N/A	N/A	N/A	19-Feb-99	12:10	N/A	N/A

Date Printed: 8/27/2004

Table I-1. Results of GC/PID Vapour and Air Testing

Sample Designation	Depth (m)	Sample Type	Sy-ringe	Syringe Wait Time Before Injection	Sample Collect Date	Sample Analysis Date	Anal-ysis Time	Injec-tion Volume (ul)	Sample Volume (L)
Syringe 1	N/A	Syringe + Valve (air)	N/A	N/A	N/A	19-Feb-99	9:23	5000	N/A
Syringe 2	N/A	Syringe + Valve (air)	N/A	N/A	N/A	19-Feb-99	9:39	5000	N/A
Syringe 3	N/A	Syringe + Valve (air)	N/A	N/A	N/A	19-Feb-99	10:01	5000	N/A
Syringe 1	N/A	Syringe + Valve (air)	N/A	N/A	N/A	22-Feb-99	9:54	N/A	N/A
Sample Tests (STATIC-FAN OFF)									
SG-BC	0.15	SG Below Greenhouse	N/A	N/A	19-Feb-99	19-Feb-99	10:43	5000	N/A
SG-BC	0.3	SG Below Greenhouse	N/A	N/A	19-Feb-99	19-Feb-99	11:13	5000	N/A
SG-BC	0.45	SG Below Greenhouse	N/A	N/A	19-Feb-99	19-Feb-99	11:51	200	N/A
SG-BC	0.57	SG Below Greenhouse	N/A	N/A	19-Feb-99	19-Feb-99	15:33	200	N/A
SG-BC	0.75	SG Below Greenhouse	N/A	N/A	19-Feb-99	19-Feb-99	16:00	200	N/A
SG-BC	0.9	SG Below Greenhouse	N/A	N/A	19-Feb-99	19-Feb-99	16:24	200	N/A
SG-BR (10mE)	0.3	SG Adjacent to Greenhouse	N/A	N/A	19-Feb-99	19-Feb-99	13:16	5000	N/A
SG-BR (10mE)	0.6	SG Adjacent to Greenhouse	N/A	N/A	19-Feb-99	19-Feb-99	13:41	5000	N/A
SG-BR (10mE)	0.75	SG Adjacent to Greenhouse	N/A	N/A	22-Feb-99	22-Feb-99	10:20	5000	N/A
SG-BR (10mE)	0.9	SG Adjacent to Greenhouse	N/A	N/A	19-Feb-99	19-Feb-99	14:21	200	N/A
SG-BR (10mE)	1.35	SG Adjacent to Greenhouse	N/A	N/A	19-Feb-99	19-Feb-99	14:48	200	N/A
SG-Adjacent to Old Building (AOB): JUNE 25, 1999									
SYRINGE BLANKS									
Syringe 1	N/A	Tube Assembly Blank	N/A	3min 45s	N/A	25-Jun-99	9:20	5000	N/A
Syringe 2	N/A	Tube Assembly Blank	N/A	3min 45s	N/A	25-Jun-99	9:37	5000	N/A
SAMPLES									
SG-AOB	0.3	SG Adjacent to Old Building	#1	3min	25-Jun-99	25-Jun-99	10:53	5000	N/A
SG-AOB	0.6	SG Adjacent to Old Building	#1	2min 55s	25-Jun-99	25-Jun-99	11:15	5000	N/A
SG-AOB	0.9	SG Adjacent to Old Building	#2	2min 54s	25-Jun-99	25-Jun-99	11:51	5000	N/A
SG-AOB	1.2	SG Adjacent to Old Building	#2	2min 50s	25-Jun-99	25-Jun-99	12:09	5000	N/A
SG-AOB	1.35	SG Adjacent to Old Building	#2	3min	25-Jun-99	25-Jun-99	12:30	5000	N/A
SG-(below) Old Building (OB): JUNE 23, 1999									
SYRINGE BLANKS									
Syringe 1	N/A	Tube Assembly Blank	N/A	15min	N/A	23-Jun-99	15:59	5000	N/A
Syringe 3	N/A	Tube Assembly Blank	N/A	15min	N/A	23-Jun-99	15:07	5000	

Date Printed: 8/27/2004

Table I-1. Results of GC/PID Vapour and Air Testing

Sample Designation	Depth (m)	Sample Type	Sy-ringe	Syringe Wait Time Before Injection	Sample Collect Date	Sample Analysis Date	Anal-ysis Time	Injec-tion Volume (ul)	Sample Volume (L)
SAMPLES									
SG-OB	0.3	SG Below Old Building	#1	2min 48s	23-Jun-99	23-Jun-99	16:29	5000	N/A
SG-OB	0.6	SG Below Old Building	#3	3min 5s	23-Jun-99	23-Jun-99	17:06	5000	N/A
SG-(below) OB: JUNE 25, 1999									
SYRINGE BLANKS									
Syringe 3	N/A	Tube Assembly Blank	N/A	3min 45s	N/A	25-Jun-99	9:54	5000	N/A
SAMPLES									
SG-OB	0.3	SG Below Old Building	#3	2min 34s	25-Jun-99	25-Jun-99	12:46	3000	N/A
SG-OB	0.3	SG Below Old Building	#3	2min 45s	25-Jun-99	25-Jun-99	14:35	500	N/A
SG-OB	0.6	SG Below Old Building	#3	3min 6s	25-Jun-99	25-Jun-99	13:06	500	N/A
SG-OB	0.9	SG Below Old Building	#3	2min 40s	25-Jun-99	25-Jun-99	15:17	400	N/A
SG-OB	1.2	SG Below Old Building	#3	2min 30s	25-Jun-99	25-Jun-99	15:37	500	N/A
SG-OB	1.35	SG Below Old Building	#3	2min 50s	25-Jun-99	25-Jun-99	0:00	500	N/A
SG-Adjacent to Building (EO): JULY 14, 1999 - Site B (Greenhouse)									
SYRINGE BLANKS									
Syringe 2	N/A	Tube Assembly Blank	#2	3min 45s	N/A	13-Jul-99	13:30	5000	N/A
SAMPLES									
SG-BE (10mE) (EO)	0.3	SG Adjacent to Greenhouse	#2	3m 40s	14-Jul-99	14-Jul-99	13:15	5000	N/A
SG-BE (10mE) (EO)	0.6	SG Adjacent to Greenhouse	#2	3m 34s	14-Jul-99	14-Jul-99	13:34	5000	N/A
SG-BE (10mE) (EO)	0.75	SG Adjacent to Greenhouse	#2	3m 30s	14-Jul-99	14-Jul-99	13:55	5000	N/A
SG-BE (10mE) (EO)	0.9	SG Adjacent to Greenhouse	#2	3m 30s	14-Jul-99	14-Jul-99	14:15	400	N/A
SG-BE (10mE) (EO)	1.2	SG Adjacent to Greenhouse	#2	5m	14-Jul-99	14-Jul-99	14:44	400	N/A
SG-BE (10mE) (EO)	1.35	SG Adjacent to Greenhouse	#2	3m 20s	14-Jul-99	14-Jul-99	15:20	400	N/A

Notes:

N/A = Not applicable, NC = not calculated,

- = not tested

Calibration Curves Used for Quantification

Calibration Curves Used for Quantification

1. March 1998

Benzene = $(7E\text{-}07R^2 + 0.0405R)/InjVol$

Tolue $E\text{-}07R^2 + 0.0496R)/InjVol$

m&p-$(8E\text{-}07R^2 + 0.0427R)/InjVol$

where R = Response

Injvol = Injection Volume

2. July 1999

Benzene = $(7E\text{-}07R^2 + 0.0218R)/InjVol$

Toluene = $(1E\text{-}06R^2 + 0.0216R)/InjVol$

m&p-Xylene = $(2E\text{-}06R^2 + 0.0228R)/InjVol$

Date Printed: 8/27/2004

Table I-1. Results of GC/PID Vapour and Air Testing

Sample Designation	Injection Conc. (ng/ul)	Mass Injected				Detector Response						Calibration Method
		Benzene (ng)	Toluene (ng)	3-fluoro toluene (ng)	m&p Xylene (ng)	Benzene (mV)	Toluene (mV)	3-fluoro toluene (ng)	Ethyl-benzene (mV)	m&p Xylene (mV)	o-Xylene (mV)	
March 1997 Program - Site E												
pid4ma14	N/A	22.5	22.5	0	22.5	ND	1033	ND	687	943	756	SPC
pid4ma9	N/A	30	30	300	30	ND	1104	3788	722	724	561	SPC
pid4ma11	N/A	45	45	0	45	2316	2062	ND	1328	170	1416	SPC
pid4ma10	N/A	75	75	0	75	ND	2836	ND	1572	2162	1833	SPC
pid4ma15	N/A	N/A	N/A	300	N/A	1826	4147	3523	ND	1449	930	SPC
pid4ma12	N/A	N/A	N/A	300	N/A	16541	3540	3910	687	2453	2329	SPC
pid4ma13	N/A	N/A	N/A	300	N/A	ND	ND	3346	ND	ND	ND	SPC
pid6mar1	N/A	N/A	N/A	250	N/A	ND	ND	3354	ND	ND	ND	SPC
pid6mar2	N/A	N/A	N/A	300	N/A	ND	336	117	ND	669	768	SPC
pidmar4	N/A	N/A	N/A	300	N/A	ND	0	311	ND	ND	ND	SPC
pid6mar5	N/A	N/A	N/A	300	N/A	ND	539	843	ND	ND	ND	SPC
pidmar9	N/A	N/A	N/A	300	N/A	N/A	N/A		N/A	N/A	N/A	SPC
pidmar8	N/A	N/A	N/A	300	N/A	N/A	N/A		N/A	N/A	N/A	SPC
pidma11	N/A	N/A	N/A	300	N/A	N/A	N/A		N/A	N/A	N/A	SPC
pidma10	N/A	N/A	N/A	300	N/A	N/A	N/A		N/A	N/A	N/A	SPC
td17ma17	N/A	N/A	N/A	300	N/A	N/A	N/A		N/A	N/A	N/A	SPC
td17ma17	N/A	N/A	N/A	300	N/A	N/A	N/A		N/A	N/A	N/A	SPC
50 ng std	N/A	50	50	50	50	875	804	-	775	895	747	SPC
100 ng std	N/A	100	100	100	100	1858	1768	-	1564	1818	1621	SPC
250 ng std	N/A	250	250	250	250	3629	3297	-	2947	3513	2946	SPC
500 ng std	N/A	500	500	500	500	6464	5616	-	4800	5897	4841	SPC
100 ng std	N/A	100	100	100	100	1904	1734	-	1527	1841	1547	SPC
Site A 0.6M QC Fail	N/A	N/A	N/A	N/A	N/A	4792	1537	-	-	465	-	SPC
Site A 0.9m QC Fail	N/A	N/A	N/A	N/A	N/A	46182	28252	-	-	10094	-	SPC
Site A 1.2m QC Fail	N/A	N/A	N/A	N/A	N/A	40706	33163	-	-	11721	-	SPC
Site A 1.2m QC Fail	N/A	N/A	N/A	N/A	N/A	48947	36272	-	-	18019	-	SPC
Site A 0.9M	N/A	N/A	N/A	N/A	N/A	9755	6752	-	-	1938	-	SPC
Site A 0.6M	N/A	N/A	N/A	N/A	N/A	27320	20643	-	-	6596	-	SPC
Site A 0.6m - 3rd	N/A	N/A	N/A	N/A	N/A	6780	5080	-	-	1255	-	SPC

Date Printed: 8/27/2004

Table I-1. Results of GC/PID Vapour and Air Testing

Sample Designation	Injection Conc. (ng/ul)	Mass Injected				Detector Response						Calibration Method
		Benzene (ng)	Toluene (ng)	3-fluoro toluene (ng)	m&p Xylene (ng)	Benzene (mV)	Toluene (mV)	3-fluoro toluene (ng)	Ethyl-benzene (mV)	m&p Xylene (mV)	o-Xylene (mV)	
												RSD
Site A 0.3m	N/A	N/A	N/A	N/A	N/A	137	260	-	-	0	-	SPC
Site A 0.3m -4th	N/A	N/A	N/A	N/A	N/A	90	109	-	-		-	SPC
												RSD
Site A 1.2 m -2nd	N/A	N/A	N/A	N/A	N/A	22075	20441	-	-	6163	-	SPC
Site A 1.2m -3rd	N/A	N/A	N/A	N/A	N/A	16772	16561	-	-	4163	-	SPC
Site A 0.3m -2nd QC Fail	N/A	N/A	N/A	N/A	N/A	0	0	-	-	0	-	SPC
Site A 0.6m -2nd QC Fail	N/A	N/A	N/A	N/A	N/A	0	0	-	-	0	-	SPC
Site B 1.2 m	N/A	N/A	N/A	N/A	N/A	24778	27859	-	-	2624	-	SPC
Site B 1.2m -2nd	N/A	N/A	N/A	N/A	N/A	28677	28201	-	-	2711	-	SPC
												RSD
Site B 0.9m	N/A	N/A	N/A	N/A	N/A	12810	16083	-	-	1348	-	SPC
Site B 0.9m -2nd	N/A	N/A	N/A	N/A	N/A	23290	24595	-	-	2559	-	SPC
												RSD
Site B 0.6m	N/A	N/A	N/A	N/A	N/A	307	618	-	-	205	-	SPC
Site B 0.6m -2nd	N/A	N/A	N/A	N/A	N/A	306	695	-	-	312	-	SPC
												RSD
Site B 0.3m	N/A	N/A	N/A	N/A	N/A	0	0	-	-	0	-	SPC
May 1997 Program - Site B -												
sg13may1	500	800	800	-	800	4741.9	5087.8	0	4895.74	5628.6	4888.62	SPC
sg13may2	250	475	475	-	475	4033.86	4106.03	0	3656	4363.87	3642.15	SPC
sg13may3	250	400	400	-	400	2830.77	3002.87	0	2875	3305.65	2813.53	SPC
sg13may4	100	160	160	-	160	1523.93	1513.2	0	1358	1589.4	1330.47	SPC
SG-BC (sg13ma24)	N/A	N/A	N/A	0	N/A	1384.52	3257.79	0	<DL	756.49	<DL	SPC
SG-BC (sg13ma25)	N/A	N/A	N/A	0	N/A	756.26	1282.82	0	<DL	213.33	<DL	SPC
SG-BC (sg13ma26)	N/A	N/A	N/A	0	N/A	-	-	0	<DL	-	<DL	SPC
SG-BC (sg13ma27)	N/A	N/A	N/A	0	N/A	22980	28626	0	<DL	1781	<DL	SPC
SG-BC (sg13ma28)	N/A	N/A	N/A	0	N/A	141.56	193.78	0	<DL	-	<DL	SPC
SG-BC (sg13ma28)	N/A	N/A	N/A	0	N/A	141.56	193.78	0	<DL	-	<DL	SPC
SG-BC (sg13ma29)	N/A	N/A	N/A	0	N/A	12021	16216	0	<DL	935.04	<DL	SPC

Date Printed: 8/27/2004

Table I-1. Results of GC/PID Vapour and Air Testing

Sample Designation	Injection Conc. (ng/ul)	Mass Injected				Detector Response						Calibration Method
		Benzene (ng)	Toluene (ng)	3-fluoro toluene (ng)	m&p Xylene (ng)	Benzene (mV)	Toluene (mV)	3-fluoro toluene (ng)	Ethyl-benzene (mV)	m&p Xylene (mV)	o-Xylene (mV)	
SG-BC (sg13ma30)	N/A	N/A	N/A	0	N/A	16802.72	23232	0	<DL	1464.77	<DL	SPC
SG-BC (sg13ma31)	N/A	N/A	N/A	0	N/A	15159.67	22188.15	0	<DL	1350.83	<DL	SPC
					RSD-SAMP	**7.3**	**3.3**			**5.7**		
SG-BC (sg13ma32)	N/A	N/A	N/A	0	N/A	15159.67	22188.15	0	1350.83	-	<DL	SPC
June 1997 Program - Site B												
sg24jun1	250	325	325	-	325	2601.35	2432.96	-	2287.79	2659.71	2263.24	SPC
sg24jun2	500	725	725	-	725	5362.51	5234.43	-	4743.91	5953.55	4721.01	SPC
sg24jun3	1500	2100	2100	-	2100	12606.81	12076.02	-	11007.53	12735.7	11293.53	SPC
SG-BC (sg24jun4)	N/A	N/A	N/A	-	N/A	<DL	<DL	-	<DL	<DL	<DL	SPC
SG-BC (sg24jun5)	N/A	N/A	N/A	-	N/A	1233.73	<DL	-	<DL	<DL	<DL	SPC
SG-BC (sg24jun6)	N/A	N/A	N/A	-	N/A	126.66	308.03	-	<DL	<DL	<DL	SPC
SG-BC (sg24jun7)	N/A	N/A	N/A	-	N/A	<DL	<DL	-	<DL	<DL	<DL	SPC
SG-BC (sg24jun8)	N/A	N/A	N/A	-	N/A	686.14	1736.68	-	<DL	103.79	<DL	SPC
SG-BC (sg24jun14)	N/A	N/A	N/A	-	N/A	1394.7	1868.7	-	<DL	110.38	<DL	SPC
SG-BC (sg24jun9)	N/A	N/A	N/A	-	N/A	7552.63	6181.36	-	<DL	152.76	<DL	SPC
SG-BC (sg24jun17)	N/A	N/A	N/A	-	N/A	12331.26	10048.08	-	<DL	290.67	<DL	SPC
SG-BC (sg24jun10)	N/A	N/A	N/A	-	N/A	13628.12	14085.84	-	<DL	425.3	<DL	SPC
SG-BC (sg24jun16)	N/A	N/A	N/A	-	N/A	14118.83	11676.58	-	<DL	370.13	<DL	SPC
						34070.3	35214.6			1063.25		
					RSD-SAMP	**58.6**	**71.0**			**68.4**		
sg24jun11	500	650	650	-	650	5983.21	5848.47	-	4836.04	5700.25	4703.95	SPC
sg24jun12	1500	1800	1800	-	1800	9467.04	8721.84	-	7957.26	9172.93	7861.59	SPC
sg24jun13	1500	1800	1800	-	1800	9101.33	8561.3	-	7729.53	8928.67	7511.29	SPC
					RSD-SYR	**2.79**	**1.31**			**1.91**		
SG-BC (sg24jun18)	N/A	N/A	N/A	-	N/A	8160.05	12646.98	-	<DL	663.58	<DL	SPC
SG-BC (sg24jun19)	N/A	N/A	N/A	-	N/A	5994.7	8878.85	-	<DL	244.57	<DL	SPC
					RSD-SAMP	**21.6**	**24.8**			**65.3**		
SG-BC (sg24jun20)	N/A	N/A	N/A	-	N/A	20276.95	19198.07	-	<DL	479.49	<DL	SPC
SG-BC (sg24jun21)	N/A	N/A	N/A	-	N/A	22899.01	23337.83	-	<DL	778.57	<DL	SPC
					RSD-SAMP	**8.6**	**13.8**			**33.6**		
July 15 1997 Program - Site												

Date Printed: 8/27/2004

Table I-1. Results of GC/PID Vapour and Air Testing

Sample Designation	Injection Conc. (ng/ul)	Mass Injected				Detector Response						Calibration Method
		Benzene (ng)	Toluene (ng)	3-fluoro toluene (ng)	m&p Xylene (ng)	Benzene (mV)	Toluene (mV)	3-fluoro toluene (ng)	Ethyl-benzene (mV)	m&p Xylene (mV)	o-Xylene (mV)	
July 15 1997 Program - Site	100	110	110	-	110	822.25	801.82	-	-	801.04	-	SPC
sg15jul15	250	300	300	-	300	1629.1	1610.75	-	-	1799.4	-	SPC
sg15jul16	250	550	550	-	550	3060.17	2926.89	-	-	3283.04	-	SPC
sg15jul17	1500	1650	1650	-	1650	7437.37	7079	-	-	7759.66	-	SPC
sg15jul18	1500	3450	3450	-	3450	12674.99	11840.49	-	-	12659.41	-	SPC
sg15jul19	100	140	140	-	140	888.13	850.03	-	-	815.93	-	SPC
sg15ju18	1500	1650	1650	-	1650	7059.29	6829.62	-	-	7402.75	-	SPC
sg15ju19	1500	1800	1800	-	1800	7254.51	6829.62	-	-	7392.92	-	SPC
sg15ju28	1500	1650	1650	-	1650	7095.22	6901.54	-	-	7345.95	-	SPC
sg15ju29	1500	1500	1500	-	1500	6496.24	6250.08	-	-	6856.98	-	SPC
sg15ju30	250	550	550	-	550	2764.96	2770.33	-	-	3057.72	-	SPC
SG-BC (sg15jul19)	N/A	N/A	N/A	-	N/A	128	261	-	<DL	<100	<DL	MPC
SG-BC (sg15jul10)	N/A	N/A	N/A	-	N/A	<100	<100	-	<DL	<DL	<DL	MPC
SG-BC (sg15jul11)	N/A	N/A	N/A	-	N/A	<100	164	-	<DL	<DL	<DL	MPC
SG-BC (sg15jul12)	N/A	N/A	N/A	-	N/A	<DL	<50	-	<DL	<DL	<DL	MPC
SG-BC (sg15jul13)	N/A	N/A	N/A	-	N/A	<100	213	-	<DL	<100	<DL	MPC
SG-BC (sg15jul14)	N/A	N/A	N/A	-	N/A	<DL	<50	-	<DL	<DL	<DL	MPC
SG-BC (sg15jul15)	N/A	N/A	N/A	-	N/A	1255	670	-	<DL	<100	<DL	MPC
SG-BC (sg15jul16)	N/A	N/A	N/A	-	N/A	<DL	<DL	-	<DL	<DL	<DL	MPC
SG-BC (sg15jul20)	N/A	N/A	N/A	-	N/A	5772	3569	-	<DL	<DL	<DL	MPC
SG-BC (sg15jul21)	N/A	N/A	N/A	-	N/A	14563	8389	-	<DL	116	<DL	MPC
												RSD
SG-BC (sg15jul22)	N/A	N/A	N/A	-	N/A	3623	4246	-	<DL	162	<DL	MPC
SG-BC (sg15jul23)	N/A	N/A	N/A	-	N/A	11510	3550	-	<DL	652	<DL	MPC
												RSD
SG-BC (sg15jul24)	N/A	N/A	N/A	-	N/A	7719	7629	-	<DL	209	<DL	MPC
SG-BC (sg15jul25)	N/A	N/A	N/A	-	N/A	<DL	<DL	-	<DL	<DL	<DL	MPC
SG-BC (sg15jul26)	N/A	N/A	N/A	-	N/A	5662	5246	-	<DL	110	<DL	MPC

Date Printed: 8/27/2004

Table I-1. Results of GC/PID Vapour and Air Testing

Z11

Sample Designation	Injection Conc. (ng/ul)	Mass Injected				Detector Response						Calibration Method
		Benzene (ng)	Toluene (ng)	3-fluoro toluene (ng)	m&p Xylene (ng)	Benzene (mV)	Toluene (mV)	3-fluoro toluene (ng)	Ethyl-benzene (mV)	m&p Xylene (mV)	o-Xylene (mV)	
SG-BC (sg15ju27)	N/A	N/A	N/A	-	N/A	10603	11057	-	<DL	265	<DL	MPC
												RSD
July 28 1997 Program - Site												
N/A	100	100	100	-	100	582.5	580.6	-	-	591.4	-	SPC
N/A	100	130	130	-	130	626.5	620.1	-	-	614.9	-	SPC
N/A	250	300	300	-	300	1265.1	1355.4	-	-	1546.7	-	SPC
N/A	250	325	325	-	325	1566.2	1624.1	-	-	1811.6	-	SPC
N/A	500	800	800	-	800	3274.8	3128.5	-	-	3367.4	-	SPC
N/A	500	900	900	-	900	3801.8	3630.5	-	-	3811.2	-	SPC
N/A	1000	1200	1200	-	1200	4237.2	4512.9	-	-	4062.2	-	SPC
N/A	1500	2700	2700	-	2700	9474.6	9199.2	-	-	9248.3	-	SPC
N/A	1500	3900	3900	-	3900	12517.8	11903.7	-	-	11622.9	-	SPC
N/A	1500	4050	4050	-	4050	12217.8	11269	-	-	11530.5	-	SPC
SG-BC	N/A	N/A	N/A	N/A	N/A	283	856	-	<DL	<100	<DL	MPC
SG-BC	N/A	N/A	N/A	N/A	N/A	<DL	<DL	-	<DL	<DL	<DL	MPC
												RSD
SG-BC	N/A	N/A	N/A	N/A	N/A	1193	1481	-	<DL	<100	<DL	MPC
SG-BC	N/A	N/A	N/A	N/A	N/A	1178	1032	-	<DL	<100	<DL	MPC
												RSD
SG-BC	N/A	N/A	N/A	N/A	N/A	<100	385	-	<DL	121	<DL	MPC
SG-BC	N/A	N/A	N/A	N/A	N/A	<100	249	-	<DL	<100	<DL	MPC
												RSD
SG-BC	N/A	N/A	N/A	N/A	N/A	1316	1913	-	<DL	131	<DL	MPC
SG-BC	N/A	N/A	N/A	N/A	N/A	1140	1648	-	<DL	<100	<DL	MPC
												RSD
SG-BC	N/A	N/A	N/A	N/A	N/A	14713	14959	-	<DL	403	<DL	MPC
SG-BC	N/A	N/A	N/A	N/A	N/A	6417	6475	-	<DL	136	<DL	MPC
												RSD
SG-BC	N/A	N/A	N/A	N/A	N/A	10644	11479	-	<DL	428	<DL	MPC
SG-BC	N/A	N/A	N/A	N/A	N/A	9178	11040	-	<DL	445	<DL	MPC
												RSD

Date Printed: 8/27/2004

Table I-1. Results of GC/PID Vapour and Air Testing

Sample Designation	Injection Conc. (ng/ul)	Mass Injected				Detector Response						Calibration Method
		Benzene (ng)	Toluene (ng)	3-fluoro toluene (ng)	m&p Xylene (ng)	Benzene (mV)	Toluene (mV)	3-fluoro toluene (ng)	Ethyl-benzene (mV)	m&p Xylene (mV)	o-Xylene (mV)	
SG-BC	N/A	N/A	N/A	N/A	N/A	11384	13196	-	<DL	432	<DL	MPC
SG-BC	N/A	N/A	N/A	N/A	N/A	9483	10873	-	<DL	336	<DL	MPC
												RSD
SG-BC	N/A	N/A	N/A	N/A	N/A	8050	8624		<DL	210	<DL	MPC
SG-BC	N/A	N/A	N/A	N/A	N/A	11429	11998		<DL	335	<DL	MPC
												RSD
September 1997 Program - S												
SG09Sep1	100	120	120	-	120	376.4	368.47		312.55	368.91	336.65	SPC
SG09Sep2	100	120	120	-	120	379.98	367.78		308.28	367.09	326.41	SPC
SG09Sep3	250	300	300	-	300	870.14	882.3		824.73	975.13	806.52	SPC
SG09Sep4	500	600	600	-	600	1510.03	1471.14		1344.98	1563.74	1313.89	SPC
SG09Sep5	1000	1800	1800	-	1800	3991.14	3894.75		3704.41	4316.52	3706.76	SPC
SG09Sep6	1500	2100	2100	-	2100	4412.4	4045.51		3732.16	4308.7	3677.16	SPC
SG09Sep6	3000	3600	3600	-	3600	5564.69	6736.86		7189.91	8634.5	7519.51	SPC
SG-BC (SG09SE19)	N/A	N/A	N/A	N/A	N/A	189.4	405.4		<DL	-	<DL	SPC
SG-BC (SG09SEP9)	N/A	N/A	N/A	N/A	N/A	147.5	275.8		<DL	-	<DL	SPC
SG-BC (SG09SE20)	N/A	N/A	N/A	N/A	N/A	622.5	2120.11		<DL	198.1	<DL	SPC
SG-BC (SG09SE11)	N/A	N/A	N/A	N/A	N/A	169.58	532.56		<DL	-	<DL	SPC
SG-BC (SG09SE12)	N/A	N/A	N/A	N/A	N/A	1274.46	1408.16		<DL	-	<DL	SPC
SG-BC (SG09SE13)	N/A	N/A	N/A	N/A	N/A	6385.92	9040.5		<DL	585.6	<DL	SPC
SG-BC (SG09SE14)	N/A	N/A	N/A	N/A	N/A	3787.39	5890.83		<DL	323.4	<DL	SPC
SG-BC (SG09SE15)	N/A	N/A	N/A	N/A	N/A	6191.97	7501.43		<DL	317.66	<DL	SPC
SG09SE16	3000	3900	3900	-	3900	5864.92	6719.35		7078.22	8441.14	7500.42	SPC
SG09SE18	1500	1800	1800	-	1800	4438.52	4456.55		4033.12	4778.84	4044.34	SPC
SG09SE21	500	700	700	-	700	1931.65	1890.9		1681.19	1994.13	1667.3	SPC
September 1997 Program - S												
SG10SE2	100	140	140	-	140	459.34	462.25		393.98	437.24	430.11	SPC
SG10SE3	250	350	350	-	350	1093.08	1090.27		1428.79	1178.05	948.59	SPC
SG10SE4	500	750	750	-	750	1938.06	1880.49		1725.8	2049.06	1744.58	SPC
SG10SE5	1000	1600	1600	-	1600	4437.41	4251.8		3919.76	4592.42	3917.33	SPC

Date Printed: 8/27/2004

Table I-1. Results of GC/PID Vapour and Air Testing

Sample Designation	Injection Conc. (ng/ul)	Mass Injected				Detector Response						Calibration Method
		Benzene (ng)	Toluene (ng)	3-fluoro toluene (ng)	m&p Xylene (ng)	Benzene (mV)	Toluene (mV)	3-fluoro toluene (ng)	Ethyl-benzene (mV)	m&p Xylene (mV)	o-Xylene (mV)	
SG10SE6	1500	2100	2100	-	2100	5326.01	4662.1		4178.88	4878.05	4130.55	SPC
SG10SE7	3000	4200	4200	-	4200	5866.85	7072.52		7466.33	8973.2	7849.67	SPC
0.17m South (sg10sep8)	N/A	N/A	N/A	N/A	N/A	1710.9	5869.3		<DL	565.2	<DL	SPC
0.17m East (sg10sep9)	N/A	N/A	N/A	N/A	N/A	1354.56	3346.38		<DL	370.44	<DL	SPC
0.4m South (sg10se10)	N/A	N/A	N/A	N/A	N/A	189.1	634.64		<DL	-	<DL	SPC
0.4m East (sg10se11)	N/A	N/A	N/A	N/A	N/A	7091.86	14184.03		<DL	1284.15	<DL	SPC
0.7m South (sg10se14)	N/A	N/A	N/A	N/A	N/A	-	462.92		<DL	-	<DL	SPC
1.6m South (sg10se15)	N/A	N/A	N/A	N/A	N/A	3973.65	8656.81		<DL	349.4	<DL	SPC
0.7m East (sg10se19)	N/A	N/A	N/A	N/A	N/A	4980.6	3958.8		<DL	145.5	<DL	SPC
1.6 m North (sg10se23)	N/A	N/A	N/A	N/A	N/A	9270.99	9266.08		<DL	475.2	<DL	SPC
0.17 m North (sg10se24)	N/A	N/A	N/A	N/A	N/A	261.8	787.7		<DL	-	<DL	SPC
0.17 m West (sg10se26)	N/A	N/A	N/A	N/A	N/A	721.16	1831.97		<DL	178.05	<DL	SPC
1.6 m West (sg10se27)	N/A	N/A	N/A	N/A	N/A	1264.2	3805.96		<DL	-	<DL	SPC
0.17m Centre (sg10se28	N/A	N/A	N/A	N/A	N/A	5710.09	5375.36		<DL	106.98	<DL	SPC
SG10SE16	500	700	700	-	700	1616.17	1613.95		1469.34	1749.34	1444.06	SPC
SG10SE17	1500	1800	1800	-	1800	4681.98	4604.89		4168.53	4915.13	4088.1	SPC
SG10SE19	1500	1800	1800	-	1800	4681.98	4604.89		4168.53	4915.13	4088.1	SPC
SG10SE29	1500	2550	2550	-	2550	5229.6	5017.96		4522.27	5232.36	4442.01	SPC
SG12SEP1	100	120	120	-	120	345.54	360.56		315.3	384.14	329.14	SPC
SG12SEP2	500	650	650	-	650	1531.75	1554.37		1444.12	1695.65	1417.38	SPC
SG12SEP3	1500	2100	2100	-	2100	4538.67	4348.21		3864.35	4590.28	3848.72	SPC
SG12SEP8	1500	3600	3600	-	3600	7427.25	7262.86		6695.61	8117.12	6734.36	SPC
SG12SEP11	1000	1200	1200	-	1200	2630.31	2838.98		2635.95	3067.29	2543.51	SPC
0.4m N Outside (SG12SEP4	N/A	N/A	N/A	N/A	N/A	370.74	980.4		<DL	-	<DL	SPC
0.7m N Outside (SG12SEP9	N/A	N/A	N/A	N/A	N/A	8207.06	4239.99		<DL	207.99	<DL	SPC
0.7m E Outside (SG12SEP6	N/A	N/A	N/A	N/A	N/A	283.94	1244.42		<DL	320.58	<DL	SPC
0.4m E Outside (SG12SEP7	N/A	N/A	N/A	N/A	N/A	2656.86	8369.45		<DL	1511.08	<DL	SPC
October 21 1997 Program - S												
SG21OCT1	100	120	120	-	120	368.86	370.03		319.98	378.39	336.74	SPC
SG21OCT2	250	325	325	-	325	937.94	912.49		867.08	978.96	813.85	SPC

Date Printed: 8/27/2004

Table I-1. Results of GC/PID Vapour and Air Testing

Sample Designation	Injection Conc. (ng/ul)	Mass Injected				Detector Response						Calibration Method
		Benzene (ng)	Toluene (ng)	3-fluoro toluene (ng)	m&p Xylene (ng)	Benzene (mV)	Toluene (mV)	3-fluoro toluene (ng)	Ethyl-benzene (mV)	m&p Xylene (mV)	o-Xylene (mV)	
SG21OCT3	500	700	700	-	700	1722.51	1701.09		1526.44	1865.79	1510.07	SPC
SG21OCT4	1000	1300	1300	-	1300	2846.17	2845.07		2572.68	3023.37	2542.54	SPC
SG21OC11	2000	4600	4600	-	4600	8363.57	8177.28		7231.25	8830.24	7449.81	SPC
SG-BC((SG21OCT5)	N/A	N/A	N/A	N/A	N/A	-	-		-	-	-	SPC
SG-BC((SG21OCT6)	N/A	N/A	N/A	N/A	N/A	-	109.07		-	<DL	-	SPC
SG-BC((SG21OCT7)	N/A	N/A	N/A	N/A	N/A	-	-		-	-	-	SPC
SG-BC((SG21OCT8)	N/A	N/A	N/A	N/A	N/A	441	1121		-	124	-	SPC
SG-BC((SG21OCT9)	N/A	N/A	N/A	N/A	N/A	8752	9259		-	376	-	SPC
SG-BC((SG21OC10)	N/A	N/A	N/A	N/A	N/A	6999	8424		-	335	-	SPC
SG-BC((SG21OC12)	N/A	N/A	N/A	N/A	N/A	6342	7561		-	330	-	SPC
SG-BC((SG21OC13)	N/A	N/A	N/A	N/A	N/A	8250	9672		-	447	-	SPC
October 28/29 1997 Program												
SG28OC22	2000	5600	5600	-	5600	7881.71	7883.84		7725.28	8773.82	8160.86	SPC
SG28OC7	2000	4400	4400	-	4400	7892.81	7964		7768.21	8728.89	7826.24	SPC
SG28OC15	2000	2800	2800	-	2800	5883.36	5990.17		4894.93	6646.75	5491.81	SPC
SG28OC6	2000	2600	2600	-	2600	4881.85	4925.34		4679.36	5514.32	4749.4	SPC
SG28OC5	1500	1950	1950	-	1950	3544.14	3801.93		4070.17	4583.28	3958.54	SPC
SG28OC4	1000	1200	1200	-	1200	2899.92	3058.24		2920.32	3541.24	3006.33	SPC
SG28OC3	500	650	650	-	650	1628.44	1728.87		1596.06	1874.89	1585.38	SPC
SG28OC2	250	350	350	-	350	1011.36	973.79		899.44	1054.7	891.66	SPC
SG28OC1	100	110	110	-	110	334.61	386.35		373.74	434.09	398.95	SPC
0.7m East (sg28oc23)	N/A	N/A	N/A	N/A	N/A	4280.9	3472.76		<DL	141.58	<DL	SPC
0.17m West (sg28oc21)	N/A	N/A	N/A	N/A	N/A	694.83	1995.14		<DL	172.57	<DL	SPC
1.6m West (sg28oc20)	N/A	N/A	N/A	N/A	N/A	4273.93	8985.06		<DL	139.73	<DL	SPC
0.17 Centre (sg28oc19)	N/A	N/A	N/A	N/A	N/A	5749.31	7886.62		<DL	219.08	<DL	SPC
0.17 North(sg28oc18)	N/A	N/A	N/A	N/A	N/A	-	111.25		<DL	-	<DL	SPC
1.6 North(sg28oc17)	N/A	N/A	N/A	N/A	N/A	7229.48	5281.43		<DL	147.97	<DL	SPC
0.7 East (sg28oc16)	N/A	N/A	N/A	N/A	N/A	16694	14154		<DL	801	<DL	SPC
0.4 East (sg28oc12)	N/A	N/A	N/A	N/A	N/A	743.7	2229		<DL	584	<DL	SPC
0.7 South (sg28oc11)	N/A	N/A	N/A	N/A	N/A	-	158		<DL	117	<DL	SPC
0.4 South (sg28oc10)	N/A	N/A	N/A	N/A	N/A	-	-		<DL	-	<DL	SPC

Date Printed: 8/27/2004

Table I-1. Results of GC/PID Vapour and Air Testing

Sample Designation	Injection Conc. (ng/ul)	Mass Injected				Detector Response						Calibration Method
		Benzene (ng)	Toluene (ng)	3-fluoro toluene (ng)	m&p Xylene (ng)	Benzene (mV)	Toluene (mV)	3-fluoro toluene (ng)	Ethyl-benzene (mV)	m&p Xylene (mV)	o-Xylene (mV)	
0.17 East (sg28oc9)	N/A	N/A	N/A	N/A	N/A	-	245		<DL	-	<DL	SPC
0.17 South (sg28oc8)	N/A	N/A	N/A	N/A	N/A	-	175		<DL	-	<DL	SPC
1.6 South (sg28oc14)	N/A	N/A	N/A	N/A	N/A	5209	9481		<DL	472	<DL	SPC
0.4 North Out (sg29oc6)	N/A	N/A	N/A	N/A	N/A	246	375		<DL	-	<DL	SPC
0.7 North Out (sg29oc8)	N/A	N/A	N/A	N/A	N/A	724	924		<DL	-	<DL	SPC
0.4 East Out (sg29oc9)	N/A	N/A	N/A	N/A	N/A	258	893		<DL	-	<DL	SPC
0.7 East Out (sg29oc7)	N/A	N/A	N/A	N/A	N/A	1808	2117		<DL	121	<DL	SPC
SG29OC10	250	350	350	-	350	849.87	882.69		766.5	846.38	828.56	N/A
SG29OC2	100	120	120	-	120	352.6	352.5		291.2	357.4	315.9	N/A
November 28 1997 (during 3												
SG-BC (SG28NOV9)	N/A	N/A	N/A	N/A	N/A	1213	3680		<DL	139	<DL	N/A
SG-BC (SG28NO10)	N/A	N/A	N/A	N/A	N/A	173	2717		<DL	13	<DL	N/A
SG-BC (SG28NO11)	N/A	N/A	N/A	N/A	N/A	522	2247		<DL	-	<DL	N/A
SG-BC (SG28NO12)	N/A	N/A	N/A	N/A	N/A	2368	2354		<DL	-	<DL	N/A
SG-BC (SG28NO14)	N/A	N/A	N/A	N/A	N/A	3436	3932		<DL	144	<DL	N/A
SG-BC (SG28NO15)	N/A	N/A	N/A	N/A	N/A	5721	7509		<DL	362	<DL	N/A
SG-BC (SG28NO15)	N/A	N/A	N/A	N/A	N/A	5721	7509		<DL	362	<DL	N/A
SG-BC (SG28NO16)	N/A	N/A	N/A	N/A	N/A	5162	6714		<DL	334	<DL	N/A
SG-BC (SG28NO17)	N/A	N/A	N/A	N/A	N/A	6373	7185		<DL	337	<DL	N/A
SG-BC (SG28NO18)	N/A	N/A	N/A	N/A	N/A	4163	5399		<DL	<DL	<DL	N/A
SG-BC (SG28NO21)	N/A	N/A	N/A	N/A	N/A	109	1842		<DL	7 mm	<DL	N/A
SG-BC (SG28NO22)	N/A	N/A	N/A	N/A	N/A	1259	3699		<DL	246	<DL	N/A
SG-BC (SG28NO23)	N/A	N/A	N/A	N/A	N/A	3806	10246		<DL	388	<DL	N/A
SG-BC (SG28NO24)	N/A	N/A	N/A	N/A	N/A	756	3152		<DL	128	<DL	N/A
SG28NOV1	100	100	100	-	100	289.02	384.51		456.48	557.74	522.89	N/A
SG28NOV7	N/A	N/A	N/A	N/A	N/A	<DL	<DL		<DL	<DL	<DL	N/A
SG28NOV2	100	120	120	-	120	492.77	614.53		578.03	696.56	635.74	N/A
SG28NOV3	500	700	700	-	700	1074.97	1157.95		1161.65	1398.31	1157.86	N/A
SG28NOV4	1000	1400	1400	-	1400	2139.32	2129.71		1985.52	2348.63	1936.92	N/A
SG28NOV5	1500	1800	1800	-	1800	2461.62	2682.04		2644.75	3195.53	2852.51	N/A
SG28NOV6	1500	3450	3450	-	3450	4268.98	4789.62		4639.31	5566.31	4694.64	N/A

Date Printed: 8/27/2004

Table I-1. Results of GC/PID Vapour and Air Testing

Sample Designation	Injection Conc. (ng/ul)	Mass Injected				Detector Response						Calibration Method
		Benzene (ng)	Toluene (ng)	3-fluoro toluene (ng)	m&p Xylene (ng)	Benzene (mV)	Toluene (mV)	3-fluoro toluene (ng)	Ethyl-benzene (mV)	m&p Xylene (mV)	o-Xylene (mV)	
SG28NO13	5000	6000	6000	-	6000	6159.08	6438.12		6320.84	7311.41	6409.83	N/A
SG28NO25	5000	11000	11000	-	11000	9791.06	10296.15		988.6	11590.56	10234.71	N/A
SG28NOV7	N/A	N/A	N/A	N/A	N/A	103.81	422.42		<DL	<DL	<DL	N/A
December 1, 1997 10 m East												
SG-BR (10mE)	N/A	N/A	N/A	N/A	N/A	9479	665		<DL	<DL	<DL	N/A
SG-BR (10mE)	N/A	N/A	N/A	N/A	N/A	377.47	296.98		<DL	mm@156 m	<DL	N/A
SG-BR (10mE)	N/A	N/A	N/A	N/A	N/A	mm@156m'	254.21		<DL	mm@156m'	<DL	N/A
SG-BR (10mE)	N/A	N/A	N/A	N/A	N/A	<DL	7 mm		<DL	<DL	<DL	N/A
SG01DEC5	N/A	N/A	N/A	N/A	N/A	<DL	152.47		<DL	<DL	<DL	N/A
SG01DEC4	1000	1400	1400	-	1400	1934.64	2028.14		1867.38	2240	1882	N/A
SG01DEC3	500	700	700	-	700	919.98	1114.35		1198.71	1446.38	1239.95	N/A
SG01DEC2	250	350	350	-	350	550.21	670.51		732.17	898.73	755.74	N/A
SG01DEC1	100	120	120	-	120	278.12	403.87		-	676.17	654.23	N/A
SG-BR (10mE) sg03dec8	N/A	N/A	N/A	N/A	N/A	3mm@156 m	112.04		<DL	<DL	<DL	N/A
SG-BR (10mE) sg03dec7	N/A	N/A	N/A	N/A	N/A	<DL	<DL		<DL	<DL	<DL	N/A
SG-BR (10mE) sg03dec9	N/A	N/A	N/A	N/A	N/A	<DL	125		<DL	<DL	<DL	N/A
SG01DEC6	N/A	N/A	N/A	N/A	N/A	<DL	mm @156 mV		<DL	<DL	<DL	N/A
October 1997 Program - Flu												
TD03OCT2 Tube 1	N/A	N/A	N/A	N/A	N/A	1709.2	23440.38	<DL	<DL	5935	<DL	SPC
TD03OCT2 Tube 2	N/A	N/A	N/A	N/A	N/A	1709.2	23440.38	<DL	<DL	5935	<DL	SPC
TD14OCT3 Tube 1	N/A	N/A	N/A	N/A	N/A	978.98	18241.5	<DL	<DL	<DL	<DL	SPC
TD14OCT4 Tube 2	N/A	N/A	N/A	N/A	N/A	11943.5	14908	<DL	<DL	<DL	<DL	SPC
TD14OCT6 Tube 1	N/A	N/A	N/A	N/A	N/A	403.92	1629.12	<DL	<DL	2203.95	<DL	SPC
TD24OCT1 Tube 2	N/A	N/A	N/A	N/A	N/A	<DL	<DL	<DL	<DL	<DL	<DL	SPC
TD24OCT5 Tube 2	N/A	N/A	N/A	N/A	N/A	499	1485	<DL	<DL	1394	<DL	SPC
TD21OCT2 Tube 1	N/A	N/A	N/A	N/A	N/A	2806.68	5089.67	<DL	<DL	8002.65	<DL	SPC
TD21OCT3 Tube 2	N/A	N/A	N/A	N/A	N/A	<DL	<DL	<DL	<DL	<DL	<DL	SPC
TD23OCT2 Tube 4	N/A	N/A	N/A	N/A	N/A	2351.56	6863.31	?	<DL	3618.03	<DL	SPC
TD23OCT3 Tube 5	N/A	N/A	N/A	N/A	N/A	<DL	<DL	?	<DL	<DL	<DL	SPC
TD23OCT1	500	500	500	-	500	1650.75	1463.59	981.74	1614.19	1302.03	-	N/A
TD22OCT1 Tube 4	N/A	N/A	N/A	N/A	N/A	<DL	<DL	<DL	<DL	<DL	<DL	SPC

Date Printed: 8/27/2004

Table I-1. Results of GC/PID Vapour and Air Testing

Sample Designation	Injection Conc. (ng/ul)	Mass Injected				Detector Response						Calibration Method
		Benzene (ng)	Toluene (ng)	3-fluoro toluene (ng)	m&p Xylene (ng)	Benzene (mV)	Toluene (mV)	3-fluoro toluene (ng)	Ethyl-benzene (mV)	m&p Xylene (mV)	o-Xylene (mV)	
TD22OCT1 Tube 5	N/A	N/A	N/A	N/A	N/A	139	<DL	<DL	<DL	<DL	<DL	SPC
TD24OCT6 Tube 4	N/A	N/A	N/A	N/A	N/A	5060.2	16147.99	<DL	<DL	16540.74	<DL	SPC
TD27OCT4 Tube 4	N/A	N/A	N/A	N/A	N/A	881.44	647.25	<DL	<DL	<DL	<DL	SPC
TD27OCT2 Tube 5	N/A	N/A	N/A	N/A	N/A	<DL	<DL	<DL	<DL	<DL	<DL	SPC
TD23OCT5 Tube 4&5	N/A	N/A	N/A	N/A	N/A	<DL	<DL	<DL	<DL	<DL	<DL	SPC
TD24OCT2	250	250	250	-	250	881.17	756.45	982.67	660.73	832.05	652.72	N/A
TD24OCT3	500	550	550	-	550	1518.73	1364.04	883.12	1178.49	1528.16	1212.9	N/A
TD24OCT4	1000	1100	1100	-	1100	2887.88	2638.44	1301.48	2251.27	2866.82	2308.04	N/A
TD27OCT1	1000	1000	1000	-	1000	2918.45	2729.8	1153.54	2410.74	2983.07	2417.5	N/A
TD27OCT3	2000	4000	4000	-	4000	8307.1	7701.75	1544.52	6649.47	8639.44	7423.81	N/A
TD30OCT3 Tube 4	N/A	N/A	N/A	N/A	N/A	566.89	2399.15	<DL	<DL	2834.57	<DL	SPC
TD30OCT4 Tube 5	N/A	N/A	N/A	N/A	N/A	<DL	<DL	894.54	<DL	<DL	<DL	SPC
TD30OCT5	1000	1100	1100	-	1100	2370.26	2177.25	1044.89	1848.54	2353.3	1888.59	N/A
TD30OCT2	500	500	500	-	500	1293.17	1291.23	912.72	1170.3	1496.38	1204.84	N/A
TD30OCT1	100	100	100	-	100	300.1	275.53	954.77	183.83	342.73	240.2	N/A
TD29OCT1 Tube 4&5	N/A	N/A	N/A	?	N/A	<DL	<DL	<DL	<DL	<DL	<DL	N/A
November 1997 Program - Ir												
TD06NO15 Tube 5	N/A	N/A	N/A	N/A	N/A	1084.25	2353.46	1058.1	<DL	427.17	<DL	SPC
TD06NO8 Tube 5	N/A	N/A	N/A	N/A	N/A	2836.51	6383.71	1323.19	190.84	1137.87	522.78	SPC
TD06NO2 Tube 5	N/A	N/A	N/A	N/A	N/A	<DL	<DL	<DL	<DL	<DL	<DL	N/A
TD06NO13 Tube 3	N/A	N/A	N/A	N/A	N/A	182.65	1404.39	371.04	<DL	158.43	<DL	N/A
TD06NO4 Tube 3&4	N/A	N/A	N/A	N/A	N/A	<DL	<DL	<DL	<DL	<DL	<DL	N/A
TD06NO10 Tube 1	N/A	N/A	N/A	N/A	N/A	<DL	<DL	<DL	<DL	<DL	<DL	N/A
TD06NO10 Tube 1	N/A	N/A	N/A	N/A	N/A	<DL	<DL	<DL	<DL	<DL	<DL	N/A
TD06NO5 Tube 1	N/A	N/A	N/A	N/A	N/A	949	2271	477.45	<DL	408.81	<DL	N/A
TD06NO5 Tube 2	N/A	N/A	N/A	N/A	N/A	949	2271	477.45	<DL	408.81	<DL	N/A
TD06NO7	100	110	110	-	110	275.73	285.66	1045.93	229.57	263.69	266.15	N/A
TD06NO16	500	550	550	-	550	1089.68	1244.33	1192.04	1353.59	1700.97	1399.15	N/A
TD06NOV1	500	550	550	-	550	1179.67	1336.68	984.14	1395.5	1791.24	1452.38	N/A
TD06NOV3	1000	1000	1000	-	1000	2145.11	2072.01	1290.43	1817.05	2334.78	1890.34	N/A
TD06NOV9	2000	2000	2000	-	2000	3840.02	3942.04	1242.48	3788.99	4903.66	4105.43	N/A
TD12NOV2 Tube 1	N/A	N/A	N/A	N/A	N/A	346.71	835.35	561.75	<DL	338.66	<DL	SPC

Date Printed: 8/27/2004

Table I-1. Results of GC/PID Vapour and Air Testing

Sample Designation	Injection Conc. (ng/ul)	Mass Injected				Detector Response						Calibration Method
		Benzene (ng)	Toluene (ng)	3-fluoro toluene (ng)	m&p Xylene (ng)	Benzene (mV)	Toluene (mV)	3-fluoro toluene (ng)	Ethyl-benzene (mV)	m&p Xylene (mV)	o-Xylene (mV)	
TD12NOV6 Tube 1	N/A	N/A	N/A	N/A	N/A	<DL	190	<DL	<DL	<DL	<DL	SPC
TD12NOV3 Tube 2	N/A	N/A	N/A	N/A	N/A	186.25	201.85	<DL	<DL	<DL	<DL	SPC
TD12NOV5 Tube 2	N/A	N/A	N/A	N/A	N/A	<DL	122.24	146.73	<DL	<DL	<DL	SPC
TD11NO3 Tube 2	N/A	N/A	N/A	N/A	N/A	<DL	<DL	<DL	<DL	<DL	<DL	N/A
TD11NOV6 Tube 4	N/A	N/A	N/A	N/A	N/A	1253.3	2167.34	322.83	594.07	2961.58	1586.9	N/A
TD12NOV9 Tube 5	N/A	N/A	N/A	N/A	N/A	N/A	N/A	909.67	N/A	N/A	N/A	N/A
TD12NOV4	250	250	250	-	250	388.77	629.24	753.48	559.78	708.07	569.8	N/A
TD11NOV5	500	500	500	-	500	1116.65	1384.91	923.98	1519.34	1951.93	1595.19	N/A
TD12NOV1	1000	1000	1000	-	1000	1862.5	1969.44	821.14	1887.28	2488.11	2005.7	N/A
TD10OCT2 Tube 4&5	N/A	N/A	N/A	N/A	N/A	<DL	<DL	<DL	<DL	<DL	<DL	N/A
TD13NOV6	N/A	N/A	N/A	N/A	N/A	230.92	1864.7	250.31	120.4	323.7	282.44	N/A
TD11NOV7 Tube 4	N/A	N/A	N/A	N/A	N/A	<DL	<DL	<DL	<DL	<DL	<DL	N/A
TD13NOV2 Tube 1	N/A	N/A	N/A	N/A	N/A	804.33	3751.44	806.17	<DL	634.25	<DL	SPC
TD12NOV8 Tube 1	N/A	N/A	N/A	N/A	N/A	<DL	<DL	<DL	<DL	<DL	<DL	N/A
TD13NOV3 Tube 2	N/A	N/A	N/A	N/A	N/A	592.13	1004.46	616.72	<DL	378.42	<DL	SPC
TD12NOV7 Tube 2	N/A	N/A	N/A	N/A	N/A	<DL	<DL	<DL	<DL	<DL	<DL	N/A
TD13NOV4	250	250	250	-	250	692.04	622.3	748.86	546.14	706.04	556.44	N/A
TD13NOV1	500	500	500	-	500	1302.49	1248.91	702.97	1318.94	1747.16	1380.63	N/A
TD13NOV5	2000	2000	2000	-	2000	3502.19	2031.34	966.14	4024.32	5117.14	4422.39	N/A
TD13NO10	N/A	N/A	N/A	N/A	N/A	717.72	4285.14	862	482	2523.92	-	N/A
TD12NO10 Tube 5	N/A	N/A	N/A	N/A	N/A	<DL	<DL	<DL	<DL	<DL	<DL	N/A
TD17NOV2 Tube 4	N/A	N/A	N/A	N/A	N/A	2354.13	5184.14	960.32	342.33	1916.02	636.74	N/A
	N/A	N/A	N/A	N/A	N/A	<DL	<DL	<DL	<DL	<DL	<DL	N/A
March 1998 Program - Site E												
Gasblk1	N/A	N/A	N/A	-	N/A	<DL	<DL	-	<DL	<DL	<DL	N/A
S100A	N/A	350	350	-	350	3015	2999	-	2762	3490	2822	N/A
S250A	N/A	350	350	-	350	7124	7099	-	6490	8069	6678	N/A
S1000A	N/A	275	275	-	275	20795	17840	-	15146	18138	15348	N/A
S1000B	N/A	600	600	-	600	36334	33421	-	29156	34934	29080	N/A
S1000C	N/A	775	775	-	775	43952	41548	-	36146	41846	37126	N/A
S100B	N/A	300	300	-	300	2676	2751	-	2572	3250	2610	N/A

Date Printed: 8/27/2004

Table I-1. Results of GC/PID Vapour and Air Testing

Sample Designation	Injection Conc. (ng/ul)	Mass Injected				Detector Response						Calibration Method
		Benzene (ng)	Toluene (ng)	3-fluoro toluene (ng)	m&p Xylene (ng)	Benzene (mV)	Toluene (mV)	3-fluoro toluene (ng)	Ethyl-benzene (mV)	m&p Xylene (mV)	o-Xylene (mV)	
S250B	N/A	300	300	-	300	6367	6327	-	5815	7313	5928	N/A
-	N/A	N/A	N/A	-	N/A	<DL	<DL	-	<DL	<DL	<DL	MPC
-	N/A	N/A	N/A	-	N/A	<DL	<DL	-	<DL	<DL	<DL	MPC
Syn #1 - Run1	N/A	N/A	N/A	-	N/A	<DL	591	-	<DL	<DL	<DL	MPC
Syn #1 - Run2	N/A	N/A	N/A	-	N/A	<DL	<DL	-	<DL	<DL	<DL	MPC
Syn #1 - Run3	N/A	N/A	N/A	-	N/A	<DL	<DL	-	<DL	<DL	<DL	MPC
Syn #3 - Run1	N/A	N/A	N/A	-	N/A	<DL	157	-	<DL	<DL	<DL	MPC
Syn #3 - Run2	N/A	N/A	N/A	-	N/A	<DL	224	-	<DL	<DL	<DL	MPC
Syn #3 - Run3	N/A	N/A	N/A	-	N/A	<DL	~40	-	<DL	<DL	<DL	MPC
Syn #3 - Run4	N/A	N/A	N/A	-	N/A	~45	242	-	<DL	<DL	<DL	MPC
Syn #4 - Run1	N/A	N/A	N/A	-	N/A	159	200	-	<DL	<DL	<DL	MPC
Syn #4 - Run2	N/A	N/A	N/A	-	N/A	579	626	-	<DL	~60	<DL	MPC
Syn #5 - Run1	N/A	N/A	N/A	-	N/A	<DL	<DL	-	<DL	<DL	<DL	MPC
Syn #5 - Run2	N/A	N/A	N/A	-	N/A	1534	3627	-	170	<DL	<DL	MPC
Syn #5 - Run3	N/A	N/A	N/A	-	N/A	<DL	<DL	-	<DL	<DL	<DL	MPC
Syn #6 - Run1	N/A	N/A	N/A	-	N/A	607	1197	-	169	<DL	<DL	MPC
Syn #6 - Run2	N/A	N/A	N/A	-	N/A	9279	9386	-	612	<DL	<DL	MPC
Syn #6 - Run3	N/A	N/A	N/A	-	N/A	437	605	-	160	<DL	<DL	MPC
Syn #6 - Run4	N/A	N/A	N/A	-	N/A	2425	3043	-	211	<DL	<DL	MPC
Syn #6 - Run5	N/A	N/A	N/A	-	N/A	233	408	-	<DL	<DL	<DL	MPC
SG-BR (10mE)	N/A	N/A	N/A	-	N/A	<DL	<DL	-	<DL	<DL	<DL	MPC
SG-BR (10mE)	N/A	N/A	N/A	-	N/A	<DL	174.5	-	<DL	<DL	<DL	MPC
SG-BR (10mE)	N/A	N/A	N/A	-	N/A	36511	16462	-	<DL	682	<DL	MPC
SG-BR (10mE)	N/A	N/A	N/A	-	N/A	45670	35302	-	<DL	1800	<DL	MPC
SG-BC	N/A	N/A	N/A	-	N/A	<DL	<DL	-	<DL	<DL	<DL	MPC
SG-BC	N/A	N/A	N/A	-	N/A	258.3	11056	-	<DL	2656	<DL	MPC
SG-BC	N/A	N/A	N/A	-	N/A	6401	48926	-	<DL	2949	<DL	MPC
SG-BC	N/A	N/A	N/A	-	N/A	41495	54658	-	<DL	7034	<DL	MPC

Date Printed: 8/27/2004

Table I-1. Results of GC/PID Vapour and Air Testing

Sample Designation	Injection Conc. (ng/ul)	Mass Injected				Detector Response						Calibration Method
		Benzene (ng)	Toluene (ng)	3-fluoro toluene (ng)	m&p Xylene (ng)	Benzene (mV)	Toluene (mV)	3-fluoro toluene (ng)	Ethyl-benzene (mV)	m&p Xylene (mV)	o-Xylene (mV)	
SG-BC	N/A	N/A	N/A	-	N/A	48211	58384	-	<DL	7369	<DL	MPC
June 1998 Program - Site B												
Standard #1	N/A	12	12	-	12	329	321	-	N/A	306	N/A	N/A
Standard #2	N/A	65	65	-	65	1519	1524	-	N/A	1700	N/A	N/A
Standard #3	N/A	150	150	-	150	3204	3554	-	N/A	3619	N/A	N/A
Standard #4	N/A	750	750	-	750	12937	13756	-	N/A	15485	N/A	N/A
Standard #5	N/A	2200	2200	-	2200	37952	39745	-	N/A	44568	N/A	N/A
Standard #6	N/A	3400	3400	-	3400	43566	47250	-	N/A	50299	N/A	N/A
Standard #7	N/A	4800	4800	-	4800	47391	52685	-	N/A	55419	N/A	N/A
SG-BC	N/A	N/A	N/A	-	N/A	158	1053	-	N/A	8 mm	N/A	SPC
SG-BC	N/A	N/A	N/A	-	N/A	7 mm	496	-	N/A	6 mm	N/A	SPC
SG-EC	N/A	N/A	N/A	-	N/A	210	696	-	N/A	10 mm	N/A	SPC
SG-EC	N/A	N/A	N/A	-	N/A	204	803	-	N/A	10 mm	N/A	SPC
SG-SC	N/A	N/A	N/A	-	N/A	205	798	-	N/A	141	N/A	SPC
SG-SC	N/A	N/A	N/A	-	N/A	252	1117	-	N/A	365	N/A	SPC
SG-WC	N/A	N/A	N/A	-	N/A	5 mm	232	-	N/A	4 mm	N/A	SPC
SG-NC	N/A	N/A	N/A	-	N/A	4 mm	223	-	N/A	5 mm	N/A	SPC
SG-O2 PROBE	N/A	N/A	N/A	-	N/A	1279	3671	-	N/A	184	N/A	SPC
SG-BC	N/A	N/A	N/A	-	N/A	185	1093	-	N/A	103	N/A	SPC
SG-BC	N/A	N/A	N/A	-	N/A	423	1157	-	N/A	210	N/A	SPC
SG-BC	N/A	N/A	N/A	-	N/A	38800	46482	-	N/A	3614	N/A	SPC
SG-BC	N/A	N/A	N/A	-	N/A	3535	5968	-	N/A	388	N/A	SPC
SG-BC	N/A	N/A	N/A	-	N/A	22975	30854	-	N/A	1296	N/A	SPC
SG-BC	N/A	N/A	N/A	-	N/A	47109	54152	-	N/A	3838	N/A	SPC
SG-EC	N/A	N/A	N/A	-	N/A	54716	54544	-	N/A	8185	N/A	SPC
SG-SC	N/A	N/A	N/A	-	N/A	low resp.	276	-	N/A	4108	N/A	SPC
SG-SC	N/A	N/A	N/A	-	N/A	2443	6496	-	N/A	388	N/A	SPC
SG-WC	N/A	N/A	N/A	-	N/A	51179	70276	-	N/A	5605	N/A	SPC
SG-NC	N/A	N/A	N/A	-	N/A	46335	46988	-	N/A	3097	N/A	SPC
SG-BR (10mE)	N/A	N/A	N/A	-	N/A	66553	59745	-	N/A	8110	N/A	SPC

Date Printed: 8/27/2004

Table I-1. Results of GC/PID Vapour and Air Testing

Sample Designation	Injection Conc. (ng/ul)	Mass Injected				Detector Response						Calibration Method
		Benzene (ng)	Toluene (ng)	3-fluoro toluene (ng)	m&p Xylene (ng)	Benzene (mV)	Toluene (mV)	3-fluoro toluene (ng)	Ethyl-benzene (mV)	m&p Xylene (mV)	o-Xylene (mV)	
December 1998 Program - S												
Calibration & Quality Contro												
Syringe 1	N/A	N/A	N/A	-	N/A	5384.56	10675.01	-	1699.52	1506.25	<DL	SPC
Syringe 1	N/A	N/A	N/A	-	N/A	129.58	242.83	-	115.33	137.74	<DL	SPC
Syringe 1	N/A	N/A	N/A	-	N/A	3204.78	8366.89	-	<DL	504.83	<DL	SPC
60ng std	N/A	60	60	-	60	3925.5	3775.05	-	3346.91	4067.13	3322.84	SPC
60ng std	N/A	60	60	-	60	3840.93	3625.95	-	3135.88	3960.52	3141.12	SPC
300ng std	N/A	300	300	-	300	16927.33	15638.25	-	13421.12	17117.12	13767.6	SPC
Sorbant Tube 1	N/A	N/A	N/A	-	N/A	<DL	251.35	-	<DL	<DL	<DL	SPC
Sorbant Tube 5	N/A	N/A	N/A	-	N/A	<DL	131.53	-	<DL	<DL	<DL	SPC
800ng std	N/A	800	800	-	800	3339.03	3047.73	-	2628.35	3176.2	2566.96	SPC
Sorbant Tube 1	N/A	N/A	N/A	-	N/A	<DL	156.91	-	<DL	<DL	<DL	SPC
Sorbant Tube 5	N/A	N/A	N/A	-	N/A	<DL	154.9	-	<DL	<DL	<DL	SPC
800ng std	N/A	800	800	-	800	3352.44	2816.19	-	2400.96	2901.28	2372.47	SPC
Sorbant Tube 1	N/A	N/A	N/A	-	N/A	<DL	113.89	-	<DL	<DL	<DL	SPC
Sorbant Tube 5	N/A	N/A	N/A	-	N/A	<DL	136.02	-	<DL	<DL	<DL	SPC
Sorbant Tube 5	N/A	N/A	N/A	-	N/A	<DL	121.11	-	<DL	<DL	<DL	SPC
575ng std	N/A	575	575	-	575	2273.16	1982.94	-	1722.1	2132.14	1690.06	SPC
115ng std	N/A	115	115	-	115	506.82	384.1	-	386.35	482.66	386.3	SPC
Sorbant Tube 5	N/A	N/A	N/A	-	N/A	<DL	<DL	-	<DL	<DL	<DL	SPC
60ng std	N/A	60	60	-	60	283.86	269.88	-	198.31	222.96	236.07	SPC
550ng std	N/A	550	550	-	550	2109.64	1968.22	-	1724.07	2055.71	1722.77	SPC
800ng std	N/A	800	800	-	800	2893.07	2569.81	-	2228.2	2682.02	2202.94	SPC
2400ng std	N/A	2400	2400	-	2400	7046.04	6885.09	-	6024.22	7190.15	5966.53	SPC
Sample Tests (DYNAMIC- -1												
Indoor Sample	N/A	N/A	N/A	-	N/A	4199.89	5918.01	-	<DL	297.25	<DL	SPC
SG-BR (10mE)	N/A	N/A	N/A	-	N/A	4377.82	864.45	-	<DL	<DL	<DL	SPC
Indoor Sample	N/A	N/A	N/A	-	N/A	343.61	4938.65	-	<DL	241.6	<DL	SPC
SG-BR (10mE)	N/A	N/A	N/A	-	N/A	390.81	122.59	-	<DL	<DL	<DL	SPC
Indoor Sample	N/A	N/A	N/A	-	N/A	1886.83	2787.32	-	<DL	159.56	<DL	SPC
SG-BR (10mE)	N/A	N/A	N/A	-	N/A	518.33	270.57	-	<DL	<DL	<DL	SPC
SG-BR (10mE)	N/A	N/A	N/A	-	N/A	1246.07	872.85	-	<DL	<DL	<DL	SPC

Date Printed: 8/27/2004

Table I-1. Results of GC/PID Vapour and Air Testing

Sample Designation	Injection Conc. (ng/ul)	Mass Injected				Detector Response						Calibration Method
		Benzene (ng)	Toluene (ng)	3-fluoro toluene (ng)	m&p Xylene (ng)	Benzene (mV)	Toluene (mV)	3-fluoro toluene (ng)	Ethyl-benzene (mV)	m&p Xylene (mV)	o-Xylene (mV)	
Indoor Sample	N/A	N/A	N/A	-	N/A	2383.58	3684.54	-	<DL	213.45	<DL	SPC
SG-BC	N/A	N/A	N/A	-	N/A	7624.33	9548.91	-	N/A	214.79	343.53	SPC
SG-NC	N/A	N/A	N/A	-	N/A	2355.19	3512.65	-	<DL	130.09	<DL	SPC
SG-SC	N/A	N/A	N/A	-	N/A	3772.88	5190.36	-	<DL	142.07	<DL	SPC
SG-EC	N/A	N/A	N/A	-	N/A	3320.35	2521.61	-	<DL	<DL	<DL	SPC
SG-WC	N/A	N/A	N/A	-	N/A	1670.71	2746.6	-	<DL	<DL	<DL	SPC
SG-MW	N/A	N/A	N/A	-	N/A	5507.2	7958.98	-	<DL	189.64	<DL	SPC
November/December 1998 P												
Calibration & Quality Contro												
Sorbant Tube 1	N/A	N/A	N/A	-	N/A	<DL	<DL	-	<DL	<DL	<DL	SPC
Sorbant Tube 5	N/A	N/A	N/A	-	N/A	<DL	<DL	-	<DL	<DL	<DL	SPC
Sorbant Tube 5	N/A	N/A	N/A	-	N/A	<DL	<DL	-	<DL	<DL	<DL	SPC
6400ng std	N/A	6400	6400	-	6400	9969.97	16099.83	-	13102.91	17175.01	14660.75	SPC
11000ng std	N/A	11000	11000	-	11000	36845.97	26469.65	-	20400.85	25955.84	22408.59	SPC
Syringe 1	N/A	N/A	N/A	-	N/A	164.51	498.32	-	<DL	250.34	<DL	SPC
12ng std	N/A	12	12	-	12	1027.6	1410.32	-	1330.76	1583.9	1287.62	SPC
300ng std	N/A	300	300	-	300	17167.51	16436.71	-	N/A	18110.16	15066.45	SPC
Sorbant Tube 1	N/A	N/A	N/A	-	N/A	<DL	<DL	-	<DL	<DL	<DL	SPC
Sorbant Tube 5	N/A	N/A	N/A	-	N/A	<DL	<DL	-	<DL	<DL	<DL	SPC
60ng std	N/A	60	60	-	60	452.94	423.21	-	318.09	352.66	355.42	SPC
60ng std	N/A	60	60	-	60	311.63	357.71	-	212.72	264.85	263.99	SPC
550ng std	N/A	550	550	-	550	2903.9	2650.1	-	2132.48	2793.18	2157.93	SPC
12000ng std	N/A	12000	12000	-	12000	35611.56	28351.87	-	21087.43	28350.79	23882.82	SPC
Syringe 1	N/A	N/A	N/A	-	N/A	<DL	214.67	-	<DL	<DL	<DL	SPC
Syringe 2	N/A	N/A	N/A	-	N/A	<DL	287.46	-	<DL	<DL	<DL	SPC
Syringe 4	N/A	N/A	N/A	-	N/A	<DL	192.33	-	<DL	<DL	<DL	SPC
12ng std	N/A	12	12	-	12	412.12	476.07	-	258.24	139.2	262.01	SPC
300ng std	N/A	300	300	-	300	1879.89	1832.62	-	N/A	1973.02	1637.52	SPC
12000ng std	N/A	12000	12000	-	12000	27462.35	26915.04	-	24998.66	28742.76	25588.71	SPC
2400ng std	N/A	2400	2400	-	2400	10628.62	10196.91	-	N/A	10544.74	9197.26	SPC
Sorbant Tube 1	N/A	N/A	N/A	-	N/A	<DL	<DL	-	<DL	<DL	<DL	SPC
4600ng std	N/A	4600	4600	-	4600	18728.8	17914.8	-	N/A	17997.92	15539.57	SPC

Date Printed: 8/27/2004

Table I-1. Results of GC/PID Vapour and Air Testing

Sample Designation	Injection Conc. (ng/ul)	Mass Injected				Detector Response						Calibration Method
		Benzene (ng)	Toluene (ng)	3-fluoro toluene (ng)	m&p Xylene (ng)	Benzene (mV)	Toluene (mV)	3-fluoro toluene (ng)	Ethyl-benzene (mV)	m&p Xylene (mV)	o-Xylene (mV)	
2400ng std	N/A	2400	2400	-	2400	11180.87	10622.71	-	N/A	11056.87	9569.81	SPC
2400ng std	N/A	2400	2400	-	2400	11085.36	10446.92	-	N/A	10898.18	9272.39	SPC
Sorbant Tube 1	N/A	N/A	N/A	-	N/A	2522.37	<DL	-	<DL	<DL	<DL	SPC
Sorbant Tube 1	N/A	N/A	N/A	-	N/A	<DL	<DL	-	<DL	<DL	<DL	SPC
Sorbant Tube2	N/A	N/A	N/A	-	N/A	<DL	<DL	-	<DL	<DL	<DL	SPC
550ng std	N/A	550	550	-	550	4354.79	3781.14	-	3072.32	4030.48	3202.64	SPC
2400ng std	N/A	2400	2400	-	2400	13789.54	12008.23	-	9767.45	13305.13	11170.7	SPC
Sorbant Tube 1	N/A	N/A	N/A	-	N/A	<DL	<DL	-	<DL	<DL	<DL	SPC
Sorbant Tube 2	N/A	N/A	N/A	-	N/A	<DL	<DL	-	<DL	<DL	<DL	SPC
Sorbant Tube 3	N/A	N/A	N/A	-	N/A	<DL	<DL	-	<DL	<DL	<DL	SPC
60ng std	N/A	60	60	-	60	714.24	610.93	-	486.03	628.03	494.77	SPC
600ng std	N/A	600	600	-	600	2421.42	2136.47	-	1707.11	4081.2	1903.07	SPC
2400ng std	N/A	2400	2400	-	2400	16468.91	13853.71	-	10901.21	14769.09	11944.32	SPC
4400ng std	N/A	4400	4400	-	4400	29013.36	24145.51	-	18831.07	25256.06	20948.22	SPC
12ng std	N/A	12	12	-	12	149.9	140.61	-	N/A	113.47	111.57	SPC
Syringe 1	N/A	N/A	N/A	-	N/A	<DL	<DL	-	<DL	<DL	<DL	SPC
Syringe 2	N/A	N/A	N/A	-	N/A	<DL	<DL	-	<DL	<DL	<DL	SPC
Syringe 2	N/A	N/A	N/A	-	N/A	<DL	<DL	-	<DL	<DL	<DL	SPC
Syringe 2	N/A	N/A	N/A	-	N/A	<DL	<DL	-	<DL	<DL	<DL	SPC
Syringe 4	N/A	N/A	N/A	-	N/A	<DL	<DL	-	<DL	<DL	<DL	SPC
12ng std	N/A	12	12	-	12	185.8	177.37	-	N/A	177.53	145.95	SPC
12ng std	N/A	12	12	-	12	170.32	162.11	-	N/A	145.22	147.5	SPC
60ng std	N/A	60	60	-	60	776.79	701.71	-	N/A	700.95	767.02	SPC
12ng std	N/A	12	12	-	12	260.07	246.91	-	178.89	175.7	204.75	SPC
60ng std	N/A	60	60	-	60	799.52	784.83	-	N/A	1005.36	847.89	SPC
Sample Tests (DYNAMIC- -1												
Indoor Sample	N/A	N/A	N/A	-	N/A	15091.92	43751.78	-	270.8	4636.76	559.97	SPC
Indoor Sample	N/A	N/A	N/A	-	N/A	12978.9	19827.06	-	N/A	1606.55	N/A	SPC
Indoor Sample	N/A	N/A	N/A	-	N/A	18253.39	48244.51	-	117.11	4497.7	316.93	SPC
Indoor Sample	N/A	N/A	N/A	-	N/A	18270.21	43541.02	-	148.35	4438.62	187.83	SPC
Outdoor Sample	N/A	N/A	N/A	-	N/A	N/A	2155.68	-	N/A	686.09	300.75	SPC
SG-BR (10mE)	N/A	N/A	N/A	-	N/A	1032.51	1485.96	-	<DL	<DL	<DL	SPC

Date Printed: 8/27/2004

Table I-1. Results of GC/PID Vapour and Air Testing

Sample Designation	Injection Conc. (ng/ul)	Mass Injected				Detector Response						Calibration Method
		Benzene (ng)	Toluene (ng)	3-fluoro toluene (ng)	m&p Xylene (ng)	Benzene (mV)	Toluene (mV)	3-fluoro toluene (ng)	Ethyl-benzene (mV)	m&p Xylene (mV)	o-Xylene (mV)	
SG-BR (10mE)	N/A	N/A	N/A	-	N/A	15312.35	5117.15	-	<DL	241.7	<DL	SPC
SG-BR (10mE)	N/A	N/A	N/A	-	N/A	15934.18	9229.36	-	<DL	686.06	<DL	SPC
SG-BR (10mE)	N/A	N/A	N/A	-	N/A	10182.59	6552.27	-	<DL	570.28	<DL	SPC
SG-BR (10mE)	N/A	N/A	N/A	-	N/A	7382.41	4890.6	-	<DL	290.16	<DL	SPC
SG-BR (10mE)	N/A	N/A	N/A	-	N/A	52459.31	38290.24	-	<DL	5058.27	<DL	SPC
SG-BC	N/A	N/A	N/A	-	N/A	7166.51	7908.84	-	<DL	222.21	<DL	SPC
SG-BC	N/A	N/A	N/A	-	N/A	18028.34	20175.64	-	<DL	812.3	<DL	SPC
SG-BC	N/A	N/A	N/A	-	N/A	10912.67	10085.74	-	343.44	168	<DL	SPC
SG-BC	N/A	N/A	N/A	-	N/A	12378.45	11112.97	-	<DL	183.29	<DL	SPC
SG-BC	N/A	N/A	N/A	-	N/A	11391.59	9762.42	-	<DL	306.62	<DL	SPC
SG-BC	N/A	N/A	N/A	-	N/A	8416.36	8320.17	-	<DL	325.11	<DL	SPC
SG-BC	N/A	N/A	N/A	-	N/A	12503.02	12314.55	-	<DL	505.85	<DL	SPC
SG-BC	N/A	N/A	N/A	-	N/A	15921.52	14971.86	-	<DL	556.68	<DL	SPC
SG-NC	N/A	N/A	N/A	-	N/A	8240.91	7709.62	-	<DL	173.08	<DL	SPC
SG-SC	N/A	N/A	N/A	-	N/A	6906.19	8142.45	-	<DL	160.74	<DL	SPC
SG-EC	N/A	N/A	N/A	-	N/A	3710.07	3009.49	-	<DL	<DL	<DL	SPC
SG-WC	N/A	N/A	N/A	-	N/A	7403.61	8456.13	-	<DL	169.91	<DL	SPC
SG-O2 PROBE	N/A	N/A	N/A	-	N/A	6896.13	7208.84	-	<DL	132.42	<DL	SPC
Indoor Sample	N/A	N/A	N/A	-	N/A	2646.11	19054.32	-	261.28	6409.44	697.43	SPC
Outdoor Sample	N/A	N/A	N/A	-	N/A	351.82	281.53	-	<DL	<DL	<DL	SPC
Indoor Sample	N/A	N/A	N/A	-	N/A	15215.03	23824.1	-	<DL	3720.26	374.52	SPC
Outdoor Sample	N/A	N/A	N/A	-	N/A	195.5	393.12	-	<DL	374.35	<DL	SPC
TD26NOV4	N/A	N/A	N/A	-	N/A	113000	92000	-	<DL	940	<DL	SPC
February 1999 Program - Sit Calibration & Quality Contro												
65ng std	N/A	65	65	-	65	255.88	252.3	-	N/A	228.88	227.72	SPC
70ng std	N/A	70	70	-	70	270.31	267.78	-	213.32	247.11	231.67	SPC
70ng std	N/A	70	70	-	70	3047.56	3045.97	-	N/A	3338.12	2677.27	SPC
350ng std	N/A	350	350	-	350	1003.15	966.27	-	N/A	1014.59	843.8	SPC
600ng std	N/A	600	600	-	600	1761.67	1737.98	-	1540.66	1810.32	1512.75	SPC
1500ng std	N/A	1500	1500	-	1500	3264.38	3171.55	-	N/A	3417.8	280.87	SPC
1500ng std	N/A	1500	1500	-	1500	3281.23	3241.13	-	2921.89	3364.93	2855.32	SPC

Date Printed: 8/27/2004

Table I-1. Results of GC/PID Vapour and Air Testing

Sample Designation	Injection Conc. (ng/ul)	Mass Injected				Detector Response						Calibration Method
		Benzene (ng)	Toluene (ng)	3-fluoro toluene (ng)	m&p Xylene (ng)	Benzene (mV)	Toluene (mV)	3-fluoro toluene (ng)	Ethyl-benzene (mV)	m&p Xylene (mV)	o-Xylene (mV)	
Syringe 1	N/A	N/A	N/A	-	N/A	<DL	<DL	-	<DL	<DL	<DL	SPC
Syringe 2	N/A	N/A	N/A	-	N/A	157.66	787.03	-	<DL	<DL	<DL	SPC
Syringe 3	N/A	N/A	N/A	-	N/A	<DL	<DL	-	<DL	<DL	<DL	SPC
Syringe 1	N/A	N/A	N/A	-	N/A	<DL	<DL	-	<DL	<DL	<DL	SPC
Sample Tests (STATIC-FAN												
SG-BC	N/A	N/A	N/A	-	N/A	139.13	337.33	-	<DL	<DL	<DL	SPC
SG-BC	N/A	N/A	N/A	-	N/A	<DL	114.75	-	<DL	<DL	<DL	SPC
SG-BC	N/A	N/A	N/A	-	N/A	426.92	3117.17	-	<DL	215.94	<DL	SPC
SG-BC	N/A	N/A	N/A	-	N/A	800.95	4076.14	-	<DL	177.4	<DL	SPC
SG-BC	N/A	N/A	N/A	-	N/A	2552.36	3858	-	<DL	168.71	<DL	SPC
SG-BC	N/A	N/A	N/A	-	N/A	4250.28	5915.8	-	<DL	299.03	<DL	SPC
SG-BR (10mE)	N/A	N/A	N/A	-	N/A	<DL	<DL	-	<DL	<DL	<DL	SPC
SG-BR (10mE)	N/A	N/A	N/A	-	N/A	260.24	157.72	-	<DL	<DL	<DL	SPC
SG-BR (10mE)	N/A	N/A	N/A	-	N/A	6051.35	2547.89	-	<DL	<DL	<DL	SPC
SG-BR (10mE)	N/A	N/A	N/A	-	N/A	1750.25	950.59	-	<DL	<DL	<DL	SPC
SG-BR (10mE)	N/A	N/A	N/A	-	N/A	4458.82	2857.35	-	<DL	208.67	<DL	SPC
SG-Adjacent to Old Building												
SYRINGE BLANKS												
Syringe 1	N/A	N/A	N/A	-	N/A	<100	123.32	-	N/A	<100	N/A	MPC
Syringe 2	N/A	N/A	N/A	-	N/A	<100	269.38	-	N/A	<100	N/A	MPC
SAMPLES												
SG-AOB	N/A	N/A	N/A	-	N/A	<100	232.47	-	N/A	<100	N/A	MPC
SG-AOB	N/A	N/A	N/A	-	N/A	<100	135.01	-	N/A	<100	N/A	MPC
SG-AOB	N/A	N/A	N/A	-	N/A	<100	206.23	-	N/A	<100	N/A	MPC
SG-AOB	N/A	N/A	N/A	-	N/A	<100	438.98	-	N/A	104.58	N/A	MPC
SG-AOB	N/A	N/A	N/A	-	N/A	<100	249.02	-	N/A	150.28	N/A	MPC
SG-(below) Old Building (OE												
SYRINGE BLANKS												
Syringe 1	N/A	N/A	N/A	-	N/A	174.22	777.36	-	N/A	<100	N/A	MPC
Syringe 3		N/A	N/A	-	N/A	421.57	2340.25	-	N/A	212.47	N/A	MPC

Date Printed: 8/27/2004

Table I-1. Results of GC/PID Vapour and Air Testing

Sample Designation	Injection Conc. (ng/ul)	Mass Injected				Detector Response						Calibration Method
		Benzene (ng)	Toluene (ng)	3-fluoro toluene (ng)	m&p Xylene (ng)	Benzene (mV)	Toluene (mV)	3-fluoro toluene (ng)	Ethyl-benzene (mV)	m&p Xylene (mV)	o-Xylene (mV)	
SAMPLES												
SG-OB	N/A	N/A	N/A	-	N/A	56887.65	>82905.76		N/A	18997.47	N/A	MPC
SG-OB	N/A	N/A	N/A	-	N/A	56242.99	>79389.30		N/A	15570.41	N/A	MPC
SG-(below) OB: JUNE 25, 19												
SYRINGE BLANKS												
Syringe 3	N/A	N/A	N/A	-	N/A	464.94	1671.97		N/A	124.38	N/A	MPC
SAMPLES												
SG-OB	N/A	N/A	N/A	-	N/A	28911.65	>87289.98		N/A	9331.78	N/A	MPC
SG-OB	N/A	N/A	N/A	-	N/A	2598.03	21919.13		N/A	719.01	N/A	MPC
SG-OB	N/A	N/A	N/A	-	N/A	6198.21	37854.92		N/A	1403.72	N/A	MPC
SG-OB	N/A	N/A	N/A	-	N/A	2164.06	18622.23		N/A	377.01	N/A	MPC
SG-OB	N/A	N/A	N/A	-	N/A	3457.52	29195.57		N/A	480.01	N/A	MPC
SG-OB	N/A	N/A	N/A	-	N/A	5768.08	34404.19		N/A	846.54	N/A	MPC
SG-Adjacent to Building (EC												
SYRINGE BLANKS												
Syringe 2	N/A	N/A	N/A	-	N/A	<100	108.34		N/A	<100	N/A	MPC
SAMPLES												
SG-BE (10mE) (EO)	N/A	N/A	N/A	-	N/A	<100	<100		N/A	<100	N/A	MPC
SG-BE (10mE) (EO)	N/A	N/A	N/A	-	N/A	<100	106.98		N/A	<100	N/A	MPC
SG-BE (10mE) (EO)	N/A	N/A	N/A	-	N/A	133.49	1199.88		N/A	662.16	N/A	MPC
SG-BE (10mE) (EO)	N/A	N/A	N/A	-	N/A	41221	24691.23		N/A	1586.9	N/A	MPC
SG-BE (10mE) (EO)	N/A	N/A	N/A	-	N/A	48819.85	35371.5		N/A	3220.7	N/A	MPC
SG-BE (10mE) (EO)	N/A	N/A	N/A	-	N/A	39423.1	22809.3		N/A	1788.94	N/A	MPC

Notes:

N/A = Not applicable, NC = no

- = not tested

Calibration Curves Used for Q

Date Printed: 8/27/2004

Table I-1. Results of GC/PID Vapour and Air Testing

Sample Designation	Soil Vapour or Indoor Air Concentration			Indoor Air Concentration						3-fluoro toluene Recov-ery (%)
	Benzene (mg/L)	Toluene (mg/L)	m&p-Xylene (mg/L)	Benzene (ug/m3)	Toluene (ug/m3)	3-fluorotolu (ug/m3)	Ethyl benzene	m&p-Xylene (ug/m3)	o-Xylene (ug/m3)	
March 1997 Program - Site E										
pid4ma14	N/A	N/A	N/A	N/A	N/A	N/A	N/A	N/A	N/A	-
pid4ma9	N/A	N/A	N/A	N/A	N/A	N/A	N/A	N/A	N/A	-
pid4ma11	N/A	N/A	N/A	N/A	N/A	N/A	N/A	N/A	N/A	-
pid4ma10	N/A	N/A	N/A	N/A	N/A	N/A	N/A	N/A	N/A	-
pid4ma15	N/A	N/A	N/A	18.32193	36.925975	24.305676	0	11.99497964	9.15038353	**80.8**
pid4ma12	N/A	N/A	N/A	90.1812	17.127145	14.657354	3.737767	11.03347821	12.4511539	**89.7**
pid4ma13	N/A	N/A	N/A	ND	ND	12.543097	ND	ND	ND	-
pid6mar1	N/A	N/A	N/A	ND	0.172889	0.0466456	ND	0.320027541	0.43666429	-
pid6mar2	N/A	N/A	N/A	ND	ND	0.1239897	ND	ND	ND	-
pidmar4	N/A	N/A	N/A	ND	4.8051774	5.8229809	ND	ND	ND	**19.3**
pid6mar5	N/A	N/A	N/A	ND	ND	22.152194	ND	ND	ND	-
pidmar9	N/A	N/A	N/A	N/A	N/A	N/A	N/A	N/A	N/A	**74.7**
pidmar8	N/A	N/A	N/A	N/A	N/A	N/A	N/A	N/A	N/A	**96.7**
pidma11	N/A	N/A	N/A	N/A	N/A	N/A	N/A	N/A	N/A	**88.2**
pidma10	N/A	N/A	N/A	N/A	N/A	N/A	N/A	N/A	N/A	**70.1**
td17ma17	N/A	N/A	N/A	N/A	N/A	N/A	N/A	N/A	N/A	**72.1**
td17ma17	N/A	N/A	N/A	N/A	N/A	N/A	N/A	N/A	N/A	**25.1**
50 ng std	N/A	N/A	N/A	N/A	N/A	N/A	N/A	N/A	N/A	-
100 ng std	N/A	N/A	N/A	N/A	N/A	N/A	N/A	N/A	N/A	-
250 ng std	N/A	N/A	N/A	N/A	N/A	N/A	N/A	N/A	N/A	-
500 ng std	N/A	N/A	N/A	N/A	N/A	N/A	N/A	N/A	N/A	-
100 ng std	N/A	N/A	N/A	N/A	N/A	N/A	N/A	N/A	N/A	-
Site A 0.6M QC Fail	0.06162512	0.02179466	0.0062031	N/A	N/A	N/A	N/A	N/A	N/A	-
Site A 0.9m QC Fail	<0.6	0.40061336	0.13465396	N/A	N/A	N/A	N/A	N/A	N/A	-
Site A 1.2m QC Fail	<1.3	<1.2	0.39089535	N/A	N/A	N/A	N/A	N/A	N/A	-
Site A 1.2m QC Fail	<1.6	1.2858424	0.60093365	N/A	N/A	N/A	N/A	N/A	N/A	-
Site A 0.9M	1.254493	0.9574336	0.2585292	N/A	N/A	N/A	N/A	N/A	N/A	-
Site A 0.6M	0.878338	0.73179435	0.2199766	N/A	N/A	N/A	N/A	N/A	N/A	-
Site A 0.6m - 3rd	0.871908	0.720344	0.167417	N/A	N/A	N/A	N/A	N/A	N/A	-

Date Printed: 8/27/2004

Table I-1. Results of GC/PID Vapour and Air Testing

Sample Designation	Soil Vapour or Indoor Air Concentration Benzene (mg/L)	Toluene (mg/L)	m&p-Xylene (mg/L)	Indoor Air Concentration Benzene (ug/m3)	Toluene (ug/m3)	3-fluorotolu (ug/m3)	Ethyl benzene	m&p-Xylene (ug/m3)	o-Xylene (ug/m3)	3-fluoro toluene Recov-ery (%)
	0.5	**1.12**	**19.2**							
Site A 0.3m	0.0088091	0.018434	0	N/A	N/A	N/A	N/A	N/A	N/A	-
Site A 0.3m -4th	0.0011574	0.00154562	0	N/A	N/A	N/A	N/A	N/A	N/A	-
	108.6	**119.54**	**#DIV/0!**							
Site A 1.2 m -2nd	2.838845	2.8985338	0.8221442	N/A	N/A	N/A	N/A	N/A	N/A	-
Site A 1.2m -3rd	2.1568792	2.3483498	0.5553442	N/A	N/A	N/A	N/A	N/A	N/A	-
Site A 0.3m -2nd QC Fail	0	0	0	N/A	N/A	N/A	N/A	N/A	N/A	-
Site A 0.6m -2nd QC Fail	0	0	0	N/A	N/A	N/A	N/A	N/A	N/A	-
Site B 1.2 m	3.1864508	3.9504062	0.3500416	N/A	N/A	N/A	N/A	N/A	N/A	-
Site B 1.2m -2nd	3.6878622	3.9989018	0.3616474	N/A	N/A	N/A	N/A	N/A	N/A	-
	10.3	**0.86**	**2.3**							
Site B 0.9m	1.647366	2.2805694	0.1798232	N/A	N/A	N/A	N/A	N/A	N/A	-
Site B 0.9m -2nd	2.995094	3.487571	0.3413706	N/A	N/A	N/A	N/A	N/A	N/A	-
	41.1	**29.6**	**43.8**							
Site B 0.6m	0.0394802	0.0876324	0.027347	N/A	N/A	N/A	N/A	N/A	N/A	-
Site B 0.6m -2nd	0.0098379	0.02463775	0.0104052	N/A	N/A	N/A	N/A	N/A	N/A	-
	85.0	**79.4**	**63.5**							
Site B 0.3m	0	0	0	N/A	N/A	N/A	N/A	N/A	N/A	-
May 1997 Program - Site B -										
sg13may1	N/A	N/A	N/A	N/A	N/A	N/A	N/A	N/A	N/A	-
sg13may2	N/A	N/A	N/A	N/A	N/A	N/A	N/A	N/A	N/A	-
sg13may3	N/A	N/A	N/A	N/A	N/A	N/A	N/A	N/A	N/A	-
sg13may4	N/A	N/A	N/A	N/A	N/A	N/A	N/A	N/A	N/A	-
SG-BC (sg13ma24)	NC	NC	NC	N/A	N/A	N/A	N/A	N/A	N/A	-
SG-BC (sg13ma25)	NC	NC	NC	N/A	N/A	N/A	N/A	N/A	N/A	-
SG-BC (sg13ma26)	NC	NC	NC	N/A	N/A	N/A	N/A	N/A	N/A	-
SG-BC (sg13ma27)	NC	NC	NC	N/A	N/A	N/A	N/A	N/A	N/A	-
SG-BC (sg13ma28)	NC	NC	NC	N/A	N/A	N/A	N/A	N/A	N/A	-
SG-BC (sg13ma28)	NC	NC	NC	N/A	N/A	N/A	N/A	N/A	N/A	-
SG-BC (sg13ma29)	NC	NC	NC	N/A	N/A	N/A	N/A	N/A	N/A	-

Date Printed: 8/27/2004

Table I-1. Results of GC/PID Vapour and Air Testing

Sample Designation	Soil Vapour or Indoor Air Concentration			Indoor Air Concentration						3-fluoro toluene Recov-ery (%)
	Benzene (mg/L)	Toluene (mg/L)	m&p-Xylene (mg/L)	Benzene (ug/m3)	Toluene (ug/m3)	3-fluorotolu (ug/m3)	Ethyl benzene	m&p-Xylene (ug/m3)	o-Xylene (ug/m3)	
SG-BC (sg13ma30)	NC	NC	NC	N/A	N/A	N/A	N/A	N/A	N/A	-
SG-BC (sg13ma31)	NC	NC	NC	N/A	N/A	N/A	N/A	N/A	N/A	-
SG-BC (sg13ma32)	NC	NC	NC	N/A	N/A	N/A	N/A	N/A	N/A	-
June 1997 Program - Site B										
sg24jun1	N/A	N/A	N/A	N/A	N/A	N/A	N/A	N/A	N/A	-
sg24jun2	N/A	N/A	N/A	N/A	N/A	N/A	N/A	N/A	N/A	-
sg24jun3	N/A	N/A	N/A	N/A	N/A	N/A	N/A	N/A	N/A	-
SG-BC (sg24jun4)	<DL	<DL	<DL	N/A	N/A	N/A	N/A	N/A	N/A	-
SG-BC (sg24jun5)	?	?	?	N/A	N/A	N/A	N/A	N/A	N/A	-
SG-BC (sg24jun6)	N/A	N/A	N/A	N/A	N/A	N/A	N/A	N/A	N/A	-
SG-BC (sg24jun7)	N/A	N/A	N/A	N/A	N/A	N/A	N/A	N/A	N/A	-
SG-BC (sg24jun8)	N/A	N/A	N/A	N/A	N/A	N/A	N/A	N/A	N/A	-
SG-BC (sg24jun14)	N/A	N/A	N/A	N/A	N/A	N/A	N/A	N/A	N/A	-
SG-BC (sg24jun9)	N/A	N/A	N/A	N/A	N/A	N/A	N/A	N/A	N/A	-
SG-BC (sg24jun17)	N/A	N/A	N/A	N/A	N/A	N/A	N/A	N/A	N/A	-
SG-BC (sg24jun10)	N/A	N/A	N/A	N/A	N/A	N/A	N/A	N/A	N/A	-
SG-BC (sg24jun16)	N/A	N/A	N/A	N/A	N/A	N/A	N/A	N/A	N/A	-
				N/A	N/A	N/A	N/A	N/A	N/A	-
sg24jun11	N/A	N/A	N/A	N/A	N/A	N/A	N/A	N/A	N/A	-
sg24jun12	N/A	N/A	N/A	N/A	N/A	N/A	N/A	N/A	N/A	-
sg24jun13	N/A	N/A	N/A	N/A	N/A	N/A	N/A	N/A	N/A	-
SG-BC (sg24jun18)	N/A	N/A	N/A	N/A	N/A	N/A	N/A	N/A	N/A	-
SG-BC (sg24jun19)	N/A	N/A	N/A	N/A	N/A	N/A	N/A	N/A	N/A	-
SG-BC (sg24jun20)	N/A	N/A	N/A	N/A	N/A	N/A	N/A	N/A	N/A	-
SG-BC (sg24jun21)	N/A	N/A	N/A	N/A	N/A	N/A	N/A	N/A	N/A	-
July 15 1997 Program - Site										

Date Printed: 8/27/2004

Table I-1. Results of GC/PID Vapour and Air Testing

Sample Designation	Soil Vapour or Indoor Air Concentration			Indoor Air Concentration						3-fluoro toluene Recov-ery (%)
	Benzene (mg/L)	Toluene (mg/L)	m&p-Xylene (mg/L)	Benzene (ug/m3)	Toluene (ug/m3)	3-fluorotolu (ug/m3)	Ethyl benzene	m&p-Xylene (ug/m3)	o-Xylene (ug/m3)	
July 15 1997 Program - Site	N/A	N/A	N/A	N/A	N/A	N/A	N/A	N/A	N/A	-
sg15jul15	N/A	N/A	N/A	N/A	N/A	N/A	N/A	N/A	N/A	-
sg15jul16	N/A	N/A	N/A	N/A	N/A	N/A	N/A	N/A	N/A	-
sg15jul17	N/A	N/A	N/A	N/A	N/A	N/A	N/A	N/A	N/A	-
sg15jul18	N/A	N/A	N/A	N/A	N/A	N/A	N/A	N/A	N/A	-
sg15jul19	N/A	N/A	N/A	N/A	N/A	N/A	N/A	N/A	N/A	-
sg15ju18	N/A	N/A	N/A	N/A	N/A	N/A	N/A	N/A	N/A	-
sg15ju19	N/A	N/A	N/A	N/A	N/A	N/A	N/A	N/A	N/A	-
sg15ju28	N/A	N/A	N/A	N/A	N/A	N/A	N/A	N/A	N/A	-
sg15ju29	N/A	N/A	N/A	N/A	N/A	N/A	N/A	N/A	N/A	-
sg15ju30	N/A	N/A	N/A	N/A	N/A	N/A	N/A	N/A	N/A	-
SG-BC (sg15jul19)	0.005	0.008	<DL	N/A	N/A	N/A	N/A	N/A	N/A	-
SG-BC (sg15jul10)	<0.005	<0.008	<DL	N/A	N/A	N/A	N/A	N/A	N/A	-
SG-BC (sg15jul11)	<0.005	0.005	<DL	N/A	N/A	N/A	N/A	N/A	N/A	-
SG-BC (sg15jul12)	<DL	<0.005	<DL	N/A	N/A	N/A	N/A	N/A	N/A	-
SG-BC (sg15jul13)	<0.005	0.006	<0.005	N/A	N/A	N/A	N/A	N/A	N/A	-
SG-BC (sg15jul14)	<DL	<0.006	<DL	N/A	N/A	N/A	N/A	N/A	N/A	-
SG-BC (sg15jul15)	0.055	0.024	<0.005	N/A	N/A	N/A	N/A	N/A	N/A	-
SG-BC (sg15jul16)	<DL	<DL	<DL	N/A	N/A	N/A	N/A	N/A	N/A	-
SG-BC (sg15jul20)	2.58	1.48	<DL	N/A	N/A	N/A	N/A	N/A	N/A	-
SG-BC (sg15jul21)	3.96	2.2	0.02	N/A	N/A	N/A	N/A	N/A	N/A	-
	29.8	**27.7**	**#DIV/0!**							
SG-BC (sg15jul22)	3.7	4.6	0.11	N/A	N/A	N/A	N/A	N/A	N/A	-
SG-BC (sg15jul23)	6.16	7.89	0.18	N/A	N/A	N/A	N/A	N/A	N/A	-
	35.3	**37.3**	**34.1**							
SG-BC (sg15jul24)	9.15	9.65	0.15	N/A	N/A	N/A	N/A	N/A	N/A	-
SG-BC (sg15jul25)	<DL	<DL	<DL	N/A	N/A	N/A	N/A	N/A	N/A	-
SG-BC (sg15jul26)	6.3	6	0.09	N/A	N/A	N/A	N/A	N/A	N/A	-

Date Printed: 8/27/2004

Table I-1. Results of GC/PID Vapour and Air Testing

Sample Designation	Soil Vapour or Indoor Air Concentration			Indoor Air Concentration						3-fluoro toluene Recov-ery (%)
	Benzene (mg/L)	Toluene (mg/L)	m&p-Xylene (mg/L)	Benzene (ug/m3)	Toluene (ug/m3)	3-fluorotolu (ug/m3)	Ethyl benzene	m&p-Xylene (ug/m3)	o-Xylene (ug/m3)	
SG-BC (sg15ju27)	13.95	15.75	0.18	N/A	N/A	N/A	N/A	N/A	N/A	-
	53.4	**63.4**	**47.1**							
July 28 1997 Program - Site										
N/A	N/A	N/A	N/A	N/A	N/A	N/A	N/A	N/A	N/A	-
N/A	N/A	N/A	N/A	N/A	N/A	N/A	N/A	N/A	N/A	-
N/A	N/A	N/A	N/A	N/A	N/A	N/A	N/A	N/A	N/A	-
N/A	N/A	N/A	N/A	N/A	N/A	N/A	N/A	N/A	N/A	-
N/A	N/A	N/A	N/A	N/A	N/A	N/A	N/A	N/A	N/A	-
N/A	N/A	N/A	N/A	N/A	N/A	N/A	N/A	N/A	N/A	-
N/A	N/A	N/A	N/A	N/A	N/A	N/A	N/A	N/A	N/A	-
N/A	N/A	N/A	N/A	N/A	N/A	N/A	N/A	N/A	N/A	-
N/A	N/A	N/A	N/A	N/A	N/A	N/A	N/A	N/A	N/A	-
N/A	N/A	N/A	N/A	N/A	N/A	N/A	N/A	N/A	N/A	-
SG-BC	0.015	0.037	<0.005	N/A	N/A	N/A	N/A	N/A	N/A	-
SG-BC	<DL	<DL	<DL	N/A	N/A	N/A	N/A	N/A	N/A	-
	70.7	**107.7**	**#DIV/0!**							
SG-BC	0.052	0.067	<0.005	N/A	N/A	N/A	N/A	N/A	N/A	-
SG-BC	0.05	0.044	<0.005	N/A	N/A	N/A	N/A	N/A	N/A	-
	2.8	**29.30**	**#DIV/0!**							
SG-BC	<0.009	0.021	0.008	N/A	N/A	N/A	N/A	N/A	N/A	-
SG-BC	<0.008	0.01	<0.005	N/A	N/A	N/A	N/A	N/A	N/A	-
	8.3	**50.18**	**32.6**							
SG-BC	0.057	0.089	0.007	N/A	N/A	N/A	N/A	N/A	N/A	-
SG-BC	0.049	0.075	<0.005	N/A	N/A	N/A	N/A	N/A	N/A	-
	10.7	**12.07**	**23.6**							
SG-BC	9.17	9.8	0.17	N/A	N/A	N/A	N/A	N/A	N/A	-
SG-BC	8.75	9.07	0.18	N/A	N/A	N/A	N/A	N/A	N/A	-
	3.3	**5.47**	**4.0**							
SG-BC	13.13	19.5	0.44	N/A	N/A	N/A	N/A	N/A	N/A	-
SG-BC	13.38	18.38	0.48	N/A	N/A	N/A	N/A	N/A	N/A	-
	1.3	**4.18**	**6.1**							

Date Printed: 8/27/2004

Table I-1. Results of GC/PID Vapour and Air Testing

Sample Designation	Soil Vapour or Indoor Air Concentration			Indoor Air Concentration						3-fluoro toluene Recov-ery (%)
	Benzene (mg/L)	Toluene (mg/L)	m&p-Xylene (mg/L)	Benzene (ug/m3)	Toluene (ug/m3)	3-fluorotolu (ug/m3)	Ethyl benzene	m&p-Xylene (ug/m3)	o-Xylene (ug/m3)	
SG-BC	17.63	21.62	0.45	N/A	N/A	N/A	N/A	N/A	N/A	-
SG-BC	13.88	17.94	0.37	N/A	N/A	N/A	N/A	N/A	N/A	-
	16.8	**13.16**	**13.8**							
SG-BC	11.38	12.69	0.25	N/A	N/A	N/A	N/A	N/A	N/A	-
SG-BC	11.83	13.92	0.36	N/A	N/A	N/A	N/A	N/A	N/A	-
	2.7	**6.54**	**25.5**							
September 1997 Program - S										
SG09Sep1	N/A	N/A	N/A	N/A	N/A	N/A	N/A	N/A	N/A	-
SG09Sep2	N/A	N/A	N/A	N/A	N/A	N/A	N/A	N/A	N/A	-
SG09Sep3	N/A	N/A	N/A	N/A	N/A	N/A	N/A	N/A	N/A	-
SG09Sep4	N/A	N/A	N/A	N/A	N/A	N/A	N/A	N/A	N/A	-
SG09Sep5	N/A	N/A	N/A	N/A	N/A	N/A	N/A	N/A	N/A	-
SG09Sep6	N/A	N/A	N/A	N/A	N/A	N/A	N/A	N/A	N/A	-
SG09Sep6	N/A	N/A	N/A	N/A	N/A	N/A	N/A	N/A	N/A	-
SG-BC (SG09SE19)	0.015	0.033	0.004	N/A	N/A	N/A	N/A	N/A	N/A	-
SG-BC (SG09SEP9)	0.047	0.09	0.011	N/A	N/A	N/A	N/A	N/A	N/A	-
SG-BC (SG09SE20)	0.054	0.196	0.016	N/A	N/A	N/A	N/A	N/A	N/A	-
SG-BC (SG09SE11)	0.013	0.043	0.008	N/A	N/A	N/A	N/A	N/A	N/A	-
SG-BC (SG09SE12)	2.53	2.87	<0.01	N/A	N/A	N/A	N/A	N/A	N/A	-
SG-BC (SG09SE13)	21.23	26.24	0.96	N/A	N/A	N/A	N/A	N/A	N/A	-
SG-BC (SG09SE14)	7.68	14.49	0.53	N/A	N/A	N/A	N/A	N/A	N/A	-
SG-BC (SG09SE15)	20.59	21.77	0.52	N/A	N/A	N/A	N/A	N/A	N/A	-
SG09SE16	N/A	N/A	N/A	N/A	N/A	N/A	N/A	N/A	N/A	-
SG09SE18	N/A	N/A	N/A	N/A	N/A	N/A	N/A	N/A	N/A	-
SG09SE21	N/A	N/A	N/A	N/A	N/A	N/A	N/A	N/A	N/A	-
September 1997 Program - S										
SG10SE2	N/A	N/A	N/A	N/A	N/A	N/A	N/A	N/A	N/A	-
SG10SE3	N/A	N/A	N/A	N/A	N/A	N/A	N/A	N/A	N/A	-
SG10SE4	N/A	N/A	N/A	N/A	N/A	N/A	N/A	N/A	N/A	-
SG10SE5	N/A	N/A	N/A	N/A	N/A	N/A	N/A	N/A	N/A	-

Date Printed: 8/27/2004

Table I-1. Results of GC/PID Vapour and Air Testing

Sample Designation	Soil Vapour or Indoor Air Concentration			Indoor Air Concentration						3-fluoro toluene Recov-ery (%)
	Benzene (mg/L)	Toluene (mg/L)	m&p-Xylene (mg/L)	Benzene (ug/m3)	Toluene (ug/m3)	3-fluorotolu (ug/m3)	Ethyl benzene	m&p-Xylene (ug/m3)	o-Xylene (ug/m3)	
SG10SE6	N/A	N/A	N/A	N/A	N/A	N/A	N/A	N/A	N/A	-
SG10SE7	N/A	N/A	N/A	N/A	N/A	N/A	N/A	N/A	N/A	-
0.17m South (sg10sep8)	0.132	0.463	0.036	N/A	N/A	N/A	N/A	N/A	N/A	-
0.17m East (sg10sep9)	0.117	0.252	0.024	N/A	N/A	N/A	N/A	N/A	N/A	-
0.4m South (sg10se10)	0.014	0.048	0.005	N/A	N/A	N/A	N/A	N/A	N/A	-
0.4m East (sg10se11)	1.02	1.68	0.09	N/A	N/A	N/A	N/A	N/A	N/A	-
0.7m South (sg10se14)	0.002	0.028	0.002	N/A	N/A	N/A	N/A	N/A	N/A	-
1.6m South (sg10se15)	7.64	25.7	0.559	N/A	N/A	N/A	N/A	N/A	N/A	-
0.7m East (sg10se19)	9.57	7.74	0.233	N/A	N/A	N/A	N/A	N/A	N/A	-
1.6 m North (sg10se23)	33.18	27.51	0.761	N/A	N/A	N/A	N/A	N/A	N/A	-
0.17 m North (sg10se24)	0.016	0.048	0.005	N/A	N/A	N/A	N/A	N/A	N/A	-
0.17 m West (sg10se26)	0.231	0.794	0.057	N/A	N/A	N/A	N/A	N/A	N/A	-
1.6 m West (sg10se27)	2.74	7.44	0.109	N/A	N/A	N/A	N/A	N/A	N/A	-
0.17m Centre (sg10se28	1.39	1.37	0.017	N/A	N/A	N/A	N/A	N/A	N/A	-
SG10SE16	N/A	N/A	N/A	N/A	N/A	N/A	N/A	N/A	N/A	-
SG10SE17	N/A	N/A	N/A	N/A	N/A	N/A	N/A	N/A	N/A	-
SG10SE19	N/A	N/A	N/A	N/A	N/A	N/A	N/A	N/A	N/A	-
SG10SE29	N/A	N/A	N/A	N/A	N/A	N/A	N/A	N/A	N/A	-
SG12SEP1	N/A	N/A	N/A	N/A	N/A	N/A	N/A	N/A	N/A	-
SG12SEP2	N/A	N/A	N/A	N/A	N/A	N/A	N/A	N/A	N/A	-
SG12SEP3	N/A	N/A	N/A	N/A	N/A	N/A	N/A	N/A	N/A	-
SG12SEP8	N/A	N/A	N/A	N/A	N/A	N/A	N/A	N/A	N/A	-
SG12SEP11	N/A	N/A	N/A	N/A	N/A	N/A	N/A	N/A	N/A	-
0.4m N Outside (SG12SEP4	0.026	0.082	0.004	N/A	N/A	N/A	N/A	N/A	N/A	-
0.7m N Outside (SG12SEP9	1.99	1.02	0.032	N/A	N/A	N/A	N/A	N/A	N/A	-
0.7m E Outside (SG12SEP6	0.025	0.13	0.025	N/A	N/A	N/A	N/A	N/A	N/A	-
0.4m E Outside (SG12SEP7	0.242	0.83	0.116	N/A	N/A	N/A	N/A	N/A	N/A	-
October 21 1997 Program - S										
SG21OCT1	N/A	N/A	N/A	N/A	N/A	N/A	N/A	N/A	N/A	-
SG21OCT2	N/A	N/A	N/A	N/A	N/A	N/A	N/A	N/A	N/A	-

Date Printed: 8/27/2004

Table I-1. Results of GC/PID Vapour and Air Testing

Sample Designation	Soil Vapour or Indoor Air Concentration			Indoor Air Concentration						3-fluoro toluene Recov-ery (%)
	Benzene (mg/L)	Toluene (mg/L)	m&p-Xylene (mg/L)	Benzene (ug/m3)	Toluene (ug/m3)	3-fluorotolu (ug/m3)	Ethyl benzene	m&p-Xylene (ug/m3)	o-Xylene (ug/m3)	
SG21OCT3	N/A	N/A	N/A	N/A	N/A	N/A	N/A	N/A	N/A	-
SG21OCT4	N/A	N/A	N/A	N/A	N/A	N/A	N/A	N/A	N/A	-
SG21OC11	N/A	N/A	N/A	N/A	N/A	N/A	N/A	N/A	N/A	-
SG-BC((SG21OCT5)	0.001	0.006	<0.001	N/A	N/A	N/A	N/A	N/A	N/A	-
SG-BC((SG21OCT6)	0.001	0.009	0.001	N/A	N/A	N/A	N/A	N/A	N/A	-
SG-BC((SG21OCT7)	<0.001	0.004	<0.001	N/A	N/A	N/A	N/A	N/A	N/A	-
SG-BC((SG21OCT8)	0.04	0.1	0.01	N/A	N/A	N/A	N/A	N/A	N/A	-
SG-BC((SG21OCT9)	4.82	5.21	0.13	N/A	N/A	N/A	N/A	N/A	N/A	-
SG-BC((SG21OC10)	19.27	23.69	0.6	N/A	N/A	N/A	N/A	N/A	N/A	-
SG-BC((SG21OC12)	16.21	21.27	0.59	N/A	N/A	N/A	N/A	N/A	N/A	-
SG-BC((SG21OC13)	22.72	27.21	0.79	N/A	N/A	N/A	N/A	N/A	N/A	-
October 28/29 1997 Program										
SG28OC22	N/A	N/A	N/A	N/A	N/A	N/A	N/A	N/A	N/A	-
SG28OC7	N/A	N/A	N/A	N/A	N/A	N/A	N/A	N/A	N/A	-
SG28OC15	N/A	N/A	N/A	N/A	N/A	N/A	N/A	N/A	N/A	-
SG28OC6	N/A	N/A	N/A	N/A	N/A	N/A	N/A	N/A	N/A	-
SG28OC5	N/A	N/A	N/A	N/A	N/A	N/A	N/A	N/A	N/A	-
SG28OC4	N/A	N/A	N/A	N/A	N/A	N/A	N/A	N/A	N/A	-
SG28OC3	N/A	N/A	N/A	N/A	N/A	N/A	N/A	N/A	N/A	-
SG28OC2	N/A	N/A	N/A	N/A	N/A	N/A	N/A	N/A	N/A	-
SG28OC1	N/A	N/A	N/A	N/A	N/A	N/A	N/A	N/A	N/A	-
0.7m East (sg28oc23)	11.4	8.91	0.18	N/A	N/A	N/A	N/A	N/A	N/A	-
0.17m West (sg28oc21)	0.08	0.25	0.015	N/A	N/A	N/A	N/A	N/A	N/A	-
1.6m West (sg28oc20)	3.64	9.93	0.071	N/A	N/A	N/A	N/A	N/A	N/A	-
0.17 Centre (sg28oc19)	1.37	2.18	0.028	N/A	N/A	N/A	N/A	N/A	N/A	-
0.17 North(sg28oc18)	0.001	0.006	0.001	N/A	N/A	N/A	N/A	N/A	N/A	-
1.6 North(sg28oc17)	20.15	13.94	0.19	N/A	N/A	N/A	N/A	N/A	N/A	-
0.7 East (sg28oc16)	9.31	7.82	0.266	N/A	N/A	N/A	N/A	N/A	N/A	-
0.4 East (sg28oc12)	0.051	0.167	0.03	N/A	N/A	N/A	N/A	N/A	N/A	-
0.7 South (sg28oc11)	0.002	0.009	0.006	N/A	N/A	N/A	N/A	N/A	N/A	-
0.4 South (sg28oc10)	<DL	0.003	<DL	N/A	N/A	N/A	N/A	N/A	N/A	-

Date Printed: 8/27/2004

Table I-1. Results of GC/PID Vapour and Air Testing

235

Sample Designation	Soil Vapour or Indoor Air Concentration			Indoor Air Concentration						3-fluoro toluene Recov-ery (%)
	Benzene (mg/L)	Toluene (mg/L)	m&p-Xylene (mg/L)	Benzene (ug/m3)	Toluene (ug/m3)	3-fluorotolu (ug/m3)	Ethyl benzene	m&p-Xylene (ug/m3)	o-Xylene (ug/m3)	
0.17 East (sg28oc9)	0.002	0.014	0.004	N/A	N/A	N/A	N/A	N/A	N/A	-
0.17 South (sg28oc8)	0.001	0.01	0.003	N/A	N/A	N/A	N/A	N/A	N/A	-
1.6 South (sg28oc14)	13.87	26.19	0.6	N/A	N/A	N/A	N/A	N/A	N/A	-
0.4 North Out (sg29oc6)	0.017	0.025	0.001	N/A	N/A	N/A	N/A	N/A	N/A	-
0.7 North Out (sg29oc8)	0.298	0.366	0.026	N/A	N/A	N/A	N/A	N/A	N/A	-
0.4 East Out (sg29oc9)	0.088	0.354	0.018	N/A	N/A	N/A	N/A	N/A	N/A	-
0.7 East Out (sg29oc7)	0.156	0.195	0.008	N/A	N/A	N/A	N/A	N/A	N/A	-
SG29OC10	N/A	N/A	N/A	N/A	N/A	N/A	N/A	N/A	N/A	-
SG29OC2	N/A	N/A	N/A	N/A	N/A	N/A	N/A	N/A	N/A	-
November 28 1997 (during 3										
SG-BC (SG28NOV9)	1.58	5.3	0.05	N/A	N/A	N/A	N/A	N/A	N/A	-
SG-BC (SG28NO10)	0.12	3.65	0.028	N/A	N/A	N/A	N/A	N/A	N/A	-
SG-BC (SG28NO11)	0.64	2.95	0.017	N/A	N/A	N/A	N/A	N/A	N/A	-
SG-BC (SG28NO12)	3.46	3.09	0.02	N/A	N/A	N/A	N/A	N/A	N/A	-
SG-BC (SG28NO14)	13.88	14.16	0.13	N/A	N/A	N/A	N/A	N/A	N/A	-
SG-BC (SG28NO15)	27.86	34.75	0.32	N/A	N/A	N/A	N/A	N/A	N/A	-
SG-BC (SG28NO15)	27.86	34.75	0.32	N/A	N/A	N/A	N/A	N/A	N/A	-
SG-BC (SG28NO16)	25.14	31.29	0.3	N/A	N/A	N/A	N/A	N/A	N/A	-
SG-BC (SG28NO17)	31.04	35.81	0.3	N/A	N/A	N/A	N/A	N/A	N/A	-
SG-BC (SG28NO18)	16.82	19.4	<DL	N/A	N/A	N/A	N/A	N/A	N/A	-
SG-BC (SG28NO21)	0.008	0.24	<0.005	N/A	N/A	N/A	N/A	N/A	N/A	-
SG-BC (SG28NO22)	0.16	0.5	0.009	N/A	N/A	N/A	N/A	N/A	N/A	-
SG-BC (SG28NO23)	1.03	3.65	0.02	N/A	N/A	N/A	N/A	N/A	N/A	-
SG-BC (SG28NO24)	0.33	1.41	0.015	N/A	N/A	N/A	N/A	N/A	N/A	-
SG28NOV1	N/A	N/A	N/A	N/A	N/A	N/A	N/A	N/A	N/A	-
SG28NOV7	N/A	N/A	N/A	N/A	N/A	N/A	N/A	N/A	N/A	-
SG28NOV2	N/A	N/A	N/A	N/A	N/A	N/A	N/A	N/A	N/A	-
SG28NOV3	N/A	N/A	N/A	N/A	N/A	N/A	N/A	N/A	N/A	-
SG28NOV4	N/A	N/A	N/A	N/A	N/A	N/A	N/A	N/A	N/A	-
SG28NOV5	N/A	N/A	N/A	N/A	N/A	N/A	N/A	N/A	N/A	-
SG28NOV6	N/A	N/A	N/A	N/A	N/A	N/A	N/A	N/A	N/A	-

Date Printed: 8/27/2004

Table I-1. Results of GC/PID Vapour and Air Testing

Sample Designation	Soil Vapour or Indoor Air Concentration			Indoor Air Concentration						3-fluoro toluene Recov-ery (%)
	Benzene (mg/L)	Toluene (mg/L)	m&p-Xylene (mg/L)	Benzene (ug/m3)	Toluene (ug/m3)	3-fluorotolu (ug/m3)	Ethyl benzene	m&p-Xylene (ug/m3)	o-Xylene (ug/m3)	
SG28NO13	N/A	N/A	N/A	N/A	N/A	N/A	N/A	N/A	N/A	-
SG28NO25	N/A	N/A	N/A	N/A	N/A	N/A	N/A	N/A	N/A	-
SG28NOV7	N/A	N/A	N/A	N/A	N/A	N/A	N/A	N/A	N/A	-
December 1, 1997 10 m East										
SG-BR (10mE)	2.13	0.03	<DL	N/A	N/A	N/A	N/A	N/A	N/A	-
SG-BR (10mE)	0.033	0.009	<0.001	N/A	N/A	N/A	N/A	N/A	N/A	-
SG-BR (10mE)	<0.001	0.009	<0.001	N/A	N/A	N/A	N/A	N/A	N/A	-
SG-BR (10mE)	<0.001	<0.005	<0.001	N/A	N/A	N/A	N/A	N/A	N/A	-
SG01DEC5	N/A	~~~ 0.01	N/A	N/A	N/A	N/A	N/A	N/A	N/A	-
SG01DEC4	N/A	N/A	N/A	N/A	N/A	N/A	N/A	N/A	N/A	-
SG01DEC3	N/A	N/A	N/A	N/A	N/A	N/A	N/A	N/A	N/A	-
SG01DEC2	N/A	N/A	N/A	N/A	N/A	N/A	N/A	N/A	N/A	-
SG01DEC1	N/A	N/A	N/A	N/A	N/A	N/A	N/A	N/A	N/A	-
SG-BR (10mE) sg03dec8	0.005	0.007	<0.001	N/A	N/A	N/A	N/A	N/A	N/A	-
SG-BR (10mE) sg03dec7	<0.001	<0.001	<0.001	N/A	N/A	N/A	N/A	N/A	N/A	-
SG-BR (10mE) sg03dec9	<0.001	0.008	<0.001	N/A	N/A	N/A	N/A	N/A	N/A	-
SG01DEC6	<0.001	~0.001	<0.001	N/A	N/A	N/A	N/A	N/A	N/A	-
October 1997 Program - Flu										
TD03OCT2 Tube 1	N/A	N/A	N/A	1.52	31.29	-	-	5.321614722	-	-
TD03OCT2 Tube 2	N/A	N/A	N/A	-	-	-	-	-	-	-
TD14OCT3 Tube 1	N/A	N/A	N/A	1.06	22.34	-	-	<DL	-	-
TD14OCT4 Tube 2	N/A	N/A	N/A	12.95	18.26	-	-	<DL	-	-
TD14OCT6 Tube 1	N/A	N/A	N/A	2.78	12.66	-	-	15.26	-	-
TD24OCT1 Tube 2	N/A	N/A	N/A	<DL	<DL	-	-	<DL	-	-
TD24OCT5 Tube 2	N/A	N/A	N/A	2.66	11.26	-	-	9.43	-	-
TD21OCT2 Tube 1	N/A	N/A	N/A	3.48	6.22	-	-	9.09	-	-
TD21OCT3 Tube 2	N/A	N/A	N/A	<DL	<DL	-	-	<DL	-	-
TD23OCT2 Tube 4	N/A	N/A	N/A	2.74	8.43	-	-	4.28	-	124
TD23OCT3 Tube 5	N/A	N/A	N/A	<DL	<DL	-	-	<DL	-	103
TD23OCT1	N/A	N/A	N/A	N/A	N/A	-	-	N/A	-	-
TD22OCT1 Tube 4	N/A	N/A	N/A	<DL	<DL	-	-	<DL	-	-

Date Printed: 8/27/2004

Table I-1. Results of GC/PID Vapour and Air Testing

Sample Designation	Soil Vapour or Indoor Air Concentration			Indoor Air Concentration						3-fluoro toluene Recov-ery (%)
	Benzene (mg/L)	Toluene (mg/L)	m&p-Xylene (mg/L)	Benzene (ug/m3)	Toluene (ug/m3)	3-fluorotolu (ug/m3)	Ethyl benzene	m&p-Xylene (ug/m3)	o-Xylene (ug/m3)	
TD22OCT1 Tube 5	N/A	N/A	N/A	<DL	<DL	-	-	<DL	-	-
TD24OCT6 Tube 4	N/A	N/A	N/A	5.23	25.28	-	-	23.09	-	-
TD27OCT4 Tube 4	N/A	N/A	N/A	0.75	0.64	-	-	<DL	-	-
TD27OCT2 Tube 5	N/A	N/A	N/A	<DL	<DL	-	-	<DL	-	83
TD23OCT5 Tube 4&5	N/A	N/A	N/A	N/A	N/A	-	-	N/A	-	-
TD24OCT2	N/A	N/A	N/A	N/A	N/A	-	-	N/A	-	-
TD24OCT3	N/A	N/A	N/A	N/A	N/A	-	-	N/A	-	-
TD24OCT4	N/A	N/A	N/A	N/A	N/A	-	-	N/A	-	-
TD27OCT1	N/A	N/A	N/A	N/A	N/A	-	-	N/A	-	-
TD27OCT3	N/A	N/A	N/A	N/A	N/A	-	-	N/A	-	-
TD30OCT3 Tube 4	N/A	N/A	N/A	0.55	3.55	-	-	3.88	-	
TD30OCT4 Tube 5	N/A	N/A	N/A	<DL	<DL	-	-	<DL	-	98
TD30OCT5	N/A	N/A	N/A	N/A	N/A	-	-	N/A	-	-
TD30OCT2	N/A	N/A	N/A	N/A	N/A	-	-	N/A	-	-
TD30OCT1	N/A	N/A	N/A	N/A	N/A	-	-	N/A	-	-
TD29OCT1 Tube 4&5	N/A	N/A	N/A	<DL	<DL	-	-	<DL	-	-
November 1997 Program - Ir										
TD06NO15 Tube 5	N/A	N/A	N/A	19.07	45.36	-	-	6.82		101
TD06NO8 Tube 5	N/A	N/A	N/A	37.88	92.81	-	-	10.01		106
TD06NO2 Tube 5	N/A	N/A	N/A	<DL	<DL	-	-	<DL		-
TD06NO13 Tube 3	N/A	N/A	N/A	0.22	1.81	-	-	0.21		38
TD06NO4 Tube 3&4	N/A	N/A	N/A	<DL	<DL	-	-	<DL		-
TD06NO10 Tube 1	N/A	N/A	N/A	<DL	<DL	-	-	<DL		-
TD06NO10 Tube 1	N/A	N/A	N/A	<DL	<DL	-	-	<DL		-
TD06NO5 Tube 1	N/A	N/A	N/A	1.06	2.62	-	-	0.41		50
TD06NO5 Tube 2	N/A	N/A	N/A	1.06	2.62	-	-	0.41		50
TD06NO7	N/A	N/A	N/A	N/A	N/A	-	-	N/A		-
TD06NO16	N/A	N/A	N/A	N/A	N/A	-	-	N/A		-
TD06NOV1	N/A	N/A	N/A	N/A	N/A	-	-	N/A		-
TD06NOV3	N/A	N/A	N/A	N/A	N/A	-	-	N/A		-
TD06NOV9	N/A	N/A	N/A	N/A	N/A	-	-	N/A		-
TD12NOV2 Tube 1	N/A	N/A	N/A	5.3	14.4	-	-	5.2		68

Date Printed: 8/27/2004

Table I-1. Results of GC/PID Vapour and Air Testing

Sample Designation	Soil Vapour or Indoor Air Concentration			Indoor Air Concentration						3-fluoro toluene Recov-ery (%)
	Benzene (mg/L)	Toluene (mg/L)	m&p-Xylene (mg/L)	Benzene (ug/m3)	Toluene (ug/m3)	3-fluorotolu (ug/m3)	Ethyl benzene	m&p-Xylene (ug/m3)	o-Xylene (ug/m3)	
TD12NOV6 Tube 1	N/A	N/A	N/A	<DL	almost <DL	-	-	<DL		-
TD12NOV3 Tube 2	N/A	N/A	N/A	5.3	14.4	-	-	5.2		Low?
TD12NOV5 Tube 2	N/A	N/A	N/A	<D:	almost <DL	-	-	<DL		-
TD11NO3 Tube 2	N/A	N/A	N/A	<DL	<DL	-	-	<DL		-
TD11NOV6 Tube 4	N/A	N/A	N/A	2.36	4.64	-	-	5.02		40
TD12NOV9 Tube 5	N/A	N/A	N/A	N/A	N/A	-	-	N/A		110
TD12NOV4	N/A	N/A	N/A	N/A	N/A	-	-	N/A		-
TD11NOV5	N/A	N/A	N/A	N/A	N/A	-	-	N/A		-
TD12NOV1	N/A	N/A	N/A	N/A	N/A	-	-	N/A		-
TD10OCT2 Tube 4&5	N/A	N/A	N/A	<DL	<DL	-	-	<DL		-
TD13NOV6	N/A	N/A	N/A	0.28	2.52	-	-	0.39		33
TD11NOV7 Tube 4	N/A	N/A	N/A	<DL	<DL	-	-	<DL		-
TD13NOV2 Tube 1	N/A	N/A	N/A	11.6	74.6	-	-	8.9		114
TD12NOV8 Tube 1	N/A	N/A	N/A	<DL	<DL	-	-	<DL		-
TD13NOV3 Tube 2	N/A	N/A	N/A	9	16.9	-	-	5.6		88
TD12NOV7 Tube 2	N/A	N/A	N/A	<DL	<DL	-	-	<DL		-
TD13NOV4	N/A	N/A	N/A	N/A	N/A	-	-	N/A		-
TD13NOV1	N/A	N/A	N/A	N/A	N/A	-	-	N/A		-
TD13NOV5	N/A	N/A	N/A	-	-	-	-	-		-
TD13NO10	N/A	N/A	N/A	1.1	8.88	-	-	3.01		115
TD12NO10 Tube 5	N/A	N/A	N/A	<DL	<DL	-	-	<DL		-
TD17NOV2 Tube 4	N/A	N/A	N/A	6.92	14.77	-	-	2.99		138
	N/A	N/A	N/A	<DL	<DL	-	-	<DL		26
March 1998 Program - Site E										
Gasblk1	N/A	N/A	N/A	N/A	N/A	N/A	N/A	N/A	N/A	-
S100A	N/A	N/A	N/A	N/A	N/A	N/A	N/A	N/A	N/A	-
S250A	N/A	N/A	N/A	N/A	N/A	N/A	N/A	N/A	N/A	-
S1000A	N/A	N/A	N/A	N/A	N/A	N/A	N/A	N/A	N/A	-
S1000B	N/A	N/A	N/A	N/A	N/A	N/A	N/A	N/A	N/A	-
S1000C	N/A	N/A	N/A	N/A	N/A	N/A	N/A	N/A	N/A	-
S100B	N/A	N/A	N/A	N/A	N/A	N/A	N/A	N/A	N/A	-

Date Printed: 8/27/2004

Table I-1. Results of GC/PID Vapour and Air Testing

Sample Designation	Soil Vapour or Indoor Air Concentration			Indoor Air Concentration						3-fluoro toluene Recov-ery (%)
	Benzene (mg/L)	Toluene (mg/L)	m&p-Xylene (mg/L)	Benzene (ug/m3)	Toluene (ug/m3)	3-fluorotolu (ug/m3)	Ethyl benzene	m&p-Xylene (ug/m3)	o-Xylene (ug/m3)	
S250B	N/A	N/A	N/A	N/A	N/A	N/A	N/A	N/A	N/A	-
-	<DL	<DL	<DL	N/A	N/A	N/A	N/A	N/A	N/A	-
-	<DL	<DL	<DL	N/A	N/A	N/A	N/A	N/A	N/A	-
Syn #1 - Run1	<DL	0.006	<DL	N/A	N/A	N/A	N/A	N/A	N/A	-
Syn #1 - Run2	<DL	<DL	<DL	N/A	N/A	N/A	N/A	N/A	N/A	-
Syn #1 - Run3	<DL	<DL	<DL	N/A	N/A	N/A	N/A	N/A	N/A	-
Syn #3 - Run1	<DL	0.002	<DL	N/A	N/A	N/A	N/A	N/A	N/A	-
Syn #3 - Run2	<DL	0.002	<DL	N/A	N/A	N/A	N/A	N/A	N/A	-
Syn #3 - Run3	<DL	<DL	<DL	N/A	N/A	N/A	N/A	N/A	N/A	-
Syn #3 - Run4	<DL	0.002	<DL	N/A	N/A	N/A	N/A	N/A	N/A	-
Syn #4 - Run1	0.001	0.002	<DL	N/A	N/A	N/A	N/A	N/A	N/A	-
Syn #4 - Run2	0.005	0.006	<DL	N/A	N/A	N/A	N/A	N/A	N/A	-
Syn #5 - Run1	<DL	<DL	<DL	N/A	N/A	N/A	N/A	N/A	N/A	-
Syn #5 - Run2	0.013	0.038	<DL	N/A	N/A	N/A	N/A	N/A	N/A	-
Syn #5 - Run3	<DL	<DL	<DL	N/A	N/A	N/A	N/A	N/A	N/A	-
Syn #6 - Run1	0.005	0.012	<DL	N/A	N/A	N/A	N/A	N/A	N/A	-
Syn #6 - Run2	0.087	0.104	<DL	N/A	N/A	N/A	N/A	N/A	N/A	-
Syn #6 - Run3	0.004	0.006	<DL	N/A	N/A	N/A	N/A	N/A	N/A	-
Syn #6 - Run4	0.020	0.031	<DL	N/A	N/A	N/A	N/A	N/A	N/A	-
Syn #6 - Run5	0.002	0.004	<DL	N/A	N/A	N/A	N/A	N/A	N/A	-
SG-BR (10mE)	<DL	<DL	<DL	N/A	N/A	N/A	N/A	N/A	N/A	-
SG-BR (10mE)	<DL	0.002	<DL	N/A	N/A	N/A	N/A	N/A	N/A	-
SG-BR (10mE)	12.1	4.90	0.147	N/A	N/A	N/A	N/A	N/A	N/A	-
SG-BR (10mE)	16.5	12.5	0.397	N/A	N/A	N/A	N/A	N/A	N/A	-
SG-BC	<DL	<DL	<DL	N/A	N/A	N/A	N/A	N/A	N/A	-
SG-BC	0.002	0.124	0.024	N/A	N/A	N/A	N/A	N/A	N/A	-
SG-BC	0.072	0.966	0.033	N/A	N/A	N/A	N/A	N/A	N/A	-
SG-BC	5.77	9.01	0.680	N/A	N/A	N/A	N/A	N/A	N/A	-

Date Printed: 8/27/2004

Table I-1. Results of GC/PID Vapour and Air Testing

240

Sample Designation	Soil Vapour or Indoor Air Concentration			Indoor Air Concentration						3-fluoro toluene Recov-ery (%)
	Benzene (mg/L)	Toluene (mg/L)	m&p-Xylene (mg/L)	Benzene (ug/m3)	Toluene (ug/m3)	3-fluorotolu (ug/m3)	Ethyl benzene	m&p-Xylene (ug/m3)	o-Xylene (ug/m3)	
SG-BC	17.9	24.7	1.79	N/A	N/A	N/A	N/A	N/A	N/A	-
June 1998 Program - Site B										
Standard #1	N/A	N/A	N/A	N/A	N/A	N/A	N/A	N/A	N/A	-
Standard #2	N/A	N/A	N/A	N/A	N/A	N/A	N/A	N/A	N/A	-
Standard #3	N/A	N/A	N/A	N/A	N/A	N/A	N/A	N/A	N/A	-
Standard #4	N/A	N/A	N/A	N/A	N/A	N/A	N/A	N/A	N/A	-
Standard #5	N/A	N/A	N/A	N/A	N/A	N/A	N/A	N/A	N/A	-
Standard #6	N/A	N/A	N/A	N/A	N/A	N/A	N/A	N/A	N/A	-
Standard #7	N/A	N/A	N/A	N/A	N/A	N/A	N/A	N/A	N/A	-
SG-BC	NC	NC	NC	N/A	N/A	N/A	N/A	N/A	N/A	-
SG-BC	NC	NC	NC	N/A	N/A	N/A	N/A	N/A	N/A	-
SG-EC	NC	NC	NC	N/A	N/A	N/A	N/A	N/A	N/A	-
SG-EC	NC	NC	NC	N/A	N/A	N/A	N/A	N/A	N/A	-
SG-SC	NC	NC	NC	N/A	N/A	N/A	N/A	N/A	N/A	-
SG-SC	NC	NC	NC	N/A	N/A	N/A	N/A	N/A	N/A	-
SG-WC	NC	NC	NC	N/A	N/A	N/A	N/A	N/A	N/A	-
SG-NC	NC	NC	NC	N/A	N/A	N/A	N/A	N/A	N/A	-
SG-O2 PROBE	NC	NC	NC	N/A	N/A	N/A	N/A	N/A	N/A	-
SG-BC	NC	NC	NC	N/A	N/A	N/A	N/A	N/A	N/A	-
SG-BC	NC	NC	NC	N/A	N/A	N/A	N/A	N/A	N/A	-
SG-BC	NC	NC	NC	N/A	N/A	N/A	N/A	N/A	N/A	-
SG-BC	NC	NC	NC	N/A	N/A	N/A	N/A	N/A	N/A	-
SG-BC	NC	NC	NC	N/A	N/A	N/A	N/A	N/A	N/A	-
SG-BC	NC	NC	NC	N/A	N/A	N/A	N/A	N/A	N/A	-
SG-EC	NC	NC	NC	N/A	N/A	N/A	N/A	N/A	N/A	-
SG-SC	NC	NC	NC	N/A	N/A	N/A	N/A	N/A	N/A	-
SG-SC	NC	NC	NC	N/A	N/A	N/A	N/A	N/A	N/A	-
SG-WC	NC	NC	NC	N/A	N/A	N/A	N/A	N/A	N/A	-
SG-NC	NC	NC	NC	N/A	N/A	N/A	N/A	N/A	N/A	-
SG-BR (10mE)	NC	NC	NC	N/A	N/A	N/A	N/A	N/A	N/A	-

Date Printed: 8/27/2004

Table I-1. Results of GC/PID Vapour and Air Testing

Sample Designation	Soil Vapour or Indoor Air Concentration Benzene (mg/L)	Toluene (mg/L)	m&p-Xylene (mg/L)	Indoor Air Concentration Benzene (ug/m3)	Toluene (ug/m3)	3-fluorotolu (ug/m3)	Ethyl benzene	m&p-Xylene (ug/m3)	o-Xylene (ug/m3)	3-fluoro toluene Recov-ery (%)
December 1998 Program - S										
Calibration & Quality Contro										
Syringe 1	0.016	0.041	0.004	N/A	N/A	N/A	N/A	N/A	N/A	-
Syringe 1	NC	NC	NC	N/A	N/A	N/A	N/A	N/A	N/A	-
Syringe 1	0.01	0.027	0.001	N/A	N/A	N/A	N/A	N/A	N/A	-
60ng std	NC	NC	NC	N/A	N/A	N/A	N/A	N/A	N/A	-
60ng std	NC	NC	NC	N/A	N/A	N/A	N/A	N/A	N/A	-
300ng std	NC	NC	NC	N/A	N/A	N/A	N/A	N/A	N/A	-
Sorbant Tube 1	NC	NC	NC	N/A	N/A	N/A	N/A	N/A	N/A	-
Sorbant Tube 5	NC	NC	NC	N/A	N/A	N/A	N/A	N/A	N/A	-
800ng std	NC	NC	NC	N/A	N/A	N/A	N/A	N/A	N/A	-
Sorbant Tube 1	NC	NC	NC	N/A	N/A	N/A	N/A	N/A	N/A	-
Sorbant Tube 5	NC	NC	NC	N/A	N/A	N/A	N/A	N/A	N/A	-
800ng std	NC	NC	NC	N/A	N/A	N/A	N/A	N/A	N/A	-
Sorbant Tube 1	NC	NC	NC	N/A	N/A	N/A	N/A	N/A	N/A	-
Sorbant Tube 5	NC	NC	NC	N/A	N/A	N/A	N/A	N/A	N/A	-
Sorbant Tube 5	NC	NC	NC	N/A	N/A	N/A	N/A	N/A	N/A	-
575ng std	NC	NC	NC	N/A	N/A	N/A	N/A	N/A	N/A	-
115ng std	NC	NC	NC	N/A	N/A	N/A	N/A	N/A	N/A	-
Sorbant Tube 5	NC	NC	NC	N/A	N/A	N/A	N/A	N/A	N/A	-
60ng std	NC	NC	NC	N/A	N/A	N/A	N/A	N/A	N/A	-
550ng std	NC	NC	NC	N/A	N/A	N/A	N/A	N/A	N/A	-
800ng std	NC	NC	NC	N/A	N/A	N/A	N/A	N/A	N/A	-
2400ng std	NC	NC	NC	N/A	N/A	N/A	N/A	N/A	N/A	-
Sample Tests (DYNAMIC- -1										
Indoor Sample	2883	4452	144	N/A	N/A	N/A	N/A	N/A	N/A	-
SG-BR (10mE)	0.0016	0.0003	<DL	N/A	N/A	N/A	N/A	N/A	N/A	-
Indoor Sample	2252	3855	113	N/A	N/A	N/A	N/A	N/A	N/A	-
SG-BR (10mE)	0.00004	0.00001	<DL	N/A	N/A	N/A	N/A	N/A	N/A	-
Indoor Sample	1243	2104	70	N/A	N/A	N/A	N/A	N/A	N/A	-
SG-BR (10mE)	0.0007	0.0005	0.00006	N/A	N/A	N/A	N/A	N/A	N/A	-
SG-BR (10mE)	0.002	0.0016	0.00014	N/A	N/A	N/A	N/A	N/A	N/A	-

Date Printed: 8/27/2004

Table I-1. Results of GC/PID Vapour and Air Testing

Sample Designation	Soil Vapour or Indoor Air Concentration			Indoor Air Concentration						3-fluoro toluene Recov-ery (%)
	Benzene (mg/L)	Toluene (mg/L)	m&p-Xylene (mg/L)	Benzene (ug/m3)	Toluene (ug/m3)	3-fluorotolu (ug/m3)	Ethyl benzene	m&p-Xylene (ug/m3)	o-Xylene (ug/m3)	
Indoor Sample	1716	2986	94	N/A	N/A	N/A	N/A	N/A	N/A	-
SG-BC	12.98	16.64	1.4	N/A	N/A	N/A	N/A	N/A	N/A	-
SG-NC	2	3.06	0.09	N/A	N/A	N/A	N/A	N/A	N/A	-
SG-SC	6.42	9.04	0.19	N/A	N/A	N/A	N/A	N/A	N/A	-
SG-EC	1.13	0.88	0.03	N/A	N/A	N/A	N/A	N/A	N/A	-
SG-WC	0.43	0.77	0.03	N/A	N/A	N/A	N/A	N/A	N/A	-
SG-MW	9.38	13.87	0.25	N/A	N/A	N/A	N/A	N/A	N/A	-
November/December 1998 P										
Calibration & Quality Contro										
Sorbant Tube 1	NC	NC	NC	N/A	N/A	N/A	N/A	N/A	N/A	-
Sorbant Tube 5	NC	NC	NC	N/A	N/A	N/A	N/A	N/A	N/A	-
Sorbant Tube 5	NC	NC	NC	N/A	N/A	N/A	N/A	N/A	N/A	-
6400ng std	NC	NC	NC	N/A	N/A	N/A	N/A	N/A	N/A	-
11000ng std	NC	NC	NC	N/A	N/A	N/A	N/A	N/A	N/A	-
Syringe 1	NC	NC	NC	N/A	N/A	N/A	N/A	N/A	N/A	-
12ng std	NC	NC	NC	N/A	N/A	N/A	N/A	N/A	N/A	-
300ng std	NC	NC	NC	N/A	N/A	N/A	N/A	N/A	N/A	-
Sorbant Tube 1	NC	NC	NC	N/A	N/A	N/A	N/A	N/A	N/A	-
Sorbant Tube 5	NC	NC	NC	N/A	N/A	N/A	N/A	N/A	N/A	-
60ng std	NC	NC	NC	N/A	N/A	N/A	N/A	N/A	N/A	-
60ng std	NC	NC	NC	N/A	N/A	N/A	N/A	N/A	N/A	-
550ng std	NC	NC	NC	N/A	N/A	N/A	N/A	N/A	N/A	-
12000ng std	NC	NC	NC	N/A	N/A	N/A	N/A	N/A	N/A	-
Syringe 1	NC	NC	NC	N/A	N/A	N/A	N/A	N/A	N/A	-
Syringe 2	NC	NC	NC	N/A	N/A	N/A	N/A	N/A	N/A	-
Syringe 4	NC	NC	NC	N/A	N/A	N/A	N/A	N/A	N/A	-
12ng std	NC	NC	NC	N/A	N/A	N/A	N/A	N/A	N/A	-
300ng std	NC	NC	NC	N/A	N/A	N/A	N/A	N/A	N/A	-
12000ng std	NC	NC	NC	N/A	N/A	N/A	N/A	N/A	N/A	-
2400ng std	NC	NC	NC	N/A	N/A	N/A	N/A	N/A	N/A	-
Sorbant Tube 1	NC	NC	NC	N/A	N/A	N/A	N/A	N/A	N/A	-
4600ng std	NC	NC	NC	N/A	N/A	N/A	N/A	N/A	N/A	-

Date Printed: 8/27/2004

Table I-1. Results of GC/PID Vapour and Air Testing

Sample Designation	Soil Vapour or Indoor Air Concentration			Indoor Air Concentration						3-fluoro toluene Recov-ery (%)
	Benzene (mg/L)	Toluene (mg/L)	m&p-Xylene (mg/L)	Benzene (ug/m3)	Toluene (ug/m3)	3-fluorotolu (ug/m3)	Ethyl benzene	m&p-Xylene (ug/m3)	o-Xylene (ug/m3)	
2400ng std	NC	NC	NC	N/A	N/A	N/A	N/A	N/A	N/A	-
2400ng std	NC	NC	NC	N/A	N/A	N/A	N/A	N/A	N/A	-
Sorbant Tube 1	NC	NC	NC	N/A	N/A	N/A	N/A	N/A	N/A	-
Sorbant Tube 1	NC	NC	NC	N/A	N/A	N/A	N/A	N/A	N/A	-
Sorbant Tube2	NC	NC	NC	N/A	N/A	N/A	N/A	N/A	N/A	-
550ng std	NC	NC	NC	N/A	N/A	N/A	N/A	N/A	N/A	-
2400ng std	NC	NC	NC	N/A	N/A	N/A	N/A	N/A	N/A	-
Sorbant Tube 1	NC	NC	NC	N/A	N/A	N/A	N/A	N/A	N/A	-
Sorbant Tube 2	NC	NC	NC	N/A	N/A	N/A	N/A	N/A	N/A	-
Sorbant Tube 3	NC	NC	NC	N/A	N/A	N/A	N/A	N/A	N/A	-
60ng std	NC	NC	NC	N/A	N/A	N/A	N/A	N/A	N/A	-
600ng std	NC	NC	NC	N/A	N/A	N/A	N/A	N/A	N/A	-
2400ng std	NC	NC	NC	N/A	N/A	N/A	N/A	N/A	N/A	-
4400ng std	NC	NC	NC	N/A	N/A	N/A	N/A	N/A	N/A	-
12ng std	NC	NC	NC	N/A	N/A	N/A	N/A	N/A	N/A	-
Syringe 1	NC	NC	NC	N/A	N/A	N/A	N/A	N/A	N/A	-
Syringe 2	NC	NC	NC	N/A	N/A	N/A	N/A	N/A	N/A	-
Syringe 2	NC	NC	NC	N/A	N/A	N/A	N/A	N/A	N/A	-
Syringe 2	NC	NC	NC	N/A	N/A	N/A	N/A	N/A	N/A	-
Syringe 4	NC	NC	NC	N/A	N/A	N/A	N/A	N/A	N/A	-
12ng std	NC	NC	NC	N/A	N/A	N/A	N/A	N/A	N/A	-
12ng std	NC	NC	NC	N/A	N/A	N/A	N/A	N/A	N/A	-
60ng std	NC	NC	NC	N/A	N/A	N/A	N/A	N/A	N/A	-
12ng std	NC	NC	NC	N/A	N/A	N/A	N/A	N/A	N/A	-
60ng std	NC	NC	NC	N/A	N/A	N/A	N/A	N/A	N/A	-
Sample Tests (DYNAMIC- -1										
Indoor Sample	1309	2457	233	N/A	N/A	N/A	N/A	N/A	N/A	-
Indoor Sample	0.045	0.072	0.002	N/A	N/A	N/A	N/A	N/A	N/A	-
Indoor Sample	1025	3403	148	N/A	N/A	N/A	N/A	N/A	N/A	-
Indoor Sample	1061	3177	150	N/A	N/A	N/A	N/A	N/A	N/A	-
Outdoor Sample	0.3	10.36	2.7	N/A	N/A	N/A	N/A	N/A	N/A	-
SG-BR (10mE)	0.03	0.05	0.001	N/A	N/A	N/A	N/A	N/A	N/A	-

Date Printed: 8/27/2004

Table I-1. Results of GC/PID Vapour and Air Testing

Sample Designation	Soil Vapour or Indoor Air Concentration			Indoor Air Concentration						3-fluoro toluene Recov-ery (%)
	Benzene (mg/L)	Toluene (mg/L)	m&p-Xylene (mg/L)	Benzene (ug/m3)	Toluene (ug/m3)	3-fluorotolu (ug/m3)	Ethyl benzene	m&p-Xylene (ug/m3)	o-Xylene (ug/m3)	
SG-BR (10mE)	0.69	0.24	0.002	N/A	N/A	N/A	N/A	N/A	N/A	-
SG-BR (10mE)	7.19	4.34	0.21	N/A	N/A	N/A	N/A	N/A	N/A	-
SG-BR (10mE)	4.6	3.08	0.18	N/A	N/A	N/A	N/A	N/A	N/A	-
SG-BR (10mE)	8.33	5.76	0.22	N/A	N/A	N/A	N/A	N/A	N/A	-
SG-BR (10mE)	22.92	17.07	1.15	N/A	N/A	N/A	N/A	N/A	N/A	-
SG-BC	7.18	8.46	0.12	N/A	N/A	N/A	N/A	N/A	N/A	-
SG-BC	20.91	25.9	0.46	N/A	N/A	N/A	N/A	N/A	N/A	-
SG-BC	10.93	10.79	0.09	N/A	N/A	N/A	N/A	N/A	N/A	-
SG-BC	12.4	11.89	0.11	N/A	N/A	N/A	N/A	N/A	N/A	-
SG-BC	12.23	11.03	0.17	N/A	N/A	N/A	N/A	N/A	N/A	-
SG-BC	9.03	9.4	0.18	N/A	N/A	N/A	N/A	N/A	N/A	-
SG-BC	13.42	13.91	0.29	N/A	N/A	N/A	N/A	N/A	N/A	-
SG-BC	19.55	19.22	0.31	N/A	N/A	N/A	N/A	N/A	N/A	-
SG-NC	4.42	4.35	0.05	N/A	N/A	N/A	N/A	N/A	N/A	-
SG-SC	7048	9.35	0.09	N/A	N/A	N/A	N/A	N/A	N/A	-
SG-EC	1.04	0.9	N/A	N/A	N/A	N/A	N/A	N/A	N/A	-
SG-WC	1.6	1.94	0.02	N/A	N/A	N/A	N/A	N/A	N/A	-
SG-O2 PROBE	7.4	8.14	0.07	N/A	N/A	N/A	N/A	N/A	N/A	-
Indoor Sample	608	645	148	N/A	N/A	N/A	N/A	N/A	N/A	-
Outdoor Sample	1.09	0.88	N/A	N/A	N/A	N/A	N/A	N/A	N/A	-
Indoor Sample	659	520	38	N/A	N/A	N/A	N/A	N/A	N/A	-
Outdoor Sample	0.6	1.48	1.37	N/A	N/A	N/A	N/A	N/A	N/A	-
TD26NOV4	1.33	1.31	0.94	N/A	N/A	N/A	N/A	N/A	N/A	-
February 1999 Program - Sit Calibration & Quality Contro										
65ng std	N/A	N/A	N/A	N/A	N/A	N/A	N/A	N/A	N/A	-
70ng std	N/A	N/A	N/A	N/A	N/A	N/A	N/A	N/A	N/A	-
70ng std	N/A	N/A	N/A	N/A	N/A	N/A	N/A	N/A	N/A	-
350ng std	N/A	N/A	N/A	N/A	N/A	N/A	N/A	N/A	N/A	-
600ng std	N/A	N/A	N/A	N/A	N/A	N/A	N/A	N/A	N/A	-
1500ng std	N/A	N/A	N/A	N/A	N/A	N/A	N/A	N/A	N/A	-
1500ng std	N/A	N/A	N/A	N/A	N/A	N/A	N/A	N/A	N/A	-

Date Printed: 8/27/2004

Table I-1. Results of GC/PID Vapour and Air Testing

215

Sample Designation	Soil Vapour or Indoor Air Concentration			Indoor Air Concentration						3-fluoro toluene Recov-ery (%)
	Benzene (mg/L)	Toluene (mg/L)	m&p-Xylene (mg/L)	Benzene (ug/m3)	Toluene (ug/m3)	3-fluorotolu (ug/m3)	Ethyl benzene	m&p-Xylene (ug/m3)	o-Xylene (ug/m3)	
Syringe 1	N/A	N/A	N/A	N/A	N/A	N/A	N/A	N/A	N/A	-
Syringe 2	N/A	N/A	N/A	N/A	N/A	N/A	N/A	N/A	N/A	-
Syringe 3	N/A	N/A	N/A	N/A	N/A	N/A	N/A	N/A	N/A	-
Syringe 1	N/A	N/A	N/A	N/A	N/A	N/A	N/A	N/A	N/A	-
Sample Tests (STATIC-FAN										
SG-BC	0.007	0.017	0.002	N/A	N/A	N/A	N/A	N/A	N/A	-
SG-BC	0.001	0.006	0.001	N/A	N/A	N/A	N/A	N/A	N/A	-
SG-BC	0.745	7.21	0.306	N/A	N/A	N/A	N/A	N/A	N/A	-
SG-BC	1.4	9.43	0.25	N/A	N/A	N/A	N/A	N/A	N/A	-
SG-BC	5.83	8.93	0.22	N/A	N/A	N/A	N/A	N/A	N/A	-
SG-BC	9.72	13.69	0.42	N/A	N/A	N/A	N/A	N/A	N/A	-
SG-BR (10mE)	0.0005	0.001	0.0003	N/A	N/A	N/A	N/A	N/A	N/A	-
SG-BR (10mE)	0.013	0.008	0.0003	N/A	N/A	N/A	N/A	N/A	N/A	-
SG-BR (10mE)	0.556	0.24	0.003	N/A	N/A	N/A	N/A	N/A	N/A	-
SG-BR (10mE)	4	1.72	0.074	N/A	N/A	N/A	N/A	N/A	N/A	-
SG-BR (10mE)	10.19	6.61	0.3	N/A	N/A	N/A	N/A	N/A	N/A	-
SG-Adjacent to Old Building										
SYRINGE BLANKS										
Syringe 1	<0.0008	0.0009	<0.0007	N/A	N/A	N/A	N/A	N/A	N/A	-
Syringe 2	<0.0008	0.002	<0.0007	N/A	N/A	N/A	N/A	N/A	N/A	-
SAMPLES										
SG-AOB	<0.0008	0.0017	<0.0007	N/A	N/A	N/A	N/A	N/A	N/A	-
SG-AOB	<0.0008	0.001	<0.0007	N/A	N/A	N/A	N/A	N/A	N/A	-
SG-AOB	<0.0008	0.0015	<0.0007	N/A	N/A	N/A	N/A	N/A	N/A	-
SG-AOB	<0.0008	0.0033	0.0007	N/A	N/A	N/A	N/A	N/A	N/A	-
SG-AOB	<0.0008	0.0019	0.001	N/A	N/A	N/A	N/A	N/A	N/A	-
SG-(below) Old Building (OE										
SYRINGE BLANKS										
Syringe 1	0.0015	0.0058	0.0007	N/A	N/A	N/A	N/A	N/A	N/A	-
Syringe 3	0.0025	0.0204	0.0014	N/A	N/A	N/A	N/A	N/A	N/A	-

Date Printed: 8/27/2004

Table I-1. Results of GC/PID Vapour and Air Testing

246

Sample Designation	Soil Vapour or Indoor Air Concentration Benzene (mg/L)	Toluene (mg/L)	m&p-Xylene (mg/L)	Indoor Air Concentration Benzene (ug/m3)	Toluene (ug/m3)	3-fluorotolu (ug/m3)	Ethyl benzene	m&p-Xylene (ug/m3)	o-Xylene (ug/m3)	3-fluoro toluene Recov-ery (%)
SAMPLES										
SG-OB	0.84	>1.366	0.4174	N/A	N/A	N/A	N/A	N/A	N/A	-
SG-OB	1.04	>1.64	0.3279	N/A	N/A	N/A	N/A	N/A	N/A	-
SG-(below) OB: JUNE 25, 19										
SYRINGE BLANKS										
Syringe 3	0.0039	0.0124	0.0008	N/A	N/A	N/A	N/A	N/A	N/A	-
SAMPLES										
SG-OB	0.711	>2.397	0.1976	N/A	N/A	N/A	N/A	N/A	N/A	-
SG-OB	0.2528	5.2718	0.047	N/A	N/A	N/A	N/A	N/A	N/A	-
SG-OB	0.7015	6.238	0.0918	N/A	N/A	N/A	N/A	N/A	N/A	-
SG-OB	0.2632	4.8415	0.0308	N/A	N/A	N/A	N/A	N/A	N/A	-
SG-OB	0.3913	4.8109	0.0314	N/A	N/A	N/A	N/A	N/A	N/A	-
SG-OB	0.6528	5.6692	0.0554	N/A	N/A	N/A	N/A	N/A	N/A	-
SG-Adjacent to Building (EC										
SYRINGE BLANKS										
Syringe 2	NC	NC	NC	N/A	N/A	N/A	N/A	N/A	N/A	-
SAMPLES										
SG-BE (10mE) (EO)	0.0004374	0.000434	0.00046	N/A	N/A	N/A	N/A	N/A	N/A	-
SG-BE (10mE) (EO)	0.0004374	0.000464443	0.00046	N/A	N/A	N/A	N/A	N/A	N/A	-
SG-BE (10mE) (EO)	0.000584511	0.005471424	0.003194832	N/A	N/A	N/A	N/A	N/A	N/A	-
SG-BE (10mE) (EO)	5.220093472	2.857468517	0.103044558	N/A	N/A	N/A	N/A	N/A	N/A	-
SG-BE (10mE) (EO)	6.831592895	5.037918531	0.235444442	N/A	N/A	N/A	N/A	N/A	N/A	-
SG-BE (10mE) (EO)	4.868375374	2.532362616	0.117971112	N/A	N/A	N/A	N/A	N/A	N/A	-

Notes:

N/A = Not applicable, NC = no

- = not tested

Calibration Curves Used for Q

APPENDIX II

EQUATION FOR VADOSE ZONE CHEMICAL TRANSPORT

APPENDIX II – Equation for Vadose Zone Chemical Transport

This appendix provides a derivation of the differential equation for vadose zone chemical transport incorporating one-dimensional advection, dispersion, diffusion and reaction. The mass conservation equation for a single chemical species in a porous media may be written as follows:

$$\frac{\partial C_T}{\partial t} = \frac{\partial}{\partial Z}\left(D\frac{\partial C_T}{\partial Z}\right) - \frac{\partial}{\partial Z}(V_Z C_T) - \mu C_T + M \qquad \text{(i)}$$

where C_T is the total chemical concentration ($mol\ M^{-1}$), t is the time (T), D is the hydrodynamic dispersion coefficient ($L^2\ T^{-1}$), V_z is the Darcy velocity ($L\ T^{-1}$), μ_T is the first-order degradation rate (T^{-1}) and M is a source sink input term ($M\ L^{-3}\ T^{-1}$). Assuming equilibrium chemical partitioning between the gas, aqueous and sorbed phase, and linear isotherms, the following relationships are developed between chemical concentrations in different phases:

$$C_T = \Theta_w C_w + \Theta_g C_g + \rho_b C_s \qquad \text{(ii)}$$

$$C_S = k_d C_w \qquad \text{(iii)}$$

$$C_g = H' C_w \qquad \text{(iv)}$$

where C_s is the mass of chemical per mass of solid (MM^{-1}), K_d is the distribution coefficient between the sorbed and aqueous phases (L^3M^{-1}), C_w is the aqueous phase concentration ($mol\ L^{-3}$), H' is Henry's Law Constant (*dimensionless*), θ_g is the gas-phase porosity (L^3L^{-3}), θ_w is the water-filled porosity (L^3L^{-3}), ρ_b is the dry bulk density of the soil (ML^{-3}) and C_g is the soil gas concentration ($mol\ L^{-3}$). Substituting equation (ii) into equation (1) and assuming that moisture content does not vary with time and that there is no solid phase transport, the following mass conservation equations are derived:

Gas: $$\Theta_g \frac{\partial C_g}{\partial t} = \frac{\partial}{\partial Z}\left[D_g \Theta_g \frac{\partial C_g}{\partial Z}\right] + \frac{\partial}{\partial Z}\left[D_{gh} \Theta_g \frac{\partial C_g}{\partial Z}\right] - \frac{\partial}{\partial Z} V_g \Theta_g C_g - \mu_g \Theta_g C_g \qquad \text{(v)}$$

Water: $$\Theta_w \frac{\partial C_w}{\partial t} = \frac{\partial}{\partial Z}\left[D_w \Theta_w \frac{\partial C_w}{\partial Z}\right] + \frac{\partial}{\partial Z}\left[D_{wh} \Theta_w \frac{\partial C_w}{\partial Z}\right] - \frac{\partial}{\partial Z} V_w \Theta_w C_w - \mu_w \Theta_w C_w \qquad \text{(vi)}$$

Solid (sorbed): $$\rho_b \frac{\partial C_s}{\partial t} = -\mu \rho_b C_s \qquad \text{(vii)}$$

where V_g is the gas-phase Darcy velocity, V_w is the aqueous-phase Darcy velocity, D_g is the gas-phase diffusion coefficient ($L^2\ T^{-1}$), D_{gh} is the gas-phase dispersion coefficient, D_w is the aqueous-phase diffusion coefficient ($L^2\ T^{-1}$), D_{wh} is the aqueous-phase dispersion coefficient, and μ_i are the first-order degradation coefficients for the three phases as denoted by the subscript *i*.

Combining terms for the gas and aqueous phases and assuming that fate and transport processes are limited to gas-phase and aqueous-phase diffusion, and that degradation occurs only in the aqueous phase results in the following equation:

$$\Theta_w \frac{\partial C_w}{\partial t} + \Theta_g \frac{\partial C_g}{\partial t} + \rho_b \frac{\partial C_s}{\partial t} = \frac{\partial}{\partial Z}\left(\Theta_g D_g \frac{\partial C_g}{\partial Z}\right) + \frac{\partial}{\partial Z}\left(\Theta_w D_w \frac{\partial C_w}{\partial Z}\right) - \mu_w \Theta_w C_w \qquad \text{(viii)}$$

Through substitution of equations (3) and (4) into equation (8), the following expressions are derived:

$$\Theta_g R \frac{\partial C_g}{\partial t} = \frac{\partial}{\partial Z}\left(\Theta_g D_g + \frac{\Theta_w}{H'} D_w\right)\frac{\partial C_g}{\partial Z} - \mu_w \frac{\Theta_w}{H'} C_g \qquad \text{(ix)}$$

$$R = 1 + \frac{\Theta_w}{\Theta_g H'} + \frac{\rho_b k_d}{\Theta_g H'} \qquad \text{(x)}$$

where R is the retardation coefficient (*dimensionless*).

APPENDIX III

ANALYSIS OF MOISTURE CONTENT DATA

APPENDIX III : ANALYSIS OF MOISTURE CONTENT DATA

Soil moisture content were measured in soil cores from below the approximate middle of the greenhouse before and after greenhouse construction. Soil cores for moisture content testing were also obtained adjacent to the greenhouse. On average, the moisture contents below the greenhouse appear to be highest between about 0.6 and 0.9 m depth. However, moisture content monitoring below the greenhouse was conducted over a one-year period and therefore is not indicative of longer-term trends.

To investigate long-term trends, a soil core was obtained from below a nearby building on the Chatterton site constructed in the 1960's (Figure III-1). Within 1 m of slab surface, the moisture content below the "old" building is consistently lower than that measured below the greenhouse. Unlike below the greenhouse, the moisture content below the building also gradually increased with depth, which is expected in the absence of surface water infiltration. The lowest moisture content below the old building (2.6 %) is likely just above the soil wilting point, estimated to be on the order of 1 to 2.5 % based on tests conducted on soil from below the greenhouse. The soil wilting point is defined as the moisture content at a matric suction of 1500 J/kg. Bioventing studies suggest that biodegradation rates are significantly reduced for soil moisture contents close to the soil wilting point (Zwick *et al.*, 1995).

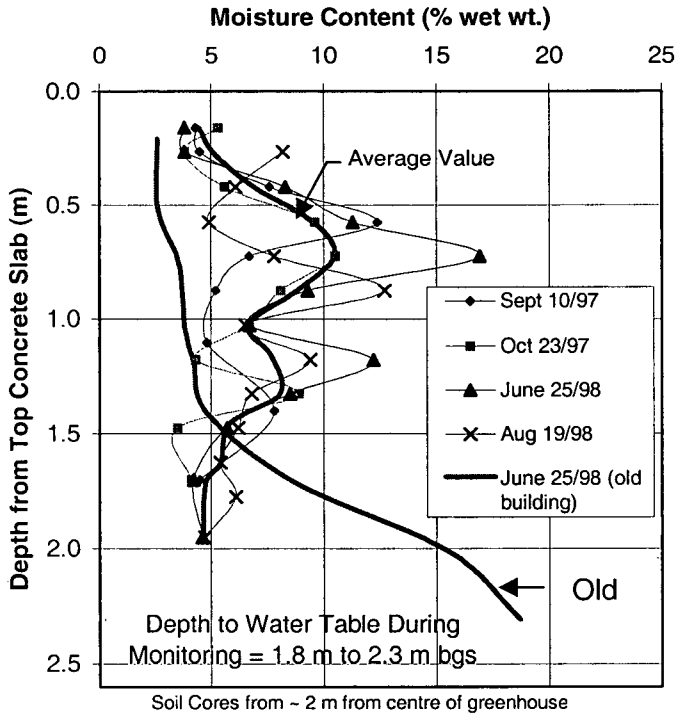

Figure III-1. Comparison Moisure Content Below Greenhouse and Old Building

The unusual shape of the moisture profile below the greenhouse leads one to question what kind of moisture regime would be expected in the absence of infiltration. After construction of the greenhouse, drying of soil would be expected since surface water infiltration would be cut off. It is difficult to predict the effect of lateral moisture transport through capillary effects;

however, based on the size of the greenhouse, lateral migration would likely not affect moisture below the middle of the greenhouse. In the absence of vertical or lateral movement of soil water, the vertical moisture content profile should be similar to the water retention curve, which plots moisture content versus the matric potential. The matric potential is equivalent to the height above the water table for this condition. Continued drying below water retention values could occur if, for example, the mean temperature below the building was higher than that adjacent to the building.

The water retention curve, based on tests conducted on samples obtained from below the greenhouse, is plotted on the moisture content profile in Figure III-1 and indicates that the moisture content measured below the greenhouse to date is significantly higher than that predicted based on the water retention curve. Possible reasons for the higher than expected moisture content include : (i) physical mechanisms (*e.g.*, variation in soil type, gradadation, sorption of water on biomass), (ii) generation of water during biodegradation, and (iii) transport of water vapour and condensation due to temperature gradients. Each possible mechanism is discussed below.

Physical Mechanisms for Moisture Content Profile

The detailed sampling program conducted in May 1999 indicated the presence of thin fin-grained silty fine sand layer at about 0.9 m depth adjacent to the greenhouse. Below the greenhouse, examination of the soil core did not reveal any distinct fine-grained layers; however, some variation in grain size is likely. Grain size analyses indicated that the sand fill below the building is relatively uniform with measured silt contents in samples collected over 0.15 m intervals ranging from 1.8 to 5.5 %. The results do not point to obvious grain size differences that would account for moisture content differences; however, the influence of thin finer-grained soils can not be ruled out.

Generation of biomass occurs as a result of biological activity. Based on a combined first-order and zero-order decay model the biodegradation rate increases with depth until concentrations reach a critical level. Therefore, the rate of biomass formation would also increase with depth up to a certain point. However, at increasing depths, biodegradation rates may decrease due to toxic effects resulting from the very high BTX concentrations. Based on this conceptual model, the greatest concentration of biomass would occur over the mid-depth zone. Biomass would tend to enhance the sorption or retention of water. The soil organic carbon content provides an indirect indication of biomass content since carbon is the main constituent of biomass. The soil organic content was estimated using the loss-on-ignition test and was found to be slightly higher in one sample adjacent to the building from 0.88 to 0.92 m depth, as described in Chapter 5.

Generation of Water Through Biodegradation

The complete mineralization of BTX through aerobic respiration will produce as end products CO_2 and water. The stochiometric equation for toluene oxidation is:

$$C_7H_8 + 9O_2 \rightarrow 7\,CO_2 + 4\,H_2O \qquad (1)$$

For every gram of benzene, toluene and m&p-xylene degraded, 0.69 gram, 0.78 gram and 0.83 gram of water is produced. Based on the mass fraction of BTX present in the subsurface, on average about 0.76 gram of water is produced for each gram of BTX degraded. Based on a first-order decay model, the biodegradation rate between 0.5 and 0.8 m depth increases significantly and therefore the water generation rate will also increase with depth. The maximum degradation rate can be approximated by the zero-order biodegradation rate obtained from the *in situ* respiration test. The maximum measured rate of 6 mg/L-hr. and an average volumetric water content of 10 % yields a water generation rate of 0.8 mg H_20 /L-soil-hr. Assuming this process occurs for one year and that all water generated is retained by soil results in a 0.007 increase in the volumetric water content. These calculations suggest that water generated through biodecay would not have a significant effect on the subsurface moisture content.

Moisture Transport Through Temperature Gradients

There are three principle modes of heat transfer consisting of conduction, convection and radiation. Conduction, the propagation of heat by internal molecular motion, is generally the primary process for heat flow (Hillel, 1980). Conduction of heat in soil can be described through the first law of heat conduction (Fourier's law), which in one-dimension can be expressed as:

$$G = - K \ \delta T / \delta z \qquad (2)$$

where G is the thermal flux ($J\ sec^{-1}\ m^{-2}$), K is the thermal conductivity ($J\ sec^{-1}\ m^{-2}$) and T is the temperature (K). To account for non-steady state conditions, the principle of energy conservation is invoked to obtain the second law of heat conduction, which in the absence of sources and sinks, can be expressed as:

$$\delta T / \delta t \ = \delta / \delta z \ (D_T \ \delta T / \delta z) \qquad (3)$$

$$D_T = K / C \qquad (4)$$

where t is the time (sec), D_T is the thermal diffusivity ($kg\ sec^{-1}\ m^{-1}$) and C is the volumetric heat capacity ($J\ K^{-1}\ m^{-3}$). The effect of diurnal or seasonal variation in air temperature and effect on soil temperature can be evaluated through an analytical solution to equations 2 and 3 assuming periodic solutions for boundary conditions (Carslaw and Jaeger, 1959), as follows:

$$T\ (0, t) = T_a \ + \ A_o \sin (\omega\ t + \alpha_o) \qquad (5)$$

$$T(\text{infinity},t) = T_a \qquad (6)$$

$$T(z,t) = T_a \ + \ A_o\ e^{-z/d} \sin (\omega\ t - z/d + \alpha_o) \qquad (7)$$

$$G(z,t) = T_a\ (\omega KC)^{\wedge 0.5}\ e^{-z/d} \sin (\omega\ t - z/d + \alpha_o + \pi/4) \qquad (8)$$

$$d = \ (2\ K / \omega\ C)^{\wedge 0.5} \qquad (9)$$

where d is the damping depth (*m*), T_a is the average soil temperature (*K*), A_o is the amplitude of the variation in air temperature (*K*), ω is equal to $2\pi / \tau$ where t is the period of the temperature change cycle (*sec*). Key assumptions are that the mean air and soil temperature is identical and that the variation in soil temperature is sinusoidal. Due to the heating effect of the greenhouse, the mean temperature in the greenhouse will be greater than that in soil. Variation in air temperature in the greenhouse is not sinusoidal and can be more closely approximated by an exponential function (*e.g.*, $f(x) = xe^{-k\pi x2}$); however, solution of this function in not straightforward.

The volumetric heat capacity of a soil can be estimated knowing the specific heat per unit mass, $(c_m)_i$, where i represents each phase, using the following equation:

$$C = \Sigma \theta_i (\rho c_m)_i \qquad (10)$$

The thermal conductivity of a soil is dependent on the mineral composition, organic matter content, and volume fractions of solid, water and air. In addition, the thermal conductivity is affected by the sizes, shapes and spatial arrangements of soil particles (Hillel, 1980). The estimation of thermal conductivity of a soil is more complex than heat capacity.

The heat capacity and thermal conductivity of quartz, water, air and concrete is given in Table III-1. Based these values, the damping depth for quartz sand with relatively low volumetric water content (as found directly below the greenhouse) is likely on the order of 0.10 to 0.15 m. The damping depth for concrete, using the average of the range of values given in Table III-1, is 0.24 m. The diurnal and seasonal variation in temperature below the greenhouse was estimated using the analytical solution to the heat flow equation (equation 7). The temperature was estimated using a two-step procedure. First the temperature variation across the concrete slab was estimated. Next, using the temperature amplitude and time lag at the base of the concrete, the temperature variation in sand was estimated.

TABLE III-1
Thermal Properties

Material	Specific Heat Capacity (c_m) (J/kg-K)	Density (ρ) (kg/m^3)	Thermal Conductivity (K) (J/sec-m-K)
Quartz[1]	800	2700	8.8
Air (20°C)[1]	1000	1.2	0.025
Water[1]	4200	1000	0.6
Concrete[2]	840-1170	2500-2600	1.4-3.6

The temperature variation in soil was estimated using a diurnal temperature amplitude of 10°C (*i.e.*, total variation of 20°C) in the greenhouse. Monitoring of greenhouse temperature indicated that a daily variation of about 20°C was common during sunny days during the summer. The results presented in Figure III-2 predict a significant variation in temperature in soil directly below the concrete slab (about 11°C). At approximately 0.2 m depth (from top of slab), the variation in temperature reduces to about 6.5°C while at 0.4 m depth, the variation is about 1.3°C. Also of note is the time-lag between temperature variation at surface and depth.

For example, there is an approximate 4 ½ hour time-lag at 0.2 m depth and 10 ½ hour time-lag at 0.4 m depth. The estimated variation in soil temperature based on seasonal temperature trends is provided in Figure III-3.

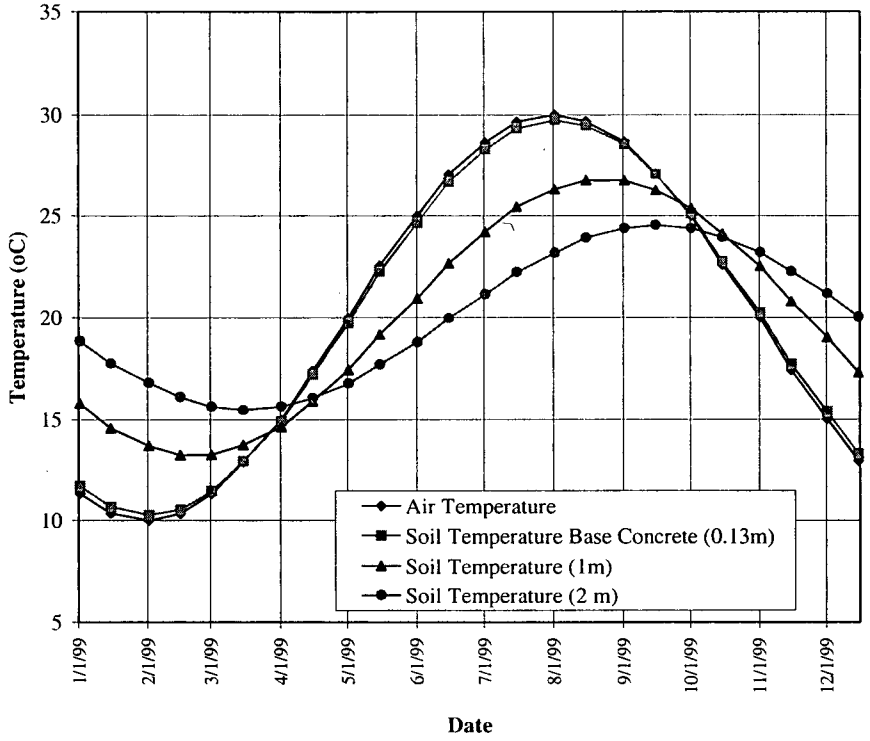

Figure III-3. Predicted Seasonal Variation in Temperature

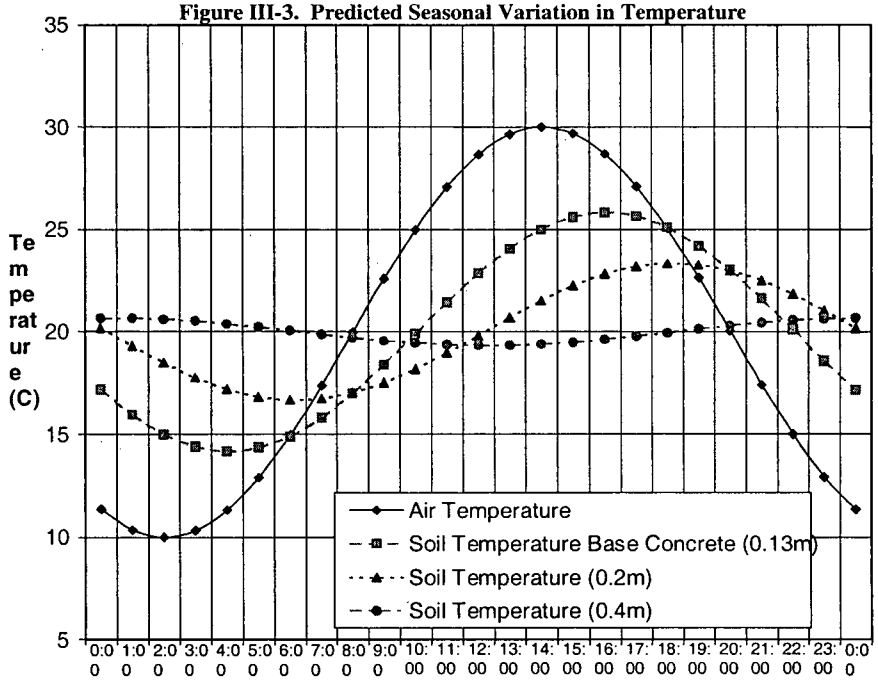

Figure III-2. Predicted Summer Fluctuations in Soil Temperature Below Greenhouse

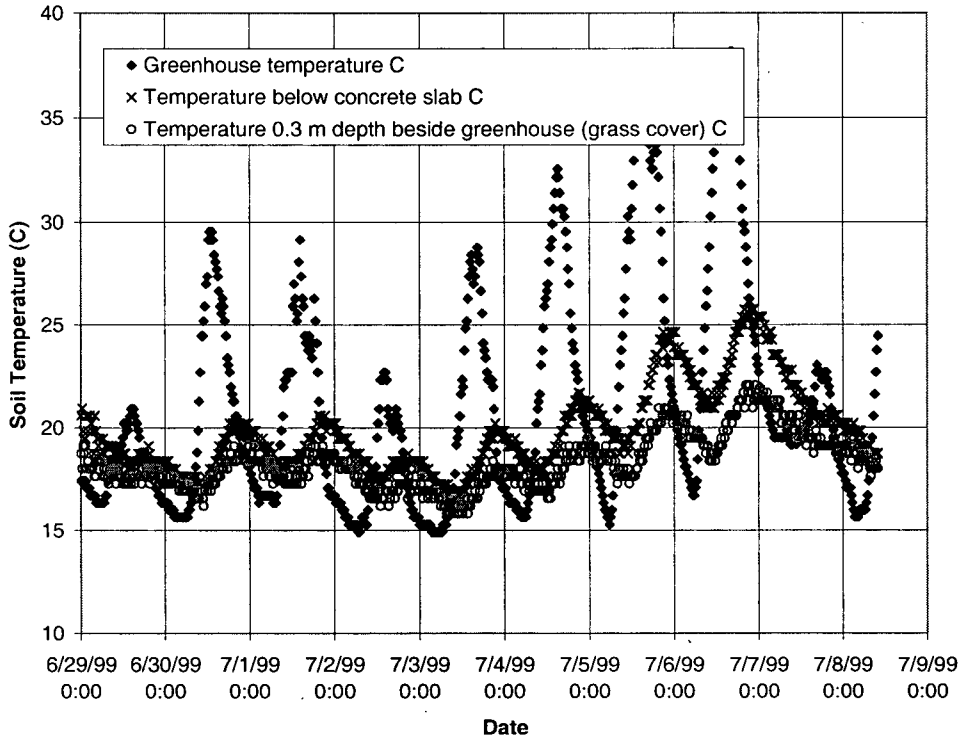

Figure III-4. Soil Temperature Below Greenhouse

The measured temperature in the greenhouse building, at about 0.25 m to 0.3 m depth below the top of slab, and at about 0.3 m depth adjacent to the greenhouse is presented in Figure III-4. When there was a 20°C variation in indoor air temperature, the variation in temperature below the slab was about 4°C, and the time-lag between indoor air and below slab temperature peaks was about 6 to 6 ½ hours. Except during cloudy weather, the sub-slab temperatures were higher than soil temperatures adjacent to the building. Overall, the model-predicted variation are reasonably close to measured values.

Water vapour diffusion will occur whenever differences in vapour pressure develop within a soil. The diffusion equation for water vapour is:

$$q_v = - D_v \delta \rho_v / \delta z \qquad \text{(I-11)}$$

where q_v is the vapour flux, D_v is the diffusion coefficient for water vapour and ρ_v is the vapour density in the gaseous phase. Vapour density will vary in response to temperature, matric potential, and osmotic or solute effects. Temperature often has the most significant effect on density. For example, a temperature difference of 0 and 20°C corresponds to a vapour pressure difference of 17.3 mbar while a change in matric suction between 0 and 100 bar is accompanied by vapour pressure change of only 1.6 mbar.

The general equation describing moisture movement under combined moisture and temperature gradients for one-dimensional vertical flow is:

$$\delta\theta_w / \delta t = \delta / \delta z \, (D_T \, \delta T / \delta z) + \delta / \delta z \, (D_W \, \delta\theta_w / \delta z) - \delta K / \delta z \qquad \text{(I-12)}$$

$$C \, \delta T / \delta t = \delta / \delta z \, (K \, \delta T / \delta z) - L \, \delta / \delta z \, (D_{W,Vap} \, \delta \theta_w / \delta z) \qquad \text{(I-13)}$$

where D_T is the water diffusivity under a temperature gradient (sum of liquid and vapour diffusivities), D_w the water diffusivity under a moisture gradient, K the hydraulic conductivity, L the latent heat of vapourization of water and $D_{w,vap}$ the diffusivity for heat conveyed by water movement. Diffusion in the above equations occurs both as a result of temperature and moisture gradients. Solution of the coupled transport equations is complicated since the diffusivities and hydraulic conductivity are dependent on volumetric water content resulting in non-linear equations. Separation of vapour from liquid flow has been attempted by monitoring salt movement in soil (Marshall and Holmes, 1980) since liquid movement includes the solutes while vapour movement does not. These studies suggest that that the rate of actual vapour movement exceeds the rate that which could be predicted through diffusion alone. A possible explanation for this occurrence was suggested by Philip and de Vries (1957) who postulated a sequential pore-scale process involving evapouration, vapour transport followed condensation.

Practical estimation of water vapour fluxes often involves simplification of equation (I-11) to just assume that vapour transport occurs as a result of temperature fluctuations. For example, Milly (1996) estimated the seasonal flux in water vapour through integration of the equation for subsurface temperature (I-7) with respect to time and substitution in the equation for vapour flux (*i.e.*, $q_v = - D_T \, \delta \, \rho_v / \delta z$). The thermal vapour diffusivity was assumed to be proportional to temperature. The maximum induced thermal flux predicted by Milly (1996) was on the order of 40 mm/yr at surface, and 18 mm/yr at 1 m depth for a A_o value of 11°C and d equal to 2.3 m.

The downward water vapour flux was estimated below the greenhouse using the simple relationship provided in equation 11. Based on the possible mean variation in annual temperature below the greenhouse (Figure I-3), it is assumed that there is on average, a 5°C temperature gradient between surface and 1 m depth over an approximate 100 day period (*i.e.*, between May and August). Assuming D_T equal to 0.2 cm^2/sec, ρ_v (25°C, 0.1 bar) equal to 23.05 x 10^{-6} g/cm^2-sec, ρ_v (20°C, 0.1 bar) equal 17.3 x 10^{-6} g/cm^2-sec, a water vapour flux of 0.1 g/cm^2 is obtained. Assuming vapour condenses as temperature decreases and that condensation is limited to a 10 cm. vertical interval, the volumetric water content within this interval would increase by 0.01 based on this vapour flux. It appears that temperature-induced downward vapour flux could have a modest effect on moisture content below the greenhouse and could account for some of the increase in the moisture content.

References

Carslaw, H.S. and J.C. Jaeger 1959. Conduction of Heat in Solids. Oxford University Press, London.

Hillel, D. 1980. Fundamentals of Soil Physics. Academic Press, New York.

Philip, J.R. and D.A. de Vries 1957. Moisure movement in porous medi under temperature gradients. *Trans. Amer. Geophys. Union*, 38: 222-232.

Marshall, T.J. and J.W. Holmes 1996. Soil Physics. Cambridge University Press, Cambridge.

Milly, P.C.D. 1996. A simulation analysis of thermal effects on evapouration from soil. *Water Resources Research*, 20: 1087-1098.

APPENDIX IV

2-D FINITE DIFFERENCE NUMBERCIAL MODEL CODE

SCREEN 8

```
LINE (50, 30)-(570, 150), , B
LOCATE 7, 10: PRINT "                                    VADBIO"
LOCATE 9, 10: PRINT "   2-D FINITE DIFFERENCE MODEL FOR GAS-PHASE DIFFU
SION,"
LOCATE 10, 10: PRINT "ADVECTION, SORPTION, BIODECAY INCORPORATING LINEA
R EQUILIBRIUM "
LOCATE 11, 10: PRINT "PARTITIONING BETWEEN SORBED, GAS AND AQUEOUS PHAS
ES; BIODECY"
LOCATE 12, 10: PRINT "   BY FIRST, ZERO ORDER OR INSTANTANEOUS REACTION
 MODEL"
LOCATE 14, 10: PRINT "V 2.1 - EXPLICIT IN TIME, CENTRAL WEIGHTING FOR A
DVECTION"
LOCATE 15, 10: PRINT "                    DEVELOPED BY IAN HERS"
LOCATE 16, 10: PRINT "              UNIVERSITY OF BRITISH COLUMBIA"

LOCATE 18, 10: PRINT "                       Type 2 to continue"
DO
LOOP UNTIL INKEY$ = "2"

CLS
LOCATE 4, 10: PRINT "ENTER FILE OUTPUT INFORMATION"
LOCATE 7, 10: INPUT "Benzene output file name (inc. path)"; ben$
LOCATE 8, 10: INPUT "Toluene output file name (inc. path)"; tol$
LOCATE 9, 10: INPUT "Xylene output file name (inc. path)"; xyl$
LOCATE 10, 10: INPUT "Oxygen output file name (inc. path)"; oxy$

OPEN ben$ FOR OUTPUT AS #1
OPEN tol$ FOR OUTPUT AS #2
OPEN xyl$ FOR OUTPUT AS #3
OPEN oxy$ FOR OUTPUT AS #4

'INPUT CHEMICAL PROPERTIES

'Diffusion Coefficients in Free Air
DAB = 8.4400000000000001D-06    'm2/sec
DAT = .0000076                  'm2/sec
DAX = .000007                   'm2/sec
DAO = .00002058#                 'm2/sec

'Diffusion Coefficients in Free Water
DWB = 1E-09    'm2/sec
DWT = 1E-09    'm2/sec
DWX = 1E-09    'm2/sec
DWO = 1E-09    'm2/sec

'Partitioning Coefficients Between Soil and Water
KOCB = 10 ^ 1.96    ' Check Values
KOCT = 10 ^ 2.12    ' Check Values
KOCX = 10 ^ 2.56    ' Check Values
```

```
'Henry's Law Coef
HB = .23   'dimensionless
HT = .28   'dimensionless
HX = .23   'dimensionless
HO = 31.6  'dimensionless

CLS
LOCATE 4, 10: PRINT "ENTER INFORMATION ON DOMAIN AND DISPERSIVITIES"

DOMX = 14
DOMY = 2
DELX = .1
DELY = .1

LOCATE 7, 10: INPUT "Domain in x-direction (0.2 m)"; DOMX
IF DOMX = 0 THEN DOMX = .2
LOCATE 8, 10: INPUT "Domain in y-direction (1.5 m)"; DOMY
IF DOMY = 0 THEN DOMY = 1.5
LOCATE 9, 10: INPUT "Grid size x-direction, integer multiple x- domain
(0.1m)", DELX
IF DELX = 0 THEN DELX = .1
LOCATE 10, 10: INPUT "Grid size y-direction, integer multiple y- domain
 (0.1m)", DELY
IF DELY = 0 THEN DELY = .1
LOCATE 11, 10: INPUT "Longitudinal dispersivity (0.1m)", DISL
IF DISL = 0 THEN DISL = .1
LOCATE 12, 10: INPUT "Tranverse dispersivity (0.01m)", DISTH
IF DISTH = 0 THEN DISTH = .1


NGRIDX = DOMX / DELX
NGRIDY = DOMY / DELY

' Dynamic arrays

X1 = NGRIDX + 1
Y1 = NGRIDY + 1
DIM CB(X1, Y1), CT(X1, Y1), CX(X1, Y1), CO(X1, Y1), MP(X1, Y1), TP(X1,
Y1)
DIM RB(X1, Y1), FOC(X1, Y1), RT(X1, Y1), RX(X1, Y1), RO(X1, Y1)
DIM DXXB(X1, Y1), DYYB(X1, Y1)
DIM DXXT(X1, Y1), DYYT(X1, Y1)
DIM DXXX(X1, Y1), DYYX(X1, Y1)
DIM DXXOX(X1, Y1), DYYOX(X1, Y1)
DIM VX(X1, Y1), VY(X1, Y1), DXY(X1, Y1)
DIM KDB(X1, Y1), KDT(X1, Y1), KDX(X1, Y1), KDO(X1, Y1)
DIM CBNEW(X1, Y1), CTNEW(X1, Y1), CXNEW(X1, Y1), CONEW(X1, Y1)
'  DIM BD(X1, Y1), AP(X1, Y1)

CLS
LOCATE 4, 10: PRINT "ENTER SOIL PROPERTIES AND GAS SPECIFIC DISCHARGE"
LOCATE 7, 10: INPUT "Number horizontal soil layers, integer (<NGRIDY)(1
```

```
)"; NLAYER
IF NLAYER = 0 THEN NLAYER = 1
LOCATE 8, 10: PRINT "Enter soil properties starting from bottom layer"

FOR K = 1 TO NLAYER
        LOCATE 10, 10: PRINT "Input Properties for Layer ="; K
        LOCATE 11, 10: INPUT "Enter first and last row of layer (bottom
 up)"; NR1, NR2
        LOCATE 12, 10: INPUT "Water-filled porosity (dimensionless)(0.1
4)"; MPTEMP
        IF MPTEMP = 0 THEN MPTEMP = .14
        LOCATE 13, 10: INPUT "Total porosity (dimensionless)(0.36)"; TP
TEMP
        IF TPTEMP = 0 THEN TPTEMP = .36
        LOCATE 14, 10: INPUT "Fraction organic carbon (dimensionless)(0
.006)"; FOC
        IF FOCTEMP = 0 THEN FOCTEMP = .006
        LOCATE 15, 10: INPUT "Specific Discharge in x-direction (m/sec)
"; QXTEMP
        LOCATE 16, 10: INPUT "Specific Discharge in y-direction(m/sec)(
5.6E-06)"; QYTEMP

        FOR J = NR1 TO NR2

           FOR I = 1 TO NGRIDX
                MP(I, J) = MPTEMP
                TP(I, J) = TPTEMP
                FOC(I, J) = FOCTEMP
                KDB(I, J) = KOCB * FOC(I, J)
                KDT(I, J) = KOCT * FOC(I, J)
                KDX(I, J) = KOCX * FOC(I, J)
                KDO(I, J) = .005   'check value for oxygen to see if re
asonable
                QX(I, J) = QXTEMP
                QY(I, J) = QYTEMP
           NEXT I

        NEXT J
NEXT K
        'Enter properties for dummy row and column along edge of domain
        'Bottom row and top row
        FOR I = 1 TO NGRIDX
                MP(I, 0) = MP(I, 1)
                TP(I, 0) = TP(I, 1)
                FOC(I, 0) = FOC(I, 1)
                MP(I, NGRIDY + 1) = MP(I, NGRIDY)
                TP(I, NGRIDY + 1) = TP(I, NGRIDY)
                FOC(I, NGRIDY + 1) = FOC(I, NGRIDY)
                KDB(I, NGRIDY + 1) = KDB(I, NGRIDY)
                QX(I, NGRIDY + 1) = QX(I, NGRIDY)
                QY(I, NGRIDY + 1) = QY(I, NGRIDY)
        NEXT I
```

```
'Left and right rows
FOR J = 0 TO NGRIDY + 1
        MP(0, J) = MP(1, J)
        TP(0, J) = TP(1, J)
        FOC(0, J) = FOC(1, J)
        MP(NGRIDX + 1, J) = MP(NGRIDX, J)
        TP(NGRIDX + 1, J) = TP(NGRIDX, J)
        FOC(NGRIDX + 1, J) = FOC(NGRIDX, J)
        KDB(NGRIDX + 1, J) = KDB(NGRIDX, J)
        QX(NGRIDX + 1, J) = QX(NGRIDX, J)
        QY(NGRIDX + 1, J) = QY(NGRIDX, J)
 NEXT J

' Due to memory constraints just enter single bulk density value
BD = 1.67
' Enter bulk density information
' FOR J = 0 TO NGRIDY + 1
'     FOR I = 0 TO NGRIDX + 1
'         BD(I, J) = 1.67    ' g/cm3
'     NEXT I
' NEXT J

' Calculate air-filled porosity
'  FOR J = 0 TO NGRIDY + 1
'     FOR I = 0 TO NGRIDX + 1
'         AP(I, J) = TP(I, J) - MP(I, J)
'     NEXT I
' NEXT J

' Calculate Dispersion Coefficient
   FOR J = 0 TO NGRIDY + 1
      FOR I = 0 TO NGRIDX + 1
          VX = QX(I, J) / (TP(I, J) - MP(I, J))
          VY = QY(I, J) / (TP(I, J) - MP(I, J))
          VV = (VX ^ 2 + VY ^ 2) ^ .5
          DXXB(I, J) = (DISL * VX ^ 2 / VV + DISTH * VY ^ 2 / VV)
 * (TP(I, J) - MP(I, J)) + (TP(I, J) - MP(I, J)) ^ (10 / 3) * DAB / TP(
I, J) ^ 2 + MP(I, J) ^ (10 / 3) * DWB / (HB * TP(I, J) ^ 2)
          DYYB(I, J) = (DISL * VY ^ 2 / VV + DISTH * VX ^ 2 / VV)
 * (TP(I, J) - MP(I, J)) + (TP(I, J) - MP(I, J)) ^ (10 / 3) * DAB / TP(
I, J) ^ 2 + MP(I, J) ^ (10 / 3) * DWB / (HB * TP(I, J) ^ 2)
          DXXT(I, J) = (DISL * VX ^ 2 / VV + DISTH * VY ^ 2 / VV)
 * (TP(I, J) - MP(I, J)) + (TP(I, J) - MP(I, J)) ^ (10 / 3) * DAT / TP(
I, J) ^ 2 + MP(I, J) ^ (10 / 3) * DWT / (HT * TP(I, J) ^ 2)
          DYYT(I, J) = (DISL * VY ^ 2 / VV + DISTH * VX ^ 2 / VV)
 * (TP(I, J) - MP(I, J)) + (TP(I, J) - MP(I, J)) ^ (10 / 3) * DAT / TP(
I, J) ^ 2 + MP(I, J) ^ (10 / 3) * DWT / (HT * TP(I, J) ^ 2)
          DXXX(I, J) = (DISL * VX ^ 2 / VV + DISTH * VY ^ 2 / VV)
 * (TP(I, J) - MP(I, J)) + (TP(I, J) - MP(I, J)) ^ (10 / 3) * DAX / TP(
I, J) ^ 2 + MP(I, J) ^ (10 / 3) * DWX / (HX * TP(I, J) ^ 2)
          DYYX(I, J) = (DISL * VY ^ 2 / VX + DISTH * VY ^ 2 / VV)
 * (TP(I, J) - MP(I, J)) + (TP(I, J) - MP(I, J)) ^ (10 / 3) * DAX / TP(
```

```
I, J) ^ 2 + MP(I, J) ^ (10 / 3) * DWX / (HX * TP(I, J) ^ 2)
                DXXOX(I, J) = (DISL * VX ^ 2 / VV + DISTH * VY ^ 2 / VV
) * (TP(I, J) - MP(I, J)) + (TP(I, J) - MP(I, J)) ^ (10 / 3) * DAO / TP
(I, J) ^ 2
                DYYOX(I, J) = (DISL * VY ^ 2 / VV + DISTH * VX ^ 2 / VV
) * (TP(I, J) - MP(I, J)) + (TP(I, J) - MP(I, J)) ^ (10 / 3) * DAO / TP
(I, J) ^ 2
                DXY(I, J) = (DISL - DISTH) * VX * VY / VV
            NEXT I
        NEXT J

    ' Calculate Retardation Coefficient
        FOR J = 0 TO NGRIDY + 1
            FOR I = 0 TO NGRIDX + 1
                RB(I, J) = 1 + (MP(I, J) / ((TP(I, J) - MP(I, J)) * HB)
) + (BD * KDB(I, J) / ((TP(I, J) - MP(I, J)) * HB))
                RT(I, J) = 1 + (MP(I, J) / ((TP(I, J) - MP(I, J)) * HT)
) + (BD * KDT(I, J) / ((TP(I, J) - MP(I, J)) * HT))
                RX(I, J) = 1 + (MP(I, J) / ((TP(I, J) - MP(I, J)) * HX)
) + (BD * KDX(I, J) / ((TP(I, J) - MP(I, J)) * HX))
                RO(I, J) = 1 + (MP(I, J) / ((TP(I, J) - MP(I, J)) * HO)
) + (BD * KDO(I, J) / ((TP(I, J) - MP(I, J)) * HO))
            NEXT I
        NEXT J


CLS
LOCATE 4, 10: PRINT "ENTER INFORMATION ON BIODEGRADATION PARAMETERS"

LOCATE 7, 10: PRINT "Indicate Type of Biodegradation Modeling"
LOCATE 8, 10: PRINT "First order decay - Enter 1"
LOCATE 9, 10: PRINT "First and zero order decay - Enter 2"
LOCATE 10, 10: PRINT "Instantaneous reaction - Enter 3"
LOCATE 11, 10: PRINT "First and zero order decay with oxygen availabili
ty check - Enter 4"
LOCATE 13, 10: INPUT "Biodegradation Model Type"; BIOTYPE

        IF BIOTYPE > 1 THEN 100

'       Enter first-order degradation rates

        LOCATE 13, 10: INPUT "Enter 1st-order degradation benzene soil-
water (sec-1)(0.00033)"; KB1
        IF KB1 = 0 THEN KB1 = .00033
        LOCATE 14, 10: INPUT "Enter 1st-order degradation toluene soil-
water (sec-1)(0.00025)"; KT1
        IF KT1 = 0 THEN KT1 = .00025
        LOCATE 15, 10: INPUT "Enter 1st-order degradation xylene soil-w
ater (sec-1)(0.00014)"; KX1
        IF KX1 = 0 THEN KX1 = .00014
        GOTO 130
```

```
100     IF BIOTYPE > 2 THEN 110

'       Enter first and zero-order degradation rates

        LOCATE 13, 10: INPUT "Enter 1st-order degradation benzene soil-
water (sec-1)(0.00033)"; KB1
        IF KB1 = 0 THEN KB1 = .00033
        LOCATE 14, 10: INPUT "Enter 1st-order degradation toluene soil-
water (sec-1)(0.00025)"; KT1
        IF KT1 = 0 THEN KT1 = .00025
        LOCATE 15, 10: INPUT "Enter 1st-order degradation xylene soil-w
ater (sec-1)(0.00014)"; KX1
        IF KX1 = 0 THEN KX1 = .00014
        LOCATE 16, 10: INPUT "Enter 0-order degradation benzene soil-wa
ter (mg/L-sec)(0.00038)"; KB0
        IF KB0 = 0 THEN KB0 = .00038
        LOCATE 17, 10: INPUT "Enter 0-order degradation toluene soil-wa
ter (mg/L-sec)(0.00029)"; KT0
        IF KT0 = 0 THEN KT0 = .00029
        LOCATE 18, 10: INPUT "Enter 0-order degradation xylene soil-wat
er (mg/L-sec)(0.00016)"; KX0
        IF KX0 = 0 THEN KX0 = .00016

    '   Above critical concentration, the first order term is adjusted
downward by ratio of
    '   critical concentration over actual concentration to obtain an e
quivalent 1st order rate

        CBCRIT = KB0 / KB1
        CTCRIT = KT0 / KT1
        CXCRIT = KX0 / KX1
        GOTO 130

110     IF BIOTYPE > 3 GOTO 120

'       Enter instantaneous-reaction rate stochiometric ratio

        LOCATE 13, 10: INPUT "Average stochiometric rate for mineraliza
tion of BTX (3.1)"; STRATIO
        IF STRATIO = 0 THEN STRATIO = 3.1
        GOTO 130

'       Enter first and zero-order degradation rates and stochiometric
ratio

120     LOCATE 13, 10: INPUT "Enter 1st-order degradation benzene soil-
water (sec-1)(0.00033)"; KB1
        IF KB1 = 0 THEN KB1 = .00033
        LOCATE 14, 10: INPUT "Enter 1st-order degradation toluene soil-
water (sec-1)(0.00025)"; KT1
        IF KBT = 0 THEN KT1 = .00025
        LOCATE 15, 10: INPUT "Enter 1st-order degradation xylene soil-w
```

```
ater (sec-1)(0.00014)"; KX1
        IF KX1 = 0 THEN KX1 = .00014
        LOCATE 16, 10: INPUT "Enter 0-order degradation benzene soil-wa
ter (mg/L-sec)(0.00038)"; KB0
        IF KB0 = 0 THEN KB0 = .00038
        LOCATE 17, 10: INPUT "Enter 0-order degradation toluene soil-wa
ter (mg/L-sec)(0.00029)"; KT0
        IF KT0 = 0 THEN KT0 = .00029
        LOCATE 18, 10: INPUT "Enter 0-order degradation xylene soil-wat
er (mg/L-sec)(0.00016)"; KX0
        IF KX0 = 0 THEN KX0 = .00016
        LOCATE 19, 10: INPUT "Average stochiometric rate for mineraliza
tion of BTX (3.1)"; STRATIO
        IF STRATIO = 0 THEN STRATIO = 3.1

   '    Above critical concentration, the first order term is adjusted
downward by ratio of
   '    critical concentration over actual concentration to obtain an e
quivalent 1st order rate

        CBCRIT = KB0 / KB1
        CTCRIT = KT0 / KT1
        CXCRIT = KX0 / KX1

130    CLS
GOTO 69
LOCATE 4, 10: PRINT "ENTER INFORMATION ON BUILDING CHARACTERISTICS"
LOCATE 7, 10: INPUT "Half Building Length (1.5 m)"; BL
IF BL = 0 THEN BL = 1.5
LOCATE 8, 10: INPUT "Ratio of cracks to total slab area(0.001)"; CRATIO
IF CRATIO = 0 THEN CRATIO = .001
LOCATE 9, 10: INPUT "Ratio of dust/dirt filled cracks to total crack ar
ea (0.25)"; DRATIO
IF DRATIO = 0 THEN DRATIO = .25
LOCATE 10, 10: INPUT "Building height (2.7)"; BH
IF BH = 0 THEN BH = 2.7
LOCATE 11, 10: INPUT "Air exchange rate per hour (1)"; AEH
IF AEH = 0 THEN AEH = 1

'  Enter diffusivity of concrete slab

        NGRIDXBE = BL / DELX

        FOR J = NGRIDY - 1 TO NGRIDY + 1
          FOR I = 0 TO NGRIDXBE
               DBTEMP = CRATIO * DRATIO * DAB
               MP(I, J) = TP(I, J) - (DBTEMP * TP(I, J) ^ 2 / DAB) ^ (
3 / 10)
               DB(I, J) = (TP(I, J) - MP(I, J)) ^ (10 / 3) * DAB / TP(
I, J) ^ 2 + MP(I, J) ^ (10 / 3) * DWB / (HB * TP(I, J) ^ 2)
               DT(I, J) = (TP(I, J) - MP(I, J)) ^ (10 / 3) * DAT / TP(
I, J) ^ 2 + MP(I, J) ^ (10 / 3) * DWT / (HT * TP(I, J) ^ 2)
```

```
                DX(I, J) = (TP(I, J) - MP(I, J)) ^ (10 / 3) * DAX / TP(
I, J) ^ 2 + MP(I, J) ^ (10 / 3) * DWX / (HX * TP(I, J) ^ 2)
                DOX(I, J) = (TP(I, J) - MP(I, J)) ^ (10 / 3) * DAO / TP
(I, J) ^ 2
            NEXT I
          NEXT J
69
CLS
'  LOCATE 4, 10: PRINT "ENTER INFORMATION ON RISK PARAMETERS"

'  LOCATE 7, 10: INPUT "Exposure duration (years)"; ED
ED = 25
'  LOCATE 8, 10: INPUT "Exposure frequency (days/year)"; EF
EF = 250
'  LOCATE 9, 10: INPUT "Daily Exposure frequency (hours/day)"; DEFF
DEFF = 8
'  LOCATE 10, 10: INPUT "Body weight (kg)"; BW
BW = 70
'  LOCATE 11, 10: INPUT "Inhalation rate (m3/hr)";IR
IR = 2.1
'  LOCATE 12,10:  INPUT "Slope factor benzene (unit)";SFB
SFB = .021
'  LOCATE 13,10:  INPUT "Reference dose benzene (unit)";RFDB
RFDB = 1
'  LOCATE 14,10:  INPUT "Reference dose toluene (unit)";RFDT
RFDT = 1
'  LOCATE 15,10:  INPUT "Reference dose xylene (unit)";RFDX
RFDX = 1

CLS
LOCATE 4, 10: PRINT "ENTER SOURCE CONCENTRATIONS (BOTTOM BOUNDARY)"

LOCATE 7, 10: INPUT "Benzene concentration in soil gas (mg/L)(15)"; SBB
IF SBB = 0 THEN SBB = 15
LOCATE 8, 10: INPUT "Toluene concentration in soil gas (mg/L)(20)"; SBT
IF SBT = 0 THEN SBT = 20
LOCATE 9, 10: INPUT "Xylene concentration in soil gas (mg/L)(0.9)"; SBX
IF SBX = 0 THEN SBX = .9

CLS
LOCATE 4, 10: PRINT "ENTER TIMESTEP INFORMATION"

MAXDISX = DXXOX(1, NGRIDY)
MAXDISY = DYYOX(1, NGRIDY)
MAXVX = QX(1, NGRIDY) / (TP(1, 1) - MP(1, 1))
MAXVY = QY(1, NGRIDY) / (TP(1, 1) - MP(1, 1))

LOCATE 7, 10: PRINT "Dispersion Stability Criteria - Max Time Step (sec
)"; .5 * RO / ((MAXDISX / DELX ^ 2) + (MAXDISY / DELY ^ 2))
LOCATE 8, 10: PRINT "Advective Stability Criteria - Max Time Step (sec)
"; RO / ((MAXVX / DELX) + (MAXVY / DELY))
LOCATE 9, 10: PRINT "Reaction Stability Criteria - Max Time Step (sec)"
```

```
; 1 / KB1
LOCATE 11, 10: INPUT "Input time step (sec)(250)"; TS
IF TS = 0 THEN TS = 250
LOCATE 12, 10: INPUT "Input number of time steps(2000)"; NTS
IF NTS = 0 THEN NTS = 2000
LOCATE 13, 10: INPUT "Input Output Frequency (timesteps/output)(500)";
FREQ
IF FREQ = 0 THEN FREQ = 500
' SET INITIAL CONDITIONS

FOR J = 0 TO NGRIDY + 1

        FOR I = 0 TO NGRIDX + 1
                CB(I, J) = .000005
                CT(I, J) = .000001
                CX(I, J) = .000003
                CO(I, J) = 279 '(mg/L)
        NEXT I

NEXT J

' SET BOUNDARY CONDITIONS

        FOR I = 0 TO NGRIDX + 1     'bottom boundary + dummy row below
                CB(I, 1) = SBB
                CB(I, 0) = SBB
                CT(I, 1) = SBT
                CT(I, 0) = SBT
                CX(I, 1) = SBX
                CX(I, 0) = SBX
        NEXT I

        FOR I = 0 TO NGRIDX + 1     'top boundary + dummy row above
                CB(I, NGRIDY) = .000005
                CB(I, NGRIDY + 1) = .000005
                CT(I, NGRIDY) = .00001
                CT(I, NGRIDY + 1) = .00001
                CX(I, NGRIDY) = .000003
                CX(I, NGRIDY + 1) = .000003
                CO(I, NGRIDY) = 279    '(mg/L)
                CO(I, NGRIDY + 1) = 279 '(mg/L)
        NEXT I

PCOUNT = 0
SCOUNT = 0
GOSUB 500

IF BIOTYPE > 1 GOTO 200

'  Calculate Concentrations  for BioType = 1

FOR K = 1 TO NTS
```

```
  PCOUNT = PCOUNT + 1                    'Counter for print control
  SCOUNT = SCOUNT + 1                    'Counter for screen display
  ETIME = (K * TS) / 60 / 60 / 24

  FOR J = 1 TO NGRIDY

     FOR I = 1 TO NGRIDX

        AB1 = TS * (-(DB(I + 1, J) + 2 * DB(I, J) + DB(I - 1, J))) / (2
 * DELX ^ 2 * (TP(I, J) - MP(I, J)) * RB(I, J)) + TS * (-(DB(I, J + 1)
+ 2 * DB(I, J) + DB(I, J - 1))) / (2 * DELY ^ 2 * (TP(I, J) - MP(I, J))
 * RB(I, J))
        AB2 = -TS * KB1 * MP(I, J) / (HB * (TP(I, J) - MP(I, J)) * RB(I
, J)) + 1
        AB = AB1 + AB2
        AT1 = TS * (-(DT(I + 1, J) + 2 * DT(I, J) + DT(I - 1, J))) / (2
 * DELX ^ 2 * (TP(I, J) - MP(I, J)) * RT(I, J)) + TS * (-(DT(I, J + 1)
+ 2 * DT(I, J) + DT(I, J - 1))) / (2 * DELY ^ 2 * (TP(I, J) - MP(I, J))
 * RT(I, J))
        AT2 = -TS * KT1 * MP(I, J) / (HT * (TP(I, J) - MP(I, J)) * RT(I
, J)) + 1
        AT = AT1 + AT2
        AX1 = TS * (-(DX(I + 1, J) + 2 * DX(I, J) + DX(I - 1, J))) / (2
 * DELX ^ 2 * (TP(I, J) - MP(I, J)) * RX(I, J)) + TS * (-(DX(I, J + 1)
+ 2 * DX(I, J) + DX(I, J - 1))) / (2 * DELY ^ 2 * (TP(I, J) - MP(I, J))
 * RX(I, J))
        AX2 = -TS * KX1 * MP(I, J) / (HX * (TP(I, J) - MP(I, J)) * RX(I
, J)) + 1
        AX = AX1 + AX2

        BB = TS * (DB(I + 1, J) + DB(I, J)) / (2 * DELX ^ 2 * (TP(I, J)
 - MP(I, J)) * RB(I, J))
        BT = TS * (DT(I + 1, J) + DT(I, J)) / (2 * DELX ^ 2 * (TP(I, J)
 - MP(I, J)) * RT(I, J))
        BX = TS * (DX(I + 1, J) + DX(I, J)) / (2 * DELX ^ 2 * (TP(I, J)
 - MP(I, J)) * RX(I, J))

        DDB = TS * (DB(I, J) + DB(I - 1, J)) / (2 * DELX ^ 2 * (TP(I, J
) - MP(I, J)) * RB(I, J))
        DDT = TS * (DT(I, J) + DT(I - 1, J)) / (2 * DELX ^ 2 * (TP(I, J
) - MP(I, J)) * RT(I, J))
        DDX = TS * (DX(I, J) + DX(I - I, J)) / (2 * DELX ^ 2 * (TP(I, J
) - MP(I, J)) * RX(I, J))

        EB = TS * (DB(I, J + 1) + DB(I, J)) / (2 * DELY ^ 2 * (TP(I, J)
 - MP(I, J)) * RB(I, J))
        ET = TS * (DT(I, J + 1) + DT(I, J)) / (2 * DELY ^ 2 * (TP(I, J)
 - MP(I, J)) * RT(I, J))
        EX = TS * (DX(I, J + 1) + DX(I, J)) / (2 * DELY ^ 2 * (TP(I, J)
 - MP(I, J)) * RX(I, J))
```

```
        FB = TS * (DB(I, J) + DB(I, J - 1)) / (2 * DELY ^ 2 * (TP(I, J)
 - MP(I, J)) * RB(I, J))
        FT = TS * (DT(I, J) + DT(I, J - 1)) / (2 * DELY ^ 2 * (TP(I, J)
 - MP(I, J)) * RT(I, J))
        FX = TS * (DX(I, J) + DX(I, J - 1)) / (2 * DELY ^ 2 * (TP(I, J)
 - MP(I, J)) * RX(I, J))

        '  Calculate concentration at next time step

        CBNEW(I, J) = AB * CB(I, J) + BB * CB(I + 1, J) + DDB * CB(I -
1, J) + EB * CB(I, J + 1) + FB * CB(I, J - 1)
        CTNEW(I, J) = AT * CT(I, J) + BT * CT(I + 1, J) + DDT * CT(I -
1, J) + ET * CT(I, J + 1) + FT * CT(I, J - 1)
        CXNEW(I, J) = AX * CX(I, J) + BX * CX(I + 1, J) + DDX * CX(I -
1, J) + EX * CX(I, J + 1) + FX * CX(I, J - 1)

     NEXT I

  NEXT J

  FOR J = 1 TO NGRIDY

    FOR I = 1 TO NGRIDX
        CB(I, J) = CBNEW(I, J)
        CT(I, J) = CTNEW(I, J)
        CX(I, J) = CXNEW(I, J)
    NEXT I

  NEXT J

' RESET BOUNDARY CONDITIONS

        FOR I = 0 TO NGRIDX + 1     'bottom boundary + dummy row below
                CB(I, 1) = SBB
                CB(I, 0) = SBB
                CT(I, 1) = SBT
                CT(I, 0) = SBT
                CX(I, 1) = SBX
                CX(I, 0) = SBX
        NEXT I

        FOR I = 0 TO NGRIDX + 1     'top boundary + dummy row above
                CB(I, NGRIDY) = .000005
                CB(I, NGRIDY + 1) = .000005
                CT(I, NGRIDY) = .00001
                CT(I, NGRIDY + 1) = .00001
                CX(I, NGRIDY) = .000003
                CX(I, NGRIDY + 1) = .000003
        NEXT I

        FOR J = 0 TO NGRIDY + 1         ' Left and right rows
                CB(0, J) = CB(1, J)
```

```
                CT(0, J) = CT(1, J)
                CX(0, J) = CX(1, J)
                CB(NGRIDX + 1, J) = CB(NGRIDX, J)
                CT(NGRIDX + 1, J) = CT(NGRIDX, J)
                CX(NGRIDX + 1, J) = CX(NGRIDX, J)
            NEXT J

        IF PCOUNT = FREQ THEN 10 ELSE 20

10      PCOUNT = 0
        PRINT #1, "Elapsed Time = "; ETIME; "    Time Step ="; K
        PRINT #2, "Elapsed Time = "; ETIME; "    Time Step ="; K
        PRINT #3, "Elapsed Time = "; ETIME; "    Time Step ="; K

        FOR I = 1 TO NGRIDX
          FOR J = 1 TO NGRIDY
            WRITE #1, CB(I, J)
            WRITE #2, CT(I, J)
            WRITE #3, CX(I, J)
            WRITE #4, CO(I, J)
          NEXT J
      NEXT I

20    IF SCOUNT = 10 THEN 15 ELSE 16

15    GOSUB 600
      SCOUNT = 0

16

NEXT K

GOTO 230

200   IF BIOTYPE > 2 GOTO 210

'   Calculate Concentrations for BioType = 2

FOR K = 1 TO NTS

  PCOUNT = PCOUNT + 1                'Counter for print control
  SCOUNT = SCOUNT + 1
  ETIME = (K * TS) / 60 / 60 / 24

  FOR J = 1 TO NGRIDY

    FOR I = 1 TO NGRIDX

        IF CB(I, J) > CBCRIT * HB THEN KB1NEW = KB1 * CBCRIT * HB / CB(
I, J) ELSE KB1NEW = KB1   'check
        IF CT(I, J) > CTCRIT * HT THEN KT1NEW = KT1 * CTCRIT * HT / CT(
I, J) ELSE KT1NEW = KT1
```

```
        IF CX(I, J) > CXCRIT * HX THEN KX1NEW = KX1 * CXCRIT * HX / CX(
I, J) ELSE KX1NEW = KX1

        AB = TS * (-(DB(I + 1, J) + 2 * DB(I, J) + DB(I - 1, J))) / (2
* DELX ^ 2 * (TP(I, J) - MP(I, J)) * RB(I, J)) + TS * (-(DB(I, J + 1) +
 2 * DB(I, J) + DB(I, J - 1))) / (2 * DELY ^ 2 * (TP(I, J) - MP(I, J))
* RB(I, J)) - TS * KB1NEW * MP(I, J)
 / (HB * (TP(I, J) - MP(I, J)) * RB(I, J)) + 1
        AT = TS * (-(DT(I + 1, J) + 2 * DT(I, J) + DT(I - 1, J))) / (2
* DELX ^ 2 * (TP(I, J) - MP(I, J)) * RT(I, J)) + TS * (-(DT(I, J + 1) +
 2 * DT(I, J) + DT(I, J - 1))) / (2 * DELY ^ 2 * (TP(I, J) - MP(I, J))
* RT(I, J)) - TS * KT1NEW * MP(I, J)
 / (HT * (TP(I, J) - MP(I, J)) * RT(I, J)) + 1
        AX = TS * (-(DX(I + 1, J) + 2 * DX(I, J) + DX(I - 1, J))) / (2
* DELX ^ 2 * (TP(I, J) - MP(I, J)) * RX(I, J)) + TS * (-(DX(I, J + 1) +
 2 * DX(I, J) + DX(I, J - 1))) / (2 * DELY ^ 2 * (TP(I, J) - MP(I, J))
* RX(I, J)) - TS * KX1NEW * MP(I, J)
 / (HX * (TP(I, J) - MP(I, J)) * RX(I, J)) + 1

        BB = TS * (DB(I + 1, J) + DB(I, J)) / (2 * DELX ^ 2 * (TP(I, J)
 - MP(I, J)) * RB(I, J))
        BT = TS * (DT(I + 1, J) + DT(I, J)) / (2 * DELX ^ 2 * (TP(I, J)
 - MP(I, J)) * RT(I, J))
        BX = TS * (DX(I + 1, J) + DX(I, J)) / (2 * DELX ^ 2 * (TP(I, J)
 - MP(I, J)) * RX(I, J))

        DDB = TS * (DB(I, J) + DB(I - 1, J)) / (2 * DELX ^ 2 * (TP(I, J
) - MP(I, J)) * RB(I, J))
        DDT = TS * (DT(I, J) + DT(I - 1, J)) / (2 * DELX ^ 2 * (TP(I, J
) - MP(I, J)) * RT(I, J))
        DDX = TS * (DX(I, J) + DX(I - I, J)) / (2 * DELX ^ 2 * (TP(I, J
) - MP(I, J)) * RX(I, J))

        EB = TS * (DB(I, J + 1) + DB(I, J)) / (2 * DELY ^ 2 * (TP(I, J)
 - MP(I, J)) * RB(I, J))
        ET = TS * (DT(I, J + 1) + DT(I, J)) / (2 * DELY ^ 2 * (TP(I, J)
 - MP(I, J)) * RT(I, J))
        EX = TS * (DX(I, J + 1) + DX(I, J)) / (2 * DELY ^ 2 * (TP(I, J)
 - MP(I, J)) * RX(I, J))

        FB = TS * (DB(I, J) + DB(I, J - 1)) / (2 * DELY ^ 2 * (TP(I, J)
 - MP(I, J)) * RB(I, J))
        FT = TS * (DT(I, J) + DT(I, J - 1)) / (2 * DELY ^ 2 * (TP(I, J)
 - MP(I, J)) * RT(I, J))
        FX = TS * (DX(I, J) + DX(I, J - 1)) / (2 * DELY ^ 2 * (TP(I, J)
 - MP(I, J)) * RX(I, J))

    ' Calculate concentration at next time step

        CBNEW(I, J) = AB * CB(I, J) + BB * CB(I + 1, J) + DDB * CB(I -
1, J) + EB * CB(I, J + 1) + FB * CB(I, J - 1)
        CTNEW(I, J) = AT * CT(I, J) + BT * CT(I + 1, J) + DDT * CT(I -
```

```
1, J) + ET * CT(I, J + 1) + FT * CT(I, J - 1)
        CXNEW(I, J) = AX * CX(I, J) + BX * CX(I + 1, J) + DDX * CX(I -
1, J) + EX * CX(I, J + 1) + FX * CX(I, J - 1)

     NEXT I

  NEXT J

  FOR J = 1 TO NGRIDY

    FOR I = 1 TO NGRIDX
        CB(I, J) = CBNEW(I, J)
        CT(I, J) = CTNEW(I, J)
        CX(I, J) = CXNEW(I, J)
    NEXT I

  NEXT J

' RESET BOUNDARY CONDITIONS

        FOR I = 0 TO NGRIDX + 1     'bottom boundary + dummy row below
                CB(I, 1) = SBB
                CB(I, 0) = SBB
                CT(I, 1) = SBT
                CT(I, 0) = SBT
                CX(I, 1) = SBX
                CX(I, 0) = SBX
        NEXT I

        FOR I = 0 TO NGRIDX + 1     'top boundary + dummy row above
                CB(I, NGRIDY) = .000005
                CB(I, NGRIDY + 1) = .000005
                CT(I, NGRIDY) = .00001
                CT(I, NGRIDY + 1) = .00001
                CX(I, NGRIDY) = .000003
                CX(I, NGRIDY + 1) = .000003
        NEXT I

        FOR J = 0 TO NGRIDY + 1         ' Left and right rows
                CB(0, J) = CB(1, J)
                CT(0, J) = CT(1, J)
                CX(0, J) = CX(1, J)
                CB(NGRIDX + 1, J) = CB(NGRIDX, J)
                CT(NGRIDX + 1, J) = CT(NGRIDX, J)
                CX(NGRIDX + 1, J) = CX(NGRIDX, J)
         NEXT J

     IF PCOUNT = FREQ THEN 11 ELSE 21

11   PCOUNT = 0
     PRINT #1, "Elapsed Time = "; ETIME; "   Time Step ="; K
     PRINT #2, "Elapsed Time = "; ETIME; "   Time Step ="; K
```

```
      PRINT #3, "Elapsed Time = "; ETIME; "    Time Step ="; K

      FOR I = 1 TO NGRIDX
        FOR J = 1 TO NGRIDY
          WRITE #1, CB(I, J)
          WRITE #2, CT(I, J)
          WRITE #3, CX(I, J)
          WRITE #4, CO(I, J)
        NEXT J
      NEXT I

21    IF SCOUNT = 10 THEN 17 ELSE 18

17  GOSUB 600
    SCOUNT = 0

18

NEXT K

GOTO 230

210    IF BIOTYPE > 3 GOTO 220

'   Calculate Concentrations for BioType = 3

FOR K = 1 TO NTS

  SCOUNT = SCOUNT + 1
  PCOUNT = PCOUNT + 1                'Counter for print control
  ETIME = (K * TS) / 60 / 60 / 24

  FOR J = 1 TO NGRIDY

    FOR I = 1 TO NGRIDX

        AB = TS * (-(DB(I + 1, J) + 2 * DB(I, J) + DB(I - 1, J))) / (2
* DELX ^ 2 * (TP(I, J) - MP(I, J)) * RB(I, J)) + TS * (-(DB(I, J + 1) +
 2 * DB(I, J) + DB(I, J - 1))) / (2 * DELY ^ 2 * (TP(I, J) - MP(I, J))
* RB(I, J)) + 1
        AT = TS * (-(DT(I + 1, J) + 2 * DT(I, J) + DT(I - 1, J))) / (2
* DELX ^ 2 * (TP(I, J) - MP(I, J)) * RT(I, J)) + TS * (-(DT(I, J + 1) +
 2 * DT(I, J) + DT(I, J - 1))) / (2 * DELY ^ 2 * (TP(I, J) - MP(I, J))
* RT(I, J)) + 1
        AX = TS * (-(DX(I + 1, J) + 2 * DX(I, J) + DX(I - 1, J))) / (2
* DELX ^ 2 * (TP(I, J) - MP(I, J)) * RX(I, J)) + TS * (-(DX(I, J + 1) +
 2 * DX(I, J) + DX(I, J - 1))) / (2 * DELY ^ 2 * (TP(I, J) - MP(I, J))
* RX(I, J)) + 1
        AO = TS * (-(DOX(I + 1, J) + 2 * DOX(I, J) + DOX(I - 1, J))) /
(2 * DELX ^ 2 * (TP(I, J) - MP(I, J)) * RO(I, J)) + TS * (-(DOX(I, J +
1) + 2 * DOX(I, J) + DOX(I, J - 1))) / (2 * DELY ^ 2 * (TP(I, J) - MP(I
, J)) * RO(I, J)) + 1
```

```
        BB = TS * (DB(I + 1, J) + DB(I, J)) / (2 * DELX ^ 2 * (TP(I, J)
 - MP(I, J)) * RB(I, J))
        BT = TS * (DT(I + 1, J) + DT(I, J)) / (2 * DELX ^ 2 * (TP(I, J)
 - MP(I, J)) * RT(I, J))
        BX = TS * (DX(I + 1, J) + DX(I, J)) / (2 * DELX ^ 2 * (TP(I, J)
 - MP(I, J)) * RX(I, J))
        BO = TS * (DOX(I + 1, J) + DOX(I, J)) / (2 * DELX ^ 2 * (TP(I,
J) - MP(I, J)) * RO(I, J))

        DDB = TS * (DB(I, J) + DB(I - 1, J)) / (2 * DELX ^ 2 * (TP(I, J
) - MP(I, J)) * RB(I, J))
        DDT = TS * (DT(I, J) + DT(I - 1, J)) / (2 * DELX ^ 2 * (TP(I, J
) - MP(I, J)) * RT(I, J))
        DDX = TS * (DX(I, J) + DX(I - I, J)) / (2 * DELX ^ 2 * (TP(I, J
) - MP(I, J)) * RX(I, J))
        PO = TS * (DOX(I, J) + DOX(I - 1, J)) / (2 * DELX ^ 2 * (TP(I,
J) - MP(I, J)) * RO(I, J))

        EB = TS * (DB(I, J + 1) + DB(I, J)) / (2 * DELY ^ 2 * (TP(I, J)
 - MP(I, J)) * RB(I, J))
        ET = TS * (DT(I, J + 1) + DT(I, J)) / (2 * DELY ^ 2 * (TP(I, J)
 - MP(I, J)) * RT(I, J))
        EX = TS * (DX(I, J + 1) + DX(I, J)) / (2 * DELY ^ 2 * (TP(I, J)
 - MP(I, J)) * RX(I, J))
        EO = TS * (DOX(I, J + 1) + DOX(I, J)) / (2 * DELY ^ 2 * (TP(I,
J) - MP(I, J)) * RO(I, J))

        FB = TS * (DB(I, J) + DB(I, J - 1)) / (2 * DELY ^ 2 * (TP(I, J)
 - MP(I, J)) * RB(I, J))
        FT = TS * (DT(I, J) + DT(I, J - 1)) / (2 * DELY ^ 2 * (TP(I, J)
 - MP(I, J)) * RT(I, J))
        FX = TS * (DX(I, J) + DX(I, J - 1)) / (2 * DELY ^ 2 * (TP(I, J)
 - MP(I, J)) * RX(I, J))
        FO = TS * (DOX(I, J) + DOX(I, J - 1)) / (2 * DELY ^ 2 * (TP(I,
J) - MP(I, J)) * RO(I, J))

        '  Calculate concentration at next time step

        CBNEW(I, J) = AB * CB(I, J) + BB * CB(I + 1, J) + DDB * CB(I -
1, J) + EB * CB(I, J + 1) + FB * CB(I, J - 1)
        CTNEW(I, J) = AT * CT(I, J) + BT * CT(I + 1, J) + DDT * CT(I -
1, J) + ET * CT(I, J + 1) + FT * CT(I, J - 1)
        CXNEW(I, J) = AX * CX(I, J) + BX * CX(I + 1, J) + DDX * CX(I -
1, J) + EX * CX(I, J + 1) + FX * CX(I, J - 1)
        CONEW(I, J) = AO * CO(I, J) + BO * CO(I + 1, J) + PO * CO(I - 1
, J) + EO * CO(I, J + 1) + FO * CO(I, J - 1)

    NEXT I

  NEXT J
```

```
'   Adjust concentrations to account for oxygen depletion

  FOR J = 1 TO NGRIDY

    FOR I = 1 TO NGRIDX

        MB = CBNEW(I, J) * (BD * KDB(I, J) / HB + MP(I, J) / HB + (TP(I
, J) - MP(I, J)))
        MT = CTNEW(I, J) * (BD * KDT(I, J) / HT + MP(I, J) / HT + (TP(I
, J) - MP(I, J)))
        MX = CXNEW(I, J) * (BD * KDX(I, J) / HX + MP(I, J) / HX + (TP(I
, J) - MP(I, J)))
        MH = MB + MT + MX
        MO = CONEW(I, J) * (MP(I, J) / HO + (TP(I, J) - MP(I, J)))

        IF MH > (MO / STRATIO) THEN 300 ELSE 301
300     MHOLD = MH
        MHNEW = MH - (MO / STRATIO)
        CO(I, J) = 0
        IF MHOLD = 0 THEN 305
        MB = MB * MHNEW / MHOLD
        MT = MT * MHNEW / MHOLD
        MX = MX * MHNEW / MHOLD
        CB(I, J) = MB / (BD * KDB(I, J) / HB + MP(I, J) / HB + (TP(I, J
) - MP(I, J)))
        CT(I, J) = MT / (BD * KDT(I, J) / HT + MP(I, J) / HT + (TP(I, J
) - MP(I, J)))
        CX(I, J) = MX / (BD * KDX(I, J) / HX + MP(I, J) / HX + (TP(I, J
) - MP(I, J)))
        GOTO 310

301     MONEW = MO - MH * STRATIO
        CO(I, J) = MONEW / (MP(I, J) / HO + (TP(I, J) - MP(I, J)))
305     CB(I, J) = 0
        CT(I, J) = 0
        CX(I, J) = 0
310
    NEXT I

  NEXT J

 ' RESET SET BOUNDARY CONDITIONS

        FOR I = 0 TO NGRIDX + 1     'bottom boundary + dummy row below
                CB(I, 1) = SBB
                CB(I, 0) = SBB
                CT(I, 1) = SBT
                CT(I, 0) = SBT
                CX(I, 1) = SBX
                CX(I, 0) = SBX
                CO(I, 0) = CO(I, 1)
        NEXT I
```

```
        FOR I = 0 TO NGRIDX + 1     'top boundary + dummy row above
                CB(I, NGRIDY) = .000005
                CB(I, NGRIDY + 1) = .000005
                CT(I, NGRIDY) = .00001
                CT(I, NGRIDY + 1) = .00001
                CX(I, NGRIDY) = .000003
                CX(I, NGRIDY + 1) = .000003
                CO(I, NGRIDY) = 279    '(mg/l)
                CO(I, NGRIDY + 1) = 279 '(mg/l)
        NEXT I

        FOR J = 0 TO NGRIDY + 1         ' Left and right rows
                CB(0, J) = CB(1, J)
                CT(0, J) = CT(1, J)
                CX(0, J) = CX(1, J)
                CO(0, J) = CO(1, J)
                CB(NGRIDX + 1, J) = CB(NGRIDX, J)
                CT(NGRIDX + 1, J) = CT(NGRIDX, J)
                CX(NGRIDX + 1, J) = CX(NGRIDX, J)
                CO(NGRIDX + 1, J) = CO(NGRIDX, J)
         NEXT J

     IF PCOUNT = FREQ THEN 12 ELSE 22

12   PCOUNT = 0
     PRINT #1, "Elapsed Time = "; ETIME; "    Time Step ="; K
     PRINT #2, "Elapsed Time = "; ETIME; "    Time Step ="; K
     PRINT #3, "Elapsed Time = "; ETIME; "    Time Step ="; K
     PRINT #4, "Elapsed Time = "; ETIME; "    Time Step ="; K

     FOR I = 1 TO NGRIDX
       FOR J = 1 TO NGRIDY
         WRITE #1, CB(I, J)
         WRITE #2, CT(I, J)
         WRITE #3, CX(I, J)
         WRITE #4, CO(I, J)
       NEXT J
    NEXT I

22  IF SCOUNT = 10 THEN 25 ELSE 26

25  GOSUB 600
    SCOUNT = 0

26

NEXT K

GOTO 230

'  Calculate Concentrations for BioType = 4
```

```
FOR K = 1 TO NTS

  SCOUNT = SCOUNT + 1
  PCOUNT = PCOUNT + 1                    'Counter for print control
  ETIME = (K * TS) / 60 / 60 / 24


  FOR J = 1 TO NGRIDY

    FOR I = 1 TO NGRIDX

        IF CB(I, J) > CBCRIT * HB THEN KB1NEW = KB1 * CBCRIT * HB / CB(
I, J) ELSE KB1NEW = KB1  'check
        IF CT(I, J) > CTCRIT * HT THEN KT1NEW = KT1 * CTCRIT * HT / CT(
I, J) ELSE KT1NEW = KT1
        IF CX(I, J) > CXCRIT * HX THEN KX1NEW = KX1 * CXCRIT * HX / CX(
I, J) ELSE KX1NEW = KX1

        AO1 = TS * (-(DXXOX(I + 1, J) + 2 * DXXOX(I, J) + DXXOX(I - 1,
J))) / (2 * DELX ^ 2 * (TP(I, J) - MP(I, J)) * RO(I, J)) + TS * (-(DXXO
X(I, J + 1) + 2 * DXXOX(I, J) + DXXOX(I, J - 1))) / (2 * DELY ^ 2 * (TP
(I, J) - MP(I, J)) * RO(I, J)) + 1
        AO2 = TS * (-(DXY(I + 1, J) + 2 * DXY(I, J) + DXY(I - 1, J))) /
 (2 * DELX * DELY * (TP(I, J) - MP(I, J)) * RO(I, J)) + TS * (-(DXY(I,
J + 1) + 2 * DXY(I, J) + DXY(I, J - 1))) / (2 * DELY * DELX * (TP(I, J)
 - MP(I, J)) * RO(I, J))
        AO3 = -TS * (-(QX(I + 1, J) + 2 * QX(I, J) + QX(I - 1, J))) / (
2 * DELX * (TP(I, J) - MP(I, J)) * RO(I, J)) - TS * (-(QY(I, J + 1) + 2
 * QY(I, J) + QY(I, J - 1))) / (2 * DELY * (TP(I, J) - MP(I, J)) * RO(I
, J))
        AO = AO1 + AO2 + AO3

        BO1 = TS * (DXXOX(I + 1, J) + DXXOX(I, J)) / (2 * DELX ^ 2 * (T
P(I, J) - MP(I, J)) * RO(I, J))
        BO2 = TS * (DXY(I + 1, J) + DXY(I, J)) / (2 * DELX * DELY * (TP
(I, J) - MP(I, J)) * RO(I, J))
        BO3 = -TS * (QX(I + 1, J) + QX(I, J)) / (2 * DELX * (TP(I, J) -
 MP(I, J)) * RO(I, J))
        BO = BO1 + BO2 + BO3

        PO1 = TS * (DXXOX(I, J) + DXXOX(I - 1, J)) / (2 * DELX ^ 2 * (T
P(I, J) - MP(I, J)) * RO(I, J))
        PO2 = TS * (DXY(I, J) + DXY(I - 1, J)) / (2 * DELX * DELY * (TP
(I, J) - MP(I, J)) * RO(I, J))
        PO3 = -TS * (QX(I, J) + QX(I - 1, J)) / (2 * DELX * (TP(I, J) -
 MP(I, J)) * RO(I, J))
        PO = PO1 + PO2 + PO3

        EO1 = TS * (DYYOX(I, J + 1) + DYYOX(I, J)) / (2 * DELY ^ 2 * (T
```

```
P(I, J) - MP(I, J)) * RO(I, J))
        EO2 = TS * (DXY(I, J + 1) + DXY(I, J)) / (2 * DELY * DELX * (TP
(I, J) - MP(I, J)) * RO(I, J))
        EO3 = -TS * (QY(I, J + 1) + QY(I, J)) / (2 * DELY * (TP(I, J) -
 MP(I, J)) * RO(I, J))
        EO = EO1 + EO2 + EO3

        FO1 = TS * (DYYOX(I, J) + DYYOX(I, J - 1)) / (2 * DELY ^ 2 * (T
P(I, J) - MP(I, J)) * RO(I, J))
        FO2 = TS * (DXY(I, J) + DXY(I, J - 1)) / (2 * DELY * DELX * (TP
(I, J) - MP(I, J)) * RO(I, J))
        FO3 = -TS * (QY(I, J) + QY(I, J - 1)) / (2 * DELY * (TP(I, J) -
 MP(I, J)) * RO(I, J))
        FO = FO1 + FO2 + FO3

        CONEW(I, J) = AO * CO(I, J) + BO * CO(I + 1, J) + PO * CO(I - 1
, J) + EO * CO(I, J + 1) + FO * CO(I, J - 1)

        '   Check if oxygen depleted, this is based on concentration at
 old time step

        MB = TS * CB(I, J) * KB1NEW * MP(I, J) / HB
        MT = TS * CT(I, J) * KT1NEW * MP(I, J) / HT
        MX = TS * CX(I, J) * KX1NEW * MP(I, J) / HX
        MH = MB + MT + MX
        MO = CONEW(I, J) * (MP(I, J) / HO + (TP(I, J) - MP(I, J)))

        IF MH > (MO / STRATIO) THEN 400 ELSE 405
400     MHDEG = MO / STRATIO
        CONEW(I, J) = 0
        IF MH = 0 THEN 410
        MB = MB * MHDEG / MH
        MT = MT * MHDEG / MH
        MX = MX * MHDEG / MH
        KB1NEW = MB * HB / (CB(I, J) * MP(I, J) * TS)
        KT1NEW = MT * HT / (CT(I, J) * MP(I, J) * TS)
        KX1NEW = MX * HX / (CX(I, J) * MP(I, J) * TS)
        GOTO 410

405     MONEW = MO - MH * STRATIO
        CONEW(I, J) = MONEW / (MP(I, J) / HO + (TP(I, J) - MP(I, J)))

410     A3SAME = TS * (-(DXY(I + 1, J) + 2 * DXY(I, J) + DXY(I - 1, J))
) / (2 * DELX * DELY * (TP(I, J) - MP(I, J)) * RB(I, J)) + TS * (-(DXY(
I, J + 1) + 2 * DXY(I, J) + DXY(I, J - 1))) / (2 * DELY * DELX * (TP(I,
 J) - MP(I, J)) * RB(I, J))
        A4SAME = -TS * (-(QX(I + 1, J) + 2 * QX(I, J) + QX(I - 1, J)))
/ (2 * DELX * (TP(I, J) - MP(I, J)) * RB(I, J)) - TS * (-(QY(I, J + 1)
+ 2 * QY(I, J) + QY(I, J - 1))) / (2 * DELY * (TP(I, J) - MP(I, J)) * R
B(I, J))
        AB1 = TS * (-(DXXB(I + 1, J) + 2 * DXXB(I, J) + DXXB(I - 1, J))
) / (2 * DELX ^ 2 * (TP(I, J) - MP(I, J)) * RB(I, J)) + TS * (-(DYYB(I,
```

```
 J + 1) + 2 * DYYB(I, J) + DYYB(I, J - 1))) / (2 * DELY ^ 2 * (TP(I, J)
 - MP(I, J)) * RB(I, J))
        AB2 = -TS * KB1NEW * MP(I, J) / (HB * (TP(I, J) - MP(I, J)) * R
B(I, J)) + 1
        AB = AB1 + AB2 + A3SAME + A4SAME

        AT1 = TS * (-(DXXT(I + 1, J) + 2 * DXXT(I, J) + DXXT(I - 1, J))
) / (2 * DELX ^ 2 * (TP(I, J) - MP(I, J)) * RT(I, J)) + TS * (-(DYYT(I,
 J + 1) + 2 * DYYT(I, J) + DYYT(I, J - 1))) / (2 * DELY ^ 2 * (TP(I, J)
 - MP(I, J)) * RT(I, J))
        AT2 = -TS * KT1NEW * MP(I, J) / (HT * (TP(I, J) - MP(I, J)) * R
T(I, J)) + 1
        AT = AT1 + AT2 + A3SAME + A4SAME

        AX1 = TS * (-(DXXX(I + 1, J) + 2 * DXXX(I, J) + DXXX(I - 1, J))
) / (2 * DELX ^ 2 * (TP(I, J) - MP(I, J)) * RX(I, J)) + TS * (-(DYYX(I,
 J + 1) + 2 * DYYX(I, J) + DYYX(I, J - 1))) / (2 * DELY ^ 2 * (TP(I, J)
 - MP(I, J)) * RX(I, J))
        AX2 = -TS * KX1NEW * MP(I, J) / (HX * (TP(I, J) - MP(I, J)) * R
X(I, J)) + 1
        AX = AX1 + AX2 + A3SAME + A4SAME

        B2SAME = TS * (DXY(I + 1, J) + DXY(I, J)) / (2 * DELX * DELY *
(TP(I, J) - MP(I, J)) * RB(I, J))
        B3SAME = -TS * (QX(I + 1, J) + QX(I, J)) / (2 * DELX * (TP(I, J
) - MP(I, J)) * RB(I, J))
        BB1 = TS * (DXXB(I + 1, J) + DXXB(I, J)) / (2 * DELX ^ 2 * (TP(
I, J) - MP(I, J)) * RB(I, J))
        BB = BB1 + B2SAME + B3SAME

        BT1 = TS * (DXXT(I + 1, J) + DXXT(I, J)) / (2 * DELX ^ 2 * (TP(
I, J) - MP(I, J)) * RT(I, J))
        BT = BT1 + B2SAME + B3SAME

        BX1 = TS * (DXXX(I + 1, J) + DXXX(I, J)) / (2 * DELX ^ 2 * (TP(
I, J) - MP(I, J)) * RX(I, J))
        BX = BX1 + B2SAME + B3SAME

        DD2SAME = TS * (DXY(I, J) + DXY(I - 1, J)) / (2 * DELX * DELY *
 (TP(I, J) - MP(I, J)) * RB(I, J))
        DD3SAME = -TS * (QX(I, J) + QX(I - 1, J)) / (2 * DELX * (TP(I,
J) - MP(I, J)) * RB(I, J))
        DDB1 = TS * (DXXB(I, J) + DXXB(I - 1, J)) / (2 * DELX ^ 2 * (TP
(I, J) - MP(I, J)) * RB(I, J))
        DDB = DDB1 + DD2SAME + DD3SAME

        DDT1 = TS * (DXXT(I, J) + DXXT(I - 1, J)) / (2 * DELX ^ 2 * (TP
(I, J) - MP(I, J)) * RT(I, J))
        DDT = DDT1 + DD2SAME + DD3SAME

        DDX1 = TS * (DXXX(I, J) + DXXX(I - I, J)) / (2 * DELX ^ 2 * (TP
(I, J) - MP(I, J)) * RX(I, J))
```

```
        DDX = DDX1 + DD2SAME + DD3SAME

        E2SAME = TS * (DXY(I, J + 1) + DXY(I, J)) / (2 * DELY * DELX *
(TP(I, J) - MP(I, J)) * RB(I, J))
        E3SAME = -TS * (QY(I, J + 1) + QY(I, J)) / (2 * DELY * (TP(I, J
) - MP(I, J)) * RB(I, J))
        EB1 = TS * (DYYB(I, J + 1) + DYYB(I, J)) / (2 * DELY ^ 2 * (TP(
I, J) - MP(I, J)) * RB(I, J))
        EB = EB1 + E2SAME + E3SAME

        ET1 = TS * (DYYT(I, J + 1) + DYYT(I, J)) / (2 * DELY ^ 2 * (TP(
I, J) - MP(I, J)) * RT(I, J))
        ET = ET1 + E2SAME + E3SAME

        EX1 = TS * (DYYX(I, J + 1) + DYYX(I, J)) / (2 * DELY ^ 2 * (TP(
I, J) - MP(I, J)) * RX(I, J))
        EX = EX1 + E2SAME + E3SAME

        F2SAME = TS * (DXY(I, J) + DXY(I, J - 1)) / (2 * DELY * DELX *
(TP(I, J) - MP(I, J)) * RB(I, J))
        F3SAME = -TS * (QY(I, J) + QY(I, J - 1)) / (2 * DELY * (TP(I, J
) - MP(I, J)) * RB(I, J))
        FB1 = TS * (DYYB(I, J) + DYYB(I, J - 1)) / (2 * DELY ^ 2 * (TP(
I, J) - MP(I, J)) * RB(I, J))
        FB = FB1 + F2SAME + F3SAME

        FT1 = TS * (DYYT(I, J) + DYYT(I, J - 1)) / (2 * DELY ^ 2 * (TP(
I, J) - MP(I, J)) * RT(I, J))
        FT = FT1 + F2SAME + F3SAME

        FX1 = TS * (DYYX(I, J) + DYYX(I, J - 1)) / (2 * DELY ^ 2 * (TP(
I, J) - MP(I, J)) * RX(I, J))
        FX = FX1 + F2SAME + F3SAME

        '  Calculate concentration at next time step

        CBNEW(I, J) = AB * CB(I, J) + BB * CB(I + 1, J) + DDB * CB(I -
1, J) + EB * CB(I, J + 1) + FB * CB(I, J - 1)
        CTNEW(I, J) = AT * CT(I, J) + BT * CT(I + 1, J) + DDT * CT(I -
1, J) + ET * CT(I, J + 1) + FT * CT(I, J - 1)
        CXNEW(I, J) = AX * CX(I, J) + BX * CX(I + 1, J) + DDX * CX(I -
1, J) + EX * CX(I, J + 1) + FX * CX(I, J - 1)

    NEXT I

  NEXT J

  FOR J = 1 TO NGRIDY

    FOR I = 1 TO NGRIDX
        CB(I, J) = CBNEW(I, J)
        CT(I, J) = CTNEW(I, J)
```

```
        CX(I, J) = CXNEW(I, J)
        CO(I, J) = CONEW(I, J)
      NEXT I

    NEXT J

' RESET SET BOUNDARY CONDITIONS

        FOR I = 0 TO NGRIDX + 1     'bottom boundary + dummy row below
                CB(I, 1) = SBB
                CB(I, 0) = SBB
                CT(I, 1) = SBT
                CT(I, 0) = SBT
                CX(I, 1) = SBX
                CX(I, 0) = SBX
                CO(I, 0) = CO(I, 1)
        NEXT I

        FOR I = 0 TO NGRIDX + 1     'top boundary + dummy row above
                CB(I, NGRIDY) = .000005
                CB(I, NGRIDY + 1) = .000005
                CT(I, NGRIDY) = .00001
                CT(I, NGRIDY + 1) = .00001
                CX(I, NGRIDY) = .000003
                CX(I, NGRIDY + 1) = .000003
                CO(I, NGRIDY) = 279    '(mg/L)
                CO(I, NGRIDY + 1) = 279 '(mg/L)
        NEXT I

        FOR J = 0 TO NGRIDY + 1         ' Left and right rows
                CB(0, J) = CB(1, J)
                CT(0, J) = CT(1, J)
                CX(0, J) = CX(1, J)
                CO(0, J) = CO(1, J)
                CB(NGRIDX + 1, J) = CB(NGRIDX, J)
                CT(NGRIDX + 1, J) = CT(NGRIDX, J)
                CX(NGRIDX + 1, J) = CX(NGRIDX, J)
                CO(NGRIDX + 1, J) = CO(NGRIDX, J)
         NEXT J

      IF PCOUNT = FREQ THEN 13 ELSE 23

13    PCOUNT = 0
      PRINT #1, "Elapsed Time = "; ETIME; "    Time Step ="; K
      PRINT #2, "Elapsed Time = "; ETIME; "    Time Step ="; K
      PRINT #3, "Elapsed Time = "; ETIME; "    Time Step ="; K
      PRINT #4, "Elapsed Time = "; ETIME; "    Time Step ="; K

      FOR I = 1 TO NGRIDX
        FOR J = 1 TO NGRIDY
          WRITE #1, CB(I, J)
          WRITE #2, CT(I, J)
```

```
          WRITE #3, CX(I, J)
          WRITE #4, CO(I, J)
        NEXT J
    NEXT I

23  IF SCOUNT = 10 THEN 27 ELSE 28

27  GOSUB 600
    SCOUNT = 0

28

NEXT K

230

999 END


500
CLS
LOCATE 12, 1: PRINT "DEPTH"
LOCATE 1, 10: PRINT "            BENZENE AND OXYGEN CONCENTRATIONS"
LOCATE 2, 10: PRINT "    BELOW BUILDING                          ADJACENT B
UILDING"
LINE (40, 20)-(320, 160), , B
LINE (330, 20)-(600, 160), , B
LOCATE 22, 10: PRINT "    C/Cinitital                1.0              C/C
initial          1.0"; ""
RETURN

600

LOCATE 23, 10: PRINT "      Elapsed Time (days)"; ETIME

FOR L = 0 TO 5

  BBCX = 40 + (320 - 40) * CB(1, NGRIDY * L / 5) / SBB
  BBCY = 160 - (160 - 20) * L / 5
  CIRCLE (BBCX, BBCY), 2, 4
  BBCX = 330 + (600 - 330) * CB(NGRIDX, NGRIDY * L / 5) / SBB
  CIRCLE (BBCX, BBCY), 2, 4
IF BIOTYPE < 2 GOTO 700
  BBCX = 40 + (320 - 40) * CO(1, NGRIDY * L / 5) / 279
  BBCY = 160 - (160 - 20) * L / 5
  CIRCLE (BBCX, BBCY), 2, 2
  BBCX = 330 + (600 - 330) * CO(NGRIDX, NGRIDY * L / 5) / 279
  CIRCLE (BBCX, BBCY), 2, 2

700
NEXT L
```

RETURN

APPENDIX V

EVALUATION OF BUILDING PARAMETERS

APPENDIX V – EVALUATION OF BUILDING PARAMETERS

This appendix provides information on key building related parameters required for models for the soil vapour transport to indoor air pathway.

Ratio of Cracks to Subsurface Foundation Area: A wide range of measured or assumed values have been reported in the literature ranging from 0.001 to 0.01 (Johnson and Ettinger, 1991) to 0.0001 to 0.000001 (VOLASOIL). The VOLASOIL model values are for a "good" and "bad" foundation, respectively. If soil gas flow rates are known, η can be backcalculated or "fitted" using a soil gas flow model. For example, the back-calculated values for a slab/wall edge crack based on air-entry rates reported in Nazaroff (1992), Revzan *et al.* (1991) and Nazaroff *et al.* (1985) range from about 0.0001 to 0.001. Another possible approach is to measure crack openings although this, in practice, is difficult to do. Figley and Snodgrass (1992) present data from ten houses where edge crack measurements were made. At the eight houses where cracks were observed, the cracks widths ranged from hairline cracks up to 5 mm wide, while the total crack length ranged from 2.5 to 17.3 m. Most crack widths were less than 1 mm.

Building Ventilation Rate: Ventilation has three components consisting of (i) infiltration, or uncontrolled leakage of air into a building through openings in the building envelope, (ii) natural ventilation through open windows and doors, and (iii) mechanical ventilation provided by fans (Nazaroff, 1992). Building ventilation rates depend on construction and seasonal factors. Figley (1997) states that the typical natural ventilation rate during the heating season for Canadian Praire Houses ranges from 0.05 to 0.1 air exchanges per hour (AEH) for an airtight new house to 0.5 to 1.0 AEH for a pre-1945 wood frame house. Lower natural ventilation rates would be expected for a climatic zone with a mild climate (Figley, 1997). The typical estimated mechanical ventilation rate ranges from 0.2 to 0.3 AEH (Figley, 1997). Nazaroff (1992), referencing a study by ASHRAE (1985), indicates that infiltration rates in U.S. single-family housing vary over an approximate range of 0.2 to 2 air exchanges per hour (AEH), with median values of 0.5 and 0.9 for two studies. In U.S. EPA (1992), quoting a study by Mueller *et al.* (1988), reports that the typical AEH for a single family residence ranges from 0.5 to 1.5, with new or energy efficient structures generally ranging from 0.5 to 0.8 but with some as low as 0.2.

Building Underpressurisation: Advective soil gas flow into buildings is induced by a negative indoor-air pressure relative to atmospheric pressure. Building underpressurization is a function of building construction, temperature differences between indoor and outdoor air, wind-loading, mechanical (forced) ventilation systems, and heating and air-conditioning systems. The effect of mechanical ventilation and heating or air-conditioning systems is dependent on the type of system installed, and in some cases positive pressures in buildings can result. Simple empirical relationships can be used to estimate building underpressurization due to wind-loading and temperature differences (Nazaroff, 1992). For example, the pressure on the wall of a building by wind blowing directly on the side of a building can be estimated assuming the wind velocity drops to zero (ignoring shear stresses between wind and ground surface) and equating this velocity drop to the change in momentum:

$$\Delta P_o = \tfrac{1}{2} C_d \rho_a v^2$$

where ΔP_o is the pressure at the wall minus the free-stream pressure, C_d is the empirical drag or pressure coefficient, ρ_a is the air density, and v is the wind velocity. Fischer *et al.* (1996) estimated that the building depressurization due to a sustained wind speed of 5.2 m/s and C_d or 0.2 to 0.3 was on order of 3 Pa for a small slab-on-grade structure. The pressure difference due to difference in indoor and outdoor temperature or stack effect is greatest at the base of the structure and decreases with height. Below the neutral pressure plane (z_o), the pressure on the outside of the building wall exceeds that on the inside of the wall. Based on a temperature difference of 20°C, a negative pressure of between about 2 and 3 Pa would be expected at the base of a two-storey structure, based on the following relationship (Nazaroff, 1992):

$$\Delta P(z) \sim \alpha [\ 1/T_i - 1/T_o\ ] (z - z_o)$$

where z is the height above base of structure (m), $T_{i,o}$ is the indoor and outdoor temperature in Kelvin, and α is equal to 3454 Pa K m^{-1}. Building underpressurization typically increases for structures with basements, for gas-fired forced-air furnaces and as the height of the building increases. Measured mean-air pressure differences for houses with basements are typically in the range of 2 to 10 Pa (Nazaroff *et al.*, 1985; Nazaroff 1992, Figley, 1997, Put and Meijer, 1989) although this pressure difference can be as high as 15 Pa. It should be noted that the climatic conditions required for the higher pressure differences are more representative of severe winter conditions in Canada (Figley, 1997). There is little data specifically for slab-on-grade structures, although studies by Scanada Consultants Limited (1993) and Fischer *et al.* (1996) suggest that a building underpressurization of 2 to 4 Pa may be reasonable for such structures.

APPENDIX VI

BACKGROUND INFORMATION ON CHATTERTON RESEARCH SITE AND PHOTOGRAPHS

TECHNICAL PAPER

Canadian Consortium Research Project - Field Validation of Soil Gas Transport to Indoor Air Pathway

Published in: Proceedings of 1998 Petroleum Hydrocarbon and Organic Chemicals in Ground Water: Prevention, Detection and Remediation. API / NGWA, Houston, Texas, November 11 to 13, 1998.

BY:

Ian Hers, University of British Columbia / Golder Associates Ltd.
Reidar Zapf-Gilje, University of British Columbia / Golder Associates Ltd.

CANADIAN CONSORTIUM RESEARCH PROJECT - FIELD VALIDATION OF SOIL GAS TRANSPORT TO INDOOR AIR PATHWAY

Ian Hers[1] and Reidar Zapf-Gilje[2]
[1] Golder Associates Ltd., Burnaby, British Columbia, Canada and University of British Columbia, [2] Golder Associates Ltd., Burnaby

INTRODUCTION

Consideration of potential risk in the remediation of sites impacted by volatile organic compounds (VOCs) is now commonplace. At many sites, the soil gas transport to indoor air pathway is an important potential exposure pathway. Relatively simple screening-level models are often used to quantify potential exposure and risk. These models are thought to incorporate conservative assumptions; however, little field data is currently available to test model accuracy. To address this limitation, a comprehensive research program is currently being conducted under the sponsorship of a consortium of governmental and industry partners at a former petrochemical plant site impacted by benzene, toluene and xylene releases, located near Vancouver, B.C. The project research objectives are to further fundamental understanding of vadose zone fate and transport of VOCs and VOC intrusion into buildings, and contribute to the process of model validation and development through comparison of measured and predicted intrusion at the test site. The project approach consists of evaluating fate and transport of VOCs in both the vadose zone, and through the building envelope (a small building has been constructed). To-date, monitoring data over an approximately one-year period has been collected.

This paper begins with a review of background information, and presents a conceptual model for this pathway based on our current understanding of soil gas transport. Next, the results of vadose zone monitoring, and monitoring of soil gas and VOC flux through the building envelope is presented. The paper concludes with a comparison of measured and model predicted VOC intrusion. Due to the extensive and on-going nature of this project, results presented are limited to an overview; additional details will be presented in other publications.

BACKGROUND

Predictive models commonly used for the soil gas transport to indoor air pathway are limited to one-dimensional steady-state analytical or semi-analytical models based on the Johnson and Ettinger (1991) framework, or one-dimensional transient analytical models based on the Jury *et al.* (1990) framework. Examples of such "screening-level" models include the *ASTM Tool Kit*, a software program based on ASTM ES-1739 and distributed by Groundwater Services Inc., the *VOLASOIL* model developed by the Dutch Ministry of Environment, the *VAPEX* model developed by Environmental Systems and Technologies, Inc., and a model developed Golder Associates Ltd. (Hers *et al.*, 1997). Significant uncertainty surrounds the accuracy of these models.

Integrated studies of vadose zone fate and transport of VOCs combined with measurement of VOC intrusion into buildings remain limited. Two studies conducted by the University of California at Berkeley in conjunction with the Lawrence Berkeley laboratory (Garbesi *et al.*, 1988; Fisher *et al.*, 1996) have consisted of field-based evaluations of soil gas VOC intrusion into buildings. The Garbesi *et al.* (1988) study included measurement of landfill-related VOC intrusion into a house while the Fischer *et al.* (1996) study involved measurement of gasoline-related VOC intrusion (*i.e.*, BTEX and other gases) into an at-grade building. Monitoring conducted by Fischer *et al.* (1996) indicated that soil gas hydrocarbon concentrations decreased sharply over a small vertical depth interval (0.1 m to 0.7 m below ground surface) within sand fill present at the site. It was postulated that a partial physical barrier to vertical transport (*i.e.*, higher moisture content zone) combined with biodegradation can account for the steep gradient. In contrast, a recent study documented by Laubacher *et al.* (1997) indicated the presence of elevated hydrocarbon concentrations in soil gas and low

oxygen levels (*i.e.*, below one percent) directly below a basement slab at a gasoline-contaminated site. Soil gas hydrocarbon concentrations adjacent to the basement (*i.e.*, at the same depth) were about two orders-of-magnitude lower and oxygen levels were about 14 %. Soils at this site consisted of uniform sand with occasional silty or clayey lenses with the water table located about 5.8 m below ground surface.

CONCEPTUAL MODEL

Research to-date indicates that vadose zone fate and transport of VOCs and intrusion into buildings is a complex phenomena. Processes within both the vadose zone and building envelope compartment affect this pathway, and are highly dependent on site specific conditions such as contaminant type and distribution (*e.g.*, is NAPL present above water table?), depth to contamination, soil properties and building characteristics. Within the vadose zone, diffusion, sorption, and in some cases, biodegradation, are generally thought to have the most significant effect on VOC fate and transport. Key factors affecting these vadose zone processes include moisture content, organic carbon and, in the case of biodegradation, the presence of indigenous microbes capable of degrading the hydrocarbon, and conditions favourable for biostimulation (for example oxygen levels). In some cases, soil gas advection through shallow soil near the building envelope, as influenced by building underpressurization and/or barometric pumping, could have a significant effect on VOC intrusion. Key factors affecting soil gas advection and building intrusion include the permeability of the subslab soil and building envelope, and potential preferential pathways (*e.g.*, utility corridors). Depending on site conditions, soil gas advection will be either primarily controlled by resistance to flow through soil, or resistance due to the building envelope.

The relative importance of various processes will depend on site specific conditions. In the case of deeper contamination, diffusion and natural attenuation processes within the vadose zone compartment are expected, in most cases, to control the overall VOC intrusion rate into a building. In the case of shallow contamination, advection and hence properties of the subslab soil (*e.g.*, permeability) and building envelope (*e.g.*, cracks) may be of greater importance.

SITE DESCRIPTION AND METHOD OVERVIEW

The field site is the former Chatterton petrochemical plant located near Delta, B.C. The plant manufactured benzoic acid, phenol and meta-toluic acid. Raw products included toluene and m&p-xylene while by-products included benzene. Near surface soils in the plant area consist of approximately 3.5 m of dredged river sand underlain by native silt. The depth to the water table generally ranges from 1.5 m to 2.5 m depth below ground surface (bgs). Release of benzene, toluene and m&p-xylene (BTX) have resulted in a laterally extensive zone of residual non-aqueous phase liquid (NAPL) (*i.e.*, smear zone) corresponding to the approximate water table fluctuation (except in source areas). Average annual precipitation at a nearby weather station (*i.e.*, 7 km from site), considered to approximate site conditions, is 1240 mm (Richmond Nature Park).

The study methods included extensive delineation of the residual NAPL concentrations at source, detailed vertical profiling of soil properties (*e.g.*, moisture content, porosity, *in situ* diffusion coefficients) and vadose zone BTX, oxygen, carbon dioxide and methane concentrations in soil gas. Regular monitoring was used to assess the effect of seasonal changes on soil gas fate and transport with vadose zone monitoring conducted between March 1997 and August 1998. To facilitate measurement of soil gas intrusion, a small building (greenhouse) with controlled building envelope features (edge crack and service penetrations) was constructed in August 1997. The greenhouse was fastened to a 6.1 m by 9.3 m concrete slab of 100 mm nominal thickness. Near-continuous monitoring of oxygen levels below the building floor slab and differential pressure between subsoils, building and ambient was implemented. Soil gas hydrocarbon intrusion rates were estimated using a flux chamber, and indirectly through air and soil gas monitoring. Soil gas monitoring and intrusion evaluation was conducted for both static and induced building underpressurizatiion (-10 and -30 Pascals (Pa)) conditions.

VADOSE ZONE FATE AND TRANSPORT

Baseline Soil Characterization

Baseline soil conditions were characterized at two locations designated as Sites A and B (Figure 1). Soils consist of a thin (0.1 to 0.3 m) laterally discontinuous soil layer consisting of sandy silt to fine sand containing some silt (henceforth referred to as "silt and fine sand crust") underlain by a medium sand fill (the ground surface is lightly vegetated with grasses). Prior to constructing the greenhouse, the silt and fine sand crust was removed to a depth of 0.3 m and replaced with 0.2 m of imported sand fill compacted to approximately 90% Modified Proctor maximum dry density (ASTM D1557). Grain size, estimated organic carbon and nutrient test results are presented in Table 1. Variability in grain size and organic carbon content was low indicating a relatively uniform sand deposit. For example, the silt content in eight samples collected from a single soil core at Site B ranged from 1.7 to 5.5 %. Grain size and organic carbon data for a vertical soil profile below the approximate centre of the greenhouse is presented in Table 2.

TABLE 1
Mean Grain Size, Organic Carbon and Soil Nutrient Properties

Soil Type	D_{50} (50 % by weight passing) (mm)	Percent finer than U.S.S. #200 sieve (silt)	Estimated Organic Carbon[3] (%)	Ammonia Nitrogen (mg/kg)	Nitrate Nitrogen (mg/kg)	Total Nitrogen (%)	Total Phosphate (mg/kg)
Silt to fine sand crust[1]	N/A	41	-	5.0	1.9	0.050	9.4
Sand fill[2]	0.33	2.5	0.63	5.4	1.1	0.014	4.4

[1] Arithmetic mean based on one to four samples. [2] Arithmetic mean based on five to thirteen samples.

[3] Estimated from organic matter content *(i.e.*, loss on ignition) using *Van Bemmelen* factor of 1.724 (Page *et al.*, 1982).

Water retention (field capacity), total porosity, air-entry tension, bulk density and saturated hydraulic conductivity were estimated using disturbed soil samples re-compacted to various densities (Table 3). Samples re-compacted to Standard Proctor and Modified Proctor density (Lambe, 1951) likely represent the range of *in situ* density for the sand, except for near surface soil. The sand field capacity values were relatively low (about 6.8 % by volume, on average) indicating the sand will drain relatively quickly to fairly low moisture contents. Air-entry tensions were also low indicating that continuous air-filled pores will form at relatively low matric suctions. Gas-phase diffusion becomes significant at matric suctions above the air-entry tension.

Soil air permeability was measured at soil gas probes below the centre of the greenhouse according to the method described in Garbesi *et al.* (1996). This test measures soil air permeability within a small radius of the probe tip (0.1 m is suggested by Fischer *et al.* (1996)). Tests were conducted using a range of flow rates (3.1 to 12.6 cm^3/sec) and pressures (43 to 160 Pa) with results presented in Table 2. Mean soil air permeability was, as expected, highest in low moisture content soils below the slab, and increased with depth. Soil air permeability at a given depth varied somewhat depending on probe pressure (between 30 to 60 %). When corrected for density and gas slippage (Klinkenberg) effects, the variation in permeability decreased slightly.

Soil samples were analyzed for benzene, toluene, ethylbenzene, xylenes (BTEX), and light hydrocarbons. The results indicate the BTX constitute essentially all hydrocarbons in soil. BTX concentrations in soil were relatively low above 1.2 m depth, but increased significantly at about 1.5 m depth indicating the presence of residual NAPL (Figure 2). At Site B, the relative proportions of individual components to total BTX were, on average, 10 % for benzene, 82 % for toluene and 8 % for m&p-xylene. The proportions did not vary significantly with depth, although data points were limited within 0.6 m of ground surface since concentrations, in many cases, were below the detection limit. Similar results were obtained for Sites A and B.

TABLE 2

Summary of Selected Soil Physical Properties Below Greenhouse

Soil Gas Probe Depth (m)	Measured Soil Air Permeability[1] (Darcy)	Measured Effective Diffusivity (cm^2/sec)	Soil Sample Depth Range (m)	Measured Silt Content (%)	Estimated Organic Carbon (%)
0.15	27	-	0.085 - 0.235	1.7	-
0.3	-	0.071	0.19 - 0.34	2.5	-
0.45	6.3	0.028	0.345 - 0.495	4.4	0.52
0.58	7.6	0.024	0.5 - 0.65	2.6	0.52
0.75	-	0.013	0.65 - 0.8	3.8	0.72
0.9	9.5	0.037	0.8 - 0.95	1.8	0.71
-	-	-	0.95 - 1.1	2.2	0.69
1.2	5.6	-	1.1 - 1.25	1.9	0.68
-	-	-	1.25 - 1.4	-	0.70
1.5	8.6	-	1.4 - 1.55	-	0.65
-	-	-	1.55 - 1.85	5.5	0.51

[1] Mean values for tests conducted at varying pressures, tests conducted in November and December 1997.

TABLE 3

Mean Soil Physical Properties[1]

Sample Preparation	Field Capacity (33 J/kg) Volumetric Water Content (% by Vol)	Total Porosity (%)	Air Entry Tension (J/kg)	Bulk Density (kg/m^3)	Saturated Hydraulic Conductivity (m/s)
1/2 Standard Proctor	12.2	37.7	0.5	1620	7.7E-04
Standard Proctor	6.8	35.6	0.8	1645	8.1E-04
Modified Proctor	6.9	35.6	1.9	1685	6.7E-04

[1] Arithmetic mean values based on analysis of two to three composite sand fill samples for each density.

Soil Moisture

Soil moisture content was measured in soil cores from below the approximate middle of the greenhouse, and in soil cores obtained prior to greenhouse construction or adjacent to the greenhouse (Figure 3). Soil moisture contents below the greenhouse are at moderate levels and correspond to air-filled porosities between about 15 and 27 %. On average, the moisture contents appear to be highest between about 0.6 and 0.9 m depth. No physically-based mechanism for the increase in moisture content appears plausible since the grain size distribution is relatively constant with depth.

Moisture content monitoring below the greenhouse has only been conducted over a one-year period and therefore is not indicative of long-term trends. The further investigate long-term trends, a soil core was obtained from below a nearby on site building constructed in the 1960's. Residual NAPL is present below the building starting at about 1.6 m depth below ground surface. Within 1 m of slab surface, the moisture content below the "old" building is consistently lower than that measured below the greenhouse and likely reflects long-term drying of soil. The lowest moisture content below the old building (2.6 %) is likely just above the soil wilting point, estimated to be on the order of 1 to 2.5 % based on tests conducted on soil from below the greenhouse. The soil wilting point is defined as the moisture content at a matric suction of 1500 J/kg. Bioventing studies suggest that biodegradation rates are significantly reduced for soil moisture contents close to the soil wilting point (Zwick *et al.*, 1995).

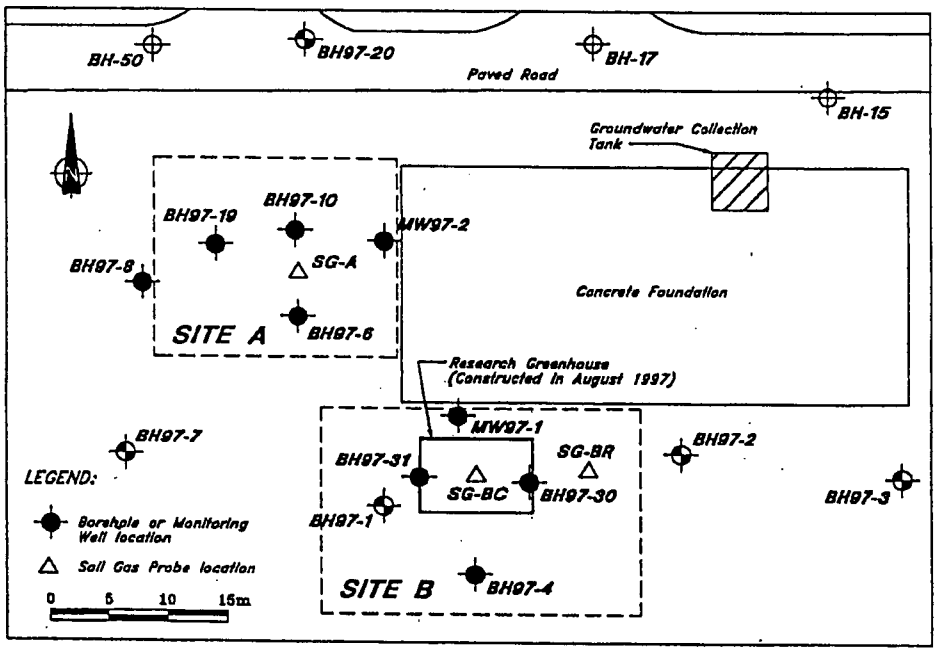

Figure 1
Site Plan

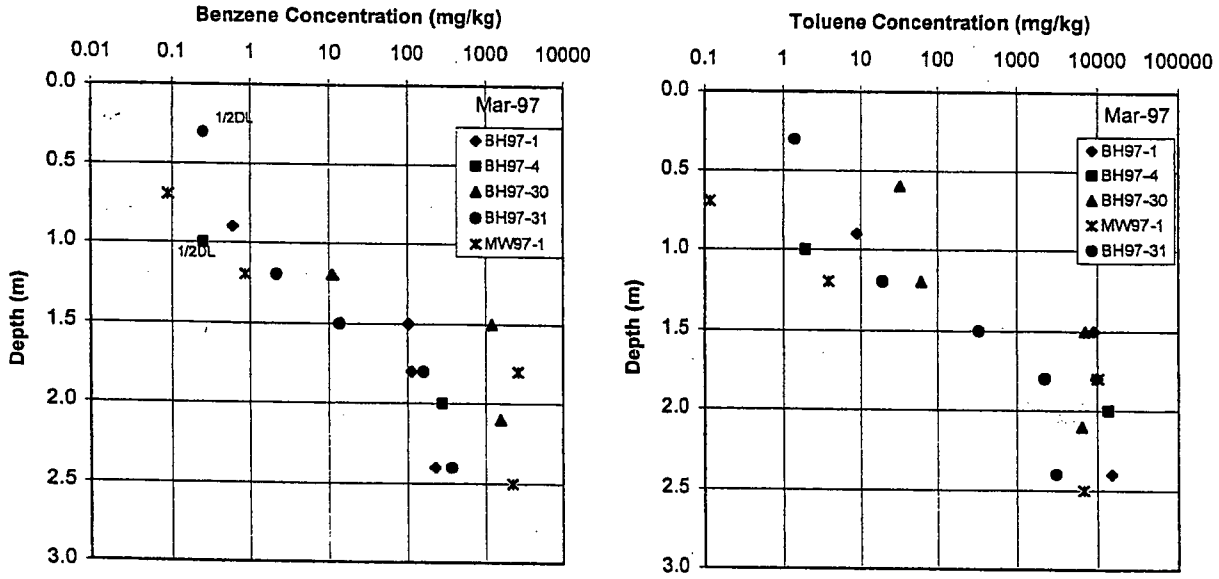

Figure 2
BTX Concentrations in Soil at Site B.

Soil Gas

Soil gas samples were analyzed for BTX and light gases (oxygen (O_2), carbon monoxide (CO), carbon dioxide (CO_2), methane (CH_4), nitrogen (N_2) and ethane). Soil gas samples were collected using 5 ml glass and Teflon syringes from either 6 mm or 12.5 mm I.D. steel probes driven to the desired depth, and analyzed for BTX on-site using a SRI 8610 gas chromatograph with photoionization detector (GC/PID). Samples for light gas analyses were collected using a 500 ml SKC Tedlar™ bag and analyzed using a GC with thermal conductivity or flame ionization detector (FID or TCD), or using a Landtec Control Technologies GA-90 field portable gas detector. Samples for BTX analysis were analyzed within four hours of collection, while samples for laboratory light gas analysis were analyzed between four and 48 hours of collection. The Landtec gas detector utilizes a galvanic cell for O_2 and infrared detector for CO_2 and CH_4. To investigate the accuracy of the field portable unit, two samples taken consecutively from selected probes were submitted for both field and laboratory analysis. The results indicate a significant bias for O_2 and CH_4. For example, Landtec O_2 concentrations were between 0.5 and 3 % lower that GC/TCD concentrations with the difference increasing at lower levels. Analysis by GC/TCD is considered more accurate than a galvanic cell.

Soil gas benzene concentrations below the building, and at probes not covered by a building (*i.e.*, below the present greenhouse before it was constructed, or adjacent to the greenhouse) are presented in Figure 4. The benzene concentration profiles below the centre of the greenhouse were relatively consistent over time and are characterized by high concentrations at depth, significant attenuation (about 3 orders-of magnitude) between about 0.4 to 0.8 m depth, and lower but variable concentrations within 0.4 m depth below slab surface. The measured soil gas concentrations below 1 m depth are close to those predicted assuming equilibrium partitioning between the NAPL and soil gas phases, and vapour pressure adjusting using the mole fraction and Raoult's Law. For example, the predicted benzene soil gas concentrations range from 13 to 26 mg/L based on a temperature range of 10 to 20°C, and benzene mole fraction of 0.08. Measured benzene concentrations ranged from 5 to 23 mg/L. The benzene concentration profiles for the no building case were somewhat more variable than those below the building. Postulated causes include variation in surface water infiltration and moisture content, and advective soil gas pumping caused by barometric pressure and/or temperature fluctuations. The low benzene concentrations for the December 1, 1997 monitoring round may have been caused by high soil moisture contents since precipitation over the previous week was about 40 mm (Richmond Nature Park station). Similar results were obtained for toluene and xylene both below and adjacent to the greenhouse with results for one typical monitoring round presented in Figure 5.

The O_2 concentrations below the building, and at probes not covered by the building are presented in Figure 6. The O_2 concentrations below the building were relatively consistent over time and indicate significant O_2 consumption is likely occurring between about 0.6 to 0.9 m depth. Oxygen levels in near surface soil below the centre of the building slab were depleted and ranged between approximately 8 and 13 %. Carbon dioxide concentrations within 0.9 m depth generally ranged from 6 to 9 %, while below 0.9 m generally ranged between 10 and 13 %. The O_2 concentration profiles for the no building case exhibit greater variability, likely for the same reasons as described above. Oxygen concentrations at a non-contaminated reference site with similar soils were close to ambient levels (*i.e.*, 20.7 %) while CO_2 concentrations were equal to or below 0.1 %.

On three occasions (October 1997, November 1997 and June 1998), BTX and light gas concentrations in soil gas were measured at other probes below the concrete slab (*i.e.*, in addition to centre probes) (Figure 7). When compared to the centre probe cluster, the results indicate BTX and light gas concentrations were similar at probes located near the north, east and south edges of the slab (SG-BNC, SG-BEC, and SG-BSC). In contrast, BTX concentrations directly below the west edge of the slab were slightly higher, and BTX concentrations at probe SG-BMW (directly below slab) were significantly higher (typically, over two orders-of-magnitude). In addition, O_2 concentrations were typically several percent lower at this location. The combined BTX and light gas results indicates significant biodegradation may be occurring below the slab. However, the lateral variability in soil gas concentrations suggest that O_2 transport in subslab soils varies spatially, and that the variation in O_2 transport may be causing lower BTX biodegradation rates below the west portion of the slab. Variable BTX concentrations at 0.3 m depth (see Figure 4) also suggest that lateral transport of soil gas below

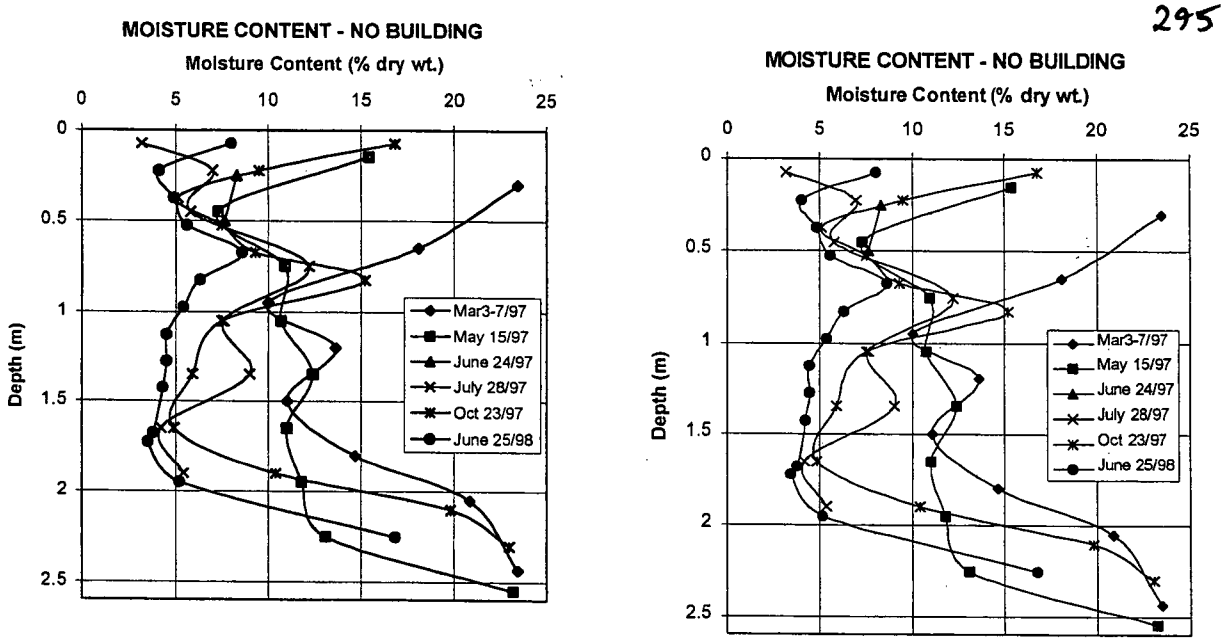

Figure 3
Moisture Content for Below Building and No Building Cases at Site B.

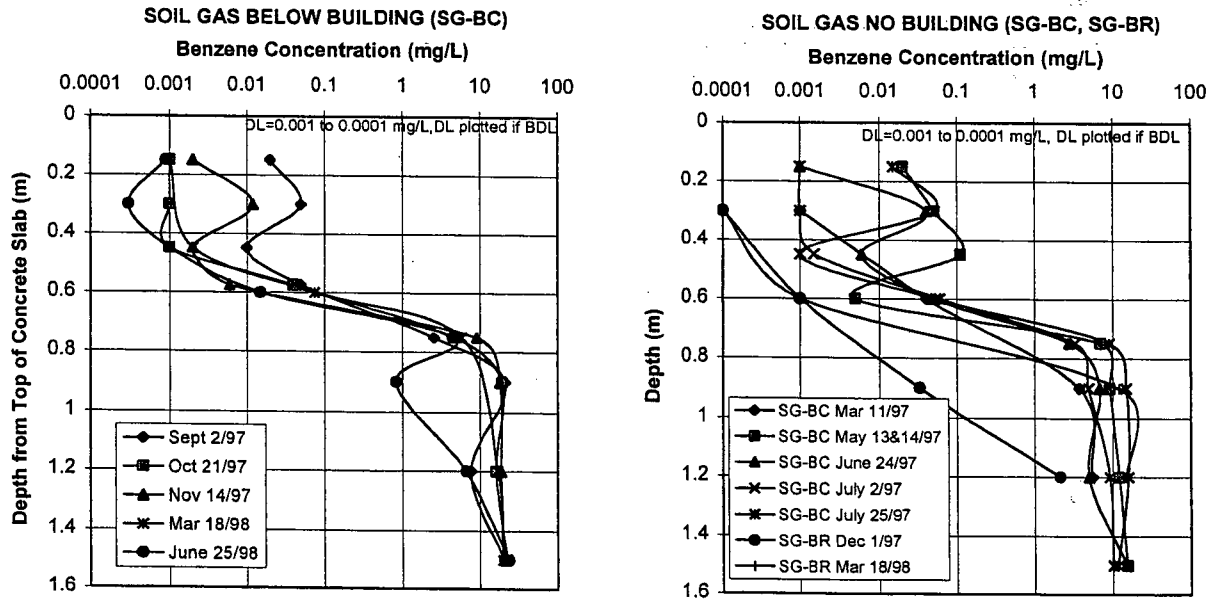

Figure 4
Soil Gas Benzene Concentrations for Below Building and No Building Cases at Site B.

the concrete slab may be occurring. It is noted that a 1 to 1.5 m strip of plastic was placed along the north, west and east edges of the greenhouse to shed rain water away from the edges of the greenhouse. This may influence O_2 replenishment toward the west end of the slab.

In Situ Diffusion Coefficients

In situ diffusion coefficients, while rarely measured, were considered important for this project due to the possible uncertainty associated with empirical relationships for effective diffusivity, and desire to accurately separate diffusive transport from other attenuation processes. *In situ* diffusion coefficients were measured at selected soil gas probe locations using a push-pull test involving injection and extraction of a non-reactive tracer gas (helium). The test is described by Johnson *et al.* (1998). The test procedure involved injection of 0.1 litre of helium followed by extraction of 1 litre of soil gas from the same probe using a Tedlar™ bag. The test was repeated several times at each probe by varying the time between injection and extraction. Helium was measured using a Mark Instruments, Inc. 9822 field portable detector. Prior to conducting each test, soil gas near the probe was purged by injecting a minimum of 15 litres of air, and a soil gas blank was collected to ensure that helium concentrations were below the detector detection limit (0.01 %).

The measured effective diffusion coefficients and tortuosities are presented in Table 4. The effective diffusion coefficients were calculated using actual air-filled porosities measured below the greenhouse. The repeatability of tests conducted at different times was relatively good with a relative standard deviation (RSD) on the order of 20 %. As expected, the effective diffusion coefficients decreased with increasing moisture. In addition, a good comparison was obtained between the measured tortuosity and that predicted using the Millington and Quirk (1961) relationship with measured values consistently about twice the predicted values. The results indicate the Millington and Quirck (1961) relationship, which is commonly used to estimate tortuosity, is appropriate over the range of moisture contents evaluated.

TABLE 4
Measured *In situ* Effective Diffusion Coefficients Based on Push-Pull Tests[1]

Location	Depth (m)	Moisture Content[3] (% wt.)	Air-filled Porosity	Measured Eff. Diffusivity - Varying Extraction Times: Time= 1.24 min (cm^2/sec)	Time= 3.24 min (cm^2/sec)	Time= 6.24 min (cm^2/sec)	Time= 11.2 min (cm^2/sec)	Time= 16.2 min (cm^2/sec)	Mean[2] Effective Diffusivity (cm^2/sec)	Mean Measured Tortuosity	Predicted Tortuosity[4] (M&Q '61)
SG-A	0.60	6.9	0.24	0.075	0.053	0.063	0.056	0.049	0.055	0.17	0.069
SG-BC	0.3	5	0.27	0.12	0.081	0.064	0.078	0.063	0.071	0.22	0.10
SG-BC	0.45	8	0.22	0.067	0.040	0.027	0.020	0.026	0.028	0.085	0.053
SG-BC	0.58	10	0.19	0.054	0.027	0.026	0.021	0.022	0.024	0.072	0.031
SG-BC	0.75	12	0.16	0.017	0.018	0.013	0.011	0.010	0.013	0.039	0.016
SG-BC	0.9	7	0.24	0.072	0.043	0.038	0.028	-	0.037	0.11	0.067

[1] Physical/chemical properties for Helium: D_{air} = 0.33 cm^2/sec, H (dimensionless) = 121; K_d = 0.002

[2] Arithmetic mean based on results for time equal to 3.24, 6.24, 11.2 and 16.2 minutes

[3] Moisture contents approximate values based on data in Figure 3, total porosity = 0.356.

[4] Predicted tortuosity based on Millington and Quirck (1961) relationship, $\tau = \phi_g^{10/3} / \phi^2$

Advective Soil Gas Transport

Potential advective soil gas transport in subslab soil was investigated by continuous monitoring of O_2 concentrations directly below the slab, differential pressure between the soil and building, soil temperature, and environmental conditions (*e.g.*, temperature, barometric pressure). Continuous O_2 concentrations were measured using an electrochemical cell (DRC XT-252) adjacent to probe SG-BMW. Significant fluctuation in O_2 levels below the slab was observed during the fall of 1997 (from less than 2 to 15 %). The following trends with respect to O_2 are noted: (i) diurnal changes in concentrations (up to 2 %) with O_2 concentrations decreasing as the greenhouse temperature increased, (ii) day-long to week-long O_2 trends that appear to be correlated to barometric pressure with O_2 concentrations proportional to pressure, and (iii) seasonal O_2 trends indicating an overall decline in O_2 concentrations between September and December 1997. Diurnal effects

were significant in September 1997 but dissipated to non-detectable levels as the daily temperature gradients decreased during the fall. The O_2 concentrations increased slowly as the barometric pressure increased, but appeared to decrease quickly in relation to a decrease in barometric pressure, which may be due to a flushing effect. It is postulated that the longer-term decrease in O_2 below the slab is due to increased precipitation during the fall, higher soil moisture content and corresponding decrease in soil air permeability. The decrease in permeability would likely be greatest for the silt and fine sand crust which would tend to retain water to a greater extent than the underlying sand, and thus hinder O_2 replenishment below the slab.

Differential pressure between the greenhouse and soil was measured below the centre of the greenhouse on a continuous basis using differential pressure transducers (Setra Systems 264) connected to soil gas probes located 0.15 and 0.58 m below the top of slab. Variation in differential pressure for the 0.15 m probe was negligible indicating that there was significant pressure coupling between the greenhouse and soil immediately below the slab, likely due to a relatively high slab permeability. Variation in differential pressure for the deeper 0.58 m probe was significant with diurnal variations in differential pressure of up to 3 Pascals. The diurnal fluctuations reflect heating (expansion) and cooling (contraction) of soil gas below the building, and result in soil gas movement into and out of soil directly below the slab. No barometric-induced variation in differential pressures were apparent.

Conceptual Model for Vadoze Zone Below Greenhouse

The conceptual model for the vadose zone processes below the greenhouse is presented in Figure 8. Based on monitoring conducted to date, processes affecting fate and transport can be divided into three zones based on depth below ground surface. In the deep zone, diffusive transport is the dominant process with likely very little bioattenuation as a result of oxygen depletion and potential toxic conditions due to high BTX concentrations. In the mid-depth zone, significant attenuation of BTX occurs below the approximate centre of the slab, but as described above, attenuation may not be spatially uniform. The BTX attenuation is attributed to be primarily due to biodecay since testing of soil properties (Table 2) and pressure gradients indicated physically-based mechanisms are unlikely to be significant. Elevated soil moisture within the mid-depth zone may be due to the generation of water as a by-product of hydrocarbon mineralization, and/or enhanced water retention within microbial biomass. In the shallow zone, advective transport is likely the dominant transport process. The driving forces for advection under static conditions (*i.e.*, no induced building depressurization) are temperature and barometric pressure fluctuations, and possibly wind-loading.

The consistent soil gas BTX profiles and relatively uniform soil physical properties suggest that fate and transport processes over the mid-depth zone are dominated by steady-state diffusion and biodecay, when sufficient O_2 is present for aerobic degradation. Based on this model and assuming homogeneous soil conditions, first order degradation coefficients were estimated by fitting model-predicted BTX concentrations based on an analytical solution for one-dimensional diffusion and reaction to measured values over the portion of the BTX profile that is approximately log-linear (*i.e.*, 0.5 to 0.8 m, see Figure 4). The first order degradation model assumes that both oxygen and hydrocarbon-degrading microbes are available in excess. Using approximate mean values for measured tortuosity and moisture content, the estimated first order degradation rate constants based on soil pore water concentrations (k_w) were on the order of 1.2 hr^{-1} for benzene and 0.9 hr^{-1} for toluene. These values compare closely to first order degradation coefficients based on laboratory and field studies, presented by DeVaull *et al.* (1997). On-going testing is being conducted to further corroborate biodegradation processes including an *in situ* respiration test and microbial enumeration of BTX-degraders.

SOIL GAS INTRUSION INTO BUILDING

Monitoring of soil gas intrusion into the greenhouse was conducted under static conditions (*i.e.*, no induced depressurization) and dynamic conditions (*i.e.*, fan-induced building depressurization) at -10 and -30 Pa relative to ambient air. For the static case, VOC intrusion into the building occurs through diffusion and potentially advective pumping caused by barometric pressure and temperature fluctuations, and/or wind loading. Possible

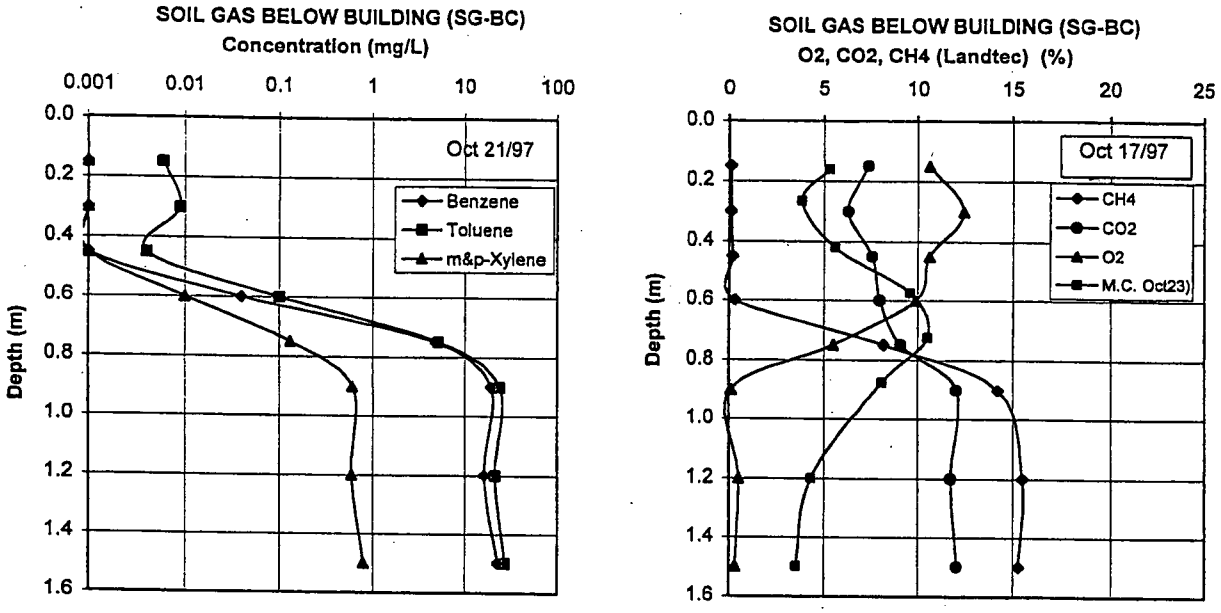

Figure 5
Soil Gas BTX and Light Gas Concentrations Below Greenhouse – October 1997.

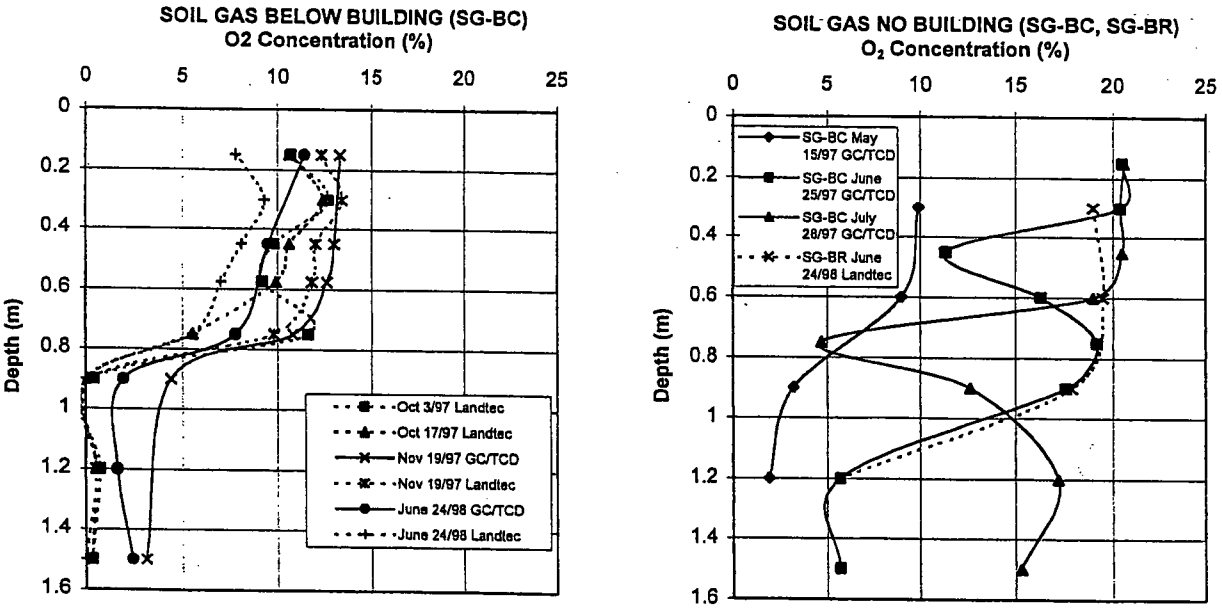

Figure 6
Soil Gas Oxygen Concentrations for Below Building and No Building Cases at Site B.

routes of soil gas entry through the building envelope are the 2-mm wide edge crack (total length of 27 m), and hairline cracks potentially surrounding soil gas probes and two capped PVC drain pipes penetrating the concrete slab. In addition, a small north-south trending shrinkage crack bisects the middle of the slab. A preliminary depressurization test conducted in October 1997 indicated that soil gas flow rates through the slab were very high with very little pressure drop across the slab. For this reason, portions of the edge crack were either sealed with concrete grout, or were covered with plastic weighted with sandbags (to enable future opening of the crack if desired) in October 1997. Four 0.9-m lengths of the crack (*i.e.*, along north, east, south and west edges) were left uncovered corresponding to a crack to slab area ratio of 0.013 %.

For the static case, the VOC flux into the building was estimated by (i) comparing indoor and outdoor BTX concentrations, and (ii) measuring potential VOC emissions through open portions of the edge crack using a stainless steel flux chamber (90 cm x 9 cm x 9 cm). Extensive chamber blanks were tested to ensure materials used were clean. The flux chamber was bolted to the concrete and sealed using a rubber gasket. After purging five chamber volumes, sampling with replacement (flow in = flow out) using a flow rate between 150 to 300 ml/min was used to obtain a sample with VOCs collected on two sorbant tubes (Supelco Inc. Carbotrap 300) in series. Inlet air to the chamber was scrubbed using a activated carbon trap. During the tests, the differential pressure between the chamber and greenhouse was periodically measured using a micromanometer (Dwyer Microtector). No pressure gradient was detected between the flux chamber and greenhouse. Indoor and outdoor air samples were also collected using sorbant tubes over a 4 to 20 hour period. During the tests, ventilation louvers in the greenhouse wall were partially open providing some natural ventilation.

For the dynamic case, flux chamber sampling without air replacement was employed to measure both soil gas advective flow through the edge crack and BTX flux. Soil gas flow rates were adjusted until there was no measurable pressure difference between the chamber and greenhouse. Soil gas samples were collected from the chamber outlet using Tedlar™ bags. In addition, soil gas flow and VOC flux were indirectly estimated using the mean indoor, outdoor and subslab BTX concentrations, and building ventilation rate (*i.e.*, mass balance approach). For the subslab BTX concentrations, the average of the four shallow probes adjacent to the edge crack was used.

The soil gas intrusion monitoring results are presented in Table 5. Statistical hypothesis testing indicated that, in all but one case, the mean indoor and outdoor concentrations were significantly different for the dynamic case (using two-tailed test and significance level of 0.10). Differences were not statistically significant for the static case, although it is recognized that only a limited number of samples were analyzed. For the static case, the low flux chamber concentrations and non-significant difference in indoor and outdoor concentrations suggest that BTX flux through the building envelope is very low and potentially not significant. In contrast, highly elevated flux chamber concentrations were measured for the dynamic case. The BTX flux rates through the edge crack were further evaluated for toluene. The estimated toluene flux based on direct measurements of concentration and flow was on the order of 0.5 mg/min (-10 Pa test). In comparison, order-of-magnitude BTX flux rates and soil gas flows backcalculated using the measured toluene concentrations and building ventilation rate, were 6.6 mg/min and 6.4 L/min (-10 Pa), and 4.3 mg/min and 3.0 L/min (-30 Pa). The higher backcalculated toluene fluxes likely reflect other potential entry routes for soil gas intrusion, in addition to the four open edge cracks, although it is noted results are relatively uncertain due to experimental inaccuracy.

The effect of induced building depressurization was further evaluated by monitoring soil gas BTX concentrations below the centre of the greenhouse nine days (-30 Pa test) to twelve days (-10 Pa test) days after building ventilation had started (Figure 9). These profiles diverge significantly from the "static" profiles obtained during previous monitoring rounds and indicate that building depressurization caused significant upward migration of soil gas. For the –30 Pa test, steady state conditions may not have been reached resulting in lower BTX concentrations. For the –10 Pa test, lower soil moisture outside the greenhouse in August 1998 may also have contributed to deeper advective soil gas transport, and therefore higher concentrations. The results demonstrate the significant effect building depressurization can have on soil gas fate and transport. However, it is cautioned that numerous factor contribute to likely "worst case" conditions with respect to induced advective transport. These include shallow contamination, relatively permeable soil, a highly

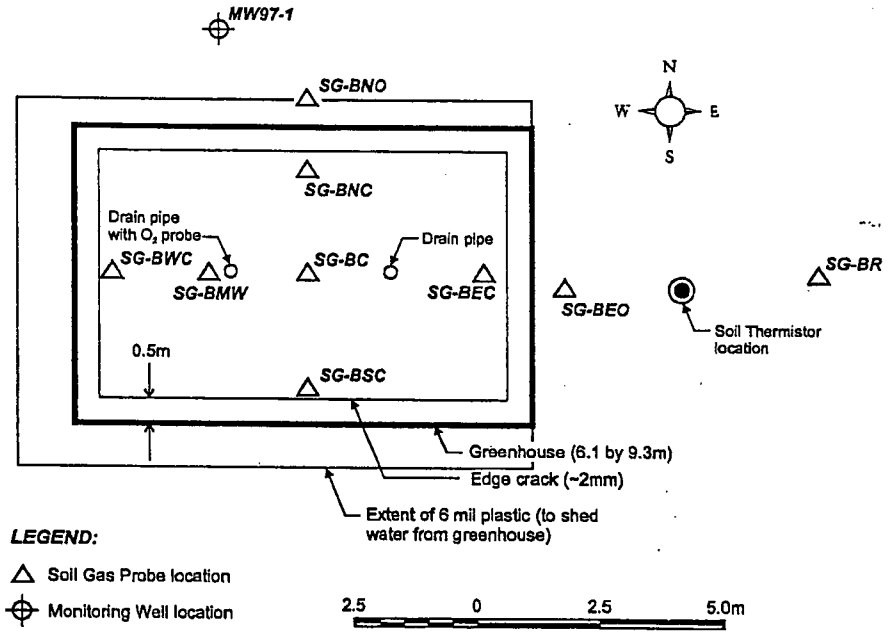

Figure 7
Greenhouse Location Plan.

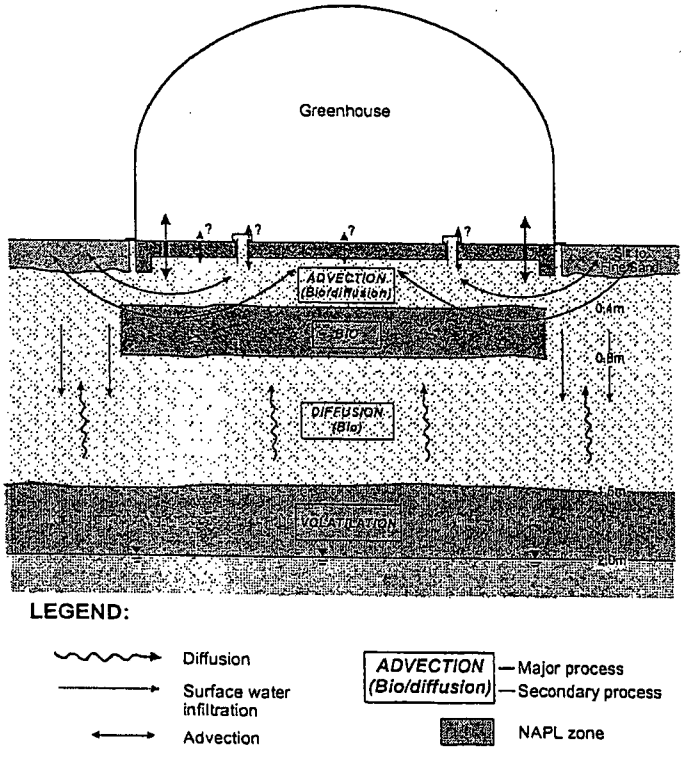

Figure 8
Conceptual Model for Vadose Zone Processes Below Greenhouse

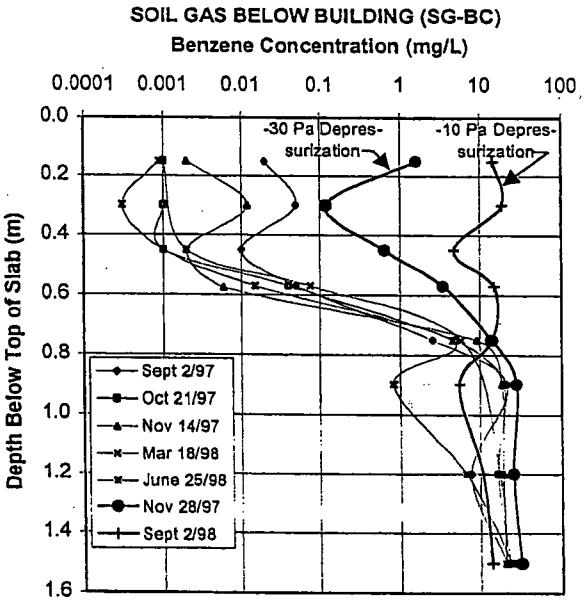

Figure 9
Effect of Depressurization on Soil Gas Benzene Profile

permeable or "leaky" concrete slab (relative to typical building construction) and relatively high building depressurizations. On-going testing is being conducted to evaluate the effect of a less permeable slab.

TABLE 5
Results of Soil Gas BTX Intrusion Monitoring[1]

Test	Location	Date	Building Ventilation Rate (m^3/min)	Soil Gas Flow Rate (L/min)	Mean Concentrations Benzene (ug/m^3)	Toluene (ug/m^3)	m&p-Xylene (ug/m^3)
No Building Depressurization (Static) Case							
Test 1	Flux Chamber Tests (4 Edge Cracks)	Nov 7-13/97	NA	NA	1.0	4.5	2.2
	Air Inside Greenhouse	Nov 7-13/97	NA	NA	18	61	8.0
	Ambient Air Outside Greenhouse	Nov 7-13/97	NA	NA	10	22	4.4
Test 2	Flux Chamber Tests (4 Edge Cracks)	NA	NA	NA	NT	NT	NT
	Air Inside Greenhouse	June 30-July 24/98	NA	NA	2.3	16	4.6
	Ambient Air Outside Greenhouse	Aug 25-Sept 3/98	NA	NA	4.5	19	3.2
Building Depressurization (Dynamic) Case							
-30 Pa	Flux Chamber Tests (4 Edge Cracks)	Nov 19-26/97	30	NT	-[3]	-[3]	-[3]
	Air Inside Greenhouse	Nov 19-26/97	30	NA	44	209	34
	Ambient Air Outside Greenhouse	Nov 19-26/97	30	NA	15	60	13
-10 Pa	Flux Chamber Tests (4 Edge Cracks)	Aug 28-Sept 1/98	10	1.84[2]	334000	294000	24000
	Air Inside Greenhouse	Aug 25 - Sept 3/98	10	NA	112	690	243
	Ambient Air Outside Greenhouse	Aug 25-Sept 3/98	10	NA	4.5	19	3.2

[1] All concentrations are arithmetic mean values for 3 to 4 measurements, NA = not applicable, NT = not tested

[2] Total gas flow rate through four 0.9 m-long open portions of edge crack (*i.e.*, not covered with plastic) measured using flux chamber.

[3] Sorbant tube breakthrough occurred.

[4] Approximate rates, volume of greenhouse = 125 m^3

Preliminary comparison of model-predicted to measured intrusion of BTX was conducted using a one-dimensional "screening-level" model based on the Johnson and Ettinger (1991) framework. The model includes steady-state diffusion in soil with no bioattenuation, and diffusion and advection through the building envelope, and is described in Hers *et al.* (1997). For the no induced building underpressurization case, BTX flux rates were very low and, in effect, could not be measured. However, comparison of predicted to measured indoor BTX concentrations provide some insight as to model accuracy. For example, the model-predicted indoor toluene concentrations (static diffusion case) are on the order of several thousand ug/m^3, depending on the input parameters chosen (*e.g.*, soil properties, natural building ventilation rate). Toluene concentrations of this magnitude are at least two orders-of-magnitude higher than actual measured values. For the dynamic case, the model-predicted values are within one order-of-magnitude of the measured values based on the input parameters used. It is noted that the overall model-predicted BTX flux into the building is controlled by the diffusive flux rate in soil.

CONCLUSIONS

Monitoring of vadose zone fate and transport of BTX and intrusion into a research greenhouse indicates that processes and factors affecting this pathway are complex with temporal and spatial variability observed. In the vadose zone, significant bioattenuation of BTX in soil gas was observed over a small depth interval below and adjacent to the greenhouse. Biodegradation below the greenhouse is dependent on oxygen transport, which for soil directly below the slab is thought to occur primarily through advective processes, as induced by temperature (*i.e.*, diurnal) and barometric pressure fluctuations. Oxygen transport rates are affected by soil permeability, and hence soil moisture, which is consistently at relatively low levels below the greenhouse but varies seasonally in surface soil adjacent to the greenhouse. Soil moisture is a critical parameter that influences all the major processes affecting vadose zone fate and transport (*i.e.*, diffusion, advection and biodegradation). Monitoring of BTX intrusion into the greenhouse indicates that under static conditions (*i.e.*, no fan-induced

building depressurization) BTX flux rates are very low and likely insignificant. Model predictions based on the Johnson and Ettinger (1991) framework were highly conservative for the static case. The BTX flux into the greenhouse was significantly higher for the dynamic case and indicates that advective processes extended to a sufficient depth to draw BTX to below and into the greenhouse. The relatively high slab and subslab soil permeability and shallow contamination contribute to the higher BTX intrusion rates for the dynamic case.

Further work that we consider important at this site include investigation of potential long-term drying of soil below a building and effects on biodegradation, O_2 transport through pumping below a building including consideration of spatial variation in O_2 and building effects, and transport processes through a building envelope including assessment of a less permeable or "leaky" slab.

ACKNOWLEDGEMENTS

Funding for this research was provided by Alberta Environmental Protection, American Petroleum Institute, B.C. Environment, Canada Mortgage and Housing Corporation, Canadian Association of Petroleum Producers, Canadian Petroleum Products Institute, Chatterton Petrochemical, Dow Chemical and Ontario Ministry of Environment. The assistance of Mr. Scott Hannam of Analytical Services Laboratory (ASL) and Mr. David Jacubcak is appreciated.

REFERENCES

DeVaull, G., Ettinger, R.A., Salanitro, J.P and Gustafson, J. 1997. *Benzene, Toluene, Ethylbenzene and Xylenes Degradation in Vadose Zone Soils During Vapor Transport: First-Order Rate Constants.* The Proceedings of the 1997 Petroleum Hydrocarbon and Organic Chemicals in Ground Water: Prevention, Detection and Remediation Conference, Houston, Texas, November, pages 365-379.

Fischer, M.L., Bentley, A.J., Dunkin, K.A., Hodgson, A.T., Nazaroff, W.W., Sextro, R.G., Daisay, J.M. 1996. *Factors Affecting Indoor Air Concentrations of Volatile Organic Compounds at a Site of Subsurface Gasoline Contamination.* Environ. Sci. Technol., 30, 2948-2957.

Garbesi, K. 1988. *Experiments and Modeling of the Soil-Gas Transport of Volatile Organic Compounds into a Residential Basement.* University of California at Berkeley, M.Sc. Thesis, December.

Garbesi, K., Sextro, R.G., Robinson, A.L., Wooley, J.D., Owens, J.A., Nazaroff, W.W. 1996. Water Resources Research, 32, 547-560.

Hers, I., Zapf-Gilje, R., Petrovic, R., Macfarlane, M., and McLenehan, R. 1997. *Prediction of Risk-Based Screening Levels for Infiltration of Volatile Subsurface Contaminants into Buildings.* Environmental Toxicology and Risk Assessment (Sixth Volume), ASTM STP 1317, F.James Dwyer, Thomas Doane, and Mark L. Hinman, Eds., American Society for Testing and Materials, 1997.

Johnson, P.C., and Ettinger, R. 1991. *Heuristic Model for Predicting the Intrusion Rate of Contaminant Vapours into Buildings.* Environ. Sci. Technol., 25, 8, 1445-1452.

Johnson, P.C., Bruce, C., Johnson, R.L., Kemblowski, M.W. 1998. *In situ* Measurement of Effective Vapor-Phase Porous Media Diffusion Coefficients. Accepted for Publication, Environ. Sci Technol.

Jury, W.A., Russo, D., Streile, G., El Abd, H. 1990. *Evaluation of Volatilization by Organic Chemicals Residing Below the Soil Surface,* Water Resources Research, 26(1), 13-20.

Lambe, W.T. (1951). *Soil Testing for Engineers.* John Wiley & Sons.

Laubacher, R.C., Bartholomae, P., Velasco, P. and Reisinger, H.J. 1997. *An Evaluation of the Vapour Profile in the Vadose Zone above a Gasoline Plume.* The Proceedings of the 1997 Petroleum Hydrocarbon and Organic Chemicals in Ground Water: Prevention, Detection and Remediation Conference, Houston, Texas, November, pages 396-409.

Zwick, T.C., Leeson, A., Hinchee, R.E., Hoeppel, R.E. and Bowling, L. 1995. *Soil Moisture Effects During Bioventing in Fuel-Contaminated Arid Soils.* In. *In situ* Aeration: Air Sparging, Bioventing and Related Remediation Processes, Batelle Press, Columbus, pp. 333-340.

APPENDIX VII

IN SITU RESPIRATION TEST DATA

Chatterton In Situ Respiration Test

1.2 m Probe West Greenhouse

1/2" Diameter

Probe Depth	1.2 West										
Date	Sept. 3, 1998							Sept. 4, 1998			Sept. 5, 1998
Time sample	Hours	7:30	9:30	11:30	13:30	15:30	17:30	19:30	11:00	13:00	15:00	8:40
Running time	Hours	0.00	2.00	4.00	6.00	8.00	10.00	12.00	15.50	17.50	19.50	37.10
		Back Ground	Peroid 1	Peroid 2	Peroid 3	Peroid 4	Peroid 5	Peroid 6	Peroid 7	Peroid 8	Peroid 9	Peroid 10
He		2.50	1.80	1.90	1.80	2.10	2.20	2.40	1.70	2.10	2.10	1.50
O2		20.00	19.30	18.90	18.90	20.50	17.30	17.30	13.90	13.50	13.30	11.30
CO2		0.00	0.20	0.10	0.10	0.30	0.60	0.90	2.80	2.80	3.10	4.80
CH4		1.50	1.60	7.10	6.40	2.20	2.20	1.70	1.50	1.50	1.60	1.20

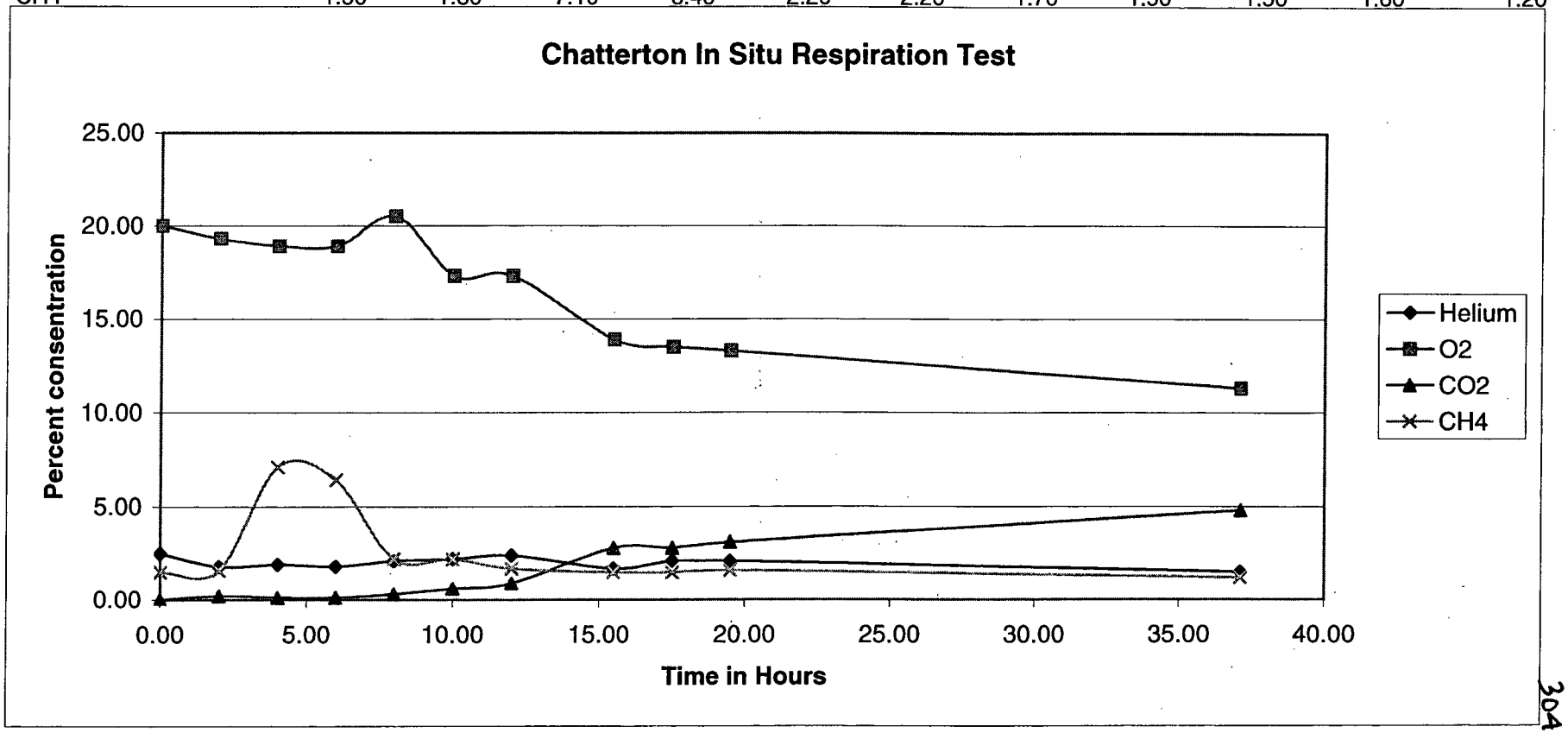

Chatterton In Situ Respiration Test

0.6 m Probe West Greenhouse

1/2" Diameter

Probe Depth	0.6 West										
Date	Sept. 3, 1998							Sept. 4, 1998			Sept. 5, 1998
Time sample Hours	7:30	9:30	11:30	13:30	15:30	17:30	19:30	11:00	13:00	15:00	8:40
Running time Hours	0.00	2.00	4.00	6.00	8.00	10.00	12.00	15.50	17.50	19.50	37.10
	Back Ground	Peroid 1	Peroid 2	Peroid 3	Peroid 4	Peroid 5	Peroid 6	Peroid 7	Peroid 8	Peroid 9	Peroid 10
He	4.10	2.60	2.40	1.90	2.00	1.90	1.90	1.40	2.10	1.20	0.86
O2	17.50	15.90	13.50	12.10	12.70	9.80	8.90	4.30	4.20	4.00	2.80
CO2	1.50	2.00	2.80	3.30	4.60	5.30	6.20	9.90	9.60	9.90	12.10
CH4	2.70	2.30	3.80	4.20	1.90	2.10	1.70	1.10	1.30	1.40	0.70

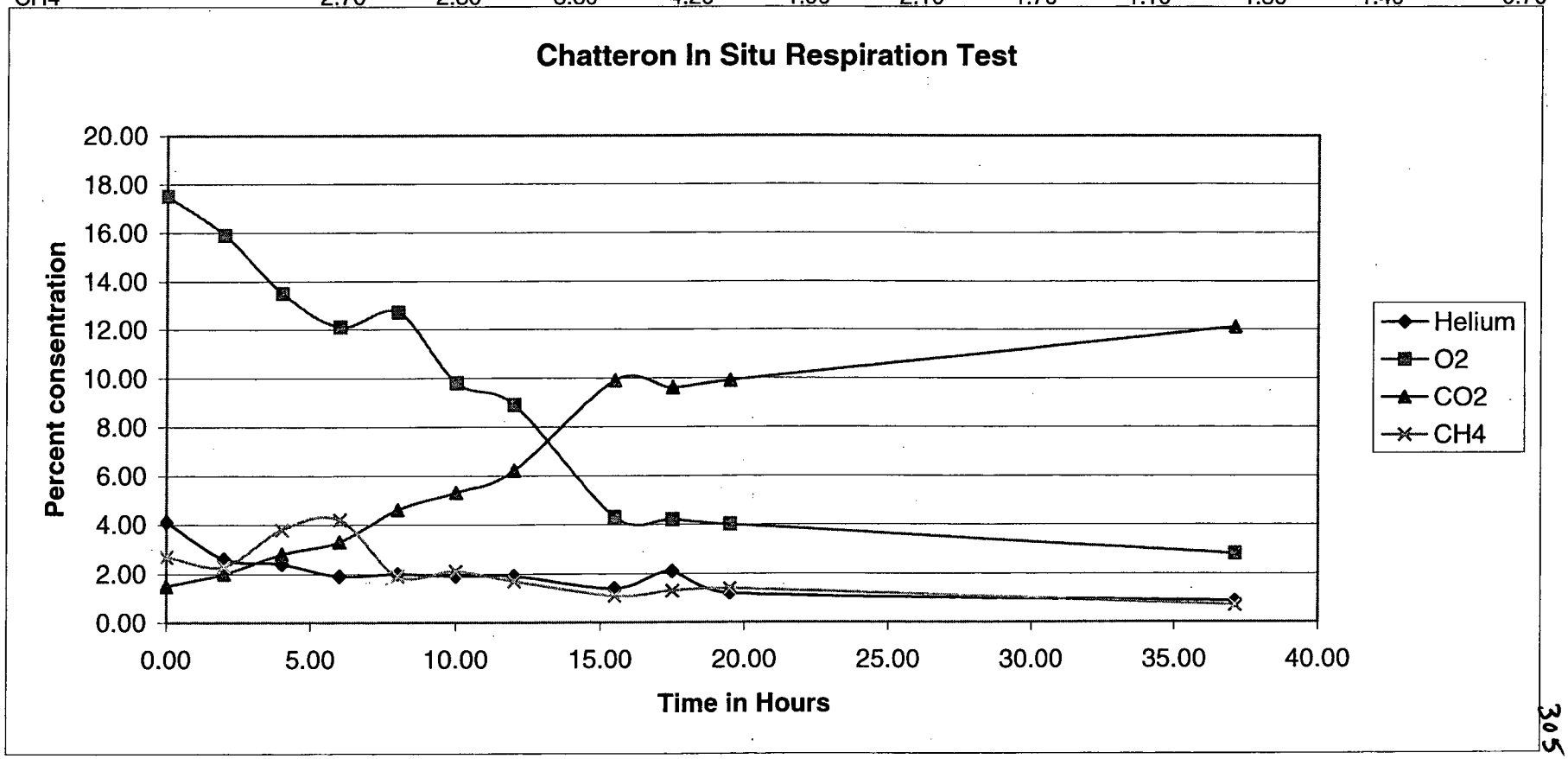

Chatterton In Situ Respiration Test 0.9 m depth below centre greenhouse

Probe Depth	0.9 Center										
Date	Sept. 3, 1998							Sept. 4, 1998			Sept. 5, 1998
Time sample Hours	7:30	9:30	11:30	13:30	15:30	17:30	19:30	11:00	13:00	15:00	8:40
Running time Hours	0.00	2.00	4.00	6.00	8.00	10.00	12.00	15.50	17.50	19.50	37.10
	Back Ground	Peroid 1	Peroid 2	Peroid 3	Peroid 4	Peroid 5	Peroid 6	Peroid 7	Peroid 8	Peroid 9	Peroid 10
He	4.60	3.30	2.60	2.00	2.10	2.10	2.10	1.60	1.40	1.40	1.00
O2	19.00	17.50	16.30	15.00	16.80	13.30	12.60	7.80	6.90	6.50	4.80
CO2	0.60	1.10	1.30	1.70	2.10	2.80	3.50	6.90	6.80	7.20	9.80
CH4	3.70	4.90	5.10	4.90	2.20	2.50	1.90	1.80	1.40	1.50	1.30

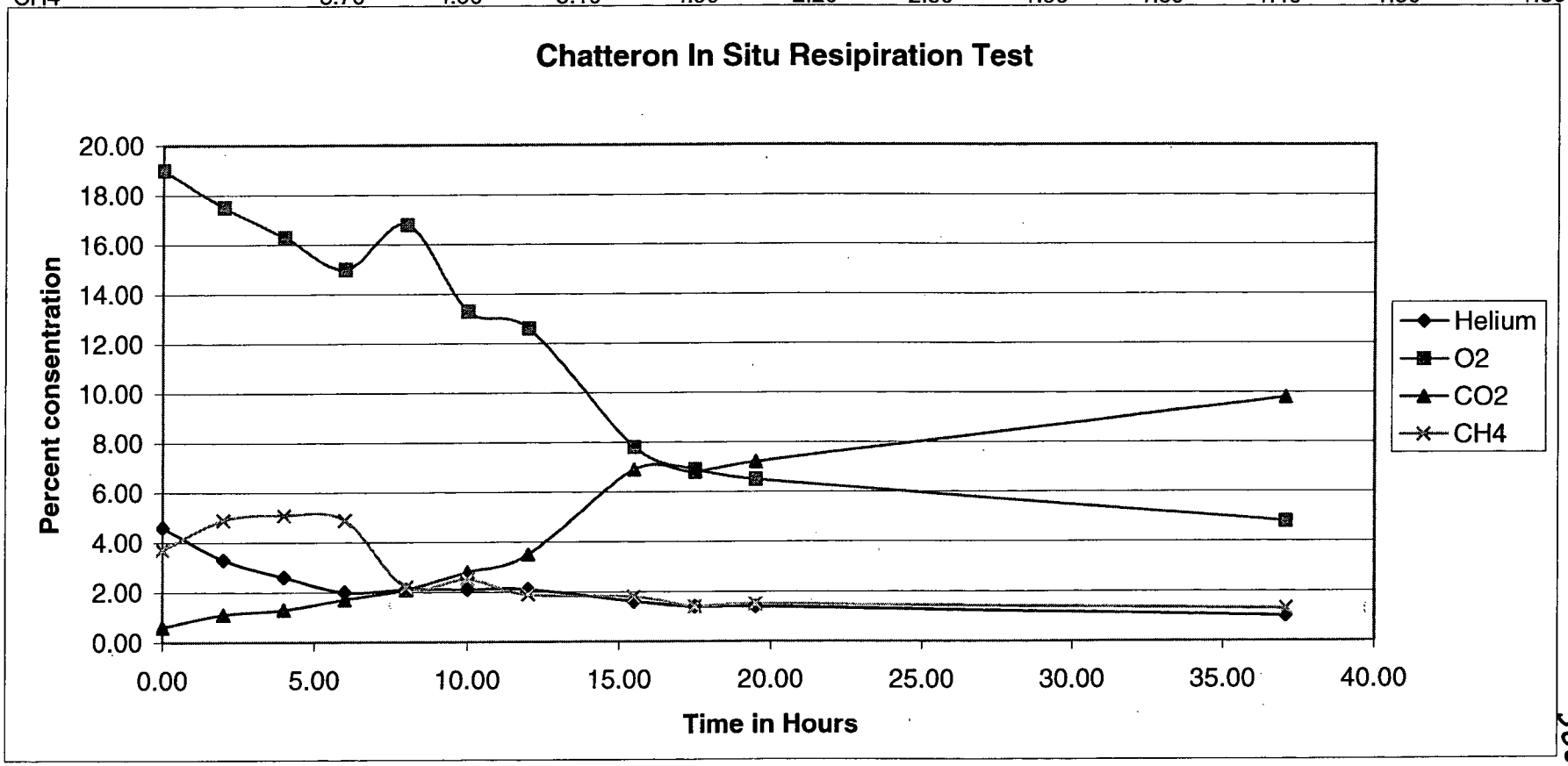

Chatterton In Situ Respiration Test

0.9 m Probe West Greenhouse

1/2" Diameter

Probe Depth	0.9 West										
Date	Sept. 3, 1998							Sept. 4, 1998			Sept. 5, 199
Time sample Hours	7:30	9:30	11:30	13:30	15:30	17:30	19:30	11:00	13:00	15:00	8:40
Running time Hours	0.00	2.00	4.00	6.00	8.00	10.00	12.00	15.50	17.50	19.50	37.10
	Back Ground	Peroid 1	Peroid 2	Peroid 3	Peroid 4	Peroid 5	Peroid 6	Peroid 7	Peroid 8	Peroid 9	Peroid 10
He	2.50	1.80	2.30	2.00	2.30	2.30	2.40	2.10	2.00	2.00	1.40
O2	20.00	19.70	18.70	18.20	20.80	16.90	16.70	13.00	12.70	12.30	10.20
CO2	0.00	1.00	0.10	0.20	0.60	0.80	1.10	3.40	3.40	3.50	5.70
CH4	1.50	0.50	1.30	4.50	1.50	1.50	1.40	1.20	1.30	1.70	0.70

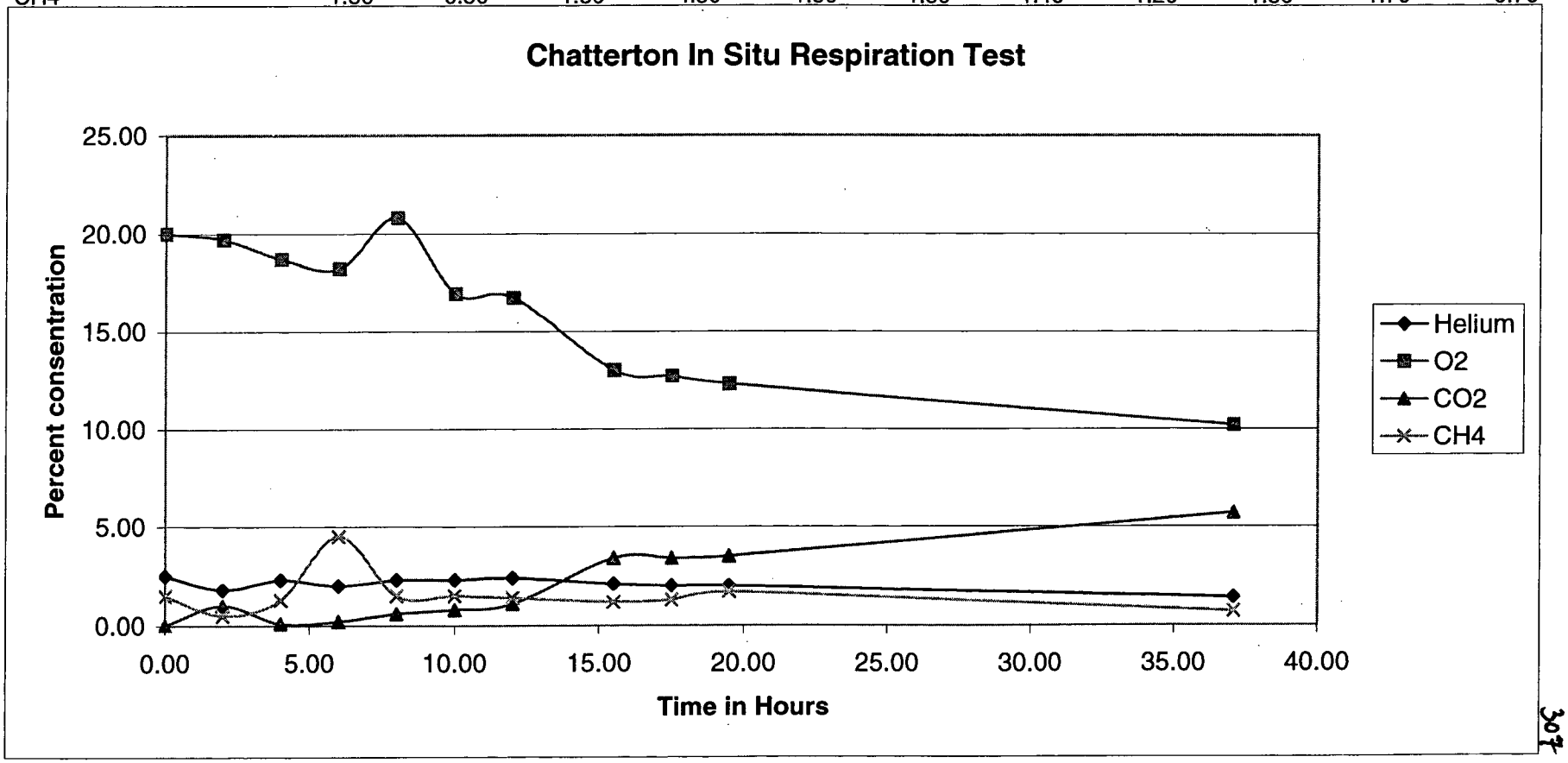

Chatterton In Situ Respiration Test 0.75 m Probe West Greenhouse

1/2" Diameter

Probe Depth 0.75 West											
Date	Sept. 3, 1998							Sept. 4, 1998			Sept. 5, 1998
Time sample Hours	7:30	9:30	11:30	13:30	15:30	17:30	19:30	11:00	13:00	15:00	8:40
Running time Hours	0.00	2.00	4.00	6.00	8.00	10.00	12.00	15.50	17.50	19.50	37.10
	Back Ground	Peroid 1	Peroid 2	Peroid 3	Peroid 4	Peroid 5	Peroid 6	Peroid 7	Peroid 8	Peroid 9	Peroid 10
He	3.90	2.60	2.30	1.80	2.10	1.90	1.20	1.30	1.20	1.00	0.44
O2	17.80	15.90	13.50	13.10	13.50	9.60	9.50	4.30	4.90	3.80	5.70
CO2	1.50	2.10	3.10	2.90	4.90	5.50	5.40	10.10	9.90	10.20	13.20
CH4	2.40	1.40	4.00	4.90	2.00	1.90	6.10	1.10	1.30	1.60	0.70

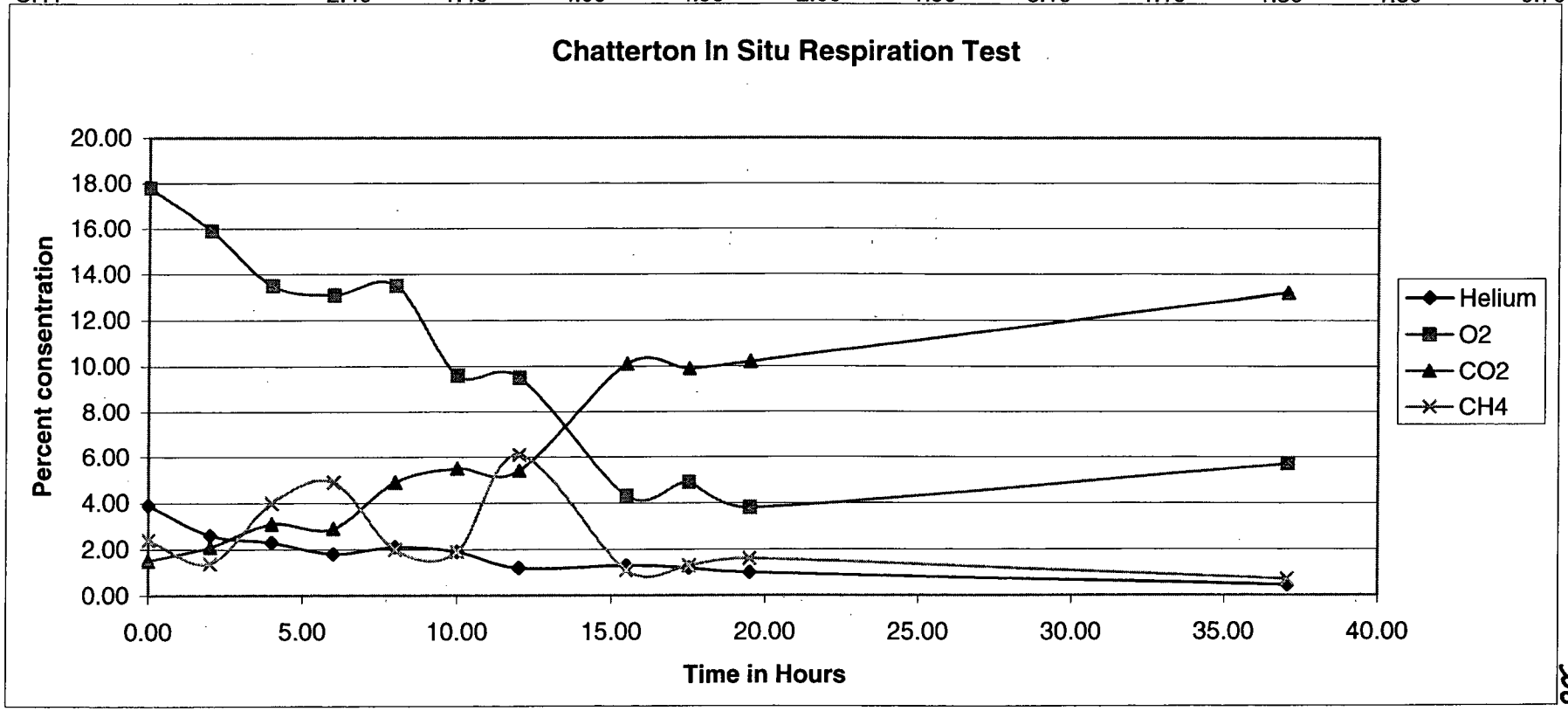

Chatterton In Situ Respiration Test

1.2 m Probe East Greenho

1/2" Diameter

Probe Depth	1.2 East										
Date	Sept. 3, 1998							Sept. 4, 1998			Sept. 5, 1998
Time sample Hours	7:30	9:30	11:30	13:30	15:30	17:30	19:30	11:00	13:00	15:00	8:40
Running time Hours	0.00	2.00	4.00	6.00	8.00	10.00	12.00	15.50	17.50	19.50	37.10
	Back Ground	Peroid 1	Peroid 2	Peroid 3	Peroid 4	Peroid 5	Peroid 6	Peroid 7	Peroid 8	Peroid 9	Peroid 10
He	3.00	2.30	2.00	1.90	2.10	2.20	2.40	2.40	2.10	2.10	1.70
O2	19.80	19.50	19.10	19.00	20.40	18.80	18.80	16.50	16.20	15.30	14.20
CO2	0.20	0.10	0.10	0.10	0.10	0.20	0.30	1.10	1.10	1.20	2.70
CH4	3.30	5.30	6.10	6.50	2.00	2.60	1.70	1.80	2.00	1.50	1.80

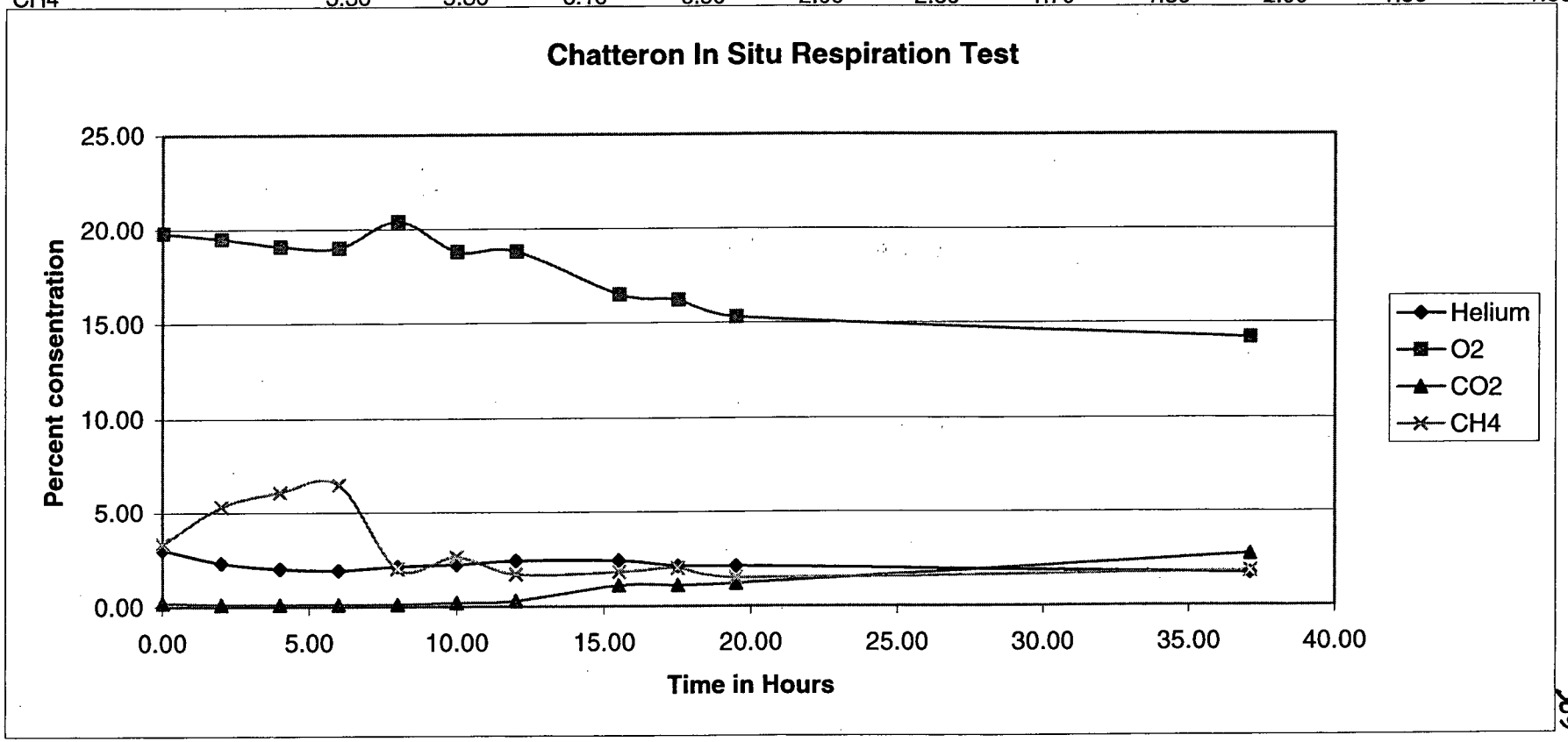

Chatterton In Situ Respiration Test 0.75 m Probe Center Greenhouse

1/4" Diameter

Probe Depth 0.75 Center											
Date	Sept. 3, 1998							Sept. 4, 1998			Sept. 5, 1998
Time sampled Hours	7:30	9:30	11:30	13:30	15:30	17:30	19:30	11:00	13:00	15:00	8:40
Running time Hours	0.00	2.00	4.00	6.00	8.00	10.00	12.00	15.50	17.50	19.50	37.10
	Back Ground	Peroid 1	Peroid 2	Peroid 3	Peroid 4	Peroid 5	Peroid 6	Peroid 7	Peroid 8	Peroid 9	Peroid 10
He	0.49	3.00	2.30	2.00	1.90	2.10	2.10	1.50	1.50	1.40	1.20
O2	19.90	19.40	18.20	17.80	19.80	17.00	16.70	14.10	13.00	12.90	11.50
CO2	0.10	0.30	0.30	0.30	0.30	0.90	1.10	2.40	2.20	2.40	4.70
CH4	2.40	4.70	5.60	5.60	1.80	2.90	2.40	1.50	1.10	1.30	1.40

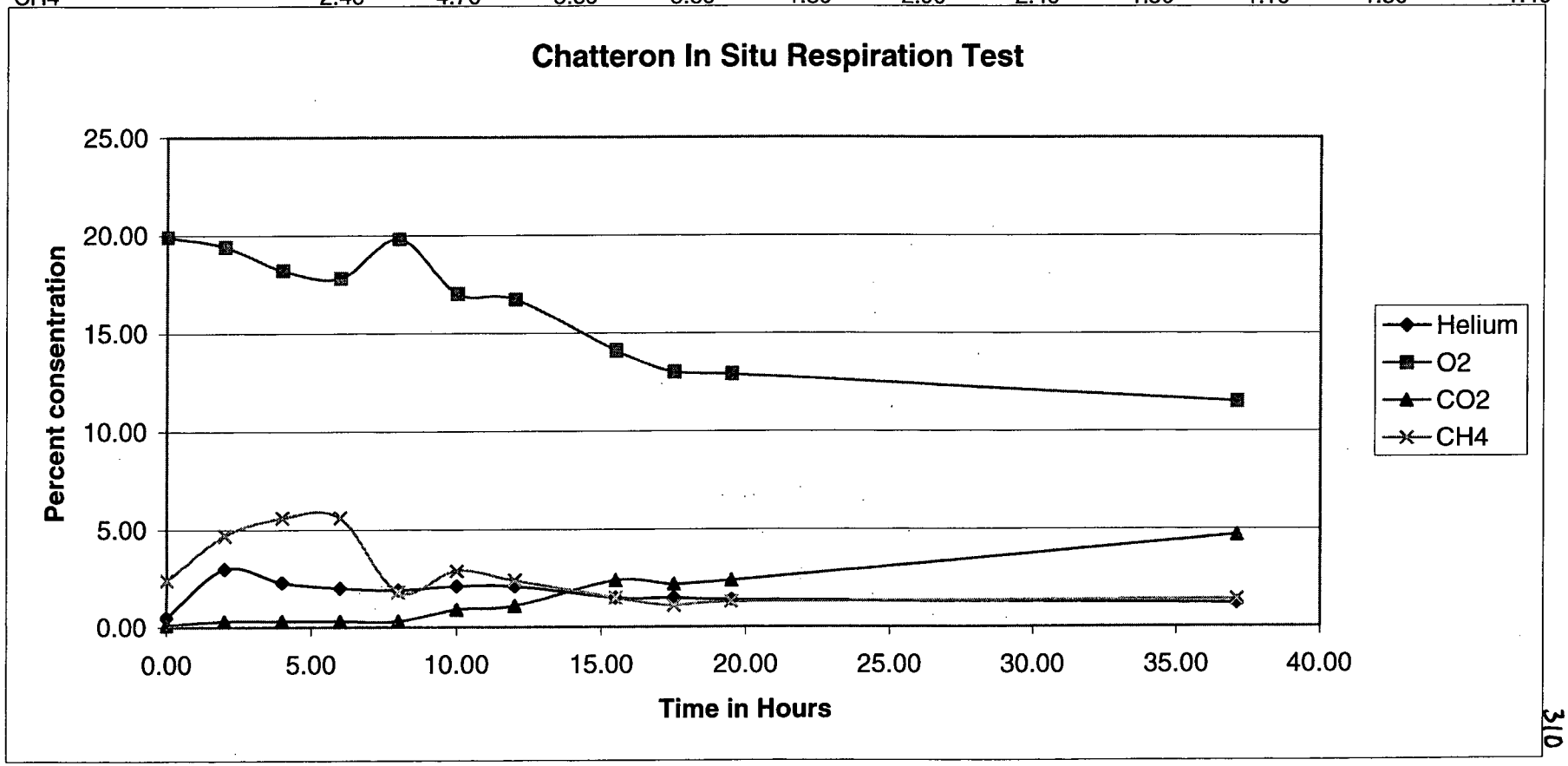

Resperation Test 0.75 Probe Center

1/2" Diameter

Probe Depth	0.75	Center										
Date		Sept. 3, 1998							Sept. 4, 1998			Sept. 5, 1998
Time sample	Hours	7:30	9:30	11:30	13:30	15:30	17:30	19:30	11:00	13:00	15:00	8:40
Running time	Hours	0.00	2.00	4.00	6.00	8.00	10.00	12.00	15.50	17.50	19.50	37.10
		Back Ground	Peroid 1	Peroid 2	Peroid 3	Peroid 4	Peroid 5	Peroid 6	Peroid 7	Peroid 8	Peroid 9	Peroid 10
He		N/A	2.60	2.20	2.10	2.20	2.10	1.90	1.00	1.40	1.40	0.64
O2		18.20	17.90	16.60	14.80	15.70	12.40	11.70	6.30	6.00	5.60	12.90
CO2		1.10	1.10	1.30	2.00	2.80	3.30	3.90	7.90	7.80	8.30	4.80
CH4		3.00	2.00	4.20	4.40	2.00	1.70	1.70	1.30	1.50	1.50	0.80

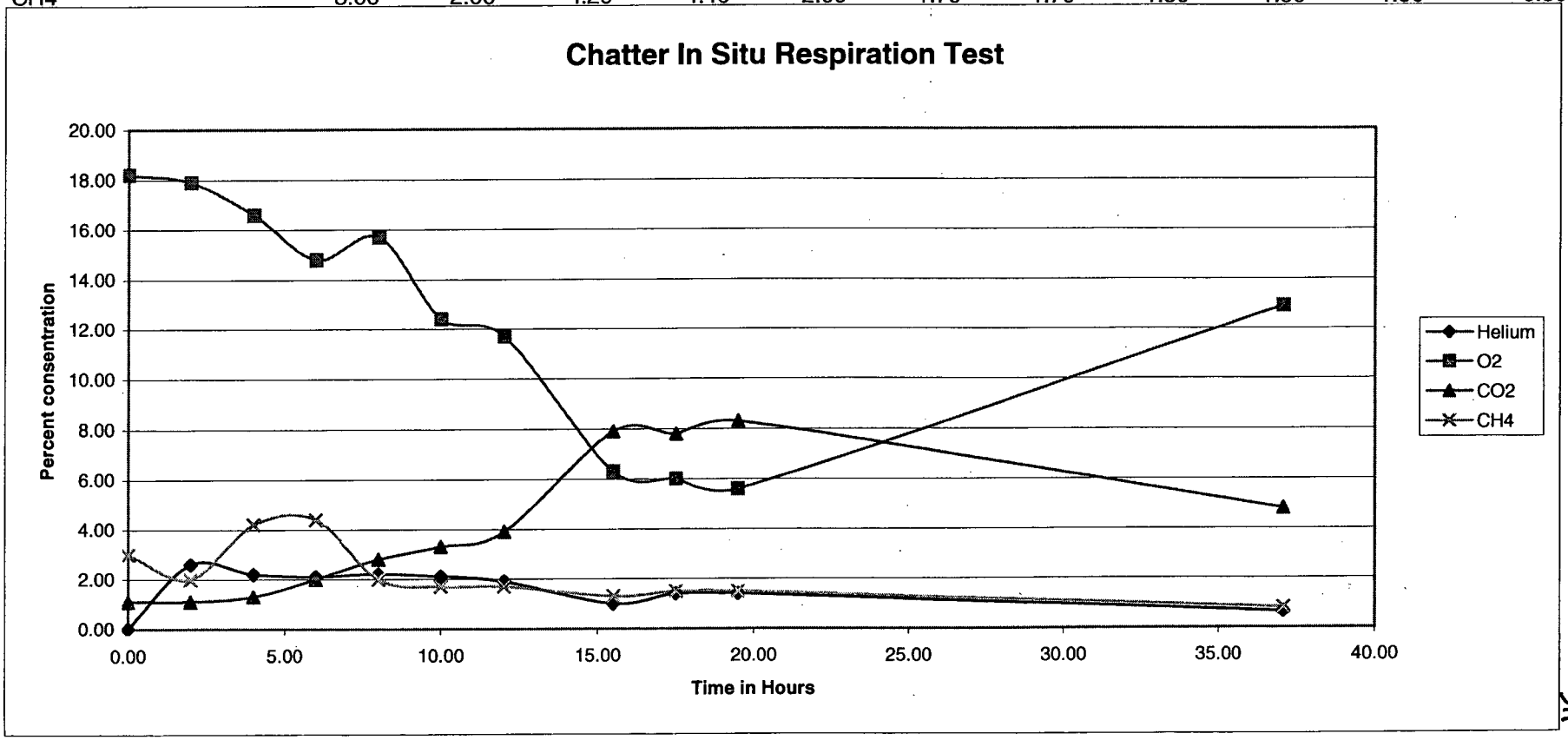

Chatterton In Situ Respiration Test 0.45 m depth below centre greenhouse

1/4" Diameter probe

Probe Depth 0.45	Center									
Date	Sept. 3, 1998						Sept. 4, 1998			Sept. 5, 1998
Time sampled-hours	7:30	11:30	13:30	15:30	17:30	19:30	11:00	13:00	15:00	8:40
Running time-hours	0.00	4.00	6.00	8.00	10.00	12.00	15.50	17.50	19.50	37.10
	Back Ground	Peroid 2	Peroid 3	Peroid 4	Peroid 5	Peroid 6	Peroid 7	Peroid 8	Peroid 9	Peroid 10
He	N/A	0.00	1.70	1.90	1.80	1.70	0.83	1.20	1.30	0.95
O2	20.00	15.70	12.60	12.90	10.40	10.80	9.20	5.50	4.70	3.60
CO2	0.20	3.00	2.90	3.90	4.50	4.40	6.80	8.20	8.90	10.90
CH4	0.40	4.00	2.80	1.70	1.50	1.60	1.10	1.20	1.40	0.90

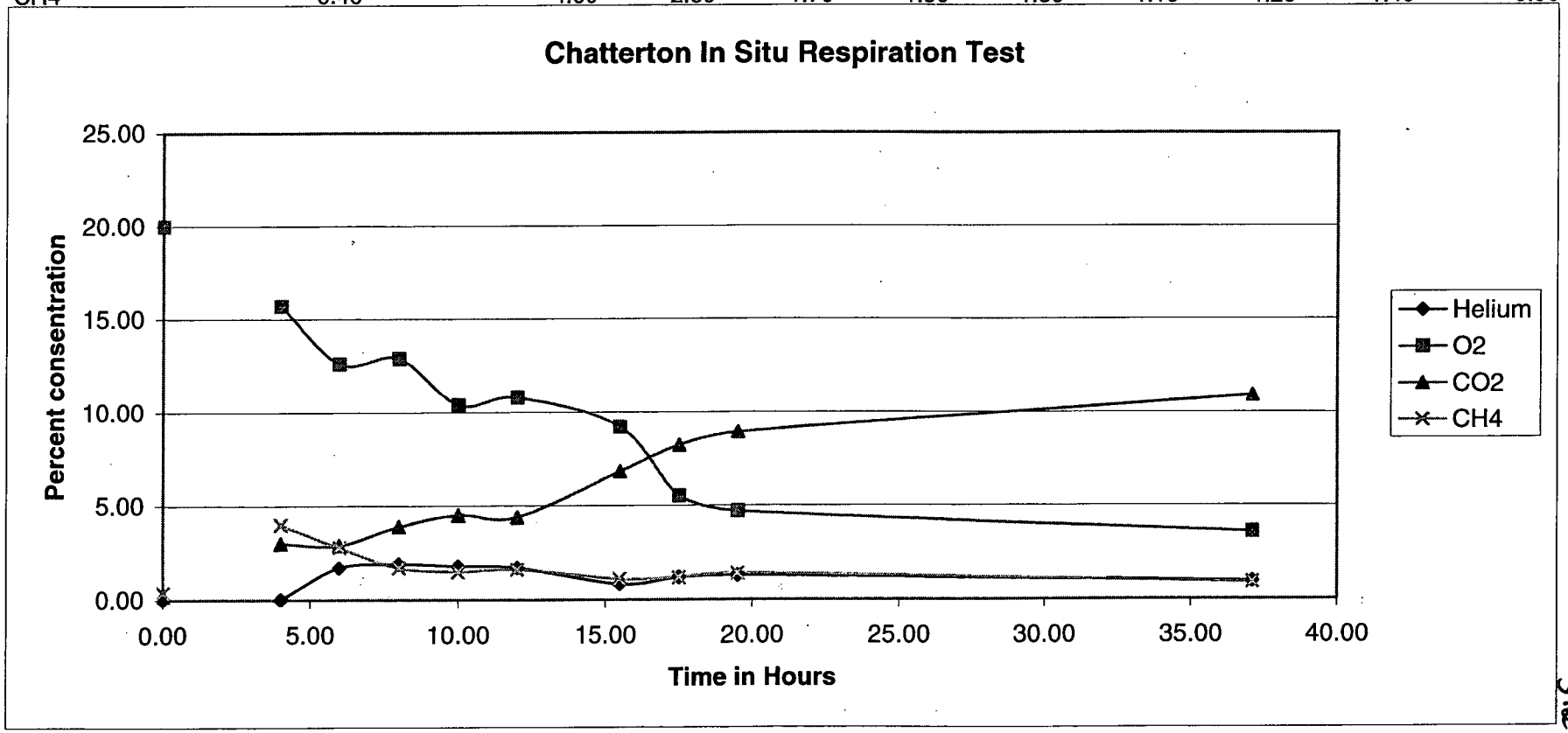

Chatterton In Situ Respiration Test 0.6 mb Probe Center Greenhouse

1/2" Diameter

Probe Depth	0.6 Center										
Date	Sept. 3, 1998							Sept. 4, 1998			Sept. 5, 1998
Time sample Hours	7:30	9:30	11:30	13:30	15:30	17:30	19:30	11:00	13:00	15:00	8:40
Running time Hours	0.00	2.00	4.00	6.00	8.00	10.00	12.00	15.50	17.50	19.50	37.10
	Back Ground	Peroid 1	Peroid 2	Peroid 3	Peroid 4	Peroid 5	Peroid 6	Peroid 7	Peroid 8	Peroid 9	Peroid 10
He	4.10	2.90	2.50	2.00	2.10	2.00	2.10	1.60	1.50	1.50	1.10
O2	17.60	17.20	15.60	14.80	16.50	13.00	12.50	8.20	7.80	7.50	5.60
CO2	1.30	1.30	1.50	1.90	2.40	2.80	3.40	6.50	6.50	6.90	9.00
CH4	1.30	2.10	3.30	2.90	2.30	1.70	1.40	1.30	1.50	1.70	1.00

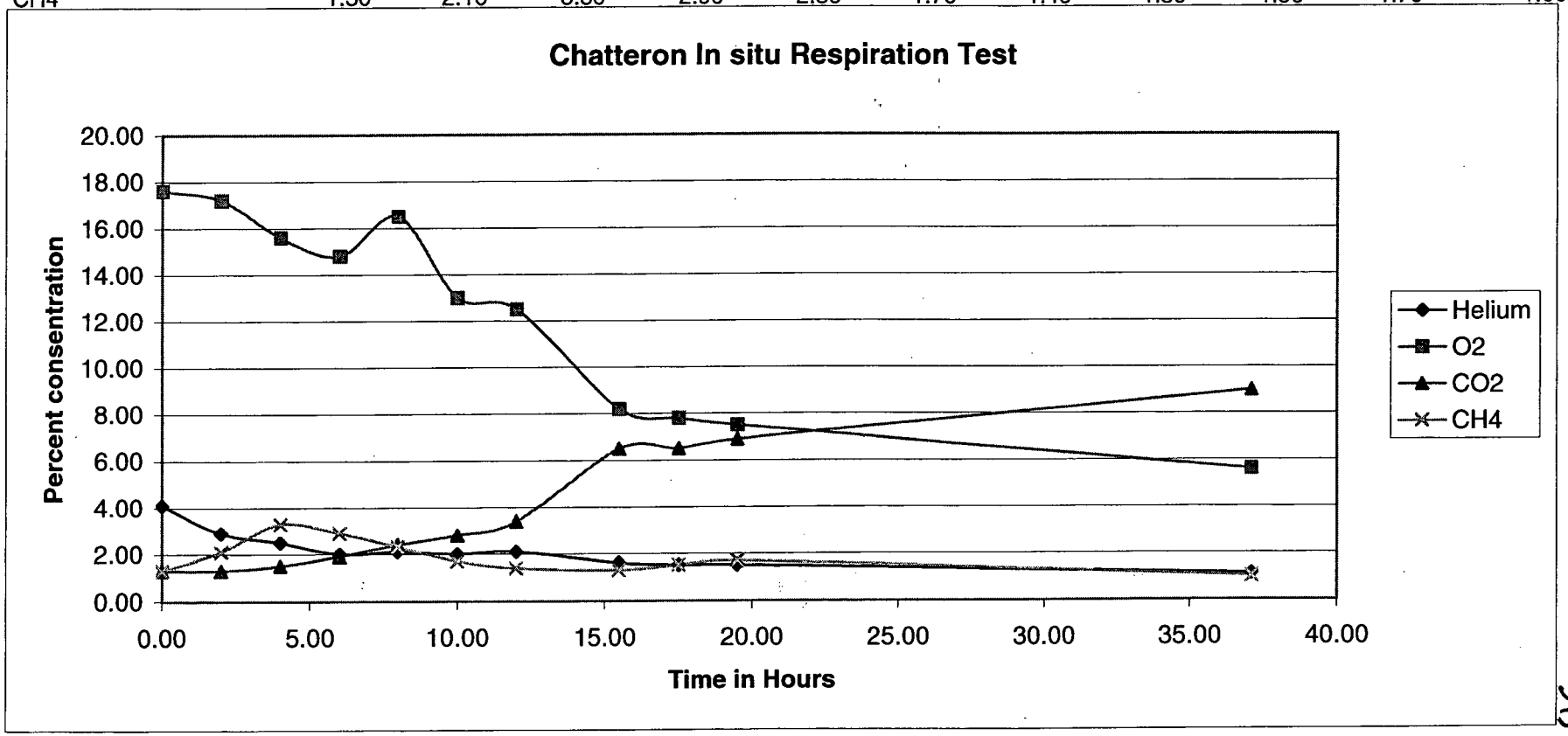

Chatterton In Situ Respiration Test 0.6m a Probe Center Greenhouse

1/2" Diameter
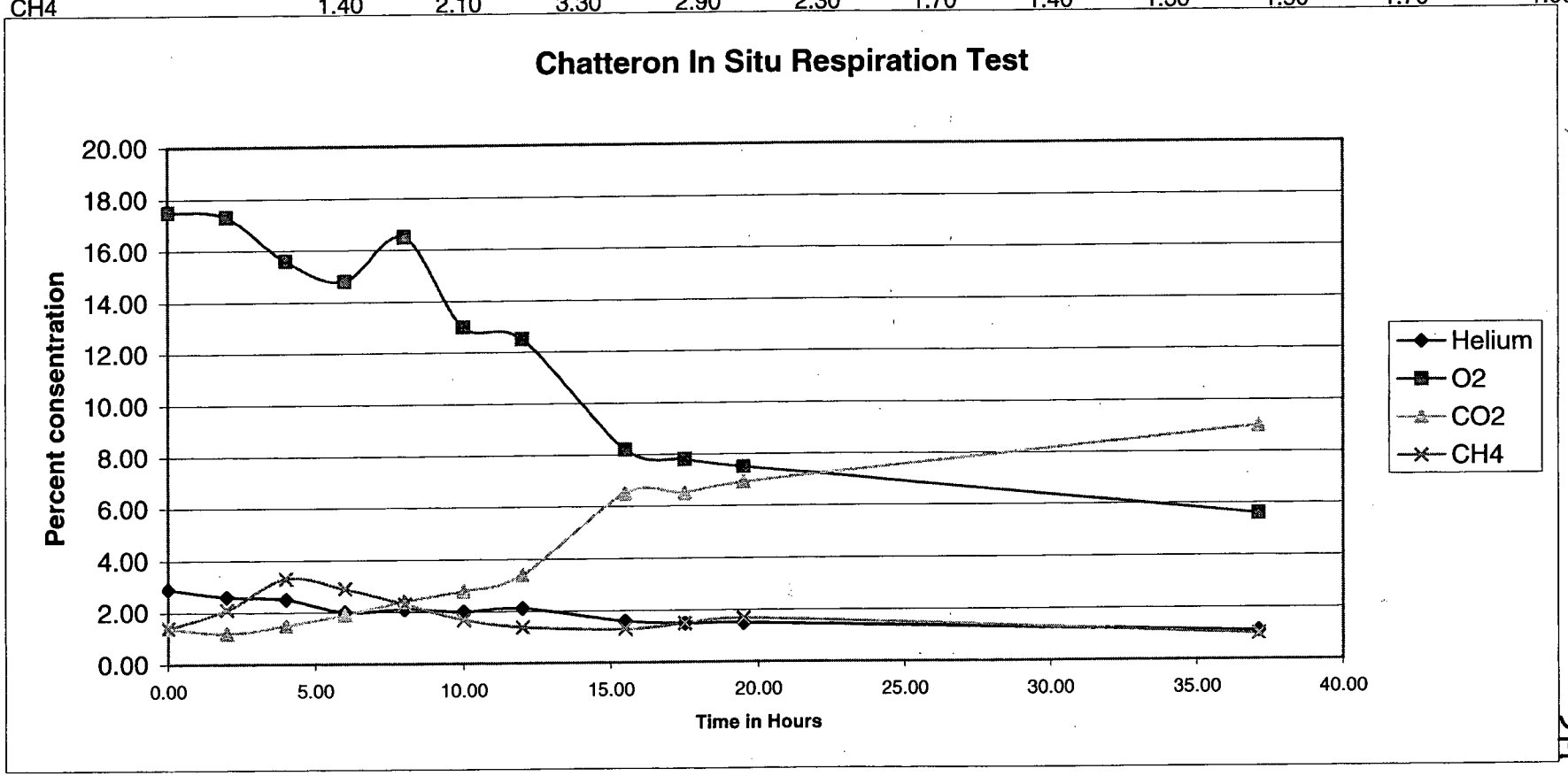
Probe Depth	0.6 Center										
Date	Sept. 3, 1998							Sept. 4, 1998			Sept. 5, 1998
Time sampled-hours	7:30	9:30	11:30	13:30	15:30	17:30	19:30	11:00	13:00	15:00	8:40
Running time-hours	0.00	2.00	4.00	6.00	8.00	10.00	12.00	15.50	17.50	19.50	37.10
	Back Ground	Peroid 1	Peroid 2	Peroid 3	Peroid 4	Peroid 5	Peroid 6	Peroid 7	Peroid 8	Peroid 9	Peroid 10
He	2.90	2.60	2.50	2.00	2.10	2.00	2.12	1.60	1.50	1.50	1.10
O2	17.50	17.30	15.60	14.80	16.50	13.00	12.50	8.20	7.80	7.50	5.60
CO2	1.40	1.20	1.50	1.90	2.40	2.80	3.40	6.50	6.50	6.90	9.00
CH4	1.40	2.10	3.30	2.90	2.30	1.70	1.40	1.30	1.50	1.70	1.00